UCDAVIS
UNIVERSITY OF CALIFORNIA

November 2011

California Cooperative Ecosystem Studies Unit, Department of Defense

Crop Water Use, Groundwater Flow, and Subsidence at Naval Air Station Lemoore, Fresno and Kings County, California

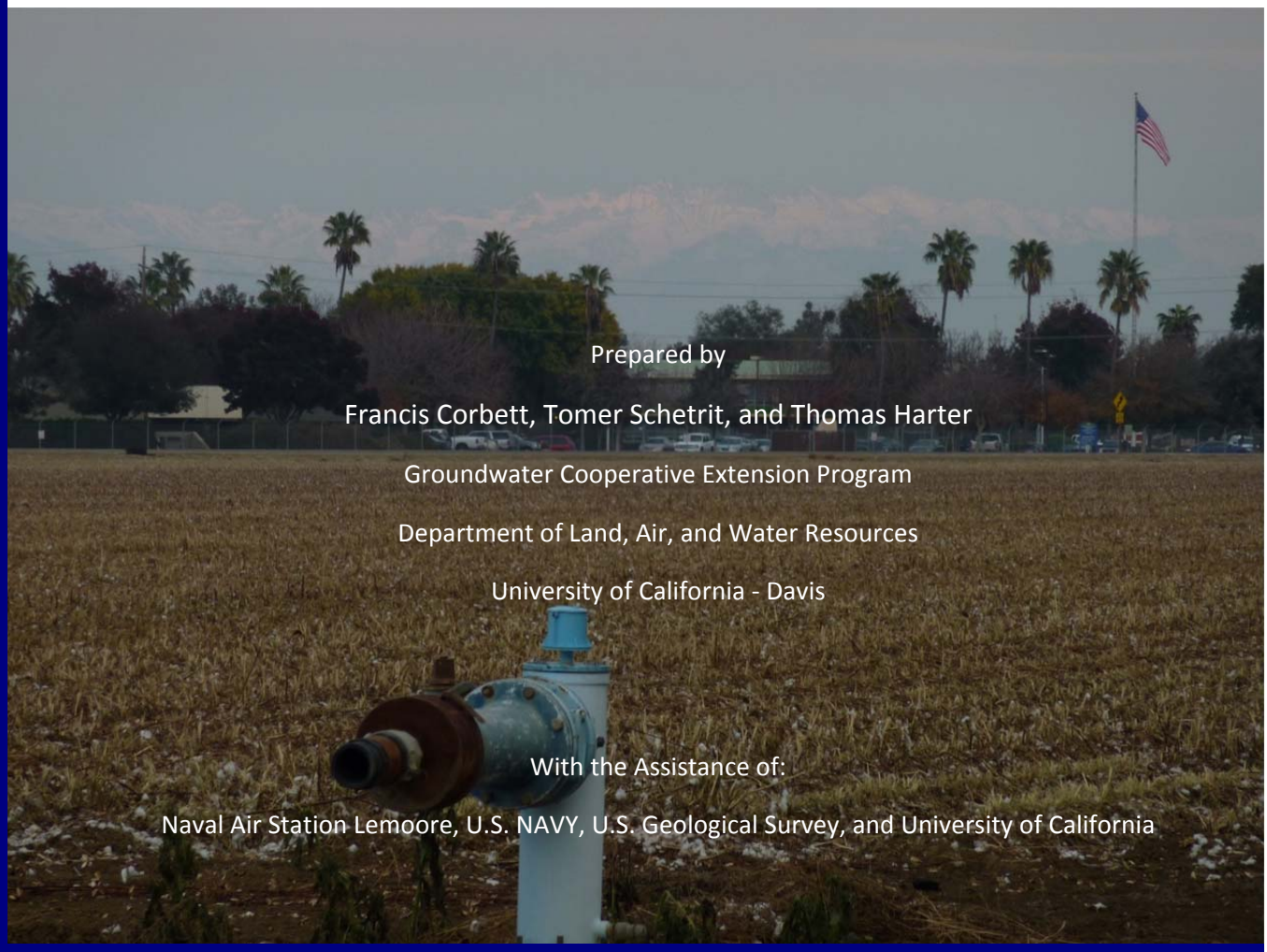

Prepared by

Francis Corbett, Tomer Schetrit, and Thomas Harter

Groundwater Cooperative Extension Program

Department of Land, Air, and Water Resources

University of California - Davis

With the Assistance of:

Naval Air Station Lemoore, U.S. NAVY, U.S. Geological Survey, and University of California

Prepared for:

Naval Air Station Lemoore

With funding by:

the U. S. Navy through the Cooperative Ecosystem Studies Unit with contracting support from the U. S. Army Corps of Engineers, Contract #W912DY-09-2-0053.

FINAL REPORT

Version 2,

November 3, 2011

ACKNOWLEDGMENTS

Preparation of this Report was assisted by:

Naval Air Station Lemoore:

Jeff Karrh, Environmental Engineer, Interim NAS Lemoore Installation Environmental Program Manager

John Crane, Natural Resources Manager, NAS Lemoore Environmental

Tim Schweizer, Natural Resource Specialist, NAS Lemoore Environmental

Richard Bottoms, Installation Environmental Program Manager, NAS Lemoore Environmental

Michelle Vieux, Commander, NAS Lemoore Public Works Officer

Robert Palmer, Fish and Wildlife Biologist

Naval Facilities Engineering Command, Southwest:

Edith Jacobsen, Environmental Planning Business Line Team Lead

Conception Flores, Natural Resource Specialist

University of California Davis:

Blaine Hanson, Ph.D., Faculty, Irrigation Cooperative Extension Specialist

Cathryn Lawrence, Ph.D., Biologist

Joseph Compte, Graduate Student

Marius Isken, Undergraduate Student

Stephen Micko, Undergraduate Student

University of California Cooperative Extension:

Don May, Fresno County, Emeritus

Dan Munk, Fresno County

U.S. Geological Survey:

Michelle Sneed, Technical Specialist, Sacramento

California Department of Water Resources:

John Kirk, Fresno; Iris Yamagata, Fresno

An electronic copy of the Final Report

is available from the following website:

http://groundwater.ucdavis.edu

For further inquiries, please contact:

Thomas Harter, Ph.D.

125 Veihmeyer Hall

University of California

Davis, CA 95616-8628

Phone: 530-752-2709

Email: ThHarter@ucdavis.edu

TABLE OF CONTENT

Figures:

Tables:

Abbreviations

CDWR	California Department of Water Resources
PLSS	Public Land Survey System
"M"	Mount Diablo base line and meridian
Central Valley	Central Valley of California
The Valley	The San Joaquin Valley
NASL	Lemoore Naval Air Station
USGS	U.S. Geological Survey
MODFLOW	U.S. Geological Survey - Modularization Concepts and the Groundwater Flow Process modeling software.
Coast Ranges	Coast Ranges of California
I-5	Interstate-5
WWD	Westland's Water District
amsl / bmsl	above mean sea level / below mean sea level
bgs	below ground surface
ags	Above ground surface
E-logs	electric logs
pdf	Portable Document Format
DRG	digital raster graphic
Corcoran or E-clay	Corcoran clay member of the Tulare formation
TDS	Total Dissolved Solids
WDL	Water Data Library
MAF	Million Acre Feet
NED	National Elevation Dataset
UTM	Universal Transverse Mercator coordinate system
NAD27	North American Datum of 1927

NAD83	North American Datum of 1983
NADCON	North American Datum Conversion Utility
ETc	Crop EvapoTranspiration
Hypo-CC	The Hypo-Corcoran Clay zone
CC	The Corcoran Clay zone
Sub-CC	The Sub-Corcoran Clay zone

Well Numbering System

Wells monitored by the California Department of Water Resources (CDWR) and cooperating agencies are identified according to the State Well Numbering system. The numbering system is based on the public land grid (PLSS), and includes the township, range, and section in which the well is located. Each section is further subdivided into sixteen 40-acre tracts, which are assigned a letter designation as shown in Figure 1. Within each 40-acre tract, wells are numbered sequentially. The final letter of the State Well Number refers to the base line and meridian of the public land grid in which the well lies. "M" refers to the Mount Diablo base line and meridian; "S" refers to the San Bernardino base line and meridian; "H" refers to the Humboldt base line and meridian (CDWR website, 2010).

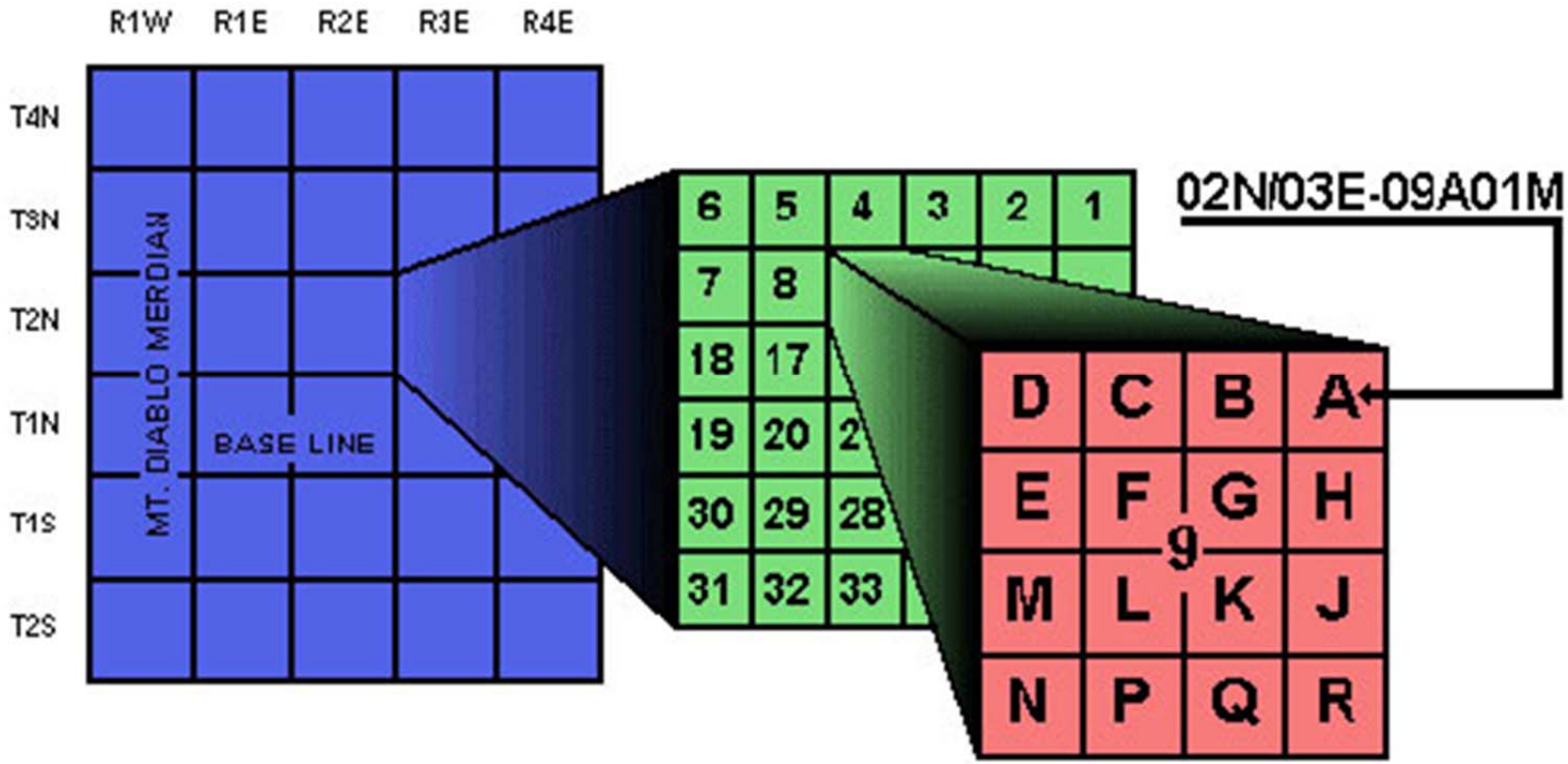

Figure 1 CDWR well-numbering system (CDWR website, 2010).

All wells within the study area covered by this report are suffixed by "M", for the Mt. Diablo base line and meridian. Wells are always referred to by their full state well number, for example 18S19E20P001M. Since all townships within the study area are to the south and east of the Mt. Diablo baseline and meridian, townships are referred to by a two-digit identifier, for example "township 18 south, range 19 east" is abbreviated as 18-19.

1 Introduction

1.1 Purpose and Scope

The goal of this project report is to provide an assessment of historic and potential future water uses, hydrogeology, and subsidence associated with groundwater pumping at the Naval Air Station Lemoore (NASL), Fresno County and Kings County, California. The report specifically considers water use of crops grown on 13,000 acres of land at NASL and provides data, data analyses, and tools to assist NASL staff with strategic planning and management of its water resources. The work area consists of all 13,000 acres of land at NASL and surrounding lands of hydrogeological significance. Strategic objectives from this study are to:

a. ensure the long-term viability and sustainability of NASL's agriculture outlease program;

b. define current base-wide water quality and quantity requirements;

c. determine to what extent NASL's agriculture outlease program and its municipal and industrial water requirements can be satisfied by supplemental groundwater resources; and

d. establish the data and conceptual technical-scientific foundation for a robust water resources management program to include or at least consider conjunctive management of both surface and groundwater resources. Concurrent ongoing studies at NASL analyze reuse/recycling of municipal and industrial wastewaters, surface and stormwater storage, and groundwater recharge/banking.

This report is structured into chapters that roughly follow the project's Task Deliverables:

Chapter 1: Introduction with outline, background and project area. Describes the purpose of this report and identifies the area of interest for a regional hydrologic analysis needed to provide a thorough assessment of the hydrology, geology, and potential future subsidence rates at NASL (Task 1-1).

Chapter 2: Historic water supply and crop water use analysis. Provides an overview of surface water deliveries and groundwater pumping, an archive of historically grown crops and an analysis of historic crop water use at NASL (Task 1-2, Task 1-3).

Chapter 3: Identification of potential alternative crop and irrigation management practices and assessment of water use under alternative practice scenarios (Task 1-4).

Chapter 4: Geology, hydrogeology, and groundwater dynamics. Describes the general geology and hydrogeology of NASL and surrounding areas and includes a detailed subsurface stratigraphy, identification of fine-textured and coarse-textured layers, historic water level

analyses, groundwater occurrence, movement, and quality, including historical trends, and identification of data gaps (Task 1-6).

Chapter 5: Assessment of historic land subsidence and subsidence related hydrogeologic properties in the region. Summarizes historic land elevation data, reviews subsurface stress-strain relationships, and estimates parametric values for elastic and inelastic storage coefficients in aquifers and aquitards (Task 1-8).

Chapter 6: Assessment and modeling of future subsidence. Provides development of a one-dimensional groundwater flow and land subsidence model for NASL, calibration to existing water level and land subsidence data, and outlines future scenarios (Task 1-9).

Chapter 7: Recommendations for future monitoring activities, crop and irrigation management, for developing water management guidelines, and for groundwater level decline management. Also include a preliminary recommendation for admin well location, base-wide monitoring protocols/guidelines to be adopted by NASL, nature/ extent/frequency of monitoring, data format and quality, and possibility/usefulness of long-term pump tests using existing wells (Task 1-10).

Ongoing but incomplete work include:

- Preliminary historic water budget analysis including estimate of storage changes for the project area with available and readily accessible data and analysis of significant data gaps (Task 1-5).
- Statistical analysis and transition probability-based geostatistical model of the aquifer stratigraphy using borehole logs for quantitative description of the sediment stratigraphy at the site. (Task 1-7)

1.2 Background: Location, Water Use, Groundwater, and Subsidence

The Naval Air Station Lemoore is located on the Westside of the Tulare Lake Basin, a closed hydrologic region within the Central Valley of California. A majority of the area is leased for irrigated agricultural production. Soils on the Station in general are well to moderately well-drained and are affected by salt and alkali. NASL is just west of the shallow trough of the Tulare Lake Basin, adjacent to and west of the diversion fork of the Kings River. The south fork of the diversion drains into the former Tulare Lake. The north fork of the diversion becomes the Fresno Slough, which is a historic overflow channel draining the historically ephemeral Tulare Lake into the San Joaquin River to the north at times when the lake reached a sufficiently high stage. Groundwater on and near NASL is pumped from depths exceeding 1,000 – 1,500 ft. below ground surface (bgs). The upper 2,000 to 3,000 ft of the subsurface within the below NASL consists of tertiary and quaternary unconsolidated sediments of predominantly alluvial, fluvial, and lacustrine origin. Unconsolidated sediment materials include clays, silts, sands, and gravels. Near-surface sediments are primarily clayey-silty, while significant amounts of coarse-

textured sediments (sands, gravels) are found at depth forming a confined aquifer systems with intercalated clay- and silt-beds (aquitards).

Groundwater is primarily used to irrigate agricultural crops. Historic pumping in the Tulare Lake Basin during the 20th century has caused significant water level declines in the area around NASL. The overdraft of the confined aquifer temporarily came to an end with the arrival of surface water through the federal Central Valley Project (San Luis Canal project), beginning in the late 1960s. However, the decline in pressure within the confined aquifer and the decline of water levels within the upper semi-confined aquifer units in the region had led to widespread and significant land subsidence in the region (Ireland et al., 1984; Galloway et al., 1999). The land subsidence observed in this region occurs as a result of the compaction of aquitard sediments, primarily clays (Poland et al., 1984). Compaction is the irreversible loss of pore space and water storage volume within the skeleton of sediment materials. Compaction occurs in response to increased effective stress onto the sediment skeleton, which is due to the loss of pressure in the pore water. The pore water pressure counterbalances the total pressure onto the sediments from the weight of the overburden (sediments and water). When water pressure decreases, the effective stress increases, leading to a mostly inelastic deformation of the sediment skeleton in clays and silts, and to a mostly elastic (reversible) deformation of the sediment skeleton in sands and gravels. The compaction (or vertical compression) of clay sediments leads to measurable land subsidence (Helm, 1975; Meinzer, 1928; Terzaghi, 1925). Maximum observed land subsidence in the region of NASL during the 20th century reached totals of as much as 30 ft. (Ireland et al., 1984).

Beginning in the late 1960s, the importation of surface water for irrigation led to significant reductions in groundwater pumping and subsequent recovery of water levels. While this did not reverse past land subsidence, the large land subsidence rates observed during the middle of the 20th century largely abated by the 1970s. However, droughts and recent court decisions concerning the delivery of water through the Sacramento-San Joaquin Delta to the federal and state water projects are significantly hampering surface water deliveries to Westlands Water District (WWD), a large irrigation district that encompasses NASL and extends to the south, west, and north of NASL. Groundwater pumping has significantly increased as a result of surface water shortages. Declining water levels threaten to lead to further compaction of fine-grained sediments within the aquifer-system surrounding NASL and leading to renewed land subsidence.

Strategically, the dual threat of long-term cuts to surface water supply, extended drought conditions, and limited groundwater pumping to avoid large-scale land subsidence can only be met by properly managing total consumptive water use within NASL and in the region surrounding NASL. This report provides the basis for developing quantifiable, rigorous strategies to establish the necessary monitoring programs and evaluate potential mitigation strategies.

1.3 Geographic and Geologic Description of the NASL Location

The NASL site is situated in Kings and Fresno Counties, California, approximately 30 miles to the southwest of the City of Fresno.

Within the Valley, NASL is located centrally in the southern portion of the Central Valley, within the Tulare Lake Basin watershed. It is located south and adjacent to the extension of the San Joaquin Valley trough, immediately north and west of the original Tulare Lake Bed. Here, the Valley is at its widest - approximately 60 miles.

Approximately 40 miles to the northeast of NASL, the Sierra Nevada runs for 400 miles from north-northwest to south-southeast, and separate the Central Valley from the Basin and Range Province to the east. Nearly, 20 miles to the west of NASL are the Coast Ranges of California, which also stretch from north-northwest to south-southeast, for a distance of more than 600 miles and separate the Valley from the Pacific Ocean. The Kettleman Hills is the closest surface feature to NASL. They crop out from the Coast Ranges to the southwest of NASL.

NASL lies adjacent to and immediately west of the shallow trough that divides the 'Westside' and the 'Eastside' of the San Joaquin Valley. Furthermore, NASL is located adjacent to and west of the fork in the Kings River that separates Kings River water flowing south into the Tulare Lake Bed and waters flowing north into Fresno Slough, which discharges into the San Joaquin River. Other major rivers of the Tulare Lake Basin are the Kaweah, Tule and Kern Rivers on the Eastside, and the ephemeral Cantua Creek and Los Gatos Creek on the Westside. With respect to groundwater sub-basins, NASL – while mostly overlying the Westside sub-basin, is immediately adjacent to the triple-junction of the Westside, Kings River, and Tulare Lake sub-basins of the Tulare Lake Basin, as identified by CDWR Bulletin 118-2003 (CDWR, 2003, p. 176).

1.4 Project Area

For a complete hydrological study, and to prepare for later development of three-dimensional groundwater flow and subsidence models at NASL, delineation of a study area containing NASL and its hydraulically connected surrounding lands was necessary. Complications arose with this, principally due to the location of NASL at the triple-junction of three sub-basins within the Tulare Lake groundwater basin: the Kings, Westside, and Tulare Lake sub-basins (Figure 2 and Table 1). To the west, a definite hydraulic boundary is the foothills of the Coast Ranges, which is used to delineate the study area wherever possible. To the south and east of NASL lies the Tulare Lake bed, which forms a less distinct hydraulic boundary. Finding a hydraulic boundary for study area delineation to the east and north of NASL was more problematic, so a sufficient number of townships within neighboring groundwater sub-basins were chosen, as necessary.

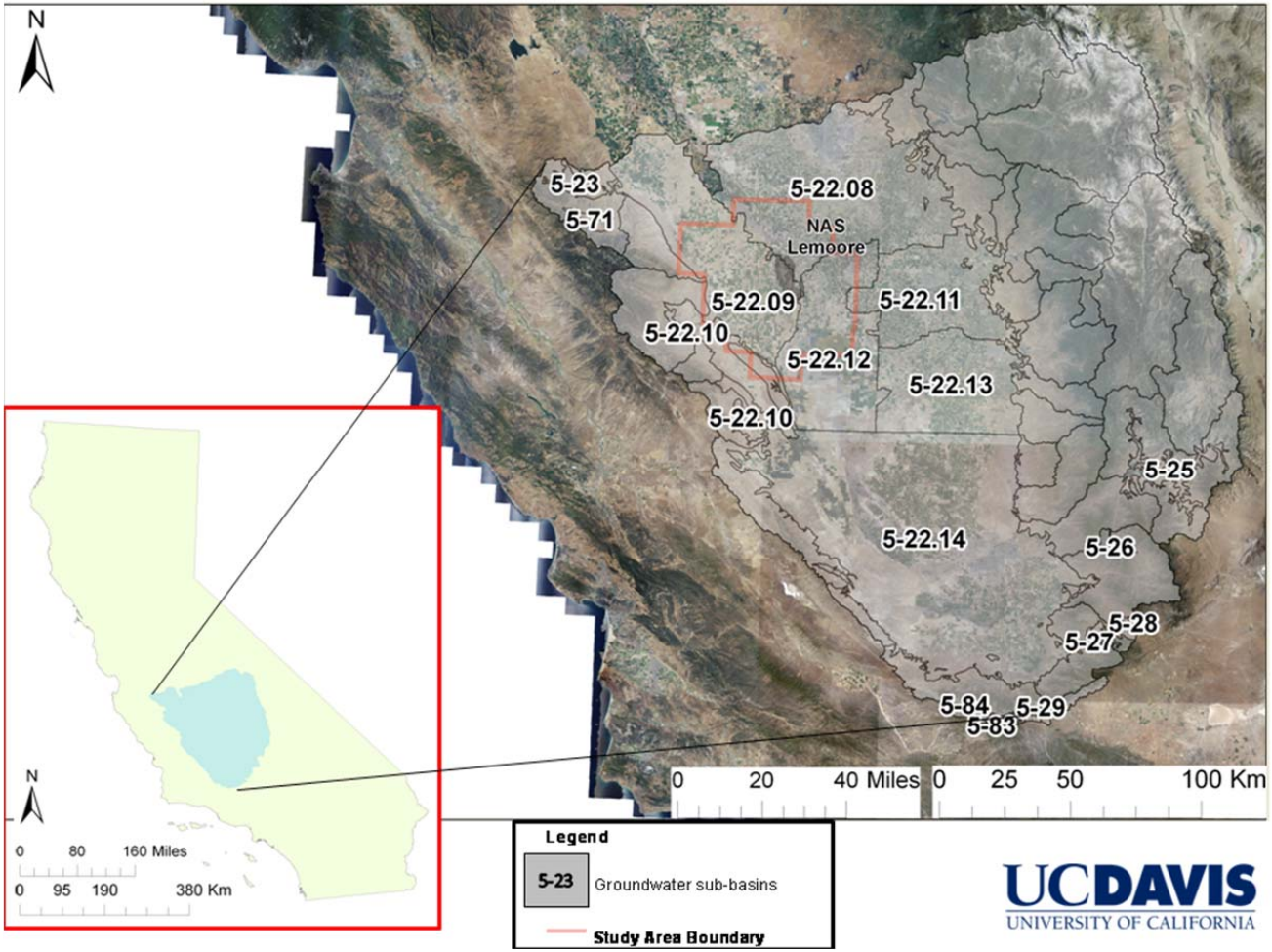

Figure 2 NASL is located adjacent to the triple junction of three CDWR groundwater basins, just west of the San Joaquin Valley thalweg, and immediately west of the Kings River fork dividing its drainage to the San Joaquin River to the north and to the Tulare Lake bed to the south. NASL is located within the Westside groundwater basin (5-22.09), but significantly influenced by the Tulare Lake (5-22.12) and Kings (5-22.08) groundwater basins to the southeast and to the northeast, respectively (*modified from*: USGS, 2003 and USGS, 2010).

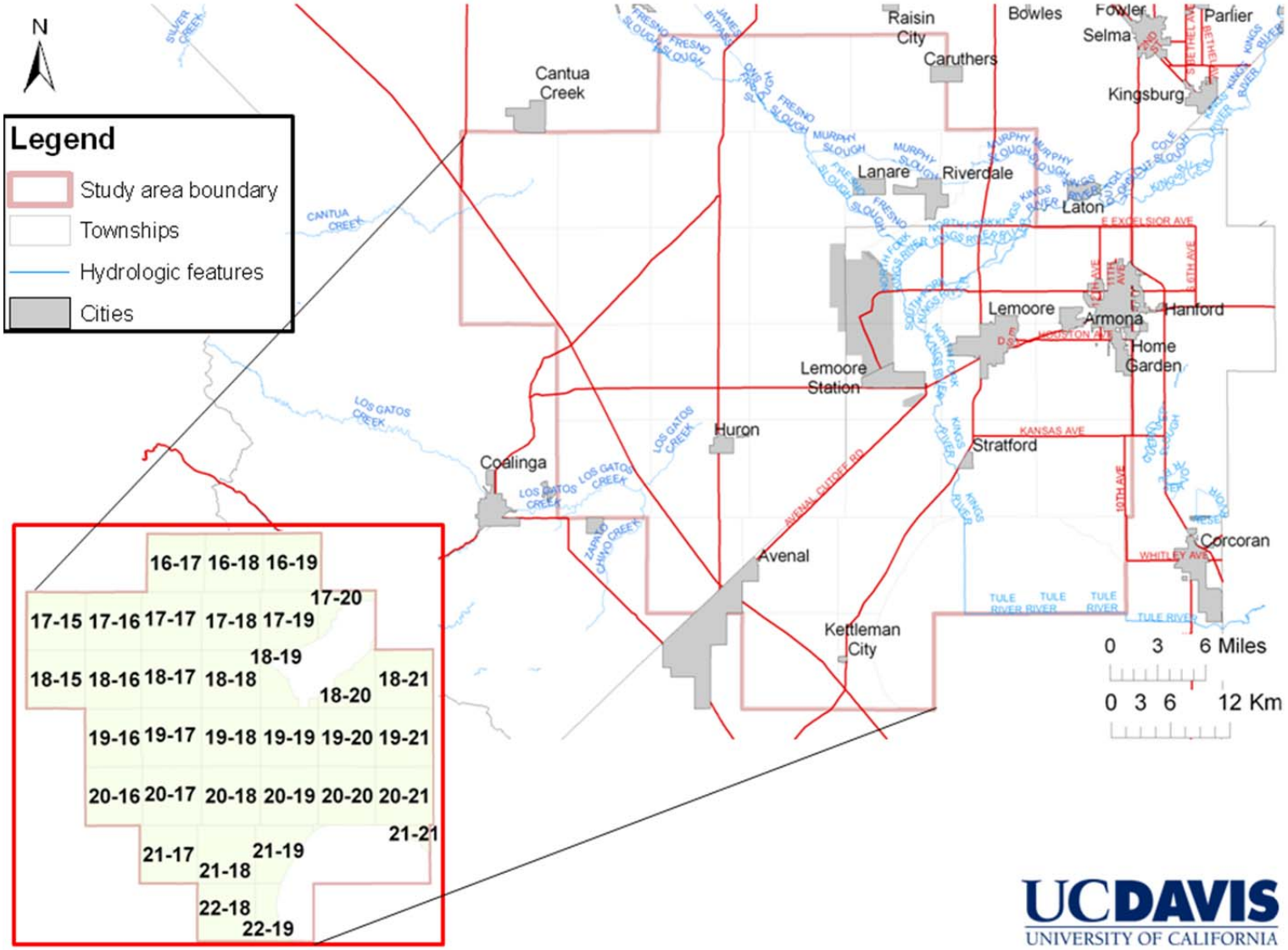

Figure 3 Study area showing local waterways, study townships and urban areas including NASL.

To simplify retrieval of data needed for this and potential follow-up studies, it was decided that the extent of the study area would be based on townships as defined by the PLSS system. As a majority of the data needed for this study was to be obtained from the CDWR this proved to be an efficient method, as CDWR data are archived by PLSS coordinates. A total of 35 townships were included in the study area, as outlined in Figure 3, NASL lies central to this area, and portions of hydraulically relevant surrounding groundwater basins are included. For the crop water use study, we focused on the lands belonging to NASL itself.

CDWR BASIN/SUB-BASIN NAME	CDWR NUMBER
San Joaquin Valley	5.22
Kings	5-22.08
Westside	5-22.09
Tulare Lake	5-22.12

Table 1 Study area groundwater basins and sub-basins.

2 Historic Water Supply and Crop Water Use Analysis

2.1 Introduction

The Naval Air Station Lemoore provides 60 agricultural leases consisting of approximately 13,000 acres to 20 local farming entities. The principle crops grown on the land are: cotton, alfalfa, tomatoes, silage corn and winter wheat. The use of land surrounding NASL accomplishes the dual purpose of optimizing utilization of natural resources on NASL federal lands and minimizing maintenance funds that must be expended, while collecting $1.2 million annual revenue from the leases. The Agriculture Outleasing Program (AGP) saves NASL approximately $2 million in cost avoidance and maintenance through cost effective compatible land or airfield management (Correspondence with NASL). Costs avoided due to the program include: dust control, bird air strike hazard (BASH) and endangered species encroachment. Maintenance savings include: weed maintenance, grounds maintenance and fire break maintenance. The AGP creates a connection between the naval air station and the surrounding community in addition to enhancing wildlife areas (i.e., 4A28's TWR Sump Project), creating natural resources stewardship projects, and salary opportunities for the local community.

The groundwater basin underlying NASL and much of Westlands Water District is generally comprised of two water-bearing zones: (1) an upper zone containing the Coastal and Sierran aquifers and (2) a lower zone containing the Sub- Corcoran confined aquifer. The two zones are separated by a low permeability aquitard comprised predominantly of clays and commonly referred to as the Corcoran Clay. The water-bearing zones are recharged by subsurface inflow from the east and northeast, the compaction of water-bearing sediments, percolation of pumped groundwater, and percolation from imported and natural surface water. Land subsidence due to groundwater overdraft ranged from one to 24 ft. between 1926 and 1972 (Westlands, 2007).

According to the Westlands Water Management Plan (2007) surface water deliveries from the San Luis Unit (SLU) began in 1968 and largely replaced groundwater for irrigation. Extensive pumping occurred in 1977, a drought year. For that year, deliveries of CVP water amounted to only 25 percent of the District's entitlement. In response to the surface water shortfall, farmers reactivated old wells and constructed new wells, pumping groundwater to irrigate their crops. During 1977, groundwater pumping in Westlands Water District rose to nearly 500,000 acre-ft. (AF) and the piezometric surface declined about 90 ft., resulting in localized subsidence of about 4 inches according to USGS officials. Groundwater pumping again increased to about 300,000 AF in 1989-90 because of decreased CVP water supplies caused by drought. Pumping during 1990-91 and 1991-92 was estimated to be about 600,000 AF annually. This increase in pumping resulted in a piezometric water surface decline of about 91 ft. from 1988 through 1991. Water level completely recovered through a series of normal and wet years by 1997.

A study by the U.S. Bureau of Reclamation, the USGS, and Westlands Water District estimated the safe yield of the deep confined aquifer underlying Westlands to be between 100,000 and 135,000 AF annually (Westlands Water District, 1980, as cited in Westlands, 2007). According to Westlands (2007), more recent district analyses of these data indicate that a better-estimated safe yield may be between 135,000 and 200,000 AF. It is not clear, to which degree these safe yield estimates rely on continued past or current groundwater recharge from agricultural return flows.

The following table (Table 2) was provided by NASL and gives a general overview of the acreage irrigated with surface water delivered through Westlands Water District (WWD) versus the acreage irrigated with water from groundwater wells. It is interesting to note that groundwater accounts for less than one third of the total irrigated acreage according to the table below.

WWD Water vs Groundwater Wells

Water Type	Number of Leases	Number of Lessees	Acres
WWD only	43	8	8,232.8
Groundwater Wells/WWD	16	13	2,956.8
Groundwater Wells only*	1	1	1,161.0

* Lease with only groundwater has an unrestricted allocation of water

Table 2 Sources of agricultural water at NASL.

Crops require irrigation water. Such agricultural water use in turn drives groundwater pumping to the degree that irrigation water demands cannot be met by surface water and precipitation. The loss of groundwater storage leads to subsidence. Agricultural practices and water use by crops are therefore intrinsically linked to land subsidence. This chapter summarizes the crop water use of historic and current crops at NASL.

2.2 Historic and Current Crop Types and Water Usage

To calculate historic crop water uses for the leased agricultural lands, crop maps of the agricultural leases dating back to 1974 and provided by NASL staff were compiled, digitized, and processed. Generally, NASL prepares four land use or crop maps each year, one each for the spring, summer, fall and winter seasons. For this project, summer crop maps were used starting from the year 1974 to extract data for the crop water use calculations. The remaining season maps were subsequently reviewed for additional crops that might have been planted and harvested before or after the summer, for example winter wheat following silage corn. It should be noted that hand-drawn and hand-colored maps dated before the year 2000 are of varying quality making it often difficult to distinguish between various crop types. This introduces potential errors into the calculated water use values.

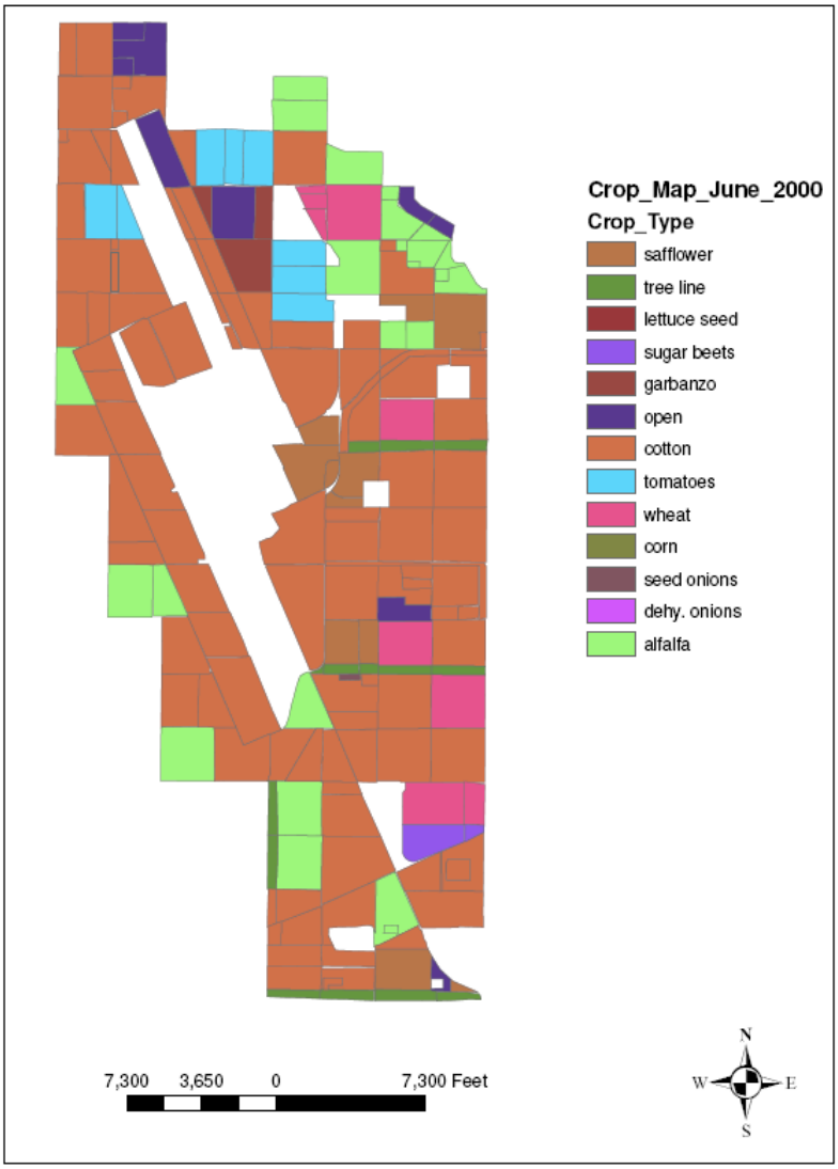

Figure 4 Example of a crop map prepared in the ArcGIS® database from hand-drawn maps provided by NASL. See Appendix G for a complete set of crop maps for 1974 through 2010.

Crop maps were scanned, and then manually digitized and georeferenced in GIS using Albers state plane projection in the NAD 1983 datum ("NAD_1983_StatePlane_California_IV_FIPS_0404_Feet"). During the digitization process leases were separated into subplots in order to better estimate the total acreage of a specific crop planted. Thus, although there are only 60 agricultural leases, a large amount of subplots were created to accurately account for the various crops grown and for their associated water demand (see example in Figure 4).

The amount and shape of subplots were reconfigured each season to account for changing acreages of crops grown. Each subplot was assigned a number symbolizing land use. Different

land uses were each given specific colors which remain constant throughout the set of maps created, representing thirty-five years of crop history at NASL. The land acreage of each subplot was calculated using GIS tools. Acreages with their associated land use were compiled in a spreadsheet (Figure 5, also see Appendices A and B).

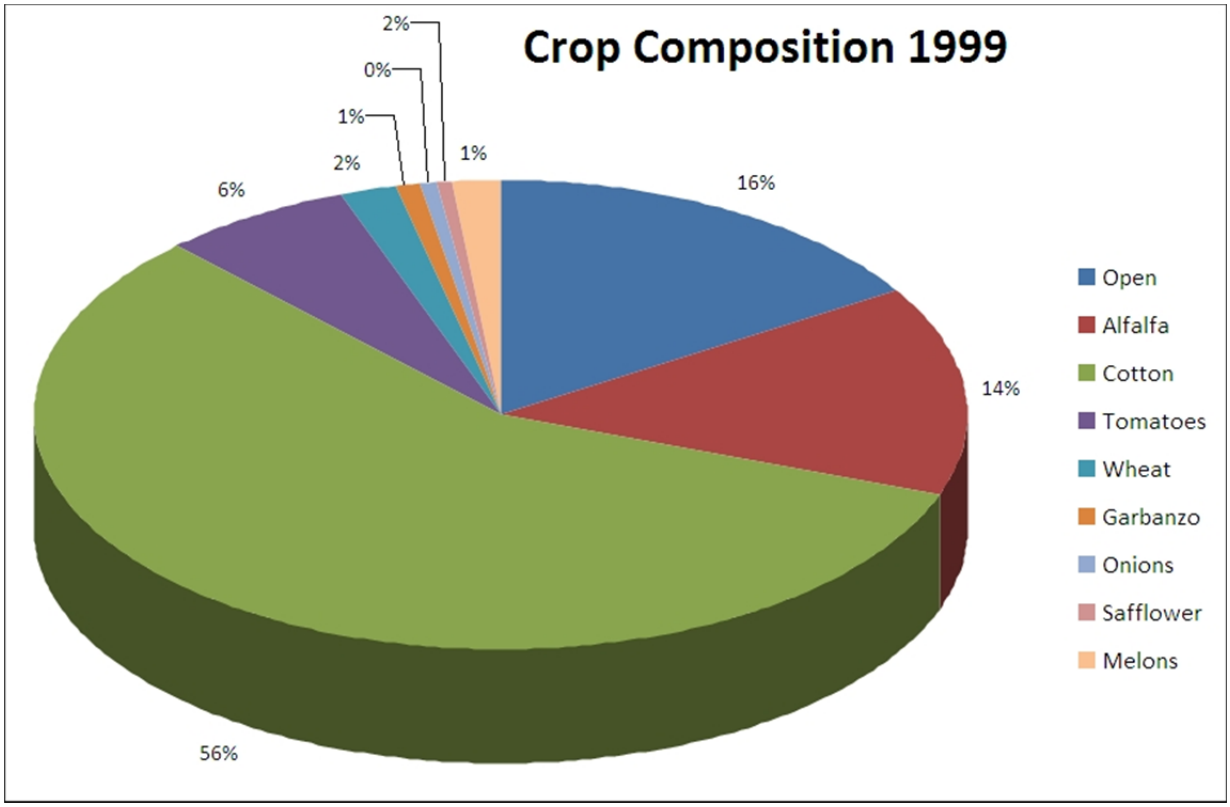

Figure 5 Computed crop type fractions, by land area, at NASL in June 1999. See appendix for a complete set of crop composition during 1974 – 2010.

Each land use (crop type) for each year was assigned an annual water application rate, which was obtained from Westlands Water District. Water application data do not cover the entire study period and only go back until 1980. For 1974-1979, water application rates were assumed to be equal to those for the earliest reported water application year, 1980. Evapotranspiration (ET) and effective precipitation data supplied by Westlands Water District had been calculated using three weather stations located within Westlands Water District: The North Weather Station (California Irrigation Management Information System (CIMIS) Westlands #105 [36°38' 02.12"N 120°22'54.26"W]) located at the District's Tranquility Field Office on Adams Ave. east of Derrick Ave. (Hwy 33). The Central Weather Station (CIMIS Five Points #002 [36°20'11"N 120°06'47"W]) located at the University of California West Side Research & Extension Center on Oakland Ave., and the South Weather Site is located on Gale Ave. at Wolfe Farming Shop (Westlands Water District owned station [36°10'51.15"N 120°07'11.02"W]).

	Alfalfa Hay	Beans	Cotton	Lettuce-Fall	Lettuce-Spring	Onions
	Estimated Applied Water *AF/Ac*	Estimated Applied Water *AF/Ac*	Estimated Applied Water *AF/Ac*	Estimated Applied Water *AF/Ac*	Estimated Applied Water *AF/Ac*	Estimated Applied Water *AF/Ac*
1980	4.48	2.73	2.47	1.49	1.04	3.26
1981	5.03	2.43	2.62	1.42	1.17	3.19
1982	4.79	2.87	2.63	1.60	1.32	3.60
1983	4.05	2.51	2.56	1.47	0.85	2.70
1984	5.42	3.09	2.92	1.65	1.36	3.25
1985	5.20	2.70	2.86	1.79	1.47	3.78
1986	4.88	2.77	2.82	1.49	1.27	3.33
1987	6.50	3.13	3.08	1.85	1.23	2.85
1988	5.56	2.80	2.69	1.94	1.47	3.66
1989	5.82	2.76	2.59	1.32	1.31	3.06
1990	5.34	2.33	2.31	1.49	1.02	3.42
1991	5.18	2.15	2.18	2.02	0.79	3.22
1992	5.72	2.03	2.14	1.32	1.13	3.88
1993	4.48	1.80	1.82	1.22	0.77	3.69
1994	6.02	2.44	2.47	0.87	0.55	4.03
1995	4.81	0.76	2.09	0.92	0.35	3.68
1996	6.05	2.80	2.63	1.01	0.66	4.70
1997	5.56	2.57	2.60	1.05	0.41	4.50
1998	3.30	2.49	2.11	0.95	0.00	2.22
1999	4.38	2.54	2.36	0.95	0.74	4.37
2000	3.63	2.18	2.05	0.88	0.45	3.49
2001	4.38	2.28	2.24	0.92	0.36	3.06
2002	3.90	2.26	2.00	0.81	0.52	3.65
2003	4.36	2.47	2.31	1.07	0.48	4.22
2004	4.56	2.47	2.25	1.06	0.57	4.01
2005	3.57	0.89	2.25	0.92	0.16	3.15
2006	4.00	1.65	1.88	0.86	0.15	3.37
2007	4.98	2.55	2.65	0.89	0.75	4.55
2008	4.50	0.05	2.32	0.40	0.43	3.29

Table 3 Estimated applied crop water, by crop and year.

	Safflower	Sugar Beets	Tomatoes-Processing	Wheat	Field Crops	Truck Crops
	Estimated Applied Water	Estimated Applied Water	Estimated Applied Water	Estimated Applied Water	Estimated Applied Water	Estimated Applied Water
	AF/Ac	*AF/Ac*	*AF/Ac*	*AF/Ac*	*AF/Ac*	*AF/Ac*
1980	2.76	3.64	2.43	1.30	2.70	2.11
1981	2.86	3.66	2.37	1.44	2.60	2.03
1982	3.05	4.03	2.37	1.55	2.86	2.24
1983	2.90	3.71	2.53	1.16	2.68	2.09
1984	3.12	4.33	2.68	1.73	2.94	2.29
1985	3.38	4.49	2.77	2.04	3.13	2.44
1986	3.08	4.17	2.57	1.39	2.93	1.44
1987	2.60	3.83	2.30	1.67	3.32	2.58
1988	2.71	4.38	2.36	1.93	3.13	2.30
1989	2.87	4.14	2.38	1.83	2.72	2.06
1990	2.53	4.11	2.06	1.69	2.52	1.91
1991	2.30	3.49	1.87	1.53	2.27	1.70
1992	2.14	3.32	1.71	1.25	2.31	1.71
1993	2.17	3.19	1.67	1.15	2.05	1.41
1994	2.45	3.89	2.08	1.71	2.70	2.06
1995	2.29	3.74	1.79	1.47	2.44	1.77
1996	2.85	4.79	2.38	2.15	2.85	2.17
1997	2.48	4.28	2.04	1.82	2.75	2.06
1998	1.65	2.78	1.74	0.89	2.61	1.84
1999	2.27	3.65	2.13	1.71	2.84	2.19
2000	1.89	3.04	1.87	1.22	2.54	1.83
2001	2.00	3.44	1.96	1.26	2.82	2.04
2002	1.92	3.11	1.82	1.42	2.45	1.77
2003	2.11	3.60	2.08	1.49	2.91	2.10
2004	2.06	3.48	1.97	1.36	2.82	2.03
2005	2.04	3.25	1.95	1.19	2.75	1.98
2006	1.60	3.15	1.36	1.08	2.79	1.99
2007	2.58	3.93	2.03	1.73	2.86	2.06
2008	1.82	3.50	1.37	1.21	2.79	2.03

Table 3 (cont). Estimated applied crop water by crop and year.

Table 3 shows the applied water demand for each crop, as estimated by Westlands Water District. These values were calculated from measured evapotranspiration rates associated with each crop, from the effective precipitation measured in the area of interest based on nearby weather station data mentioned above, and by accounting for the associated leaching requirements (irrigation efficiency) reported by Westlands Water District. In Table 3**Error! Reference source not found.**, truck crops are considered to be: melons, peppers, peas, eggplant, and sweet-corn. Field crops are considered to be: field-corn, grains-sorghum, grain-hay and oats. Garbanzo beans are classified as beans, sweat peas as peas, endive lettuce and lettuce seed as fall lettuce. Onion values were adjusted to reflect soil surface evaporation where an additional 6.3" average preplant ET was

Year	Open Land (Ac)	Cropped Land (Ac)	Estim. Applied Water (Af/Ac)	Estim. Applied Water (AF)	Estim. Crop Water Requirement (Af/Ac)	Estim. Crop Water Require-ment (AF)	Estim. Recharge (Af/Ac)	Estim. Recharge (AF)	Irrigation Efficiency
2010	1,554	12,128	2.87	34,864	2.47	29,998	0.53	6,370	86.0%
2009	6,382	8,377	2.89	24,245	2.47	20,681	0.59	4,925	85.3%
2008	1,447	12,605	2.88	36,312	2.31	29,074	0.74	9,375	80.1%
2006	430	13,092	2.31	30,296	1.99	26,013	0.40	5,192	85.9%
2005	2,344	12,045	2.53	30,468	2.14	25,825	0.47	5,652	84.8%
2004	1,153	12,653	2.61	33,053	2.26	28,632	0.43	5,384	86.6%
2003	1,507	12,358	2.76	34,128	2.35	28,982	0.49	6,067	84.9%
2002	991	12,976	2.44	31,714	2.42	31,372	0.13	1,671	98.9%
2001	2,991	12,607	2.45	30,842	2.13	26,865	0.39	4,876	87.1%
2000	521	11,974	2.22	26,540	2.11	25,241	0.17	2,038	95.1%
1999	2,423	12,507	2.68	33,544	2.31	28,941	0.45	5,581	86.3%
1998	685	14,427	2.18	31,385	1.93	27,896	0.31	4,451	88.9%
1997	848	14,313	2.66	38,045	2.14	30,566	0.57	8,176	80.3%
1996	3,116	12,188	2.62	31,934	2.18	26,606	0.47	5,767	83.3%
1995	1,443	13,801	2.07	28,557	1.76	24,345	0.34	4,735	85.3%
1994	1,552	13,688	2.47	33,794	2.15	29,393	0.38	5,140	87.0%
1993	1,257	13,822	1.90	26,210	1.69	23,387	0.24	3,296	89.2%
1992	1,556	13,518	2.11	28,485	1.93	26,108	0.24	3,281	91.7%
1991	1,041	13,806	2.37	32,715	2.24	30,908	0.22	3,005	94.5%
1990	1,198	13,514	2.56	34,533	2.30	31,108	0.33	4,509	90.1%
1989	914	13,577	2.88	39,164	2.37	32,227	0.63	8,510	82.3%
1988	754	13,824	2.88	39,745	2.31	31,915	0.68	9,424	80.3%
1987	1,501	13,033	3.21	41,898	2.44	31,804	0.89	11,568	75.9%
1986	745	13,785	2.41	33,219	1.91	26,274	0.58	8,031	79.1%
1985	1,539	12,978	2.86	37,140	2.33	30,193	0.64	8,358	81.3%
1984	470	14,354	2.87	41,136	2.44	35,017	0.54	7,730	85.1%
1983	927	12,005	2.59	31,050	2.38	28,582	0.31	3,771	92.1%
1982	869	12,029	2.73	32,840	2.32	27,967	0.51	6,155	85.2%
1981	1,436	11,391	2.69	30,680	2.51	28,642	0.46	5,273	93.4%
1980	408	12,366	2.58	31,961	2.29	28,356	0.40	4,900	88.7%
1979	1,961	10,800	2.53	27,342	2.29	24,678	0.36	3,869	90.3%
1978	2,717	9,828	2.81	27,577	2.52	24,718	0.43	4,179	89.6%
1977	4,044	8,504	2.77	23,570	2.51	21,315	0.39	3,353	90.4%
1976*	11,408	2,590	2.88	7,452	2.49	6,453	0.52	1,347	86.6%
1975	1,234	11,412	2.13	24,300	1.83	20,898	0.37	4,227	86.0%
1974	755	11,761	1.58	18,541	1.39	16,380	0.24	2,847	88.3%
1978-2010	**1,521**	**12,699**	**2.58**	**32,669**	**2.23**	**28,197**	**0.45**	**5,664**	**86.7%**

Table 4 Annual open and harvested acreage, estimated crop water requirements [acre-ft.], estimated applied water [acre-ft.], and estimated groundwater recharge [acre-ft.]. These values were computed by adding the annual acreage, crop water requirements, applied water, and groundwater recharge for individual crops at NAS Lemoore. Crop water requirements, crop

[Table 4 Caption, continued] evapotranspiration, effective precipitation, and applied water were provided for each crop and year by Westlands Water District (2007). Crop acreages were obtained by digitizing hand-drawn crop maps for June, July, or August of each year at NAS Lemoore. Recharge was computed for each crop, in each year, as the difference between (applied water plus effective precipitation) minus crop evapotranspiration. The spatially averaged irrigation efficiency (right column) is obtained by dividing the crop water requirement by the amount of applied water. *Note: only October crop maps were available for 1976, and only September crop maps were available for 1985, 1995, 1996, and 2001. The 1976 numbers are not representative for that year. No crop maps were available for 2007.

added. In all cases, conservative estimates were made if a range of values was available, meaning that the highest estimate for applied water was used for the computation.

Land in production – estimated annually from digitized summer crop maps for 1974-2010 – ranged from 8,377 acres in 2009 (the third year in a three-year drought period) to 14,427 acres in 1998 (following two very wet winters). On average (1978-2010), production areas cover 12,700 acres of NASL's land with an average of just over 1,500 acres left open (Table 4). Data for crop acreage in 1976 are underestimating the actually cropped acreage, as no summer crop map was available for that year and the crop acreages were based on October maps, when much of the crops had been harvested. Note that summer crop maps were also not available for the following years: 1985, 1995, 1996, and 2001. For these latter four crop years, we used September crop maps to estimate crop acreages, all of which are recorded at above 12,000 acres.

The estimated applied water demand (Table 4 and Figure 6) for the land leased by NASL has historically ranged from as little as 24,000 AF (1975, 1977, and 2009) to as much as 42,000 AF (1987). Average applied water demand for crop irrigation at NASL is 32,700 AF per year for the period 1978-2010. The average applied water demand per acre of cropland is 2.6 AF/acre, for that same period, and ranges from 1.9 AF/acre (1993, following a major prolonged drought) to as much as 3.2 AF/acre (1987).

Groundwater use was calculated by assuming that the total applied water demand is met by two sources: water supplied to NASL by WWD and groundwater pumped on site. Water delivery data from WWD to NASL were available only for the period from 2003 to current (not including 2007 and 2008). During that time period, annual groundwater pumping (estimated by: applied water demand minus surface water delivered) for irrigation at NASL has ranged from 4,000 AF to 26,000 AF or 0.3 AF/acre to 2.5 AF/ac. The short time period is not sufficiently long to extrapolate any groundwater pumping trends. But a drastic increase in pumping was observed in 2009 and 2010 due to the significantly decreased amounts of water supplied by WWD.

Figure 7 shows the total amount of water that WWD has supplied to its customers within the nearly one-million acre district over the past 30 years as well as the total amount of groundwater pumped by the district to meet water demands. Despite significant variability, a significant trend showing a decrease in surface water supplied and an increase in groundwater pumping can be observed. Surface water restrictions due to drought conditions and other environmental factors have increased the reliance on groundwater at a time when the precipitation needed to recharge these aquifers is in short supply. Also, comparing Figure 6 to Figure 7, it can be seen that the relative annual variations in groundwater pumping at NASL mirror those observed for WWD as a whole. Given this similarity, an extrapolation of the groundwater pumping patterns in WWD, observed prior to 2003, and applying it to NASL yields past groundwater pumping rates that varied typically from 8,000 AF/yr to 13,000 AF/yr, not including some very wet and very dry periods. In years with low surface water supplies (dry years) significantly higher pumping would have been observed at NASL (~30,000 AF/yr).

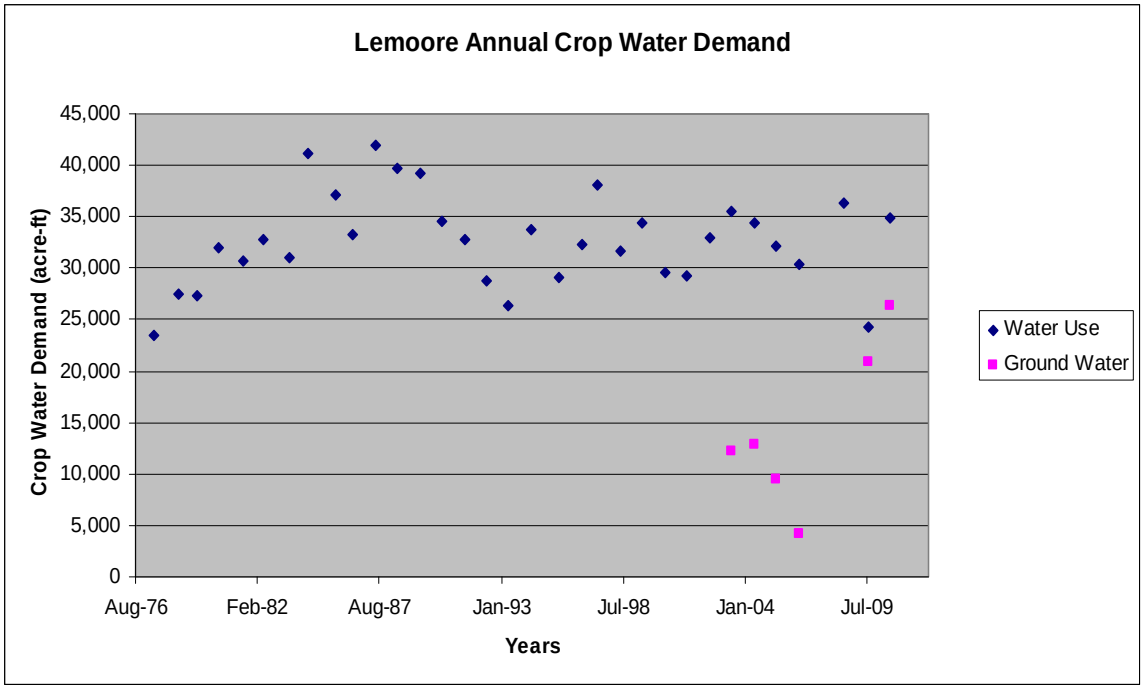

Figure 6 Annual applied water demand for irrigating the crops at NASL from 1974 through 2010.

In addition to irrigation water, NASL uses approximately 3 million gallons per day or 3,400 AF/yr of additional water to meet its municipal and non-agricultural, operational water supply needs. The additional water need is met through surface water supplies from WWD.

Groundwater pumping stresses are partially alleviated through groundwater recharge at NASL, which primarily originates from irrigation water returns (applied irrigation water that is not used by the crop). We used two methods to estimate groundwater recharge: Groundwater recharge in Table 4 represents the recharge at NASL, totalized over the acreage of all crops. For individual crops in a given year, recharge was estimated by subtracting crop-specific annualized

evapotranspiration from the sum of crop-specific applied water (estimated) and crop-specific effective precipitation (precipitation that is used by the crop to meet its evapotranspiration demand). The resulting recharge varies from 2,000 AF or less (2000 and 2002) to more than 11,000 AF (in 1987) (see Figure 8). The average recharge is 5,600 AF/yr, or 0.45 acre-ft. per cropped acre, reflecting the relatively high irrigation efficiency at NASL and in WWD.

Importantly, this estimate neglects recharge from winter precipitation. Average annual precipitation at NASL is 8.0 inches with as much as 1 inch already being accounted for in the above recharge estimate as effective precipitation. Of the remaining precipitation, perhaps as much as 2 inches will become recharge in normal years (approximately 2,000 acre-ft. for NASL), increasing NASL's average recharge to an estimated 7,000 to 8,000 acre-ft. per year. The remainder will largely evaporate or be transpired by winter plants.

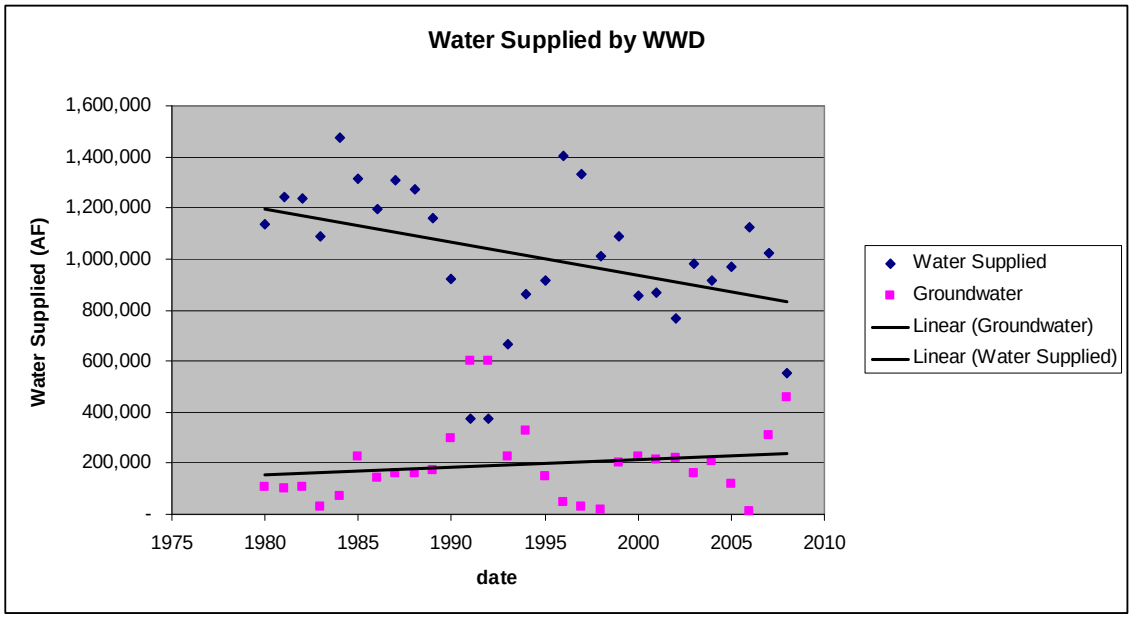

Figure 7 Total water supplied by Westlands Water District to its customers and estimated groundwater pumping in Westlands Water District (WWD, 2008).

Twenty years ago, the U.S. Geological Survey derived a different recharge rate for a large area of Westlands Water District north of NASL. The estimated recharge rate on agricultural lands, in a normal water year (and prior to large-scale conversion of irrigation systems to higher efficiency technology) was estimated to be in the range of 0.84 – 0.96 AF/acre/year (Table 4 in Belitz et al., 1994; Table 1 in Belitz et al., 1995). For the average summer acreage in crops (12,600 acres), their alternative recharge estimate would yield a total annual recharge on NASL agricultural land on the order of 11,000 AF/yr. However, this estimate is based on an irrigation efficiency of 65% (*ibid.*), while reported values by Westlands Water District (2007) typically range between 80% and 90% (Figure 9). At an average of 33,000 acre-ft. of applied water, the difference between 65% and 85% irrigation efficiency corresponds to 0.5 AF/acre/year of additional recharge under the lower irrigation efficiency scenario. On the other hand, Belitz et

al., 1995, also assume, as we did for the estimates in Table 4, that additional recharge from winter precipitation is negligible. Hence, we consider the recharge rate found by Belitz et al. (1994) to be a upper bound for the likely range of recharge at NASL.

In wet years, or years with large supplies of surface water, recharge can be somewhat higher. In dry years, or years with very small surface water supplies, recharge can be significantly less, particularly if much of the land remains fallow (no recharge from agricultural return water).

Groundwater recharge via NASL's non-agricultural water uses are mostly associated with lawn irrigation on approximately 200 to 300 acres of residential land and wastewater recharge from its wastewater ponds, which cover approximately 300 acres. Recharge from these land uses are estimated to be on the order of 500 AF/year or less.

Long-term total average groundwater recharge from NASL over the past 35 years is estimated to be in the range of 7,500 to 11,500 AF/year. At NASL, over the past 35 years, groundwater pumping in normal and wet years has therefore been of similar magnitude as groundwater recharge. Importantly, in dry years, groundwater pumping increases two- to three-fold, while recharge is likely lower due to higher irrigation efficiency and more land acreage out of production, and hence without groundwater recharge. The imbalance of groundwater pumping relative to groundwater recharge that occurs during these drought periods is not being balanced by equivalent amounts of recharge surplus at NASL during normal and wet years.

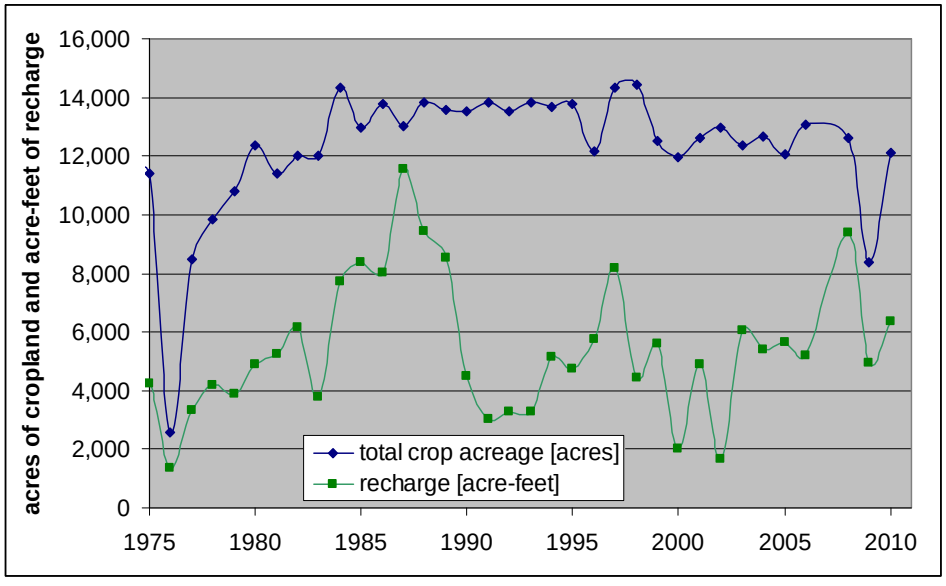

Figure 8 Comparison of total crop acreage and total recharge from 1975 to 2010. Recharge here is estimated as the difference between the sum of applied water plus effective precipitation and crop evapotranspiration.

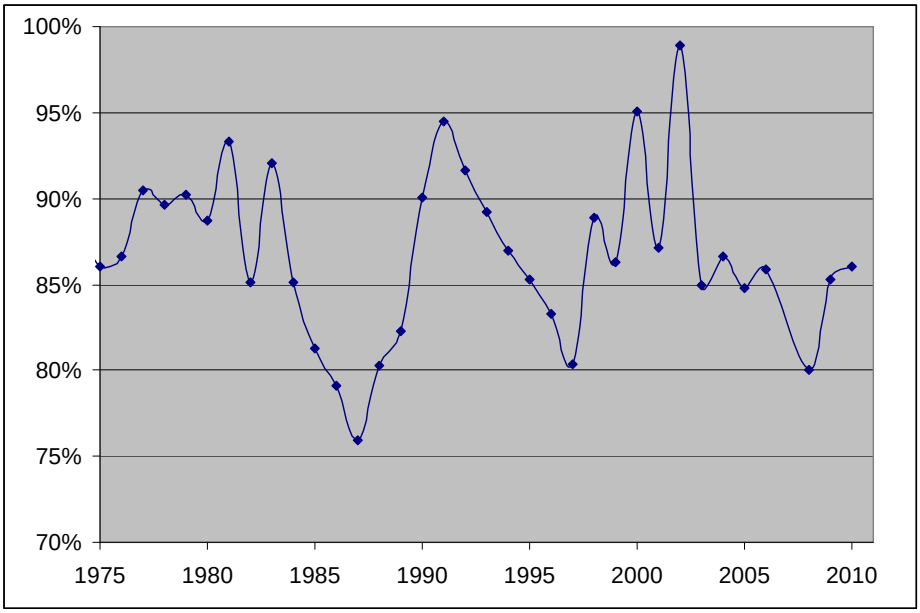

Figure 9 Irrigation efficiency [in %] at NAS Lemoore, where irrigation efficiency here is defined as the ratio of estimated crop consumptive water need to estimated applied (irrigation) water.

3 Alternative Future Crop Types and Water Usage

The probability of decreased surface water availability in the future is very significant. Climate change, increasing population, increasing energy needs, and decreasing ground water levels all contribute to an outcome dictated by less available water for the agricultural needs of the lessees on NASL land.

A 2010 report prepared by Tetra Tech (2010) performed a countrywide analysis using annual water use data at the U.S. county level, and using global climate model outputs for temperature and precipitation, both projected 20-40 years into the future. The report found that, under the business-as-usual scenario of demand growth, water supplies in 70% of counties in the U.S. may be at risk to climate change, and approximately one-third of counties may be at high or extreme risk with Kings and Fresno counties being one of the counties at extreme and high risk of demanding an unsustainable water supply (Figure 10).

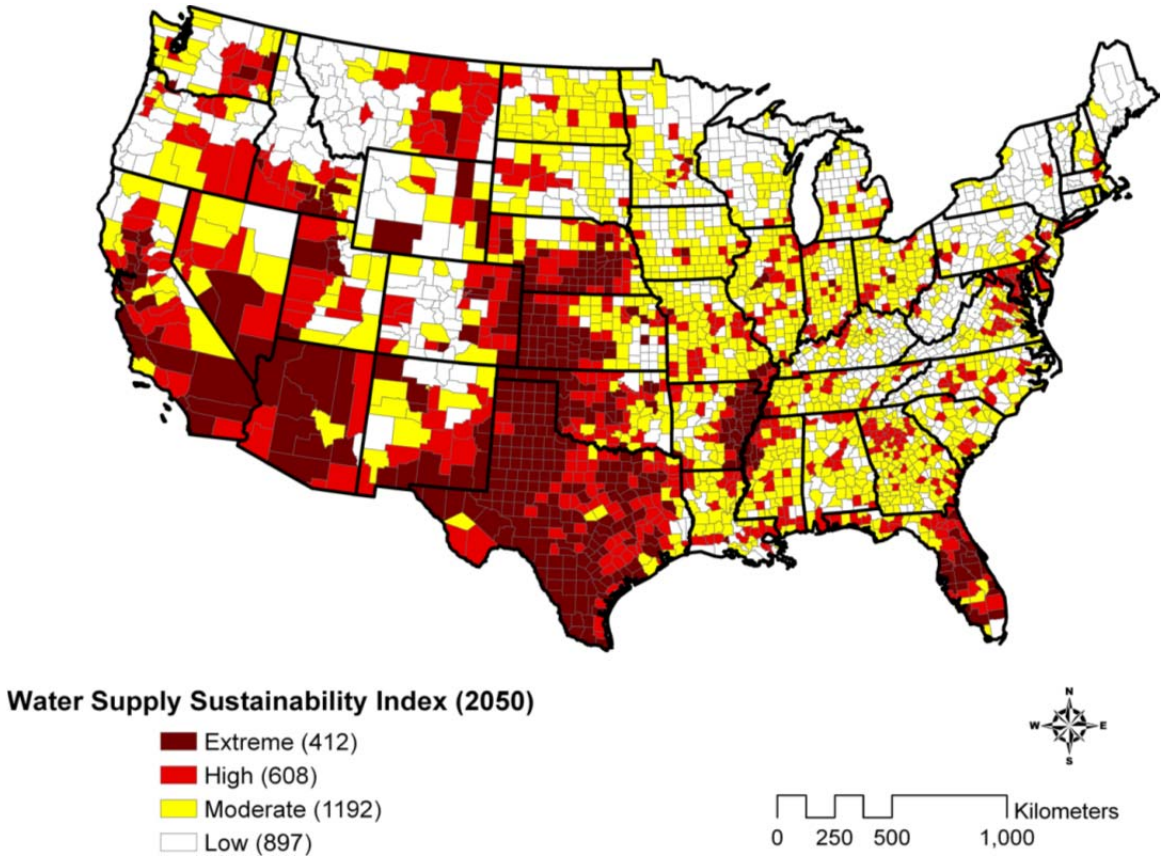

Figure 10 Water Supply Sustainability Index (2050) (Tetra Tech, 2010).

Although the report shows relatively small absolute changes in precipitation (from -1 inch to +1-2 inches) as a result of climate change over the next 40 years, the uncertainty in

precipitation projections is great. The relative inter-quartile ratio (RIQR) for the 2050 precipitation based on analysis of monthly data from 16 GCMs can be seen in Figure 11. The RIQR is a quantitative measure of the variation in projected precipitation across different GCMs defined as (75th percentile value -25th percentile value)/Median. Low values of the ratio at a given location imply that the 16 GCM projections for this location are in agreement, whereas large values of this ratio suggest differences across models. The RIQR shows agreement in annual precipitation projections for most of the country with the Southwest and the Great Plains being the exceptions (Tetra Tech, 2010). The area of interest of this report is in a geographic region for which the variation in projected precipitation is greatest (Figure 11). However, it is unclear if water transport projects such as the California State Water Project are taken into account in the water supply sustainability index. If water is transported from areas that have a relatively moderate to low precipitation projection the severity shown in Figure 11 will change dramatically.

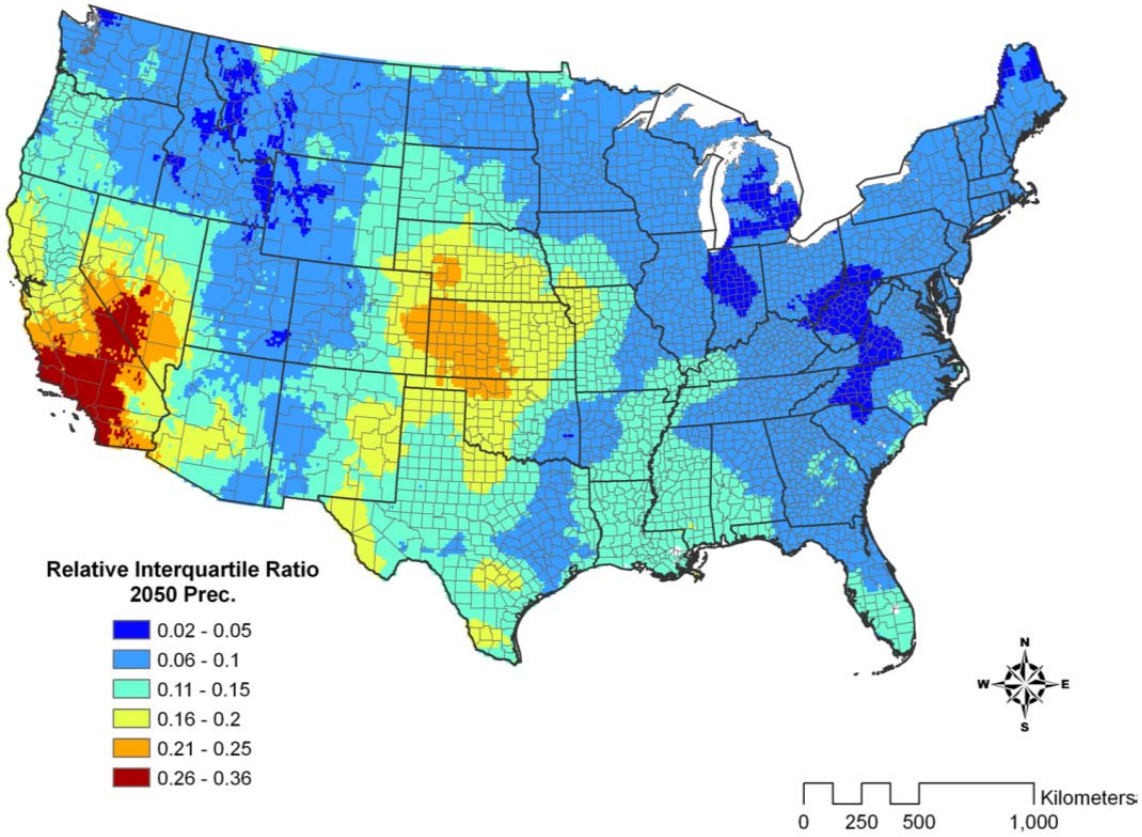

Figure 11 Relative Interquartile Ratio (Tetra Tech,2010).The projected total freshwater withdrawal as a percentage of available precipitation in 2050, assuming climate change impacts, and also relative to historical precipitation (1934-2000) is shown in Figure 12 and Figure 13. These maps can be used to compare directly the location and magnitude of impacts due to climate change. In some arid regions (e.g., Texas and California) and agricultural areas, water withdrawals are estimated to be greater than 100% of the available precipitation. Kings County, according to the map in Figure 12, is at over 500% of the available precipitation.

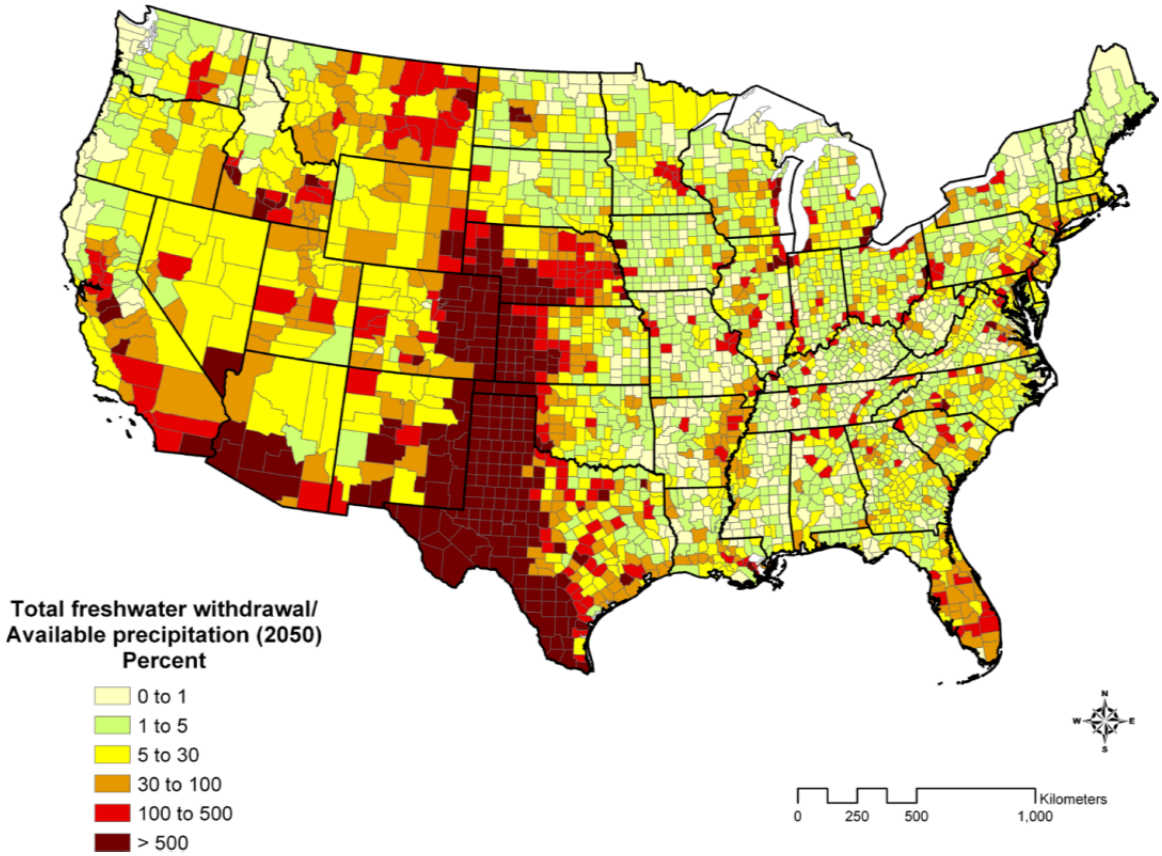

Figure 12 The total freshwater withdrawals for industrial, municipal, and agricultural uses, normalized by the amount of available precipitation for 2050 (Tetra Tech, 2010).

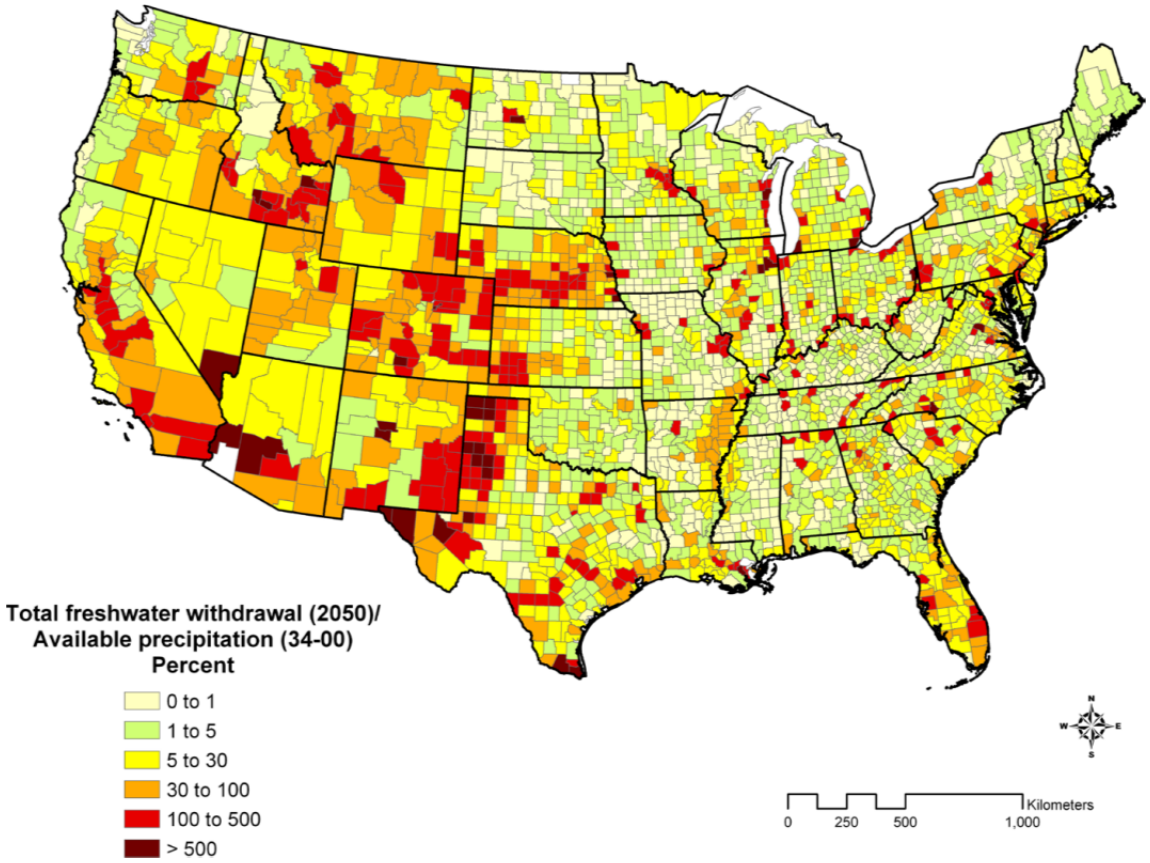

Figure 13 Total freshwater withdrawals for industrial, municipal, and agricultural uses in 2050 normalized by currently available precipitation, averaged from 1934-2000 (Tetra Tech, 2010).

In 1992 the Central Valley Project Improvement Act (CVPIA) reduced the Basic Water Allocation (a theoretical maximum water delivery) from 5.2 AF/acre to 2.6 AF/acre. Westlands Water District is the water provider for NASL, delivering NASL's annual water amount, which is an annually varying fraction of the Basic Water Allocation. The Basic Water Allocation is the amount of water delivered in a year with 100% water allocations. NASL and WWD entered into a Supplemental Water Agreement to secure an additional 10,000 AF of water for NASL Lessees (above the 2.6 AF/acre allocation). Actually delivered Supplemental Water is adjusted by the same annually varying delivery fraction applicable to the Basic Water Allocation deliveries from WWD. Westlands Water District receives its water from Northern California reservoirs via the Delta and the California Aqueduct and the Delta-Mendota Canal. Recent U.S. Environmental Protection Agency (EPA) and a court decision related to the U.S. Endangered Species Act (ESA) have affected the pumping of Delta water into the California Aqueduct and into the Delta-Mendota Canal and will potentially reduce the Basic Water Allocation from 2.6 AF to 1.82 AF for future years (30% reduction). The EPA's and Fish and Wildlife Service's (FWS) Steelhead Trout Biological Opinion (BO) will potentially reduce the Basic Water Allocation by an additional 5 – 10%. It is currently still unclear how this BO will affect the water allocations in the Central Valley. The following table summarizes past and present Basic Water Allocation by the WWD.

	Allocation Percentage	Allocation [Acre-Ft.]
Pre-CVPIA Basic Water Allocation	100%	5.2
Post-CVPIA Basic Water Allocation	100%	2.6
Average year allocation	60%	1.56
Typical drought year allocation, pre-2009	30% - 40%	0.78 – 1.04
Record-low allocation, pre-2009 (1977 & 1992)	25%	0.65
Post-Delta Smelt allocation, wet year	70%	1.82
Post-Delta Smelt allocation, average year	40%	1.04
Post-Delta Smelt drought year allocation	0 – 10%	0 – 0.26
2009 allocation, actual	10%	0.26
2010 allocation, actual	30%	0.78

Table 5 Surface water allocation to NASL from Westlands Water District (right column is acre-ft. per cropped acre). The first two rows are theoretical allocations for water rights purposes (*from:* NAS Agriculture Program Summary, 2010).

Future cropping patterns will be influenced by (1) changes in average farm size, (2) increases in water costs, (3) increases in acreage of high-value crops, (4) increases in double-cropping, (5) lands taken out of production, (6) substantially reduced subsidies for crops and water, and (7) the extent of fallow acreage (Westlands, 2008).

Prior to the delivery of Project water, Westlands' farmers primarily grew cotton and grain crops, such as wheat and barley, and some vegetables. However, between 1980 and 1996, the acreage devoted to vegetables increased to more than 220,000 acres, while grains declined by some 100,000 acres. Part of the increase in vegetable production is attributed to the fact that traditional "salad bowl" growing areas, such as the Salinas-Monterey area and the Central Coastal counties of California, are becoming urbanized and water scarce. In addition, some coastal areas are faced with groundwater pumping limitations brought about by seawater intrusion.

Figure 14 below shows the crop acreage trends in WWD over the past 30 years. There has been a visible increase in the production of both, fruits and vegetables as well as grains. However if one looks to future crop trends as shown in Table 6 one notes an overall decrease in the total acreage planted due increases in fallowed land and a steep decrease in cotton production forecasted.

Cooley et al. (2008) summarized the fraction of acreage, water use, and production value for field crops, vegetable crops, and fruits and nut crops in the San Joaquin Valley (including the Tulare Lake Basin) as shown in Figure 15. While the report assessed the potential to improve agricultural water-use efficiency, with a focus on the effects to Sacramento-San Joaquin Delta flows, some of their recommendations and models are relevant to the water and agriculture issues challenging the area surrounding NASL. According to Cooley et al. (2008), field crops accounted for 56% of total irrigated acreage in 2008 in the San Joaquin Valley. Field crops use

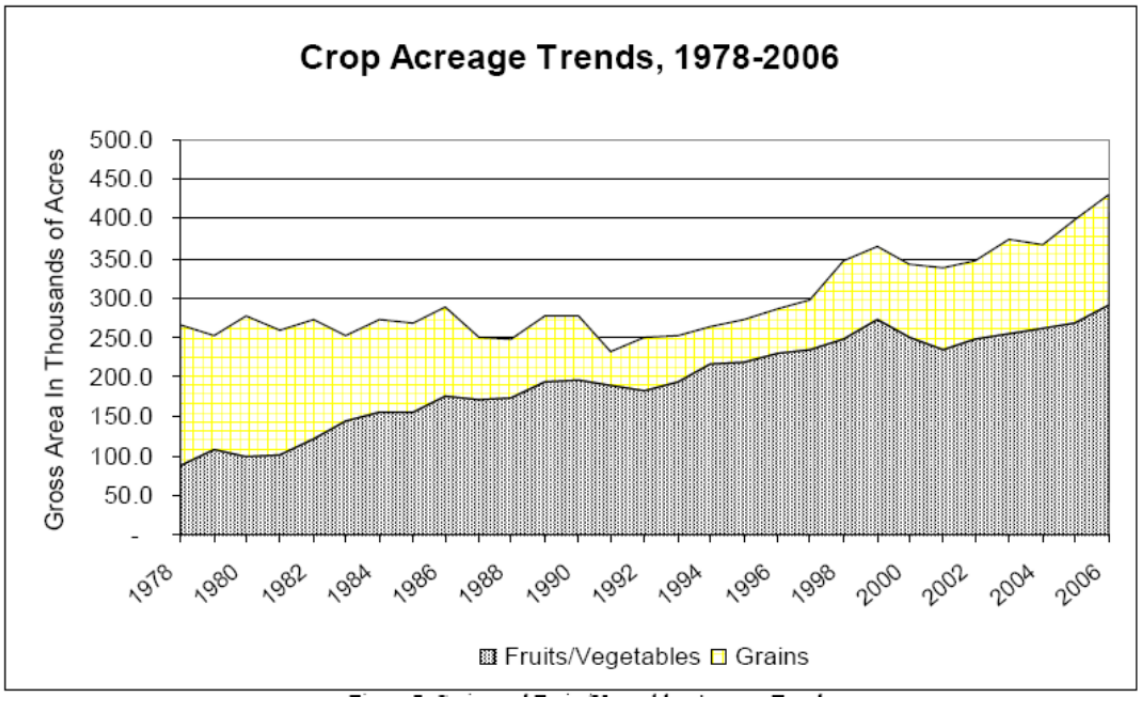

Figure 14 Crop acreage trends (*from:* Westlands Water Management Plan 2008).

Crop	2006 Present Ac	2020 Future Ac
Alfalfa Hay	13,305	10,000
Cotton	130,886	70,000
Field Crops	87,466	90,000
Grain	35,037	5,000
Trees	75,309	90,000
Vegetables	170,641	200,000
Vines	12,468	15,000
Fallow	54,944	125,000
Subtotal	580,056	605,000
Double Crop	(20,312)	(30,000)
Total	559,744	450,000

Table 6 Present and projected cropping patterns (*from:* Westlands Water Management Plan 2008).

63% of the applied water but generate only 17% of California's crop revenue. Vegetables, however, produce substantially more revenue both, per unit land and per unit water use: vegetables account for only 16% of the irrigated acreage but use 10% of the applied water and generate 39% of California's crop revenue.

At NASL, the difference in the total acreage of field crops versus vegetable crops is much larger than Valley wide (Figure 16). The definitions of field and vegetable crops are the same as in Figure 15. In some of the more recent years, NASL has seen significant conversion to vegetable crops (primarily tomatoes, beans, and onions).

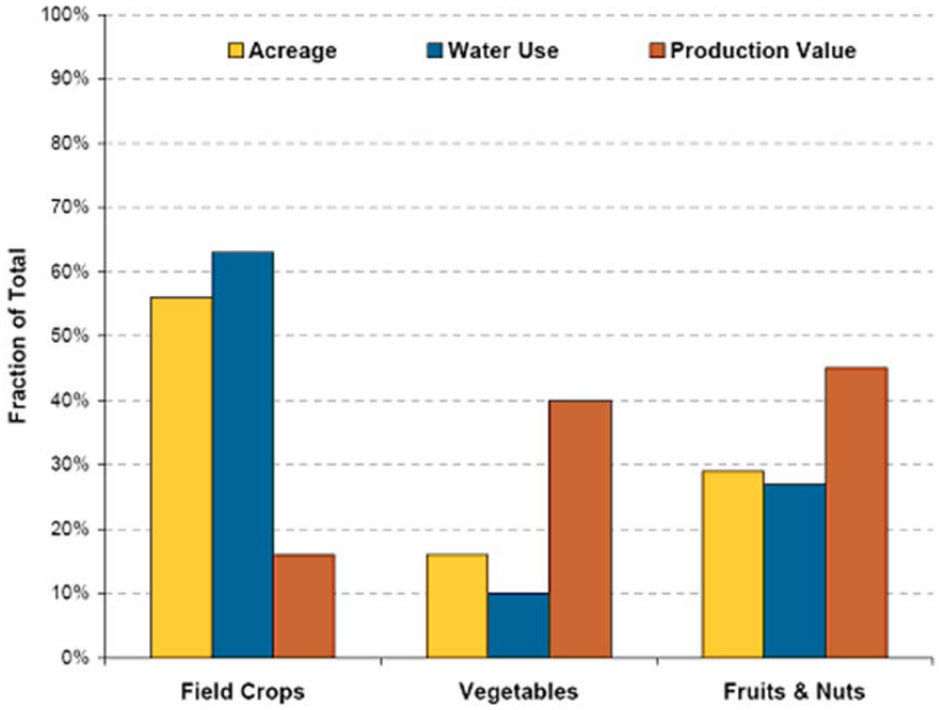

Note: Nursery products account for a large proportion of agricultural revenue but are excluded here because of insufficient data on irrigated acreage and water use.
Source: Gross production value is based on crop production values for 2003 (USDA 2007a). The applied water and irrigated acreage values were based on 2003 estimates from the DWR 2008c.

Figure 15 Percent of irrigated acreage, gross production value, and applied water for each major crop type in the San Joaquin Valley, 2003.

The trend of growing crops with high water demand and relatively low revenue is an unsustainable venture as water prices rise and availability becomes uncertain. It is paramount for the agricultural sector to be as efficient as possible in terms of water conservation which in turn plays a significant role in the financial viability of the sector.

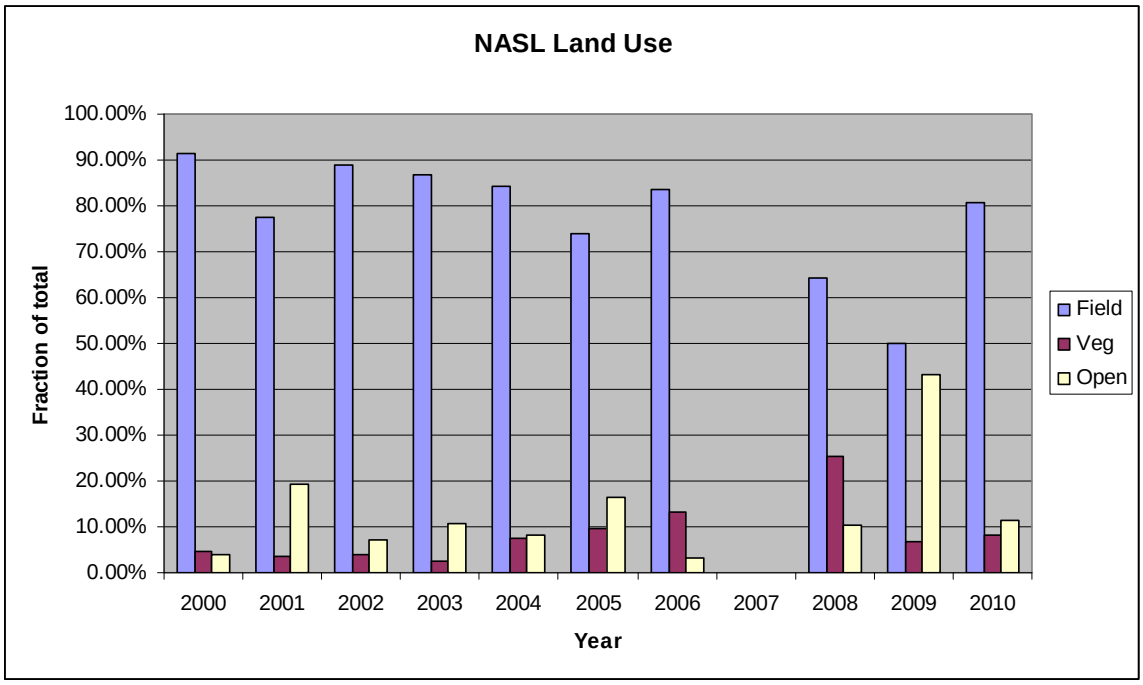

Figure 16 NASL land use distribution over the past decade with crops categorized as field crops and vegetable crops.

Cooley et al. (2008) tested the viability of four alternative scenarios for water conservation in the agriculture sector. The following section is a summary of those alternative scenarios with changes made to account for the specific area of NASL:

- **Modest Crop Shifting** – shifting a small percentage of lower-value, water-intensive crops to higher-value, water-efficient crops, possibly decreasing consumptive use.
- **Smart Irrigation Scheduling** – utilizing irrigation scheduling information to help farmers more precisely irrigate to meet crop water needs, decreasing both, consumptive and non-consumptive water use
- **Advanced Irrigation Management** – applying advanced management methods that save water, such as regulated deficit irrigation, reducing consumptive water use due to decrease in evapotranspiration
- **Efficient Irrigation Technology** – shifting a fraction of the crops irrigated using flood irrigation to sprinkler and drip systems, reducing both, consumptive and non-consumptive use

It is important to note that when looking at methods for conserving agricultural water at NASL we are looking at ways that could possibly reduce the reliance on groundwater, thus keeping groundwater storage at sustainable levels. The methods mentioned above do not take into account groundwater pumping further “downstream” or “upstream” from NASL that could continue to affect groundwater storage at NASL into the future.

Modest Crop Shifting Scenario

Under the modest crop shifting scenario, replacing crops that are associated with high rates of applied water per unit area with those that use less water can result in substantial water savings. Because plant water requirements in much of California are met by irrigation, water saved from crop shifting can reduce both, water withdrawals and consumptive water use. Crop shifting may also provide economic advantages to the region. Field crops are generally more water-intensive and generate lower value per acre compared with other crop types with alfalfa being the most water intensive at 4.5 AF/acre and cotton being the major crop of the region at 2.32 AF/acre. Some field crops such as safflower (as low as 1.15 AF/acre) and grain (as low as 1.19 AF/acre) are less water intensive than alfalfa. In the 1970s, 1980s, and 1990s, cotton dominated the landscape at NASL. Over the past decade, a significantly higher acreage at NASL is in alfalfa. Together, alfalfa and cotton typically constitute well over half of the total acreage planted at NASL. It is important to note that field crops can provide important benefits including, but not limited to: price stability for farmers (in comparison to other commodities); nitrogen fixation (in the case of alfalfa, lotus species, and legumes); lower fertilizer and pesticide inputs (depending on farm management); and, in some cases, wildlife habitat (Putnam et al. 2001).

Cooley et al. (2008) estimated that shifting 25% of irrigated field crop acreage to irrigated vegetable crop acreage created a 4% decrease in consumptive water use in the Tulare Lake Basin with a 36% increase in production value in comparison to their baseline estimates which were based upon water use from the delta system for total area irrigated in the Sacramento River, San Joaquin River and Tulare Lake regions in the year 2000.

	Water Withdrawals (1,000 AF)	**Production Value** (2005$ billions)
Sacramento River	-545 (-6%)	$1.7 (57%)
San Joaquin River	-240 (-3%)	$1.3 (33%)
Tulare Lake	-440 (-4%)	$2.1 (36%)
Total	-1,225 (-5%)	$5.1 (40%)

Table 7 Modest Crop Shifting Scenario: Shifting 25% of Field Crop Acreage to Vegetable Acreage.

There are increased operation and maintenance costs associated with particular crop types, which are not reflected in the gross estimates because net estimates are not available by crop type. However, a shift to crops that are more economically viable but also consume less water could prove to be profitable both in terms of water conservation and economically.

Importantly, groundwater recharge may also be affected by changing to crops with lower water use. Depending on the farmer's ability and willingness to adjust irrigation practices to reflect the lower consumptive water use, groundwater recharge may increase, decrease, or remain the same.

Smart Irrigation Scheduling Scenario

Crop water requirements vary throughout the crop life cycle and depend on weather and soil conditions. Irrigation scheduling provides a means to evaluate and apply an amount of water sufficient to meet crop requirements at the right time. While proper scheduling can either increase or decrease water use, it will likely increase yield and/or quality, resulting in an improvement in water-use efficiency (Clemens et al, 2008) which is defined as yield per unit of applied water. Despite the promise of irrigation scheduling and other new technologies, farmers frequently rely primarily on visual inspection or personal experience to determine when to irrigate. A survey by the Department of Agriculture and Resource Economics at the University of California, Berkeley evaluated the applied water use and yield of all the major crop types of 55 growers across California who used CIMIS to determine water application timing and rates (Eching, 2002). Their study concluded that the use of CIMIS increased yields by 8% and reduced applied water use by 13% on average (DWR, 1997).

This scenario assumes that farmers are able to apply the necessary amount of water to crop requirements when needed. "Inadequacies in the irrigation system and poor management of the water supply result in inadequate and unreliable water supplies to the field, frustrating any attempts at accurate crop irrigation scheduling" (FAO 1996).

With respect to groundwater, smart irrigation scheduling at NASL, which has no tile drains, has two significant advantages given that surface water supplies are fixed and the difference between available surface water and crop water needs are supplemented with groundwater: 1. it has the potential to reduce the amount of groundwater pumping (less water and energy use), especially on leases with a dual water source, and 2. it reduces the amount of farm chemicals (nutrients, pesticides) potentially leaching into groundwater.

From a groundwater budgeting perspective, smart irrigation scheduling may have varying effects depending on other changes in agronomic practices that often come along with smart irrigation scheduling. The most likely effect is that the groundwater balance is unaffected, because the savings in groundwater pumping are matched by reductions in groundwater recharge from irrigation water return flow. If yields and, hence, crop water consumption increase due to reduction in plant stress during critical growth period, net groundwater use may actually increase, because the decrease in groundwater recharge due to reduced irrigation return flows is even larger than the decrease in groundwater pumping due to lower applied water demand.

Advanced Irrigation Management Scenario

Evan and Sandler (2008) point to production increases due to improved uniformity increasing crop production in previously water-short areas in the field and the capacity for improved irrigation schedules that minimize short-term drought stresses. These improvements do not necessarily save water on the regional level because the same of amount of water still needs to

be applied to produce high yields. Cooley et al. (2008) emphasize that water conservation occurs only when total diversions to the farm are reduced, without increasing groundwater pumping. We point out that this statement is incorrect: It does not take into account the balance of groundwater pumping and groundwater recharge. Correctly stated, true water conservation occurs only when a reduction occurs in the difference between total applied water and groundwater recharge from irrigation water return flow. The total applied water includes surface water deliveries and pumped groundwater water. For example, if irrigation technology allows the farmer to reduce his percolation losses (groundwater recharge) by 0.75 AF/ac, he must reduce his applied water rate by an amount that is larger than 0.75 AF/ac, otherwise there is no real water conservation.

The most important approach to achieve such water conservation is by applying methods through which consumptive plant water use is reduced without significant reduction in yield. A growing body of international work shows that consumptive water use can be reduced in orchards and vineyards without negative impacts on production. The concept of "deficit irrigation," defined as the application of water below the level of traditional, full crop ET, can be an important tool to both, reduce applied water and increase revenue (Chaves et al. 2007, Fereres and Soriano 2006).

A specific example of combining a crop shift in addition to application of advanced irrigation management techniques is the Olive. Olive (*Olea europaea L.*) is considered drought tolerant and trees can survive on shallow soils with little supplemental water beyond winter rainfall. However, olive fruit production and the economic survival of the orchard operation do not depend solely on tree survival. In table olive production, maximum fruit size and fruit yield must be maintained, while in olive oil production, oil yield and quality must be maximized if an orchard is to remain economically viable (University of California, 2008). The following table shows mature olive water use at full irrigation, that is at 100% of the crop ETc (crop EvapoTranspiration).

San Joaquin Valley	Month	Jan.	Feb.	Mar.	Apr.	May	Jun.	Jul.	Aug.	Sep.	Oct.	Nov	Dec.
	gal/acre/day	683	1186	2181	3333	4375	5261	5564	4822	3700	2280	1011	526

Table 8 Crop Water Use (ETc) for Olive when fully irrigated (Beede and Goldhamer, 2005).

The total annual water use, computed from Table 8, is 3.2 AF. For NASL, such water use would be among the largest given the current crop mix planted around NASL. However research has shown that when water was cut by 50% from June 1st to August 15th up to nearly 21% (0.6 AF) of the season's water requirement was saved. This irrigation strategy led to no differences in gross fresh fruit yield, fruit size, or gross revenue when this mild to moderate regulated deficit irrigation approach was employed over four years (Goldhamer, 1999).

When considering olive oil, irrigation management has a profound influence on olive oil production and on olive oil quality but with some flexibility over a broad range of water applications below full ETc (University of California, 2008). Since the price received for olive oil is not related to fruit size, oil olives can be irrigated less than table olives and still produce good olive oil (University of California, 2008).

A comparative study evaluating the influence of seven different levels of water applied by drip irrigation to 'Arbequina I-18' olive trees grown in a super high density orchard (670 trees per acre) in the Sacramento Valley of California was conducted in the early 2000's (Grattan et al, 2006). The reduced percentages of ETc applied were imposed during the irrigation season from roughly May to October. By October, seasonal rainfall once again began to contribute to ETc demands in all treatments prior to harvest. Full ETc was met in the Spring by annual rainfall and a fully recharged soil profile until the irrigation season began in late April to early May.

A study on oil quality measured fruitiness, bitterness and pungency of oils produced at various levels of water stress. Results showed that stressing olives to between 33 and 40% ETc produced oils that had a better balance of pungency and bitterness, were pleasantly fruity, held both ripe and green character, had more complexity and depth, and boasted higher polyphenol content. High levels of irrigation lowered oil extractability and produced bland oils with significantly less fruitiness and almost no bitterness or pungency (Berenguer et al, 2006).

The volume of water that can be saved using a deficit irrigation strategy depends on many factors, such as crop sensitivity to stress, climatic demand, stored available water at bud break, spring-summer rains, and the particular irrigation strategy. Cooley et al. (2008) estimate that deficit irrigation can reduce applied water by 20% for almonds, pistachios, and citrus trees according to a review of papers listed in Table 9.

According to Evan and Sandler (2008), a 30% to 40% decrease in water applied may result in only a 5% to 10% yield reduction depending on the relationship between yield and water use of a specific crop.

For NASL agricultural lands, an effective deficit irrigation strategy would become a necessary option, if NASL and its lessees decided on long-term leasing options that make permanent orchard crops a viable alternative, at least on some of the leased lands. The benefit of switching to an orchard crop grown under an effective deficit irrigation strategy would be a potential reduction (10% - 20%) in applied water demand from the current average of 2.6 AF/acre, but more importantly, a potentially significant increase in crop value. Tree crops use significantly less water than alfalfa, but their water use is approximately 25% higher than the average water use in field crops. Of the crops listed above, almonds and citrus are unlikely to be grown at NASL due to soil conditions including elevated soil and water salinity conditions. However, Pistachios are a potential tree crop that can be grown at NASL under regulated deficit irrigation, with 33% reduction in consumptive water use and a total applied water need of 2.3 AF/ac/yr instead of 2.9 AF/ac/yr at full irrigation (Iniesta et al., 2008).

Study	Location & Year	Crop	Change in Applied Water	Change in Yield
Goldhamer et al. 2006	San Joaquin Valley 1993-1995	Almonds (high density)	-20%	-7%
Goldhamer et al. 2006	San Joaquin Valley 1993-1995	Almonds (low density)	-12%	-4%
Goldhamer et al. 2003	San Joaquin Valley 2001	Almonds	-5%	+4 %
Goldhamer et al. 2003	San Joaquin Valley 2001	Almonds	-42%	-9%
Goldhamer and Beede 2004	San Joaquin Valley 1998-1992	Pistachios	-23%	NA[(a)]
Average water savings for almonds and pistachios = -20%				
Goldhamer and Salinas 2000	San Joaquin Valley 1997-2000	Citrus (Navel orange)	-25%	-5%[(b)]
González-Altozano and Castel 2000	Valencia, Spain 1997-1998	Citrus (Clementine)	-12%	+4%
González-Altozano and Castel 2000	Valencia, Spain 1997-1998	Citrus (Clementine)	-22%	+1%
Average water savings for citrus = -20%				

Table 9 Literature review of deficit irrigation studies in orchards (Cooley et al., 2008).

The disadvantage of permanent crops is that the water savings relative to current water use may be insufficient and that orchard crops lock up future water supplies, particularly during drought/water shortage years. A potential option may be to allow for permanent crops managed under deficit irrigation on a fraction of the total acreage.

Deficit irrigation practices are not limited to tree crops. Regulated deficit irrigation practices have been developed for some of the major field crops grown at NASL: cotton (Munk et al., 2004, 2007), processing tomatoes (Hanson and May, 2006) and alfalfa (Orloff et al., 2004). Water savings can be of similar magnitude as in regulated deficit irrigated tree crops.

Efficient Irrigation Technology Scenario

Numerous irrigation methods are currently available to deliver water where and when it is needed. These methods are typically divided into three categories: flood, sprinkler, and drip/micro-irrigation systems. In WWD the irrigation methods are divided as shown below:

Type of System	Percentage of Land Irrigated						
	1985	1990	1996	2000	2004	2005	2006
Surface							
Furrow	60	38	34	28	23	21	20
Border Strip	3	5	2	2	2	2	2
Combination sprinkler/furrow	15	38	43	43	39	35	31
Pressurized							
Sprinkler	21	16	15	14	11	16	11
Drip/Trickle	1	3	6	13	25	26	36
Total	100	100	100	100	100	100	100

Table 10 Irrigation type used in Westlands Water District (Westlands Water District, 2008).

As seen in Table 10 above the use of drip irrigation has steadily increased over the past 20 years. It is currently even higher due to the continued conversion to drip irrigation, particularly in tomatoes. Although traditionally applied to specialty crops such as vegetables and grapes, drip irrigation systems are increasingly applied to row crops, and there are examples of use on field crops such as cotton, corn, alfalfa, and potatoes. With proper management and design, drip and micro irrigation are the most efficient at maximizing crop-yield-per-unit water use; flood irrigation is the least efficient because of the larger volumes of unproductive evaporative losses that occur and due to water application to non-targeted surface areas. In furrow irrigation there is the propensity for deep percolation. With respect to NASL's groundwater storage, groundwater recharge from excess irrigation is not an immediate disadvantage. However, due to the depth of the aquifer and the relatively high amounts of clays in the top soil, the increased salinity of the recharge water is a potential water quality issue. Also, the cost of water (for pumping or delivery from surface water sources) makes it economically desirable to minimize the amount of water leaching to groundwater.

Sprinkler irrigation often claims a benefit for improving efficiency, however in some settings, the additional evaporation caused by frequent irrigation and spray evaporation may result in more net consumption than field runoff losses from other irrigation systems that are recoverable (Clemens et al, 2008).

One of the major disadvantages to converting to drip is the initial investment, which is estimated at $500 to $2,000 per acre (Bisconer, I., Chair of the Drip/Micro Common Interest Group, Irrigation Association, personal communication, August 6, 2008). However, these costs can be offset with a reduction in operation costs and/or increase in crop revenue. The "Drip-Micro Irrigation Payback Wizard," can be used to compare the costs and benefits associated with converting from flood to drip/micro for cotton and almonds in Central California. The Payback Wizard estimates that the payback period for converting all of the cotton planted around NASL is 1.86 years, suggesting that a conversion to drip/micro is an economically very viable alternative to reduce the gross water usage at NASL.

The economic savings associated with conserving water is relatively small because water for agriculture is typically inexpensive in California. While conserving water may not be an economic driver for converting to drip, the additional revenue provided by increased yields and/or quality often make these investments worthwhile. Cooley et al. (2008) had further suggested that saved water may be applied elsewhere to increase overall production, resulting in no applied water savings but an overall increase in agricultural production and income.

For NASL, this latter argument poses a significant problem as it does not address the underlying concern of groundwater overdraft: Increasing irrigation efficiency through smart irrigation scheduling, improved irrigation management, or conversion to drip irrigation or micro-irrigation systems will significantly decrease the amount of applied irrigation water demand at NASL, including the amount of groundwater pumped, while keeping yields at current levels or even improving yields. But it will – by design – also drastically reduce the amount of groundwater recharge from NASL crop lands. Estimated irrigation efficiencies (applied crop water demand per unit of irrigation water) in some of the drip/micro-irrigated regions of WWD, for example in tomatoes, are on the order of 90% to 95%, leaving 5% to 10% of the applied water for groundwater recharge. Under typical practices for the study period (1975 – 2010), groundwater recharge was estimated to be on the order of 0.45 to 0.9 AF/acre. With higher irrigation efficiencies, groundwater recharge may be as small as 0.15 – 0.3 AF/acre. For tomatoes in Westlands Water District, the conversion to drip irrigation has decreased the applied water demand from 2.4 AF/ac/yr in the 1980s to 1.8 AF/ac/yr in the 2000s (Table 3), with a likely increase in production and possibly consumptive water use. Effectively, groundwater recharge from tomatoes has therefore drastically decreased.

Without regulated deficit irrigation or switching to crops with reduced water demand (e.g., winter cropping only), increased irrigation efficiency in the current set of cropping patterns will decrease the applied water demand, but not the crop consumptive water use, which means that the net groundwater use (pumping minus recharge) will remain the same. Net groundwater use may even increase, if annual surface water supplies continue to be below their 1975 – 2000 average to a degree that is not matched by a reduction of applied water demands.

For NASL, conversion to highly efficient and smart irrigation systems is a necessary step, not to "fix" its groundwater overdraft potential, but merely to address the immediate shortage of surface water supplies due to the reductions in water deliveries through the Sacramento-San Joaquin Delta system. In the longer term, NASL and its neighbors – assuming a continued shortage of water imports - will need to move to cropping systems that yield a significantly lower consumptive water use across NASL and – by extension - across the entire Westside region affected by surface water shortages in the California Aqueduct and Delta-Mendota Canal systems. Lower consumptive water use is achieved mainly by shifting to low water use crops (see Table 3), partial fallowing, and deficit-irrigation.

Data Gaps

A significant data gap exists in our database regarding the water supplied to NASL by WWD for agricultural use. Data are available for only six years of the nearly forty years of crop water deliveries. Additionally, for the best model results an accurate picture of all groundwater use in the area needs to be available including groundwater pumping from regions adjacent to the NASL area (Figure 3). For example, if NASL reduces its pumping of the aquifer, it is unlikely to stop land subsidence with other pumping in the region continuing to decrease aquifer water levels. For improved future water use scenario assessment, we need to better account for past and current irrigation practices, for the role of tail water systems, and of any other water recycling schemes that have been or are currently in effect. We foresee using the above outlined scenarios as a basis for further discussion with local growers and experts in irrigation management and technology and experts in agronomy and agricultural economics.

4 Geology, Hydrogeology, and Groundwater Dynamics

4.1 Introduction

In the earlier part of the twentieth century, extensive groundwater development began in most areas of the Central Valley of California (referred to hereinafter as the "the Central Valley"), especially within the San Joaquin Valley ("the Valley") (Poland et al, 1975, p. 8). The agricultural fertility of the area led to large scale withdrawal of groundwater for crop and municipal uses. As is the present case, over some periods in the 20th century, groundwater withdrawal has been greater than the groundwater recharge rate, and a consequence of this has been subsidence of the land surface over large portions of the Central Valley floor. This type of subsidence is believed to have begun in the mid-1920s, with the beginning of groundwater development in the Valley. Other causes of land subsidence exist within the Valley, but subsidence due to excessive groundwater pumping is the main cause (Poland et al, 1975, p. 8).

A key purpose of this report is to study the historical and present-day causes of this type of subsidence. This is primarily achieved by performing a literature review of available reports conducted by other investigating parties, in particular those that study the same or similar phenomena in close vicinity to the Naval Air Station Lemoore (NASL). Of particular interest to this report are the major local and regional geological formations found beneath this part of the Valley floor. The main focus of our investigation is the upper portion of the valley fill that contain the aquifer systems with water of acceptable quality. This portion of the total valley fill thickness is thought to be responsible for most of the subsidence experienced at NASL. Historical and current surface hydrology features are noted and their importance to the subsidence problem at NASL is considered. Groundwater levels and direction of groundwater flow, from predevelopment times to the present, are also studied. Regional aquifer systems are largely delineated and defined by groundwater quality. The findings of previous hydrogeology and subsidence studies in the Valley are discussed, in particular those that study the type of subsidence resulting from groundwater pumping overdraft.

Besides literature review, multiple datasets were gathered, processed and utilized for the hydrogeology and subsidence study at the Lemoore Naval Air Station (NASL). The type of subsidence that has historically occurred at NASL and surrounding lands (the study area) is believed to be mostly due to a change in water levels directly attributable to groundwater pumping. To gain further understanding of the extent of potential groundwater level decline within the study area, contoured groundwater elevation maps and hydrographs representative of specific aquifer layers were completed. Groundwater elevation data was compiled to create groundwater contour maps, so that regional and local groundwater flow patterns could be mapped and visualized. Flow patterns were observed over a period of time beginning in 1956, and conditions described for a variety of scenarios. Details of this analysis were also used for a 1-D subsidence model at NASL. The same dataset was used to complete 'idealized' hydrographs from paired pumping wells located on NASL lands. The hydrographs were completed from

measured and estimated data. The aquifer systems beneath the study area were divided into their two main systems: the 'upper' (or hypo-Corcoran) and 'lower' (or sub-Corcoran) aquifers and separate hydrographs were drawn for each. Data used to complete the hydrographs was available for dates as far back as 1925.

Well logs were collected for delineation of major and minor geologic units beneath the study area. Logs collected were electric logs (E-logs) and well completion reports (driller's logs) which included more detailed geologic reports. E-logs in conjunction with geologic logs proved to be the most valuable and reliable data source for this investigation. The results of E-Log interpretation were also used for the 1-D subsidence model at NASL.

Historical land surface elevation data was collected from a variety of sources (chapter 5) to determine the total amount of subsidence within the study area believed to have occurred since predevelopment times. Information relating to land surface elevation within the study area began in 1947, and was paired with later measurements from a variety of sources to provide a more or less continuous record of land surface elevation change to present times. Using the assumption that 1925 was representative of predevelopment conditions, subsidence rates between this date and 1947 were estimated.

4.2 Previous Studies

Several hydrogeologic and subsidence studies of areas surrounding NASL have been undertaken. A number of these reports cover areas surrounding NASL, whilst others cover areas that are a large proportion of the Valley.

The USGS has published several reports on regional hydrology and geology for areas that include NASL. Two of these reports proved particularly useful, the first being the report entitled "Subsurface geology of the late tertiary and quaternary water-bearing deposits of the southern part of the San Joaquin Valley" prepared by M.G. Croft and published in 1969 (Croft, 1969); the second being "Geology, hydrology, and quality of water in the Hanford-Visalia area San Joaquin Valley, California" (Croft and Gordon, 1968). Both of these reports covered areas larger than, but inclusive of, the study area that is the subject of this report. These reports were used to place NASL within a regional hydrogeologic context, and of particular interest was the area immediately surrounding NASL.

Two reports prepared by Kenneth D. Schmidt and Associates were also used; "Groundwater conditions beneath district owned lands in the Westlands Water District" published in April 2009 (Kenneth D. Schmidt and Associates, 2009) and " Groundwater conditions and reuse of City of Lemoore WWTF effluent in the Westlake Farms area " published in March 2002 (Kenneth D. Schmidt and Associates, 2002). These reports were very useful, as they contained a great deal of very local hydrogeological information and analysis.

4.3 Regional Hydrogeology

The Sierra Nevada mountains to the east of NASL are westward-tilted, ranging in elevation from 1,000 ft. in the foothills to more than 14,000 ft. at the crest of the range. They are composed of consolidated igneous and metamorphic, crystalline rocks of pre-Tertiary age.

The Coast Ranges to the west of NASL consist of a series of folded and faulted marine and volcanic rocks rising to approximately 6,000 ft. in elevation at their highest point. The mountains consist mainly of complexly folded and faulted consolidated marine and non-marine sedimentary rocks of Jurassic, Cretaceous, and Tertiary age, dipping eastward to overlie the basement complex. The range that forms the western boundary of the San Joaquin Valley adjacent to the study area is the Diablo Range, and is the most easterly of the Coast Ranges.

The hydrogeology of the San Joaquin Valley has been drastically changed by anthropogenic intervention. In pre-development times, groundwater recharge was mainly from the Valley flanks, particularly the Sierra Nevada foothills. The general groundwater flow direction was from the Valley margins to beneath the Valley trough in the center of the Valley, where under natural conditions it would feed streams and other water-bodies. Regionally extensive restricting clay layers, produce a system of confined aquifers, where pre-development heads where often artesian. Development for agricultural purposes has led to much lower heads in theses confined aquifers, reversing the upward groundwater flow direction. The two aquifer systems have also become much more hydraulically connected, due to the large number of wells penetrating both aquifer systems (Figure 17).

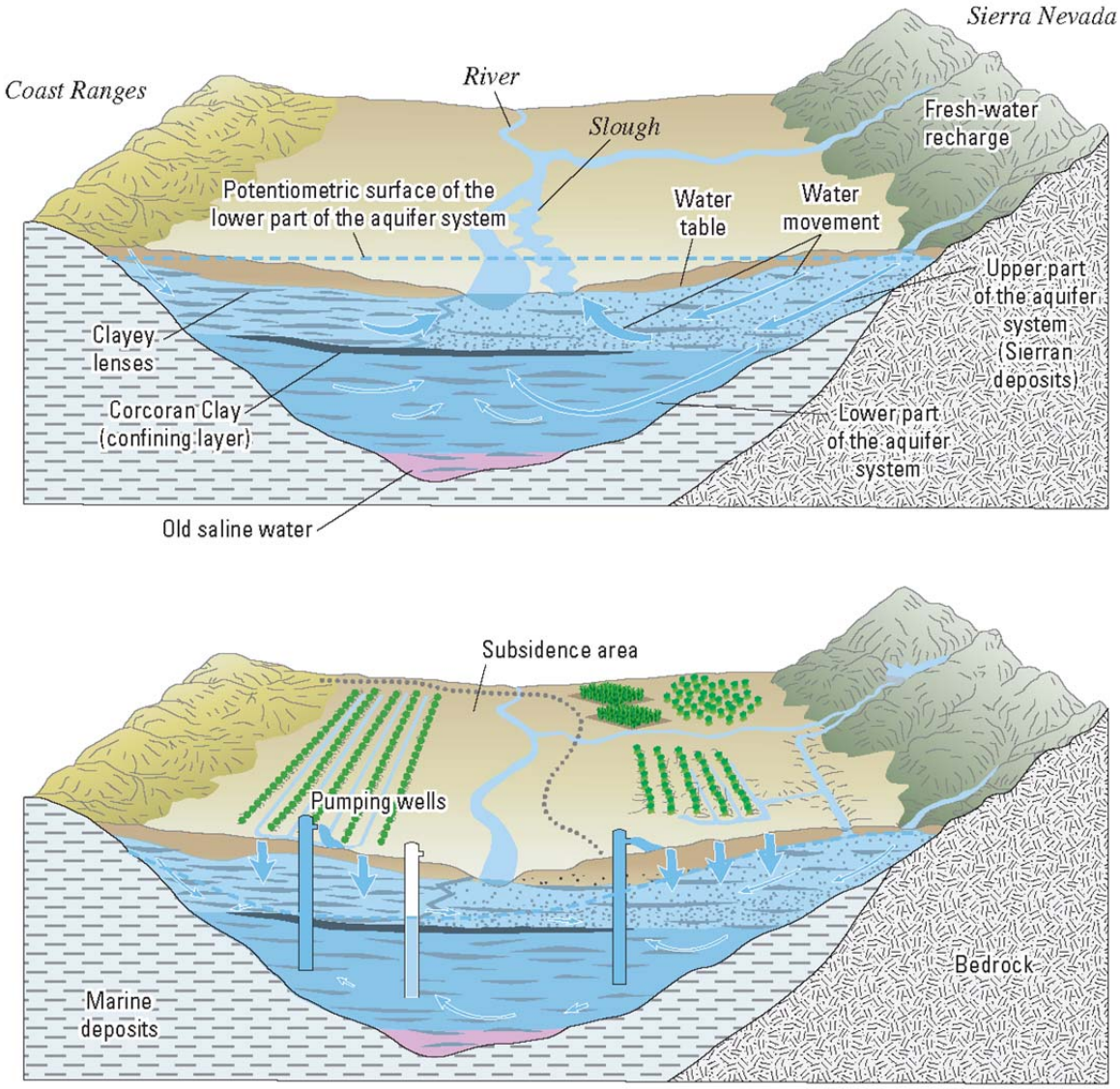

Figure 17 Pre- and post-development groundwater conditions in the San Joaquin Valley, showing generalized geology (Faunt, 2009).

The basement complex, of pre-Tertiary age, consists of metamorphic and igneous rocks. Below the ground surface, they slope steeply downwards and westwards from the Sierra Nevada. An E-log obtained for this study for a well drilled to 12,300 ft. bgs in township 19-17 fails to reach the bedrock. Below the western side of the Valley, and parts of the eastern side, the rocks are believed to be mafic and ultramafic (Sun et al, 1991). Beneath the Tulare Lake Bed, the basement complex is found beneath more than 14,000 ft. of Cretaceous, Tertiary and quaternary age sediments. In this area a well failed to penetrate the basement complex at

14,642 ft. below sea level. Along the western flank of the Valley, marine rocks and deposits of pre-Tertiary age crop out. The basement complex is of little hydrogeologic significance beneath the study area, as its rocks are mainly impermeable and at too great a depth to be penetrated by wells. In the Valley, the marine rock units overlying the basement complex are thought to be as thick as 20,000 ft. (Repenning, 1960).

The western flank of the Valley between the Kettleman Hills and Los Banos is primarily underlain by fine-grained sediments which extend eastwards into the Valley. Through time, these were probably deposited at the distal parts of alluvial fans and floodplains, and also in small marshes and lakes (Sun et al, 1991). The following provides a more detailed description.

The marine rocks and deposits that crop out to the west and south of NASL are beneath the Kettleman Hills and the Coast Ranges and are Eocene, Oligocene, Miocene and Pliocene in age. Primarily, they consist of sand, clay, silt, sandstone, shale, mudstone, and siltstone. In places, gypsum and limestone are found. The Kettleman Hills are northwest-southeast-trending and lie directly to the west of the Tulare Lake Bed. In places, these units are fractured and sometimes saturated. However, they normally contain saline water and are capable only of small yields (Sun et al, 1991).

Underlying the Los Banos-Kettleman City area is the Etchegoin Formation of Miocene and Pliocene age, overlain by the San Joaquin Formation. They are both of continental and marine origin, cropping out along the hills on the flank of the Valley and dipping in a northeasterly direction. The Etchegoin Formation varies greatly in texture, from sand, gravel and sandstone to clay and silt whilst the San Joaquin Formation is also variable in texture, but is mainly comprised of silt and silty sandstone. The part of the deep San Joaquin Formation to the northeast of the Kettleman Hills is considered to be the shoreline phase of the Formation.

The Tulare Formation is defined by Woodring and others (Woodring, Stewart et al., 1940) as the youngest folded strata exposed in the Kettleman Hills. It overlies the San Joaquin Formation, where present beneath the Valley floor. Beneath and to the west of the study area, the depth and thickness of the Tulare Formation is unknown, but is 3,500 ft. thick in the Kettleman Hills.

The Kings, Kaweah, Tule, and Kern Rivers are the only major perennial streams in the Tulare Lake Basin (the southern part of the San Joaquin Valley). The Kings River forks immediately east of NASL, where it discharges northwards to the Fresno Slough and southwards to a southern fork of the Kings River. The Fresno Slough meanders along the northwest-southeast extension of the San Joaquin River valley trough, from the Kings River diversion fork at the eastern boundary of NASL in the south, to the San Joaquin River near Firebaugh in the north. The San Joaquin River is the major river draining much of the northern part of the San Joaquin Valley. The southern fork of the Kings River, together with the Kaweah and Tule Rivers discharge onto the drained Tulare Lake Bed. The Kings River is the largest river to discharge onto the Tulare Lake Bed. Presently, due to water diverted for irrigation, the Tulare Lake Bed lies dry. The Tulare Lake Basin is essentially an endorheic basin, with the Tulare Lake Bed at the lowest elevation. Historically, prior to water regulation in the San Joaquin Valley, the shallow, but

extensive Tulare Lake would sufficiently fill to occasionally discharge water from the Tulare Lake Basin to the north via Fresno Slough. The Kern River flows to the Kern and Buena Vista Lake Beds, part of the endorheic Tulare basin. The streams that drain the Coast Ranges are not perennial, flowing only during the rainy season.

The origin of the Tulare Lake itself has been discussed in previous reports (Sun et al, 1991). Some authors believe the lake was formed by natural damming of the Kings River and Los Gatos Creek via deposition of their alluvial fans, whilst others believe that it was formed by structural down-warping due to tectonic subsidence. The area now known as the Tulare Lake Bed has been successively covered by lakes and marshes for more than 2 million years.

4.4 Local Hydrogeology

The valley floor to the northwest of the present-day dry Tulare Lake Bed, including NASL, is formed by a large alluvial fans formed by ephemeral streams originating in the Coast Ranges. In contrast, directly to the north and east of NASL and overlapping with the study area is the Kings River alluvial fan formed by the Kings River, which originates in the granitic Sierra Nevada. The wideness of the valley at this point, along with the connection to high elevation glaciated areas of the Sierra Nevada, and the high tectonic basin subsidence rates are the main reasons for the Kings River fan to consist of relatively thick deposits. The total area covered by the Kings River alluvial fan is approximately 950 square miles. NASL is bordered on the northeast side by the distal and lowest alluvial fan deposits of the Kings River, generally consisting of finer-grained sediments than the higher alluvial fan of the Kings River. These deposits variably interfinger with the distal fan deposits from the coast range underlying NASL.

Historically, the less incised and less entrenched reach of the Kings River downstream of Laton was subject to flooding before levees were constructed. As a result, groundwater levels in the area tend to be consistently higher than in anywhere else within the study area (see below).

The trough of the Valley has shifted over time, and micaceous sands from the Sierra Nevada can be found as far as 17 miles to the west of the present-day position of the Valley axis. These periodic shifts have been attributed to changing climates and geology over time.

The unconsolidated deposits found on the Westside of the valley, at NASL and west of NASL, originated in the Coast Ranges and consist of undifferentiated alluvium. Flood-basin, lacustrine (lake) and paludal (marsh) deposits can be found in the centre of the valley, and interfinger with deposits from both sides of the valley. These deposits together form most of the water-bearing formations in the study area. Beneath the valley trough the unconsolidated deposits are at least 3,000 ft. thick. On the east side of the valley, these deposits are grouped in three stratigraphic units: continental deposits, older alluvium, and younger alluvium. Oxidized deposits generally represent subaerial deposition, and reduced deposits generally represent subaqueous deposition (Croft and Gordon, 1968).

Reduced continental deposits of Pliocene and Pleistocene age extend from the eastern side of the valley beneath the trough to the western side. These deposits are moderately permeable and consist of micaceous sand, silt, and clay (Croft and Gordon, 1968). Of the reduced deposits, the coarsest are believed to be deposited on deltaic and flood-plain environments, whilst the finer-grained deposits are interpreted as lacustrine, flood-basin and paludal deposits. Water found in these deposits is fresh in the upper two-thirds, but is generally slightly brackish in the lowest third (below 2,000 ft. depth). Beneath the present location of the Tulare Lake Bed, the reduced continental deposits form the only aquifer.

Older alluvium of Pleistocene and Recent age unconformably overlie the continental deposits, being of moderate to high permeability and hence forming the largest aquifer system in the area. The older alluvium can be divided into reduced and oxidized deposits.

The reduced deposits consist mainly of moderately permeable, unweathered, fine to medium sand, silty sand, and clay, sporadically cemented with calcium carbonate. Between Riverdale and Stratford, within the study area, the reduced older alluvium forms the main aquifer (Croft and Gordon, 1968).

The oxidized deposits consist of reddish-mottled, highly permeable, crossbedded, fluviatile arkosic sand with lenses of gravel and, rarely, thick beds of silt or clay. The beds of oxidized older alluvium in the subsurface beneath the Kaweah, Tule and Kings Rivers are shown in electric logs to be very coarse. At the northern end of the Tulare Lake Bed, the older alluvium interfingers with the undifferentiated alluvium.

Younger alluvium of Recent age consists of arkosic beds, of moderate to highly permeability, fluviatile sand beneath broad, nearly featureless flood plains. The unit formed by the younger alluvium is less than 55 ft. thick, and forms an aquifer only in the vicinity of Hanford and Lemoore, where it is about 40 ft. thick and lies above the A-clay. The principal water source for this aquifer is seepage from the Last Chance Ditch, Lemoore Canal and irrigation return. To the southeast of NASL, driller's logs report blue or grey deposits on the toe of an alluvial fan (Croft and Gordon, 1968).

In general, groundwater is confined in the reduced continental deposits and reduced older alluvium below and between impermeable lacustrine clays in the vicinity of the Tulare Lake Bed; groundwater is semi-confined in the reduced and some of the oxidized older alluvium; and unconfined in the oxidized older alluvium, the younger alluvium and floodplain deposits (Croft and Gordon, 1968).

Flood-basin deposits underlie the Tulare Lake Bed and the surrounding overflow lands and slough areas at the valley trough. They overlie the lacustrine and marsh deposits and are mainly composed of grey, fossiliferous clay. They are less than 50 ft. thick, and are considered Recent in age. Synclines exist to the north and south of the Tulare Lake Bed.

Lacustrine and paludal deposits, of Pliocene and Pleistocene age, consisting of blue, green, or grey silty clay and fine sand underlie the flood-basin deposits. These deposits extend to around

3,000 ft. in depth in the subsurface beneath parts of the Tulare Lake Bed, cropping out in the Kettleman Hills to the southwest of NASL. Where the equivalent beds crop out in the Kettleman Hills, they were named the Tulare Formation by Anderson (Anderson, 1905), and their origin has been debated (Croft and Gordon, 1968). At least one of the fine-grained deposits beneath the Tulare Lake Bed has been shown to be a distal portion of an alluvial fan , but most of the fine-grained deposits are lacustrine, paludal or deltaic in origin (Sun et al, 1991).

Undifferentiated alluvium, exists to the south of NASL, in a narrow projection from the Kettleman Hills to the Tulare Lake Bed. This formation overlies the lacustrine and paludal deposits that crop out in the Kettleman Hills and is composed of oxidized, poorly sorted, lenticular, gypsiferous clay, silt, sand, and gravel. Because of its small areal extent, this formation is considered unimportant in a hydrologic sense.

In the subsurface of the region surrounding the Tulare Lake Bed, lacustrine and paludal deposits form six extensive tongues that interfinger with the more permeable continental deposits; alluvium, undifferentiated; and older alluvium. These are referred to by Croft and Gordon as the A-, B-, C-, D-, E- and F-clays (Croft and Gordon, 1968) and all of these clay layers are present within the study area. Other zones of clay are found in the area, but are not as aerially extensive, and are not assigned names in other reports.

These clay layers are important hydrogeologically, as they restrict the flow of water, especially vertically. They are also associated with much of the subsidence seen in the area. Of these clays, the F-clay is considered of least hydrogeological importance, whilst the E-, C- and A-clays are most aerially extensive.

F-Clay: The F-clay is found approximately 500 ft. below sea level beneath the area to the south of NASL, where it interfingers with the reduced deposits of the older alluvium within the limits of the Tulare Lake Bed. The layer is characterized as having thin layers of sand between the clay layers, with southward plunging synclines and anticlines (Croft and Gordon, 1968).

E-Clay: The E-clay is one of the largest and well-known of the clay layers in the San Joaquin Valley. In part it is equivalent to the Corcoran Clay member of the Tulare Formation (sometimes referred to as "the Corcoran Clay" in the remainder of this report). It is dark greenish-grey, silty and diatomaceous, often described in well completion reports studied for this report as the "Blue Clay" or "Corcoran clay". In general the E-Clay is 60-120 ft. above the F-Clay. Underlying approximately 3,500 square miles to the west of U.S. Highway 99, the beds were probably deposited in lakes formed by a diastrophism in the Coast Ranges, believed to be in the Pliocene to mid-Pleistocene ages. The average thickness of the clay bed is 75 ft thick, being thickest to the south of NASL near Corcoran and beneath the study area. Warping of the E-Clay is similar to that found in the F-clay below. To the south of the study area, the E-Clay becomes bifurcated and the sand layer between the clay layers thickens. In general the clay deepens from north to south; beneath the Tulare Lake Bed it is found at its greatest depth of 900 ft. bgs. It is also at its thickest at 160 ft. here (Sun et al, 1991).

D-Clay: Croft and Gordon only map this clay unit in a narrow band between Lemoore and Corcoran, where it ranges in thickness between 5 and 20 ft.. To the southeast of NASL, the D-Clay merges with lacustrine and marsh deposits.

C-Clay: The C-Clay is of Pleistocene age and thought to be found from near Mendota to Goose Lake Bed to the south of the study site. It underlies the Valley trough, with thicknesses ranging from 5-45 ft. and depths ranging from 100-330 ft. bgs. A theory suggests this clay was deposited by a lake during a period of glaciation in the Sierra Nevada (Sun et al, 1991). This clay layer is similar in extent to the D-Clay, interfingering with the older alluvium to the south and also to the northeast and probably east of NASL. Generally, the C-Clay is found 250 ft. bgs and is thickest at its southernmost extent (100 ft. near Corcoran) and thinnest at its northernmost extent (10 ft. near Riverdale). This clay layer has a similar shape to the D-, E- and F-Clays, but the amplitude of its deformations are smaller in size.

B-Clay: The B-Clay is similar in aerial extent to the D-Clay, extending from the Tulare Lake Bed in a northerly direction to Lemoore and Corcoran, about 140 ft. bgs, and averaging 15 ft. in thickness. On the edges of this unit, the clay layer merges with the older alluvium, but the unit itself does not seem to be affected by the same warping forces experienced by the lower units.

A-Clay: The A-Clay is of Pleistocene and possibly Holocene age. It is found in the same area as the C-Clay, but all the way down to the Kern Lake bed in the south. In general, the thickness of the A-clay ranges from 5-70 ft. and in depth from less than 10 ft. to around 70 ft.. It is thought the A-Clay was deposited by a lake during the Wisconsin Glaciation period (Sun et al, 1991). The shallowest of all clay tongues, the A-Clay can be found below the younger alluvium at around 40-50 ft. bgs. The thickness of this clay unit ranges from 20-50 ft., and it also appears to be unaffected by the warping forces experienced by lower clay units. The A-Clay occurs mainly near the trough of the valley, and commonly has shallow groundwater pooled on top of it. To the south of the study area, the A-Clay is partially bifurcated and averages about 30-40 ft. in thickness.

Surface fissures are a general concern when land subsidence is induced by groundwater pumping and subsequent subsidence due to compaction of clays. If the vertical distribution and total thickness of clays varies significantly over short lateral distances, land subsidence is highly uneven across the land surface, resulting in extensive surface fissuring, such as that observed at Edwards Air Force Base southeast of the Valley at the Rogers Lake Bed, and at other locations in the Valley (Sneed et al, 2000; Poland and others, 1975). However, despite the significant amount of subsidence observed in study area and especially to the west of the NASL, there is no evidence of past and present surface fissuring at NASL and its associated agricultural lands or in any other area within the study region. This is thought to be the result of the large depth of the bedrock complex and the relatively smoothly varying lateral changes in total clay layer thickness and vertical distribution. To test this hypothesis specifically for the NASL location, we conducted a detailed analysis of well logs to generate a representative geologic cross-section of the NASL study area.

4.5 Site-Specific Geology: Analysis of Well Logs

Three main types of well log were collected for this study, driller's logs (well completion reports filed by drilling contractors - example shown in Figure 18), geologic logs (prepared by geologists or hydrogeologists, also filed as well completion reports (Figure 19)) and geophysical logs. For the construction of a representative site stratigraphy at NASL, only E-logs were used and matched with corresponding well completion reports. For later analysis of the regional aquifer stratigraphy, a more complete set of driller's and geologic logs was digitized into a database. Driller's logs and geologic logs were requested from the CDWR for the entire 35 township study area (Figure 3). Approximately 7,500 well logs were obtained for the study area in digital scan format. Additional geologic logs and driller's logs were scanned and collected from the CDWR in Fresno when E-Logs were collected.

The quality of the stratigraphic information contained in driller's logs is largely dependent on the qualifications of the driller who completed the report in question. A system was needed to grade logs in terms of their usefulness. A modified method developed by Laudon and Belitz (Laudon and Belitz, 1991) was used to accomplish this task. Logs were rated as poor, fair, good or excellent based on the level of detail and suitability of the language used to describe the geologic texture for each depth interval (see Table 11). The best description used in at least one depth interval description set the classification of the log, if the textural information was clearly legible. In some cases scan/photocopy quality or handwriting issues prevented this from being possible and in this case the log was rejected.

DESCRIPTION	RATING
Clay, sand	Poor
Silty clay, fine sand	Fair
Bluish silty clay, brownish-yellow fine sand	Good
Clay, light-olive grey 5Y5/2, silty, laminated; sand, olive-grey 5Y4/1, very fine to fine, some silt	Excellent

Table 11 Rating criteria for driller's and geologic logs

Only 'good' or 'excellent' well logs were selected as suitable for entry into a Microsoft Access database. Logs rated as excellent were almost exclusively geologic logs.

Aerial photos were used to delineate primarily irrigated agricultural areas within the study area. Several areas bordering the Coast Ranges and Kettleman Hills to the west and southwest of the study area contained areas partially covered by rangeland. Well logs within these sections were omitted for entry into the database.

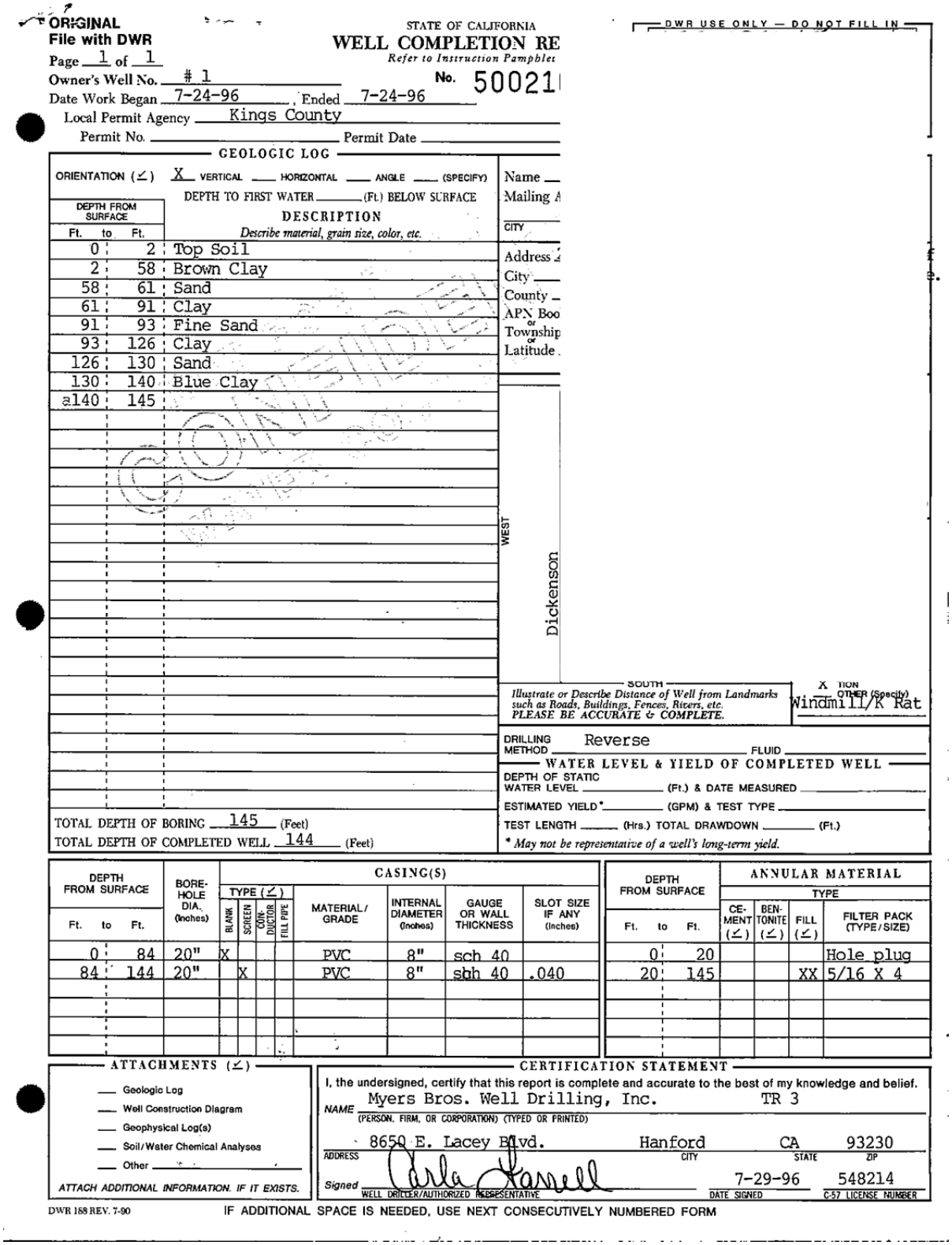

ORIGINAL
File with DWR

STATE OF CALIFORNIA
WELL COMPLETION RE
Refer to Instruction Pamphlet

DWR USE ONLY — DO NOT FILL IN

Page 1 of 1
Owner's Well No. # 1
No. 50021
Date Work Began 7-24-96 Ended 7-24-96
Local Permit Agency Kings County
Permit No. _____ Permit Date _____

GEOLOGIC LOG

ORIENTATION (✓) X VERTICAL ___ HORIZONTAL ___ ANGLE ___ (SPECIFY)
DEPTH TO FIRST WATER _____ (Ft.) BELOW SURFACE

DEPTH FROM SURFACE Ft.	to Ft.	DESCRIPTION *Describe material, grain size, color, etc.*
0	2	Top Soil
2	58	Brown Clay
58	61	Sand
61	91	Clay
91	93	Fine Sand
93	126	Clay
126	130	Sand
130	140	Blue Clay
a140	145	

Name
Mailing A
CITY
Address
City
County
APN Boo
or
Township
or
Latitude

WEST
Dickenson

SOUTH
Illustrate or Describe Distance of Well from Landmarks such as Roads, Buildings, Fences, Rivers, etc. PLEASE BE ACCURATE & COMPLETE.

X TION
___ OTHER (Specify)
Windmill/K Rat

DRILLING METHOD Reverse FLUID _____

WATER LEVEL & YIELD OF COMPLETED WELL

DEPTH OF STATIC WATER LEVEL _____ (Ft.) & DATE MEASURED _____
ESTIMATED YIELD* _____ (GPM) & TEST TYPE _____
TEST LENGTH _____ (Hrs.) TOTAL DRAWDOWN _____ (Ft.)
* *May not be representative of a well's long-term yield.*

TOTAL DEPTH OF BORING 145 (Feet)
TOTAL DEPTH OF COMPLETED WELL 144 (Feet)

DEPTH FROM SURFACE Ft.	to Ft.	BORE-HOLE DIA. (Inches)	CASING(S) TYPE (✓) BLANK	SCREEN	CONDUCTOR	FILL PIPE	MATERIAL/ GRADE	INTERNAL DIAMETER (Inches)	GAUGE OR WALL THICKNESS	SLOT SIZE IF ANY (Inches)
0	84	20"	X				PVC	8"	sch 40	
84	144	20"		X			PVC	8"	sch 40	.040

DEPTH FROM SURFACE Ft.	to Ft.	ANNULAR MATERIAL TYPE CEMENT (✓)	BENTONITE (✓)	FILL (✓)	FILTER PACK (TYPE/SIZE)
0	20				Hole plug
20	145			XX	5/16 X 4

ATTACHMENTS (✓)
___ Geologic Log
___ Well Construction Diagram
___ Geophysical Log(s)
___ Soil/Water Chemical Analyses
___ Other _____
ATTACH ADDITIONAL INFORMATION, IF IT EXISTS.

CERTIFICATION STATEMENT
I, the undersigned, certify that this report is complete and accurate to the best of my knowledge and belief.
NAME Myers Bros. Well Drilling, Inc. TR 3
(PERSON, FIRM, OR CORPORATION) (TYPED OR PRINTED)
ADDRESS 8650 E. Lacey Blvd. CITY Hanford STATE CA ZIP 93230
Signed Carla Farrell
WELL DRILLER/AUTHORIZED REPRESENTATIVE
DATE SIGNED 7-29-96
C-57 LICENSE NUMBER 548214

DWR 188 REV. 7-90
IF ADDITIONAL SPACE IS NEEDED, USE NEXT CONSECUTIVELY NUMBERED FORM

Figure 18 Example well completion report obtained from the CDWR (w/o location info.)

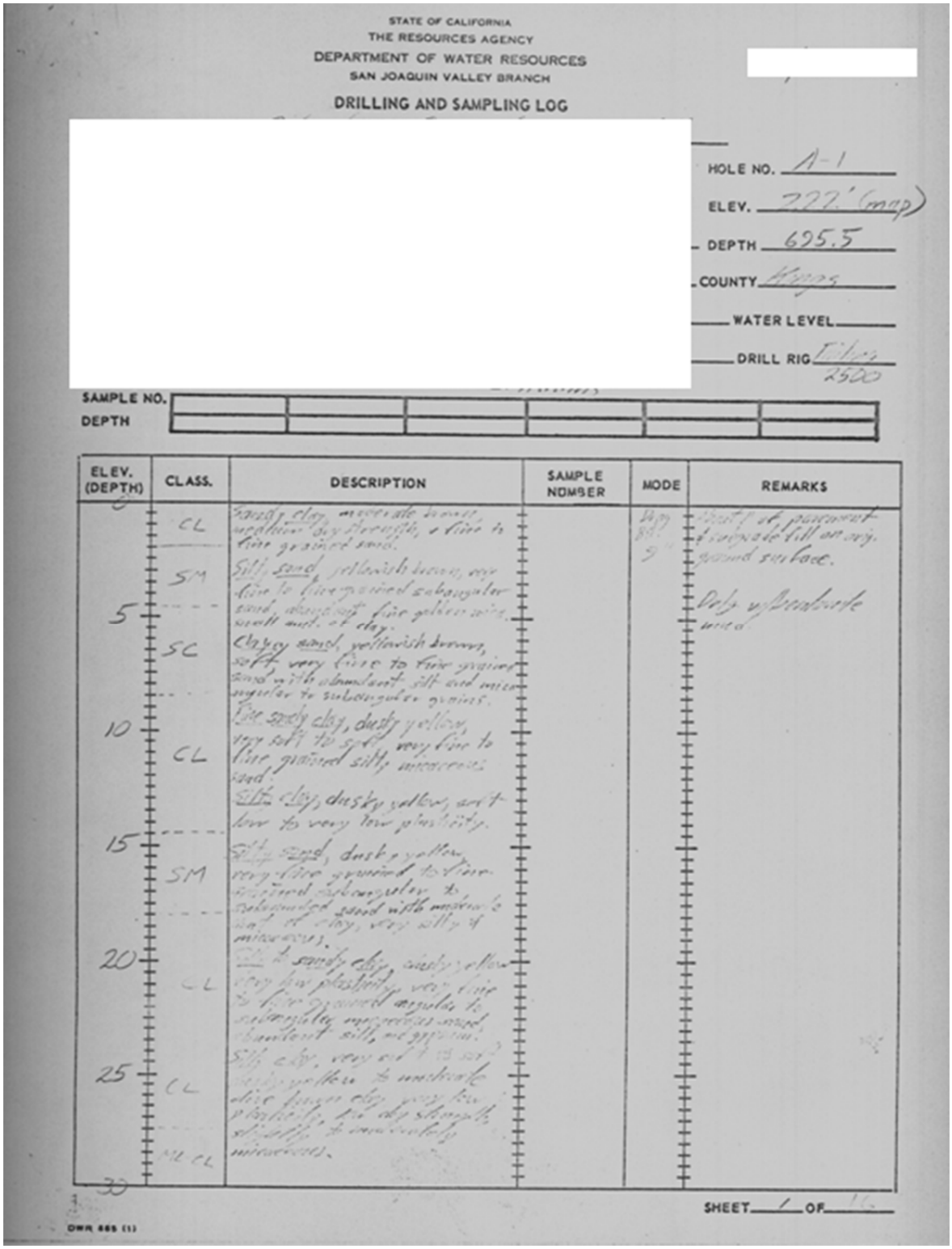

STATE OF CALIFORNIA
THE RESOURCES AGENCY
DEPARTMENT OF WATER RESOURCES
SAN JOAQUIN VALLEY BRANCH

DRILLING AND SAMPLING LOG

HOLE NO. A-1
ELEV. 222' (map)
DEPTH 695.5
COUNTY Kings
WATER LEVEL
DRILL RIG Failing 2500

SAMPLE NO.
DEPTH

ELEV. (DEPTH)	CLASS.	DESCRIPTION	SAMPLE NUMBER	MODE	REMARKS
0	CL	Sandy clay, moderate brown, medium dry strength, slight to fine grained sand.		Auger	Base of pavement & upgrade fill on orig. ground surface.
	SM	Silty sand, yellowish brown, very fine to fine grained subangular sand, abundant fine yellow mica, small amt. of clay.			
5	SC	Clayey sand, yellowish brown, soft, very fine to fine grained sand with abundant silt and micaceous to subangular grains.			Only graduate used.
10	CL	Fine sandy clay, dusky yellow, very soft to soft, very fine to fine grained silty micaceous sand.			
		Silty clay, dusky yellow, soft, low to very low plasticity.			
15	SM	Silty sand, dusky yellow, very fine grained to fine grained subangular to subrounded sand with moderate amt. of clay, very silty & micaceous.			
20	CL	Silty sandy clay, dusky yellow, very low plasticity, very fine to fine grained angular to subangular micaceous sand, abundant silt, micaceous.			
25	CL	Silty clay, very soft to soft, dusky yellow to moderate olive brown clay, very low plasticity, dry strength, slightly to moderately micaceous.			
30	ML CL				

SHEET 1 OF 11

DWR 668 (1)

Figure 19 Example geologic log obtained from the CDWR.

The database template used for well log entry was modified from a U.S.G.S. version. The resulting database was designed so that all available pertinent information available in well logs for each selected well could be entered. Of primary concern were information relating to stratigraphy and casing. Casing type, casing depth intervals and casing diameter, along with perforated (screened) intervals of casings were entered. Other pertinent well information, such as well location, the drilling company responsible for completing the well, whether an E-Log was made for the well, and total well depth were also recorded, if available.

For textural analysis at NASL, we relied primarily on electric logs (E-logs). Based on careful interpretation of these E-logs, two geologic cross-sections for the four townships encompassing NASL and also an idealized stratigraphy for a 1-D subsidence model were developed.

An E-log is an example of a geophysical log. Geophysical logs include E-logs, caliper logs, gamma logs and neutron logs amongst other types. E-logs were the only geophysical logs that were interpreted and used for this study, with the resistivity and spontaneous potential curves proving useful for delineation of stratigraphy (Figure 20).

Most of the E-logs obtained consisted of curves from two different electrical measurements, spontaneous potential and resistivity. Resistivity measurements are most often made using a so-called short normal resistivity sensor setup. Long normal and single point resistivity are due to alternative sensor arrangements also encountered in resistivity logs.

Geophysical logs for the NASL study area were filed at the CDWR office in Fresno, California, in their original paper format. The selected logs were scanned with a large format scanner. Whenever possible, each E-Log was scanned as a single page in Portable Document Format (pdf). This was completed between March 24th and 26th, 2010. All available E-logs were scanned regardless of quality/legibility and brought to UC Davis for processing and filing. Poor quality or illegible E-logs were rejected.

For effective E-log interpretation, geologic logs were paired with their associated E-logs and used as a "calibration target". The short normal resistivity curve was used (whenever available), for more detailed delineation of aquifer materials (to differentiate coarser-grained water-bearing materials from laterally discontinuous aquitard materials). The long normal resistivity curve was used for identifying major textural layers such as regionally continuous clay layers (A-F clays) and major water-bearing zones. In general, geologic materials become more resistive with depth, which was accounted for in the interpretation. Interpretation of E-logs is often qualitative rather than quantitative, with sharp and spiky deflections of the resistivity curve to the left (low resistivity measurements) representative of thin aquitards and sustained deflections to the left indicative of thicker confining units. As a rule of thumb, resistivity values of 10 ohm-m or less were found to be indicative of clayey (aquitard-type) materials (Figure 20).

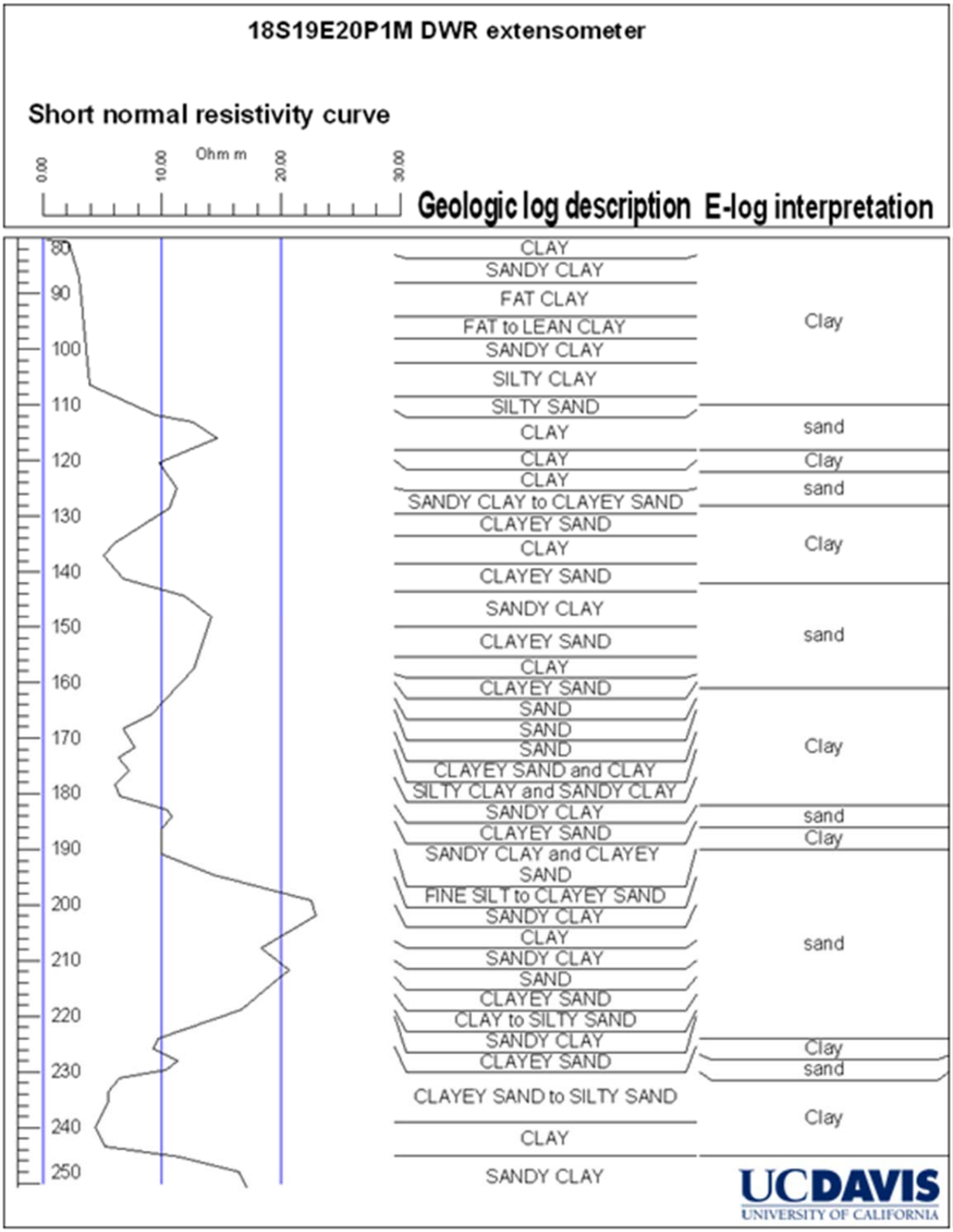

Figure 20 E-log interpretation.

To construct a geologic cross-section for the four townships encompassing NASL, a suitable subset of E-logs and geologic logs were identified and chosen. These townships were 18S-18E, 18S-19E, 19S-18E and 19S-19E. Chosen E-logs were required to be fully locatable on a map; however this information was rarely obtainable from the E-log itself. Driller's logs often contain location information in the form of sketches, descriptions with respect to local infrastructure or latitude-longitude coordinates. In some cases pairing E-logs with driller's logs proved problematic due to lack of pertinent identifying information. Often the full state well number was not included on either the E-log or driller's log (e.g. 18S19E rather than 18S19E20P001M). In these cases CDWR's Integrated Water Resources Information System (IWRIS) database (CDWR, 2010) and Google Earth© software by Google Inc. were used to geolocate the log.

Within the four township study area, a total of 42 E-logs were chosen (Figure 21). Their locations were digitally recorded as a GIS layer. Two additional geographic data layers were created, a topographic map and a digital elevation model map of the area. The topographic map was created from a cropped selection of digital raster graphics (DRGs) obtained from the Cal-Atlas geospatial clearinghouse website (Cal-Atlas website, 2010). The DEM GIS layer was obtained from the U.S. Geological Survey National Elevation Dataset (USGS NED) website (USGS seamless website, 2010). The DEM with the best resolution available (⅓ arc second, 10m resolution) was chosen. The 'Project Raster' tool in ArcMap 9.3 was then used to assign each well an elevation on the cross-section. Didger 3 by Golden Software was used to digitize the E-logs for representation in the geologic cross-sections.

Cross-sections were created in east to west and northeast to southwest directions such that cross-sections intersected the largest concentration of chosen wells (Figure 21). Wells represented in an individual cross-section included all those wells located within 0.5 miles of the cross-section lines. The selected wells were projected on to the line at the nearest orthogonal point. The cross-section lines designated A-A' and B-B' include 10 and 9 wells, respectively.

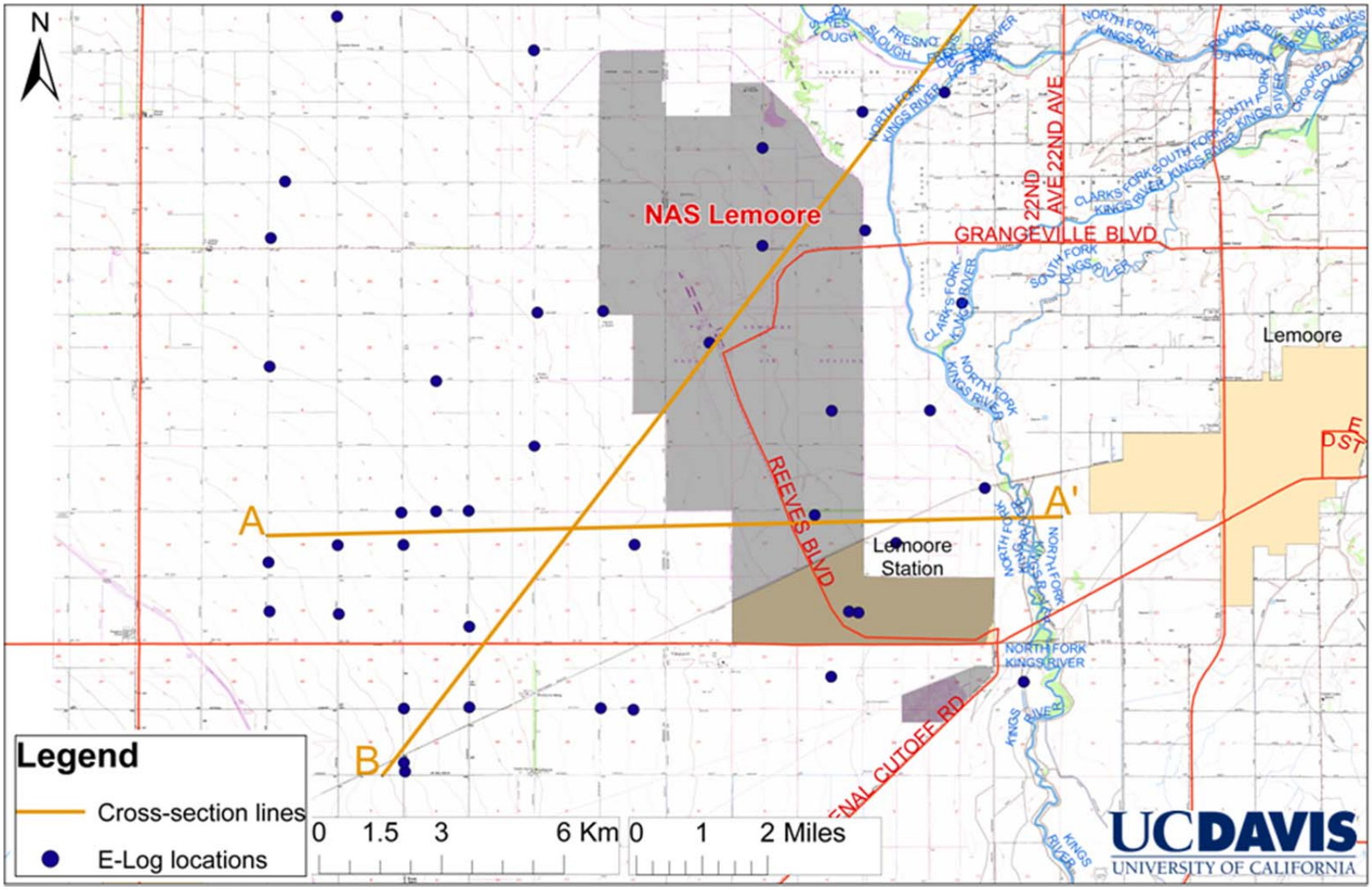

Figure 21 NASL geologic cross-section location (orange lines) and location of E-logs selected for analysis (blue dots).

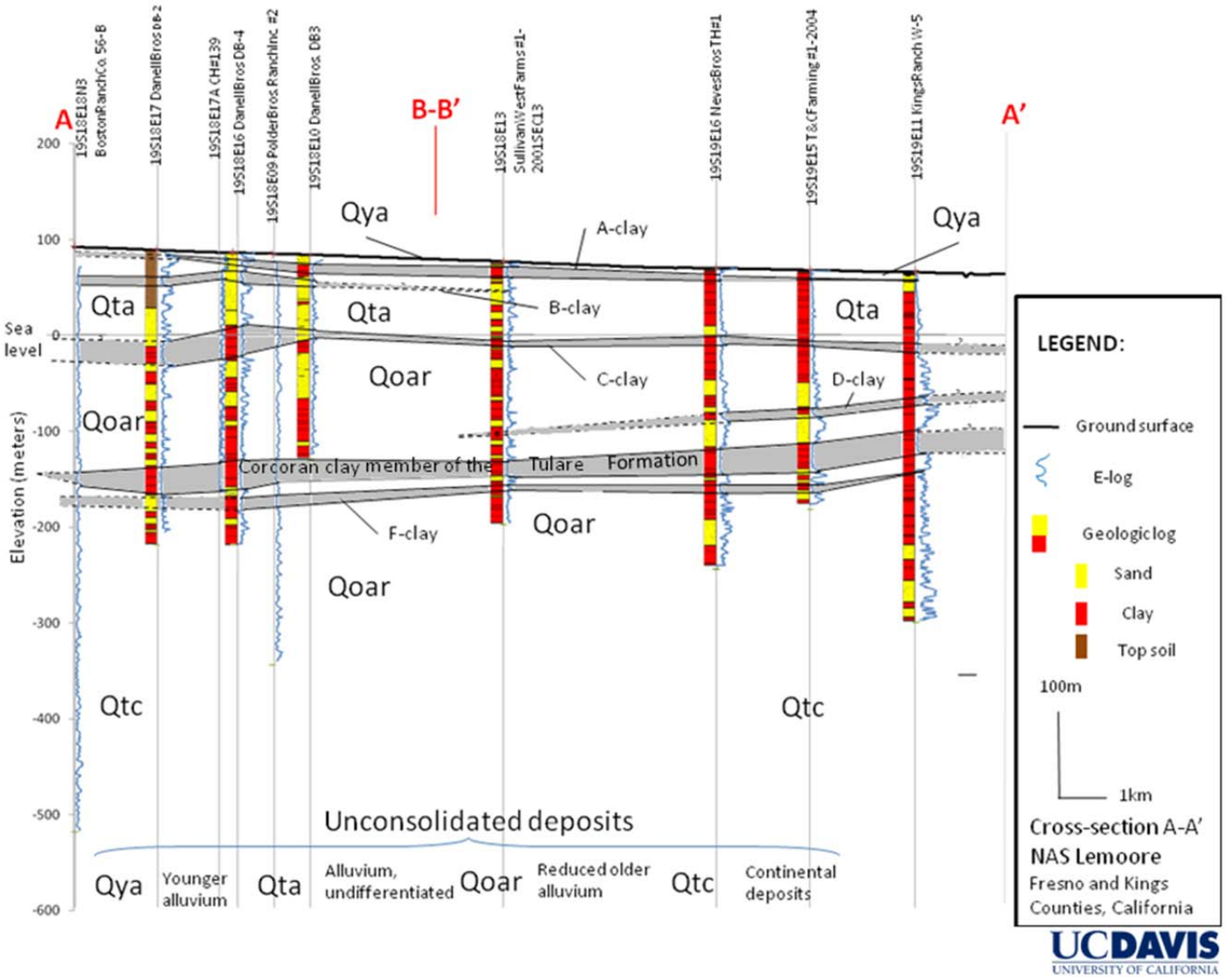

Figure 22 Geologic cross-section A-A' (lines dashed where inferred).

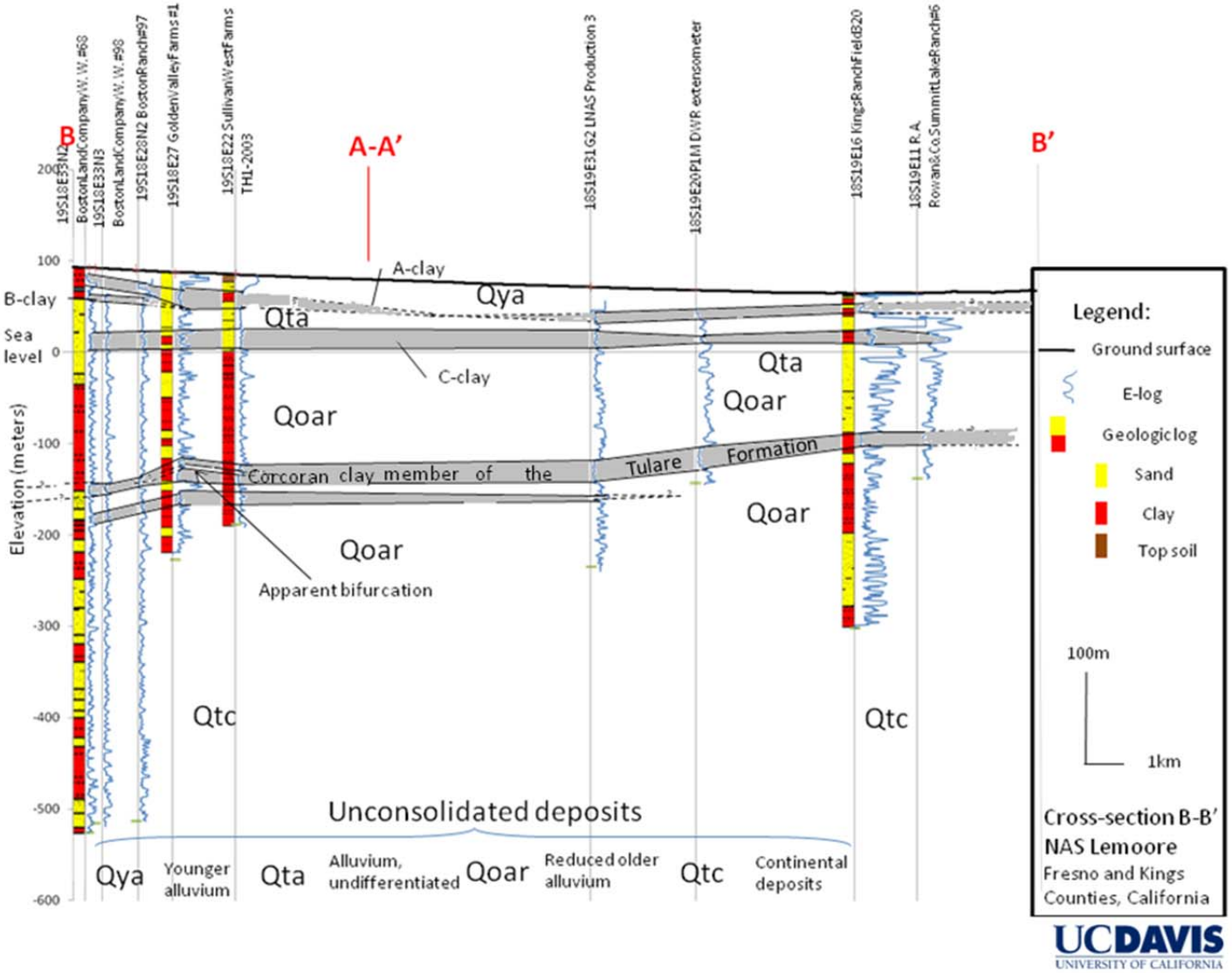

Figure 23 Geologic cross-section B-B' (lines dashed where inferred).

The prominent clay layers (Corcoran-, C- and A-Clays) and major geologic formations named in other reports (Croft, 1969; and Croft and Gordon, 1968) are represented in the cross-sections in Figure 22 and Figure 23. Contoured plots for the base of the Corcoran- (E-), C- and A-Clays for a large section of the Valley are included in Plates 4, 5 and 6 of Croft, 1969, respectively; and the major geologic formations are included in a geologic cross-section that passes in close proximity to the eastern boundary of NASL, from Plate 5 of Croft and Gordon, 1968. The method to complete the cross-sections in Figure 22 and Figure 23 was to note low deflections within more than one E-log resistivity curves at similar depths, and to link them with clay layer A-F.

As can be seen from Figure 22 and Figure **23**, the Corcoran (E-) clay is continuous beneath all four study townships, at an average depth of approximately 650 ft. bgs. The Corcoran clay is by far the most prominent clay layer in terms of extent and thickness. The thickness of this unit averages 80 ft., but can be as thick as 100 ft., mainly to the southwest of NASL; and as thin as 60 ft. in areas to the east of NASL. A small vertical bifurcation within the Corcoran clay appears to exist within a small area beneath the Golden Valley Farms/Boston Ranch area.

The F-clay is continuous beneath most of the cross-section study area, and follows a similar pattern of warping to the Corcoran Clay, the bottom boundary of which can be found approximately 30-40 ft. above the top boundary of the F-clay. The F-clay is hard to delineate, or absent, in the northeast areas of the cross-section study area. The F-clay is a great deal thinner than the Corcoran clay, averaging approximately 20-30 ft. in thickness.

A thin discontinuous clay lens can be found beneath the southern portions of the NASL runway area and stretching to the east. This is assumed to be the full extent of the D-clay beneath this area. The average depth of the D-clay is approximately 500 ft bgs with an average thickness of 20-30 ft..

The C-clay is continuous throughout the four-township study area, generally at a depth of sea-level, or approximately 230-260 ft. bgs. It is thickest in the southwest of the study area, at approximately 60 ft., and quickly thins to the northerly and easterly sub-areas. The C-clay is separated from the D- and Corcoran clays by a thick layer of aquifer materials of mainly reduced older alluvium.

The B-clay appears to be semi-continuous, generally appearing absent in northeastern parts of the study area. Where it exists, it is approximately 100 ft. bgs and approximately 20 ft. in thickness.

Like the Corcoran clay, the A-clay is known from other reports to exist below most of the NASL area. It is the shallowest of the named clay layers, and appears at depths of approximately 20-100 ft. bgs. The A-clay separates the unconfined aquifer from lower confined aquifers where it exists, creating perched aquifers which are exploited for groundwater resources.

4.6 Regional Groundwater Flow and Occurrence

Under natural conditions, the structural trough of the Central Valley is the principal controlling structure of groundwater movement and occurrence in the entire Valley. In general, higher heads on the flanks of the Valley (and hence the flanks of the trough) cause groundwater to flow to the lower heads found in the Valley trough. Heads are generally higher at the flanks due to natural recharge from creeks and rivers here, and the confining structures are generally shallower here. Once groundwater reaches the Valley trough, it generally discharged to local streams or lakes. However, due to groundwater development, local flow patterns differ from these general rules, and in some places flow is towards pumping depressions.

To the west and south of the study area, groundwater is restricted by the anticlinal folds of Anticline Ridge, the Guijarral Hills and the Kettleman Hills. These are known to restrict groundwater flow.

Post-Eocene continental deposits and rocks contain most of the fresh water in the Central Valley, cropping out at regular intervals throughout the San Joaquin Valley. In the majority of instances, these rocks and deposits overlie or contain saline water that has migrated from the marine rocks. In this report , the base of fresh groundwater is defined as having a conductance of 3,000 micromhos per centimeter (approximately 2,000 milligrams per liter dissolved solids) (Page, 1973).

The Etchegoin Formation is greater than 3,000 ft. below the surface beneath the Valley floor and varies from tens of ft. to greater than 2,000 ft.. A few deep wells derive fresh water from this formation, but due to its depth it is not considered a major aquifer in the area.

Whilst the continental rocks and deposits to the south of the Tulare Lake Bed contain saline water, those to the north of the lake bed contain mostly fresh water. In places throughout the Valley, the saline water has been flushed from the rocks and deposits that bear it, and have been replaced with fresh water.

In a most of the San Joaquin Valley, the fresh groundwater is mostly contained within the principally unconsolidated Pliocene to Holocene age continental deposits. These deposits extend to depths ranging from approximately 100 ft. to depths greater than 3,500 ft. bgs, but are believed to extend to approximately 3,000 ft. in the study area (Page, 1973). In the study area, the base of fresh water reflects the shape of the synclines to the north and south of the Tulare Lake Bed.

The E-clay is considered to be the principal confining bed in the Tulare Lake Basin, but confined aquifers do exist above the E-clay as well within it in the study area. The groundwater quality beneath the E-Clay is generally better than above, with lower Total Dissolved Solids (TDS) and salts encountered.

Within the study area, groundwater is pumped from the unconfined aquifer above the A-Clay as well as from the confined aquifers between the A- and E-Clays. Groundwater is also pumped from below the E-Clay.

To the south of NASL, in the Lakeside subarea of the Westlands Water District, there is no hypo-Corcoran aquifer system productive enough to supply large-capacity irrigation wells. Substantial groundwater supplies can be found to the north of this subarea, below a depth of 1,200 ft.. The base of freshwater is believed to be 2,000-2,100 ft. bgs here, limiting the depth to which large-capacity water supply wells can be drilled. In the southern part of this subarea, the Corcoran Clay has little hydrologic significance, as clays and other fine-grained deposits from the former Tulare Lake Bed dominate. The depth to the base of freshwater beneath most of this subarea generally ranges from 2,000-2,100 ft. bgs.

Northwest of NASL, in the Five Points subarea of the WWD, both aquifers (above and below the Corcoran Clay) are tapped in most of the subarea. In the southwest of this subarea, substantial clay deposits are present in the Coast Range deposits above and below the Corcoran Clay, limiting productivity of wells in the vicinity. Brackish water is present in the Five Points subarea, above and below the freshwater. The base of freshwater varies from about 2,200 ft. to below 3,000 ft. bgs in this subarea.

Sand dunes are present to the northeast of the study area across the Kings River, but are not an important source of groundwater, as they lie above the water table.

A review of available hydrogeologic literature for the 'Westside' of the Valley concludes that two main basic conceptualizations for aquifer system structure beneath the NASL site and surrounding areas persist. A majority of the reports divide the production aquifers into two main water-bearing zones: referred to as the 'upper' and 'deep' aquifers in this report (Figure 24). The upper aquifer was assumed to confine with depth due to the locally extensive horizontal clay layers present within this aquifer system. Below the regionally extensive Corcoran clay layer, the deep aquifer is found. The deepest boundary of the aquifer system is delineated by an idealized groundwater quality boundary. Water with a specific conductivity greater than 3,000 µmhos/cm is considered too low a quality for most applications, and this value is commonly exceeded below depths of 2,500-3,000 ft bgs.

Other reports use the same main division of aquifer materials, but with the upper aquifer split into two separate aquifers, with localized perched aquifers existing above the A-clay confining unit and a 'middle' or 'intermediate' aquifer between the A-clay and the Corcoran clay (Figure 25).

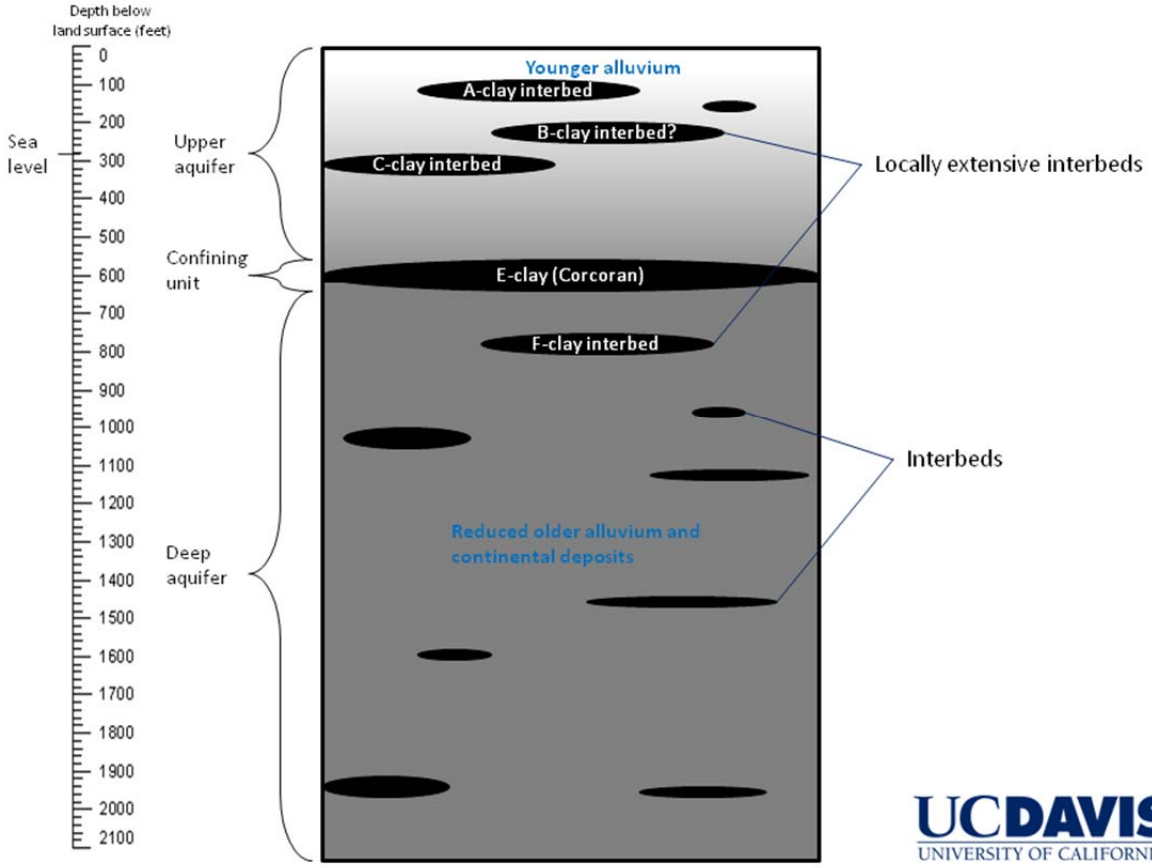

Figure 24 Simplified study area stratigraphy as presented in several available reports showing upper aquifer that confines with depth due to the A-C-Clay layers, and the deep aquifer.

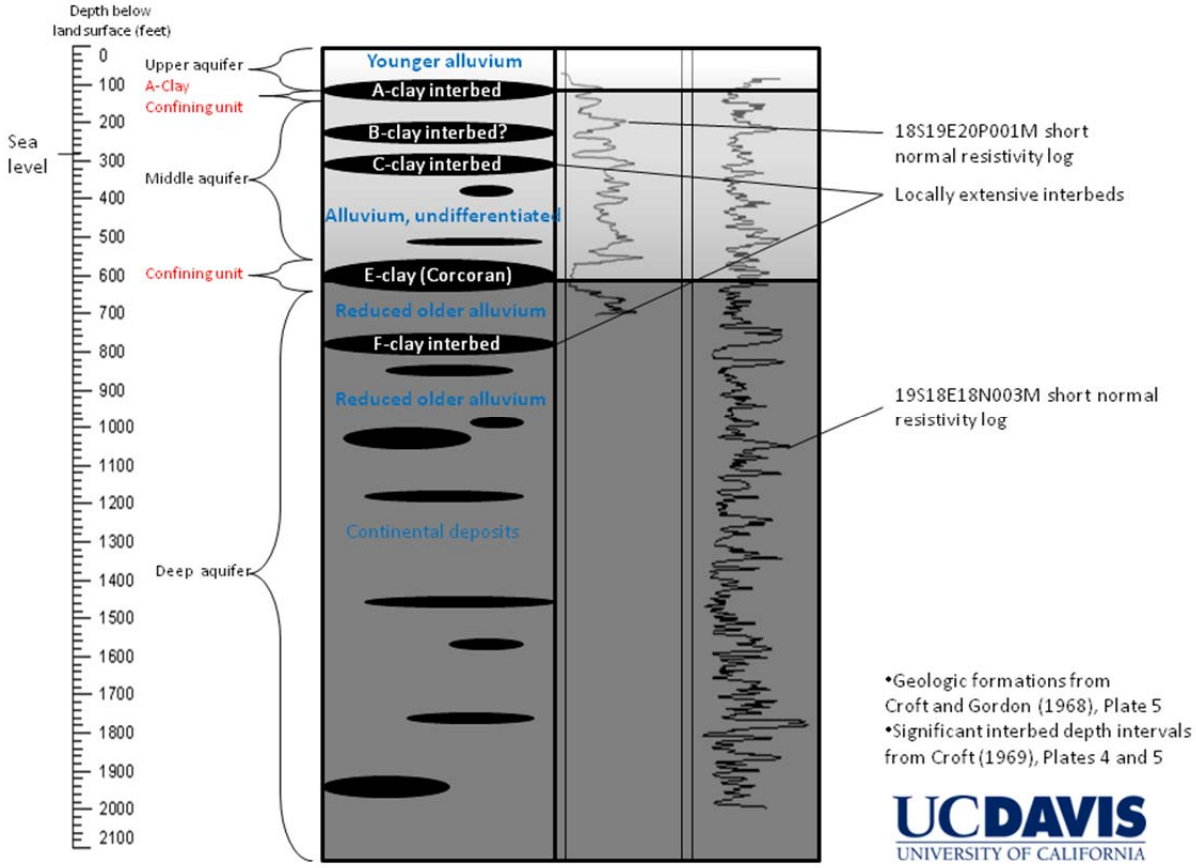

Figure 25 Detailed study area stratigraphy interpreted from site-specific E-Logs showing upper aquifer above the A-clay confining unit and a middle aquifer that confines with depth due to the B- and C-Clay layers, and the deep aquifer.

4.7 Local Groundwater Elevation and Groundwater Flow

The NASL property is situated within two separate administrative regions for which groundwater elevation contour maps are available: the Tulare Lake Region as defined by the California Department of Water Resources (CDWR), and the Westlands Water District (WWD). The Tulare Lake Region covers the lower two-thirds of the San Joaquin Valley, including the Kings, Westside, Pleasant Valley, Kaweah, Tulare Lake, Tule, Kern County, Panoche Valley, Kern River Valley, Walker Basin Creek Valley, Cummings Valley, Tehachapi Valley West, Castac Lake Valley, Vallecitos Creek Valley, Brite Valley, Cuddy Canyon Valley, Cuddy Ranch Area, Cuddy Valley and Mil Potrero Area sub-basins. Large-scale contoured groundwater elevation maps are available for the Tulare Lake Region. As described earlier in this report, the study area lies at the triple-junction of the 'Westside', 'Kings' and 'Tulare Lake' groundwater sub-basins, contained within the Tulare Lake Region (Figure 2). Maps for the Tulare Lake Region and the three

groundwater sub-basins of concern are available for dates as far back as 1958 at the CDWR website (CDWR website, 2010) (see Table 12). All groundwater elevation contour maps for these areas were downloaded from the CDWR website and are included in Appendix E. All maps provided by the CDWR are completed using data collected in Spring (usually January-March) (personal communication, Mike McGinnis, CDWR Fresno office) and are only available for the hypo-Corcoran aquifer system.

Contoured groundwater elevation maps are also available for the WWD and are available at the WWD website (WWD website, 2010) (Table 12). These maps are available for dates between 1993 and the present and are included in Appendix A. Maps for this area are divided for three aquifer systems: for wells screened in the shallow perched aquifers and deeper wells screened in aquifers referred to as the 'upper' and 'lower' aquifers (above and below the Corcoran clay confining layer). These three aquifer systems are referred to as the 'upper', 'middle' and 'deep' aquifers respectively in this report.

CDWR maps provided a regional overview of groundwater flow over areas much larger than the NASL study area, but lacked the small-scale detail needed for identifying groundwater flows at NASL. They were also available only for the upper, unconfined to semi-confined aquifer. Examples for the Kings, Westside and Tulare Lake basins are shown in Figure 26, Figure 27 and Figure 28. The WWD maps provided better resolution, but for a smaller time period. Because of the position of NASL within the WWD, coverage of the study area was often not complete. In light of these factors, additional maps of contoured groundwater elevation were completed with available data from the CDWR; with better coverage, covering a larger time-frame and with better resolution.

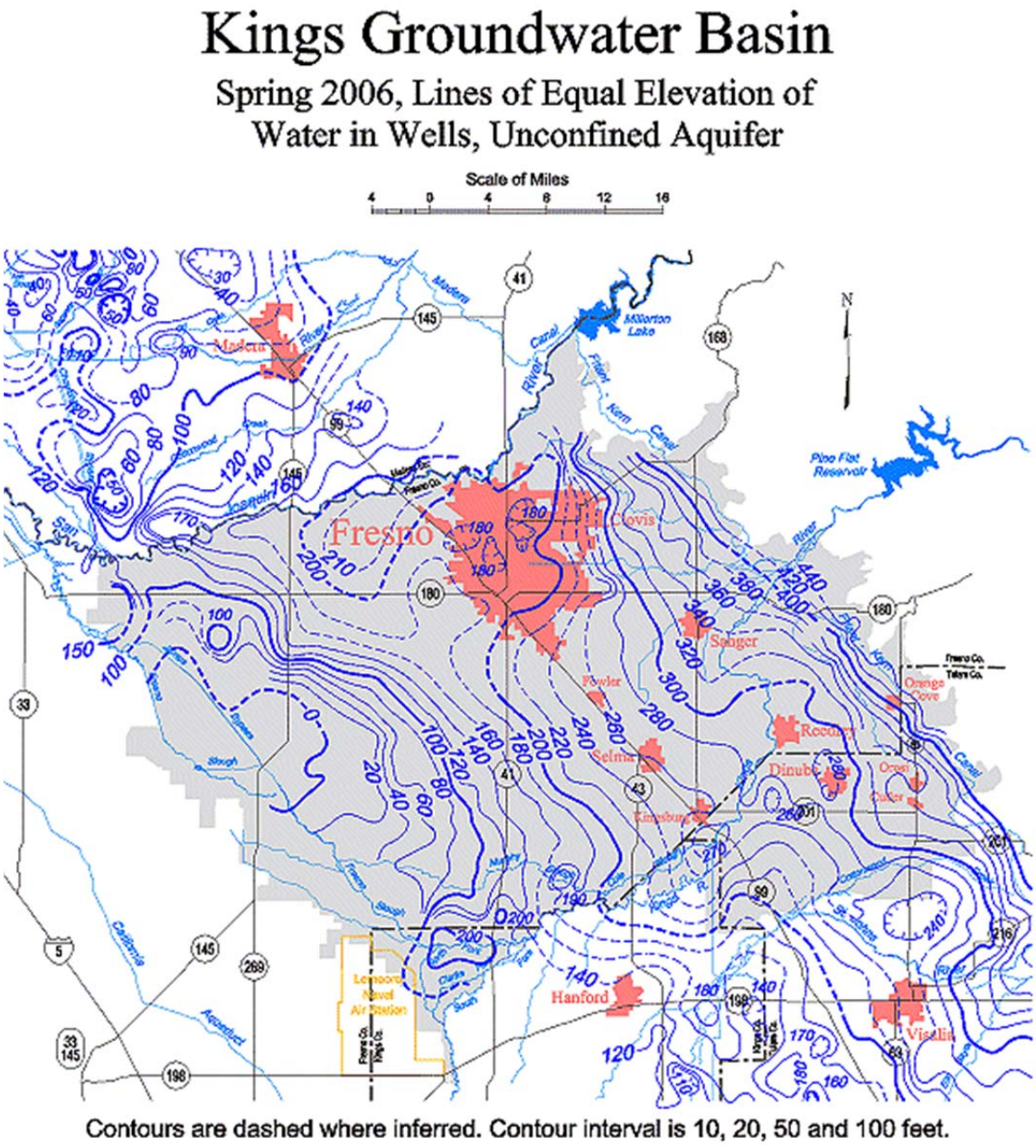

Figure 26 Latest CDWR groundwater contour map Kings groundwater basin (CDWR website, 2010).

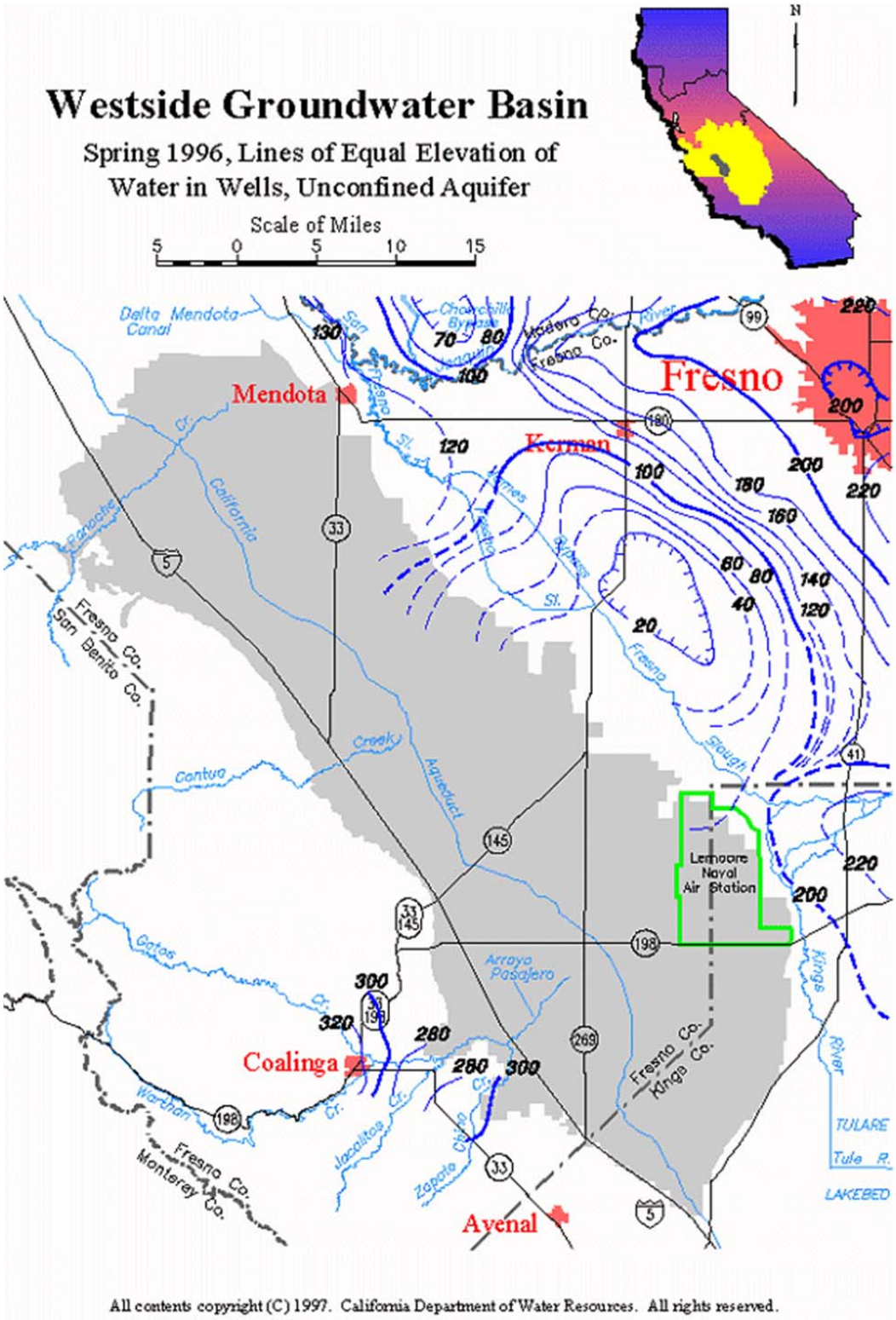

Figure 27 Latest CDWR groundwater contour map for Westside groundwater basin (CDWR website, 2010).

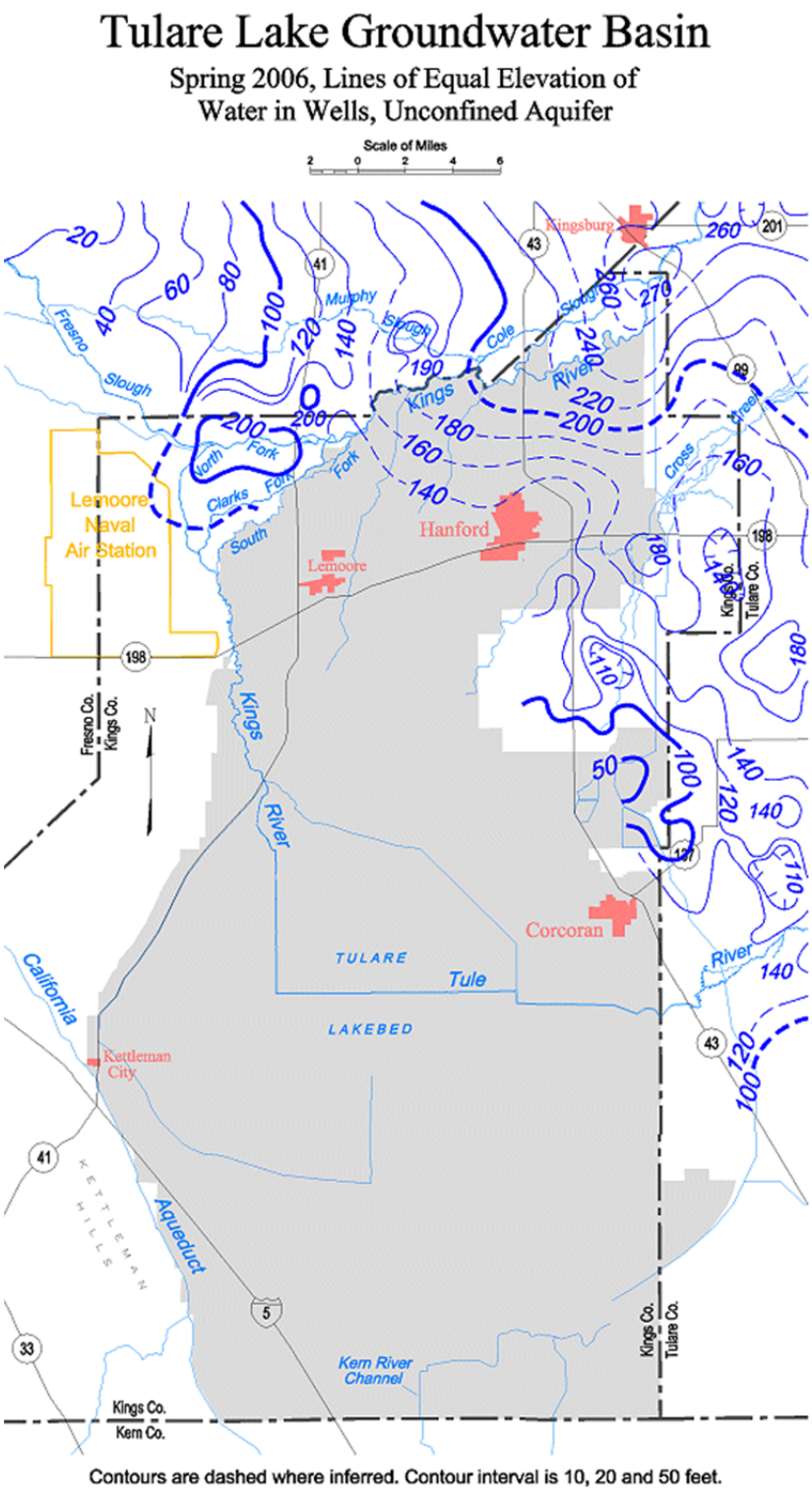

Figure 28 Latest CDWR groundwater contour map for Tulare Lake groundwater basin (CDWR website, 2010).

REGION [CDWR NUMBER IF APPLICABLE]	AQUIFER	DATE FROM	DATE TO	NUMBER OF MAPS	SOURCE
San Joaquin River and Tulare Lake Basin	Unconfined	1952	2008	49	CA DWR Website
Kings [5-22.08]	Unconfined	1958	2006	24	CA DWR Website
Westside [5-22.09]	Unconfined	1996	1996	1	CA DWR Website
Tulare Lake [5-22.12]	Unconfined	1958	2006	24	CA DWR Website
WWD	Shallow	1993	2009	32	WWD Website
WWD	Unconfined	1994	2009	16	WWD Website
WWD	Confined	1993	2009	17	WWD Website
WWD	Confined	1956	1993	3	Schmidt, 2009

Table 12 Availability and coverage of regional contoured groundwater elevation maps

Individual groundwater level records were retrieved from the CDWR water data library (WDL) website (CDWR website, 2010). All records for the 35 townships in the study area (Figure 3) were retrieved into Microsoft Excel spreadsheets. Data obtained include water level measurement date, and associated water and ground surface elevations (Figure 29). Depth to water was measured from a reference point chosen for its permanence (such as the top of the well casing). Ground surface elevation was usually measured by interpolation using U.S. Geological Survey (USGS) 7.5-minute topographic maps, but in a few cases was determined by surveying methods. Some water level elevation measurements were deemed questionable by the field technician, and in some cases no measurements were taken. In these cases, reasons were given in the form of questionable measurement and no measurement codes (QMCs and NMCs respectively) (Table 13) or a reason was given in the comments field. This field was used to eliminate inconsistent data. Location data for each well was provided in latitude-longitude coordinates and often in UTM coordinates as well. Since the groundwater level data was collected by multiple government agencies, the datum used for well locations was not always consistent. The most common datum used was North American Datum of 1927 (NAD27), but in some cases North American Datum of 1983 (NAD83) was used. To convert location data to a consistent datum the North American Datum Conversion Utility (NADCON) developed by the National Geodetic Survey (NGS) was used. This location data was used to compile a Geographic Information System (GIS) map showing locations of wells within the study area.

Information that was needed to complete contoured maps of groundwater elevation (State Well Number, groundwater elevation and well location) was obtained from the individual records and used to compile all records into a database (Microsoft Access). Years were chosen between 1956 and the present, with the aim of completing contour maps in approximately five year intervals (depending on data availability and precipitation scenario). Spring water levels were chosen, as little groundwater pumping takes place at this time of year and groundwater levels are generally at their highest due to wet season groundwater recharge. For the purposes of this report, Spring is defined as January, February and March (after communication with Mike McGinnis at CDWR, Fresno office).

QUESTIONABLE MEASUREMENT CODES (QMCS)		NO MEASUREMENT CODES (NMCS)	
Code	**Definition**	**Code**	**Definition**
0	Caved or deepened	0	Discontinued
1	Pumping	1	Pumping
2	Nearby pump operating	2	Pumphouse locked
3	Casing leaking or wet	3	Tape hung up
4	Pumped recently	4	Cannot get tape in casing
5	Air or pressure gauge measurement	5	Unable to locate well
6	Other	6	Well destroyed
7	Recharge operation at near well	7	Special
8	Oil in casing	8	Casing leaking or wet
9	Acoustical sounder measurement	9	Temporarily inaccessible
		D	Dry well
		F	Flowing well

Table 13 Questionable measurement and no measurement codes.

State Well Number	Measurement Date	RP Elevation	GS Elevation	RPWS	WSE	GSWS	QM Code	NM Code	Agency	Comment
18S19E05K001M	5/6/1961	210	209	123.4	86.6	122.4			5000	
18S19E05K001M	3/27/1962	210	209	115	95	114			5050	
18S19E05K001M	12/19/1963	210	209					2	5050	

Well Coordinate Information

Projection	Datum	Easting	Northing	Units	Zone
UTM	NAD27	237204	4031394	metres decimal	11
LL	NAD27	119.93	36.3936	degrees	

Well Use: Undetermined

Figure 29 Example groundwater level record (well 18S19E05K001M).

This time period is an operational idealization of Spring, as the climate is unpredictable from year to year and farmer's irrigation practices vary with the climate and range of crops grown. Years for which maps were drawn were chosen based on the number and coverage of data points. 'Good' years were chosen if there were more data points covering a larger portion of the study area than preceding and succeeding years. Data availability over time was variable for wells in the study area. A proportion of the wells had more or less continuous coverage over large spans of time, whereas others had sporadic data coverage. Information regarding perforated (screened) intervals of wells was extracted from well completion reports.

To select wells with water level data that represent the deep and intermediate aquifers, the well water level records needed to be matched to well logs. Matching well logs to associated groundwater elevation data records was not always a straightforward process as driller's logs often do not state the full state well number. Water elevation data records, however, always contain a full state well number (e.g. '16S17E36P001M') in comparison to a typically incomplete driller's log entry that may abbreviate the state well number to '16S17E' or '16S17E36'. Where well water level data could not be matched with well logs that identified screen depth, a manual procedure for selecting wells representing the deep and intermediate portion of the aquifer was applied: Utilizing all data, contour maps were completed; then, obvious spikes (localized high water levels) and deep depressions (localized low water levels) that were not consistent with surrounding data points were eliminated. This method was in line with methods used by CDWR personnel when completing contour maps (verbal communication, Mike McGinnis CDWR).

ArcMap © software by ESRI was applied to complete contoured maps of groundwater elevation. A total of 10 groundwater elevation contour maps were created from CDWR data between the years of 1956 and 2009. Data from dates prior to 1956 were generally too sparse to complete meaningful contour maps and time intervals between the contour maps that were completed varied from three to seven years. Examples were chosen to be representative of wet, normal (average), and dry years as well as conditions representative of water levels both before and after surface water deliveries became available to WWD in 1968. Drought periods were defined by comparing average runoff from the major rivers in the San Joaquin Valley. The average runoff from the major San Joaquin Valley rivers (Stanislaus, Tuolomne, Merced and San Joaquin) is 6 MAF. During the course of the 20th century eight major droughts have occurred with those over the last half century being the 1959-1961, 1976-1977, 1987-1992, and 2007-2009 drought periods (Figure 30).

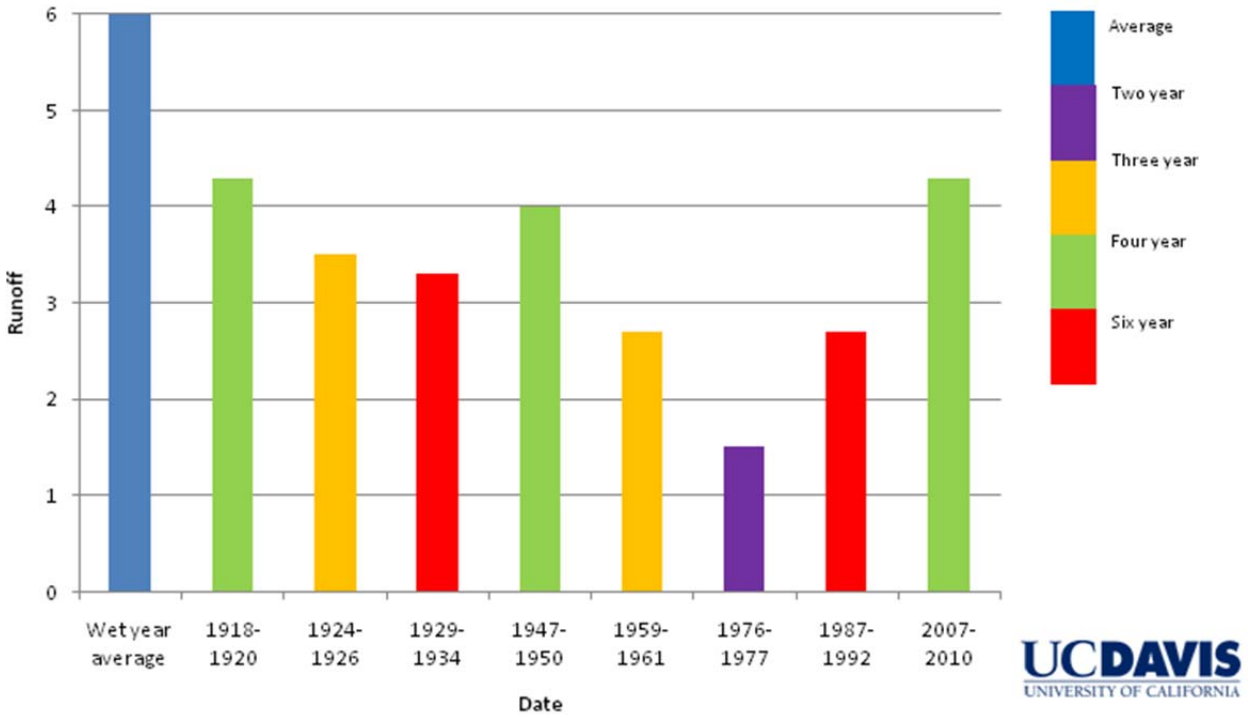

Figure 30 Average annual runoff [in million AF per year] from the Stanislaus, Tuolomne, Merced and San Joaquin Rivers. Shown are a typical average year (left bar) and several drought periods of varying lengths. The major drought periods during the last half century were 1959-1961, 1976-1977, 1987-1992, and 2007-2010.

The following provides an interpretation of two sets of water level contour maps: three historic water level maps available from WWD, either directly from their website or through the reports of Kenneth D. Schmidt and Associates (2009); and the water level maps constructed from CDWR data as described above.

Interpretation of Westlands Water District Groundwater Level Maps of the Lower Aquifer System

In 1951, the average hydraulic gradient along the entire inflow boundary to the WWD, on which NASL lies, was estimated to be 18 ft. per mile in a northeasterly direction (Schmidt, 2009).

A study by Davis and Poland in 1957 (Davis and Poland, 1957) estimated that approximately 80% of groundwater pumpage in the Westlands Water District was from the lower aquifer.

A subset of the WWD groundwater elevation contour maps representing a variety of scenarios, and listed in Table 12 were analyzed. Additional groundwater elevation contour maps that were not analyzed, are appended. In addition, several maps listed as available on the website, were unavailable for various reasons.

A groundwater contour map from December 1965 (Figure 31) represented a period indicative of the heaviest pumping within the study area. The map shows groundwater elevations varying from 25 ft. amsl to sea level (0 ft. amsl) across NASL, with a cone of depression centered approximately 8-10 miles to the southwest of NASL where water levels are less than -200 ft. amsl, and another cone of depression (sink) centered approximately 20 miles to the northwest of NASL with water levels as deep as -300 ft. amsl. Water from the Los Gatos Creek passing through the Pasajero Gap to the west of Huron and directly south of the sink mentioned above, acted as a local recharge point for the area.

A groundwater contour map from December 1986 (Figure 32) showed a partial recovery in regional groundwater levels, largely attributed to a decrease in groundwater pumping and an increase of surface water deliveries from the San Luis Canal. Groundwater elevations directly to the north of NASL are approximately 100 ft (bgs) (100 ft amsl), with groundwater flow to three sinks to the north and west of NASL. A small sink exists to the north in the Five Points subarea of the WWD, where groundwater elevations are -50 ft. amsl; another sink still exists to the north of the Pasajero Gap recharge area, where water elevations have recovered to -50 ft. amsl. At this time, the cone of depression to the southwest of NASL has moved further west (5-10 miles southwest of the City of Huron), with groundwater elevations recovering to greater than sea level.

The year 1993 followed the prolonged drought from 1987-92 in the Valley. A groundwater contour map from November-December 1993 (Figure 33) was chosen and studied as representative of the deeper water elevations found following drought conditions. Groundwater flows into the WWD from the northeast, to sinks to the southwest and northwest of NASL. Groundwater elevations at NASL are generally between sea level and greater than 20 ft. amsl, whilst elevations at the two sinks are -120 and -140 ft. amsl, respectively. The Pasajero Gap recharge area is greater in extent compared to previous contour map studies, and is still the major recharge area to the west of NASL, with groundwater levels of -40 ft amsl.

An important recharge area for the aquifer system beneath the study area is beneath the Kings River upstream (east) from NASL near Hardwick. Along with water from other recharge areas, this groundwater flows to areas of lower head, such as the aquifers beneath the Tulare Lake Bed.

A large pumping depression lies to the north of NASL, along the McMullin Grade near Helm. Groundwater from the north of the study area generally flows to this depression, along with other depressions in and to the north and east of the Five Points Area.

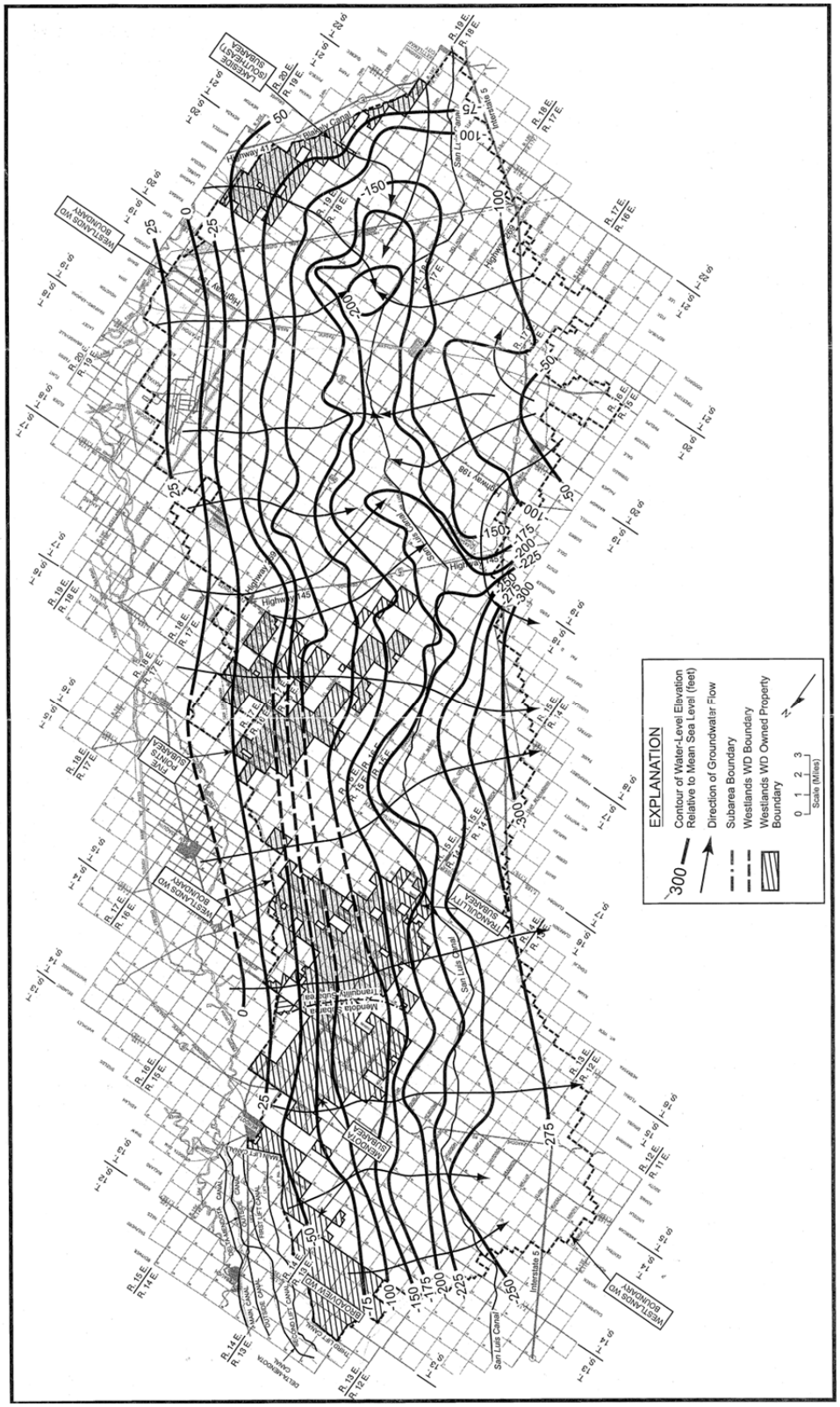

Figure 31 WWD Lower aquifer groundwater contour map, December 1965 (Schmidt, 2009).

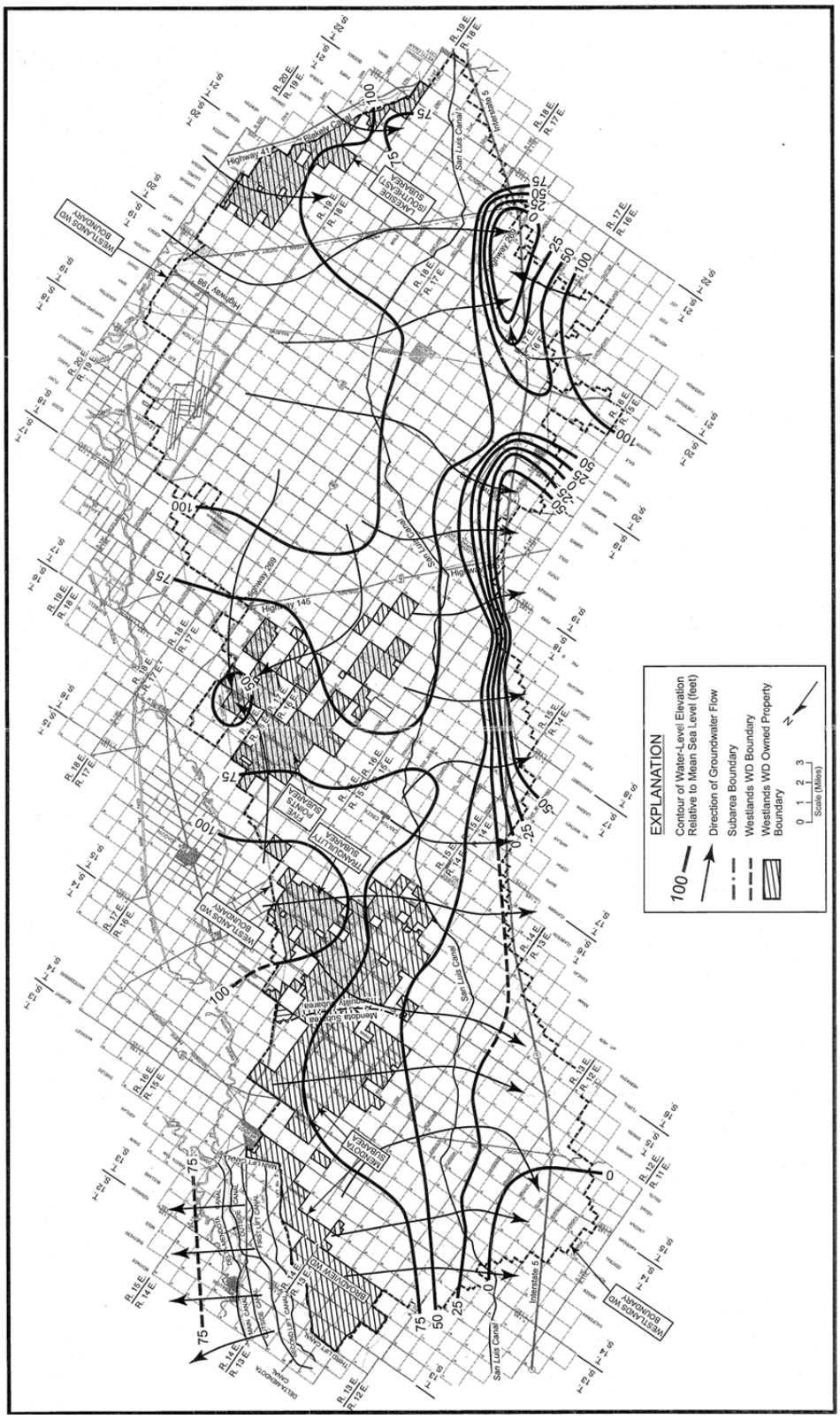

Figure 32 WWD Lower aquifer groundwater contour map, December 1986 (Schmidt, 2009).

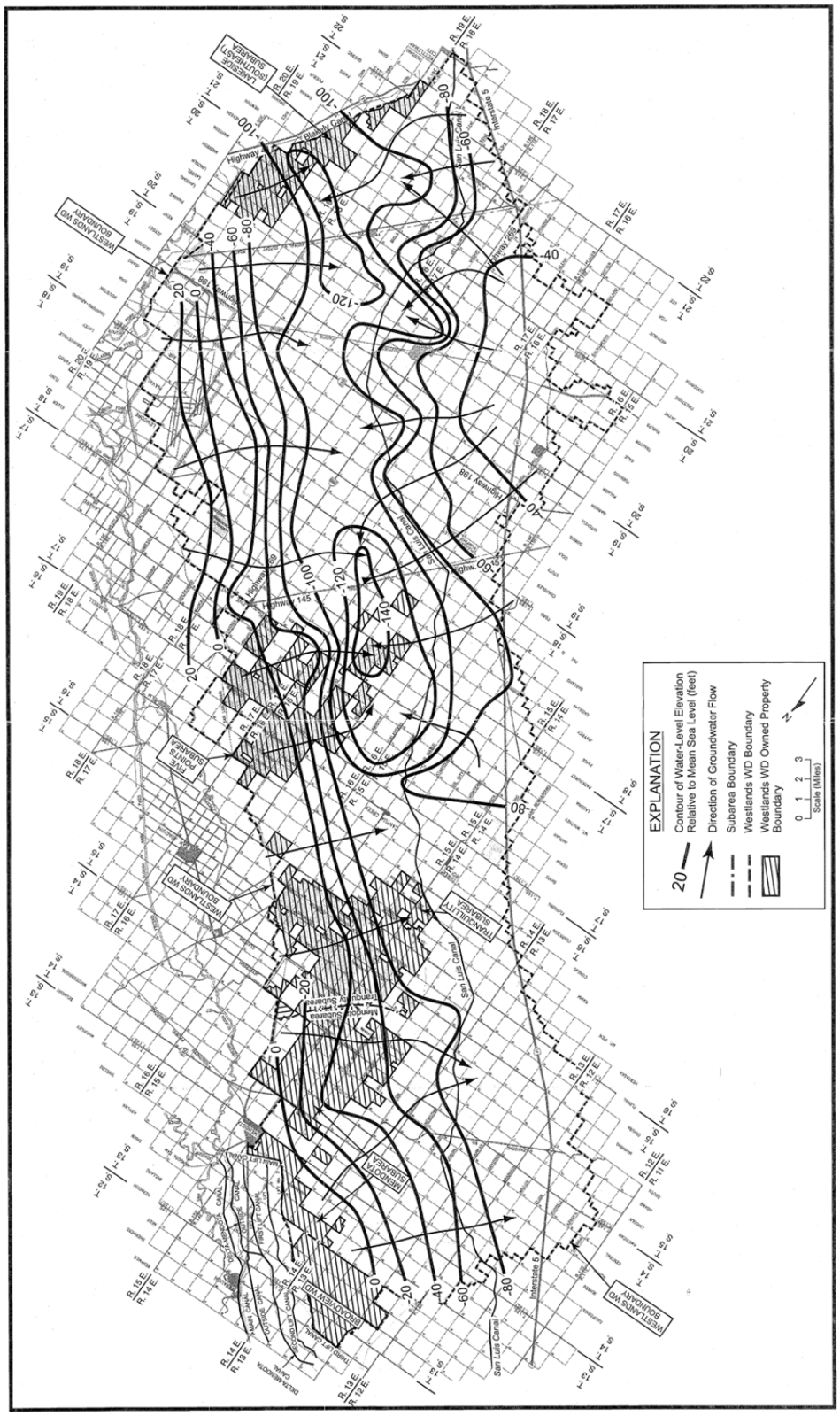

Figure 33 WWD Lower aquifer groundwater contour map, December 1993 (Schmidt, 2009).

Water Level Maps of the Study Area Constructed from CDWR WDL Data Representing the Sub-Corcoran Aquifer System

In 1956, groundwater flow patterns are assumed to be in early development conditions. Groundwater is pumped, but generally at smaller scales than later withdrawals. Groundwater flow is generally from the east of the study area and flows to points to the west of NASL (Figure 34). The primary recharge point lies to the north of the midway point between the cities of Lemoore and Hanford, near Laton. Here the groundwater elevation is approximately 220 ft.. Two cones of depression exist to the northwest and northeast of Huron, with elevations of -20 ft. and 30 ft. respectively. Groundwater elevations at NASL vary between approximately 140 ft. and 80 ft. from the eastern side to the west side of the property.

Spring 1961 was chosen to represent a development period drought scenario (Figure 35). In general groundwater is found at deeper levels than previously, as is expected in post-drought conditions. Groundwater generally flows from the east to points to the southwest and west of the study area. The Laton recharge area referred to previously still exists, but there are more numerous and larger cones of depression. Two cones of depression lie to the south of the study area, with groundwater elevations of approximately -50 and 50 ft. amsl. Two deep and extensive cones of depression lie in the Huron area, one slightly to the north and the other to the southwest. Groundwater elevation at both these areas is approximately -100 ft. amsl. Groundwater elevation at the recharge area is approximately 200 ft. amsl. Groundwater elevations at NASL vary between approximately 125 ft. amsl and 25 ft. amsl from the eastern side to the west side of the property, a significant decrease from previous years.

Spring 1972 is the first drought year to follow the beginning of surface water deliveries. Groundwater conditions are similar to the previous drought in 1961, and no large differences in groundwater elevations are evident (Figure 36). Recharge occurs near Laton, while one small cone of depression exists just to the north of Huron and a larger one further to the west, outside the study area. Groundwater elevations remain at 200 ft. amsl at the recharge area near Laton, and -100 ft. and -350 ft. amsl at the two cones of depression. Groundwater elevations at NASL are similar to the previous drought, at approximately 100 ft. amsl on the eastern side of NASL's property and approximately 25 ft. amsl on the western side.

After 1980, the area to the west and northwest of NASL appears to experience a significant recovery in water levels (Figure 37). By the end of the 1990s, the deep depressions and sub-sea level water levels have largely disappeared (Figure 38). Near Huron, water levels have recovered to levels around 50 ft. amsl; at NASL, water levels have recovered to 110 ft. (at the western boundary) to 150 ft. amsl (at the eastern boundary).

In the 2000s, water levels in the WWD area to the west and northwest of NASL recover to levels that exceed the elevation of high groundwater near Laton: In 2005, water levels near Huron recover to over 250 ft. amsl (Figure 39). The regional groundwater gradient is reversed with groundwater flowing across NASL from west-southwest to the east-northeast and water levels

at NASL ranging from over 200 ft. amsl at its western boundary to 180 ft. amsl at its eastern boundary.

The 2007-2009 drought reinitiates the groundwater decline in the WWD sub-area west of NASL. In 2009, water levels near Huron have dropped from over 250 ft. amsl in 2005 to under 150 ft. amsl (Figure 40).

In summary, the mid 1900s saw significant groundwater development in the WWD and its surrounding areas. Prior to this, groundwater in most of the hypo-Corcoran aquifer flowed northeasterly towards the Fresno Slough. In early 1952, this was still the case in much of the District. By 1965, however, flow direction had reversed, flowing southwest and into the District. By the late 1990s, nearly three decades after groundwater pumping had been reduced due to surface water deliveries from the San Luis Canal, groundwater flow reverted to its natural northeasterly direction in the area of the district east of the San Luis Canal. However, as the 2007-2009 drought has shown, these groundwater recoveries on the Westside of the valley trough are quickly eliminated by prolonged drought conditions and shortages of surface water supply.

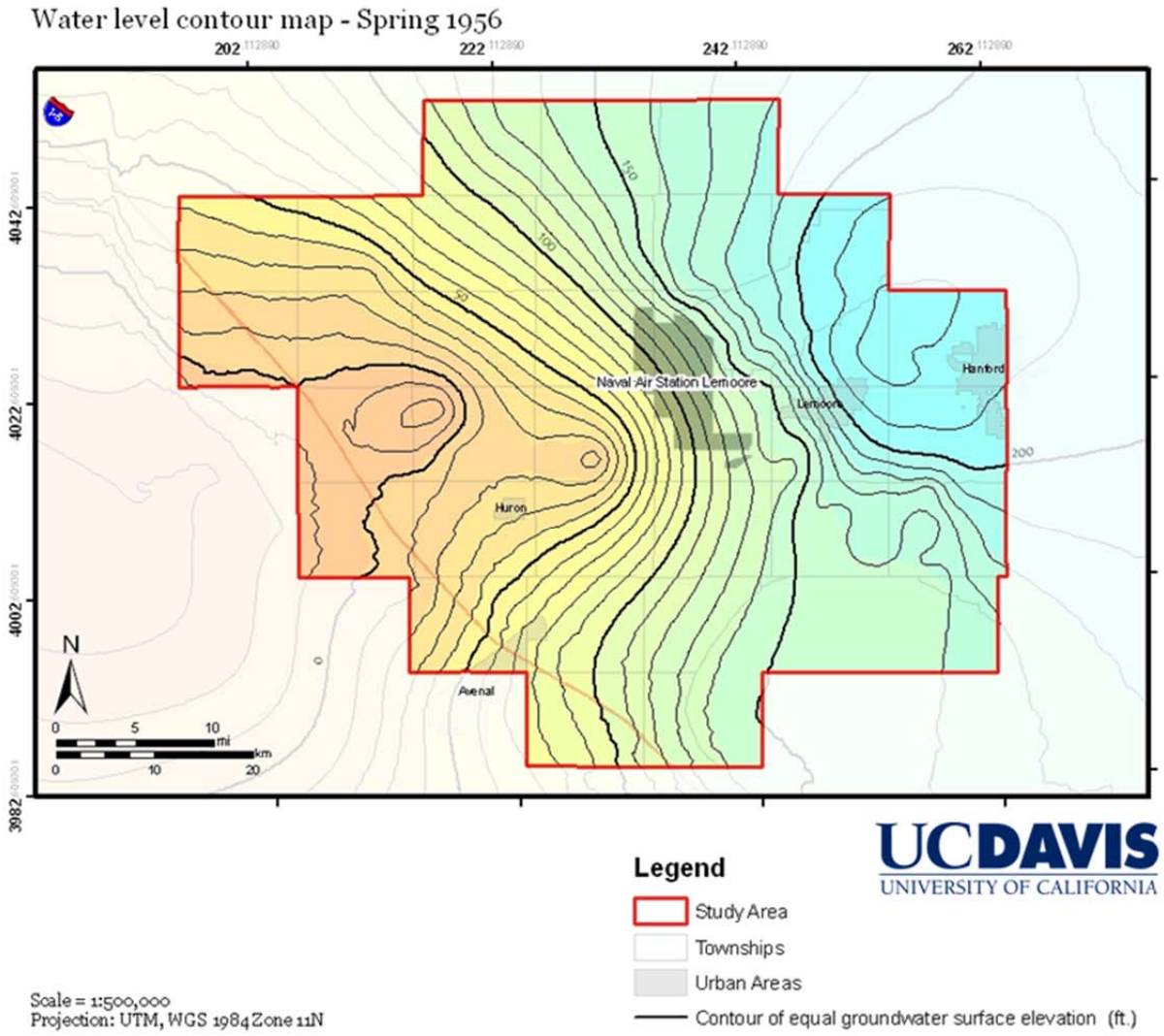

Figure 34 Water level contour map for the intermediate and deep aquifer for Spring 1956. Data obtained from the California Department of Water Resources.

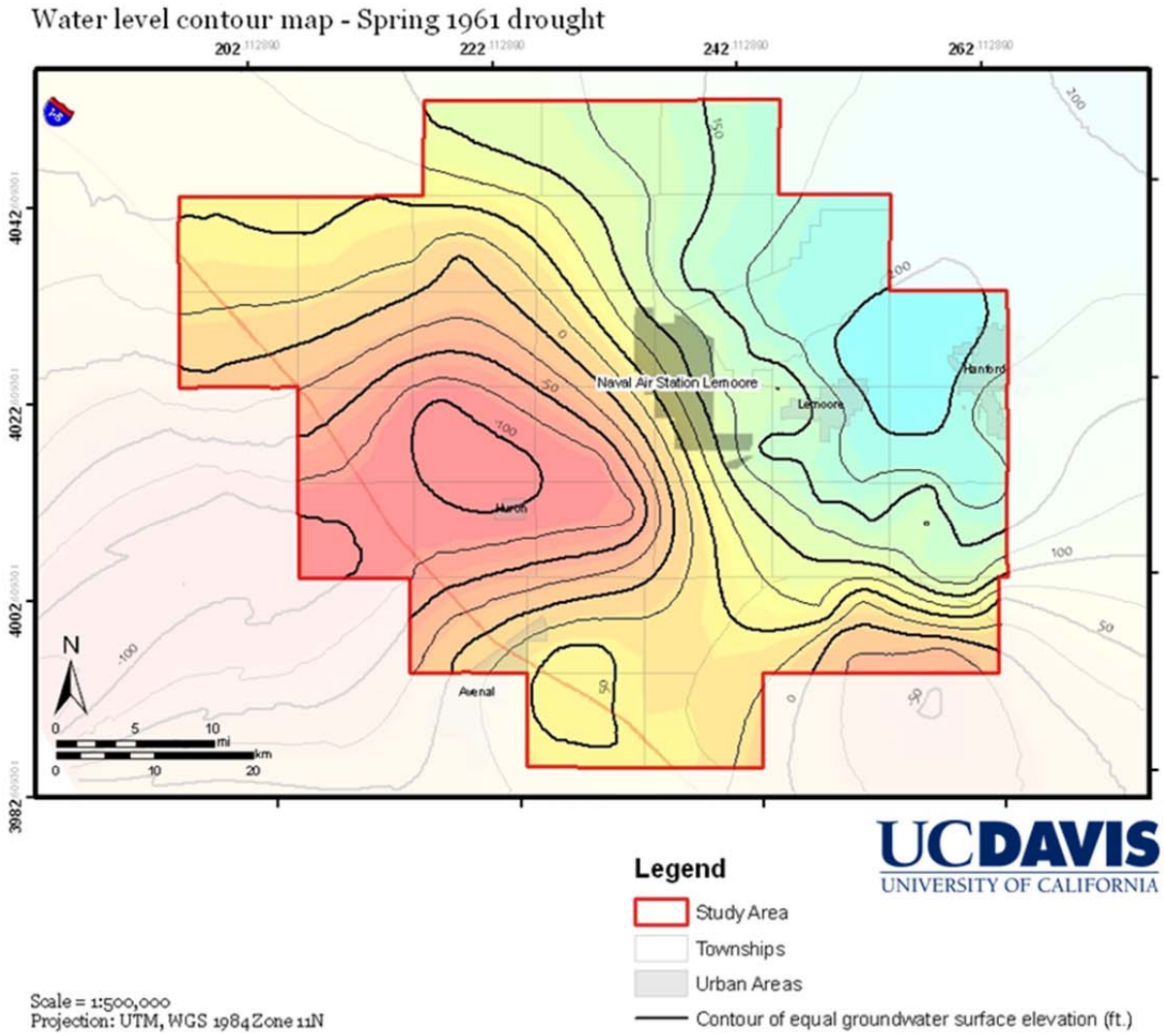

Figure 35 Water level contour map for the intermediate and deep aquifer for Spring 1961. Data obtained from the California Department of Water Resources.

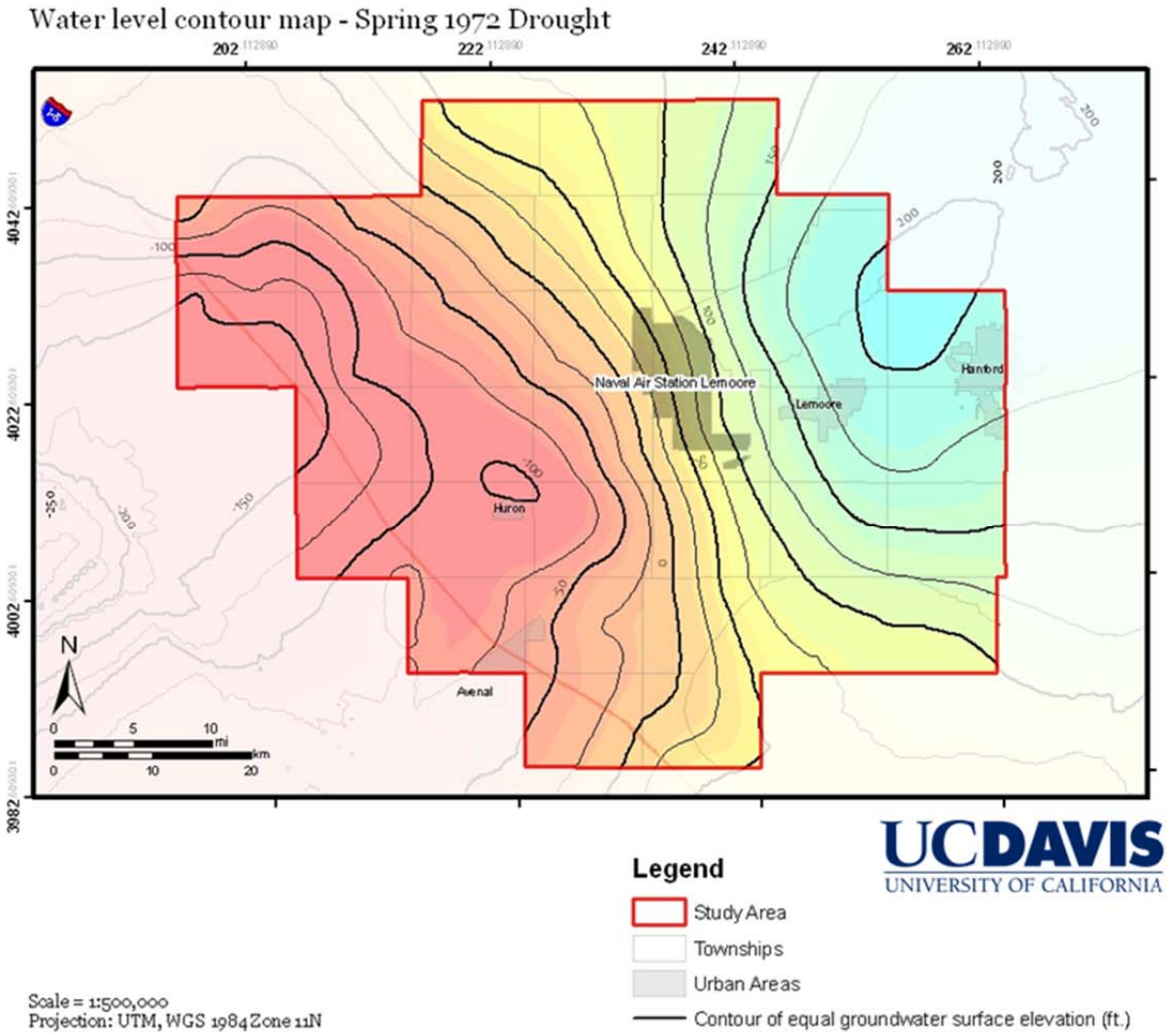

Figure 36 Water level contour map for the intermediate and deep aquifer for Spring 1972. Data obtained from the California Department of Water Resources.

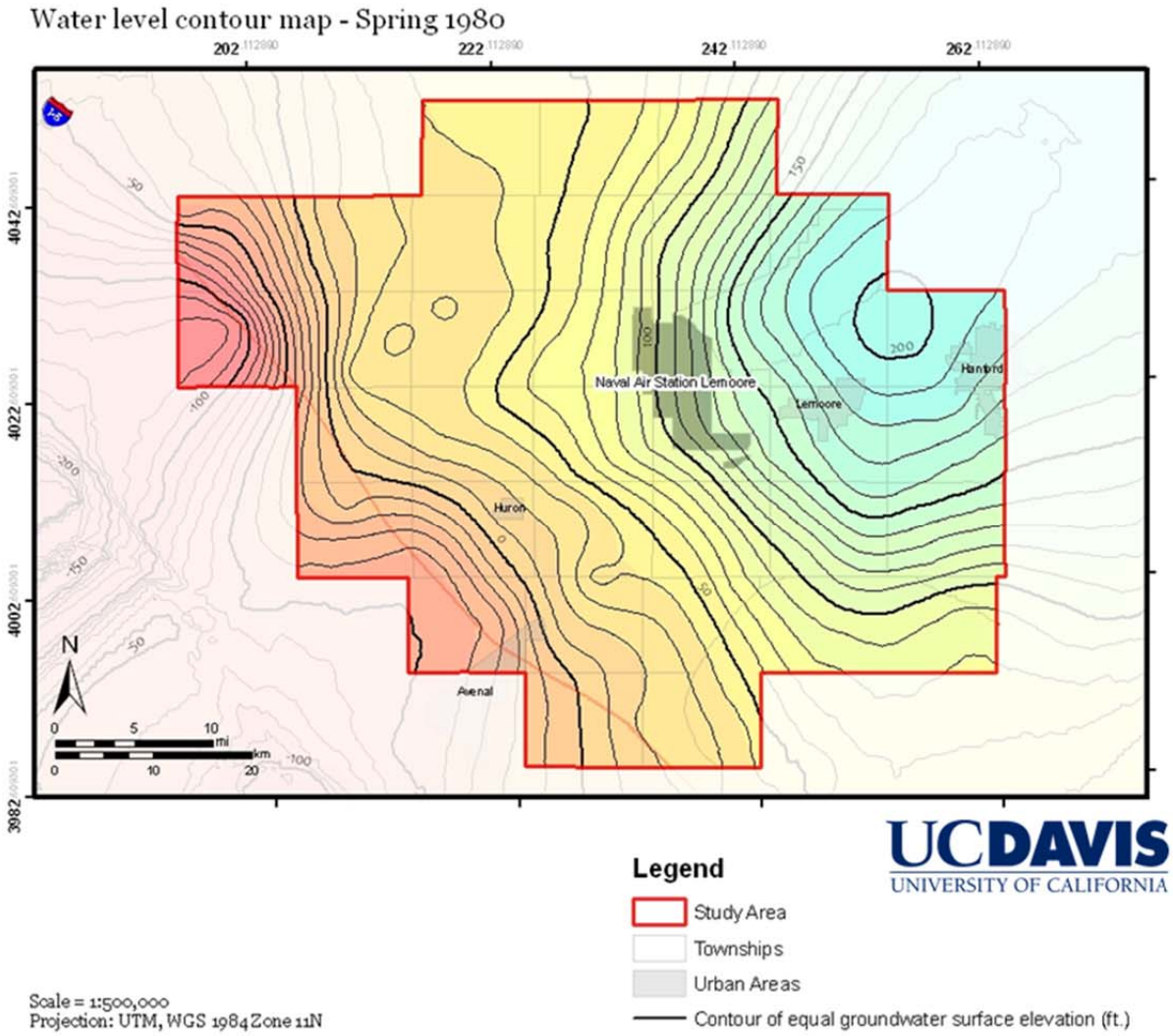

Figure 37 Water level contour map for the intermediate and deep aquifer for Spring 1980. Data obtained from the California Department of Water Resources.

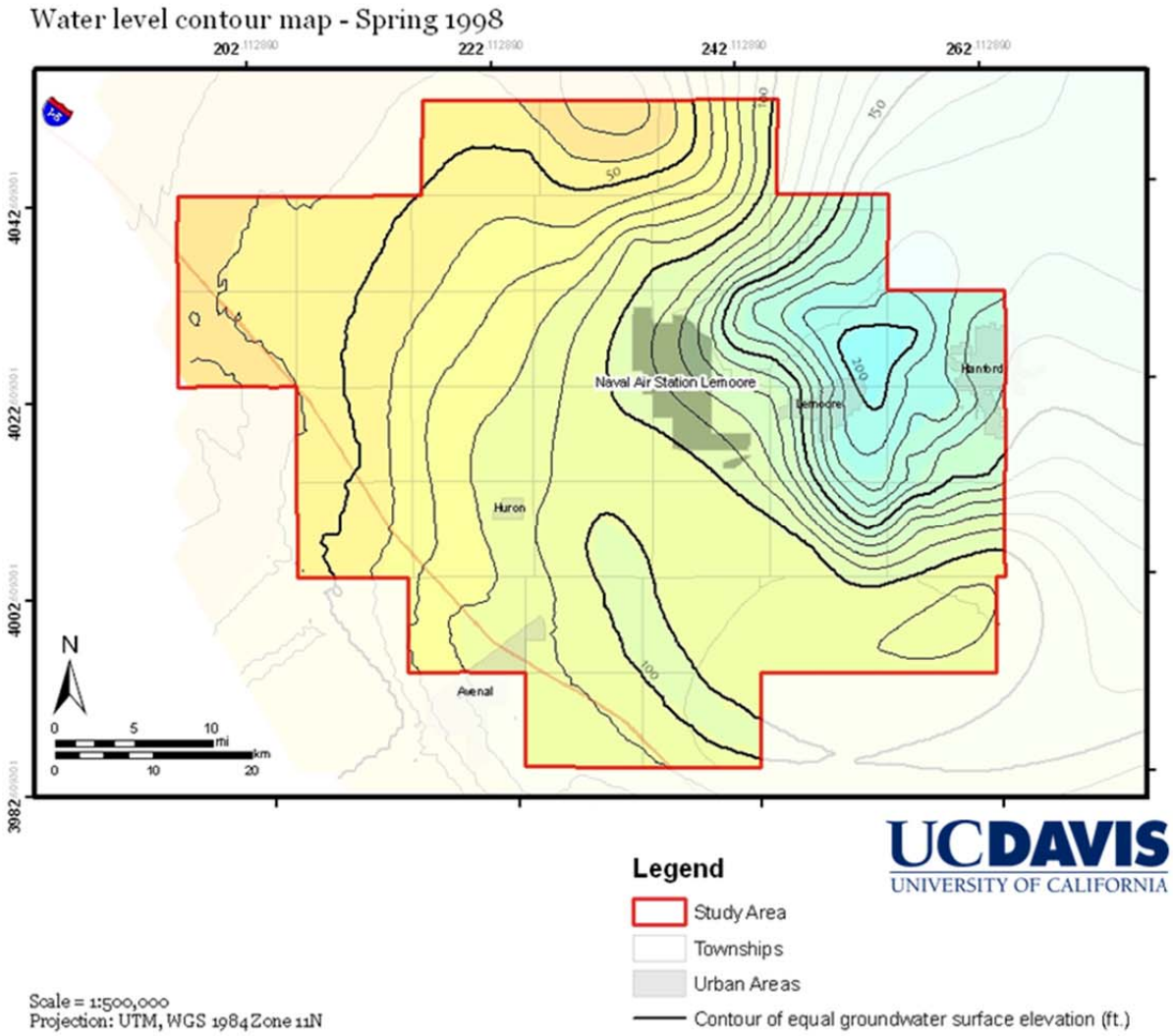

Figure 38 Water level contour map for the intermediate and deep aquifer for Spring 1998. Data obtained from the California Department of Water Resources.

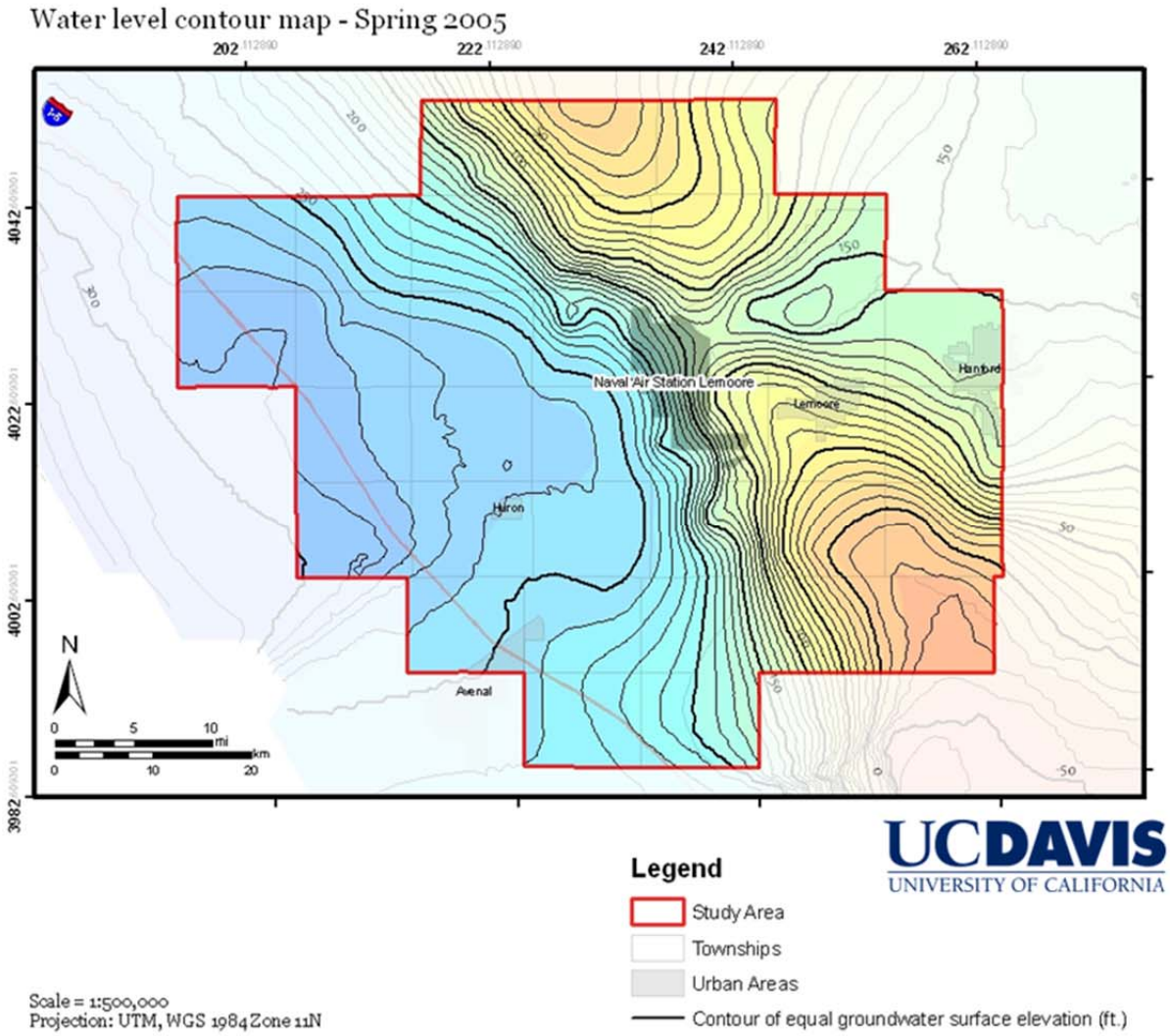

Figure 39 Water level contour map for the intermediate and deep aquifer for Spring 2005. Data obtained from the California Department of Water Resources.

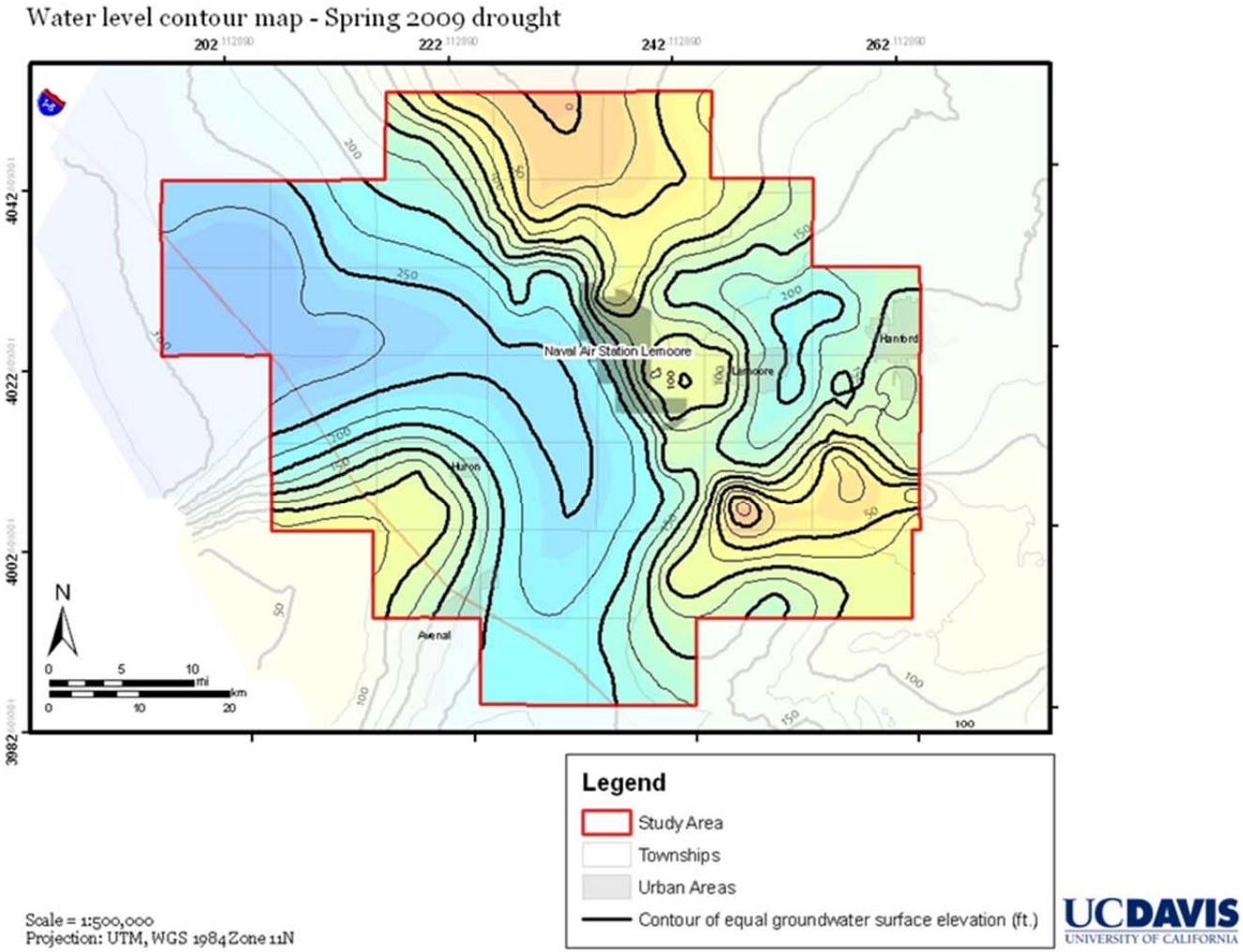

Figure 40 Water level contour map for the intermediate and deep aquifer for Spring 2009. Data obtained from the California Department of Water Resources.

4.8 Generalized Hypo-Corcoran and Sub-Corcoran Aquifer Hydrographs

As before, aquifer materials above the Corcoran clay are collectively designated as the hypo-Corcoran aquifer system, and aquifer materials located below the Corcoran clay named the Sub-Corcoran aquifer system. A subset of groundwater elevation data records were selected to complete representative hydrographs in the hypo-Corcoran and sub-Corcoran aquifers. First, to complete representative hydrographs of the hypo-Corcoran and sub-Corcoran aquifers, it was necessary to separate wells that were screened in each of these aquifers. As before, groundwater elevation data records were not always easily geo-locatable. In particular, it was not always possible to identify screened depths from water level data records. A number of wells drilled within township T18S-R19E, typically in the 1950s, and screened from approximately 700-2,100 ft. bgs were used to complete a composite hydrograph for the sub-Corcoran aquifer (Figure 42). A number of wells screened at various depth intervals in the hypo-Corcoran zone where found in the NASL vicinity and used to complete a composite hydrograph for this aquifer system (Figure 41). QMCs (Table 13) and outliers (data points that lay significantly outside of normal trends) were removed from these hydrographs. Hypo-Corcoran aquifer hydrographs displayed linear characteristics, with typical groundwater surface depths of 0 to 25 ft. bgs for the whole period of data availability (1958-present). Deeper aquifer wells showed far greater variability, rapidly declining to depths greater than 500 ft bgs before recovering in the late 1960s due to canal water imports.

For the Hypo-Corcoran aquifer, less data was available for use, as most of the wells with driller's logs tap the deeper aquifer. Data is also available for a shorter date range, and a large proportion of the measurements are only available for later dates (2004-present). An overall linear trend can be observed with water levels roughly at 10 ft. bgs. Surface water deliveries from the San Luis Canal become available in 1968. Before this time, water levels decline to below 20 ft. bgs, but rebound quickly in the early 1970s before stabilizing (Figure 41).

Water level data for the sub-Corcoran aquifer is more numerous, and available for a longer period (mid-1940s-present). Most of these data are available post-1950. Pre-1947 measurements are estimated, starting at ground level. When measurement data becomes available in 1947, sub-Corcoran water levels rapidly decline to a low of 528 ft bgs in 1967. A strong recovery occurs, lasting until 1988, when water levels fluctuate due to droughts and wt years. The latest trend is downwards, as groundwater pumping again increases to make up for the shortfall in surface water deliveries.

Figure 41 Hydrograph representative of Hypo-Corcoran Aquifer wells.

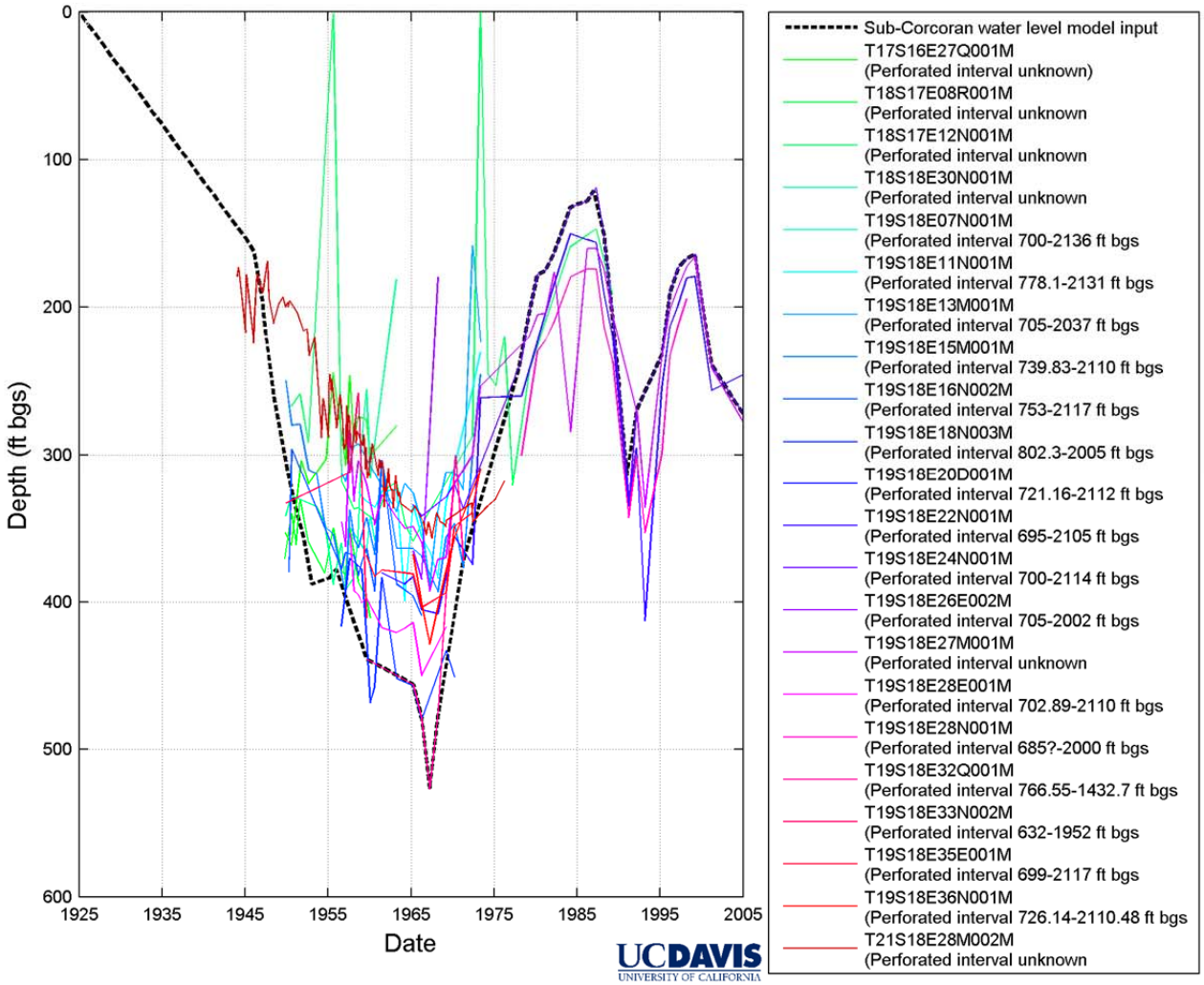

Figure 42 Lower aquifer well hydrographs and their screened intervals.

4.9 Well Production – Hypo-Corcoran and Sub-Corcoran Aquifers

An analysis of pumping tests within the WWD is carried out in Schmidt (2009). Transmissivity values for the hypo-Corcoran aquifer where found to vary between 60,000 and 280,000 gallons per day per foot (gpd/ft), with an average value of 125,000 gpd/ft. For the coarse deposits, hydraulic conductivity values varied between 500 and 2,000 gpd/ft^2 with extremes at several wells of 3,600 to 5,700 gpd/ft^2. The average hydraulic conductivity was found to be comparable to that of the Sierran sands in the area, at 1,900 gpd/ft^2.

In 1926, a three-month long "mega" aquifer test was carried out to the southwest of NASL, in the sub-Corcoran aquifer. Fifty-four wells belonging to the Boston Land Co. were pumped for a prolonged period, and then pumping was suspended for three months whilst water elevation recovery was measured. From this test, a transmissivity of 120,000 gpd/ft was calculated. The average hydraulic conductivity of the entire 1,100 ft. thick clay and sand layers that constitute the sub-Corcoran aquifer was calculated as 110 gpd/ft^2. Within the Lakeside subarea, approximately 10 miles to the south of NASL, aquifer tests were completed at three sub-Corcoran aquifer wells. Transmissivities varied between 59,000 to 84,000 gpd/ft, whilst hydraulic conductivities varied between 260 and 300 gpd/ft^2 in the sand layers (Schmidt, 2009). A Leaky Aquifer Test conducted in 1997 at Hamburg Farm, approximately 2 miles to the north of the Fresno-Merced county line. The transmissivity was calculated to be 160,000 gpd per foot, the storage coefficient 0.001 and the vertical hydraulic conductivity of the Corcoran Clay at his site 0.001 gpd per square foot. From this, it was estimated that the storage coefficient for the entire sub-Corcoran aquifer in the WWD range from 10^{-3}-10^{-4}.

We further note that, to the west of NASL, in the Anticline Ridge/Cantua Creek area, wells are often drilled through the upper alluvial fan materials to tap the more productive Etchegoin and San Joaquin Formations.

4.10 Regional and Local Groundwater Quality

Croft and Gordon (1968) conducted a study of groundwater quality in the Hanford-Visalia area in 1968. Their categorization of groundwater types are used in this report. Calcium bicarbonate water is defined as having a proportion of 50 percent or greater of the cations as calcium and 50 percent or greater of the anions as bicarbonate. Calcium sodium carbonate type water contains calcium and sodium as the first and second most abundant cation constituents respectively, but with each as less than 50 percent of the total cation count. Calcium bicarbonate sulfate water contains bicarbonate and sulfate as its two most common constitutent anions, respectively, also with each as less than 50 percent of the total anion amount. When the principal water cations (or anions) are present in approximately equal proportions, the water is described as intermediate cation (or anion) composition.

Within the study area, groundwater chemical quality is largely associated with surface water quality in local streams and rivers that recharge the aquifers. The water found in the Kaweah,

Kings and Tule Rivers (all of which originate in the Sierra Nevada mountains and its foothills) is of calcium carbonate type with low dissolved-solids (TDS) content. Of these three rivers, the Kings River originates at the highest elevation in the Sierra Nevada mountains and has a larger magnesium percentage and lower TDS than the other two rivers. The Kings River has been shown to have a larger proportion of its catchment area underlain by magnesium-rich geologic materials. The Croft and Gordon study showed only small seasonal variations in concentrations of TDS in these rivers. As expected, the concentration was smallest at times of highest discharge, during the Spring and early summer snowmelt, with smaller concentrations at all other times. Groundwater chemical measurements from intermittent streams originating in the Coast Ranges were not analyzed for the Croft and Gordon study, but several intermittent streams originating in the Sierra Nevada foothills showed TDS concentrations of 2-10 times that of perennial streams when they were sampled during the Winter and Spring seasons.

Several studies adopt a system for delineating groundwater chemical quality sub-areas first used in an early study by Mendenhall (Mendenhall and others, 1916). This study divided the section of the Valley in which NASL is located into three main areas with distinct groundwater types: 'east-side', 'west-side' and 'axial-trough'. NASL lands straddle the west-side and axial-trough groundwater type sub-areas. West-side groundwater samples are highly mineralized (high TDS) and of mainly sulfate type, whereas axial-trough groundwater is alkaline with differing chemical character and concentration found within its subareas. These contrast with groundwater encountered below the east-side, which is classified as bicarbonate type with a low TDS content.

Davis and others (1959) furthered Mendenhall's concept of using divisions of groundwater type by geographic region, by noting the groundwater quality change with depth bgs. Groundwater was divided vertically into three zones: the unconfined to semi-confined zone between the land surface and the Corcoran clay, the confined zone below the Corcoran clay and above lower confining beds, and brackish-saline connate or modified connate water found beneath the lower confining beds to the basement complex deep below the valley floor.

Bulletin 118, CDWR's comprehensive report on groundwater in California last updated in 2003 (CDWR, 2003), outlines groundwater quality impairments directly attributable to anthropogenic activities. The primary Constituents of Concern (COCs) listed for the Tulare Lake Hydrologic Region are high TDS, nitrate, arsenic, and organic compounds (CDWR, 2003, p.196). In particular, high TDS is seen as a problem along the western sides and axial trough area of the region. High TDS problems in the axial trough are mainly due to the marine origins of the Coast Ranges and their associated alluvial fan soils west of the Valley thalweg. Problems are amplified due to the evaporation of groundwater from shallow water table areas and poor drainage. Groundwater quality is generally higher beneath the Corcoran Clay. High nitrate levels due to

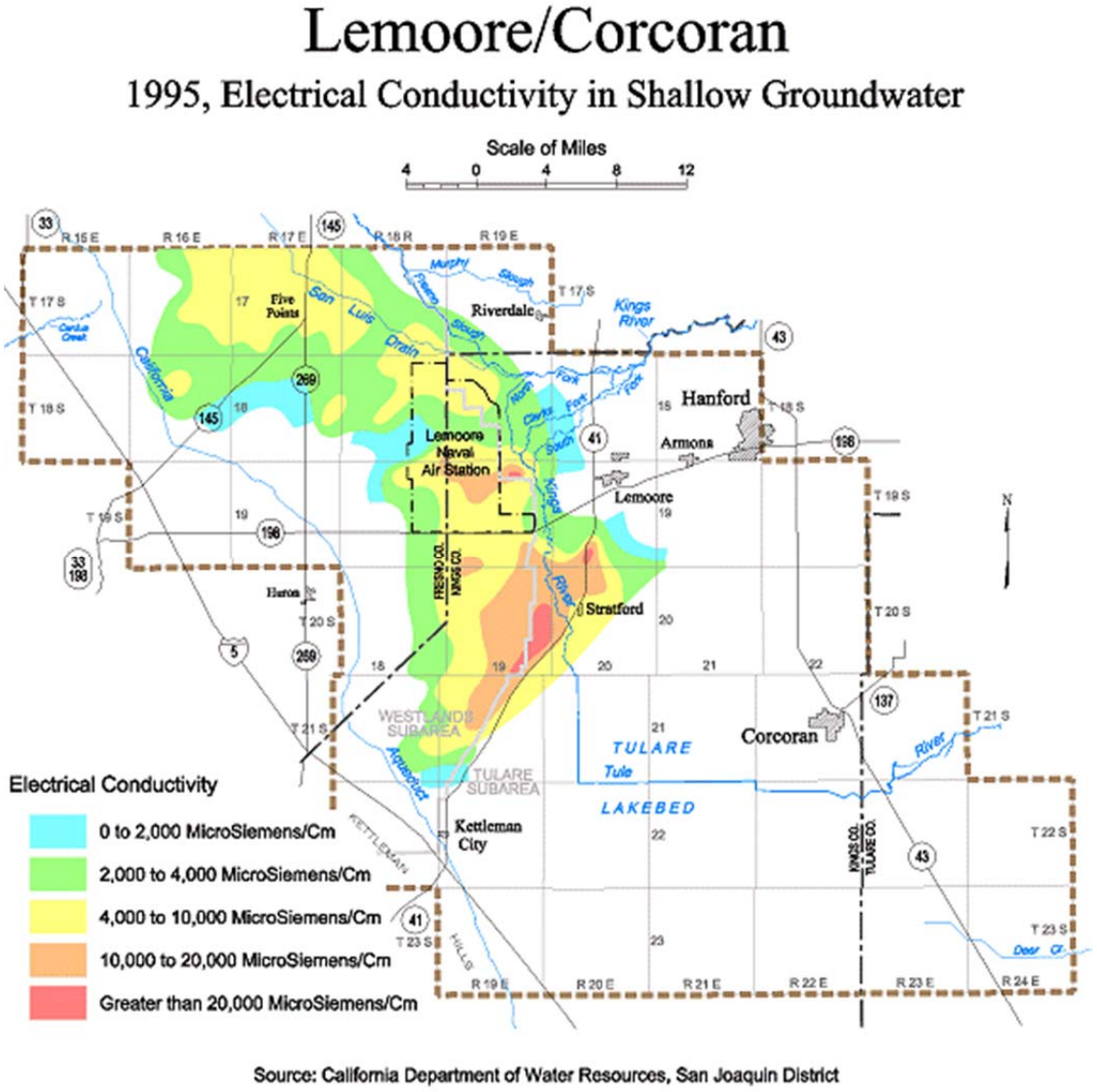

Figure 43 Electrical conductivity in the Lemoore/Corcoran area in 1995 (CDWR groundwater data and monitoring website, 2010).

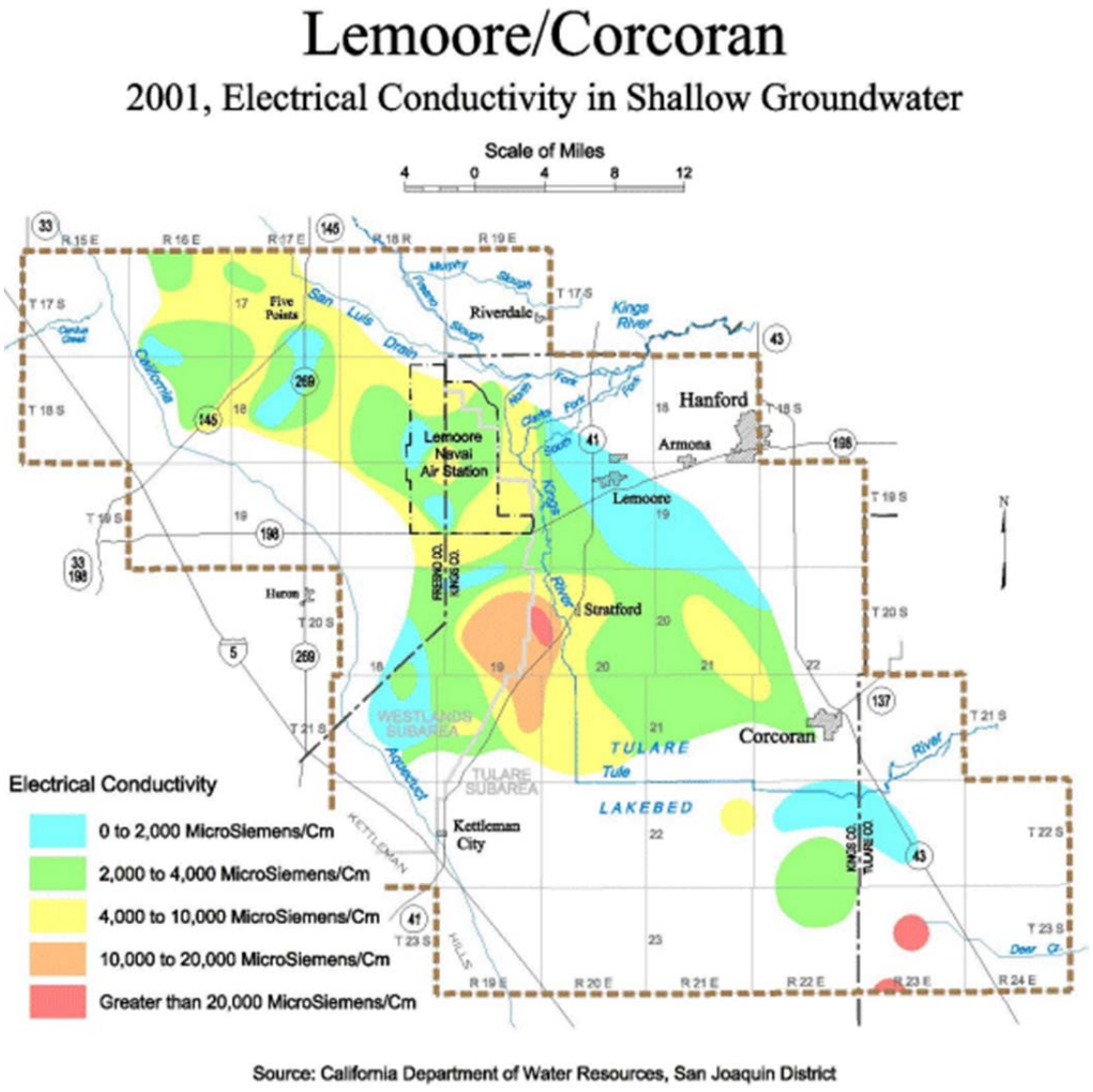

Figure 44 Electrical conductivity in the Lemoore/Corcoran area in 2001 (CDWR groundwater data and monitoring website, 2010).

human and animal waste and crop fertilization, are present in distinct locations throughout the Valley. High arsenic levels can also be found throughout the Valley, mainly in fine-grained lake bed sediments.

Maps showing specific conductivity for shallow groundwater in the NASL vicinity (designated as area Lemoore/Corcoran) were available from the CDWR website (CDWR groundwater data and monitoring website, 2010). Maps for 1995 and 2001 were available (Figure 43 and Figure 44).

In 1995, the highest specific conductivity (EC) can be found in a small area beneath NASL and in a larger area next to Stratford. Here, measurements of greater than 20,000 µmhos/cm can be found, though by 2001 the high EC readings beneath NASL have been greatly reduced to small and medium detections, and the area of high measurements near Stratford has retracted in size. Areas with medium measurements (4,000-10,000 µmhos/cm) are dispersed throughout the whole Lemoore/Corcoran area and are numerous beneath NASL in both 1995 and 2001. For both years, the best water quality (0-2,000 µmhos/cm) can be found in localized areas to the west and east of the NASL boundaries, as well as other localized areas within the Lemoore/Corcoran area.

5 Land Subsidence

5.1 The Subsidence Problem

This chapter provides an overview of the land subsidence problem, a summary of existing literature knowledge, an analysis of the various existing data sources used to estimate historic land subsidence within the NASL study area to date, and concludes with a synthesis of these data.

Land subsidence (the lowering of a land surface) can be caused by mining (physical removal of water and other fluids, deposits, or gases from the subsurface) and dissolution of carbonate and limestone (the forming and collapsing of subsurface voids or caves/caverns). It can also be caused by geological processes such as faulting as a result of differential stresses within the Earth's crust and isostatic subsidence due to the buoyancy of the Earth's crust floating on the asthenosphere. Subsidence due to any of these factors, combined with a few other relatively insignificant subsidence drivers, affect an estimated area larger than 44,000 km^2 in 45 states within the USA. More than 80 percent of this subsidence is related to groundwater removal (Hoffmann et al, 2003).

In agricultural areas, large volumes of irrigation water are required during the long, hot and dry summers, including in California's San Joaquin Valley ("Valley"), where a significant percentage of U.S. food crops are grown. Agricultural development within the Valley began in the mid-1920s, leading to large-scale groundwater withdrawal, and subsequent subsidence (Sneed, 2001). By 2002, it was estimated that the Central Valley, whilst forming less than 1 percent of the nation's farmland, produced 8 percent of the nation's agricultural output by value (approximately $17 billion) (Reilly, 2008). In addition, many of the most agriculturally productive counties constitute and directly surround the study area. The projected population growth within the study area has the potential to add further stresses to groundwater supplies.

Large-scale groundwater pumping within the study area began after new pumping technologies were introduced before the onset of the Second World War. Groundwater pumping diminished significantly when surface water deliveries from the San Luis Canal began in the late 1960s. By 1983, groundwater levels in most of the subsidence regions in the Valley had recovered to levels measured in the 1940s and 1950s. In recent years, surface water deliveries have again declined (see Figure 42).

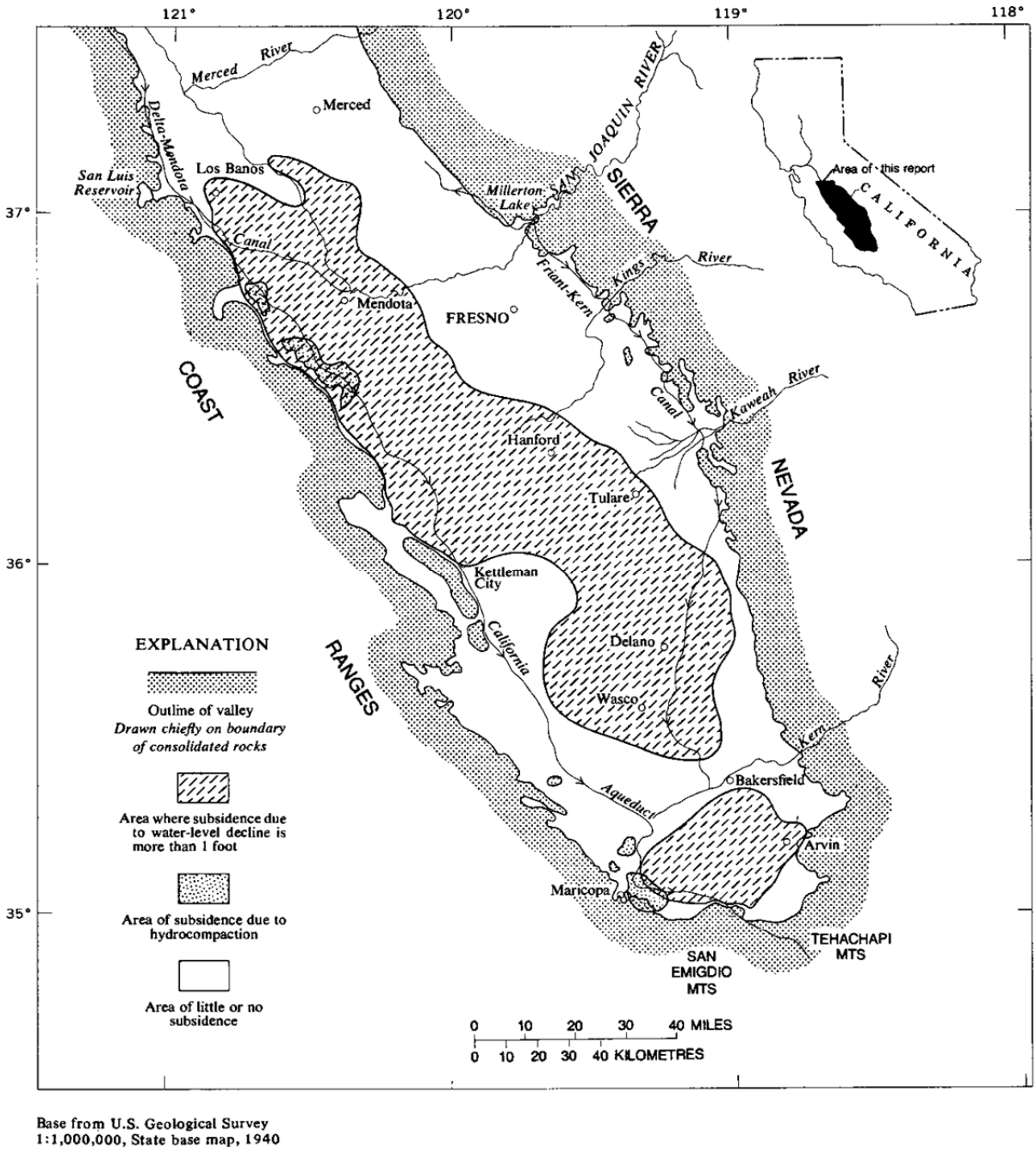

Figure 45 Major subsidence areas within the San Joaquin Valley, California (Poland et al, 1975).

The most significant potential problems caused by subsidence are infrastructure damage (e.g., damage to roads, levees, building foundations, pipelines etc.) and a loss of groundwater storage capacity within the affected aquifer. Natural waterways, including wetlands and riparian habitats and riparian courses, as well as constructed waterways (canals, ditches, etc.) are also significantly affected by land subsidence. Land subsidence has the potential to cause unrecoverable damage to these areas.

Land subsidence related to groundwater can be the result of different processes: Irrigation or excessive wetting of dry, clay-rich soils in arid and semi-arid climates can cause hydrocompaction and subsequent land subsidence (Figure 45). Hydrocompaction has been encountered in areas of the western San Joaquin Valley, west of the project area, and affected the construction of the San Luis Canal, which passes to the west of the NASL property. To minimize post-construction damage to the canal structure, pre-wetting of several canal reaches was performed.

Subsidence due to the draining of peats in the Sacramento - San Joaquin River Delta for agricultural purposes has led to the need for islands to be protected by levees due to their subsea-level elevations. In some areas, land surface levels of 15 ft. and more below sea-level have been measured.

Subsidence is also caused by other types of fluid removal including hydrocarbons, for example in some areas of Southern California.

By far the most widespread form of land subsidence, in terms of magnitude and area affected within California, is subsidence due to large scale groundwater withdrawal from aquifers that contain, in various quantities, unconsolidated fine-grained sediments. This form of subsidence provides the focus of this research report.

A particular damaging aspect of subsidence is differential (uneven) subsidence across a groundwater basin. Differential subsidence is particularly strong, where the thickness of clay beds in the subsurface varies significantly over short distances. Within the Valley, differential subsidence is a significant problem, causing damage estimated to be hundreds of millions of dollars annually. California sites outside the Valley, such as the Rogers Lake Bed at Edwards Air Force Base (Sneed & Galloway, 2000) have also been affected by differential subsidence. This form of subsidence brings its own set of potentially serious problems, and is especially damaging to infrastructure such as runways. The damage it inflicts on canals and levees, etc., can lead to a loss in conveyance capacity.

5.2 Previous Subsidence Studies

Within the San Joaquin Valley, there are three main regions of subsidence, referred to by J.F. Poland and others as the Los Banos-Kettleman City, Arvin-Maricopa, and Tulare-Wasco subsidence regions (see Figure 46) (Poland et al, 1975, p.2). NASL lies in the southeastern portion of the narrow and long northwest-southeast trending Los Banos-Kettleman City (LB-KC) subsidence region. To the southeast of LB-KC region, lies first the Tulare-Wasco subsidence region, followed by the Arvin-Maricopa subsidence region further to the south. The maximum subsidence measured within the LB-KC subsidence region (also the maximum measured in the Central Valley) can be found to the northwest of the NASL site, near Mendota. Here, subsidence

approached 30 ft. in 1981 (Sneed, 2001). Within the Valley, an area estimated at 13,500 km^2 (5,200 square miles) of mostly agricultural lands has been subject to subsidence greater than 1 ft (Figure 46).

Subsidence in all of these areas has been studied extensively, especially during the 1960s and 1970s. Joseph Poland was instrumental in raising awareness of the subsidence problems within California. With his colleagues at the U.S.G.S, he studied the major subsidence regions within the Valley. The series of reports that were produced as a result of this work (USGS Open File Reports 437-A-I) contained information and data that proved very useful for this report.

Bull (1964) reported that the interfan areas in the Western Valley were often surficial mudflow deposits. These deposits were studied prior to construction of the San Luis Canal, and six compaction recorders (extensometers) were built by the late 1960s to monitor subsidence. Wetting from initial irrigation can cause the mudflow deposits to compact irreversibly. As these mudflow deposits are not found as far east as NASL, this form of subsidence is not considered to be a major problem within the study area.

Ireland, Poland & Riley included a map showing total subsidence measured between 1926 and 1972 (Figure 46). As shown, in this assessment, NASL is located within an area that experiences between 4 ft. and 8 ft. of subsidence during the 1926-1972 period. Large-scale subsidence occurs approximately 10 miles to the west and southwest of NASL, near the San Luis Canal, where subsidence measurements of 20 ft. have been recorded. Other subsidence 'hotspots' within the Los Banos – Kettleman subsidence area occurred to the north along the California Aqueduct, the most extensive measurement located 5 miles to the southwest of Mendota. A maximum of 28 ft. of subsidence has historically been measured here.

Michelle Sneed, also at the U.S.G.S, has been and is currently engaged in subsidence modeling at sites located in Southern and Central California. The modeling efforts completed by Sneed and Galloway (Sneed and Galloway, 2000) at the Holly Site (at Edwards Air Force Base) in the Antelope Valley were very useful, as many of the methods employed were similar to those used for this study. Concurrent to this work, a subsidence model is being developed based on data at Oro Loma, between Los Banos and Mendota, to the northwest of NASL.

The Central Valley Hydrologic Model (CVHM), outlined in Faunt, 2009 is a multi-faceted, large-scale groundwater flow model. As part of the CVHM project, subsidence is modeled over the entire Central Valley. The NASL model was completed to add further detail to this large scale regional model.

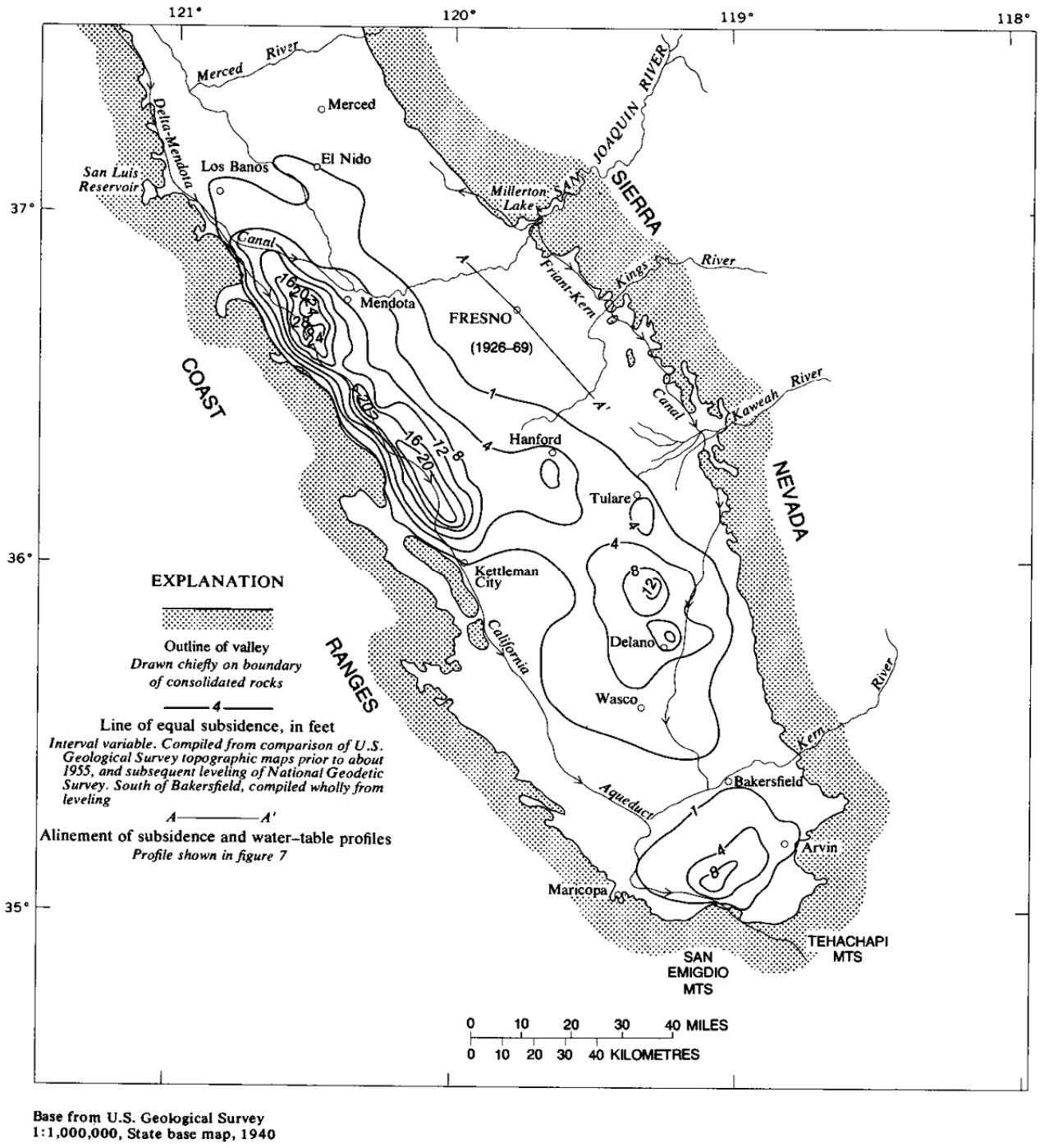

Figure 46 J.F. Poland's map showing contours of equal land surface subsidence between 1926 and 1970 (Poland et al, 1975).

5.3 Reconstructing Subsidence

Reconstructing historic land subsidence from existing land elevation and compaction-measuring equipment was not straightforward. There was no single land elevation data source at NASL that would provide continuous data for the whole model timeframe.

There were three main sources of subsidence/compaction data that were used for this modeling project: land surface elevation data, extensometer data, and existing subsidence contour plots completed by other investigators. Leveling data obtained from the NGS was deemed unusable, as it was unadjusted. Reliable sources of adjusted leveling data used in this study were collected from Poland's (Ireland, Poland and Riley, 1984) report on major subsidence areas within the Tulare Lake Basin and a land elevation survey by Caltrans along Highway 198 to the south of NASL. Poland's report also includes elevation data for several extensometers within the NASL vicinity, complete with their respective compaction/subsidence ratios. Further land elevation data for a number of these extensometers was obtained from electronic files at the USGS in Sacramento.

Historical subsidence data indicate that, within the WWD, each foot of subsidence has been caused by groundwater level declines of 20-45 ft.. The areas in the west and south of the WWD have seen the least subsidence per foot of groundwater level decline, whilst the Mendota area to the north has seen the most. Given that approximately 200 ft. of drawdown had occurred by the early 1970s and again in recent years at NASL, a total subsidence of 4-10 ft. since groundwater development began in the early 20th century, is consistent with our land level data.

The following paragraphs describe the details of the data collection and interpretation methods used for this study, and provide further details on land subsidence reconstruction at NASL.

Highway 198 Survey. A very useful dataset was obtained from a land elevation study completed by the California Department of Transportation (Caltrans) along Highway 198 in 2004. This study was completed using adjusted data from survey benchmarks along the Valley section of Highway 198, using elevation measurements covering the period approximately 30-50 years before 2004. Highway 198 enters the Valley at the Harris Ranch junction on the I-5 freeway and traverses to the East side of the Valley. The Highway passes NASL directly to the south, before heading in an east-northeasterly direction to Hanford, where it again heads east through Visalia and to the Sierra foothills (Figure 47). The survey data was provided courtesy of John Kirk at CDWR, Fresno. The benchmarks in this study that are on Highway 198 directly to the south of NASL are GT1050, GT1729, GT1036 and GT0979 and were all measured in the mid-1960s and again in 2004.

DATA TYPE	DATA SOURCE	STATION/WELL ID	DATA FROM	DATA TO
Highway 198 leveling survey	Survey benchmark	GT1050	1963	2004
		GT1729	1966	2004
		GT1036	1966	2004
		GT0979	1966	2004
Extensometer data from Poland and Sneed	Extensometer	20S18E06D001M	1/11/1965	11/8/2010
		18S19E20P002M	2/28/1967	1/8/1980
		20S18E11Q001M	7/24/1964	12/31/1979
Poland's subsidence contours and profiles	Subsidence contour plot	Figure 4, Ireland et al, 1984	1926	1972
	Subsidence profile	Various, Figure 19, Ireland et al, 1984	1947	1972

Table 14 Land surface elevation data coverage.

HIGHWAY 198 BENCHMARK	DATE FIRST MEASURED	DATE LAST MEASURED	SUBSIDENCE (M.)	SUBSIDENCE (FT.)
GT1050	1963	2004	1.2	4
GT1729	1966	2004	1.1	3.5
GT1036	1966	2004	1.2	3.9
GT0979	1966	2004	1.3	4.2

Table 15 Highway 198 benchmark data availability.

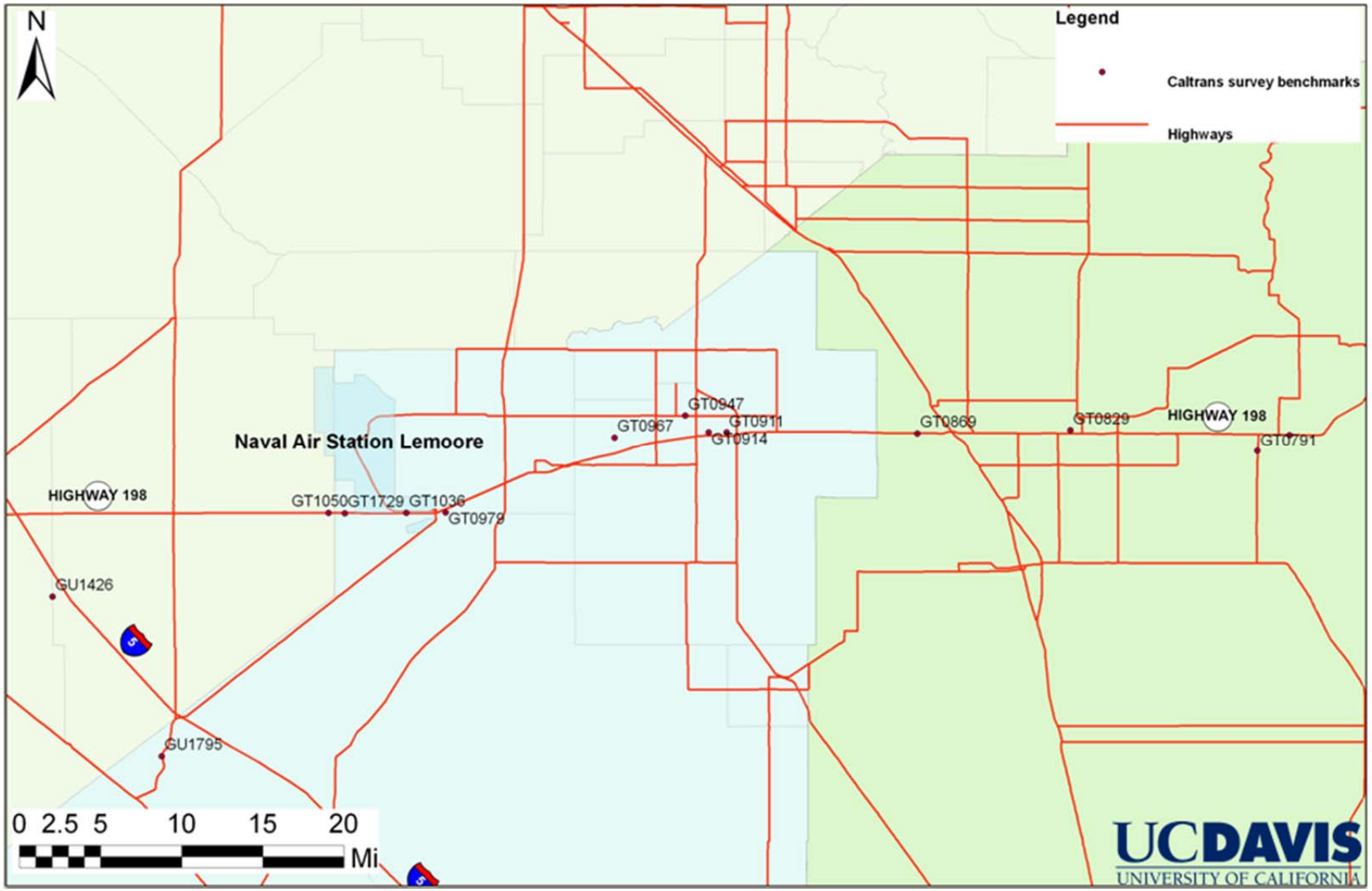

Figure 47 Highway 198 survey benchmark locations.

Results of the Caltrans land elevation survey showed that approximately 3.5-4.0 ft. of subsidence occurred along the portion of Highway 198 adjacent to NASL. A benchmark located midway between the cities of Lemoore and Hanford (GT0967) showed the greatest amount of total subsidence within the Caltrans study timeframe at approximately 9.5 ft. (Figure 48).

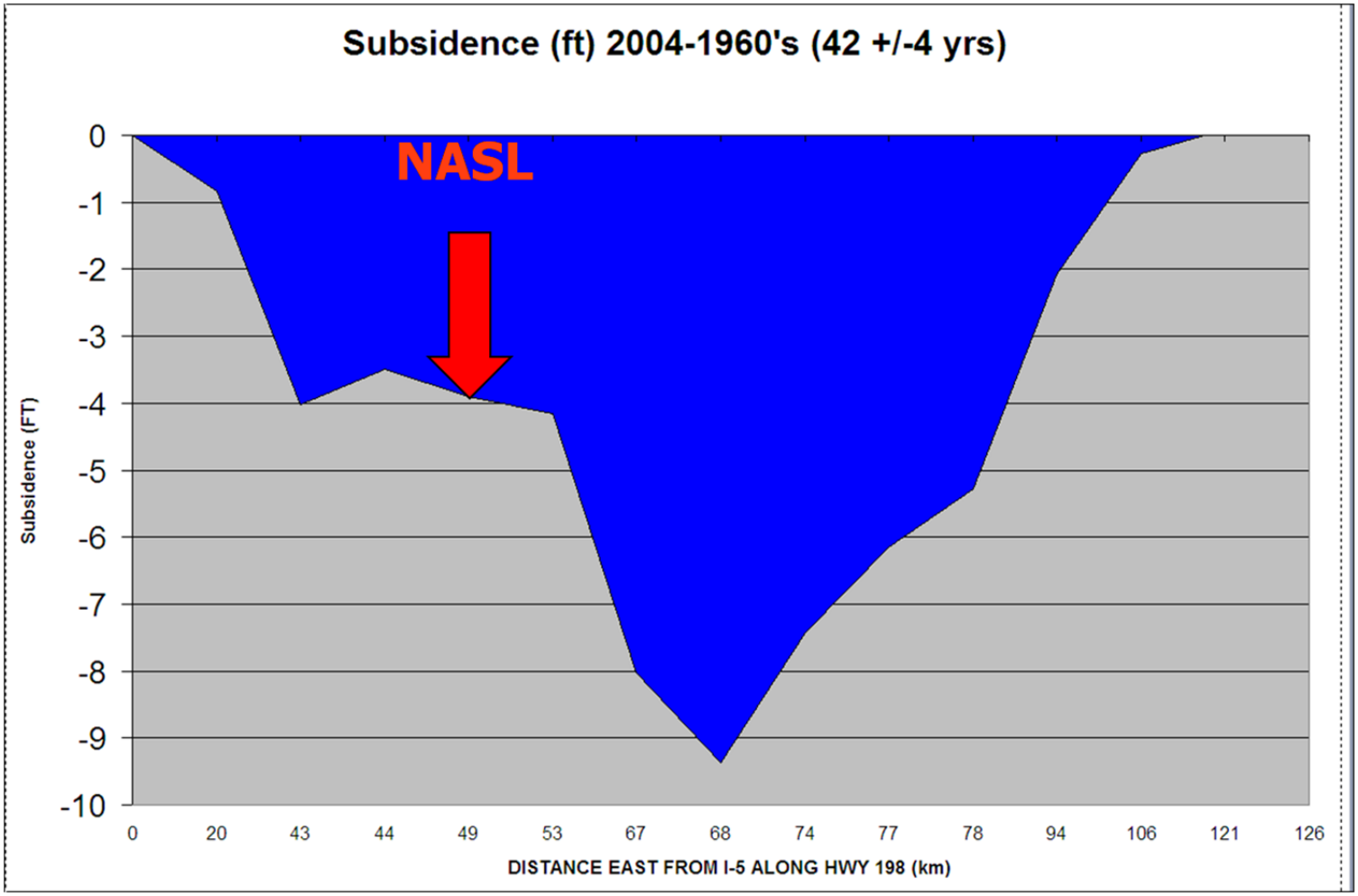

Figure 48 Subsidence at NASL estimated by Caltrans Highway 198 study.

Extensometers. Extensometers are commonly used for measuring and calculating land subsidence. They are installed within a completed well, which in most instances are specially drilled for extensometry. Calculation of the extension/compaction in the formation surrounding the well is achieved by measuring the corresponding change in the above-ground portion of a cable suspended within a deep well casing anchored effectively at the bottom of the well (Figure 49).

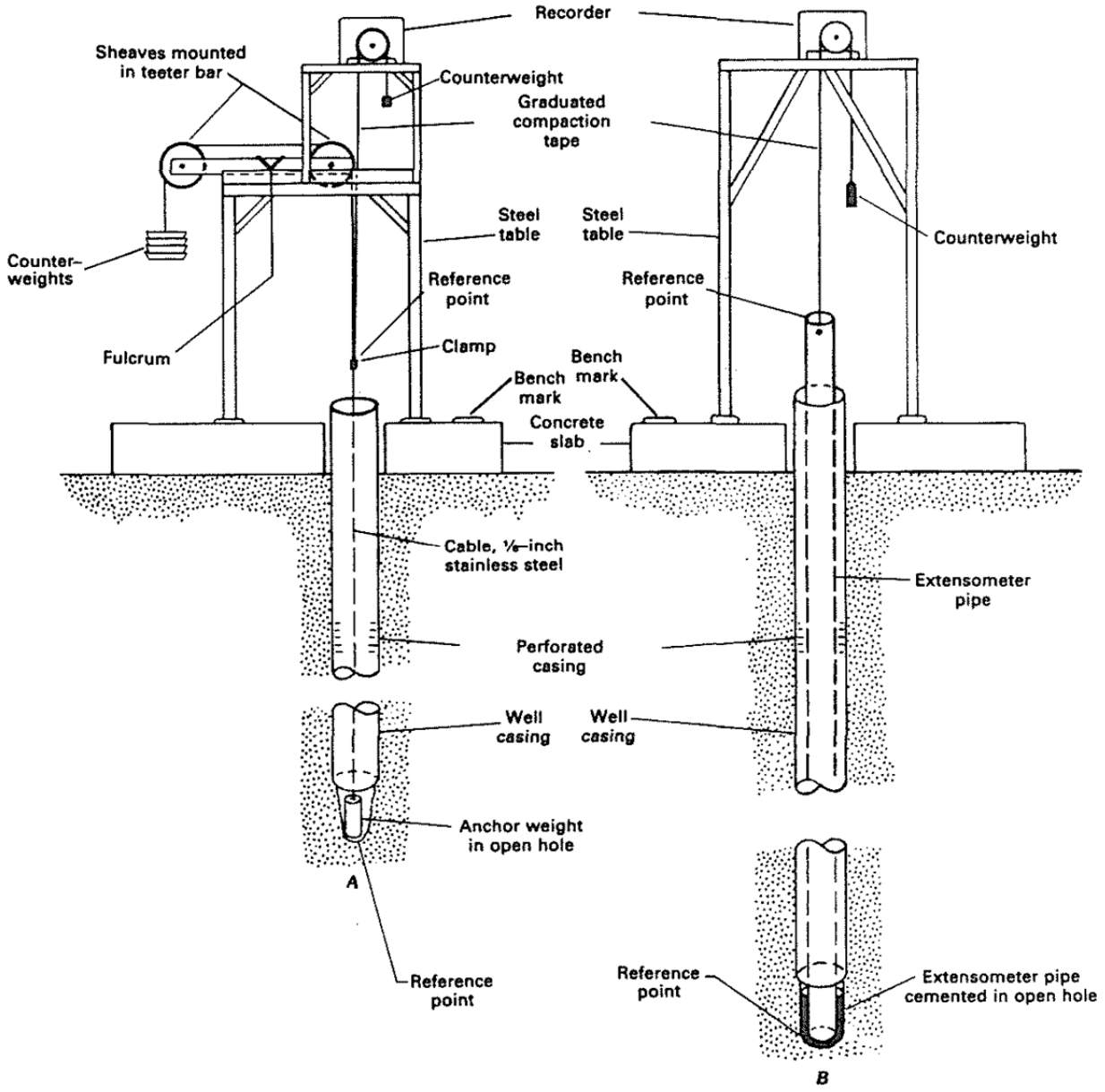

Figure 49 Typical extensometer construction (Riley, 1984).

A total of 15 compaction recorders (extensometers) were originally installed in the WWD (including 6 along the San Luis Canal). Some of these compaction recorders were decommissioned or not maintained further when imported surface water became available after 1967. However, operation of the compaction recorders along the SLC continued until 1989.

Extensometers can be found within the study area, including the extensometer designated 18S19E20P002M (20P2) located on NASL property (Figure 50). Data for this extensometer, along with two other extensometers located within the study area was obtained from the USGS and Poland's reports (Ireland, Poland and Riley, 1984). The timeframe of data availability is shown in Table 16.

EXTENSOMETER NAME (abbreviation)	DATA FROM	DATA TO	MEASURE-MENTS	DEPTH INTERVAL (FT.)	COMPACTION/ SUBSIDENCE RATIO (%)
20S18E06D001M (6D1)	1/11/1965	11/8/2010	148	0-867 (possibly 0-1007)	42
18S19E20P002M (20P2)	2/28/1967	1/8/1980	4698	0-578	33
20S18E11Q001M (11Q1)	7/24/1964	12/31/1979	17	0-710	46

Table 16 Historical extensometer data availability.

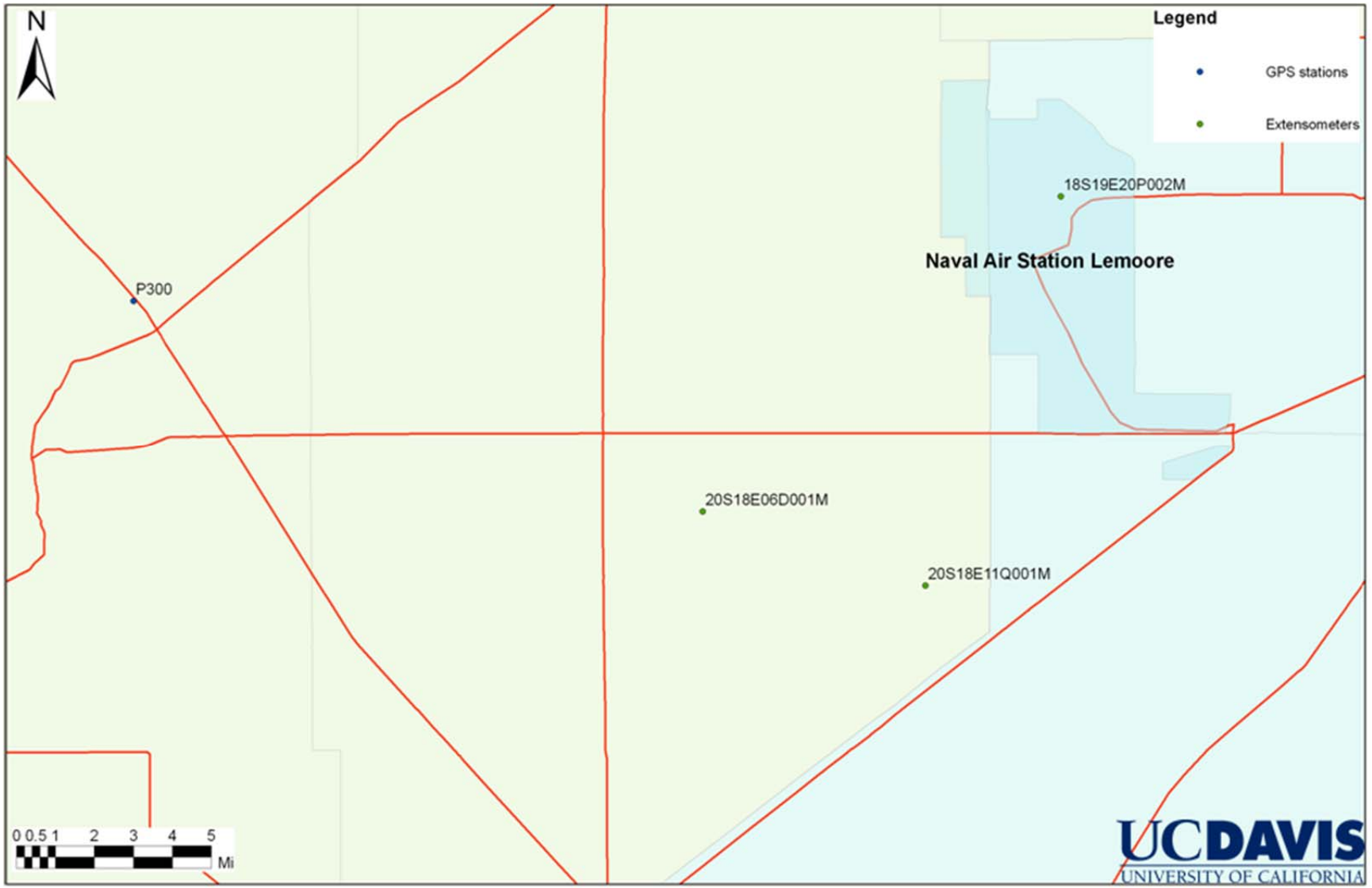

Figure 50 Study area extensometer and GPS station locations.

Extensometer 20P2 was chosen due to its location directly on NASL lands and its period of data availability. Measurements at this extensometer were usually made at daily intervals throughout the period from 1967-1980, the best temporal resolution for any subsidence data source in the NASL vicinity. Data from extensometer 20S18E06D001M (6D1) was chosen for its long data period between 1965 and 2010, and its close proximity to NASL.

Poland's subsidence studies (Ireland, Poland and Riley, 1984). Poland and others completed several reports outlining the results of subsidence studies within the Tulare Lake Basin. Of particular interest was a subsidence contour plot for the entire Los Banos - Kettleman City subsidence area, including NASL properties, completed using adjusted leveling data from 1926 and 1972 (Figure 51 (Figure 4 in original report)). This figure also includes the location of the detailed cross-section (H-H') completed to the north of NASL, with subsidence profiles created for March 1947, January 1954, November 1955, January 1958 and 1960, March 1963, 1966 and 1969, February 1972 and 1978 (Figure 52). Due to the close proximity and similar subsidence traits to NASL, the data contained within the subsidence profile H-H' was deemed useful for this study.

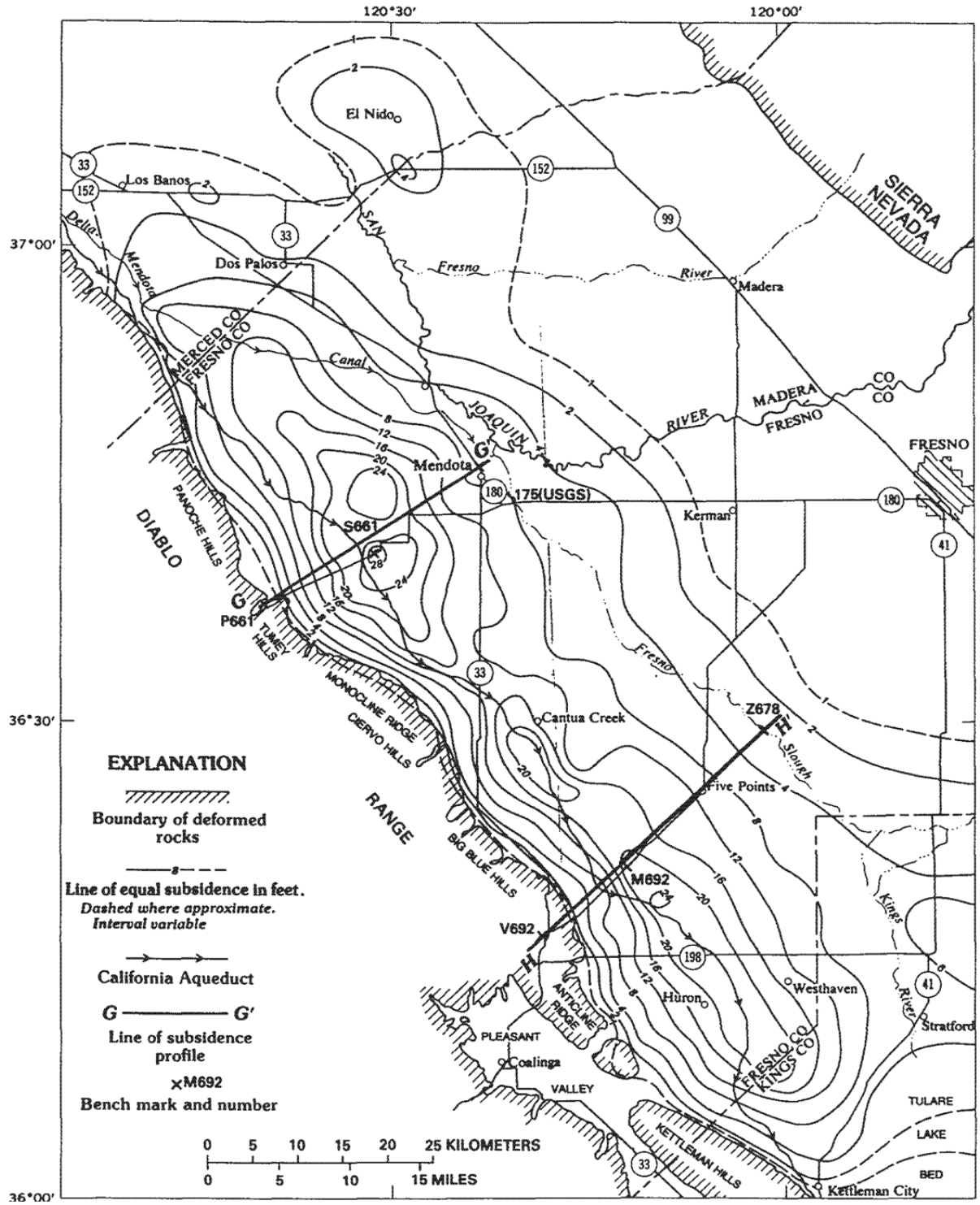

Figure 51 Land subsidence between 1926 and 1972 in the Los Banos - Kettleman City subsidence area (modified from Ireland, Poland and Riley, 1984, figure 4).

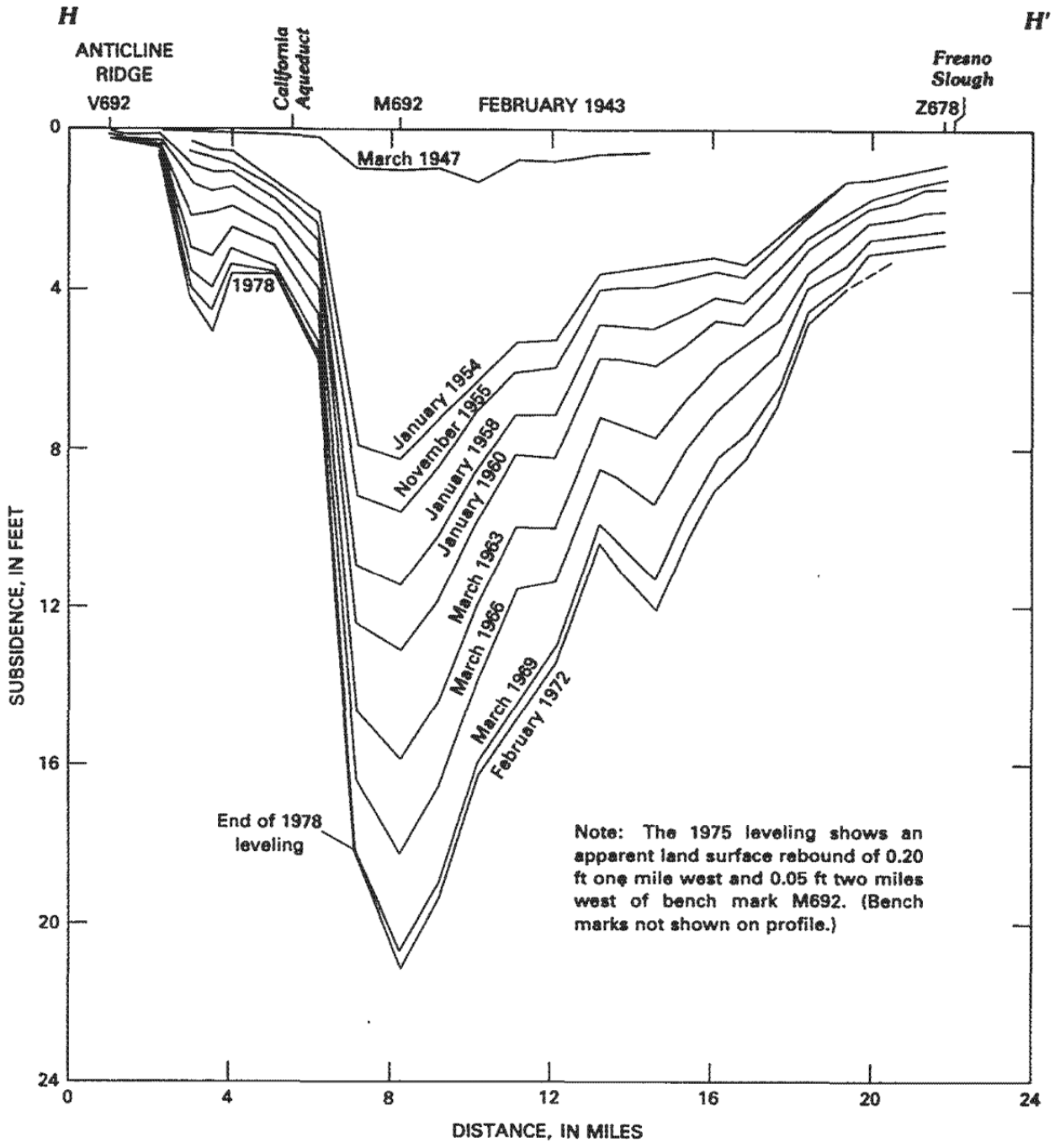

Figure 52 Subsidence profile H-H' (1943-78) (Ireland, Poland and Riley, 1984, figure 19).

GPS. In recent years, data from GPS stations has become available at the UNAVCO website (UNAVCO GPS data website, 2010). The UNAVCO website was searched for data from GPS stations located within the study area vicinity with the hope of filling data gaps from other sources. However, the nearest GPS station is at Harris Ranch (designated P300) with data

availability beginning in 2004 (Figure 50 and Figure 53). This station is not in the NASL vicinity (in an area with very different subsidence characteristics, so is of limited use for this study). P300 lies at a point that experienced less than 1 ft of subsidence between 1926 and 1972 (Figure 54) and has experienced no permanent subsidence since 2004 (Figure 53).

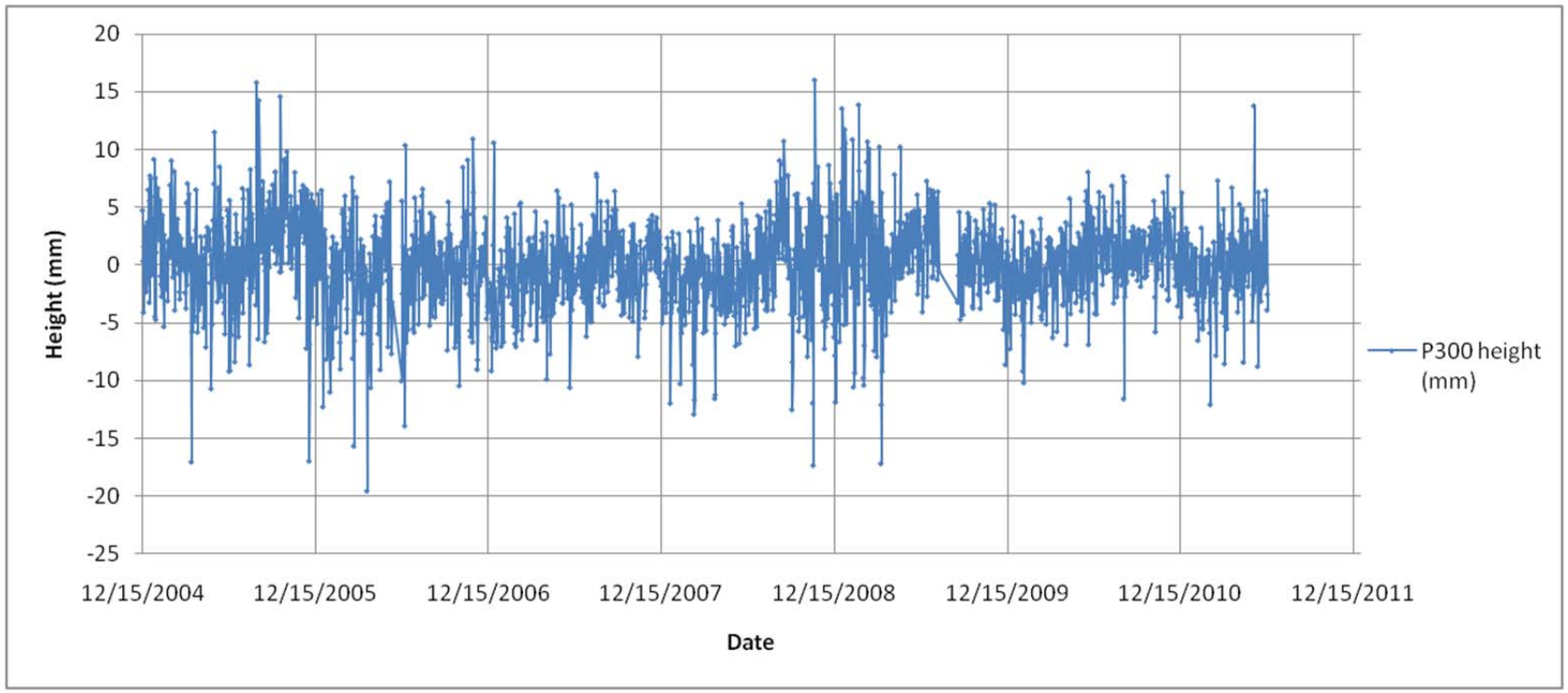

Figure 53 GPS station P300 vertical height change (2004-2011) (UNAVCO website, 2010).

Synthesis. Poland's subsidence calculations were coupled with extensometer data and the Caltrans Highway 198 leveling data to obtain a subsidence history spanning the whole model time-frame (1925-present).

As a starting point Poland's subsidence contours for the Los Banos - Kettleman City subsidence region were geo-referenced using ArcGIS (Figure 54).

To determine the subsidence history at NASL, we needed to combine time series of land subsidence available several tens of miles north of NASL, with the one-time 1960s-2004 totalized subsidence data available on or immediately adjacent to NASL from the Highway 198 benchmarks. Poland (Ireland, Poland and Riley, 1984) reports subsidence trends relative to the original land surface elevation in 1925 for the years 1947, 1954, 1955, 1958, 1960, 1963, 1969, and 1972 (Figure 52).

In his report, these data are reported only graphically (Figure 19 in Ireland, Poland and Riley, 1984) for two cross-sections, the closest of which is located along a SW-NE transect 15 miles northwest of the NASL boundary (Figure 54). In addition, the same report maps the total 1926-1972 subsidence (Figure 4 in Ireland, Poland and Riley, 1984).

To create a subsidence history of the Highway 198 benchmarks for the period prior to the 1960s, we first identified the location of the Highway 198 benchmarks on Poland's 1926-1972 subsidence map (Figure 51), then read the total 1926-1972 subsidence at those locations (e.g., 10 ft), then identified the corresponding 1972 subsidence level (e.g., 10 ft) on the A-A' cross-section (Figure 52), and then read the subsidence history prior to the 1960s from that graph.

For each of the Highway 198 benchmarks the year of measurement in the 1960s is approximately known (see Table 16). We assumed that the subsidence history of the Highway 198 benchmark prior to their 1960s measurement was identical to the corresponding locations on the A-A' cross-section during the same time period. Thus we were able to create a complete 1925 to 2004 subsidence history for the four Highway 198 benchmarks immediately adjacent to NASL. From the process outlined above, it was possible to build a subsidence history estimate at each NASL benchmark in 1926, 1947, 1954, 1955, 1958, 1960, 1963, 1966, 1969, and 1972 (Figure 59).

To obtain estimates between 1972 and 2004, and again between 2004 and the present, extensometer data was utilized. The three extensometers outlined above (20P2, 6D1 and 11Q1) all have known compaction/subsidence ratios. These ratios can be used to estimate their subsidence histories, using the assumption that the ratios remain valid at dates outside the timeframe used in the original calculation.

The key advantages of 20P2 are the detailed and reasonably long period of data availability and its location directly on NASL. The extensometer at 6D1, however, has a longer period of data availability, but is located further from NASL property than 20P2 (approximately 11 miles to the southwest of 20P2, Figure 50). Between 1967 and 1980, 20P2 experienced an estimated 1.56 ft of subsidence, compared to 2.11 ft. at 6D1. 11Q1, located approximately 10 miles south-southwest (Figure 50), was subject to an estimated 2.65 ft. in roughly the same period (Figure 57). This is possibly due to a variety of reasons, such as location (differential subsidence between the different locations) , different forms of subsidence (this may cause differential subsidence) or simply extensometer errors.

Estimated subsidence at 6D1 between 1966 and 2004 compares reasonably well to the subsidence calculated at the NASL benchmarks (3.83 ft at 6D1, in comparison to 2.84 ft (estimated) at GT1050, 3.5 ft. at GT1729, 3.63 ft. (estimated) at DH6731, 3.9 at GT1036, and 4.2 at GT0979). The ratio of subsidence experienced at 6D1 to each NASL benchmark between 1966 and 2004 was computed, and used to scale estimated subsidence at 6D1 to each NASL benchmark between 1966 and 2010.

Using this methodology, subsidence histories at the NASL benchmarks were created and are shown in Figure 58 and Figure 59. The total subsidence at NASL amounts to approximately 10 ft. between the early 1900s and current time. Much of that subsidence occurred during the middle of the 20th century, but significant subsidence has also occurred since the 1970s: the extended drought during the early 1990s triggered nearly two feet of subsidence at NASL, and the recent 2008-2010 drought appeared to be accompanied with approximately 0.5 feet of subsidence. Earlier in the 2000s, an equivalent land-rise was measured by nearby extensometers, possibly due to increasing groundwater levels.

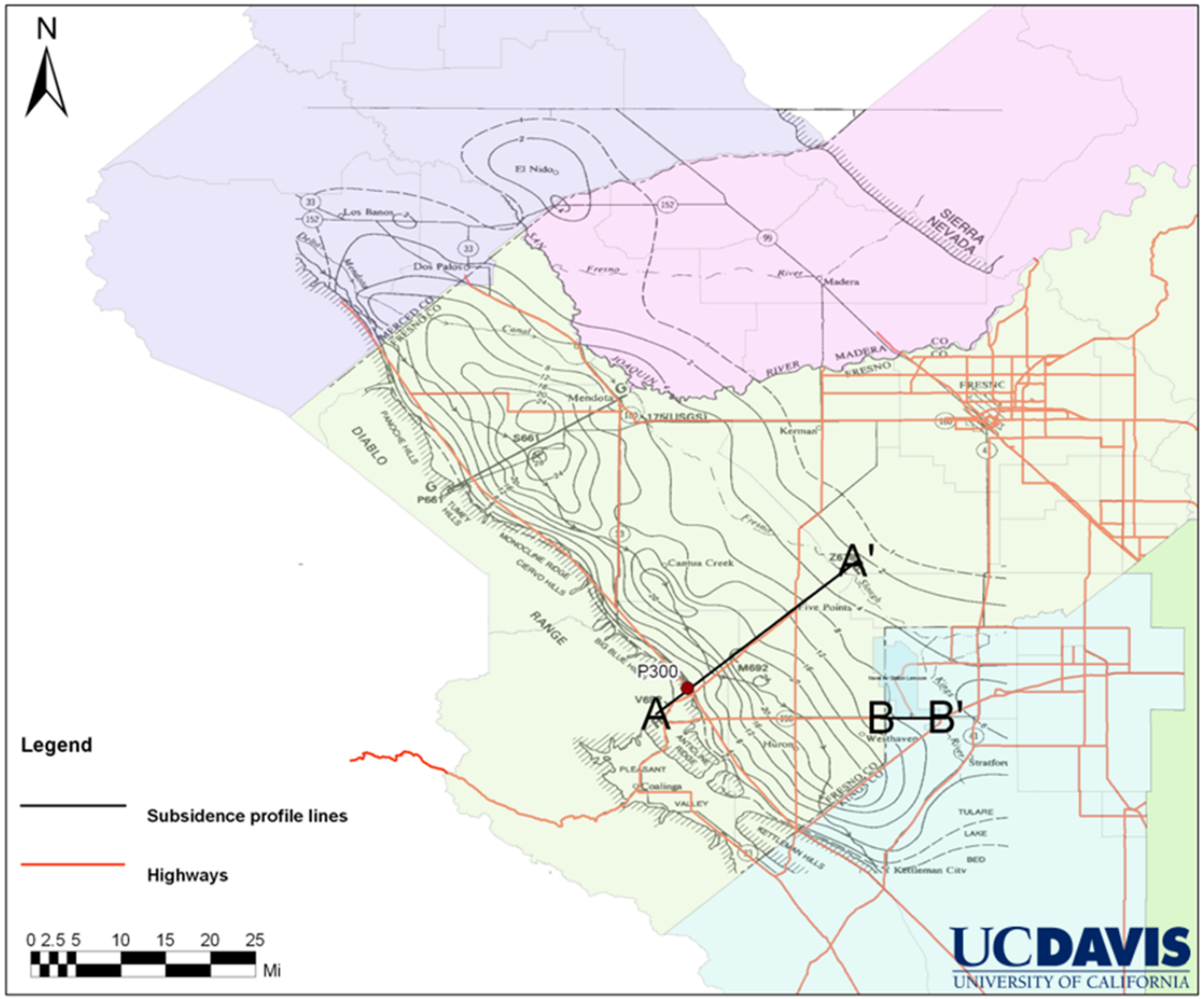

Figure 54 Geo-referenced Figure 4 from Poland (Ireland, Poland and Riley, 1984).

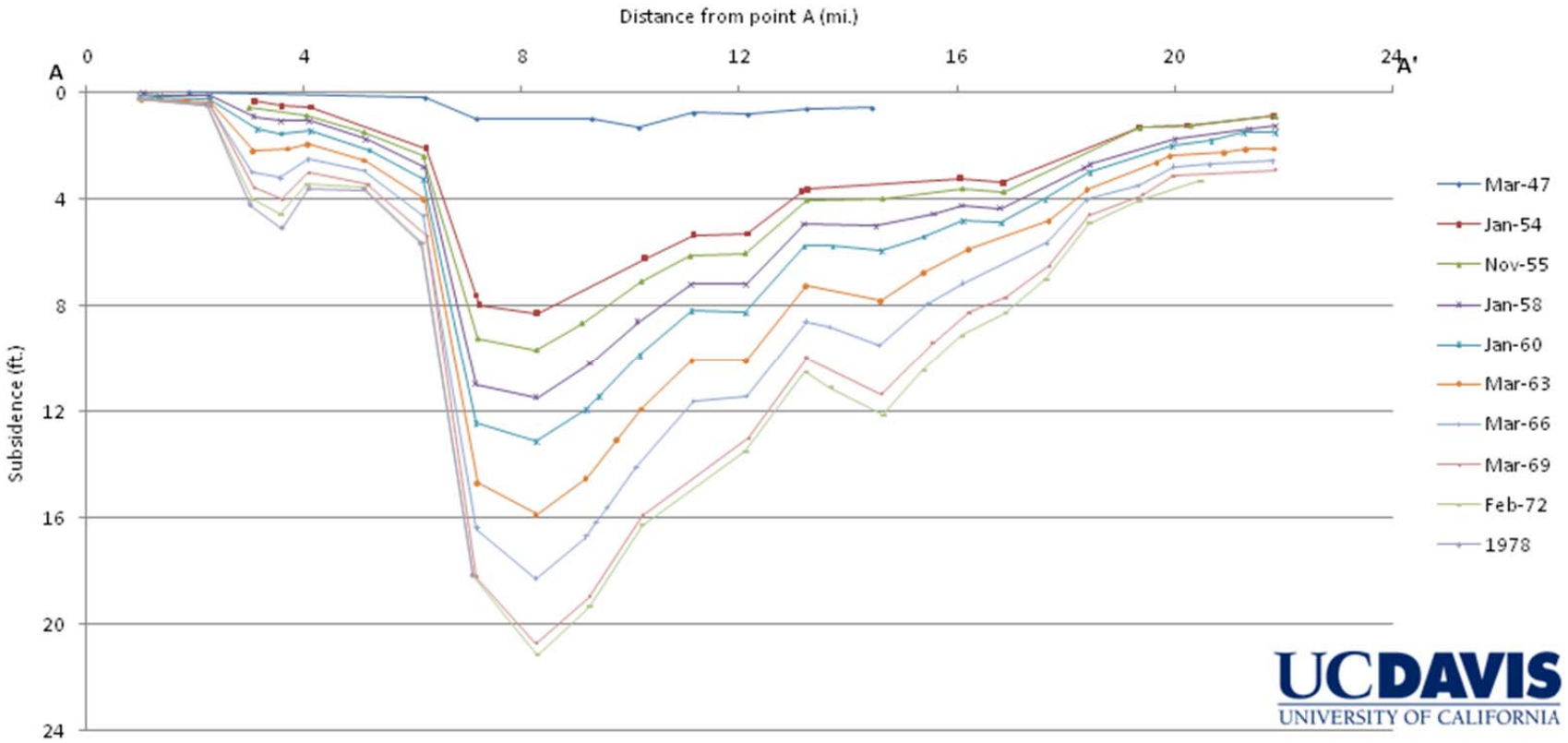

Figure 55 Subsidence profile line A-A' (digitized version of H-H' shown in Figure 52).

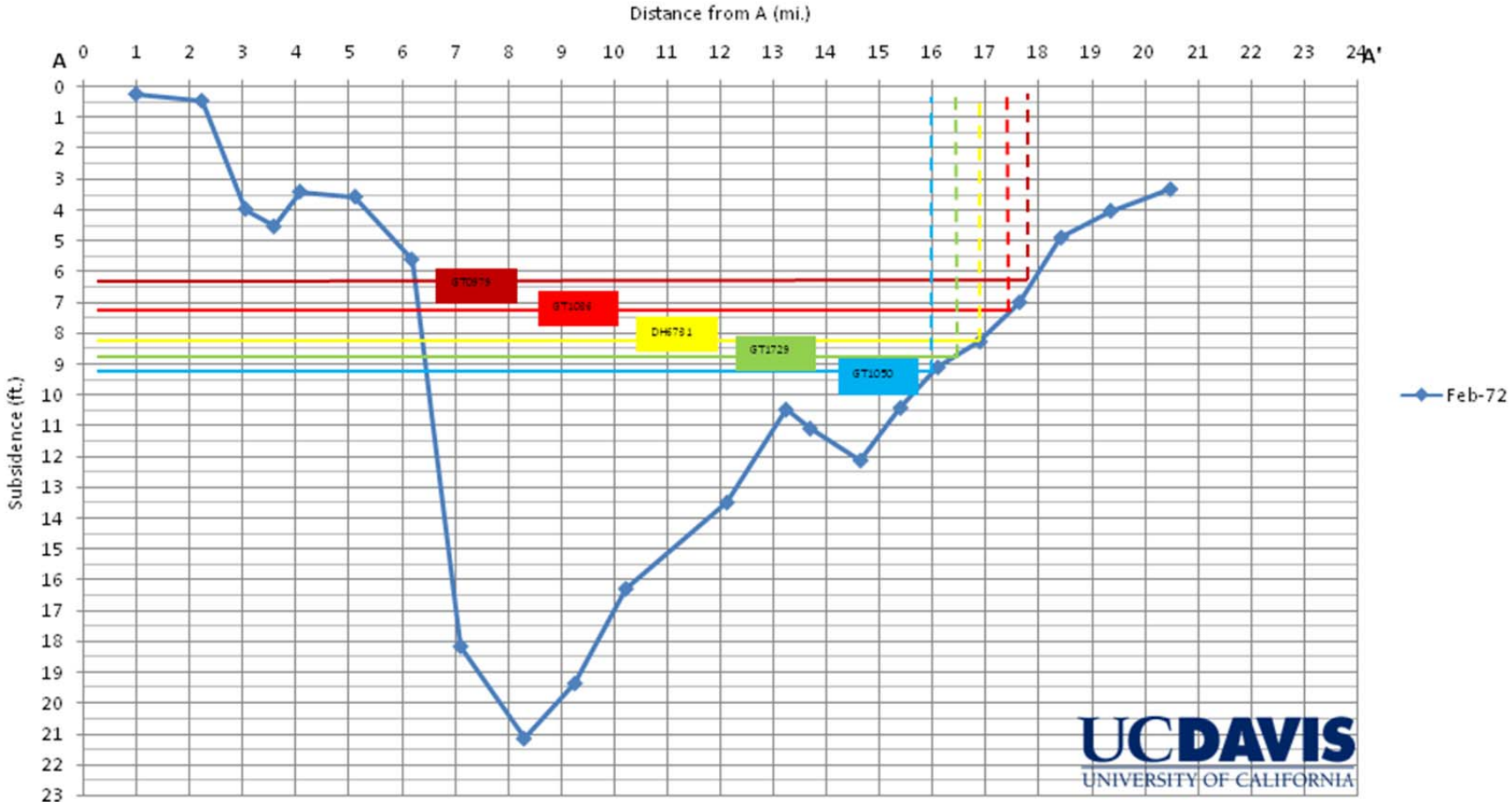

Figure 56 Digitized 1972 subsidence profile (A-A') showing method for locating NASL benchmarks.

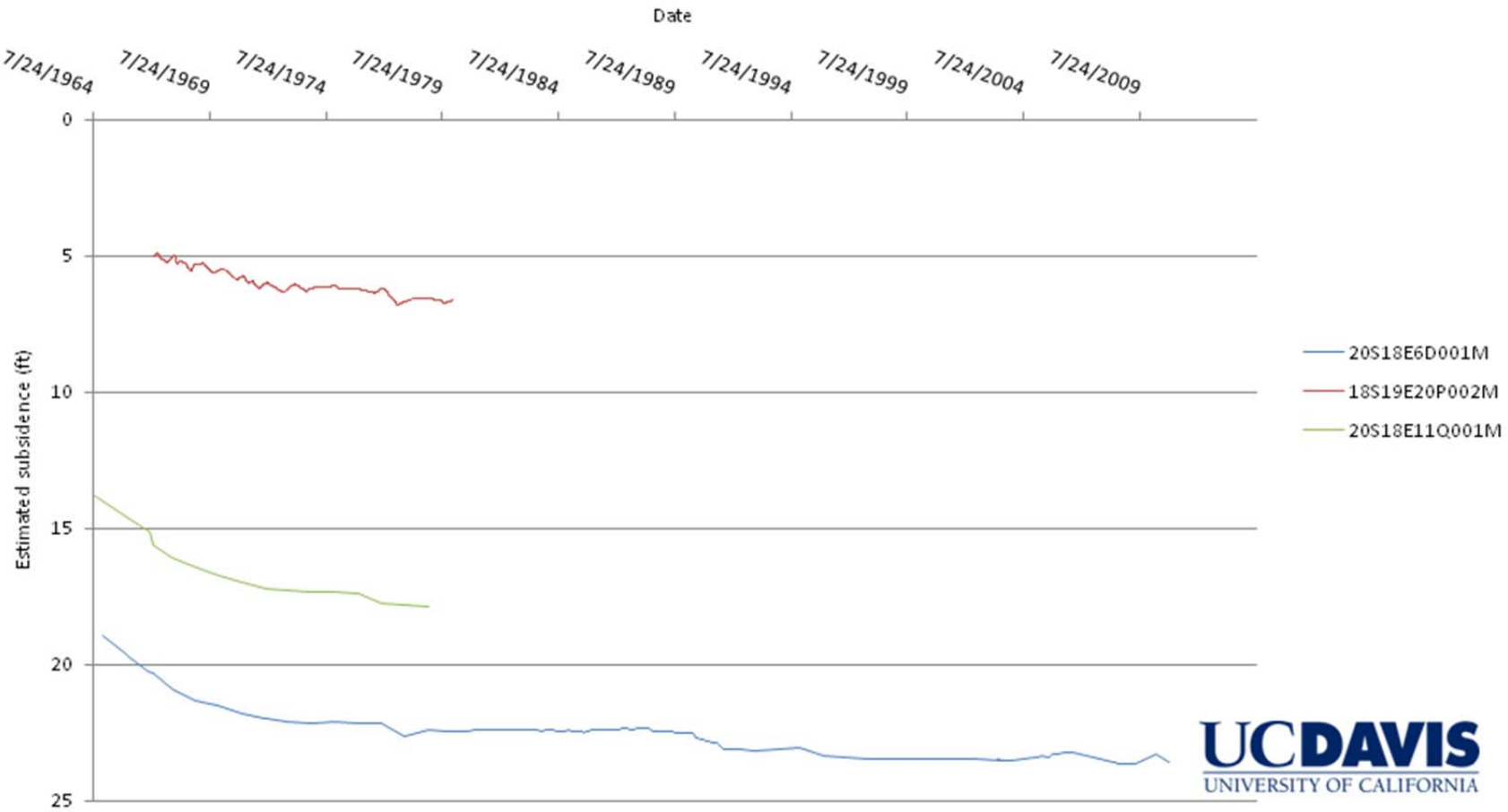

Figure 57 Estimated compaction at study area extensometers

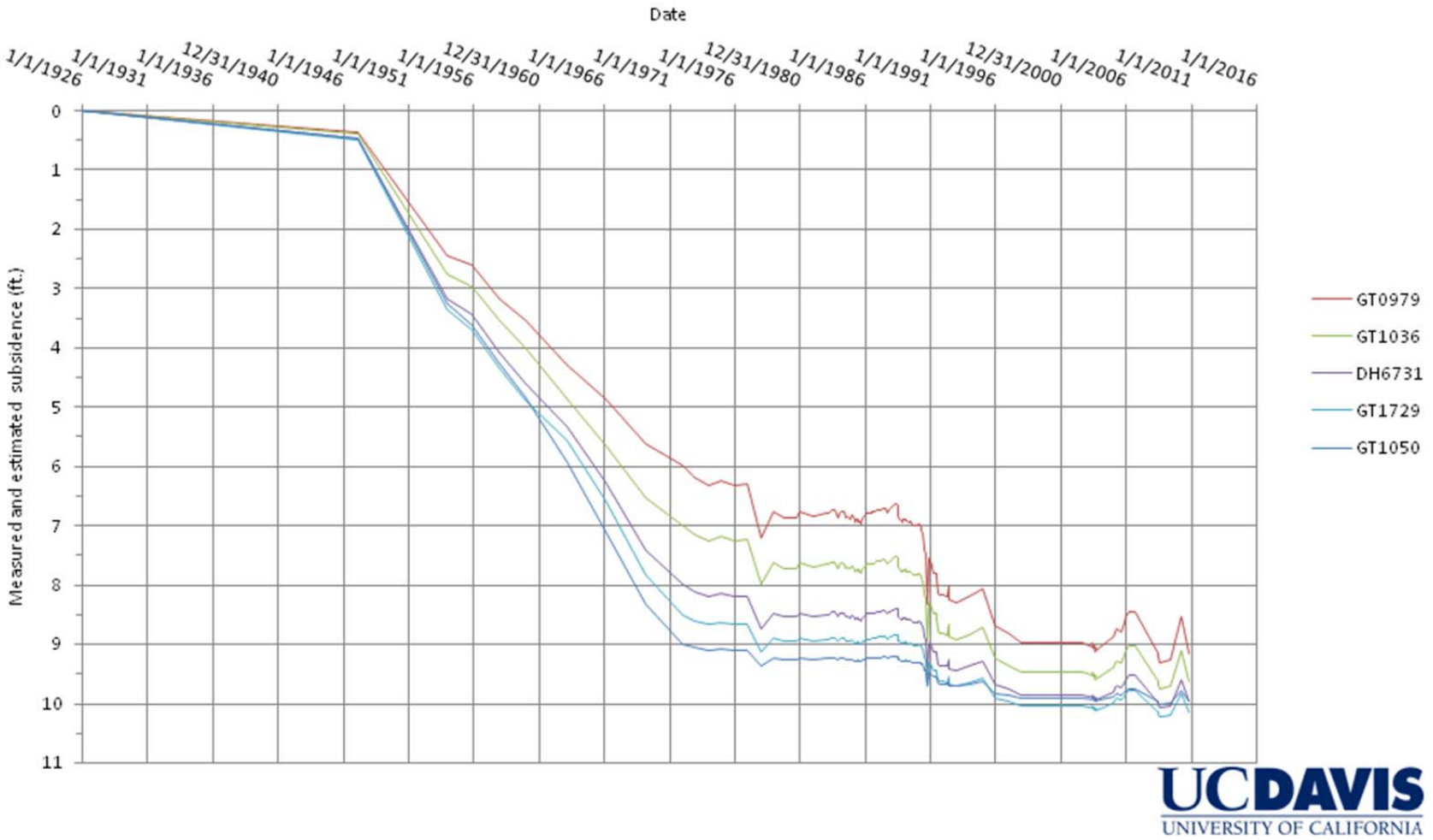

Figure 58 Estimated and measured subsidence at the NASL benchmarks.

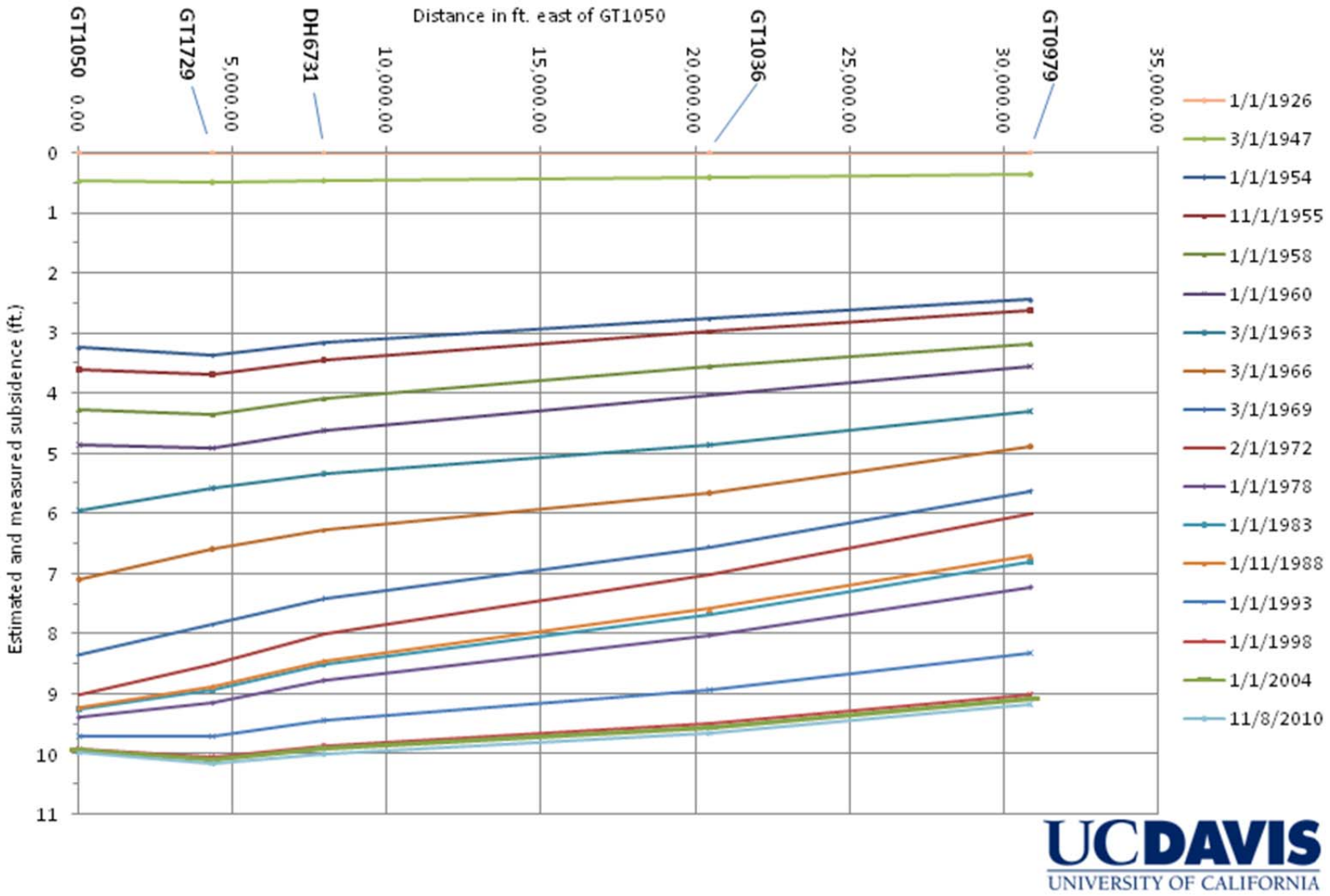

Figure 59 Selected NASL benchmark subsidence profiles from estimated and measured data.

6 Subsidence Modeling

6.1 Purpose

Subsidence records, from a variety of sources, show that a total of approximately 10 ft. of subsidence has occurred at NASL between 1925 and 2010. To gain an understanding of potential future subsidence, all available datasets were collated to develop a subsidence model.

The data gathering processes are described in earlier chapters of this report. The purpose of this modeling chapter is to describe how these data were used to formulate a subsidence model at NASL. Pertinent datasets collected were groundwater level, stratigraphy, and aquifer compaction and land subsidence data records. This chapter describes the development of a MODFLOW-2000 subsidence model and its calibration by comparing measured datasets to simulated values. The aims of this model were to adequately match the historically measured magnitudes and timing of subsidence, primarily through the refining of parameter estimates obtained from other studies. The model output is controlled principally by the aquifer stratigraphy and by historic changes in groundwater levels. This chapter therefore builds extensively on the stratigraphical model development and historic water level reconstruction described in chapter 4. The stratigraphic model is primarily based on geophysical logs that provide information on the thicknesses and depths of fine-grained and coarse-grained materials. Groundwater level records were assembled, analyzed, and simplified to generate a representative water level history as the key driver of land subsidence.

6.2 Subsidence Theory

In unconsolidated (loose) and partially consolidated sedimentary aquifers such as the alluvial aquifers in the California's Central Valley and other groundwater basins, sediment particles buried at depth experience a significant pressure due to the weight of the overlying sediments and water. Similarly, the groundwater contained within the pores of these sediments, between the individual grains of clay, silt, sand, or gravel, experiences significant pressure due to the overlying column of water, which extends to the water table. At the grain-pore water contact, the weight of the sedimentary overburden balances the pressure of the water column. A change in the water level due to groundwater pumping causes the pore water pressure in groundwater at depth to become lower. The water is therefore not able to counterbalance the weight of the overburden on the sedimentary grains. As a result, the sedimentary grains move closer together, that is, their packing arrangement becomes tighter, leading to sediment compaction. In the process, the pore space becomes slightly smaller, extruding water at the same time.

When water levels rise, pore water pressure in groundwater at depth increases. In sands and gravels, the increase in pore pressure acts on the grain surfaces and forces sediment grains

further apart, thus regaining some or all of the original volume lost. Hydrogeologists refer to this phenomenon as elastic storage change. However, in clays (fine-grained sediment particles), the increased pore pressure is not sufficient to press these very small particles apart. Hence, the compaction that occurs in clays as a result of a drop in water levels and pore pressure is irreversible. Hydrogeologists call this inelastic storage change. It is this inelastic compaction that leads to permanent subsidence over long time-frames (Hoffmann et al, 2003).

The combined effect of compression and expansion of a sedimentary basin due to water level changes leads to changes in land surface elevation. For sands and gravels alone, these changes are relatively small. But where clays are frequent within or below the aquifer system, the loss in land elevation can be significant and moreover is irreversible, hence the name land subsidence.

Clays (fine-grained sediments) inherently have two important properties: they typically have much higher compressibility than sands and gravels (they compact more under the same drop in water pressure when compared to sands and gravels). They also have much lower hydraulic conductivity (permeability) than sands and gravels, that is, water moves much slower in clays.

Groundwater levels decline when total groundwater pumping exceeds the overall groundwater recharge into the aquifer, either seasonally or as a long-term trend. Water is first drawn from areas of the aquifer system with the lowest resistance to withdrawal (sandy and gravelly sediments, which have high hydraulic conductivity). These are the first to compact – and the first to expand, however little.

Simultaneously, water is also released, albeit at a slower rate, from clay interbeds and confining units (aquitards), which begin to compact. As the extent of an aquifer-system that is drained becomes large in size, it is possible that a significant amount of the water that is subsequently withdrawn is derived from interbeds and aquitards (Poland and others, 1975). Due to the overall difference in thickness, the water contained within thick, continuous aquitard units takes even longer to drain that that from interbeds, which are generally less thick than confining units, and laterally discontinuous.

When heads stabilize and rise, the lowest head prior to the time of stabilization or trend reversal is defined as the preconsolidation head. In the case of the Central Valley, prior to large scale groundwater development, water levels would rise and fall due to minor development of groundwater prior to the 1920s. The lowest water level during this predevelopment period is referred to as the predevelopment preconsolidation head.

As the water levels begin to rise after an extended multi-year or decadal period of water level decline, subsidence rates usually slow down, but do not necessarily stop. This is due to the very slow water release from within thick clay beds (aquitards) that continue to compact as their internal pressure has not fallen as far as that in the surrounding aquifer. This is referred to as residual subsidence, and is a prominent feature in developed aquifers that contain thick interbeds of finer-grained materials. Vertical hydraulic conductivity, K_v, describes the ease with which water can pass through the pore space of a material. It is a very important parameter in

characterizing subsidence problems, as its value governs the timing of the compaction within sediments.

Heads naturally change seasonally, generally rising with groundwater recharge during the wet season, and lowering during the dry summer months, when recharge is low or non-existent. In California, the summer months coincide with the crop-growing season, when potentially large volumes of groundwater are withdrawn from the subsurface for crop irrigation, and to supplement surface water supplies. By the end of the growing season, groundwater levels are generally at their lowest, and winter month recharge may not be large enough to overcome this groundwater overdraft. This is especially true in the latter stages of a prolonged multi-year drought. Longer-term changes in groundwater levels can also be more complex, driven by anthropogenic surface-water supply issues. In the late 1960s, the San Luis Unit of the Central Valley Project was completed, to deliver water to water districts in Western Fresno, Kings and Merced Counties, including the Westlands Water District. Groundwater levels at NASL rebounded after deliveries began. More recently, due to environmental and judicial decisions in addition to drought, surface water deliveries have decreased, leading again to heavy pumping within the study area and sharply declining water levels.

A confined aquifer is one which has a confining unit as its upper boundary. Water that is obtained from such an aquifer is gained from expansion, due to pressure in the aquifer caused by the compressibility of the so-called aquifer skeleton. It is usual for the skeletal compressibility of interbeds and confining units to be as much as several orders of magnitude greater than that of the coarser-grained areas within the aquifer system. The corresponding storativities are also larger, by the same factor. These storage coefficients largely govern the overall magnitude of subsidence. Subsidence from other factors is deemed negligible (Hoffmann et al, 2003).

Karl (or Charles) von Terzaghi, a famous Austrian civil engineer active in the earlier part of the last century, was instrumental in formulating many of the modern theories in soil mechanics. In particular, his conceptualizations of clay settlement and consolidation are of direct relevance to the causes of subsidence due to groundwater withdrawal. Many of the theories and equations laid out below were developed by Terzaghi.

Terzaghi had a large role in developing the concept of effective stress, σ_e, which at a given point is described by:

$$\sigma_e = \sigma_T - p \qquad 1$$

where σ_T is the geostatic load and *p* is the pore-fluid pressure. The geostatic load is the total load of sediments and water found above this given point. Terzaghi reasoned that if an interbed is large in aerial extent relative to its thickness, then the changes in pore-pressure gradients will be mainly vertical in orientation. On the aquifer-scale this is true, but on smaller scales, for example within the area directly surrounding a pumping well, the resulting displacements can be horizontal as well. These pore-pressure gradients cause an increase in skeletal stresses, ultimately resulting in skeletal compression, that contribute to vertical compaction, particularly

in the finer aquifer and aquitard materials. In general, unconsolidated alluvial aquifers are composed of coarse-grained materials such as sand and gravel, and fine-grained materials including silts and clays. The finer-grained beds are responsible for the vast majority of overall subsidence. Aquifer-system stresses cause elastic deformations until the preconsolidation head is reached. Once the preconsolidation head (or stress) is reached or exceeded, aquifer-system deformation can be inelastic too. As the preconsolidation stress is exceeded within aquitards, resultant compaction can be 20-100 times greater in magnitude (Riley, 1998).

Specific storage is defined as the volume of fluid gained, or lost, from a discrete volume of aquifer-system sediments, per unit change in head. Head (*h*) is defined in terms of *p*, *ρ* (the density of pore water) and *g* (acceleration due to gravity):

$$h = p/\rho g \qquad 2$$

The source of this exchanged water is attributable to two sources: the expansion (or compression) of sediments due to a change in effective stress (σ_e) and/or the expansion (or compression) of fluid due to a change in pore-fluid pressure (*p*). The former of these is the dominant process experienced by unconsolidated alluvial aquifer systems. The skeletal specific storage (S_{sk}) describes the former of these processes, and since magnitudes of skeletal specific storages vary by several orders of magnitude for coarse- and fine-grained materials depending on σ_e and preconsolidation head, they are defined separately. S'_{sk} (aquitard skeletal specific storage) is defined:

$$S'_{sk} = \begin{cases} S'_{ske} = \alpha'_{ke}\rho g, & \sigma_e < \sigma_{e(max)} \\ S'_{skv} = \alpha'_{kv}\rho g, & \sigma_e > \sigma_{e(max)} \end{cases} \qquad 3$$

where S'_{ske} and S'_{skv} are elastic and inelastic aquitard skeletal specific storage properties, respectively; α'_{ke} and α'_{kv} are aquitard elastic and inelastic compressibility; and $\sigma_{e(max)}$ is the preconsolidation stress. Aquifer-system compressibility, α, is given by:

$$\alpha = \frac{-\frac{dV}{V}}{d\sigma'} \qquad 4$$

where *dV* is the incremental volume change of a volume *V*; and $d\sigma'$ is the incremental change in effective stress (σ_e). Negative compaction is termed expansion. Using the assumption that compaction is vertical gives $\bar{\alpha}$, vertical displacement:

$$\bar{\alpha} = \frac{-\frac{db}{b}}{d\sigma'_{zz}} \qquad 5$$

where *db* is the incremental thickness change of a thickness *b*; and $d\sigma'_{zz}$ is the incremental change in vertical displacement.

It can be shown, using the assumptions that hydraulic gradients within interbeds are vertical, that this delay in head equilibration, can be described by the one-dimensional heat diffusion equation:

$$\frac{\partial^2 h}{\partial z^2} = \frac{1}{D'}\frac{\partial h}{\partial t} \qquad 6$$

where z is the vertical spatial coordinate; D' is the interbed vertical hydraulic diffusivity, the ratio of the interbed vertical hydraulic conductivity (K'_v) and the interbed inelastic specific skeletal storage (S'_{skv}); and t is time from a known datum. Solving this equation, it can be shown that the time delay, $\tau_{0,}$ for an aquitard that drains from its upper and lower surfaces (a doubly-draining aquitard) is given by:

$$\tau_0 = \frac{(\frac{b0}{2})^2}{D'} \qquad 7$$

τ_0 is the time taken for approximately 93 percent of ultimate compaction to take place for a given head decline (Riley, 1969) and b_0 is the interbed thickness.

6.3 Model Formulation and Conceptual Model

Generally, the aquifer systems beneath NASL are divided into two main systems, the Hypo-Corcoran and Sub-Corcoran Aquifer systems. The sediments found above the Corcoran Clay Member of The Tulare Formation (commonly referred to as the Corcoran Clay or E-Clay) constitute the hypo-Corcoran Aquifer, and due to the interbed systems and larger, laterally discontinuous clay layers (such as the A and C-Clays) found within it, the Hypo-Corcoran Aquifer confines with depth. Due to the very large areal extent of the Corcoran Clay, the aquifer system found below this aquitard within the study area is wholly confined. For water quality and economic reasons, groundwater is seldom pumped from below 2000 ft. bgs. Shallow groundwater quality within the study area, particularly beneath NASL has been affected by a variety of anthropogenic water-quality issues. Historically, this has led to a high concentration of wells drilled to tap the more reliable sub-Corcoran aquifer-systems. As a result, historical groundwater level records for wells tapping the sub-Corcoran aquifer are plentiful, for the majority of the model simulation time-frame. Hydraulic heads within the sub-Corcoran aquifer show large temporal variations (see Figure 42), mainly caused by the large swings in historical groundwater demands due to droughts and wet period conditions.

A conceptual framework was developed for the NASL subsidence model, based on one developed by Sneed and Galloway (2000) and USGS Open File Reports 437-A-I (1964-1984), and based on on-site and nearby geophysical logs, well completion reports, and historical water level data all obtained from CA DWR. Geophysical logs and the majority of well completion reports (driller's logs) were retrieved from the CA DWR office in Fresno, CA, as detailed in chapter 4. Relevant subsidence data for NASL, to be used for model output calibration, were hard to obtain. Sources for this included Ireland and Poland's work (Ireland et al, 1984) and a subsidence study completed for Highway 198 (outlined in the previous chapter).

MODFLOW-2000 (Harbaugh et al., 2000), a finite-difference flow model developed by the U.S.G.S to solve the groundwater flow equation, was used for the modeling aspect of this subsidence study. MODFLOW-2000 was chosen, along with the subsidence and aquifer-system

compaction (SUB) package (Hoffman et al., 2003), for its modular design and successful track record in providing solutions for similar subsidence problems in California and other subsidence regions in the southwestern United States (Sneed and Galloway, 2000; Holzer, 1981). MODFLOW-2000 and the SUB package work by solving for hydraulic head and vertical displacement (the sum of compaction within a layer and all its underlying layers). The SUB package supersedes the Interbed Storage Packages (IBS1 and IBS2), and has been shown to provide better model results (verbal communication, Michelle Sneed). Parameters were constrained by values obtained from other studies, and refined by trial-and error calculations and simulations. In addition to the SUB package, the Transient Specified-Flow and Specified-Head Boundaries (FHB1) Package (Leake and Lilly, 1997), Basic 6 (BAS6) Package, Block-Centered Flow 6 (BCF6) Package, Discretization (DIS) Package, Output Control (OC) Package and Strongly Implicit Procedure (SIP) Package (all, Harbaugh et al., 2000; McDonald and Harbaugh, 1988; and Harbaugh and McDonald, 1996) were used.

MODFLOW solves the three-dimensional groundwater-flow equation given by:

$$\frac{\partial}{\partial x}(K_{xx}\frac{\partial h}{\partial x})+\frac{\partial}{\partial y}(K_{yy}\frac{\partial h}{\partial y})+\frac{\partial}{\partial z}(K_{zz}\frac{\partial h}{\partial z})\text{-}W=S_s\frac{\partial h}{\partial t} \qquad 8$$

where *x*, *y*, and *z* are Cartesian coordinates in the x-, y-, and z-directions, respectively; K_{xx}, K_{yy}, and K_{zz} are the components of hydraulic conductivity tensors in the x-, y-, and z-directions, respectively; *W* is the volumetric flux per unit volume of sources and/or sinks of water, with positive values of *W* for flow into the groundwater system, and negatives values for out-flow; S_s is the specific storage; and *t* is time from a given datum.

When an aquifer system includes compressible sediments, the term on the right hand side of equation 8 is multiplied by (1-*γ*) where *γ* is the volume fraction of compressible sediments in the aquifer system. The water entering the system from interbeds is incorporated into the *W* term on the left hand side.

In the IBS1 Package, water is assumed to have exited or entered storage in interbeds within the time-frame of a single model time-step. Therefore, interbed heads are assumed to instantaneously equilibrate with those in the adjacent aquifer. This is appropriate for thin interbeds (No-Delay- [ND-] interbeds). The SUB package adds extra functionality, with the addition of Delay- (D-) interbeds; thicker interbeds that drain over a time-frame of one time-step or greater. For ND-interbeds $\tau_0 \leq TS$, where *TS* is the model time-step length.

,$\hat{q}$ the flow per unit volume, for ND- and D-interbeds are defined as:

$$\hat{q}=\gamma S'_{sk}\frac{\partial h}{\partial t} \quad \text{with } S'_{sk}=\begin{cases}S'_{ske} & for\ h>h_{min},\\ S'_{skv} & for\ h\leq h_{min}\end{cases} \qquad 9$$

where S'_{ske} and S'_{skv} are the elastic and inelastic (or virgin) aquitard skeletal specific storages, respectively; and h_{min} is the preconsolidation stress in terms of preconsolidation head. Assuming preconsolidation stress is equivalent to preconsolidation head is only feasible if σ_T (the total stress or geostatic load) is assumed to be constant. Elastic and inelastic skeletal storage coefficients, S'_{ke} and S'_{kv}, respectively, are calculated by multiplying S'_{ske} and S'_{skv} by

b_0 (the interbed thickness). For ND-interbeds, S'_k and (the cumulative skeletal storage coefficients for a system of *N* ND-interbeds), are entered into the SUB Package, given by:

$$S'_k = \sum_{i=0}^{n} S'_{k_i} = \sum_{i=0}^{n} S'_{k_i}\ b_i \qquad 10$$

storage attributable to the compressibility of water, S_{sw}, though usually considered negligible compared to skeletal storage, is accounted for by entry in to the BCF Package. This is achieved by formulation of the variable *SF1*, the product of S_{sw} and the cumulative thickness of the confined aquifer-system including interbeds.

D-interbeds are always thicker than ND-interbeds assuming equivalent hydraulic properties, and are characterized by $\tau_0 > TS$, or practically, $\tau_0 \gg TS$ (the model time-step length). The slow dissipation of transient heads and pressures from these interbeds must be accounted for in simulations. A method for solving equation 6 at every time-step is needed. To reduce potentially long computation times, D-interbeds are aggregated into systems, with the same or similar K'_v, S'_{ske} and S'_{skv} values. B_{equiv}, the equivalent thickness of a system of *N* D-interbeds, each of individual thickness b_1,...b_N, is calculated as:

$$B_{equiv} = \sqrt{\frac{1}{N}\sum_{i=1}^{N} {b_i}^2} \qquad 11$$

given by Helm (1975). Correspondingly, $\boldsymbol{N_{equiv}}$, the multiplication factor required to provide the total thickness (and hence appropriate compaction and water budget) of D-interbeds is given by:

$$N_{equiv} = \frac{\sum_{i=1} b_i}{B_{equiv}} \qquad 12$$

Both B_{equiv} and N_{equiv} are required for entry into the SUB Package input file. They greatly decrease the computational load, as equation 6 is solved only for each ND-interbed system. In doing so, the assumption is made that heads at the top and bottom boundaries are equal at all times to the surrounding coarse-grained materials within the same model layer.

Initial conditions include prescribed heads given in the FHB1 file. The model computes heads at subsequent time-steps. The head at the beginning of the time-step is assumed constant over the full extent of the interbed surface. The dissipation of heads and compaction within the interbed are therefore assumed to occur symmetrically about its center-plane. MODFLOW-2000 exploits this by calculating solutions for the half-thickness of the interbed, with the center-plane as a no-flow boundary. A finite-difference approximation of equation 6, utilizing these boundary conditions, yields one equation for each of the *NN* cells representing the half-thickness of the interbed:

$$[A]^m[h]^m = [r]^m \qquad 13a$$

where $[A]^m$ is an *NN*x*NN* symmetric tridiagonal matrix, $[h]^m$ is an *NN*x1 vector of head values and $[r]^m$ is an *NN*x1 vector of known quantities defined in equations 13f-13h.

Elements of $[A]^m$ are:

$$A_{ij}^{m} = \frac{K_v'}{\Delta z} \quad for\ i \neq j \tag{13b}$$

$$A_{11}^{m} = -3\frac{K_v'}{\Delta z} - \frac{\Delta z}{\Delta t} S'^{m}_{sk_1} \tag{13c}$$

$$A_{ii}^{m} = -2\frac{K_v'}{\Delta z} - \frac{\Delta z}{\Delta t} S'^{m}_{sk_1} \quad \text{for } 1 < i < NN \tag{13d}$$

$$A_{NN\,NN}^{m} = \frac{K_v'}{\Delta z} - \frac{\Delta z}{2\Delta t} S'^{m}_{sk_{NN}} \tag{13e}$$

$$r_1^m = \frac{\Delta z}{\Delta t}[-S'^{m}_{sk}\, H'^{m-1}_{1} + S'_{ske}(H'^{m-1}_{1} - h'^{m-1}_{1})] - 2\frac{K_v'}{\Delta z} h_j^m \tag{13f}$$

$$r_i^m = \frac{\Delta z}{\Delta t}[-S'^{m}_{sk}\, H'^{m-1}_{i} + S'_{ske}(H'^{m-1}_{i} - h'^{m-1}_{i})] \quad \text{for } 1 < i < NN \tag{13g}$$

$$r_{NN}^m = \frac{\Delta z}{2\Delta t}[-S'^{m}_{sk}\, H'^{m-1}_{NN} + S'_{ske}(H'^{m-1}_{NN} - h'^{m-1}_{NN})] \tag{13h}$$

where K_v' is the vertical hydraulic conductivity of interbed material (assumed constant for each system); Δz is the distance between two finite-difference nodes (assumed constant as the percentage decrease in interbed thickness is small); Δt is the time-step length; $S'^{m}_{sk_1}$ is the skeletal specific storage at node *i* and time-step *m*; h_j^m is the head in the aquifer cell *j* to which the node at the interbed boundary is coupled at the end of time -step *m*; H'^{m-1}_{i} is the preconsolidation head at node i at the end of time-step *m-1*; and - h'^{m-1}_{1} is the head at node i at the end of time-step *m-1*.

Equations 13 are solved iteratively for each system, layer etc. at every time-step. When the SUB Package is used, these equations are coupled with the three-dimensional groundwater flow equation (equation 8). The solutions at each time-step must converge to a solution, or the simulation will not terminate correctly.

The simulation time-frame was chosen to begin at a time preceding large-scale groundwater development in the Valley. As discussed earlier, 1925 was chosen, and studies by Poland and others of subsidence-prone areas within the Valley used data from as early as 1920. The simulation time was extended to late 2010, and into the near future (2015) based on water levels measured at NASL in 2010.

Parameters were constrained using values from various subsidence studies, mainly completed within the NASL vicinity. A particularly useful source was 'Hydraulic and Mechanical Properties Affecting Ground-Water Flow and Aquifer-System Compaction, San Joaquin Valley, California' (Sneed, 2001), a report that includes parameters calculated by Poland directly at NASL.

Spatial and temporal discretizations were chosen based on data availability and feasibility. Beneath NASL, sediments comprise the Valley fill to depths in the neighborhood of 14,000 ft. bgs, before the basement complex is reached. A literature review was performed, based primarily on a recent modeling study of the Central Valley (Faunt, 2009), to ascertain the thicknesses of developed aquifer-systems, and the model domain and discretization were accordingly chosen. The one-dimensional, vertical model domain extends from 12 to 2012 ft. bgs. A no-flow boundary exists at the bottom of the model domain. The groundwater below approximately 2000 ft bgs is rarely pumped due its low quality. A temporal discretization

consisting of 85 annual (each 365.25 days) stress periods (from 1925-2010), was sub-divided into 12 monthly (30.4375 day) time steps. These time-frames are used by MODFLOW-2000 to calculate volumetric budgets for each model cell, and hence for the model domain as a whole. This discretization was deemed adequate to characterize the temporal water-level measurements, balancing the potential mass balance errors with computation time.

The MODFLOW-2000 Discretization Package input was used to divide the domain into layers. For the SUB Package, each layer is sub-divided based on its material properties, such as clayey interbeds and coarser-grained sediments. Each layer is also horizontally divided into rows and columns, forming model cells. For the NASL model, 3 geologic layers (hypo-Corcoran, Corcoran, and sub-Corcoran) are divided into 8 discrete model layers to characterize the vertical domain. Since we do not consider horizontal changes in stratigraphy, our 1-dimensional model is based on an arbitrary uniform lateral model extent (1 foot by 1 foot) (Figure 60).

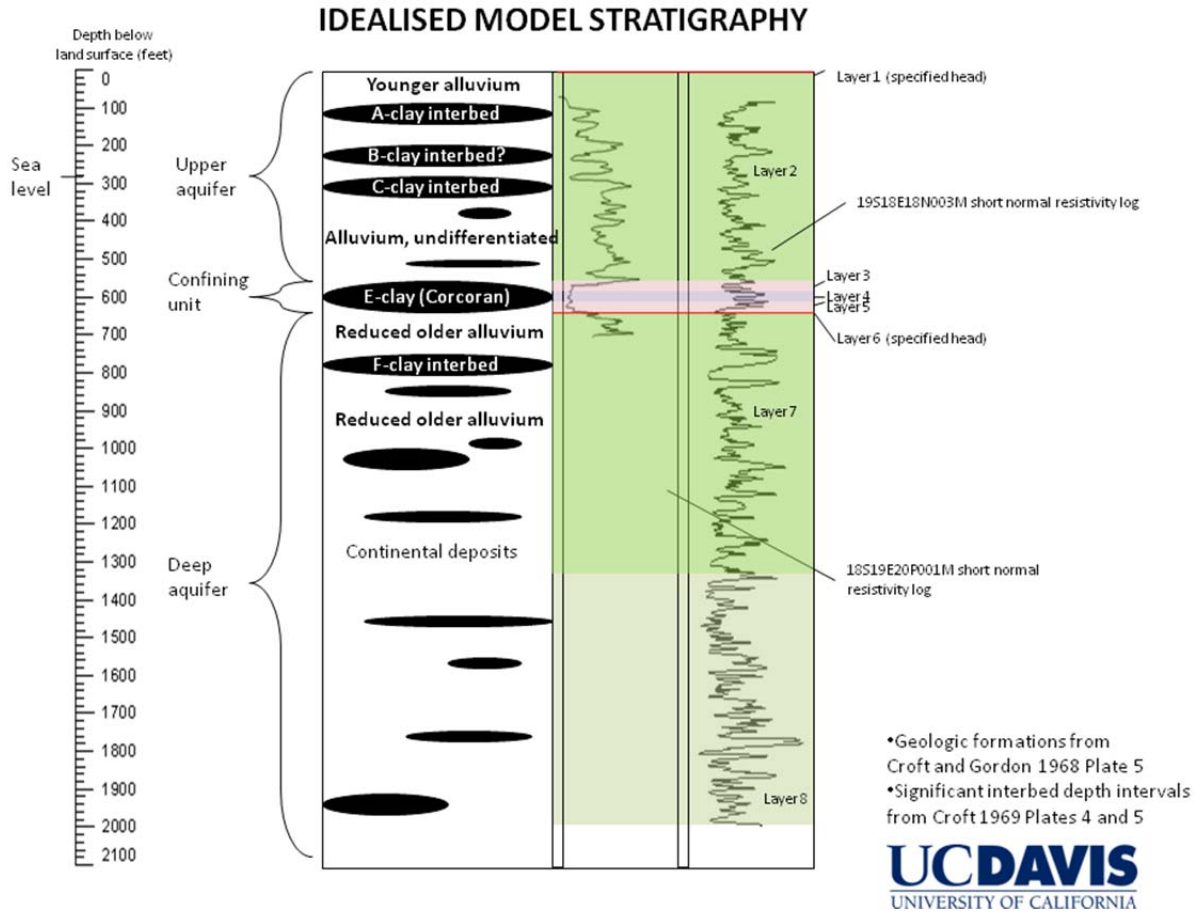

Figure 60 Model spatial discretization.

Confining units are defined using whole layers, whilst interbeds are grouped together with water-bearing sediments and incorporated into aquifer-system layers. These confining unit layers are described using both elastic and inelastic storage coefficients, whereas the coarser aquifer layers are described only by their elastic storage coefficients. The interbeds are grouped into systems of ND- and D-interbeds, as described above. Interbed time constants for chosen thicknesses using calibrated data are shown in Table 19. The only confining unit represented within the model domain is the Corcoran Clay, a regionally extensive - and in many locations, thick - clay layer. Beneath the NASL site, the Corcoran Clay, is approximately 80 ft. thick. The SUB Package documentation (Hoffman and others, 2003) recommends the splitting of thick aquitards into multiple layers, to increase the accuracy in computing flow and storage changes. This, however, also increases computation time and requires an increase in computer memory allocation (not a significant concern in the case of the NASL model).

The FHB1 package is used to incorporate water-level data into the subsidence model. Data for all wells were collated and plotted using Matlab Software by Mathworks. Separate water level trajectories were computed for the hypo- and sub-Corcoran aquifer systems using these data, as described in earlier chapters. For the period of data availability, groundwater levels for the hypo-Corcoran Aquifer have remained relatively constant (see Figure 41). Because of this, the initial groundwater level measurement of 3 ft. was used for all water-level inputs between 1925 and 1957, starting at the beginning simulation time (1925). The FHB1 Package was used to assign these groundwater level records, along with interpolated estimates, at approximate yearly intervals, to certain specified-head layers. Layer 1 (the uppermost model layer), was used to assign measured and estimated groundwater levels to the hypo-Corcoran Aquifer. Layer 6 (the top-most model layer within the sub-Corcoran Aquifer) was used to assign sub-Corcoran Aquifer groundwater levels. Both of these model layers were limited to one foot in thickness as explained later in model assumptions and limitations.

The DIS Package was used to enter spatial and temporal model discretization data. The total number of layers (8) was determined empirically, as this configuration produced smooth model runs and allowed sufficient geologic detail. The hypo-Corcoran aquifer system was divided into two layers. Layer 1 was used as a 1 foot thick specified-head layer (as described above) and layer 2 was chosen to incorporate the remaining mixed aquifer sediments between layer 1 and the Corcoran Clay layers. Layers 3, 4 and 5, all 24 foot in thickness, represent the Corcoran Clay. As per SUB Package documentation instructions, these layers were assigned as ND-interbeds within the SUB Package input file (multiple adjacent ND layers account for the delay). Immediately below the Corcoran Clay layers, layer 6 was set as a 1 foot thick specified-head layer. Layers 7 and 8 make up the remaining portion of the sub-Corcoran aquifer-system. Layer 7 is 685 ft. thick, whilst layer 8 is 679 ft. thick.

The BC6 input file is used to input the variables *SF1* (the primary storage coefficient - described above), transmissivity and equivalent vertical leakance (*VCONT*) for each layer. *VCONT* is given by:

$$(K_v/b)_{k+1/2} = \frac{2}{b_k/(K_v)_k + b_{k+1}/(K_v)_{k+1}} \quad 14$$

where b_k is the thickness and $(K_v)_k$ is the vertical hydraulic conductivity of model layer *k*. As *VCONT* for model layer *k* is calculated by using values from the model layer below (*k+1*), a *VCONT* value for the bottom model layer is not needed.

The SIP solver Package was used also used in NASL subsidence model simulations. A head change criterion of was 1.00×10^{-3} was specified in the SIP Package input file, meaning that when the maximum absolute value of head change from all nodes is less than or equal to this value, model iteration ceases.

Parameter values used in equations to describe aquifer-system properties by MODFLOW-2000 were required for model input. Estimates for K_v, S_{skv} and S_{ske} were obtained from various sources, the most useful being the report 'Hydraulic and Mechanical Properties Affecting Ground-Water Flow and Aquifer-System Compaction, San Joaquin Valley, California' (Sneed, 2001). This report was completed to summarize parameters to be used in the development of the WESTSIM model (a U.S. Bureau of Reclamation combined ground- and surface-water model), and includes K_v, S_{ske} and S_{skv} values measured and estimated at sites close to or directly at NASL. Laboratory, field and calibrated model parameter values are presented and discussed. Parameter values from previous studies, including Poland's multiple subsidence studies within the Tulare Basin, are also included.

Parameter estimates: Beginning in 1961, Poland and others studied sites within the LB-KC subsidence area, with the focus being on storage properties derived from aquifer tests. The problems of using short-term aquifer tests are also discussed.

Riley (1969) developed a graphical method for computing elastic and inelastic storage coefficients (S_{ske} and S_{skv}) whilst completing a study at the prominent Pixley site (about 3 mi. to the south of Pixley, within the Tulare-Wasco subsidence region). His method involves plotting applied stress (head) on the y-axis, versus compaction (strain) on the x-axis. For aquifer-systems where pressure equilibrations between the aquitards and aquifer-systems can occur rapidly, the inverse slope of the predominant linear stress-strain trajectory are representative of the skeletal storage coefficients. This generally holds true for interbeds, but not thicker aquitards, such as the Corcoran Clay, that have slower pressure equilibration rates.

Bull and Poland (1975) performed stress-strain analyses, using Riley's method described above, on a well located on NASL lands (well 18S19E20P2M). From this, values for S^*_{sk} and S^*_{ske} (aquifer-system elastic skeletal storage coefficient and aquifer-system elastic skeletal specific storage, respectively) were calculated for the portion of the aquifer between 230 and 577 ft bgs. Bull and Poland (1975) also report S^*_{ske} results from well 19S16E23P2 (southwest of NASL) for the complete modeled aquifer thickness of 0-3,300 ft. bgs. The mean value is included in Table 17, but it is reported that this value may be too small.

Laboratory consolidation tests (CTRs) have also been completed at multiple sites within the Valley. Terzaghi's (1943) soil consolidation theories are used to calculate the coefficient of

consolidation (for the inelastic range), C_v, and K_v. In CTRs, saturated soil samples are subjected to a variety of loads. Initially, the water within the sample bears the entire load due to its relative incompressibility. As water escapes, the load is transferred to the sample sediments, resulting in reduction in overall volume. The rate of transfer is slower for finer-grained sediments (Sneed, 2001). C_v is calculated by:

$$C_v = (T_{50}{H_{50}}^2)/t_{50} \quad 15$$

where T_{50} is the time factor at 50 percent consolidation; H_{50} is the half-thickness of the sample at 50 percent consolidation; and t_{50} is the time needed for 50 percent consolidation. At maximum loading, K_v is calculated as:

$$K_v = C_v\gamma_w(e_0 - e)/\Delta p(1+e_0) \quad 16$$

where γ_w is the specific weight of water, e_0 is the void ratio at the starting load, e is the final void ratio, and Δp is the increment of load. S_{skv}, is defined as:

$$S_{skv} = K_v/C_v \quad 17$$

CTR results are available for wells 19S17E22J1M and 19S17E22J2M, located within the study area at Huron. Results are included for multiple depth intervals, and multiple load ranges. Originally, the CTR results used in this report where reported in Johnson and others (1968). Differing parametric values were assigned to model layers within the hypo-Corcoran, Corcoran, and sub-Corcoran aquifer sub-systems (Table 18). Two criteria were used to obtain relevant parameter values from the CTR results.

1. Fine-grained samples were of most interest, so only samples with >90 percent clay were used.

2. Generally, sample results are reported for several load ranges for each sample. Care was taken to select relevant load ranges for each depth interval, to adequately represent the geostatic load. In general, deeper samples are likely to be subjected to a larger geostatic load, so the appropriate (higher) load ranges were chosen.

Sample results were collected for each aquifer-system - hypo-Corcoran, Corcoran Clay and sub-Corcoran - that met the above criteria. The average of these K_v and S_{skv}values was calculated for each aquifer system. Other Central Valley subsidence modelers (verbal communication, Michelle Sneed, March 2011) have found that these averaged parametric values need to be multiplied by a factor of approximately 5 during model calibration.

Model parameters were further constrained by the modeling results of previous calibrated model simulations. Helm (1975, 1976, 1977 and 1978) completed inverse model simulations for several extensometer sites within the Valley, in the vicinity of the Pixley site. These values, whilst not in the immediate vicinity of NASL, are useful due to the similarity in geology at the two sites. When Helm (1976) used stress-dependant parameters, K_v' values were assigned as $3.4\text{x}10^{-3}$ ft/yr near the midplane of an idealized aquitard, and almost an order of magnitude less at the drainage faces ($3.0\text{x}10^{-4}$ ft/yr). However, the calibrated scenario, for compaction without expansion, returned a K_v' value of $2.5\text{x}10^{-3}$ ft/yr. Corresponding S_{kv}' were also reported. Helm

argues that even though simulations run with stress-dependant parameters match measured compaction more closely over the short term, carefully chosen values of K_v' and S_{skv}' have the potential to provide good and even better results over longer time-periods (Helm, 1976).

Larger-scale models, with a wide range of modeling interests that include subsidence, have also been completed. The U.S.G.S.'s Regional Aquifer-System Analysis (RASA) models, initiated in 1978 and completed in 1995, have very large spatial domains and were designed to cover each of the nationally important aquifer systems. A total of 25 aquifer-systems were studied, of which the Central Valley is included (Williamson et al., 1989). The WESTSIM model (mentioned above), has a far smaller domain than the RASA Central Valley domain, covering the west-side of the S.J. Valley from the City of Tracy at its northern boundary and the City of Avenal as its southern boundary. The Central Valley Hydrologic Model (CVHM) (Faunt, 2009), like the RASA model, covers the whole areal extent of the Central Valley, and incorporates subsidence modeling as a component.

CONSTRAINING PARAMETER VALUES						
Method	**Source well**	**Subsidence region**	**K_v (ft/day)**	**S_{ske} (ft^{-1})**	**S_{skv} (ft^{-1})**	**D depth interval bgs (ft bgs)**
Stress-strain analyses	23S/25E-16N	Tulare-Wasco	8.21x10^{-6}	-	1.4e^{-4}-3.0e^{-4}	355-760
	18/19-20P2	Los Banos - Kettleman City	-	6e^{-7}-3.5e^{-6}	-	230-577
			-	7e^{-7}-3.1e^{-6}		0-2,200
Calibrated models	18/19-20P2	Los Banos - Kettleman City	-		6.70E-04	0-578
	19S16E23P2		-		3.00E-04	0-3,300
	20S18E11Q1		-	-	1.40E-04	0-710
	12S12E16H1		2.10E-05	1.70E-06	5.80E-04	30-380
			1.75E-06	1.70E-06	1.75E-03	380-467.1
			1.70E-05	1.70E-06	6.50E-04	467.1- 1,200
Laboratory consolidation tests (LCTs)	19S17E22J1,2	Los Banos - Kettleman City	7.12E-06		1.70E-04	311.5-311.9
			1.20E-05		8.4E-05	734.6-734.9
			1.58E-06		3.8E-05	904.9-2,021

Table 17 List of selected constraining parameters from previously conducted stress-strain analyses and calibrated models (Sneed, 2001, and written communication, Michelle Sneed, USGS Sacramento).

Model layer temporal discretization						SUB Package input								BC6 Package input	
Aquifer system	Layer	Layer top depth (ft)	Layer bottom depth (ft)	Layer thickness (ft)	Cumulative interbed thickness (ft) [%]	K'_v (ft/d)	Sfv (ND layers)	S'_{skv} (ft^{-1})	Sfe (ND layers)	S'_{ske} (ft^{-1})	HC (ft)	B_{equiv} (D layers) (ft)	N_{equiv} (D layers) (ft)	Sf1	VCONT (d^{-1})
Hypo-Corcoran	1	12	13	1	0 [0.00%]	7.10E-06	N/A	1.70E-05	N/A	4.00E-06	-3	N/A	N/A	4.42E-06	1.08E-04
	2	13	565	552	134 [10.58%]	7.10E-06	5.10E-05	1.70E-05	2.21E-03	4.00E-06	-3	15.91	7.86	2.32E-04	9.95E-07
Corcoran	3	565	589	24	24 [1.89%]	1.20E-05	8.40E-03	3.50E-04	9.60E-05	4.00E-06	-2.25	N/A	N/A	1.01E-05	5.02E-07
	4	589	613	24	24 [1.89%]	1.20E-05	8.40E-03	3.50E-04	9.60E-05	4.00E-06	-1.5	N/A	N/A	1.01E-05	5.02E-07
	5	613	637	24	24 [1.89%]	1.20E-05	8.40E-03	3.50E-04	9.60E-05	4.00E-06	-0.75	N/A	N/A	1.01E-05	1.00E-06
Sub-Corcoran	6	637	638	1	0 [0.00%]	1.60E-06	N/A	1.30E-05	N/A	1.20E-06	0	N/A	N/A	1.62E-06	8.75E-05
	7	638	1323	685	485 [38.28%]	1.60E-06	7.80E-05	1.30E-05	8.22E-04	1.20E-06	0	42.39	11.30	2.88E-04	4.40E-05
	8	1323	2002	679	576 [45.46%]	1.60E-06	N/A	1.30E-05	N/A	1.20E-06	0	44.13	13.05	2.85E-04	N/A

Table 18 List of calibrated model parameters. Underlined values were entered into the SUB and BC6 packages.

Holzer, 1981, reported on subsidence conditions in various parts of the USA, namely in Texas, Arizona, Nevada and California. Water level decline before preconsolidation stress, or preconsolidation head, is reached at these sites vary from as little as 16 m (52.5 ft) bgs to as much as 63 m (approximately 207 ft) bgs. Preconsolidation head is reported as 26 m (85 ft) bgs at a site within the Tulare-Wasco subsidence region. For the calibrated NASL subsidence model, -3 ft. bgs and 0 ft.bgs (initial heads) were applied to the hypo-Corcoran and sub-Corcoran aquifer systems, respectively, with linearly varying numbers assigned to the Corcoran Clay layers in between.

AQUIFER SUB-SYSTEM	3 ft. interbed (days)	4 ft. interbed (days)	7 ft. interbed (days)	8 ft. interbed (days)	10 ft. interbed (days)
Hypo-Corcoran	5.4	9.6	29.3	38.3	59.9
Corcoran (72 ft thickness)	----------37,800----------				
Sub-Corcoran	18.3	32.5	99.5	130.0	203.1

Table 19 Interbed time constants for chosen depths.

6.4 Model Results

Trial-and-error calculations were completed, with differing parameter combinations, until the difference between measured and simulated subsidence time-series data was minimized. Calibrated values are shown in Table 18.

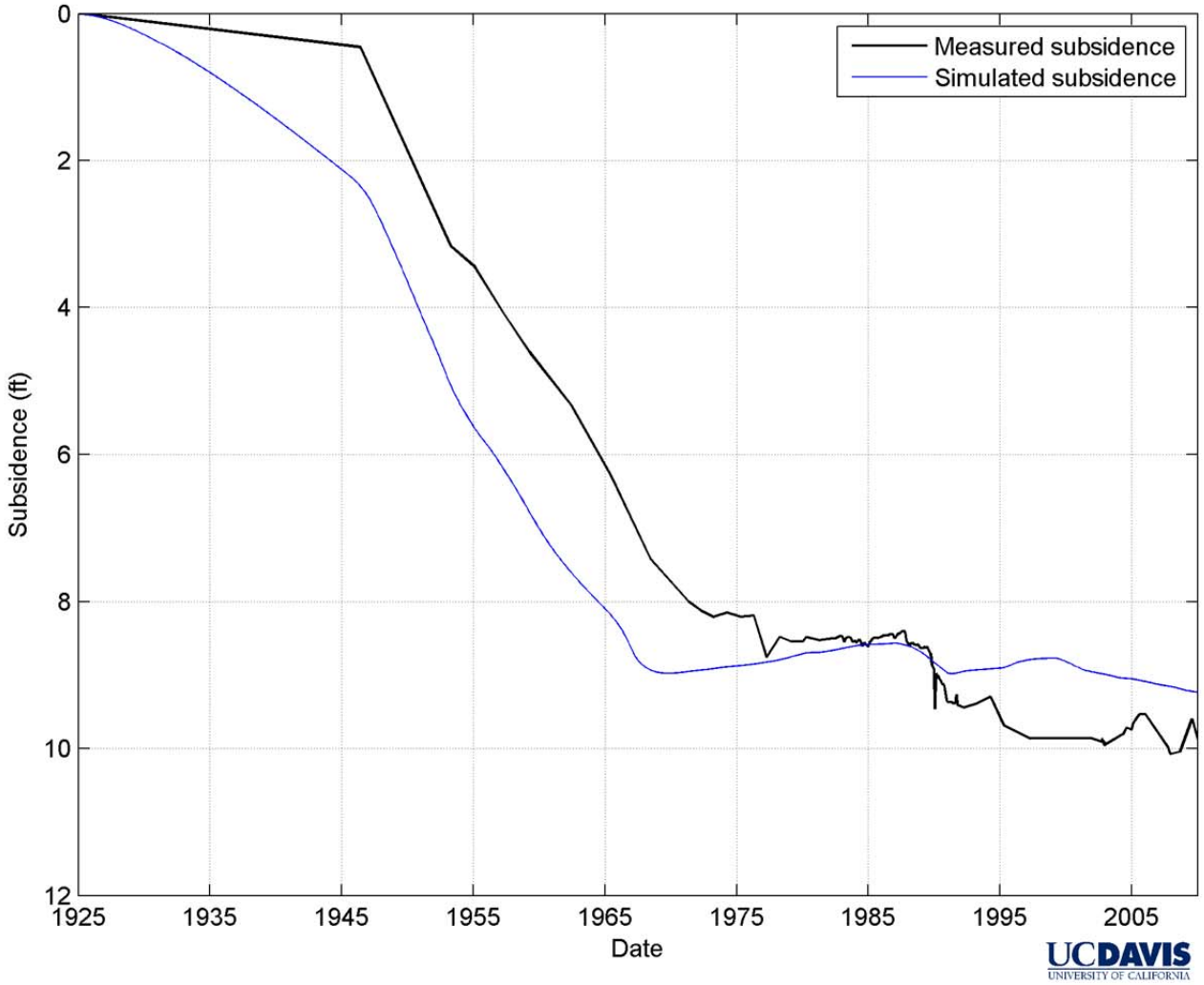

Figure 61 Simulated and measured subsidence results at NASL

Subsidence data (described earlier) from various sources was compiled to complete a continuous subsidence record from 1925 to 2010. As can be seen in Figure 61, measured and simulated subsidence are a reasonably good match. Simulations show that subsidence rates greatly accelerated between 1945 and 1975. As mentioned earlier, pumping technologies greatly improved in the mid-1930s, and as a result subsidence was initially realized as a problem within the San Joaquin Valley (Johnson and others, 1968). The majority of subsidence occurred within this same time-frame (approximately 8.0 ft.). The effects of surface water deliveries from the SLC, beginning in the late 1960s, are evidenced in the form of a reduced subsidence rate. After the completion of the SLC in the late 1960s, subsidence rates greatly decrease, though they do not cease entirely. Between 1975 and 2010, simulations indicate approximately 1.8 ft of net subsidence took place. This period is also characterized by periods of uplift, before subsidence is re-established, though these uplift periods and are not reflected in simulated results.

Overall, the measured and estimated subsidence characteristics are mirrored in simulated results. Differences in these characteristics can probably be explained by limitations in reconstructing historical subsidence and water level records.

Starting in 2007, surface water deliveries from the SLC have declined, mainly as a result of drought and complex environmental litigation. So far this has not led to major subsidence, but if extensive pumping continues, it may. To investigate potential future subsidence, several simulations were undertaken, with a variety of theoretical water level prescriptions.

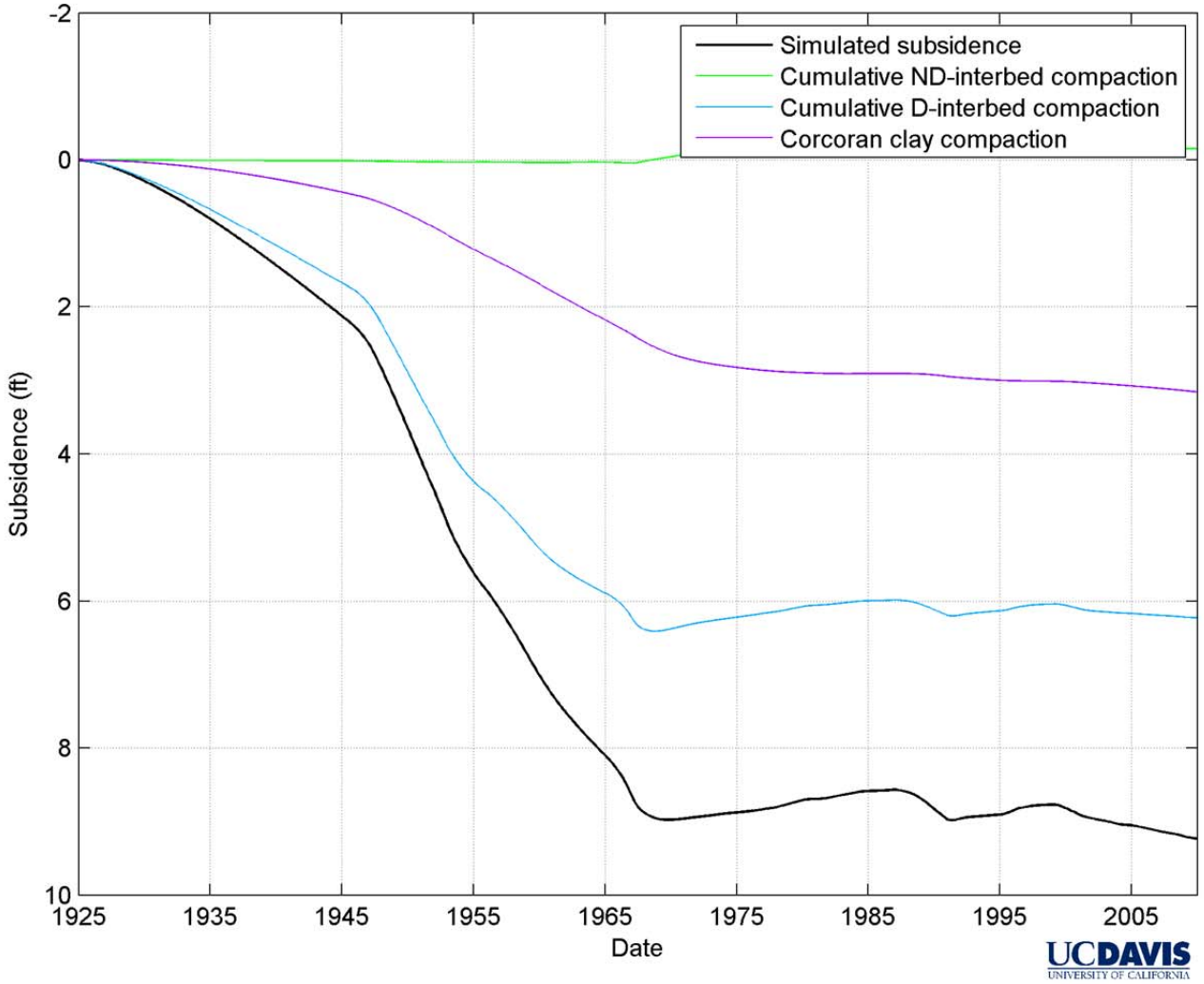

Figure 62 Compaction by interbed type.

Figure 62 shows compaction by interbed type - no-delay, delay and Corcoran Clay. From this, it can be seen that D-interbed compaction accounts for the largest portion of ultimate subsidence (6.12 ft or approximately 59.1 percent). Corcoran Clay compaction accounts for a further 3.16 ft or approximately 30.5 percent of ultimate subsidence. This relatively small percentage is due to the long time delay factor, $\boldsymbol{\tau_o}$ of approximately 37,800 days (103.5 years). The compressible sediments of the Corcoran Clay are important to the subsidence problem at NASL, but only a small portion of ultimate subsidence has taken place within the modeling time-frame. ND interbeds are responsible for the remaining 10.4 percent of total subsidence. ND interbeds constitute only a small portion of the model domain (0.35%), so this is to be expected.

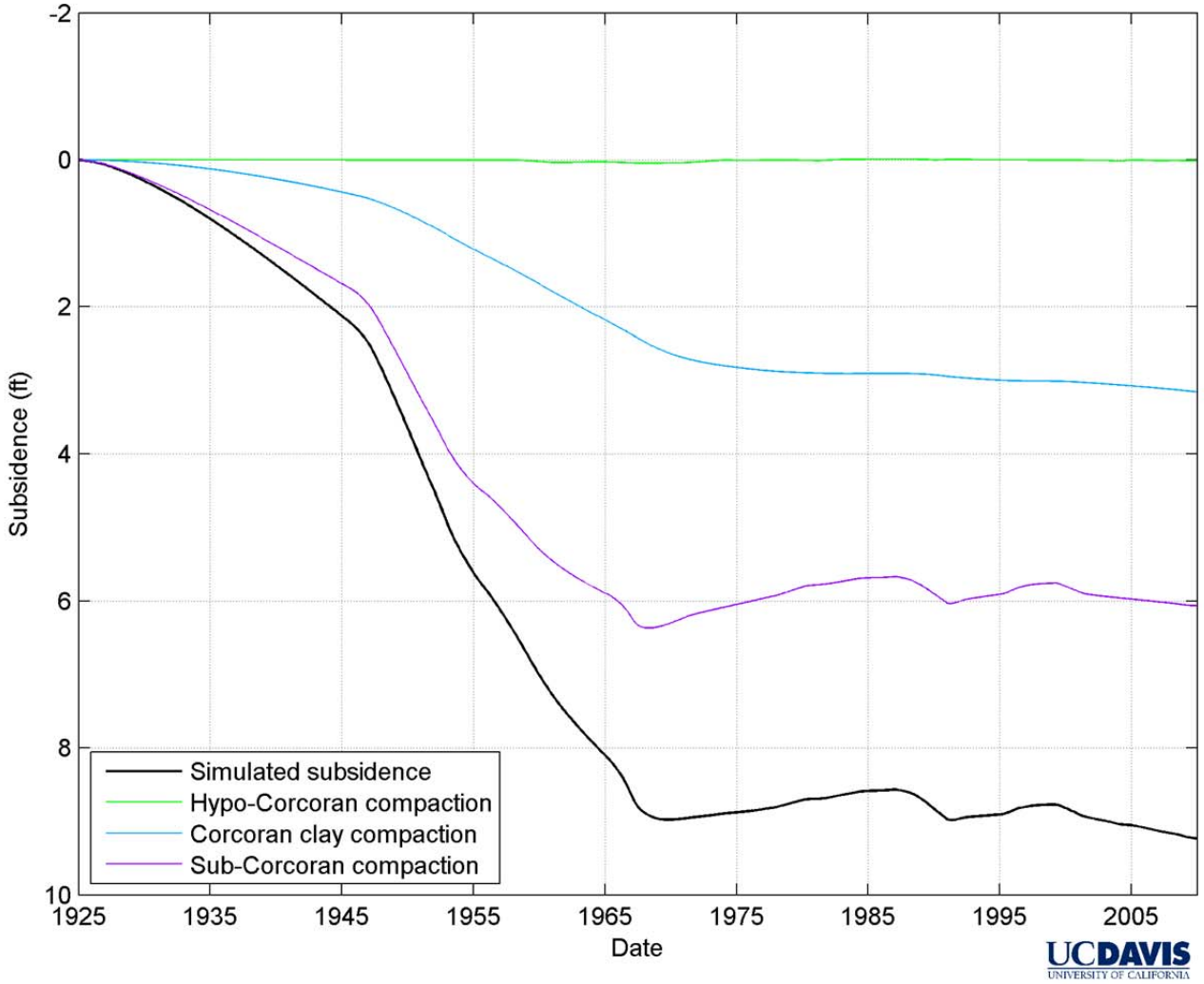

Figure 63 Compaction by aquifer system.

Figure 63 shows the simulated subsidence characteristics within each aquifer system at NASL - hypo-Corcoran, Corcoran and sub-Corcoran. A tiny percentage (0.84 percent, or 0.087 ft) of ultimate subsidence takes place in the hypo-Corcoran zone). The sub-Corcoran aquifer system accounts for the vast majority of overall subsidence, at 7.12 ft (approximately 69 percent).

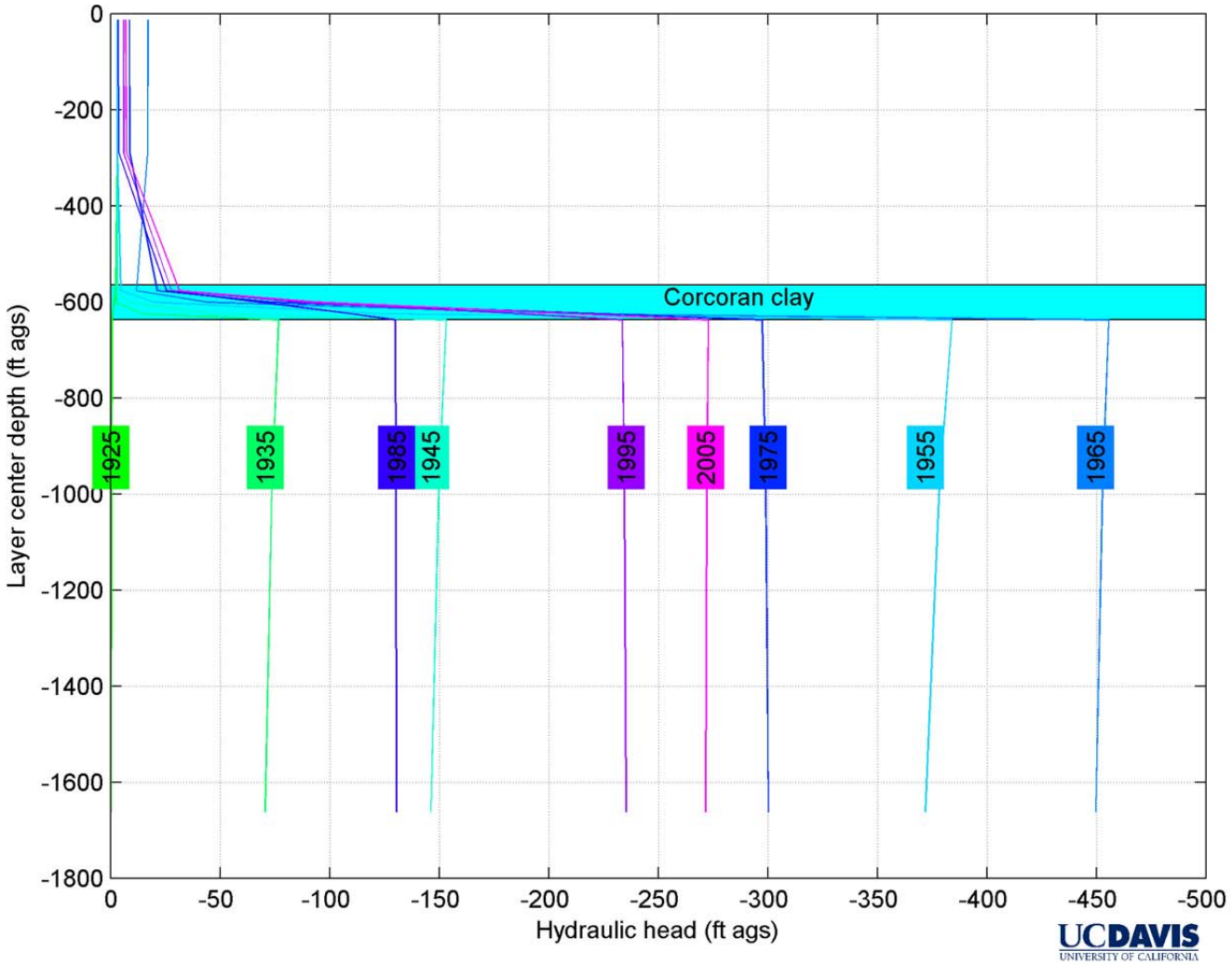

Figure 64 Evolution of simulated hydraulic-head profiles.

Figure 64 shows the evolution of simulated throughout the temporal and spatial model domain. Hypo-Corcoran heads remain low and relatively constant throughout the simulation time-frame as expected. Heads within the sub-Corcoran aquifer system, are much lower. As time progresses, these heads become lower, and are at their lowest in 1965. By 2005, a large portion of this head loss has been regained. The distribution of hydraulic heads is indicative of residual compaction (Riley,1998).

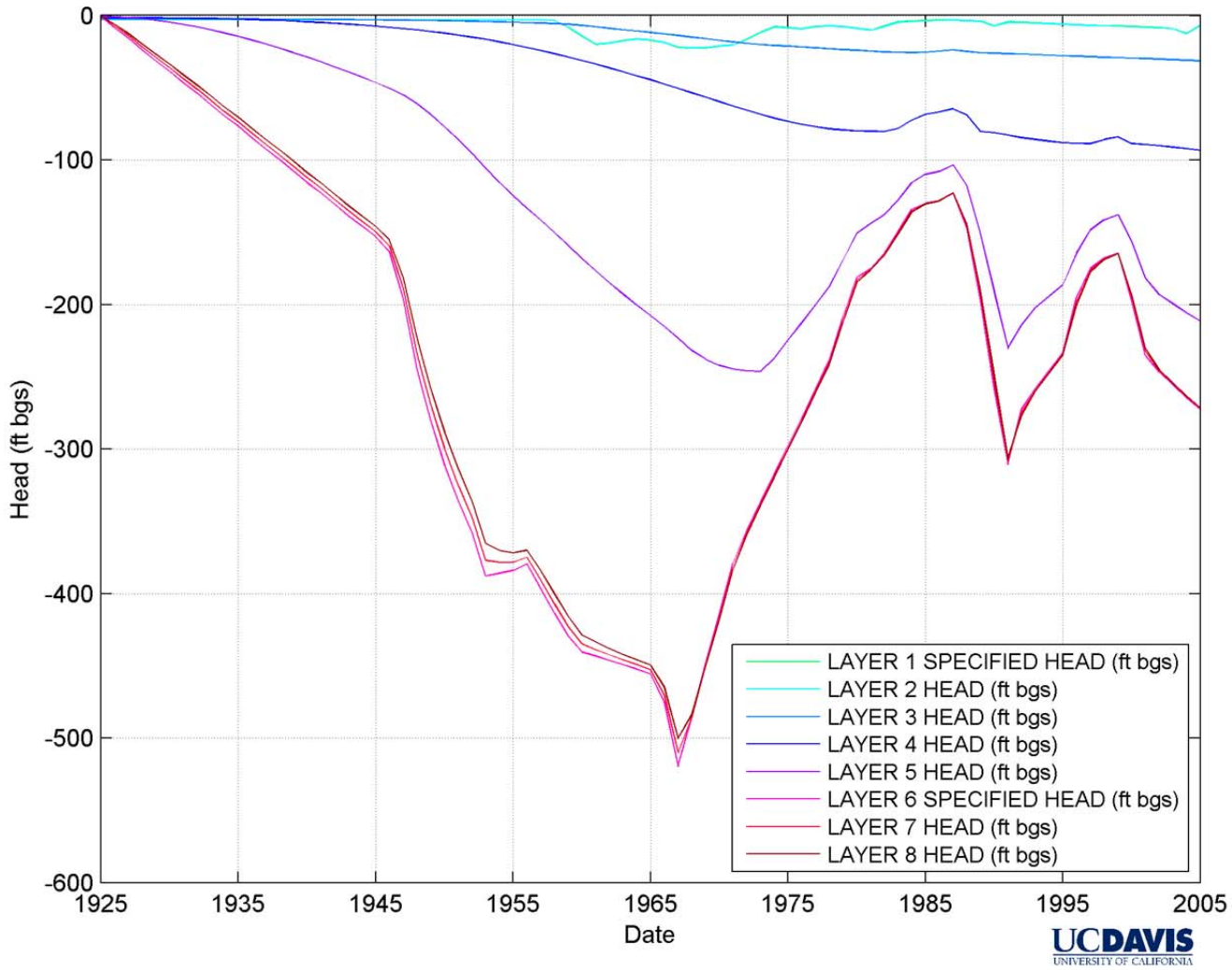

Figure 65 Simulated head by layer.

6.5 Sensitivity Analysis

To investigate the sensitivity of the NASL subsidence model to individual parameter changes used within the NASL model, a sensitivity analysis was completed. Preconsolidation head (HC), elastic and inelastic skeletal storages (S'_{ske} and S'_{skv}, respectively) and vertical hydraulic conductivity (K'_v) were all varied from their calibrated values, separately within the three aquifer systems (hypo-Corcoran, Corcoran and sub-Corcoran). Additionally, differing K'_v and S'_{skv} values were trialed, for constant diffusivity (D') ($D' = K'_v/S'_{skv}$). S'_{ske}, S'_{skv}, and K'_v were all varied between an order of magnitude smaller to an order of magnitude larger than calibrated parameter values. The error between simulated and measured subsidence was computed using:

$$Error = \sqrt{\frac{(\mu_{z0} - \mu_{zs})^2}{n-1}} \qquad 18$$

where μ_{z0} is observed displacement, μ_{zs} is simulated displacement, and *n* is the number of comparisons between the observed and simulated time-series.

Calibrated parameters are shown in Table 20, below.

Layer	K'$_v$ (ft/d)	S'$_{skv}$ (ft^{-1})	S'$_{ske}$ (ft^{-1})	HC (ft bgs)
1	7.10E-06	1.70E-05	4.00E-06	-3
2	7.10E-06	1.70E-05	4.00E-06	-3
3	1.20E-05	3.50E-04	4.00E-06	-2.25
4	1.20E-05	3.50E-04	4.00E-06	-1.5
5	1.20E-05	3.50E-04	4.00E-06	-0.75
6	1.60E-06	1.30E-05	1.20E-06	0
7	1.60E-06	1.30E-05	1.20E-06	0
8	1.60E-06	1.30E-05	1.20E-06	0

Table 20 Calibrated model parameters used as a starting point for sensitivity analysis.

First, preconsolidation head (HC) sensitivity was investigated, within the three aquifer sub-systems. This was achieved by varying HC values from 10 ft below to 10 ft above calibrated values. Corcoran (layers 3-5) HC is very insensitive, hypo-Corcoran (layers 1-2) HC is slightly sensitive in the negative direction, whilst sub-Corcoran (layers 6-8) HC shows the greatest sensitivity. Simulations do not change for positive changes in HC, as the SUB package changes HC values that are greater than starting head to starting head. HC sensitivities are shown in Figure 66. Potentially, smaller values of sub-Corcoran HC would lead to smaller model errors, but not necessarily better subsidence trajectories matches.

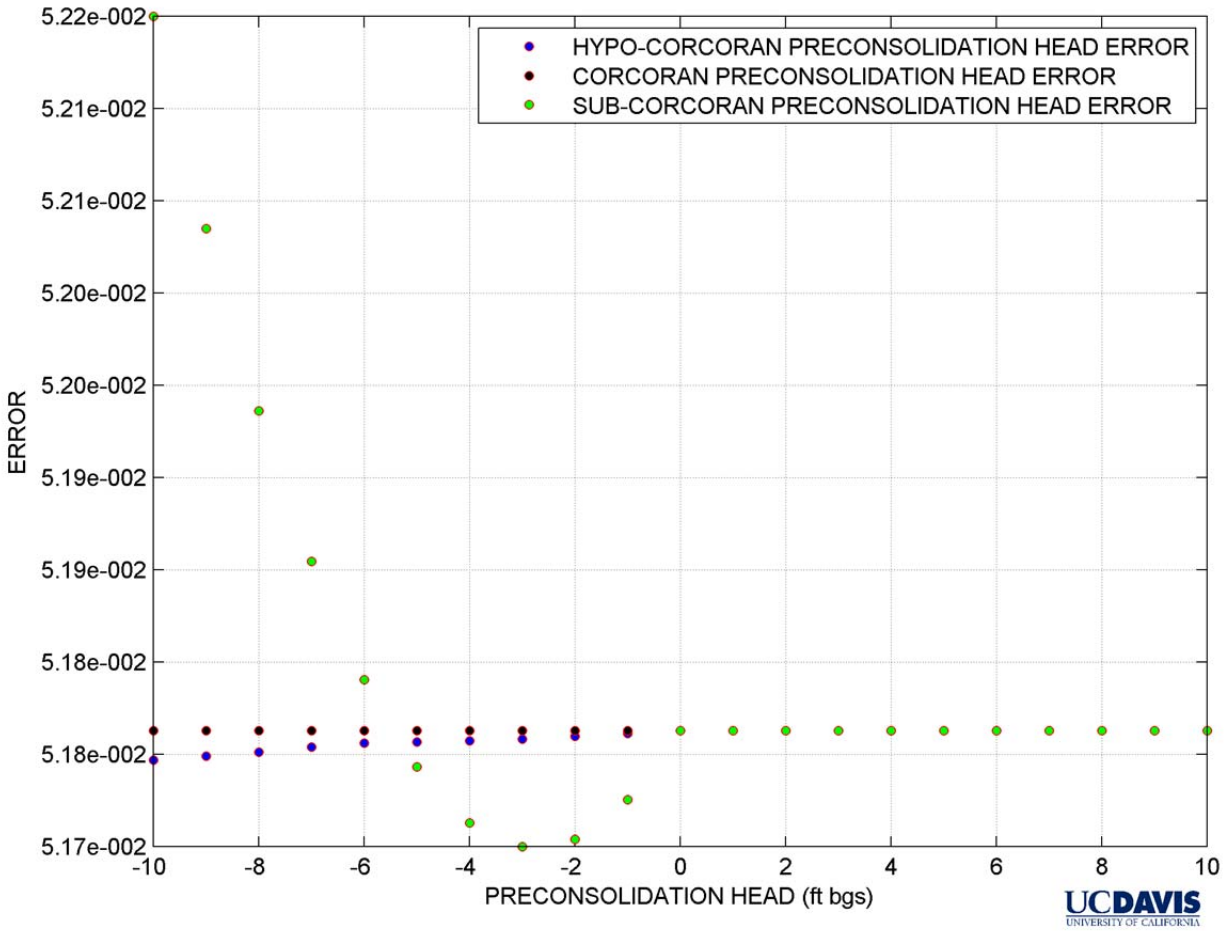

Figure 66 Preconsolidation head error distribution between measured and simulated parameter values. Hypo-Corcoran, Corcoran and sub-Corcoran K'_v values are 7.10E-06, 1.20E-05 and 1.60E-06 ft/day, respectively. Hypo-Corcoran, Corcoran and sub-Corcoran S'_{skv} values are 1.70E-05, 3.50E-04 and 1.30E-05 $\mathbf{ft}^{-1}$, respectively. Hypo-Corcoran, Corcoran and sub-Corcoran S'_{ske} values are 4.00E-06, 4.00E-06 and 1.20E-06 $\mathbf{ft}^{-1}$, respectively.

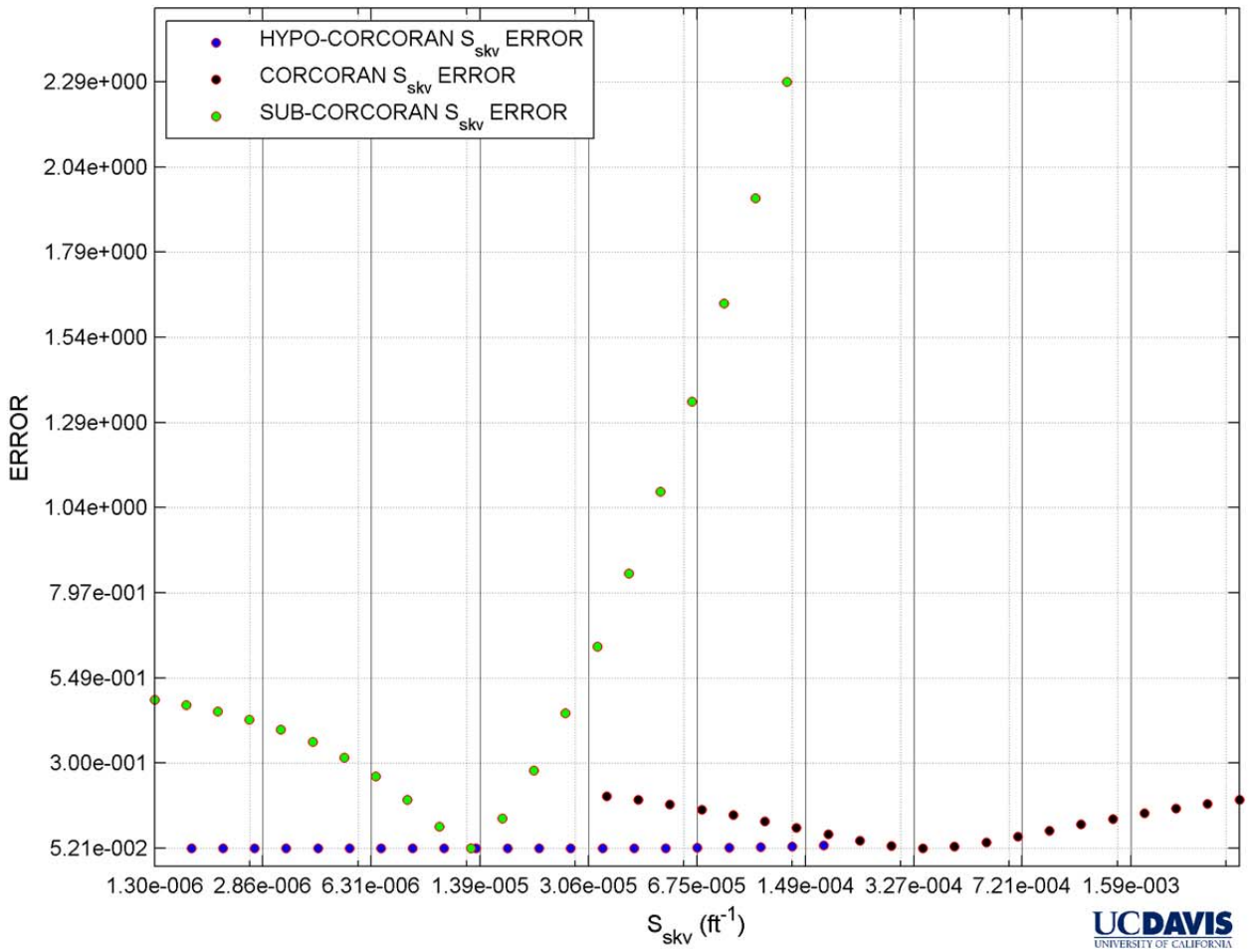

Figure 67 Inelastic skeletal specific storage error distribution between measured and simulated parameter values. Hypo-Corcoran, Corcoran and sub-Corcoran $\boldsymbol{K'_v}$ values are 7.10E-06, 1.20E-05 and 1.60E-06 ft/day, respectively. Hypo-Corcoran, Corcoran and sub-Corcoran $\boldsymbol{S'_{ske}}$ values are 4.00E-06, 4.00E-06 and 1.20E-06 $\mathbf{ft^{-1}}$, respectively.

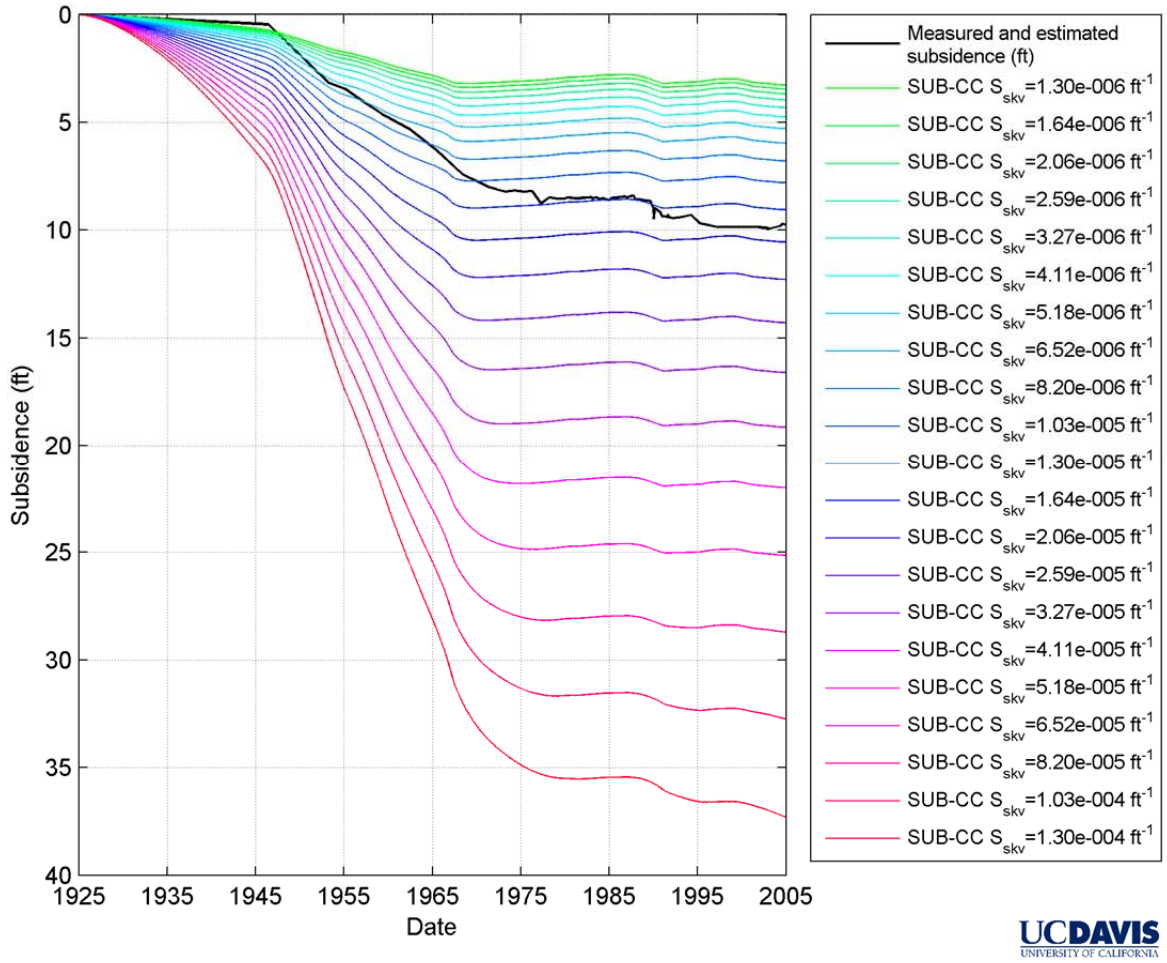

Figure 68 Sub-Corcoran inelastic skeletal specific storage compaction trajectories. Hypo-Corcoran, Corcoran and sub-Corcoran K'_v values are 7.10E-06, 1.20E-05 and 1.60E-06 ft/day, respectively. Hypo-Corcoran, and Corcoran S'_{skv} values are 1.70E-05 and 3.50E-04 $\mathbf{ft^{-1}}$, respectively. Hypo-Corcoran, Corcoran and sub-Corcoran S'_{ske} values are 4.00E-06, 4.00E-06 and 1.20E-06 $\mathbf{ft^{-1}}$, respectively.

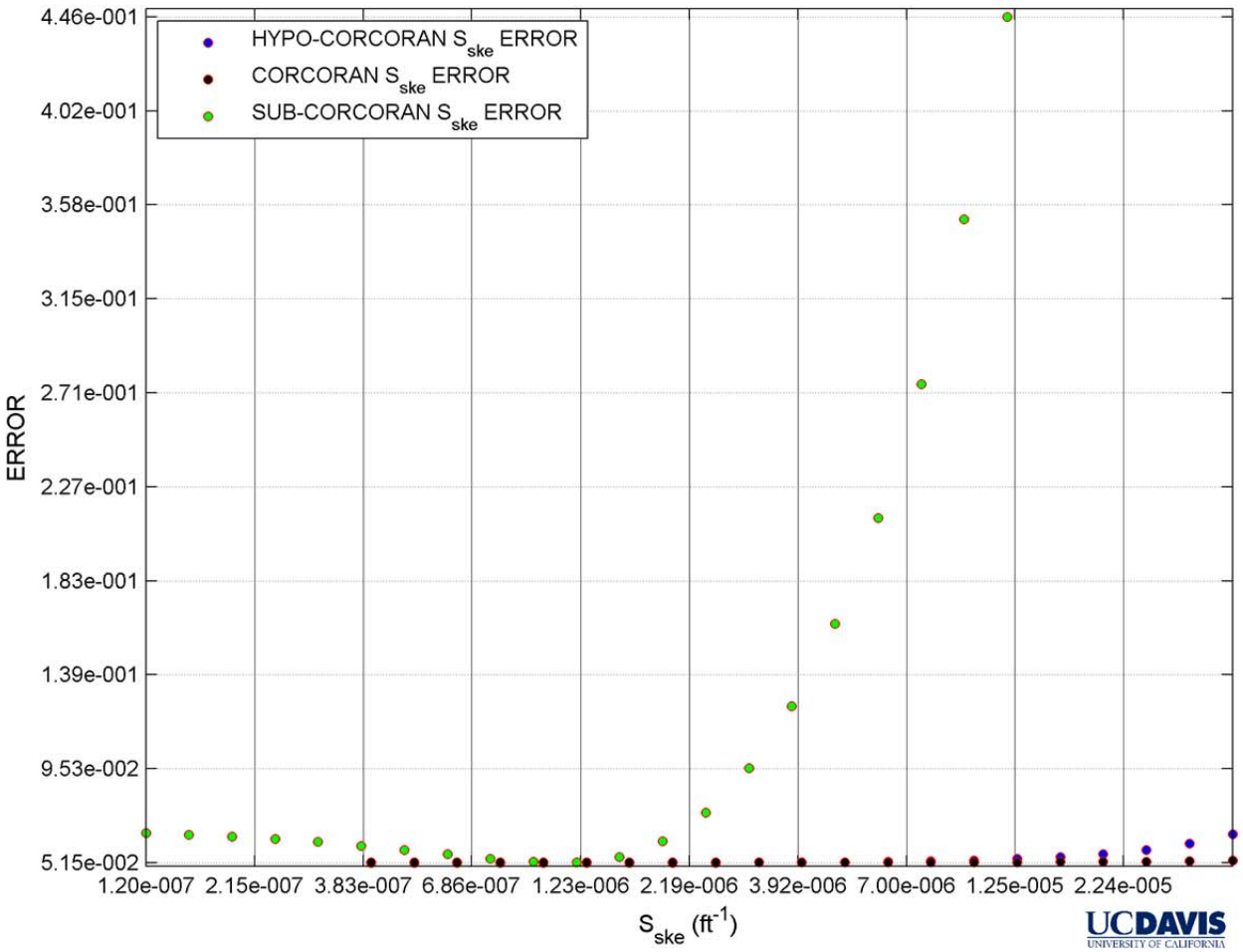

Figure 69 Elastic skeletal specific storage error distribution between measured and simulated parameter values. Hypo-Corcoran, Corcoran and sub-Corcoran $\boldsymbol{K'_v}$ values are 7.10E-06, 1.20E-05 and 1.60E-06 ft/day, respectively. Hypo-Corcoran, Corcoran and sub-Corcoran $\boldsymbol{S'_{skv}}$ values are 1.70E-05, 3.50E-04 and 1.30E-05 $\mathbf{ft^{-1}}$, respectively.

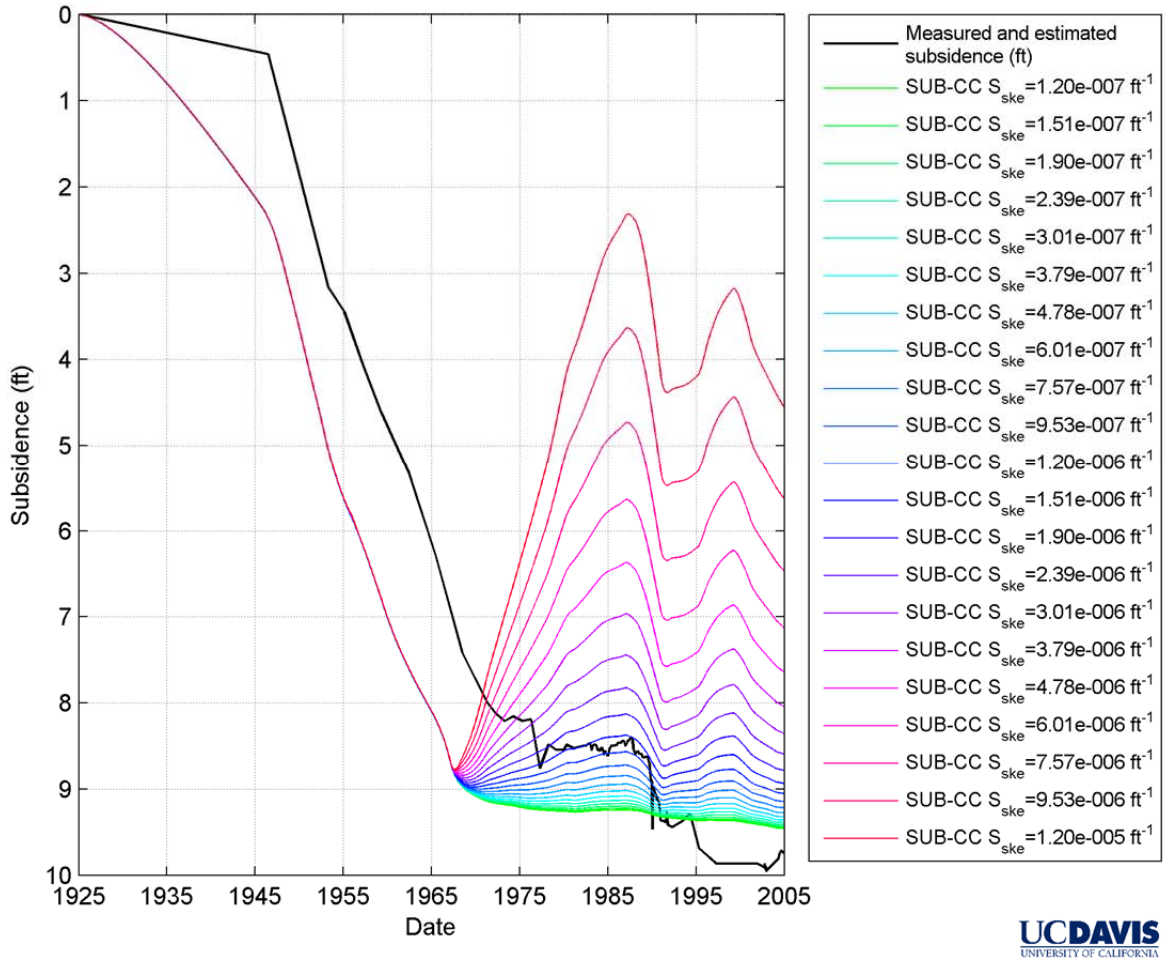

Figure 70 Sub-Corcoran elastic skeletal specific storage compaction trajectories. Hypo-Corcoran, Corcoran and sub-Corcoran K'_v values are 7.10E-06, 1.20E-05 and 1.60E-06 ft/day, respectively. Hypo-Corcoran, Corcoran and sub-Corcoran S'_{skv} values are 1.70E-05, 3.50E-04 and 1.30E-05 $\mathbf{ft^{-1}}$, respectively. Hypo-Corcoran and Corcoran S'_{ske} values are 4.00E-06 $\mathbf{ft^{-1}}$.

Aquitard inelastic skeletal specific storage (S'_{skv}) sensitivity was investigated by varying S'_{skv} between an order of magnitude lower to an order of magnitude larger than calibrated values within each aquifer sub-system. Again, the sub-Corcoran aquifer sub-system is the most sensitive to changes in S'_{skv} , especially when S'_{skv} is increased. The hypo-Corcoran zone is very insensitive to this parameter, only slightly so when multiplied by a factor close to 10. The Corcoran layers show a moderate sensitivity (Figure 67). In calibrating the NASL model, this parameter was very important, and its effect on timing and magnitude of compaction in the sub-Corcoran zone can clearly be seen in Figure 68.

A study of aquifer-system elastic skeletal specific storage (S_{ske}) sensitivity was completed by varying S_{ske} through the same range of coefficients as S'_{skv}. Hypo-Corcoran and Corcoran sensitivities are very small for this parameter - the hypo-Corcoran zone only displays small errors at the upper end of the coefficient range (Figure 69). The sub-Corcoran zone shows a great deal of sensitivity to positive changes in S_{ske}, but is far more restrained when decreased. Sub-Corcoran S_{ske} compaction trajectories are shown in Figure 70. This figure shows how pre-1970s compaction is almost unaffected by changes in this parameter, but once sub-Corcoran heads rebound post-1970s (Figure 65), this parameter controls how much land elevation recovery occurs.

Vertical hydraulic conductivity (K_v) is another key sensitivity parameter. To investigate this, K_v was multiplied by the same coefficient as S_{skv} within the three aquifer sub-systems. The hypo-Corcoran and Corcoran zones both show very little sensitivity (Figure 71), whereas the sub-Corcoran sensitivity is very high, especially to values lower than calibrated ones. This is because the Corcoran clay, whilst being very fine-grained, has a very high time delay due to its thickness, and only realizes a small amount of its ultimate compaction within the model time frame. Sub-Corcoran vertical hydraulic conductivity compaction trajectories are shown in Figure 72, and show the effect of this parameter on timing (and to a lesser extent) magnitude.

The sensitivity of diffusivity was investigated by varying K_v and S_{skv} in unison through the same ranges as described above, for constant diffusivity. Hypo-Corcoran and Corcoran both show a small amount of sensitivity to this parameter combination, whilst the sub-Corcoran sub-system shows a great deal of sensitivity, especially to positive increases. Diffusivity sensitivities are shown in Figure 73.

Though model head inputs are not a parameter of concern, and their values are considered well-defined (when available), a sensitivity analysis was undertaken for head inputs to the three aquifer sub-systems. As expected all three zones are sensitive to these scenarios, see Figure 74.

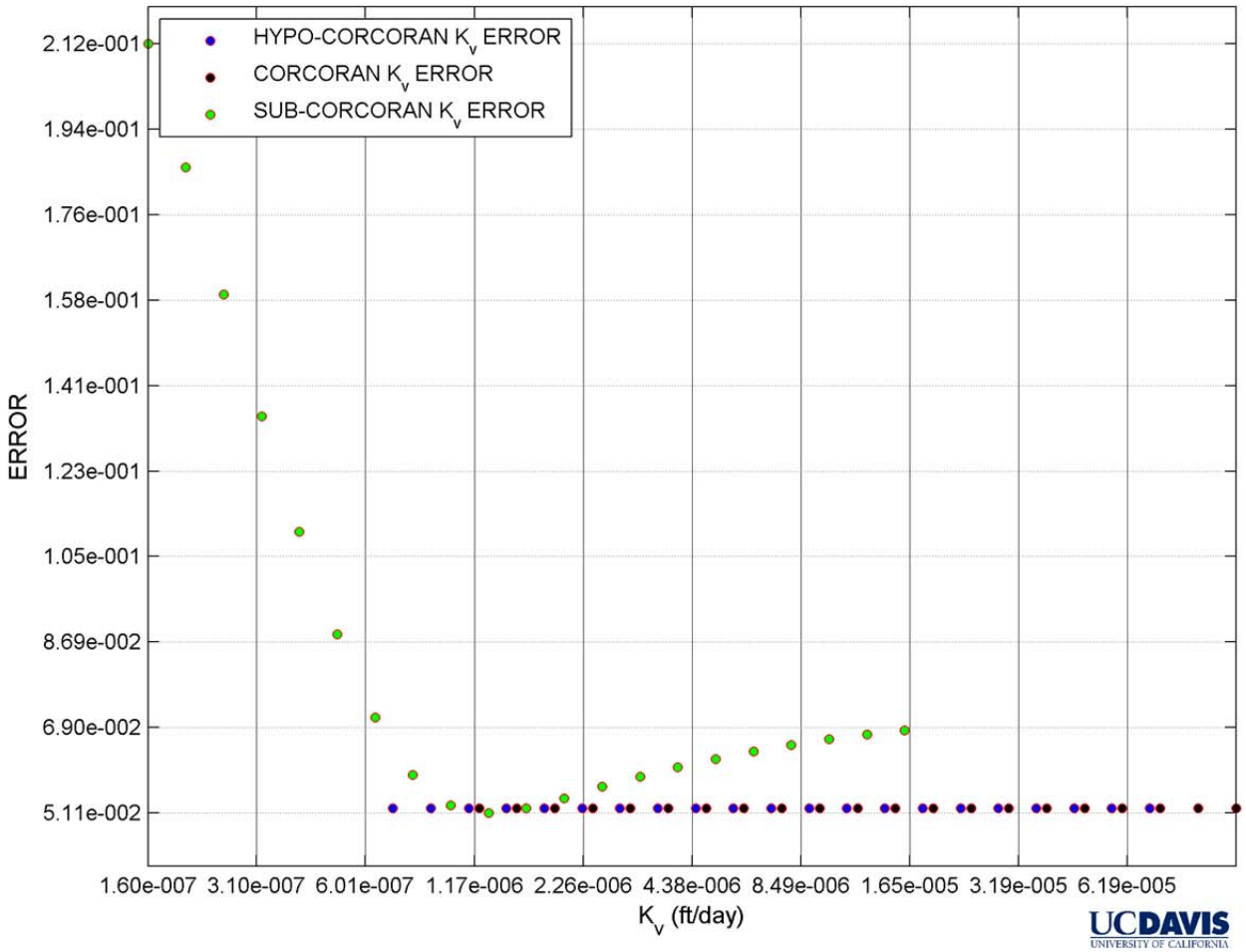

Figure 71 Vertical hydraulic conductivity error distribution between measured and simulated parameter values. Hypo-Corcoran, Corcoran and sub-Corcoran $\boldsymbol{S'_{skv}}$ values are 1.70E-05, 3.50E-04 and 1.30E-05 $\mathbf{ft^{-1}}$, respectively. Hypo-Corcoran, Corcoran and sub-Corcoran $\boldsymbol{S'_{ske}}$ values are 4.00E-06, 4.00E-06 and 1.20E-06 $\mathbf{ft^{-1}}$, respectively.

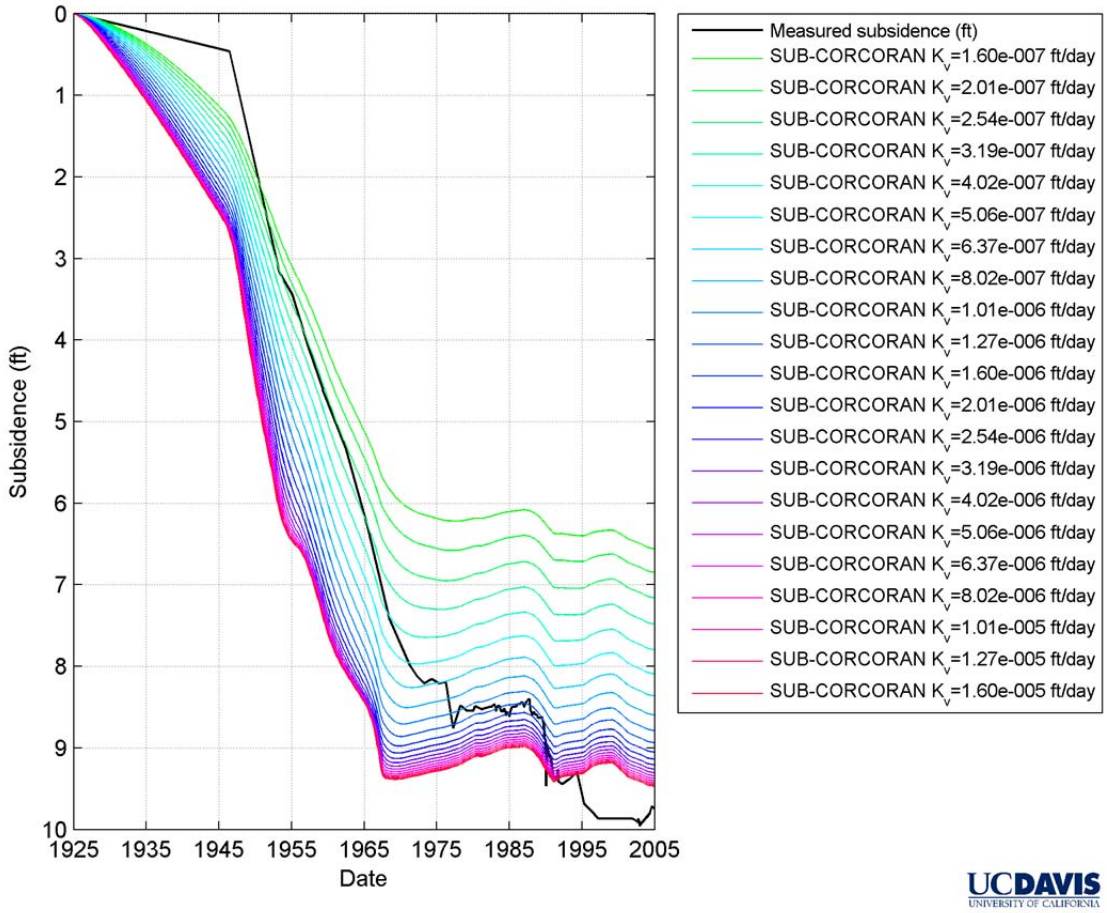

Figure 72 Sub-Corcoran vertical hydraulic conductivity compaction trajectories. Hypo-Corcoran and Corcoran $\boldsymbol{K'_v}$ values are 7.10E-06 and 1.20E-05 ft/day, respectively. Hypo-Corcoran, Corcoran and sub-Corcoran $\boldsymbol{S'_{skv}}$ values are 1.70E-05, 3.50E-04 and 1.30E-05 $\mathbf{ft^{-1}}$, respectively. Hypo-Corcoran, Corcoran and sub-Corcoran $\boldsymbol{S'_{ske}}$ values are 4.00E-06, 4.00E-06 and 1.20E-06 $\mathbf{ft^{-1}}$, respectively.

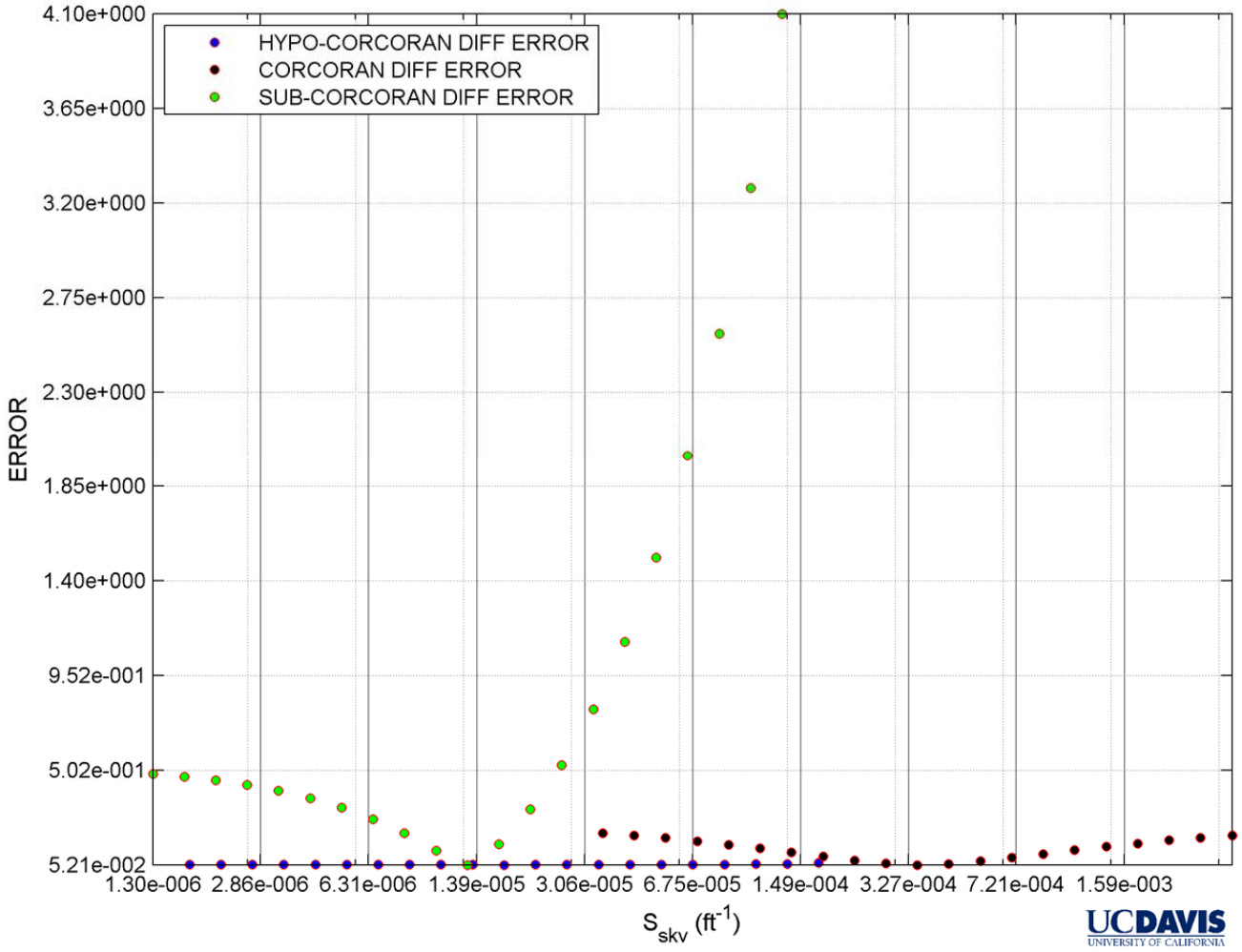

Figure 73 Diffusivity error distribution between measured and simulated parameter values. Hypo-Corcoran, Corcoran and sub-Corcoran $\boldsymbol{S'_{ske}}$ values are 4.00E-06, 4.00E-06 and 1.20E-06 $\mathbf{ft^{-1}}$, respectively.

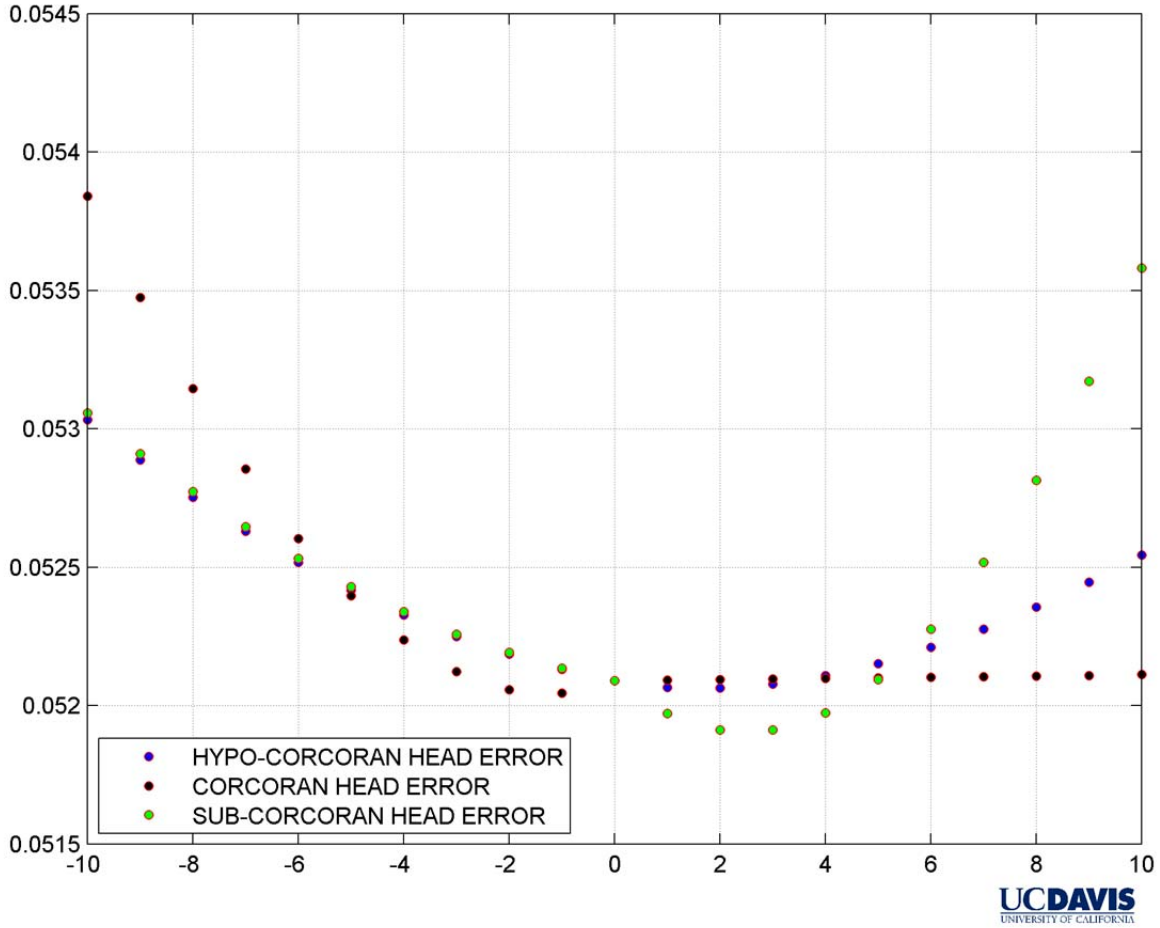

Figure 74 Head input error distribution between measured and simulated parameter values. Hypo-Corcoran, Corcoran and sub-Corcoran K'_v values are 7.10E-06, 1.20E-05 and 1.60E-06 ft/day, respectively. Hypo-Corcoran, Corcoran and sub-Corcoran S'_{skv} values are 1.70E-05, 3.50E-04 and 1.30E-05 $\mathbf{ft}^{-1}$, respectively. Hypo-Corcoran, Corcoran and sub-Corcoran S'_{ske} values are 4.00E-06, 4.00E-06 and 1.20E-06 $\mathbf{ft}^{-1}$, respectively.

As expected, parameters show the greatest sensitivity within the sub-Corcoran aquifer sub-system. This zone is the thickest, and contains the largest cumulative interbed thickness (Table 18). The sensitivity of all parameters included in the analysis are much smaller in the hypo-Corcoran and Corcoran systems. Diffusivity and the inelastic skeletal storage coefficient are the most sensitive parameters in the sub-Corcoran aquifer-system, whilst vertical hydraulic conductivity is the least sensitive.

6.6 Assumptions and limitations

Translating the real-life subsidence problem at NASL lead to assumptions and limitations in the development of the MODFLOW model. These can be broken down into two basic categories: those made by the SUB package and those made by the modeler.

In the SUB package, delay beds and no-delay beds are defined upon the simplification that no-delay beds have hydraulic heads that equilibrate with hydraulic heads in the surrounding aquifer within a single time step. This means that no residual compaction is simulated for no-delay aquitards and compaction may be miscalculated by the SUB Package. In the NASL model, time-steps of 30.4375 days were defined, with interbeds of less than 8 ft. in thickness in the hypo-Corcoran and less than 4 ft. in thickness in the sub-Corcoran being simulated as no-delay . A very small amount of such no-delay interbeds are found in the NASL, model, so this error is believed to be minimal. Additionally, lateral flow within the aquitards is ignored and simulated as Darcian. This is appropriate for models where permeability variances between aquifer and aquitards vary by several orders of magnitude (Hanson, 1989). Another assumption is that specific storage and K_v terms are simulated as constant throughout the model time-frame. However, these parameters vary with effective stress, so this can lead to smaller rates of late-time compaction than occurs in reality. Additionally, the SUB Package does not calculate compaction for layers that are being used to specify head (layers 1 and 6 in this model). As other subsidence modelers have done (eg. Sneed and Galloway, 2000), these layers were limited to 1 ft. thicknesses of aquifer material. A very small quantity of mainly elastic subsidence would occur within this type of layer, so this potential error is believed to be largely mitigated.

More tightly defined K_v, S_{skv} and S_{ske} values would have greatly aided in modeling efforts. As can be seen from sensitivity analysis results, the selection of these parameters greatly affects subsidence characteristics at NASL. Table 17 shows their variability, and K_v and S_{skv} are especially important in model formulation. Selections of preconsolidation head values are less important as can be seen from the sensitivity analysis. Data relating to this parameter is also hard to find, as discussed earlier.

A key constraint to better modeling results was the lack of historical subsidence data. Additional elevation measurements between 1925 to 2010 for a point directly on NASL lands would have provided a far superior target for model calibration. Such a long timeline of subsidence data was not available, as outlined in earlier chapters. In calculating the subsidence measured by extensometers, it was assumed the compaction/subsidence ratio held for all times, include those outside the period in which the ratio was calculated. This is justified, as the ratios were calculated over relatively long time-frames, and were not believed to change measurably. For optimal comparison of simulated results with measurable data, it would have been very beneficial to obtain high resolution land elevation data, as was obtained at the Holly site (Sneed and Galloway, 2000), for at least a portion of the model simulation time-frame. Measured and simulated subsidence values obtained at the Holly site were very close both in magnitude and timing, and high resolution data greatly aided the analysis of simulation results.

Measured groundwater level data were defined well for the last third of the 20th century and later times, but was estimated for earlier times. Since water levels are key for subsidence modeling, it is possible that this problem contributed to errors between simulated and measured subsidence results. If groundwater level records were received with well construction details (in particular, which aquifer-system each well was screened in) it is likely that a better water level history could be formed.

6.8 Future modeling

Several additional long-term modeling scenarios were completed to guide potential current and future pumping management decisions at NASL. Four scenarios were simulated with a variety of future prescribed head values for the hypo- and sub-Corcoran aquifer-subsystems, ending in the year 2200 (a 275 year total simulation period). These simulations are named scenarios 1a-1d. Scenario 1a shows the result of a managed situation where heads are kept at present levels. Scenario 1b outlines the outcome of a management decision to allow sub-Corcoran hydraulic heads to recover to levels measured in 2000 and remain at this level until 2200. Scenarios 1c and 1d show the outcome of declining sub-Corcoran water levels, at different rates: 'business-as-usual' scenarios. Head inputs are shown in Figure 76.

Scenario 1a was completed with prescribed hydraulic heads measured at the last date available (2010) for the remaining simulation time-frame (2010-2200). As in earlier simulations, the FHB1 Package was used to specify these heads to layers 1 and 6 for the hypo- and sub-Corcoran aquifer systems respectively. Layer 1 was prescribed a head of 10.7 ft bgs, and layer 6 was prescribed a head of 314 ft. bgs. This scenario leads to a small quantity of residual subsidence occurring post-2010 that levels out over time. Total subsidence by 2200 is approximately 10.1 ft. The continued increase in subsidence is due to residual subsidence in delay interbeds and within the Corcoran Clay (Figure 75).

Scenario 1b was completed using the same heads as scenario 1a for layer 1, but heads specified for layer 6 were increase steadily to 2000 levels (195 ft bgs) between the years 2010 and 2015,

and then kept at this level until 2200. This scenario results in the immediate onset of uplift to approximately 9 ft. and this quantity is sustained until the end of the simulation (Figure 75).

Scenarios 1c and 1d again use the same prescribed heads for layer 1 as scenario 1a, but heads in layer 6 were decreased at an annualized rate of 3 ft/yr, until a depth representing the top of the Corcoran is reached, and this level is sustained until the ending simulation time. Estimated water levels within the sub-Corcoran aquifer-system decreased at average rate of 3.7 ft/yr between 1925 and 2010. Scenario 1c shows subsidence continues at a steady rate post-2010. By approximately 2090 (when heads reach their lowest point at the top of the Corcoran Clay), subsidence rates ease off. By 2200, ultimate subsidence is approximately 15 ft. Scenario 1d was constructed exactly as scenario 1c, but layer 6 heads were decreased at annualized rate of 5 ft/yr until a level corresponding to the top of the Corcoran Clay was reached. The post-2010 subsidence trend output by this simulation scenario is similar to that of scenario 1c, but the rate is initially more aggressive, and it reaches its terminal subsidence value sooner. However, terminal subsidence is approximately the same as scenario 1c, at approximately 15 ft. (Figure 75). These latter two scenarios show that there remains a large potential for further subsidence at NASL depending on how groundwater is managed. If groundwater levels are allowed to decline further, subsidence could become a significant problem at NASL and in surrounding areas.

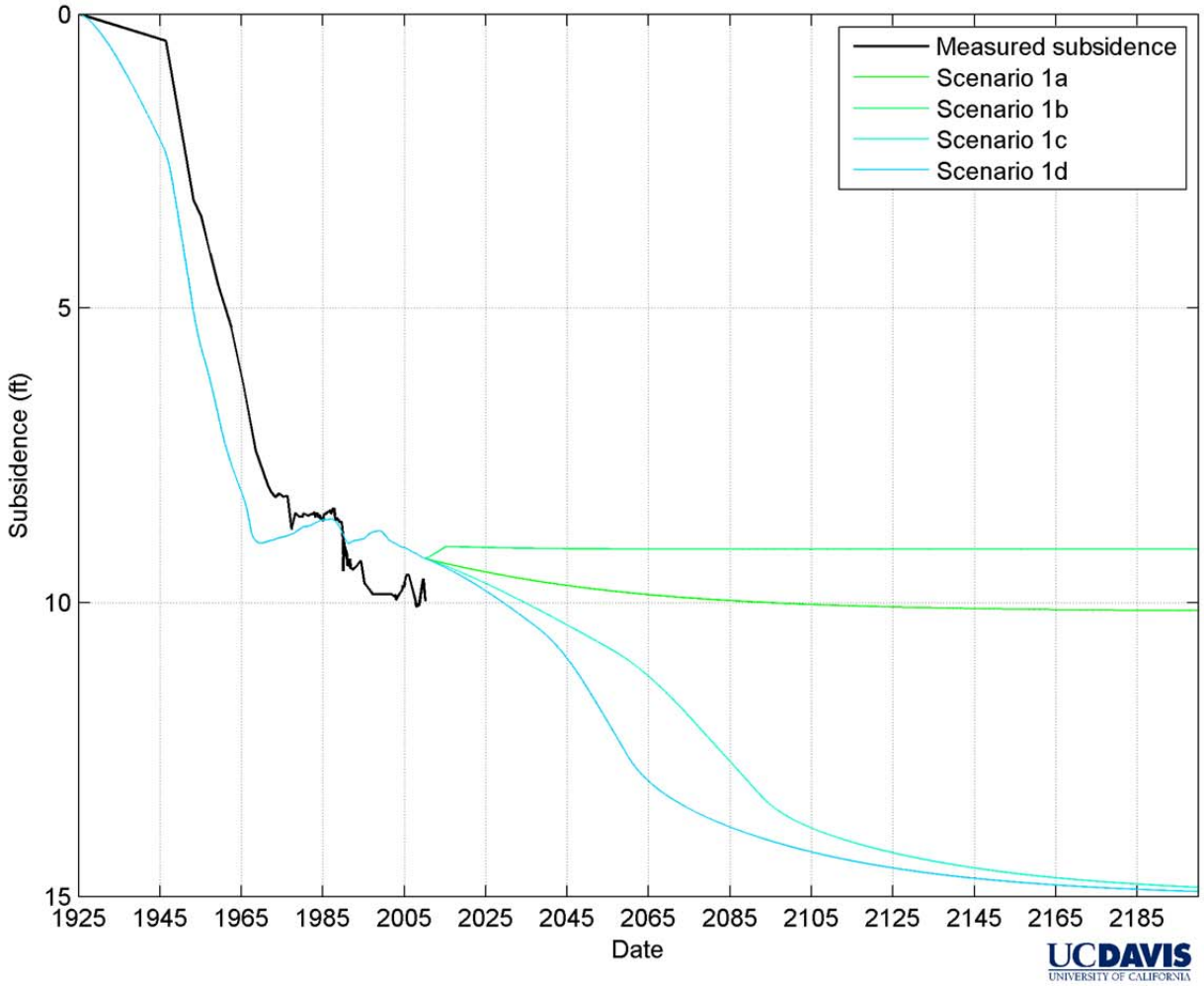

Figure 75 Future simulation scenarios 1a-1d.

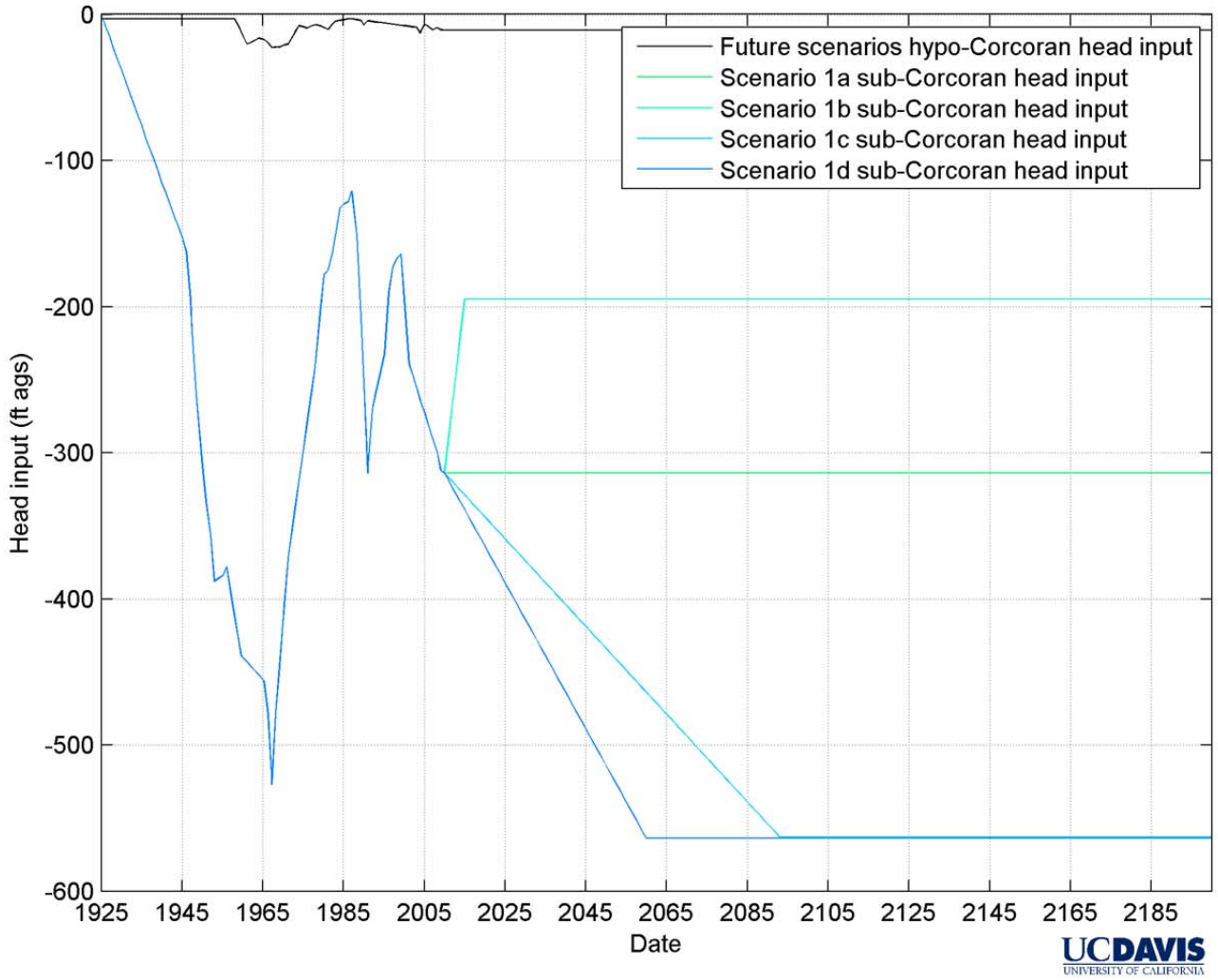

Figure 76 Head input data for future modeling scenarios.

6.7 Conclusions

Based on extensive data review and collection, described in chapters 4 and 5, we developed a thorough understanding of historic water levels and their variations with depth, on the geologic stratigraphy at the NASL site, and on the historic subsidence rates. Using these data, we developed a 1-dimensional groundwater flow and subsidence model that was used to make future land subsidence predictions based on hypothetical future water level scenarios.

Stratigraphy data are used to define the architecture of the groundwater model. Historic groundwater levels are used to drive the groundwater pumping intrinsically in the model. Model output is projected land subsidence. For the historic simulation portion, modeled data were matched against actually measured land subsidence data. The manual sensitivity and calibration analysis showed that, on one hand, the model results are very sensitive to the critical model parameters (vertical hydraulic conductivity, elastic storage coefficient, inelastic storage coefficient), on the other hand, the historic time series of land subsidence and the field estimates of the aquifer parameters provide a solid constraint. Future predictions of subsidence are not highly sensitive to the range of parameters that provide a reasonable match to historic subsidence rates. All future prediction suggest that further lowering of groundwater levels may induce subsidence on the order of 5 feet. Even larger amount of subsidence would occur, if water levels were allowed to drop below the Corcoran Clay.

Suggested future work includes preparation of a fully three-dimensional groundwater flow and subsidence model for the region surrounding NASL. This would allow for a comprehensive evaluation and assessment of the effects of various agricultural water management scenarios on regional groundwater flows and provide a fully three-dimensional assessment of subsidence.

7 Summary and Recommendations

7.1 Water Management

- NASL's average applied water demand is 32,700 AF/yr, varying from 24,000 AF/yr to 42,000 AF/yr depending on surface water supplies. Of this, groundwater pumping, on average, provides between 8,000 AF/yr and 13,000 AF/yr, but may be as little as 5,000 AF/yr and as high as 30,000 AF/yr.
- NASL and its surrounding region rely on a combination of stream recharge (particularly from the Kings River) and percolation of excess irrigation water as their source of groundwater recharge. Recharge from the NASL lands is estimated to be on the order of 7,500 AF/yr to 11,500 AF/yr with most of the recharge being agricultural return flows.
- To avoid long-term massive land subsidence, groundwater levels at NASL must be maintained to not exceed depths reached during previous drought periods, when spring water levels reached 250 ft below ground surface (bgs): Historically, spring groundwater levels in the lower aquifer wells gradually fell from 30 ft to approximately 100 ft bgs during the first half of the 20th century. After 1950, water levels at NASL declined at an accelerated pace to approximately 200-250 ft bgs by the late 1960s, then recovered over the following two decades until the late 1980s, when water levels returned to 1950 levels (~100 ft bgs), only briefly interrupted by the 1977 drought. In the 20 years following this first forty year water level decline and recovery cycle, three droughts and two relatively wetter periods followed in successively more rapid periods (1988-1999 cycle, 2000-2006 cycle, and 2006-current), with each cycle being shorter than the previous one, yet reaching both lower groundwater levels and higher groundwater levels at increasingly more rapid rates: The high 1950-equivalent groundwater level was briefly achieved in 1999 (100 ft bgs), but not in 2006 (150 ft bgs). Water levels dropped to nearly 250 ft bgs at the end of droughts in 1991, 2003, and 2009. The increasingly rapid water level decline is due to a combination of high groundwater pumping and loss of groundwater storage because of sediment compaction.
- Given the long-term trend, the increasingly rapid groundwater level fluctuations, the loss of groundwater storage, and the uncertainty about refilling the groundwater basin, NASL will likely experience historically low groundwater levels significantly exceeding 250 ft bgs during upcoming drought periods, unless a stringent collaborative program on-site as well as with neighboring groundwater users is implemented that caps groundwater pumping to avoid increases in spring groundwater levels below a target of 250 ft bgs.
- Approximately two-thirds (8,200 acres) of the current agriculture-leases depend solely on surface water delivered through Westlands Water District (WWD), another nearly 3,000 acres are variably irrigated with surface water or groundwater; NASL must

continue close cooperation with WWD to ensure sufficient water supply, as there are no additional available groundwater resources to rely on permanently.

- The main use of groundwater at NASL is as a water bank to supplement and replace temporary (1- to 5-year) shortages in surface water supplies. Apart from land subsidence management, NASL has a high stake and interest in long-term maintenance of these groundwater levels to manage periodic surface water shortfalls. For management purposes, groundwater must be considered a water bank and is best managed jointly with surface water (conjunctive use).
- Due to the location of NASL near the triple-junction of three groundwater basins (Westside, Kings River, and Tulare Lake), the management of this water bank would be done jointly with neighboring water districts and groundwater users, particularly WWD and KRCD.
- A fundamental paradigm for NASL and its neighbors managing groundwater must be to maximize the recharge of high quality surface water to the aquifer, while minimizing the amount of groundwater pumping.
    - In dry years, when surface water supplies are limited, consumptive water use must be limited to meet maximum groundwater level decline targets, while also minimizing the amount of percolating water from irrigation (high irrigation efficiency).
    - In wet years or during wet seasons, NASL and its neighbors must create opportunities for recharging good quality surface water in recharge basins and – perhaps more importantly – via excess irrigation on agricultural lands, provided that nitrate and pesticide leaching is minimal. Dual irrigation systems (furrow and drip/sprinkler) may be considered for this purpose. This is an area of irrigation, water, and nutrient management for which there is currently little guidance and further research is needed.
- It is critical that the region continue recharging excess surface water via irrigation or, alternatively, in recharge basins on highly permeable non-saline soils to maintain a groundwater banking reserve for drought periods. Such recharge management must consider minimizing salt, nitrate, and pesticide leaching.
- NASL may consider contracting water supplies from the Kings River Conservation District (KRCD), which is located immediately to the east of the property and is not subject to Delta regulations. The water is of very high water quality with significantly lower salinity than water delivered by WWD through SLU. Particularly in wet years, NASL may be able to take advantage of surplus water for additional recharge. Such a contract may involve significant legal, political, and financial investments, and any proposal to move forward along such a venue should be prepared carefully, and with full participation of various stakeholders (e.g., WWD, Fresno County, Kings County, farm community, groundwater management plans, integrated regional water management plans).
- NASL's principal crop water management options include:
    - Partial land fallowing, possibly on a rotating basis: NASL has considerable experience in adjusting crop acreages from year to year to adjust to varying

water supplies. Annual average applied water demand varies from 1.9 AF/yr to 3.2 AF/yr, with an average of 2.6 AF/yr. Depending on drought and surface water supply conditions, future land fallowing may need to be expanded on a year-by-year basis.

- Conversion to crops with significantly lower consumptive use and applied water demand: Wheat (and other cold season grains) have the lowest consumptive water use and applied water demand among currently grown crops. The economic gains for wheat and similar crops are limited, except under high price conditions, but the crop would provide for the necessary land cover and use sought by NASL.
- Use of regulated deficit irrigation on selected crops: The most promising crop for which deficit irrigation protocols exist and that can be grown under the soil and climate condition at NASL are pistachios and field crops. With regulated deficit irrigation, the applied water need for pistachios is approximately 2.3 AF/yr (rather than 2.9 AF/yr without deficit irrigation), which is significantly higher than some field crops, but lower than alfalfa or regularly irrigated tree crops. Planting permanent tree crops reduces land fallowing management options. But the dedication of a limited and carefully selected acreage of NASL agricultural lands to a permanent crop under a long-term contract may provide economic incentives and balance economic costs for growing lower value crops elsewhere on NASL lands. The choice of planting pistachios must be weight against growing other high value (annual) vegetable (truck) crops, especially tomatoes, which have similar applied water demand to pistachios, and which can be rotated into fallow land as needed. Regulated deficit irrigation programs may also be developed for key field crops at NASL, including tomatoes, cotton, and alfalfa.
- Improvements in irrigation technology and irrigation timing: Conversion to sprinkler and drip irrigation is common within WWD and appropriate for NASL. This will reduce applied water demand, but also reduce recharge to groundwater while not significantly affecting the consumptive crop water use. Conversion to center-pivot irrigation reduces irrigated acreage by 20%, if the corners are not separately irrigated, thus amounting to partial fallowing without the disadvantage to NASL of land abandonment.
- Conjunctive use of water
    - in dry years, water use should be minimized by reducing crop consumptive use and minimizing leaching from irrigation
    - in average years, groundwater pumping should be minimized while taking advantage of available surface water for irrigation and intentional recharge
    - in wet years, intentionally high recharge should be considered when excess surface water supplies are available, for example by over-applying water on agricultural lands; this management practice must carefully consider management of fertilizer and pesticide, and soil salinity

7.2 Monitoring Activities

- We recommend that NASL shall continue its ongoing quarterly crop reporting and crop mapping program to assess and evaluate crop water use.
- We recommend adding information about the irrigation system during the quarterly crop reporting and mapping survey, because growers increasingly shift from furrow and flood irrigation to micro-sprinkler and drip irrigation. Having irrigation system information available will provide additional information on potential irrigation efficiency and groundwater recharge.
- NASL shall continue and expand its twice annual groundwater level monitoring program at all of its existing wells. Groundwater level monitoring frequency is best maintained at a quarterly or even monthly surveying cycle. Monthly reporting will allow development of a database that may provide the basis for evaluating groundwater pumping limitations during the following crop year as early as January, which supports growers in their crop year planning efforts.
- At very low cost, a groundwater salinity monitoring program could be added to the water level surveying program to monitor fluctuations and trends in water quality that have significance to the irrigation program.
- NASL shall install groundwater flow meters on all production wells for identification of relationships between groundwater pumping rates and water level drawdown for planning purposes.
- NASL must continue any mandatory groundwater level and groundwater quality monitoring programs under existing agreements with regulatory and planning state agencies (CDWR, SWRCB/RB).
- We strongly recommend that NASL reactivate or install an extensometer system on-site for long-term monitoring of land subsidence.
- We further recommend that any well drilling activities require detailed core drilling, core description and geologic analysis to clearly identify the depth and extent of finer-grained clay and clayey interbeds and aquitards. Any drilling activities must be supervised by a professional, experienced hydrogeologist that can manage the recovery of a full sediment core description, and the acquisition of all appropriate geophysical logs. The base best maintains its own database of groundwater well logging information.
- Potential groundwater contaminants include salinity, arsenic, and nitrate. Nitrate and shallow salinity problems in the produced water can be avoided by drilling sufficiently deep water wells that are sealed off at shallow depths. Native salinity in deeper sediment section must be identified using depth-specific water sampling during the drilling process. Arsenic problems are best avoided by obtaining sediment samples at various depths that can be tested for arsenic leaching. Depth intervals that potentially yield or leach high salinity, nitrate, or arsenic must be sealed off, even at depth. We recommend us of stainless steel screens placed only in highly productive sediment section that have tested negatively for contaminants of interest. Each well may have

multiple screen intervals. Appropriate design criteria shall be included in the bid for well drilling contractors and consulting hydrogeologists.

- Long-term pumping tests may provide important information on aquifer hydraulic properties useful for the construction of groundwater models.

7.3 Administration of Groundwater Data

- We recommend that NASL locally maintain a complete electronic database of historic and current groundwater and other environmental data.
- Efficient data management and analysis at NASL requires the development, purchase, or acquisition of an environmental database management system, including a spatial mapping system, and an efficient data retrieval portal, maintained by knowledgeable personnel locally. For efficiency and economy of scales, NASL may consider providing equivalent (contracted) services to neighboring water districts as part of a collaborative agreement.
- At a minimum, the environmental database would include the following attributes:
    - Capable of storing a wide range of environmental data in one-dimensional, two-dimensional, or three-dimensional spatial systems and in spatio-temporal (time dependent) systems
    - Compatibility with ESRI ArcGIS data formats
    - Compatibility with common spreadsheet and database formats
    - Ease of use and maintenance of meta-data
    - Data quality assurance/quality control capability
    - Relative ease of use and broad capabilities for rapid visualization
    - Provides for basic statistical, geostatistical, and mathematical analysis of data
- The geospatial environmental database shall include all of the following groundwater related information from location onsite or from surrounding locations:
    - Well completion reports for all existing wells
    - Well construction details for all existing wells
    - Well status (active, inactive, abandoned, maintenance records)
    - Groundwater level data, with clear identification of the well and specific depth interval represented by the water level information
    - Groundwater quality data, with clear identification of the well and specific depth interval represented by the water quality information
    - Land elevation data from various sources
        - Extensometers
        - Survey benchmarks
        - Remote sensing data (e.g., INSAR)
        - GPS data
    - Quarterly crop and irrigation information
    - Groundwater pumping and surface water delivery information (monthly)

8 References

Anderson, F.M. (1905). A stratigraphic study in the Mount Diablo Range of California. Proceedings of the California Academy of Sciences.3d series. Geology, vol. 2, no. 2.

Beede, R. H.; and D. A. Goldhamer (2005) Olive irrigation management. In: Olive Production Manual, Second Edition, G. S. Sibbett; and L. Ferguson, eds. University of California Publication 3353. pp. 61-69.

Belitz, K.; S. P. Phillips; and J.M. Gronberg (1993), Numerical Simulation of Ground-Water Flow in the Central Part of the Western San Joaquin Valley, California, U.S. Geological Survey Water Supply Paper 2396, 69 p.

Belitz, K., and S. P. Phillips (1995), Alternative to agriculture drains in California's San Joaquin valley: Results of a regional-scale hydrogeologic approach, Water Resour. Res., 31, 1845– 1862.

Bull, W.B. (1964). Alluvial fans and near-surface subsidence in Western Fresno County, California. U.S. Geological Survey Prof. paper 437-A.

Bull, W.B.; and J.F. Poland, (1975), Land subsidence due to groundwater withdrawal in the Los Banos-Kettleman City area, California, Part 3. Interrelations of water-level change, change in aquifer-system thickness, and subsidence. U.S. Geological Survey Professional Paper 437-G, 62 p.

Cal-Atlas geospatial clearinghouse (2010). Available: http://atlas.ca.gov/imagerySearch.html. Accessed: June 2010.

California Department of Water Resources website (2010). Groundwater level data by township, range, and section. Available: http://www.water.ca.gov/waterdatalibrary/groundwater/hydrographs/index_trs.cfm. Accessed: April 2010.

California Department of Water Resources (1997) Fifteen Years of Growth and a Promising Future: The California Irrigation Management Information System. Sacramento, California.

California Department of Water Resources (2010). Integrated Water Resources Information System (IWRIS). Available: http://www.water.ca.gov/iwris/. Accessed: June 2010.

California Department of Water Resources groundwater data and monitoring website (2010). Available: http://www.water.ca.gov/groundwater/data_and_monitoring/south_central_region/GroundwaterLevel/gw_level_monitoring.cfm. Accessed: November 2010.

California Department of Water Resources groundwater data and monitoring website (2010).. Available: http://www.water.ca.gov/groundwater/data_and_monitoring/south_central_region/GroundwaterQuality/gw_quality_monitoring.cfm. Accessed: November 2010.

California Department of Water Resources website, State well numbering system (2010) Available: http://www.water.ca.gov/waterdatalibrary/includes/StateWellNumber.cfm. Accessed 11/28/2010.

California Department of Water Resources. Bulletin 118 - Update 2003. Available: http://www.water.ca.gov/pubs/groundwater/bulletin_118/california%27s_groundwater__bulletin_118_-_update_2003_/bulletin118_entire.pdf. Accessed: July 2010.

Chaves, M.M.; T.P. Santos; C.R. Souza; M.F. Ortuno; M.L. Rodrigues; and C.M. Lopes; and J.P.

Clemmens, A. J.; R. G. Allen; and C. M. Burt (2008), Technical concepts related to conservation of irrigation and rainwater in agricultural systems, Water Resour. Res., 44, W00E03, doi:10.1029/2007WR006095.

Cooley, H.; Christian-Smith, J.; Glieck, P.H. (2008) More with less: Agricultural water conservation and efficiency in California. A special focus on the delta. Pacific Institute. Available: www.pacinst.org/reports/more_with_less_delta

Croft, M.G; (1969). Subsurface geology of the late tertiary and quaternary water-bearing deposits of the southern part of the San Joaquin Valley. U.S Geological Survey open file report.

Croft, M.G; and G. V. Gordon (1968). Geology, hydrology, and quality of water in the Hanford-Visalia area San Joaquin Valley, California. U.S Geological Survey open file report.

Davis, G.H.; and J.F. Poland (1957). Ground-water conditions in the Mendota-Huron area, Fresno and Kings Counties, California. U.S. Geological Survey water-supply paper 1360-G.

Davis, S.N.; and F.R. Hall (1959). Water quality of eastern Stanislaus and Northern Merced Counties, California. Stanford Univ. Pub., Geol. Sci., v. 6, no. 1.

Eching, S. (2002) Role of Technology in Irrigation Advisory Services: The CIMIS Experience. Irrigation Advisory Services and Participatory Extension in Irrigation Management Workshop, FAO – ICID. Montreal, Canada.

Evans, R. G.; and E. J. Sadler (2008), Methods and technologies to improve efficiency of water use, Water Resour. Res., 44, W00E04, doi:10.1029/2007WR006200.

Faunt, C.C., ed., (2009) Groundwater Availability of the Central Valley Aquifer, California. U.S. Geological Survey Professional Paper 1766, 225 p.

Fereres, E.; and M.A. Soriano (20062007). Deficit irrigation for reducing agricultural water use. Journal of Experimental Botany, 58 (2), pp. 147-159. DOI: 10.1093/jxb/erl165

Galloway, D.L.; D.R Jones; and S.E. Ingebritsen, (1999) Land subsidence in the United States: U.S. Geological Survey Circular 1182, 177 p. http://pubs.usgs.gov/circ/circ1182/

Goldhamer, D.A. (1999) Regulated deficit irrigation for California canning olives. ISHS Acta Horticulturae 474(1), pp. 369-372.

Goldhamer, D.A.; and M. Salinas (2006). Goldhamer, D.A.; and M. Salinas (2000). Evaluation of regulated deficit irrigation on mature orange trees grown under high evaporative demand. Proc. Intl. Soc. Citrucult. IX Congress, pp. 227-231.

Goldhamer, D.A.; and R.H. Beede (2004). Regulated deficit irrigation effects on yield, nut quality and water-use efficiency of mature pistachio trees. The Journal of Horticultural Science and Biotechnology, 79 (4), pp. 538-545.

Goldhamer, D.A.; E. Fereres, M. Salinas (2003). Can almond trees directly dictate their irrigation needs? California Agriculture, 57(4), pp. 138-144.

Goldhamer, D.A.; M. Viveros; and M. Salinas (2006). Regulated deficit irrigation in almonds: effects of variations in applied water stress timing on yield and yield components. Irrigation Science, Vol. 24(2), pp. 101-114. DOI: 10.1007/s00271-005-0014-8.

González-Altozano, P.; and J.RL. Castel (2000). Effects of regulated deficit irrigation on 'Clementina de Nules' citrus trees growth, yield, and fruit quality. ISHS Acta Horticulturae, 537, pp. 749- 758.

Grattan, S.R.; M.J. Berenguer; J.H. Connell; V.S. Polito; and P.M. Vossen (2006). Olive oil production as influenced by different quantities of applied water. Agric. Water Mang. Vol. 85 (1-2), pp. 133-140. doi:10.1016/j.agwat.2006.04.001.

Hanson, R.T., (1989). Aquifer-System Compaction, Tucson Basin and Avra Valley, Arizona. U.S. Geological Survey Water-Resources Investigations Report 88-4172, 69 p.

Hanson, B.R. and D.M. May. 2006. Crop evapotranspiration of processing tomato in the San Joaquin Valley of California, USA. Irrig Sci. 24: 211–221.

Harbaugh, A.W.; E.R. Banta; M.C. Hill; and M.G. McDonald (2000). Modflow-2000, the U.S. Geological Survey modular ground-water model—user guide to modularization concepts and the ground-water flow process. U.S. Geological Survey Open-File Report 00-92, 192 p.

Harbaugh, A.W.; and M.G. McDonald, (1996). User's documentation for MODFLOW-96, an update to the U.S. Geological Survey modular finite-difference ground-water flow model. U.S. Geological Survey Open-File Report 96-485, 56 p.

Helm, D.C. (1975), One-dimensional simulation of aquifer system compaction near Pixley, California. 1, Constant parameters, Water Resources Research, v. 11, no. 3, pp. 465–478.

Helm, D.C. (1976), One-dimensional simulation of aquifer-system compaction near Pixley; California. 2, Stress-dependent parameters: Water Resources Research, v. 12, no. 3, pp. 375-391.

Helm, D.C. (1977), Estimating parameters of compacting fine-grained interbeds within a confined aquifer system by a one-dimensional simulation of field observations, In Land subsidence symposium. Proceedings of the Second International Symposium on Land Subsidence, held at Anaheim, California, 13-17 December 1976. International Association of Hydrologic Sciences, IAHS-AISH Publication series, no. 121, p. 145-156.

Helm, D.C. (1978), Field verification of a one-dimensional mathematical model for transient compaction and expansion of a confined aquifer system, in verification of mathematical and physical models in hydraulic engineering. Proceedings, 26th annual Hydraulics Division specialty conference, University of Maryland, College Park, Maryland, August 9-11, 1978, New York, American Society of Civil Engineers, p. 189-196.

Hoffmann, J.; S.A. Leake; D.L. Galloway; and A.M. Wilson (2003), MODFLOW-2000 ground-water model -- User guide to the subsidence and aquifer-system compaction (SUB) Package. U.S. Geological Survey Open-File Report 03-233, 44 p.

Holzer, T.L., (1981), Preconsolidation Stress of Aquifer Systems in Areas of Induced Land Subsidence. Water Resources Research, Vol. 17, No. 3, pages 693-704.

Iniesta, F.; L. Testi; D. A. Goldhamer; and E. Fereres (2008), Quantifying reductions in consumptive water use under regulated deficit irrigation in pistachio (*Pistacia vera* L.), Agric. Water Mgmt 95, pp. 877-886.

Ireland, R.L.; J.F Poland; and F.S. Riley (1984), Land subsidence in the San Joaquin Valley, California, as of 1980, U.S. Geological Survey Professional Paper 437-I, 93 p.

Johnson, A.I., (1984). Laboratory tests for properties of sediments in subsiding areas, pt. 1, chap. 4 of Poland, J.F.., ed., Guidebook to studies of land subsidence due to ground-water withdrawal. Paris, UNESCO, Studies and reports in Hydrology 40, p 55-88.

Johnson, A.I.; R.P. Moston; and D.A. Morris, (1968). Physical and hydrologic properties of water-bearing deposits in subsiding areas in Central California. U.S. Geological Survey Professional Paper 497-A, 71 p., 14 pls.

Johnson, T.; and K. Belitz (2003) Hydrogeologic Provinces for California based upon established groundwater basins and watershed polygons. U.S. Geological Survey open file report 03-470 edition 1.0. Retrieved from: http://water.usgs.gov/lookup/getspatial?ca_provinces. Accessed 11/1/2010.

Kenneth D. Schmidt and Associates (2002). Groundwater conditions and reuse of City of Lemoore WWTF effluent in the Westlake Farms area. Prepared by Kenneth D. Schmidt and Associates, Fresno, California for Westlands Water District, California.

Kenneth D. Schmidt and Associates (2009). Groundwater conditions beneath district owned lands in the Westlands Water District. Prepared by Kenneth D. Schmidt and Associates, Fresno, California for Westlands Water District, California.

Laudon, J.; and K. Belitz (1991). Texture and depositional history of late Pleistocene-Holocene alluvium in the central part of the Western San Joaquin Valley, California. California: Bulletin of the Association of Engineering.

Leake, S.A.; and M.R. Lilly, (1997). Documentation of a computer program (FHB1) for assignment of transient specified-flow and specified-head boundaries in applications of the modular finite- difference ground- water flow model (MODFLOW). U.S. Geological Survey Open-File Report 97-571, 50 p.

Lofgren, B.E., (1975). Land subsidence due to ground-water withdrawal, Arvin-Maricopa area, California. U.S. Geological Survey professional paper 437-D.

Maroco, and J.S. Pereira. (2007). Deficit irrigation in grapevine improves water-use efficiency while controlling vigour and production quality, Annals of Applied Biology, Vol. 150, Issue 2, pp. 237-252.

McDonald, M.G.; and A.W. Harbaugh, (1988), A modular three- dimensional finite-difference ground-water flow model. U.S. Geological Survey Techniques of Water-Resources Investigations, book 6, chap. A1, 586 p.

Meinzer, O.E. (1928), Compressibility and elasticity of artesian aquifers, Economic Geology, v. 23, no. 3, p. 263-291. DOI: 10.2113/gsecongeo.23.3.263.

Mendenhall, W.C.; R.B. Dole; and H. Stabler (1916). Ground water in San Joaquin Valley, California. U.S. Geological Survey water-supply paper 398.

Munk, D.S., J.F. Wroble and R.B. Hutmacher. Crop Responses to Water Deficits in High Yielding Pima and Acala Cotton. 2007. Beltwide Cotton Production Conferences. p. 31-32.

Munk, D., J. Wroble, R. Snyder, J. Robb, and R. Hutmacher. 2004. Comparative evaluation of Pima and Upland cotton transpiration in the San Joaquin Valley. Acta Hort. Vol. 664:419-426.

National Geodetic Survey datasheet page (2010). Available: http://www.ngs.noaa.gov/cgi-bin/datasheet.prl. Accessed: August 2010.

Orloff, S., D.H. Putnam, B. Hanson and H. Carlson. 2004. Controlled Deficit Irrigation of Alfalfa (Medicago sativa): A Strategy for Addressing Water Scarcity in California. 2004 12th AAC, 4th ICSC.

Page, R.W. (1973). Base of fresh ground water (approximately 3,000 micromhos) in the San Joaquin Valley, California. U.S. Geological Survey Hydrologic investigations atlas HA-489.
Poland, J. F.; B. E. Lofgren; R. L. Ireland; and R. G. Pugh (1975) Land subsidence in the San Joaquin Valley, California, as of 1972, U.S. Geological Survey Professional Paper 437-H.

Poland, J.F., ed., 1984, Guidebook to studies of land subsidence due to ground-water withdrawal, v. 40 of UNESCO Studies and Reports in Hydrology: Paris, Frane, United Nations Educational, Scientific and Cultural Organization, 305 p., 5 appendixes.

Putnam, D.; M. Russelle; S. Orloff; J. Kuhn; L. Fitzhugh; L. Godfrey; A. Kiess; and R. Long (2001). Alfalfa, Wildlife, and the Environment. California Alfalfa and Forage Association, Novato, California.

Reilly, Thomas E., (2008). Ground-Water Availability in the United States. U.S. Geological Survey Circular 1323, 84p.

Riley, F.S., (1969). Analysis of borehole extensometer data from central California. International Association of Scientific Hydrology Publication 89.
Riley, F.S. (1984). Developments in borehole extensometry. U.S .Geological Survey, Menlo Park, CA.

Riley, F.S., (1998). Mechanics of aquifer systems—The scientific legacy of Dr. Joseph F. Poland, in Borchers, J.W., ed., Land subsidence case studies and current research: Proceedings of the Dr. Joseph F. Poland Symposium on Land Subsidence, Association of Engineering Geologists Special Publication no. 8.

Repenning, C. A. (1960). Geologic summary of the Central Valley of California, with reference to disposal of liquid radioactive waste. U.S. Geological Survey open file report.

Ruud, N. C.; T. Harter; and A.W. Naugle, (2004) Estimation of groundwater pumping as closure to the water balance of a semi-arid, irrigated agricultural basin. Journal of Hydrology 297, pp. 51-73.

Sneed, M.; and D.L Galloway, (2000) Aquifer-system compaction and land subsidence: Measurements, analyses, and simulations-the Holly Site, Edwards Air Force Base, Antelope Valley, California, U.S. Geological Survey Water-Resources Investigations Report 00-4015, 65 p.

Sneed, M., (2001) Hydraulic and mechanical properties affecting ground-water flow and aquifer system compaction, San Joaquin Valley, California. U.S. Geological Survey Open-File Report 01-35. 26p.

Sun, R.J; J.B. Weeks; and H.F. Grubb (1991). Regional aquifer-system analysis--Central Valley, California. U.S. Geological Survey Water-Resources Investigations Report 97-4074.

Terzaghi, K. (1925) Principles of soil mechanics: IV: settlement and consolidation of clay, Erdbaummechanics, v. 95, no. 3, pp. 874-878.

Terzaghi, K., (1943). Theoretical soil mechanics. New York, Wiley, 510 p.

U.S Geological Survey seamless data warehouse (2010). Available: http://seamless.usgs.gov. Accessed: June 2010.

U.S. Geological Survey NED 1 arc second and NED 1/3 arc second Download Tool (2010). Available: http://cumulus.cr.usgs.gov/webappcontent/neddownloadtool/NEDDownloadToolDMS.html. Accessed 11/1/2010.

UNAVCO GPS data website (2010). Available: http://www.unavco.org/. Accessed: August 2010.

University of California (2008) Available: http://ucmanagedrought.ucdavis.edu/Olives.cfm. Accessed: 8/10/2010.

Westlands Water District (2007). Water Management Plan.

Williamson, A.K.; D.E. Prudic; and L.A. Swain, (1989). Ground-water flow in the Central Valley, California. U.S. Geological Survey Professional Paper 1401-D, 127 p.

Woodring, W. P., R. Stewart; and R.W. Richards (1940). Geology of the Kettleman Hills oil field, California; stratigraphy, paleontology, and structure. U.S. Geological Survey professional paper 195.

WWD Maps website (2010) Available: http://www.westlandswater.org/wwd/pages/general.asp?title=Maps&page=Maps&index=1&cwide=896 . Accessed: November 2010.

Zhang, H.; T. Harter; and B. Sivakumar (2006). Nonpoint source solute transport normal to aquifer bedding in heterogeneous, Markov chain random fields, Water Resour. Res., Vol. 42, No. 6, W06403, DOI: 10.1029/2004WR003808

Appendix A Crop acreage and water use data at NASL, by year, from 1974 to 2010

2010.00 Crop Type	Total Acreage	Estimated Applied Water (Af/Ac)	Estimated Applied Water (AF)	Estimated Crop Water Requirement (Af/Ac)	Estimated Crop Water Requirement (AF)	Estimated Recharge (Af/Ac)	Estimated Recharge (AF)	Estimated Application Efficiency (%)	Estimated Uptake Efficiency (%)
Open	1554								
Alfalfa	3414	4.50	15363	4.01	13690	0.76	2597	89.2	84.7
Cotton	6052	2.32	14019	2.07	12499	0.29	1744	89.2	89.5
Tomatoes	408	1.37	560	1.16	471	0.41	168	84.2	77.5
Wheat	530	1.21	642	0.96	509	0.27	146	79.2	83.8
Corn	158	2.79	442	2.07	328	0.79	126	74.2	71.6
Garbanzo	321	0.05	15	0.03	11	0.02	5	74.2	90.4
Onions	697	3.29	2291	1.95	1355	1.65	1150	59.2	55.1
Oats	548	2.79	1531	2.07	1136	0.79	435	74.2	71.6
Total	12128	2.87	34864	2.47	29998	0.53	6370	86.0	

2009.00 Crop Type	Total Acreage	Estimated Applied Water (Af/Ac)	Estimated Applied Water (AF)	Estimated Crop Water Requirement (Af/Ac)	Estimated Crop Water Requirement (AF)	Estimated Recharge (Af/Ac)	Estimated Recharge (AF)	Estimated Application Efficiency (%)	Estimated Uptake Efficiency (%)
Open	6382								
Alfalfa	3707	4.50	16682	4.01	14865	0.76	2820	89.2	84.7
Cotton	1193	2.32	2763	2.07	2463	0.29	344	89.2	89.5
Tomatoes	292	1.37	401	1.16	337	0.41	121	84.2	77.5
Wheat	1679	1.21	2036	0.96	1612	0.27	461	79.2	83.8
Garbanzo	799	0.05	37	0.03	28	0.02	12	74.2	90.4
Onion	707	3.29	2326	1.95	1376	1.65	1167	59.2	55.1
Total	8377	2.89	24245	2.47	20681	0.59	4925	85.3	

2008.00 Crop Type	Total Acreage	Estimated Applied Water (Af/Ac)	Estimated Applied Water (AF)	Estimated Crop Water Requirement (Af/Ac)	Estimated Crop Water Requirement (AF)	Estimated Recharge (Af/Ac)	Estimated Recharge (AF)	Estimated Application Efficiency (%)	Estimated Uptake Efficiency (%)
Open	1447								
Alfalfa	3457	4.50	15554	4.01	13860	0.76	2629	89.2	84.7
Cotton	2654	2.32	6148	2.07	5481	0.29	765	89.2	89.5
Tomatoes	656	1.37	901	1.16	758	0.41	271	84.2	77.5
Wheat	2327	1.21	2821	0.96	2233	0.27	639	79.2	83.8
Corn	223	2.79	623	2.07	462	0.79	177	74.2	71.6
Onion	2912	3.29	9577	1.95	5666	1.65	4805	59.2	55.1
Safflower	377	1.82	689	1.63	614	0.24	89	89.2	89.8
Total	12605	2.88	36312	2.31	29074	0.74	9375	80.1	

2006.00 Crop Type	Total Acreage	Estimated Applied Water (Af/Ac)	Estimated Applied Water (AF)	Estimated Crop Water Requirement (Af/Ac)	Estimated Crop Water Requirement (AF)	Estimated Recharge (Af/Ac)	Estimated Recharge (AF)	Estimated Application Efficiency (%)	Estimated Uptake Efficiency (%)
Open	430								
Alfalfa	2809	4.00	11222	3.52	9899	0.62	1731	88.2	86.5
Cotton	7451	1.88	14012	1.66	12360	0.24	1785	88.2	89.8
Tomatoes	1458	1.36	1981	1.13	1649	0.40	584	83.2	78.4
Wheat	342	1.08	369	0.84	288	0.25	84	78.2	83.8
Corn	383	2.79	1070	2.04	783	0.79	303	73.2	71.7
Onion	334	3.37	1126	1.96	655	1.63	546	58.2	57.5
Garbanzo	314	1.65	517	1.21	379	0.51	159	73.2	76.5
Total	13092	2.31	30296	1.99	26013	0.40	5192	85.9	

2005.00 Crop Type	Total Acreage	Estimated Applied Water (Af/Ac)	Estimated Applied Water (AF)	Estimated Crop Water Requirement (Af/Ac)	Estimated Crop Water Requirement (AF)	Estimated Recharge (Af/Ac)	Estimated Recharge (AF)	Estimated Application Efficiency (%)	Estimated Uptake Efficiency (%)
Open	2344								
Alfalfa	2265	3.57	8088	3.20	7253	0.54	1231	89.7	85.7
Cotton	6372	2.25	14308	2.01	12832	0.26	1661	89.7	89.0
Tomatoes	504	1.95	981	1.65	831	0.50	254	84.7	75.7
Wheat	325	1.19	385	0.94	307	0.26	84	79.7	82.8
Corn	551	2.75	1518	2.06	1133	0.75	416	74.7	72.6
Garbanzo	373	0.89	333	0.67	248	0.27	102	74.7	70.5
Onion	839	3.15	2645	1.88	1578	1.53	1285	59.7	55.7
Sugar Beets	164	3.25	533	2.42	398	0.86	141	74.7	75.8
Lettuce Seed	63	0.92	58	0.55	34	0.54	34	59.7	41.7
Oats	588	2.75	1621	2.06	1210	0.75	444	74.7	72.6
Total	12045	2.53	30468	2.14	25825	0.47	5652	84.8	

2004.00 Crop Type	Total Acreage	Estimated Applied Water (Af/Ac)	Estimated Applied Water (AF)	Estimated Crop Water Requirement (Af/Ac)	Estimated Crop Water Requirement (AF)	Estimated Recharge (Af/Ac)	Estimated Recharge (AF)	Estimated Application Efficiency (%)	Estimated Uptake Efficiency (%)
Open	1153								
Alfalfa	2162	4.56	9850	4.01	8663	0.77	1662	87.9	83.8
Cotton	8473	2.25	19048	1.98	16751	0.30	2537	87.9	87.5
Tomatoes	940	1.97	1853	1.63	1537	0.54	509	82.9	74.3
Wheat	580	1.36	787	1.06	614	0.32	185	77.9	78.8
Corn	262	2.82	739	2.06	539	0.82	215	72.9	70.9
Onion	55	4.01	220	2.32	128	1.99	109	57.9	52.4
Sugar Beet	151	3.48	524	2.54	382	0.98	148	72.9	73.0
Lettuce Seeds	30	1.06	32	0.61	19	0.62	19	1.1	57.9
Total	12653	2.61	33053	2.26	28632	0.43	5384	86.6	

2003.00 Crop Type	Total Acreage	Estimated Applied Water (Af/Ac)	Estimated Applied Water (AF)	Estimated Crop Water Requirement (Af/Ac)	Estimated Crop Water Requirement (AF)	Estimated Recharge (Af/Ac)	Estimated Recharge (AF)	Estimated Application Efficiency (%)	Estimated Uptake Efficiency (%)
Open	1507								
Alfalfa	2894	4.36	12611	3.73	10800	0.83	2402	85.6	81.7
Cotton	8146	2.31	18844	1.98	16138	0.36	2939	85.6	85.3
Tomatoes	330	2.08	686	1.68	554	0.61	201	80.6	72.4
Wheat	605	1.49	902	1.13	682	0.38	232	75.6	76.4
Corn	129	2.91	374	2.06	264	0.91	117	70.6	68.7
Sugar Beets	118	3.60	425	2.54	300	1.10	130	70.6	70.7
Safflower	136	2.11	286	1.80	245	0.34	46	85.6	85.0
Total	12358	2.76	34128	2.35	28982	0.49	6067	84.9	

2002.00 Crop Type	Total Acreage	Estimated Applied Water (Af/Ac)	Estimated Applied Water (AF)	Estimated Crop Water Requirement (Af/Ac)	Estimated Crop Water Requirement (AF)	Estimated Recharge (Af/Ac)	Estimated Recharge (AF)	Estimated Application Efficiency (%)	Estimated Uptake Efficiency (%)
Open	991								
Alfalfa	3302	3.90	12877	3.89	12836	0.28	915	99.7	93.1
Cotton	7835	2.00	15679	1.99	15630	0.04	330	99.7	98.0
Tomatoes	535	1.82	975	1.73	923	0.32	173	94.7	83.1
Wheat	852	1.42	1211	1.27	1086	0.18	150	89.7	88.2
Corn	162	2.45	395	2.07	335	0.45	72	84.7	81.8
Onion	11	3.65	42	2.54	29	1.48	17	69.7	60.2
Safflower	279	1.92	535	1.91	533	0.05	14	99.7	97.5
Total	12976	2.44	31714	2.42	31372	0.13	1671	98.9	

2001.00 Crop Type	Total Acreage	Estimated Applied Water (Af/Ac)	Estimated Applied Water (AF)	Estimated Crop Water Requirement (Af/Ac)	Estimated Crop Water Requirement (AF)	Estimated Recharge (Af/Ac)	Estimated Recharge (AF)	Estimated Application Efficiency (%)	Estimated Uptake Efficiency (%)
Open	2991								
Alfalfa	1348	4.38	5904	3.88	5228	0.77	1032	88.6	83.8
Cotton	8546	2.24	19129	1.98	16940	0.29	2493	88.6	87.6
Tomatoes	338	1.96	661	1.63	552	0.54	184	83.6	0.5
Wheat	283	1.26	358	0.99	281	0.29	83	78.6	81.1
Corn	139	2.82	391	2.07	287	0.82	113	73.6	71.0
Onion	207	3.06	634	1.79	371	1.56	323	58.6	52.3
Safflower	1448	2.00	2900	1.77	2568	0.27	391	88.6	87.8
Sugar Beets	160	3.44	551	2.53	405	0.96	154	73.6	73.6
Garbanzo	139	2.28	316	1.67	232	0.75	104	73.6	69.4
Total	12607	2.45	30842	2.13	26865	0.39	4876	87.1	

2000.00 crop	Total acreages	Estimated Applied Water (Af/Ac)	Estimated Applied Water (AF)	Estimated Crop Water Requirement (Af/Ac)	Estimated Crop Water Requirement (AF)	Estimated Recharge (Af/Ac)	Estimated Recharge (AF)	Estimated Application Efficiency (%)	Estimated Uptake Efficiency (%)
Open	521								
Alfalfa	1653	3.63	5994	3.48	5753	0.34	556	96.0	91.2
Cotton	8790	2.05	18028	1.97	17301	0.11	975	96.0	94.6
Tomatoes	625	1.87	1167	1.70	1062	0.38	236	91.0	79.9
Wheat	676	1.22	825	1.05	710	0.19	129	86.0	87.0
Garbanzo	212	2.18	464	1.77	375	0.54	115	81.0	75.1
Onions	18	3.49	62	2.30	41	1.49	27	66.0	59.3
Total	11974	2.22	26540	2.11	25241	0.17	2038	95.1	

1999.00 Crop	Total Acreages	Estimated Applied Water (Af/Ac)	Estimated Applied Water (AF)	Estimated Crop Water Requirement (Af/Ac)	Estimated Crop Water Requirement (AF)	Estimated Recharge (Af/Ac)	Estimated Recharge (AF)	Estimated Application Efficiency (%)	Estimated Uptake Efficiency (%)
Open	2423								
Alfalfa	2139	4.38	9373	3.83	8190	0.76	1631	87.4	82.8
Cotton	8562	2.36	20214	2.06	17663	0.33	2805	87.4	86.1
Tomatoes	977	2.13	2081	1.76	1715	0.59	573	82.4	72.5
Wheat	286	1.71	489	1.32	379	0.41	118	77.4	76.6
Garbanzo	142	2.54	362	1.84	262	0.84	119	72.4	67.1
Onions	64	4.37	278	2.51	160	2.18	139	57.4	50.6
Safflower	98	2.27	223	1.98	195	0.32	32	87.4	85.8
Melons	238	2.19	523	1.59	378	0.69	165	72.4	68.4
Total	12507	2.68	33544	2.31	28941	0.45	5581	86.3	

1998.00 Crop	Total Acreages	Estimated Applied Water (Af/Ac)	Estimated Applied Water (AF)	Estimated Crop Water Requirement (Af/Ac)	Estimated Crop Water Requirement (AF)	Estimated Recharge (Af/Ac)	Estimated Recharge (AF)	Estimated Application Efficiency (%)	Estimated Uptake Efficiency (%)
Open	685								
Alfalfa	1499	3.30	4941	2.96	4441	0.50	743	89.9	87.2
Cotton	10440	2.11	22037	1.90	19808	0.24	2514	89.9	89.1
Tomatoes	2055	1.74	3581	1.48	3039	0.46	950	84.9	74.9
Wheat	141	0.89	126	0.71	101	0.19	27	79.9	87.1
Corn	188	2.61	491	1.95	367	0.71	133	74.9	73.8
Onions	50	2.22	112	1.33	67	1.10	55	59.9	60.4
Melons	53	1.84	97	1.38	73	0.54	28	74.9	73.7
Total	14427	2.18	31385	1.93	27896	0.31	4451	88.9	

1997.00 Crop	Total Acreages	Estimated Applied Water (Af/Ac)	Estimated Applied Water (AF)	Estimated Crop Water Requirement (Af/Ac)	Estimated Crop Water Requirement (AF)	Estimated Recharge (Af/Ac)	Estimated Recharge (AF)	Estimated Application Efficiency (%)	Estimated Uptake Efficiency (%)
Open	848								
Alfalfa	237	5.56	1319	4.54	1077	1.27	301	81.6	78.9
Cotton	12276	2.60	31888	2.12	26032	0.51	6231	81.6	82.0
Tomatoes	1163	2.04	2372	1.56	1818	0.68	790	76.6	69.9
Wheat	52	1.82	94	1.30	67	0.54	28	71.6	72.1
Onions	11	4.50	48	2.32	25	2.48	26	51.6	48.1
Sugar Beets	542	4.28	2324	2.86	1548	1.47	800	66.6	67.2
Trees	31								
Total	14313	2.66	38045	2.14	30566	0.57	8176	80.3	

1996.00 Crop	Total Acreages	Estimated Applied Water (Af/Ac)	Estimated Applied Water (AF)	Estimated Crop Water Requirement (Af/Ac)	Estimated Crop Water Requirement (AF)	Estimated Recharge (Af/Ac)	Estimated Recharge (AF)	Estimated Application Efficiency (%)	Estimated Uptake Efficiency (%)
Open	3116								
Cotton	11792	2.63	31067	2.21	26010	0.46	5478	83.7	83.3
Corn	304	2.85	868	1.96	596	0.95	290	68.7	67.7
Trees	91								
Total	12188	2.62	31934	2.18	26606	0.47	5767	83.3	

1995.00 Crop	Total Acreages	Estimated Applied Water (Af/Ac)	Estimated Applied Water (AF)	Estimated Crop Water Requirement (Af/Ac)	Estimated Crop Water Requirement (AF)	Estimated Recharge (Af/Ac)	Estimated Recharge (AF)	Estimated Application Efficiency (%)	Estimated Uptake Efficiency (%)
Open	1443								
Cotton	12822	2.09	26862	1.79	23000	0.33	4275	85.6	86.2
Tomatoes	451	1.79	809	1.45	652	0.55	248	80.6	74.2
Corn	177	2.44	432	1.72	305	0.78	137	70.6	72.0
Trees	153								
Safflower	198	2.29	454	1.96	388	0.37	74	85.6	85.7
Total	13801	2.07	28557	1.76	24345	0.34	4735	85.3	

1994.00 Crop	Total Acreages	Estimated Applied Water (Af/Ac)	Estimated Applied Water (AF)	Estimated Crop Water Requirement (Af/Ac)	Estimated Crop Water Requirement (AF)	Estimated Recharge (Af/Ac)	Estimated Recharge (AF)	Estimated Application Efficiency (%)	Estimated Uptake Efficiency (%)
Open	1552								
Cotton	11987	2.47	29613	2.17	26049	0.34	4031	88.0	86.8
Tomatoes	913	2.08	1895	1.72	1572	0.57	517	83.0	74.0
Wheat	50	1.71	86	1.33	67	0.41	21	78.0	78.4
Onions	128	4.03	516	2.33	299	2.04	262	58.0	50.5
Safflower	481	2.45	1180	2.16	1038	0.34	166	88.0	86.6
Sugar Beets	130	3.89	504	2.84	368	1.11	144	73.0	72.9
Total	13688	2.47	33794	2.15	29393	0.38	5140	87.0	

1993.00 Crop	Total Acreages	Estimated Applied Water (Af/Ac)	Estimated Applied Water (AF)	Estimated Crop Water Requirement (Af/Ac)	Estimated Crop Water Requirement (AF)	Estimated Recharge (Af/Ac)	Estimated Recharge (AF)	Estimated Application Efficiency (%)	Estimated Uptake Efficiency (%)
Open	1257								
Cotton	11169	1.82	20338	1.66	18491	0.20	2178	90.9	90.9
Tomatoes	57	1.67	96	1.44	83	0.44	25	85.9	79.9
Wheat	480	1.15	552	0.93	447	0.24	116	80.9	86.6
Onions	83	3.69	307	2.25	187	1.78	148	60.9	55.6
Safflower	1375	2.17	2978	1.97	2708	0.24	333	90.9	91.0
Sugar Beets	607	3.19	1938	2.43	1472	0.82	496	75.9	78.7
Tree Line	51								
Total	13822	1.90	26210	1.69	23387	0.24	3296	89.2	

1992.00 Crop	Total Acreages	Estimated Applied Water (Af/Ac)	Estimated Applied Water (AF)	Estimated Crop Water Requirement (Af/Ac)	Estimated Crop Water Requirement (AF)	Estimated Recharge (Af/Ac)	Estimated Recharge (AF)	Estimated Application Efficiency (%)	Estimated Uptake Efficiency (%)
Open	1556								
Cotton	8785	2.14	18774	1.98	17353	0.21	1856	92.4	91.4
Tomatoes	998	1.71	1708	1.50	1493	0.45	448	87.4	78.0
Corn	164	2.31	377	1.79	292	0.61	99	77.4	76.7
Tree Line	89								
Safflower	3324	2.14	7100	1.97	6563	0.23	748	92.4	90.9
Sugar Beets	158	3.32	526	2.57	407	0.82	130	77.4	78.1
Total	13518	2.32	28485	1.96	26108	0.46	3281	91.7	

1991.00 Crop	Total Acreages	Estimated Applied Water (Af/Ac)	Estimated Applied Water (AF)	Estimated Crop Water Requirement (Af/Ac)	Estimated Crop Water Requirement (AF)	Estimated Recharge (Af/Ac)	Estimated Recharge (AF)	Estimated Application Efficiency (%)	Estimated Uptake Efficiency (%)
Open	1041								
Alfalfa	895	5.18	4638	4.97	4452	0.68	606	96.0	87.8
Cotton	9153	2.18	19926	2.09	19128	0.14	1278	96.0	94.2
Tomatoes	154	1.87	288	1.70	262	0.42	64	91.0	80.3
Wheat	862	1.53	1320	1.32	1135	0.26	221	86.0	86.4
Corn	72	2.27	163	1.84	132	0.52	37	81.0	79.4
Safflower	1832	2.30	4205	2.20	4037	0.16	298	96.0	93.7
Melons	424	1.70	722	1.38	585	0.45	192	81.0	76.8
Sugar Beets	416	3.49	1453	2.83	1177	0.74	309	81.0	80.6
Total	13806	2.37	32715	2.24	30908	0.22	3005	94.5	

1990.00 Crop	Total Acreages	Estimated Applied Water (Af/Ac)	Estimated Applied Water (AF)	Estimated Crop Water Requirement (Af/Ac)	Estimated Crop Water Requirement (AF)	Estimated Recharge (Af/Ac)	Estimated Recharge (AF)	Estimated Application Efficiency (%)	Estimated Uptake Efficiency (%)
Open	1198								
Alfalfa	949	5.34	5073	4.88	4631	0.86	819	91.3	84.4
Cotton	10994	2.31	25415	2.11	23201	0.25	2713	91.3	89.9
Tomatoes	315	2.06	649	1.78	560	0.52	164	86.3	76.6
Corn	156	2.52	391	1.92	299	0.68	105	76.3	74.8
Garbanzo	274	2.33	637	1.78	486	0.74	203	76.3	69.8
Safflower	330	2.53	836	2.31	763	0.28	94	91.3	89.4
Melons	233	1.91	445	1.46	339	0.57	133	76.3	72.4
Sugar Beets	264	4.11	1087	3.14	829	1.05	277	76.3	75.5
Total	13514	2.56	34533	2.30	31108	0.33	4509	90.1	

1989.00 Crop	Total Acreages	Estimated Applied Water (Af/Ac)	Estimated Applied Water (AF)	Estimated Crop Water Requirement (Af/Ac)	Estimated Crop Water Requirement (AF)	Estimated Recharge (Af/Ac)	Estimated Recharge (AF)	Estimated Application Efficiency (%)	Estimated Uptake Efficiency (%)
Open	914								
Alfalfa	946	5.82	5502	4.97	4703	1.19	1122	85.5	80.3
Cotton	10009	2.59	25930	2.21	22163	0.47	4710	85.5	82.6
Tomatoes	217	2.38	516	1.92	415	0.69	150	80.5	72.7
Wheat	513	1.83	939	1.38	709	0.48	247	75.5	76.1
Corn	20	2.72	53	1.92	38	0.87	17	70.5	69.7
Onions	538	3.06	1647	1.70	914	1.64	884	55.5	48.0
Safflower	143	2.87	410	2.46	351	0.47	68	85.5	84.1
Melons	369	2.06	760	1.45	536	0.71	261	70.5	68.0
Sugar Beets	823	4.14	3406	2.92	2400	1.28	1051	70.5	70.6
Total	13577	2.88	39164	2.37	32227	0.63	8510	82.3	

1988.00 Crop	Total Acreages	Estimated Applied Water (Af/Ac)	Estimated Applied Water (AF)	Estimated Crop Water Requirement (Af/Ac)	Estimated Crop Water Requirement (AF)	Estimated Recharge (Af/Ac)	Estimated Recharge (AF)	Estimated Application Efficiency (%)	Estimated Uptake Efficiency (%)
Open	754								
Alfalfa	662	5.56	3680	4.60	3046	1.28	846	82.8	78.4
Cotton	11563	2.69	31117	2.23	25757	0.56	6489	82.8	79.7
Wheat	381	1.93	734	1.40	534	0.56	212	72.8	74.2
Corn	86	3.13	269	2.12	182	1.08	93	67.8	66.0
Onions	648	3.66	2376	1.93	1254	2.04	1323	52.8	45.5
Safflower	192	2.71	521	2.24	431	0.52	100	82.8	81.4
Melons	112	2.30	258	1.56	175	0.85	95	67.8	63.8
Sugar Beets	180	4.38	791	2.97	536	1.47	266	67.8	67.3
Total	13824	2.88	39745	2.31	31915	0.68	9424	80.3	

1987.00 Crop	Total Acreages	Estimated Applied Water (Af/Ac)	Estimated Applied Water (AF)	Estimated Crop Water Requirement (Af/Ac)	Estimated Crop Water Requirement (AF)	Estimated Recharge (Af/Ac)	Estimated Recharge (AF)	Estimated Application Efficiency (%)	Estimated Uptake Efficiency (%)
Open	1501								
Alfalfa	523	6.50	3397	5.04	2636	1.82	952	77.6	73.3
Cotton	11046	3.08	33994	2.39	26374	0.80	8809	77.6	74.1
Wheat	427	1.67	712	1.13	481	0.57	242	67.6	71.6
Onions	147	2.85	418	1.36	199	1.74	256	47.6	43.3
Melons	31	2.58	80	1.62	50	1.08	33	62.6	58.1
Sugar Beets	860	3.83	3297	2.40	2063	1.48	1276	62.6	64.4
Total	13033	3.21	41898	2.44	31804	0.89	11568	75.9	

1986.00 Crop	Total Acreages	Estimated Applied Water (Af/Ac)	Estimated Applied Water (AF)	Estimated Crop Water Requirement (Af/Ac)	Estimated Crop Water Requirement (AF)	Estimated Recharge (Af/Ac)	Estimated Recharge (AF)	Estimated Application Efficiency (%)	Estimated Uptake Efficiency (%)
Open	745								
Alfalfa	459	4.88	2239	4.02	1845	1.15	527	82.4	78.7
Cotton	7404	2.82	20887	2.33	17216	0.60	4447	82.4	79.4
Wheat	5122	1.39	7104	1.00	5145	0.41	2084	72.4	78.4
Corn	180	2.93	528	1.97	356	1.03	185	67.4	66.1
Safflower	111	3.08	343	2.54	283	0.60	67	82.4	81.6
Sugar Beets	508	4.17	2118	2.81	1428	1.42	721	67.4	68.2
Total	13785	2.41	33219	1.91	26274	0.58	8031	79.1	

1985.00 Crop	Total Acreages	Estimated Applied Water (Af/Ac)	Estimated Applied Water (AF)	Estimated Crop Water Requirement (Af/Ac)	Estimated Crop Water Requirement (AF)	Estimated Recharge (Af/Ac)	Estimated Recharge (AF)	Estimated Application Efficiency (%)	Estimated Uptake Efficiency (%)
Open	1539								
Cotton	12930	2.86	36961	2.33	30101	0.64	8256	81.4	77.7
Onions	48	3.78	179	1.94	92	2.16	102	51.4	44.4
Total	12978	2.86	37140	2.33	30193	0.64	8358	81.3	

1984.00 Crop	Total Acreages	Estimated Applied Water (Af/Ac)	Estimated Applied Water (AF)	Estimated Crop Water Requirement (Af/Ac)	Estimated Crop Water Requirement (AF)	Estimated Recharge (Af/Ac)	Estimated Recharge (AF)	Estimated Application Efficiency (%)	Estimated Uptake Efficiency (%)
Open	470								
Cotton	13391	2.92	39075	2.50	33467	0.53	7159	85.6	81.7
Tomatoes	110	2.68	295	2.16	238	0.77	85	80.6	71.2
Wheat (Grains)	741	1.73	1282	1.31	970	0.45	337	75.6	77.6
Sugar Beets	112	4.33	484	3.06	342	1.34	149	70.6	70.5
Total	14354	2.87	41136	2.44	35017	0.54	7730	85.1	

1983.00 Crop	Total Acreages	Estimated Applied Water (Af/Ac)	Estimated Applied Water (AF)	Estimated Crop Water Requirement (Af/Ac)	Estimated Crop Water Requirement (AF)	Estimated Recharge (Af/Ac)	Estimated Recharge (AF)	Estimated Application Efficiency (%)	Estimated Uptake Efficiency (%)
Open	927								
Cotton	11705	2.56	29935	2.37	27718	0.30	3502	92.6	88.3
Sugar Beets	300	3.71	1114	2.88	865	0.89	269	77.6	78.3
Total	12005	2.59	31050	2.38	28582	0.31	3771	92.1	

1982.00 Crop	Total Acreages	Estimated Applied Water (Af/Ac)	Estimated Applied Water (AF)	Estimated Crop Water Requirement (Af/Ac)	Estimated Crop Water Requirement (AF)	Estimated Recharge (Af/Ac)	Estimated Recharge (AF)	Estimated Application Efficiency (%)	Estimated Uptake Efficiency (%)
Open	869								
Alfalfa	121	4.79	579	4.20	507	0.91	110	87.7	82.4
Cotton	10143	2.63	26728	2.31	23431	0.43	4412	87.7	83.5
Wheat	275	1.55	427	1.21	332	0.38	104	77.7	79.6
Lettuce	60	1.60	96	0.92	55	0.90	54	57.7	43.8
Sugar Beets	789	4.03	3177	2.93	2309	1.17	922	72.7	72.4
Oats (Barley)	640	2.86	1833	2.08	1332	0.86	553	72.7	69.9
Total	12029	2.73	32840	2.32	27967	0.51	6155	85.2	

1981.00 Crop	Total Acreages	Estimated Applied Water (Af/Ac)	Estimated Applied Water (AF)	Estimated Crop Water Requirement (Af/Ac)	Estimated Crop Water Requirement (AF)	Estimated Recharge (Af/Ac)	Estimated Recharge (AF)	Estimated Application Efficiency (%)	Estimated Uptake Efficiency (%)
Open	1436								
Alfalfa	125	5.03	632	4.79	601	0.62	78	95.2	88.6
Cotton	10045	2.62	26358	2.50	25083	0.43	4369	87.7	83.5
Sugar Beets	489	3.66	1791	2.93	1435	0.79	388	80.2	79.4
Oats	731	2.60	1900	2.08	1523	0.60	438	80.2	77.0
Total	11391	2.69	30680	2.51	28642	0.46	5273	93.4	

1980.00 Crop	Total Acreages	Estimated Applied Water (Af/Ac)	Estimated Applied Water (AF)	Estimated Crop Water Requirement (Af/Ac)	Estimated Crop Water Requirement (AF)	Estimated Recharge (Af/Ac)	Estimated Recharge (AF)	Estimated Application Efficiency (%)	Estimated Uptake Efficiency (%)
Open	408								
Cotton	10044	2.47	24855	2.28	22880	0.31	3093	92.1	87.6
Sugar Beets	881	3.64	3209	2.81	2473	0.90	793	77.1	77.2
Oats	1441	2.70	3897	2.08	3003	0.70	1014	77.1	74.0
Total	12366	2.58	31961	2.29	28356	0.40	4900	88.7	

1979.00 Crop	Total Acreages	Estimated Applied Water (Af/Ac)	Estimated Applied Water (AF)	Estimated Crop Water Requirement (Af/Ac)	Estimated Crop Water Requirement (AF)	Estimated Recharge (Af/Ac)	Estimated Recharge (AF)	Estimated Application Efficiency (%)	Estimated Uptake Efficiency (%)
Open	1961								
Alfalfa	169	4.48	758	4.13	698	0.68	116	92.1	86.6
Cotton	9419	2.47	23308	2.28	21456	0.31	2900	92.1	87.6
Corn	244	2.70	660	2.08	509	0.70	172	77.1	74.0
Oats	968	2.70	2616	2.08	2016	0.70	681	77.1	74.0
Total	10800	2.53	27342	2.29	24678	0.36	3869	90.3	

1978.00 crop	Total Acreages	Estimated Applied Water (Af/Ac)	Estimated Applied Water (AF)	Estimated Crop Water Requirement (Af/Ac)	Estimated Crop Water Requirement (AF)	Estimated Recharge (Af/Ac)	Estimated Recharge (AF)	Estimated Application Efficiency (%)	Estimated Uptake Efficiency (%)
Open	2717								
Alfalfa	1275	4.48	5714	4.13	5260	0.68	871	92.1	86.6
Cotton	7034	2.47	17407	2.28	16024	0.31	2166	92.1	87.6
Sugar Beets	371	3.64	1353	2.81	1042	0.90	334	77.1	77.2
Oats	1148	2.70	3104	2.08	2392	0.70	808	77.1	74.0
Total	9828	2.81	27577	2.52	24718	0.43	4179	89.6	

1977.00 crop	Total Acreages	Estimated Applied Water (Af/Ac)	Estimated Applied Water (AF)	Estimated Crop Water Requirement (Af/Ac)	Estimated Crop Water Requirement (AF)	Estimated Recharge (Af/Ac)	Estimated Recharge (AF)	Estimated Application Efficiency (%)	Estimated Uptake Efficiency (%)
Open	4044								
Alfalfa	850	4.48	3812	4.13	3509	0.68	581	92.1	86.6
Cotton	6954	2.47	17210	2.28	15842	0.31	2142	92.1	87.6
Sugar Beets	700	3.64	2548	2.81	1964	0.90	630	77.1	77.2
Total	8504	2.77	23570	2.51	21315	0.39	3353	90.4	

1976.00 crop	Total Acreages	Estimated Applied Water (Af/Ac)	Estimated Applied Water (AF)	Estimated Crop Water Requirement (Af/Ac)	Estimated Crop Water Requirement (AF)	Estimated Recharge (Af/Ac)	Estimated Recharge (AF)	Estimated Application Efficiency (%)	Estimated Uptake Efficiency (%)
Open	11408								
Alfalfa	404	4.48	1813	4.13	1669	0.68	276	92.1	86.6
Cotton	1182	2.47	2924	2.28	2692	0.31	364	92.1	87.6
Corn	476	2.70	1287	2.08	992	0.70	335	77.1	74.0
Oats	528	2.70	1428	2.08	1100	0.70	372	77.1	74.0
Total	2590	2.88	7452	2.49	6453	0.52	1347	86.6	

1975.00 crop	Total acreages	Estimated Applied Water (Af/Ac)	Estimated Applied Water (AF)	Estimated Crop Water Requirement (Af/Ac)	Estimated Crop Water Requirement (AF)	Estimated Recharge (Af/Ac)	Estimated Recharge (AF)	Estimated Application Efficiency (%)	Estimated Uptake Efficiency (%)
Open	1234								
Alfalfa	176	4.48	787	4.13	724	0.68	120	92.1	86.6
Cotton	4656	2.47	11521	2.28	10605	0.31	1434	92.1	87.6
Wheat	5030	1.30	6562	1.07	5385	0.26	1323	87.1	85.0
Sugar Beets	1318	3.64	4800	2.81	3698	0.90	1187	77.1	77.2
Oats	233	2.70	630	2.08	485	0.70	164	77.1	74.0
Total	11412	2.13	24300	1.83	20898	0.37	4227	86.0	

1974.00 crop	Total acreages	Estimated Applied Water (Af/Ac)	Estimated Applied Water (AF)	Estimated Crop Water Requirement (Af/Ac)	Estimated Crop Water Requirement (AF)	Estimated Recharge (Af/Ac)	Estimated Recharge (AF)	Estimated Application Efficiency (%)	Estimated Uptake Efficiency (%)
Open	755								
Alfalfa	283	4.48	1270	4.13	1169	0.68	194	92.1	86.6
Cotton	4200	2.47	10394	2.28	9569	0.31	1293	92.1	87.6
Wheat	1519	1.30	1982	1.07	1626	0.26	400	87.1	85.0
Oats (Barley)	5759	0.85	4895	0.70	4017	0.17	960	82.1	87.2
Total	11761	1.58	18541	1.39	16380	0.24	2847	88.3	

Appendix B Distribution of crops across NASL lands, by year, from 1974 to 2010

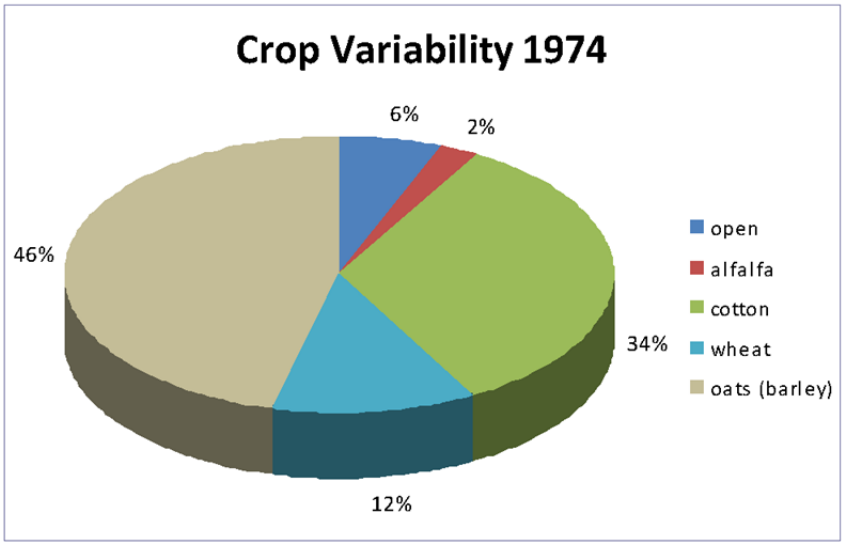

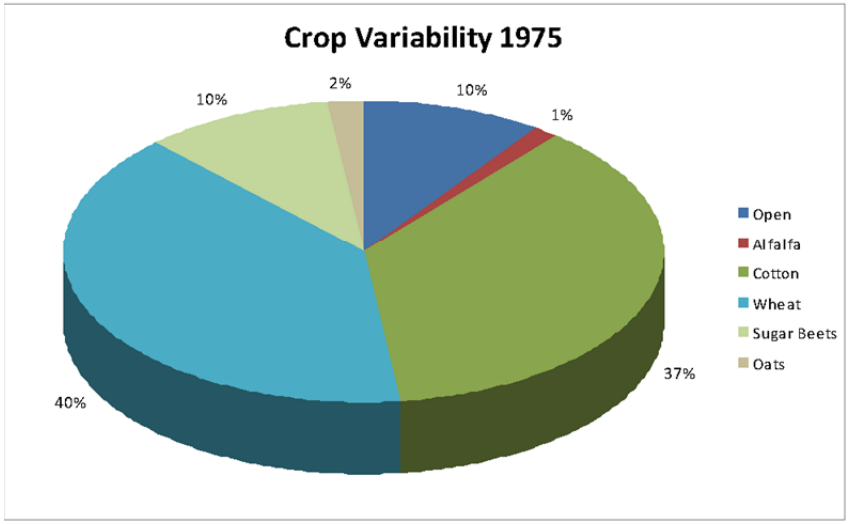

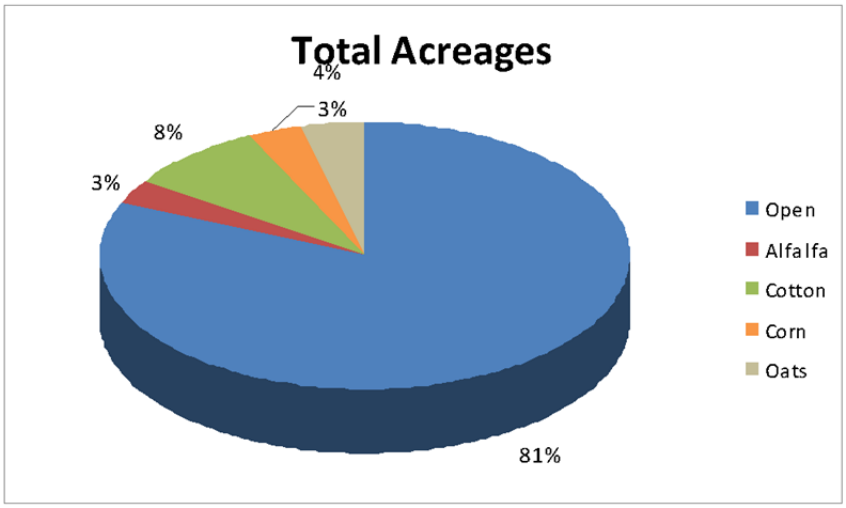

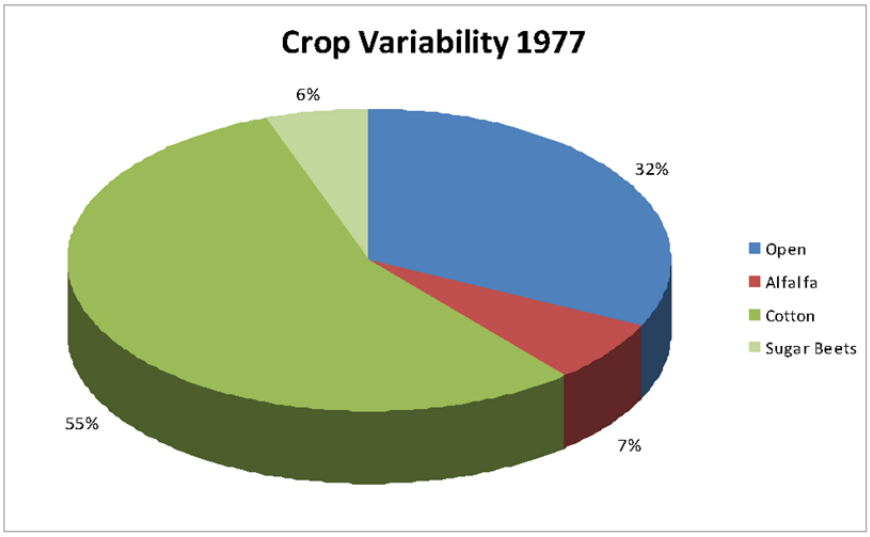
Crop Variability 1977
6%
32%
55%
7%
Open
Alfalfa
Cotton
Sugar Beets

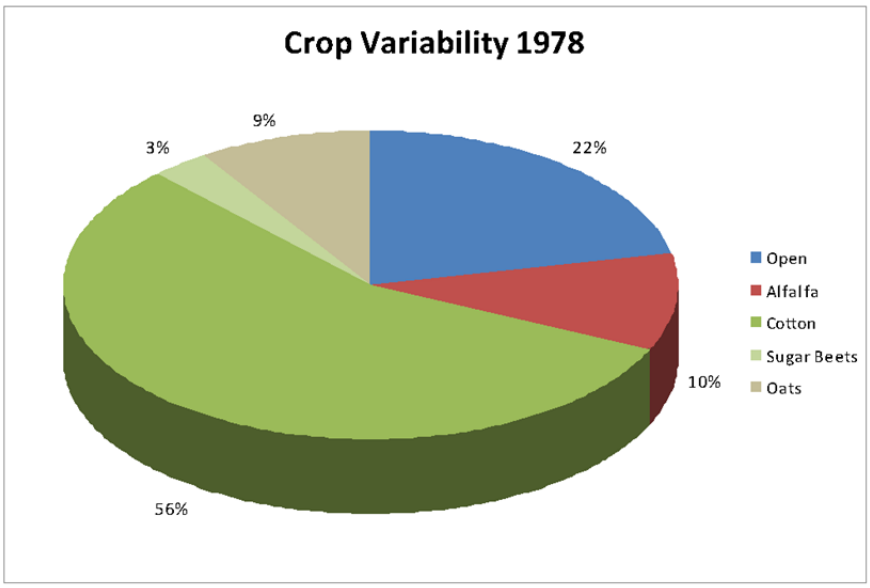
Crop Variability 1978
9%
3%
22%
10%
56%
Open
Alfalfa
Cotton
Sugar Beets
Oats

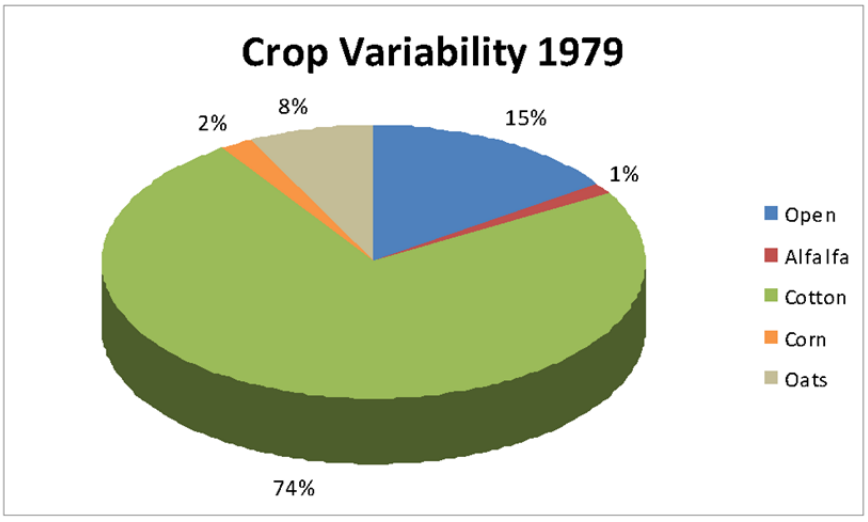
Crop Variability 1979
8%
2%
15%
1%
74%
Open
Alfalfa
Cotton
Corn
Oats

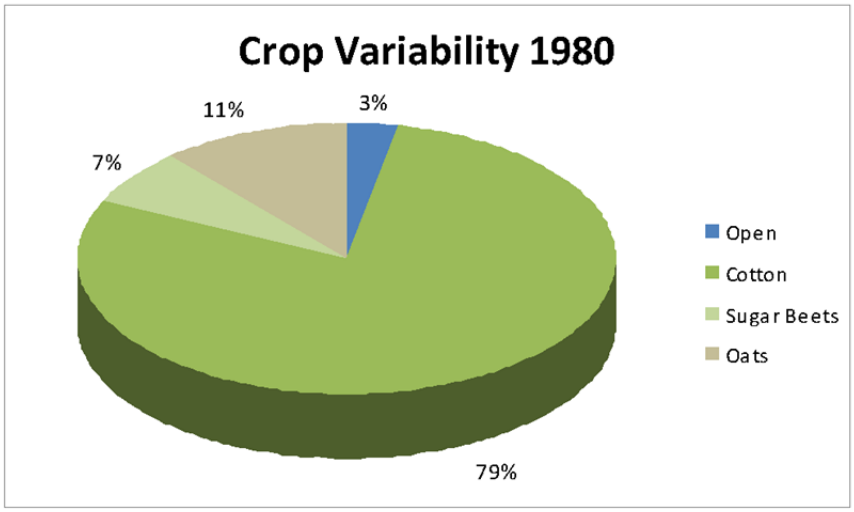
Crop Variability 1980
11%
3%
7%
79%
Open
Cotton
Sugar Beets
Oats

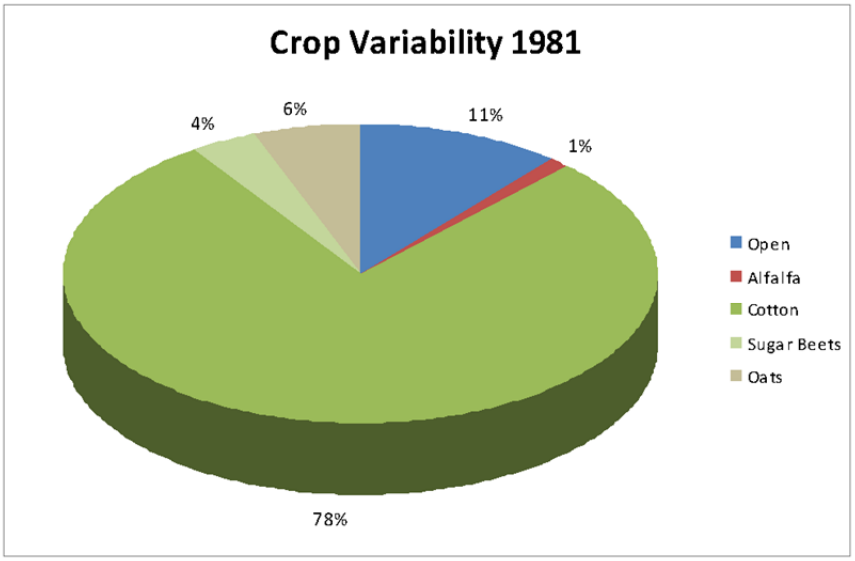
Crop Variability 1981
4%
6%
11%
1%
78%
Open
Alfalfa
Cotton
Sugar Beets
Oats

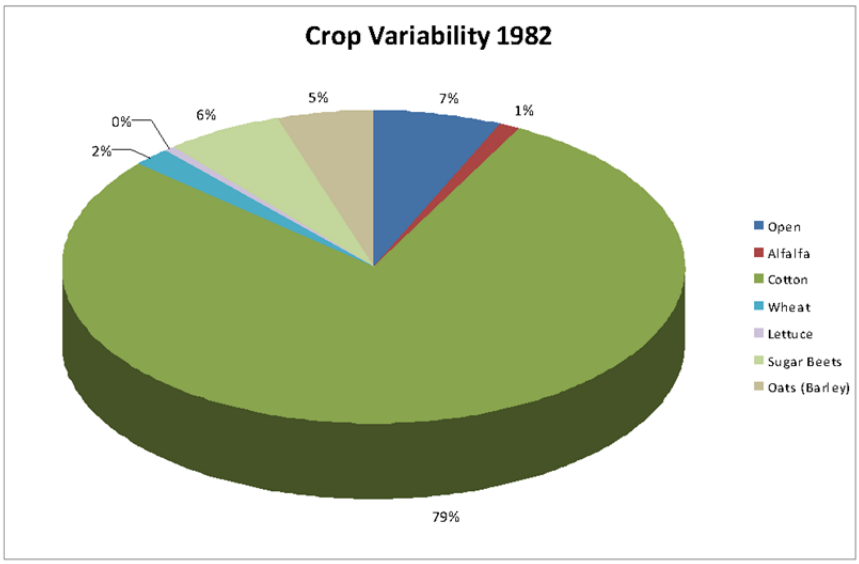
Crop Variability 1982
0%
6%
5%
7%
1%
2%
79%
Open
Alfalfa
Cotton
Wheat
Lettuce
Sugar Beets
Oats (Barley)

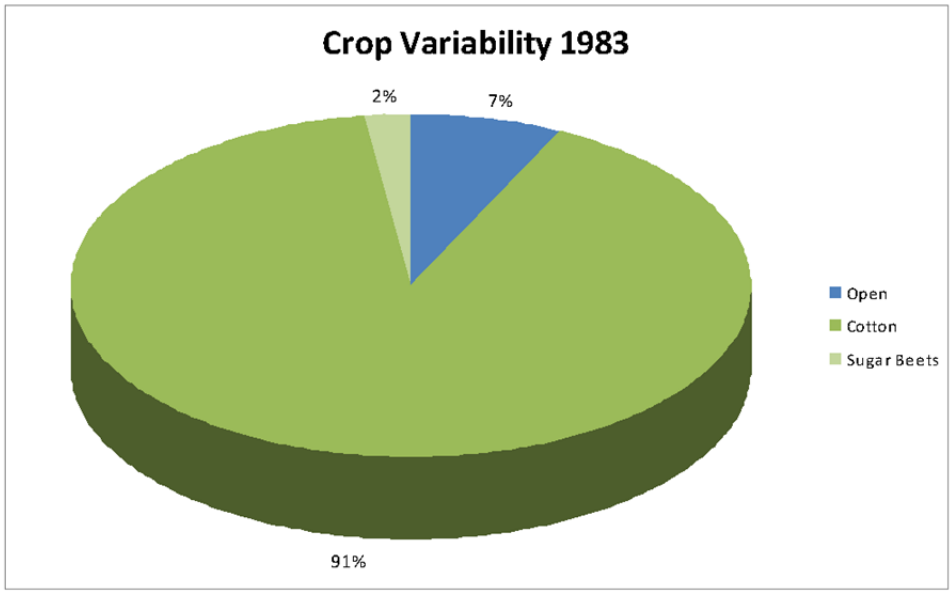
Crop Variability 1983
2%
7%
91%
Open
Cotton
Sugar Beets

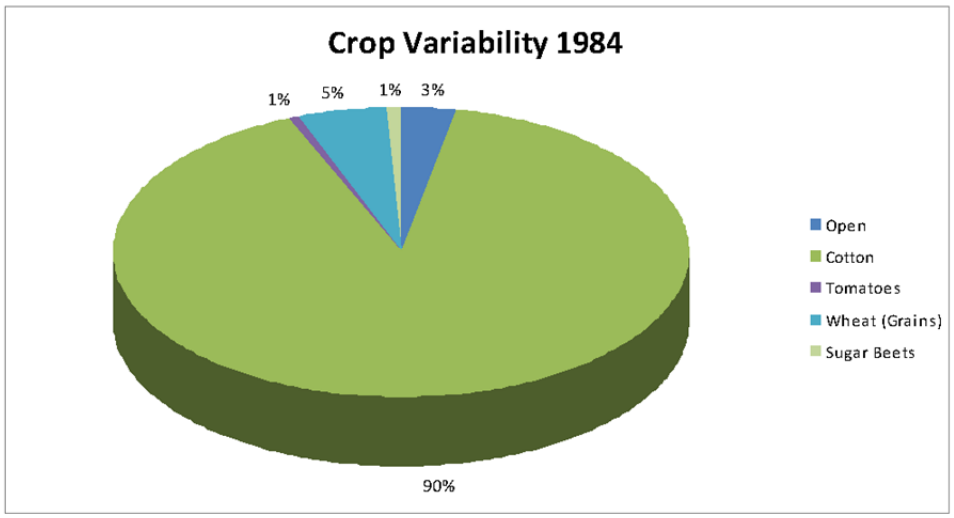
Crop Variability 1984
1%
5%
1%
3%
90%
Open
Cotton
Tomatoes
Wheat (Grains)
Sugar Beets

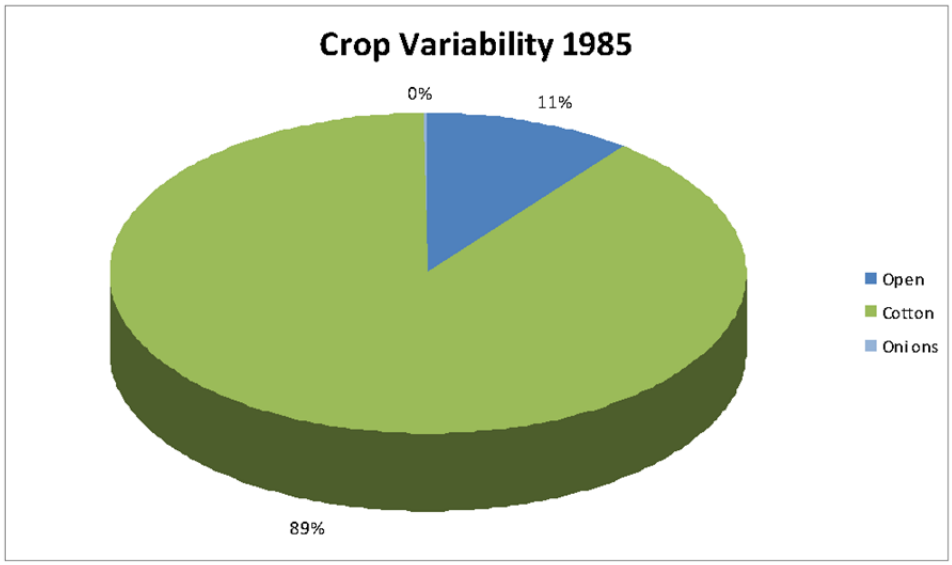
Crop Variability 1985
0%
11%
89%
Open
Cotton
Onions

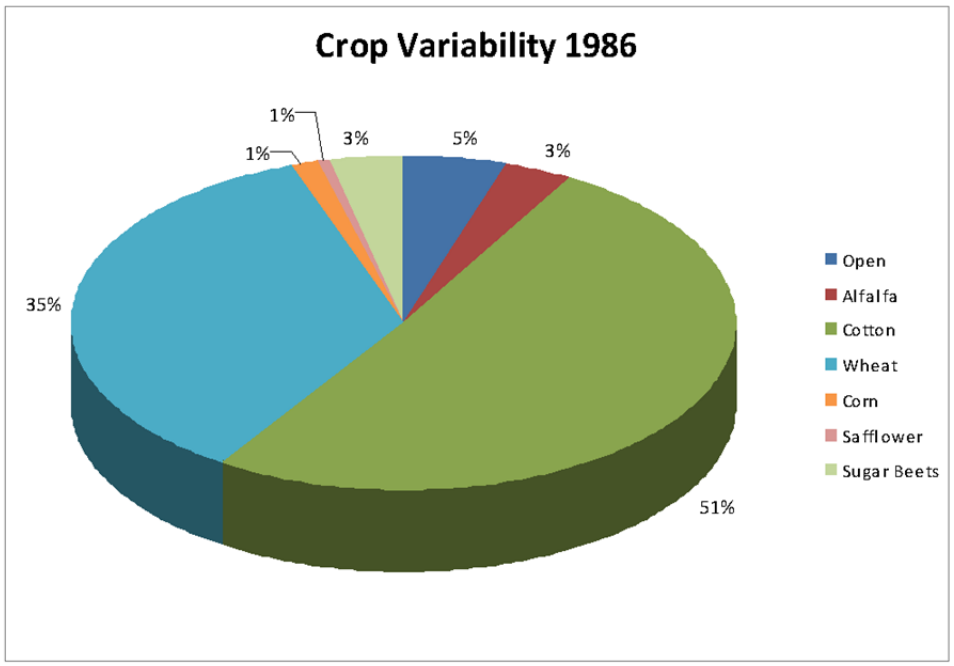
Crop Variability 1986
1%
1%
3%
5%
3%
35%
51%
Open
Alfalfa
Cotton
Wheat
Corn
Safflower
Sugar Beets

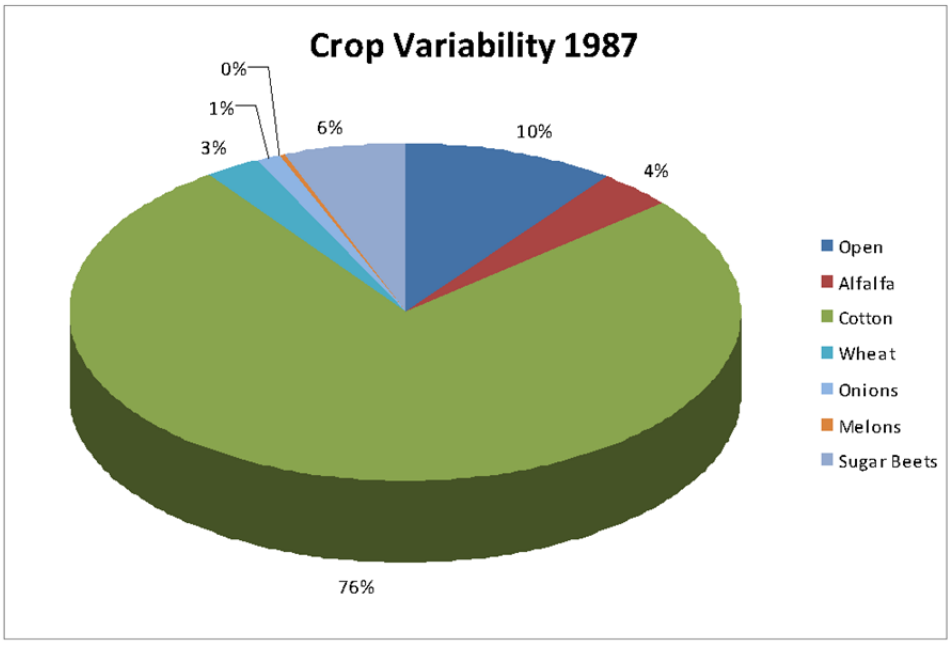
Crop Variability 1987
0%
1%
3%
6%
10%
4%
76%
Open
Alfalfa
Cotton
Wheat
Onions
Melons
Sugar Beets

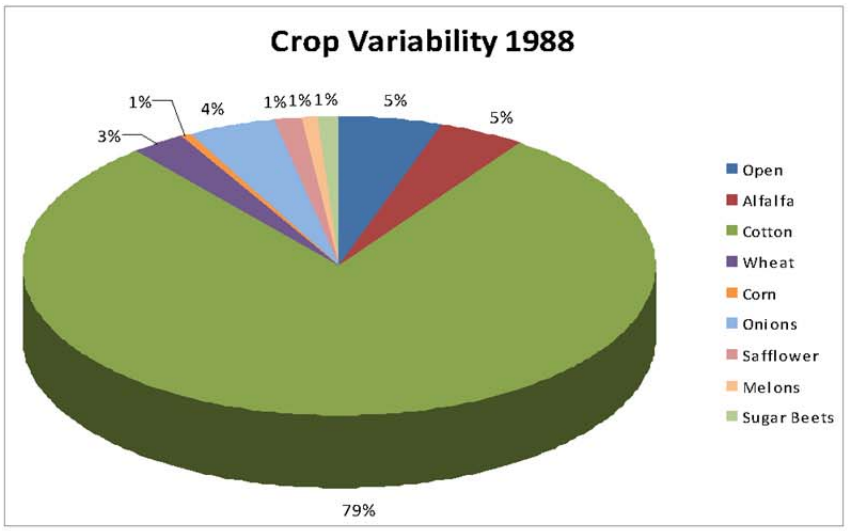
Crop Variability 1988
1%
4%
1%
1%
1%
5%
3%
5%
79%
Open
Alfalfa
Cotton
Wheat
Corn
Onions
Safflower
Melons
Sugar Beets

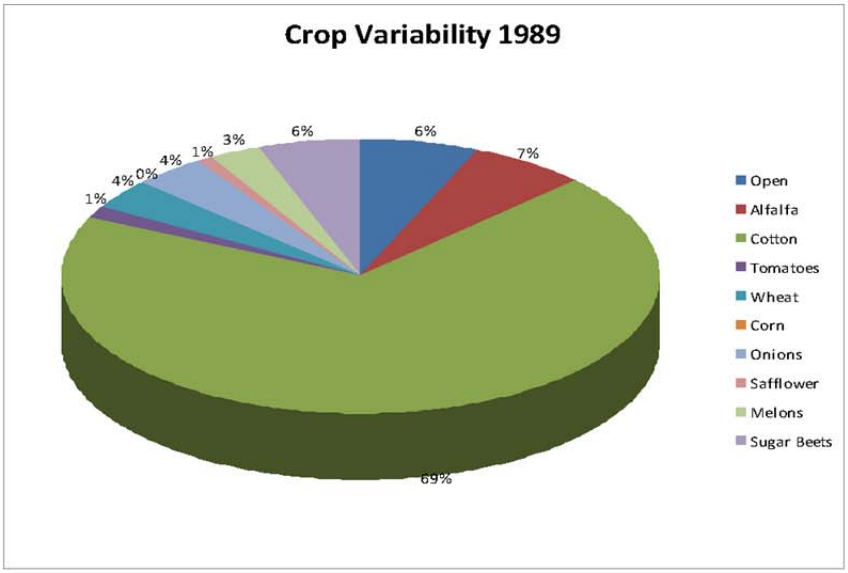
Crop Variability 1989
6%
6%
7%
3%
1%
4%
0%
4%
1%
69%
Open
Alfalfa
Cotton
Tomatoes
Wheat
Corn
Onions
Safflower
Melons
Sugar Beets

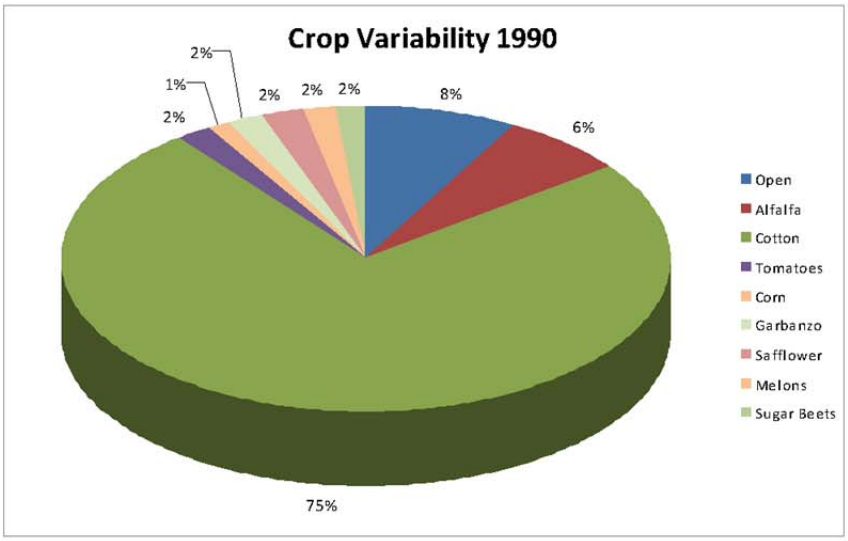
Crop Variability 1990
2%
1%
2%
2%
2%
2%
8%
6%
75%
Open
Alfalfa
Cotton
Tomatoes
Corn
Garbanzo
Safflower
Melons
Sugar Beets

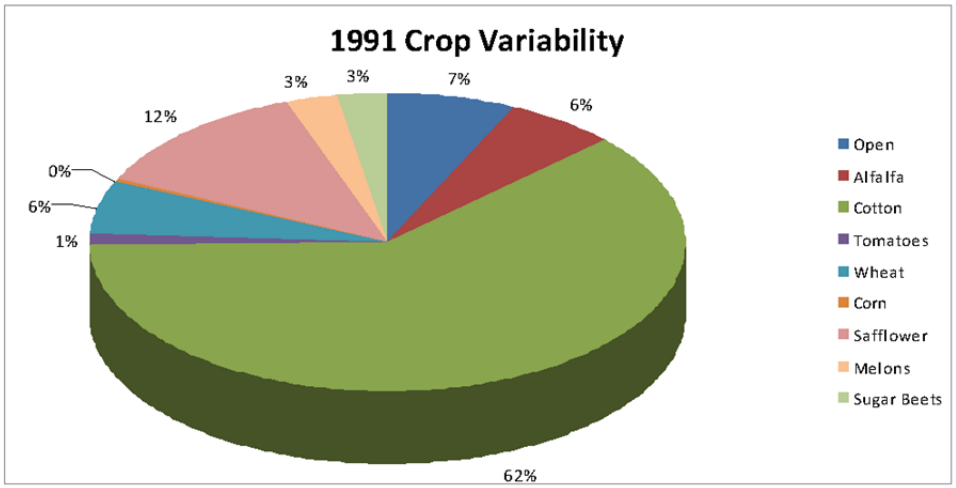
1991 Crop Variability
7%
6%
3%
3%
12%
0%
6%
1%
62%
Open
Alfalfa
Cotton
Tomatoes
Wheat
Corn
Safflower
Melons
Sugar Beets

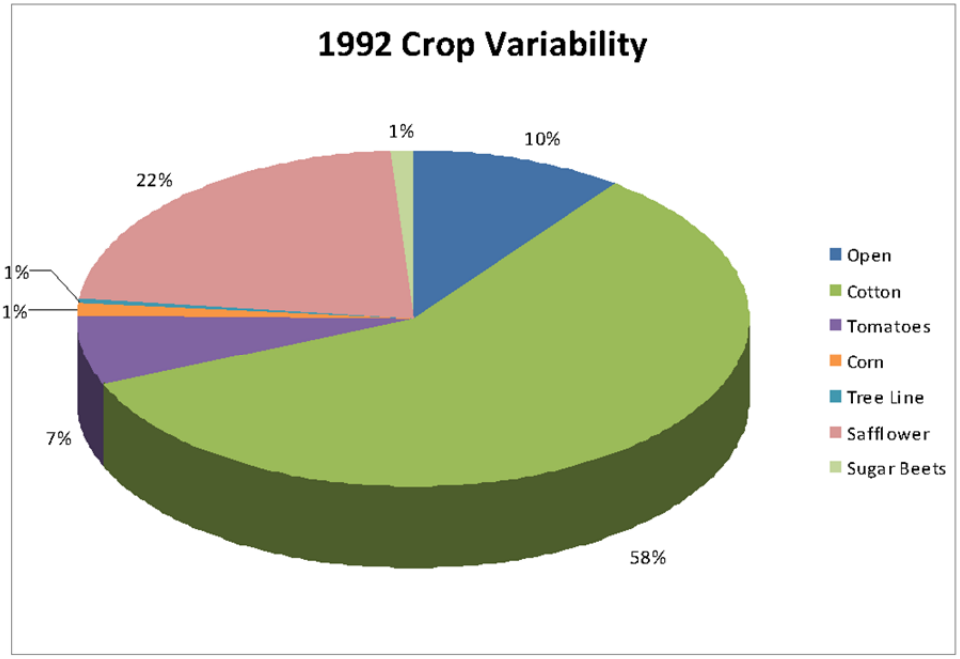
1992 Crop Variability
1%
10%
22%
1%
1%
7%
58%
Open
Cotton
Tomatoes
Corn
Tree Line
Safflower
Sugar Beets

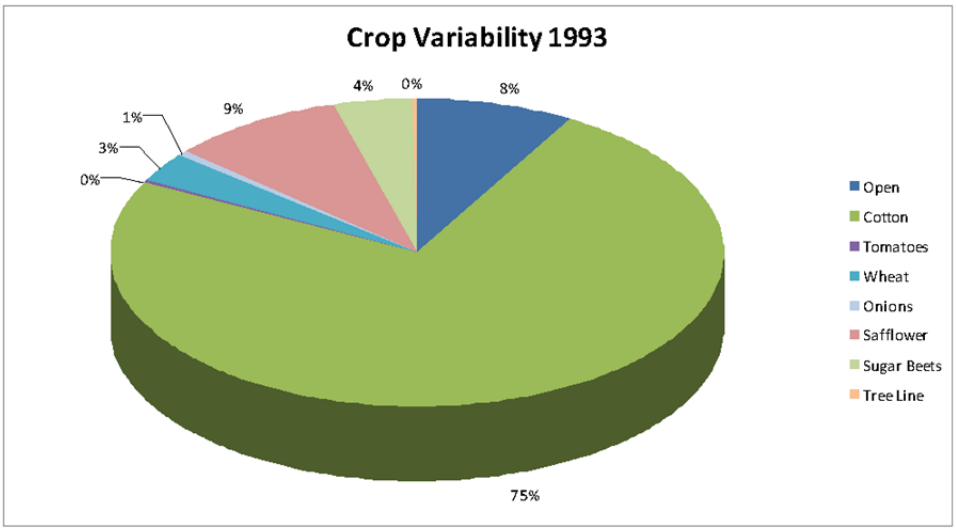
Crop Variability 1993
4%
0%
8%
9%
1%
3%
0%
75%
Open
Cotton
Tomatoes
Wheat
Onions
Safflower
Sugar Beets
Tree Line

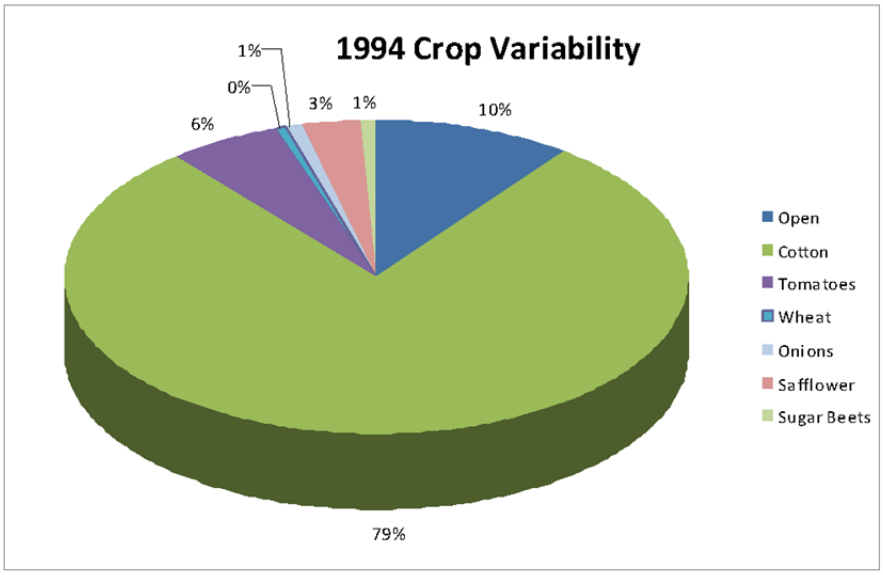
1994 Crop Variability
1%
0%
3%
1%
10%
6%
79%
Open
Cotton
Tomatoes
Wheat
Onions
Safflower
Sugar Beets

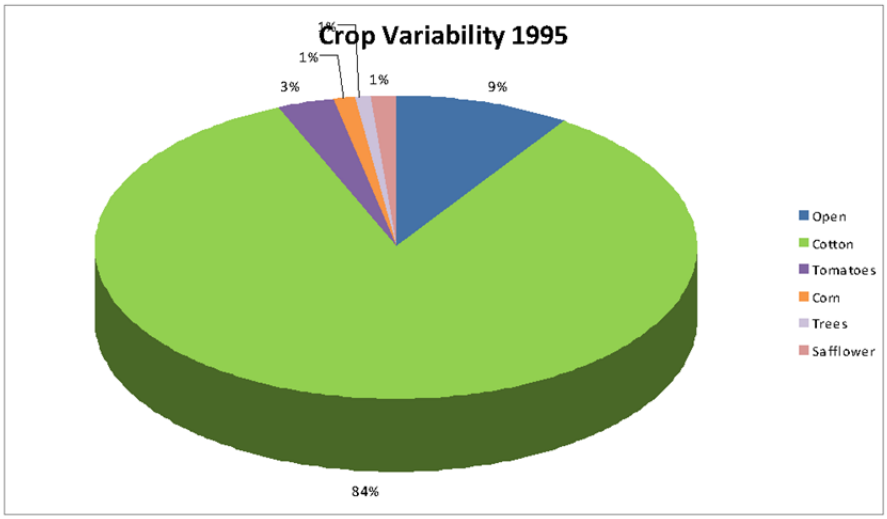
Crop Variability 1995
1%
3%
1%
9%
84%
Open
Cotton
Tomatoes
Corn
Trees
Safflower

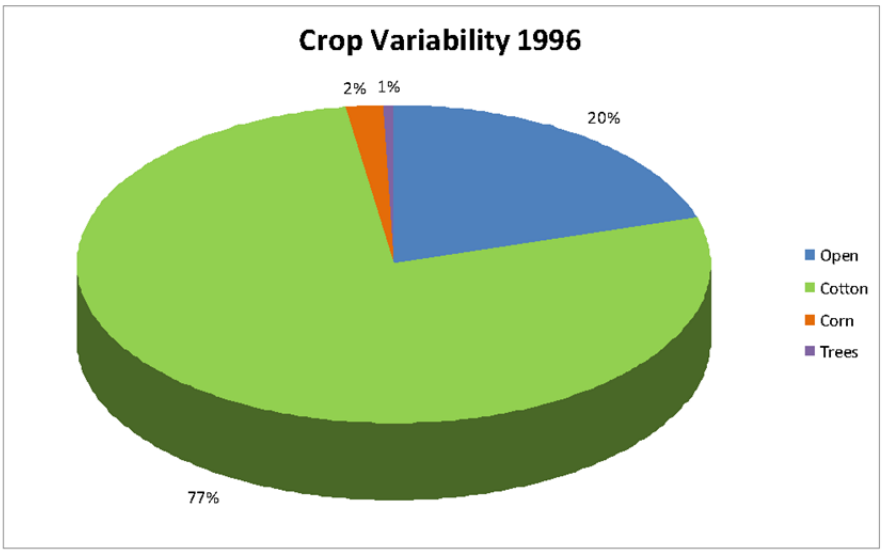
Crop Variability 1996
2%
1%
20%
77%
Open
Cotton
Corn
Trees

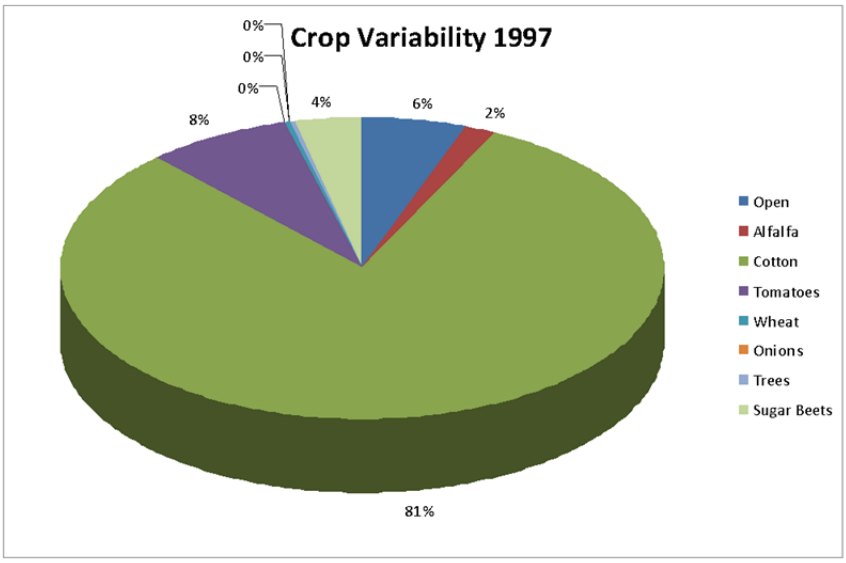
Crop Variability 1997
0%
0%
0%
4%
6%
2%
8%
81%
Open
Alfalfa
Cotton
Tomatoes
Wheat
Onions
Trees
Sugar Beets

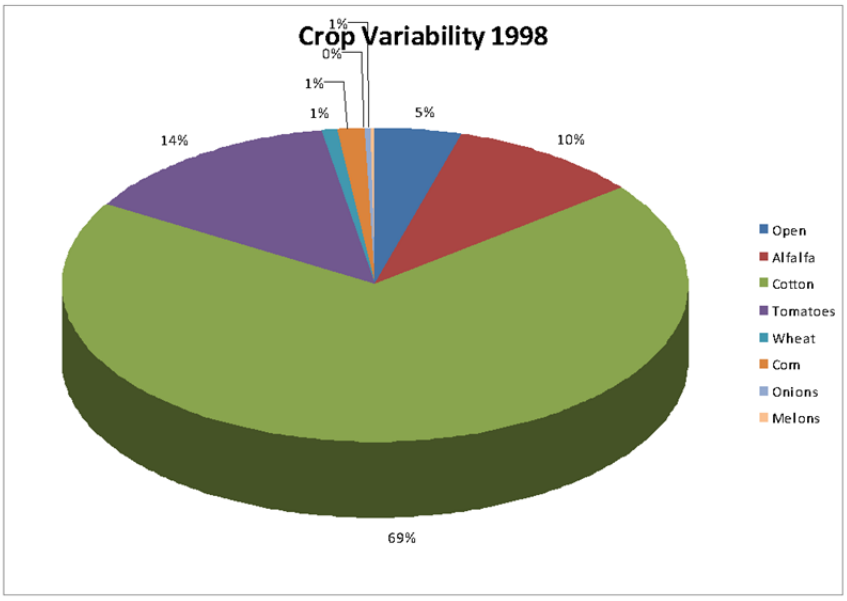
Crop Variability 1998
1%
0%
1%
1%
5%
10%
14%
69%
Open
Alfalfa
Cotton
Tomatoes
Wheat
Corn
Onions
Melons

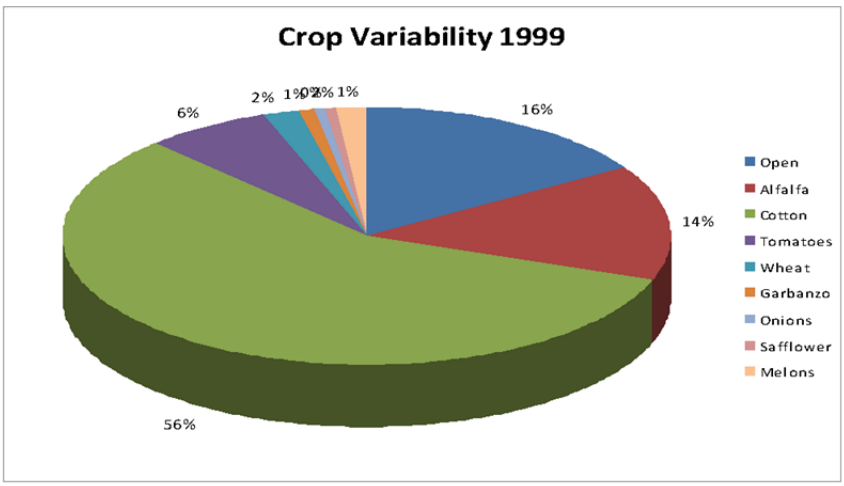
Crop Variability 1999
6%
2%
1%
1%
1%
16%
14%
56%
Open
Alfalfa
Cotton
Tomatoes
Wheat
Garbanzo
Onions
Safflower
Melons

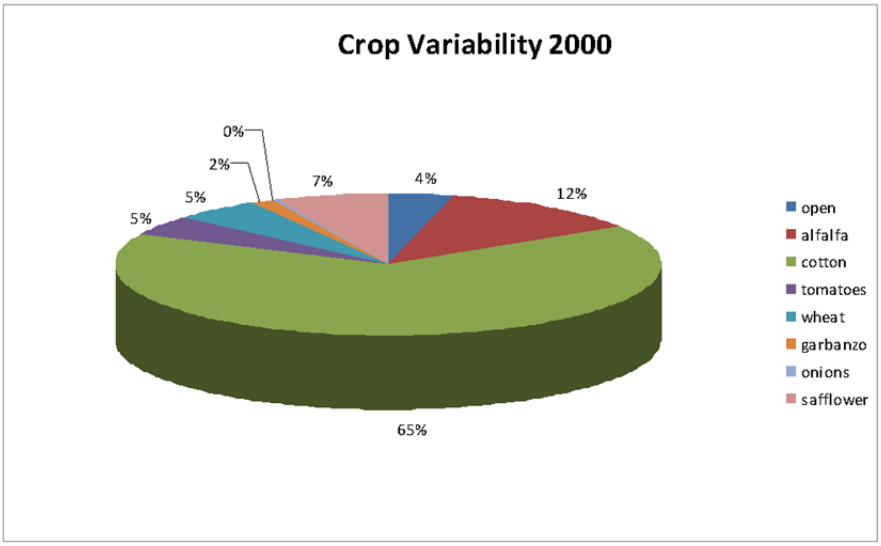
Crop Variability 2000
0%
2%
7%
4%
5%
12%
5%
65%
open
alfalfa
cotton
tomatoes
wheat
garbanzo
onions
safflower

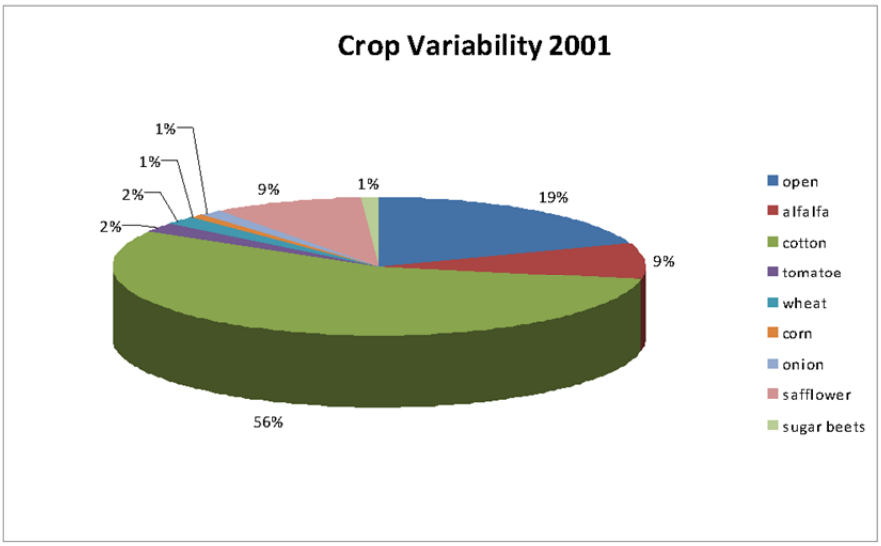
Crop Variability 2001
1%
1%
2%
9%
1%
19%
2%
9%
56%
open
alfalfa
cotton
tomatoe
wheat
corn
onion
safflower
sugar beets

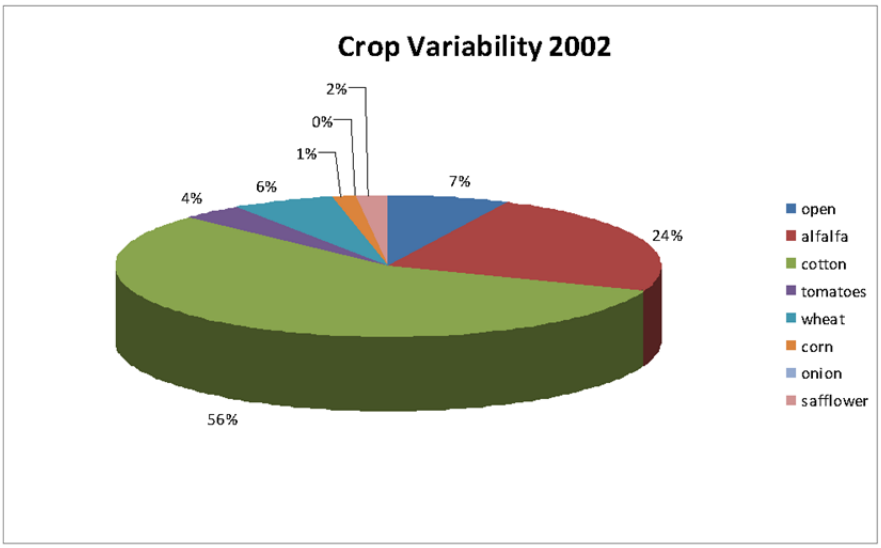
Crop Variability 2002
2%
0%
1%
7%
4%
6%
24%
56%
open
alfalfa
cotton
tomatoes
wheat
corn
onion
safflower

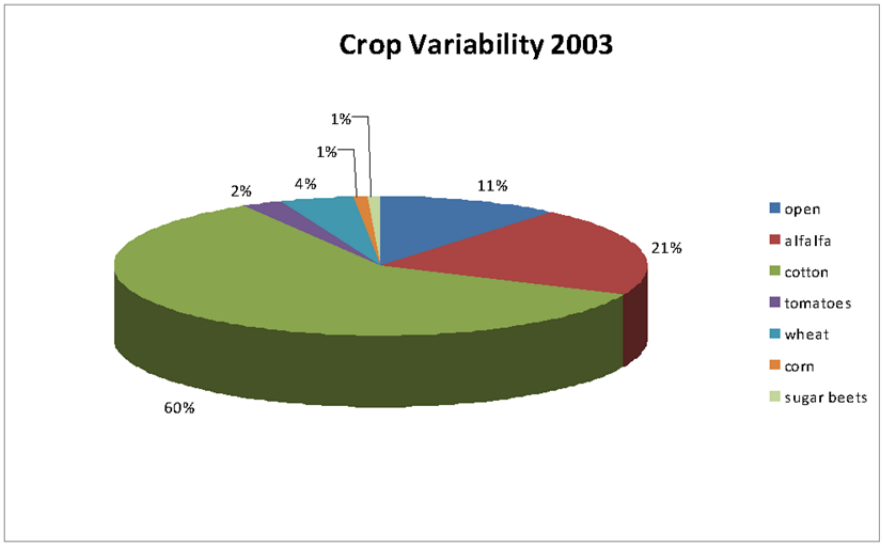
Crop Variability 2003
1%
1%
2%
4%
11%
21%
60%
open
alfalfa
cotton
tomatoes
wheat
corn
sugar beets

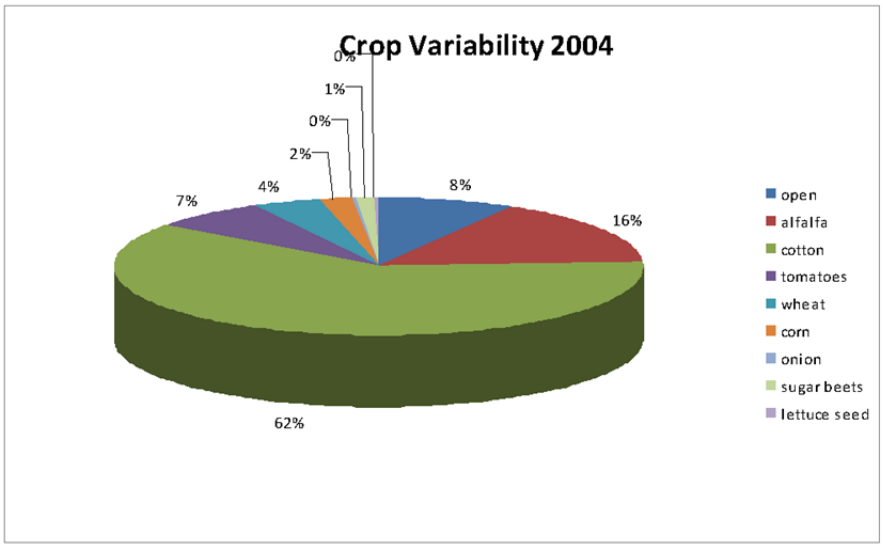
Crop Variability 2004
0%
1%
0%
2%
4%
7%
8%
16%
62%
open
alfalfa
cotton
tomatoes
wheat
corn
onion
sugar beets
lettuce seed

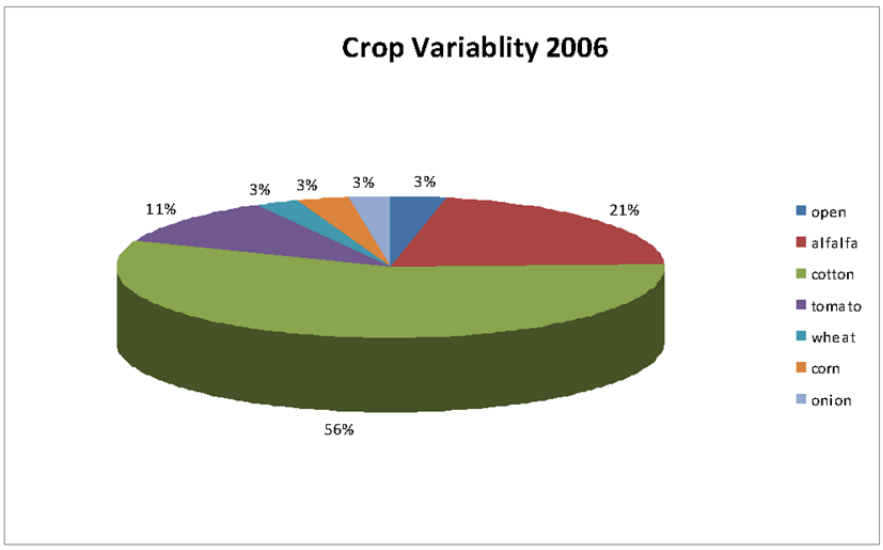
Crop Variablity 2006
3%
3%
3%
3%
11%
21%
56%
open
alfalfa
cotton
tomato
wheat
corn
onion

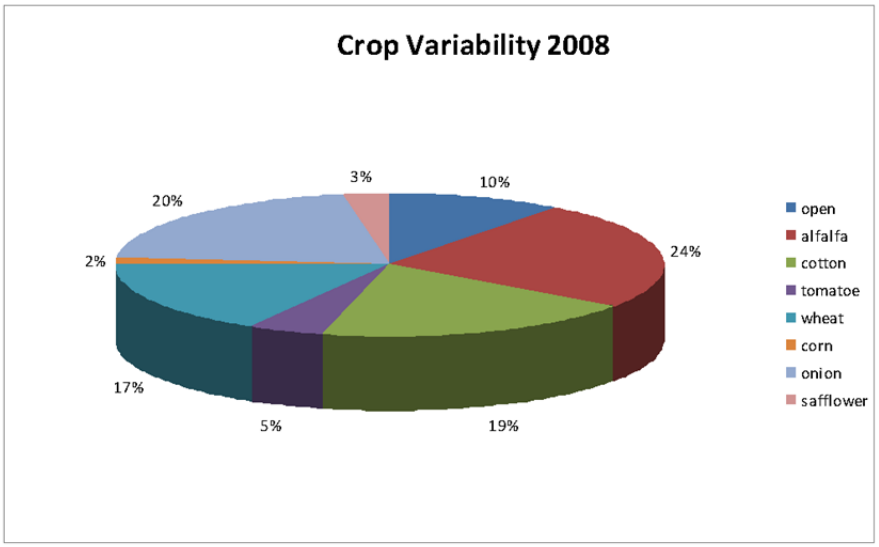
Crop Variability 2008
3%
10%
20%
24%
2%
17%
5%
19%
open
alfalfa
cotton
tomatoe
wheat
corn
onion
safflower

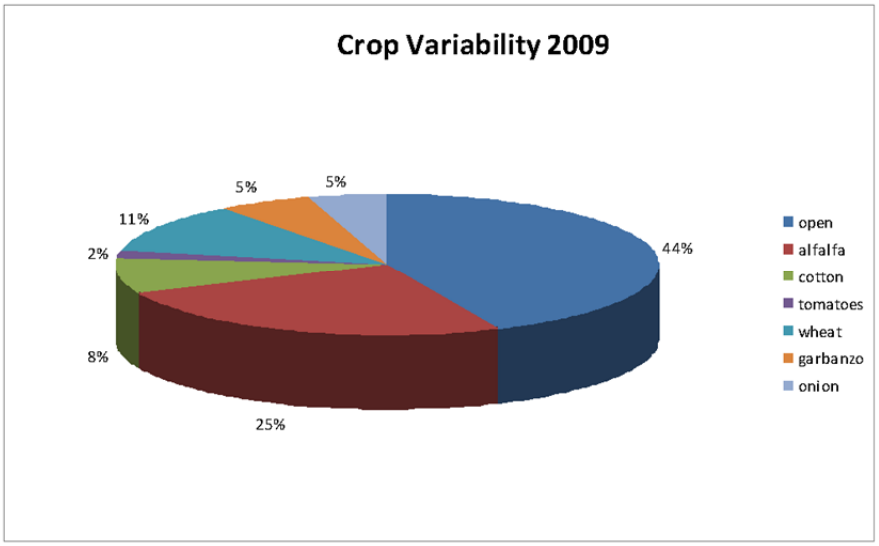
Crop Variability 2009
5%
5%
11%
44%
2%
8%
25%
open
alfalfa
cotton
tomatoes
wheat
garbanzo
onion

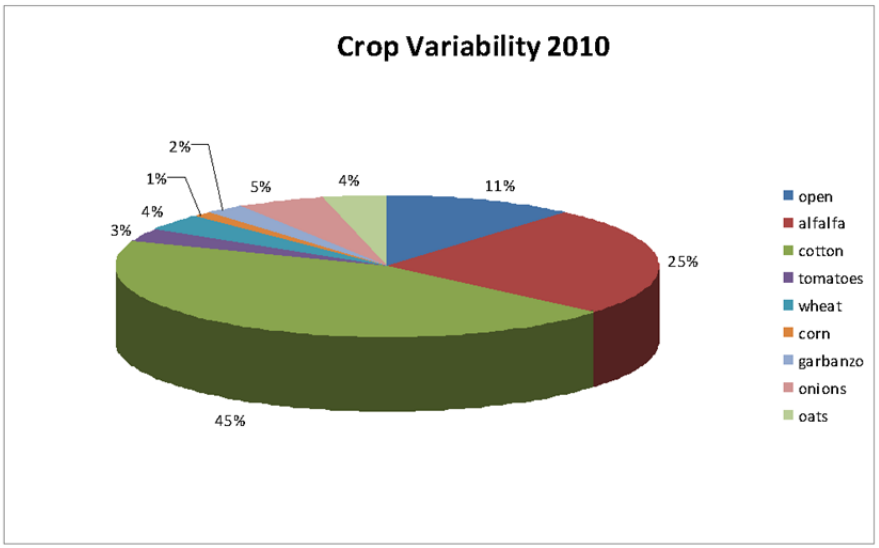
Crop Variability 2010
2%
1%
5%
4%
11%
4%
3%
25%
45%
open
alfalfa
cotton
tomatoes
wheat
corn
garbanzo
onions
oats

Appendix C: NASL groundwater elevation contour maps

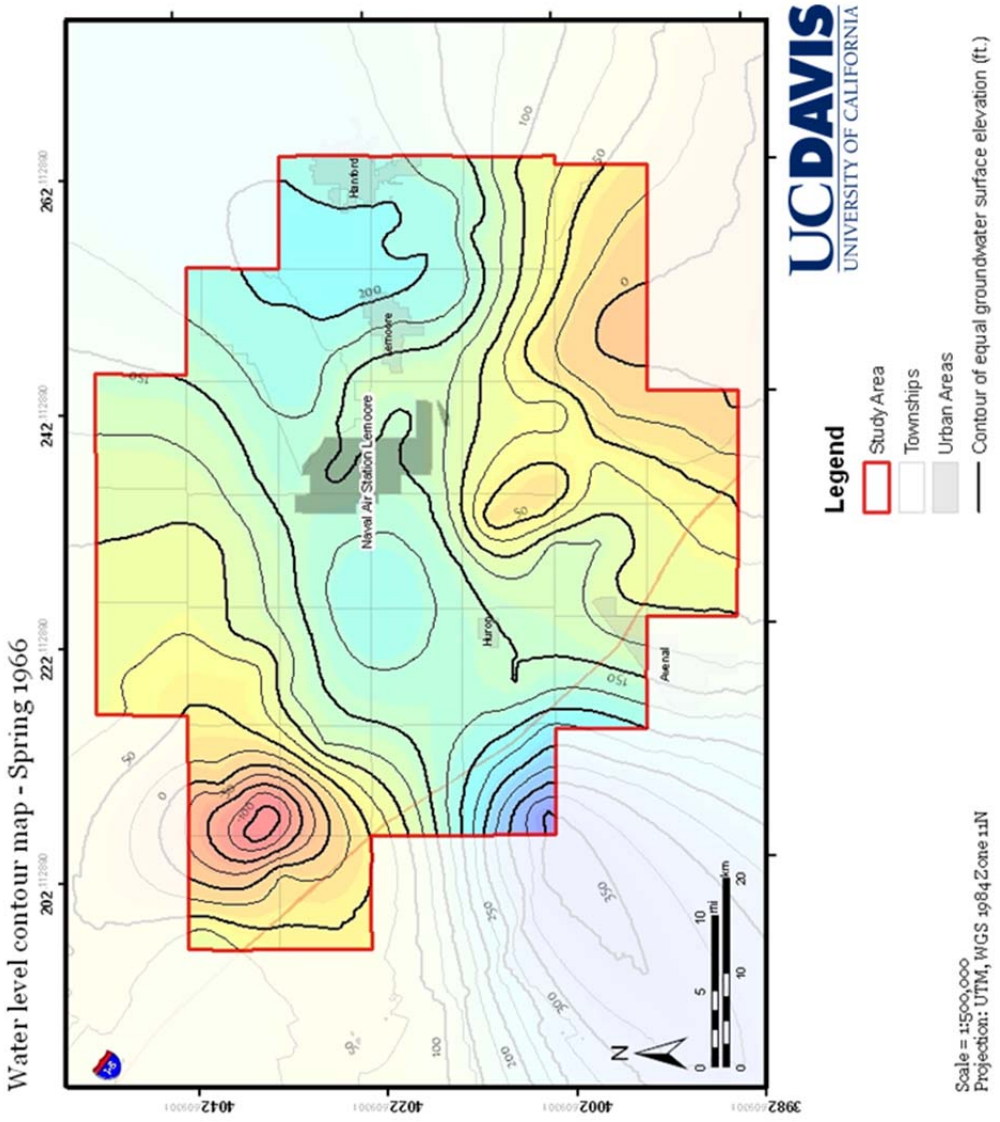

C 1 Water level contour map for the intermediate and deep aquifer for Spring 1966. Data obtained from the California Department of Water Resources.

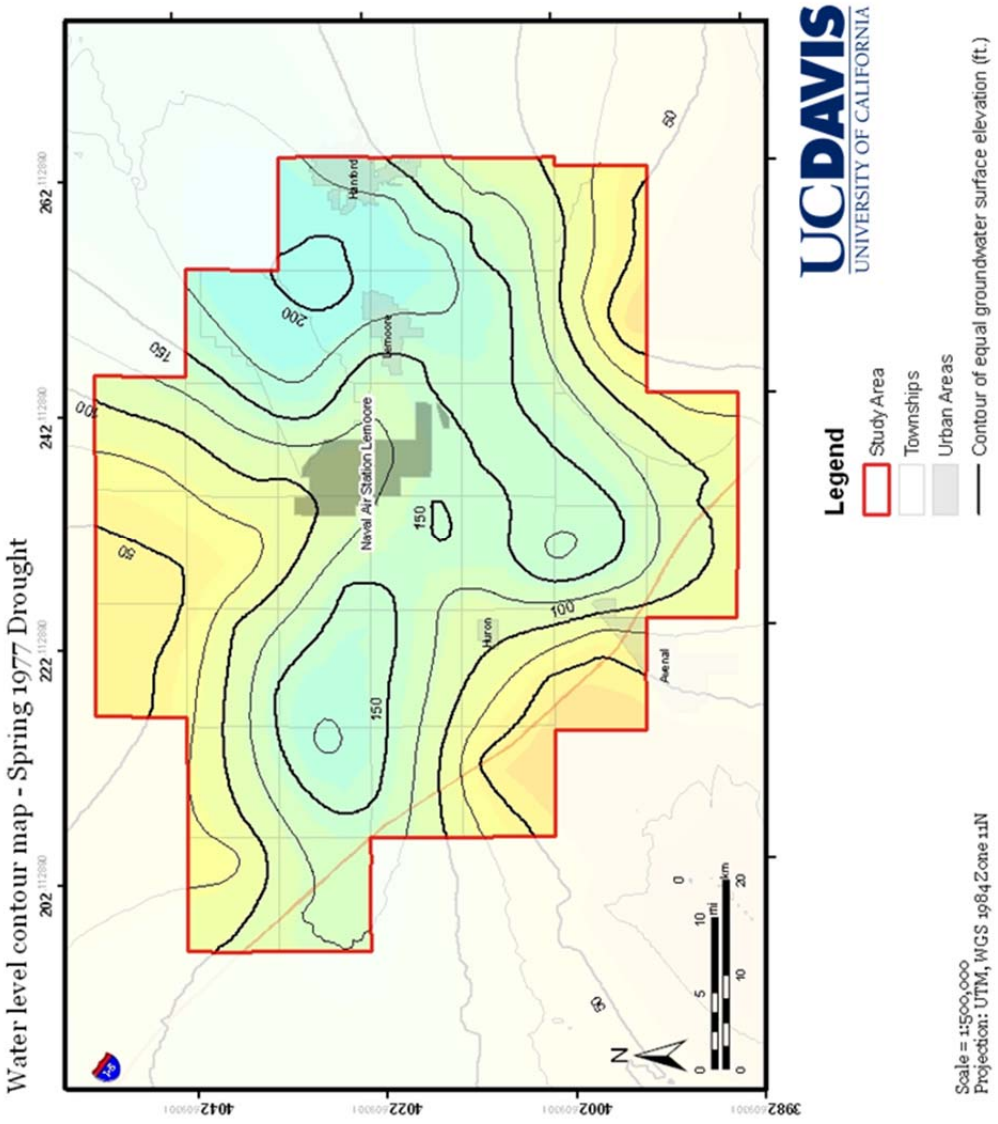

C 2 Water level contour map for the intermediate and deep aquifer for Spring 1977. Data obtained from the California Department of Water Resources.

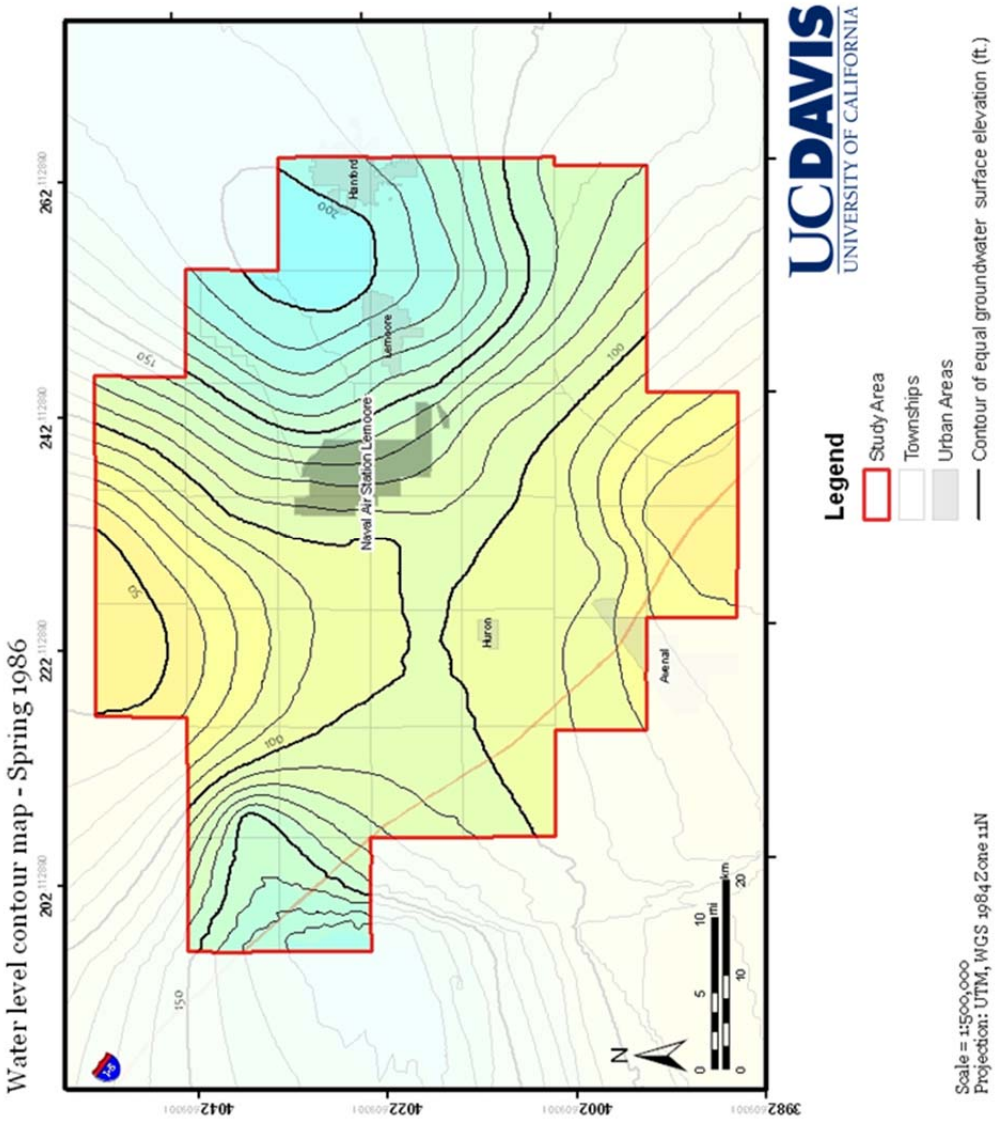

C 3 Water level contour map for the intermediate and deep aquifer for Spring 1986. Data obtained from the California Department of Water Resources.

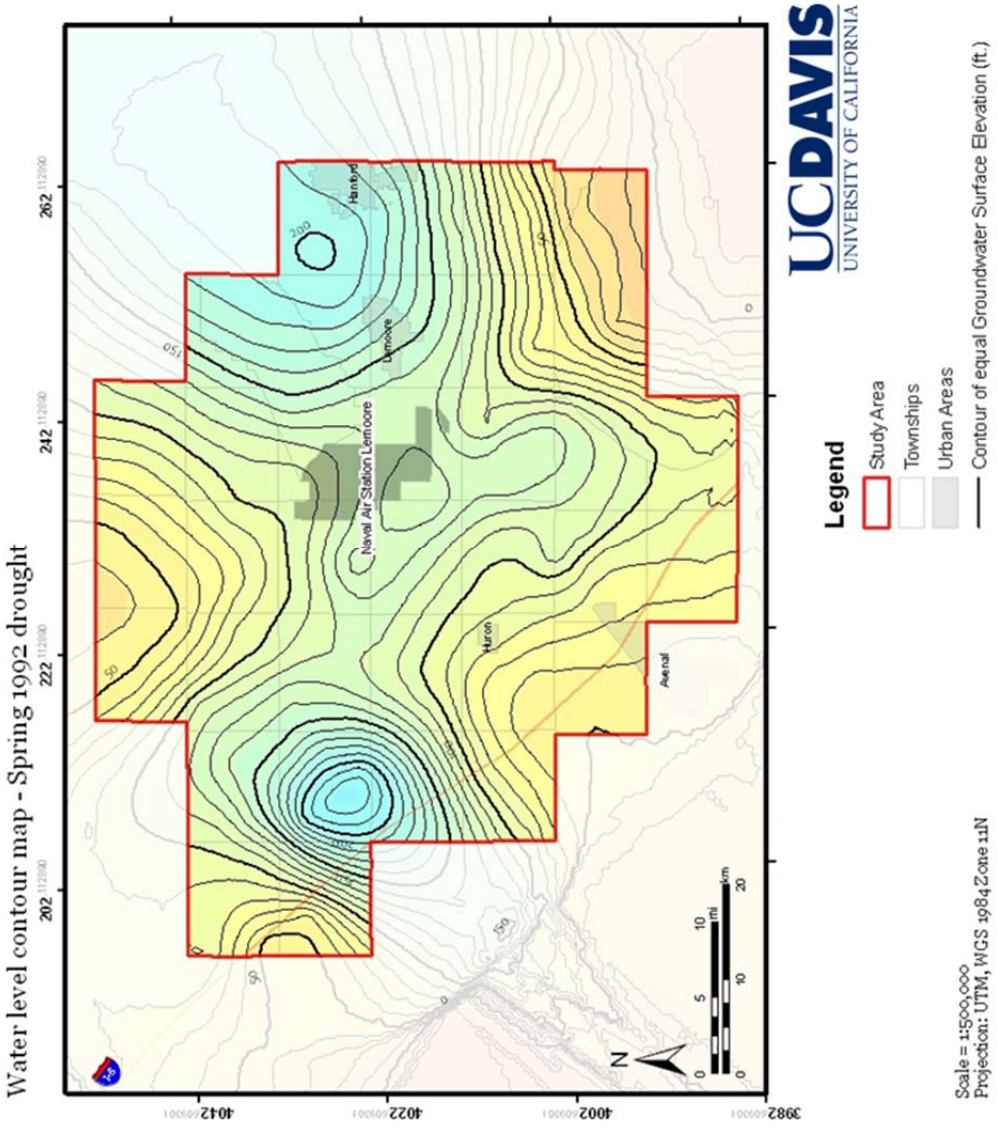

C 4 Water level contour map for the intermediate and deep aquifer for Spring 1992. Data obtained from the California Department of Water Resources.

Appendix D Additional NASL groundwater elevation contour maps

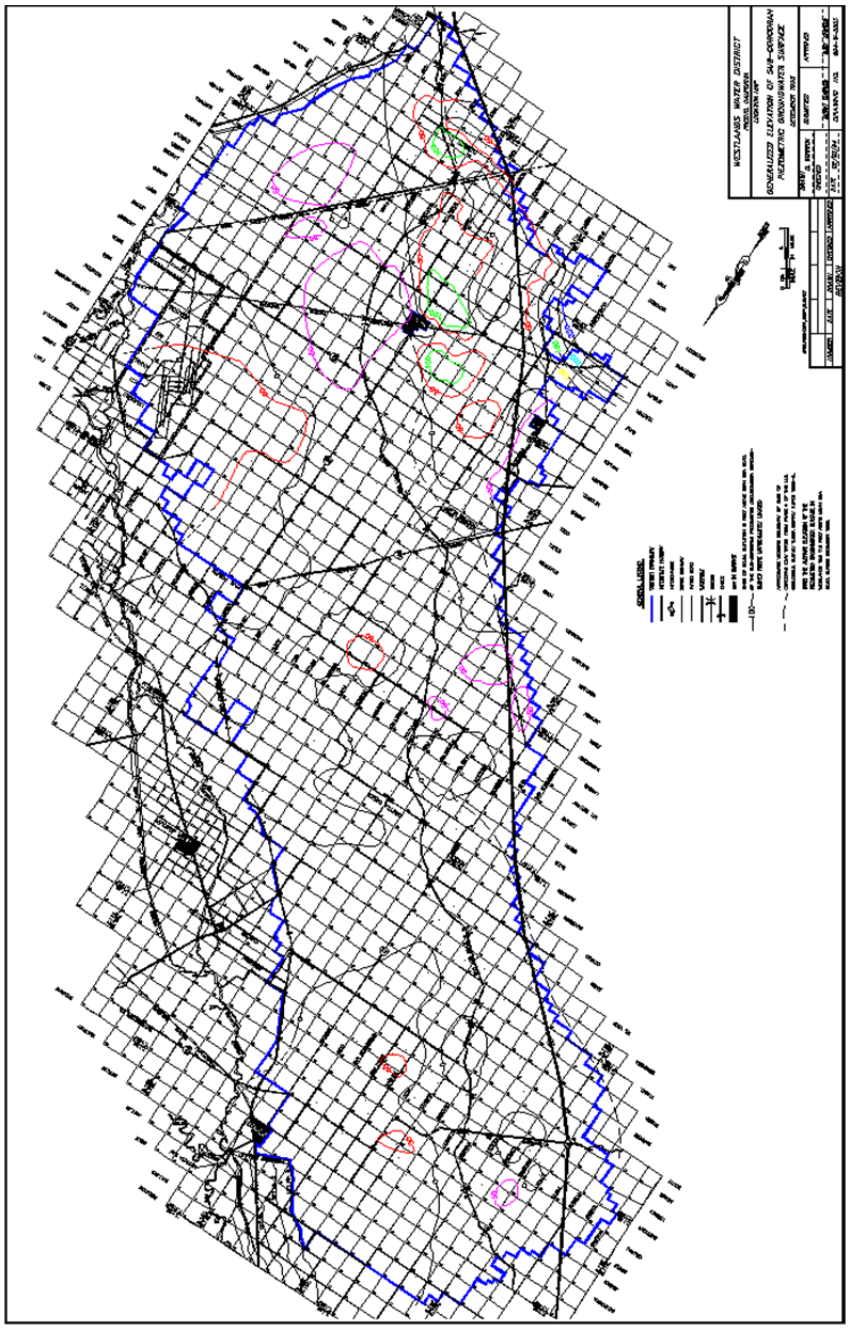

D 1 Confined aquifer groundwater contour map, December 1993.

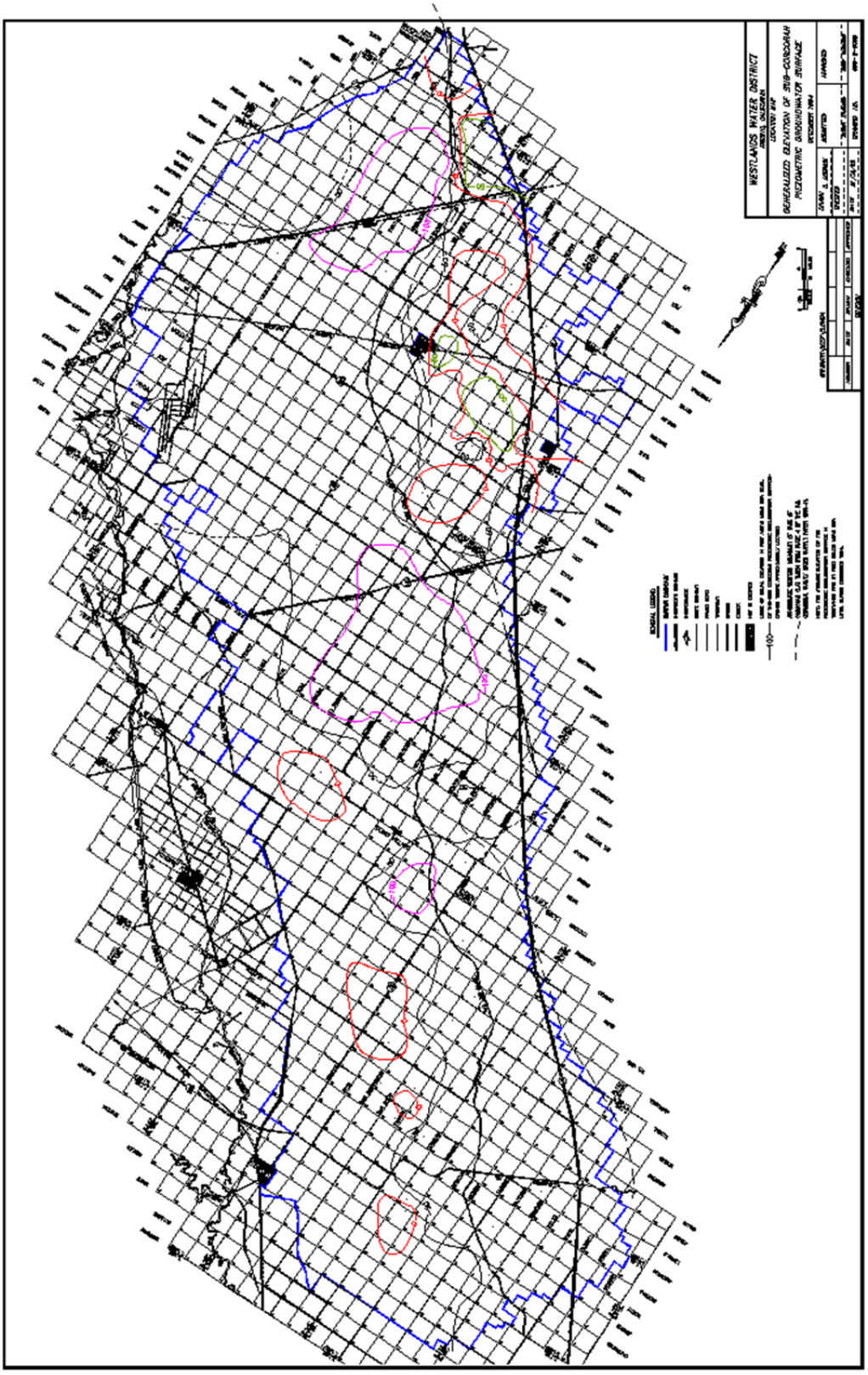

D 2 Confined aquifer groundwater contour map, December 1994.

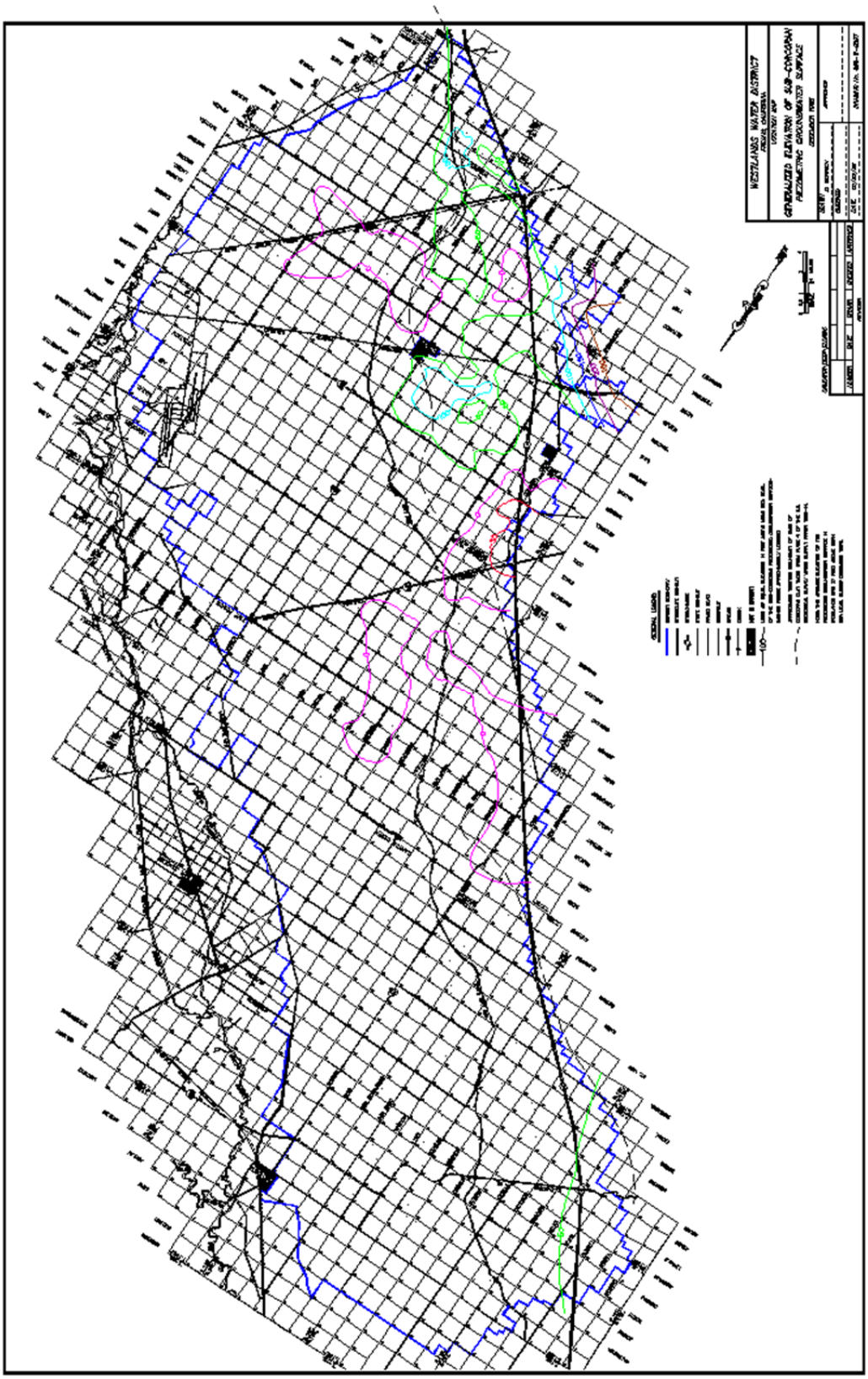

D 3 Confined aquifer groundwater contour map, December 1995.

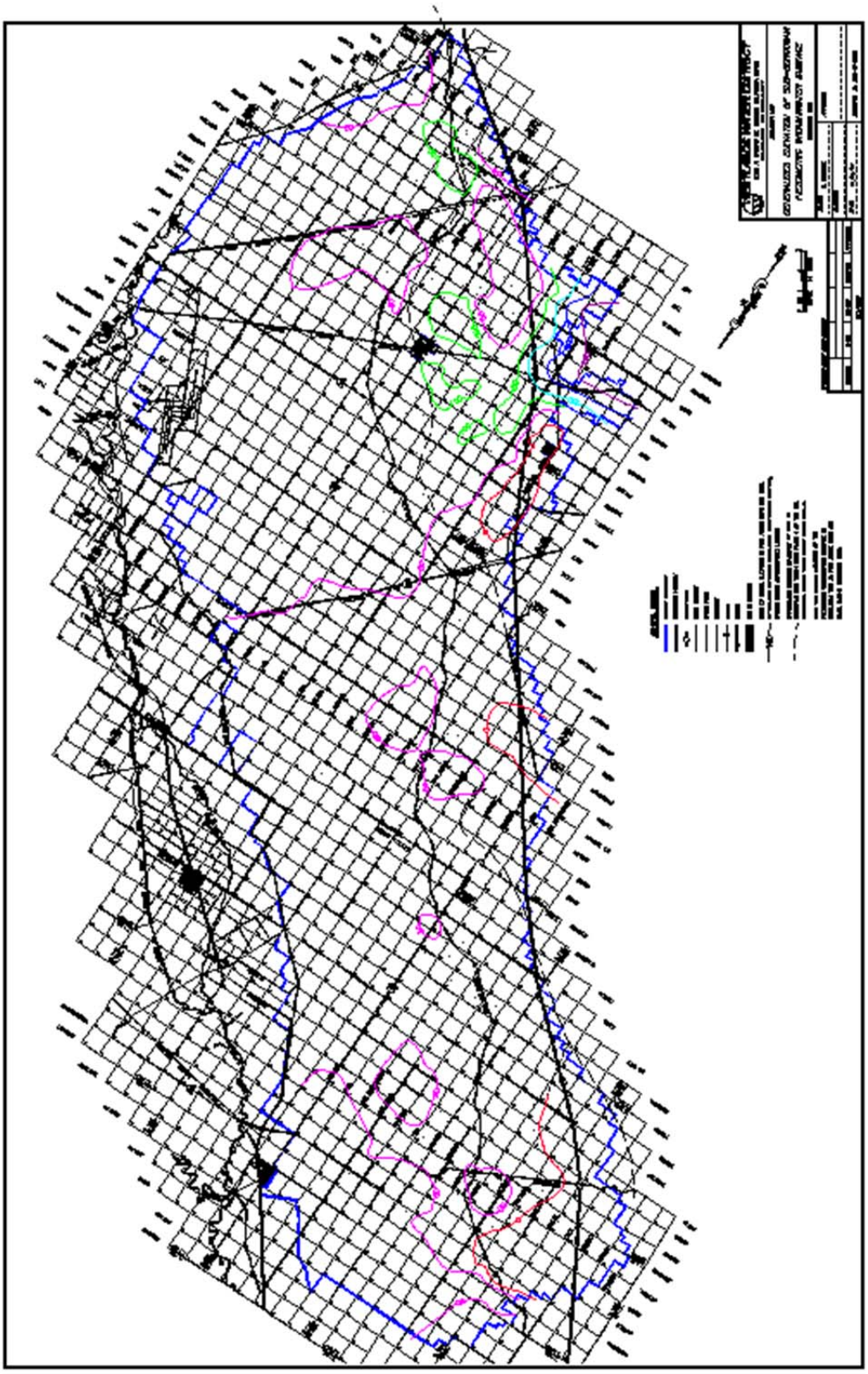

D 4 Confined aquifer groundwater contour map, December 1996.

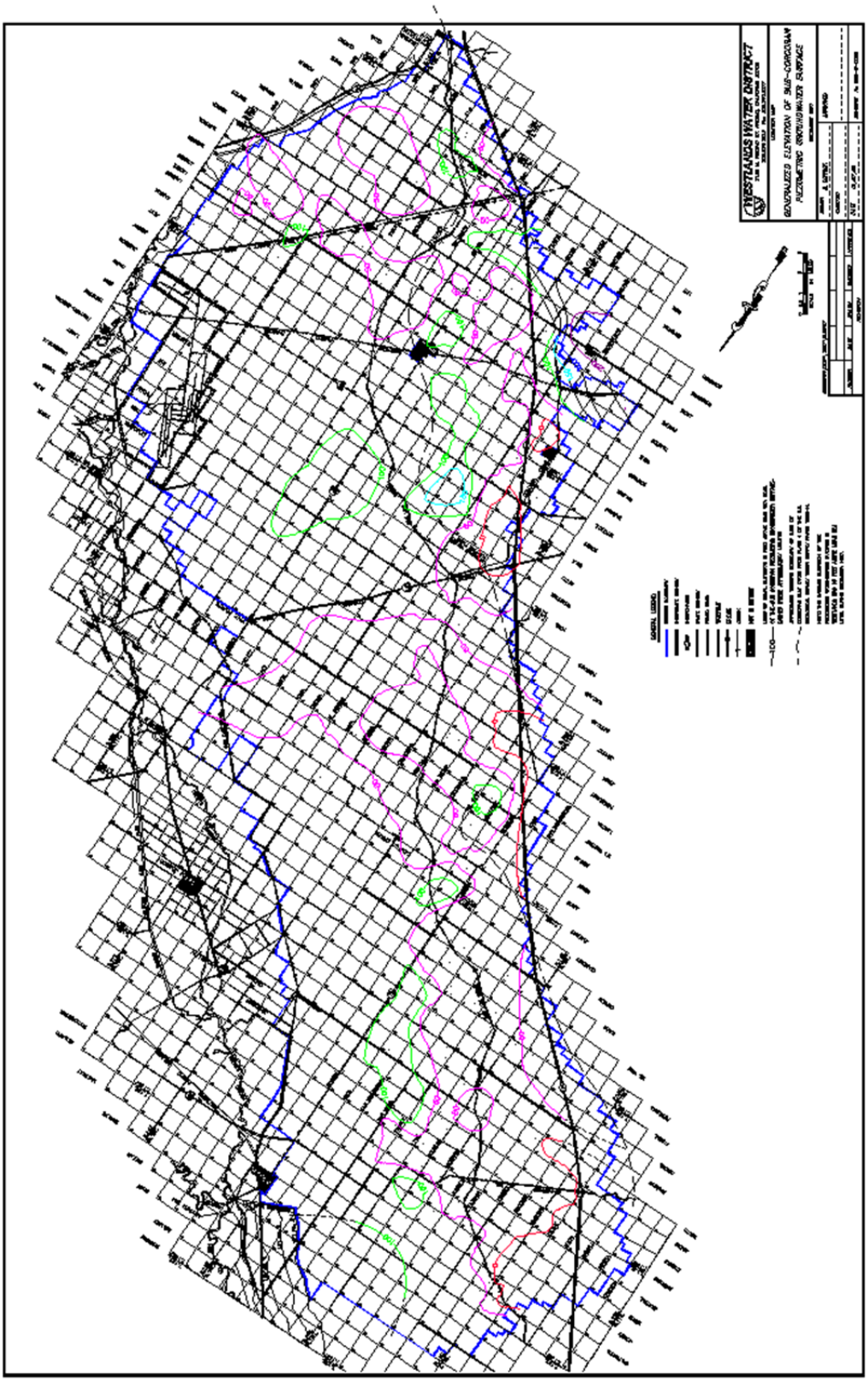

D 5 Confined aquifer groundwater contour map, December 1997.

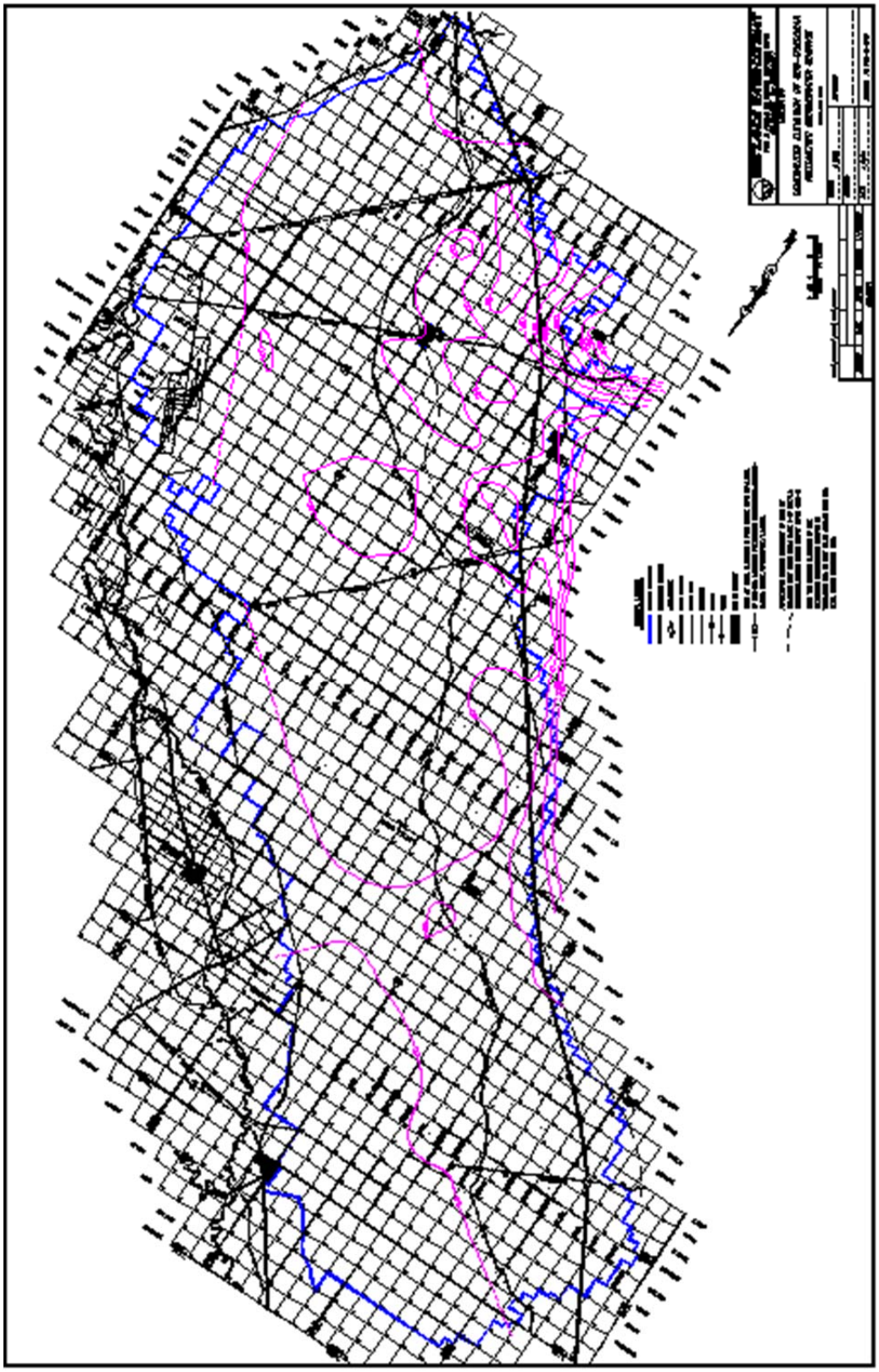

D 6 Confined aquifer groundwater contour map, December 1998.

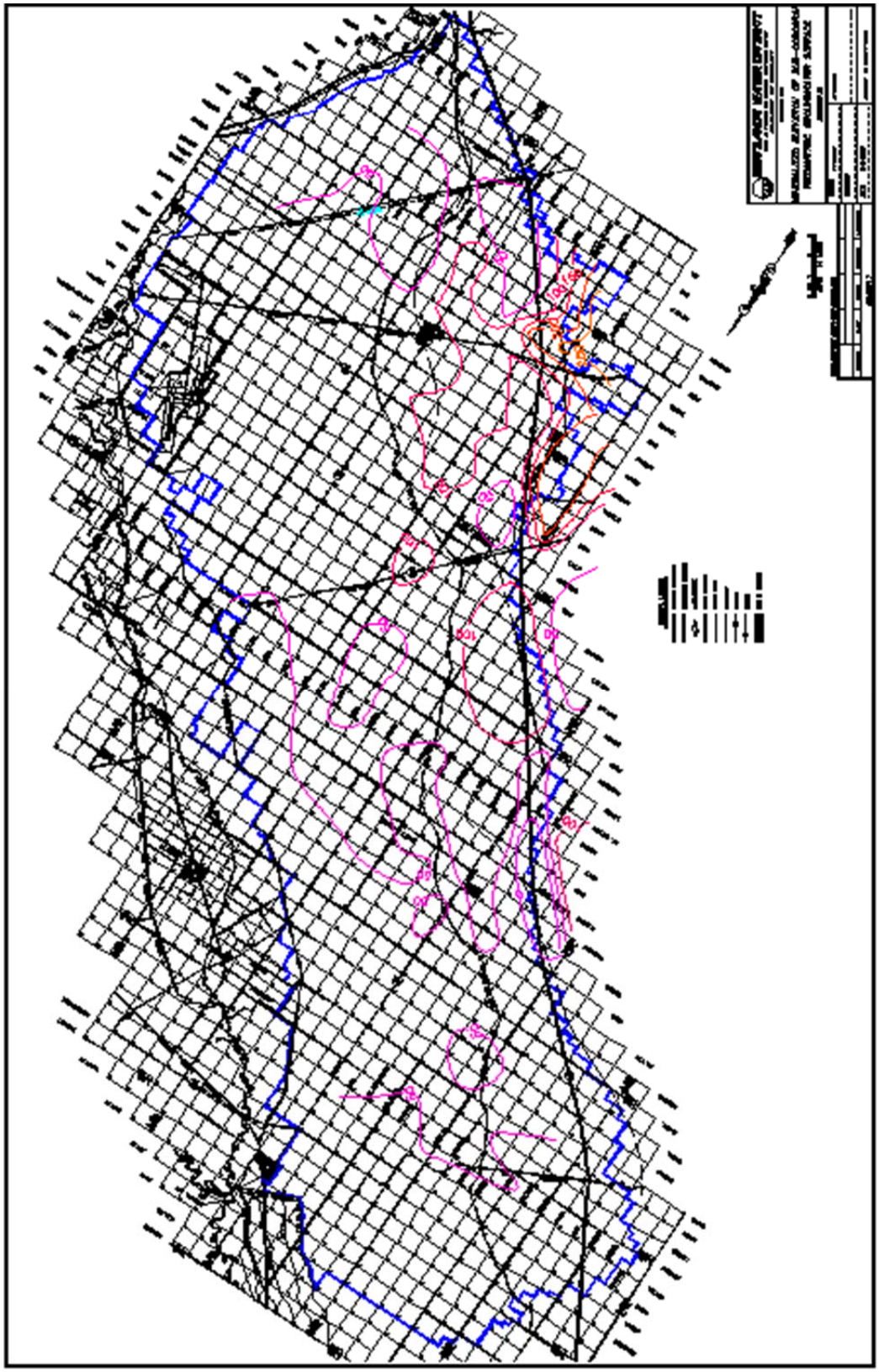

D 7 Confined aquifer groundwater contour map, December 1999.

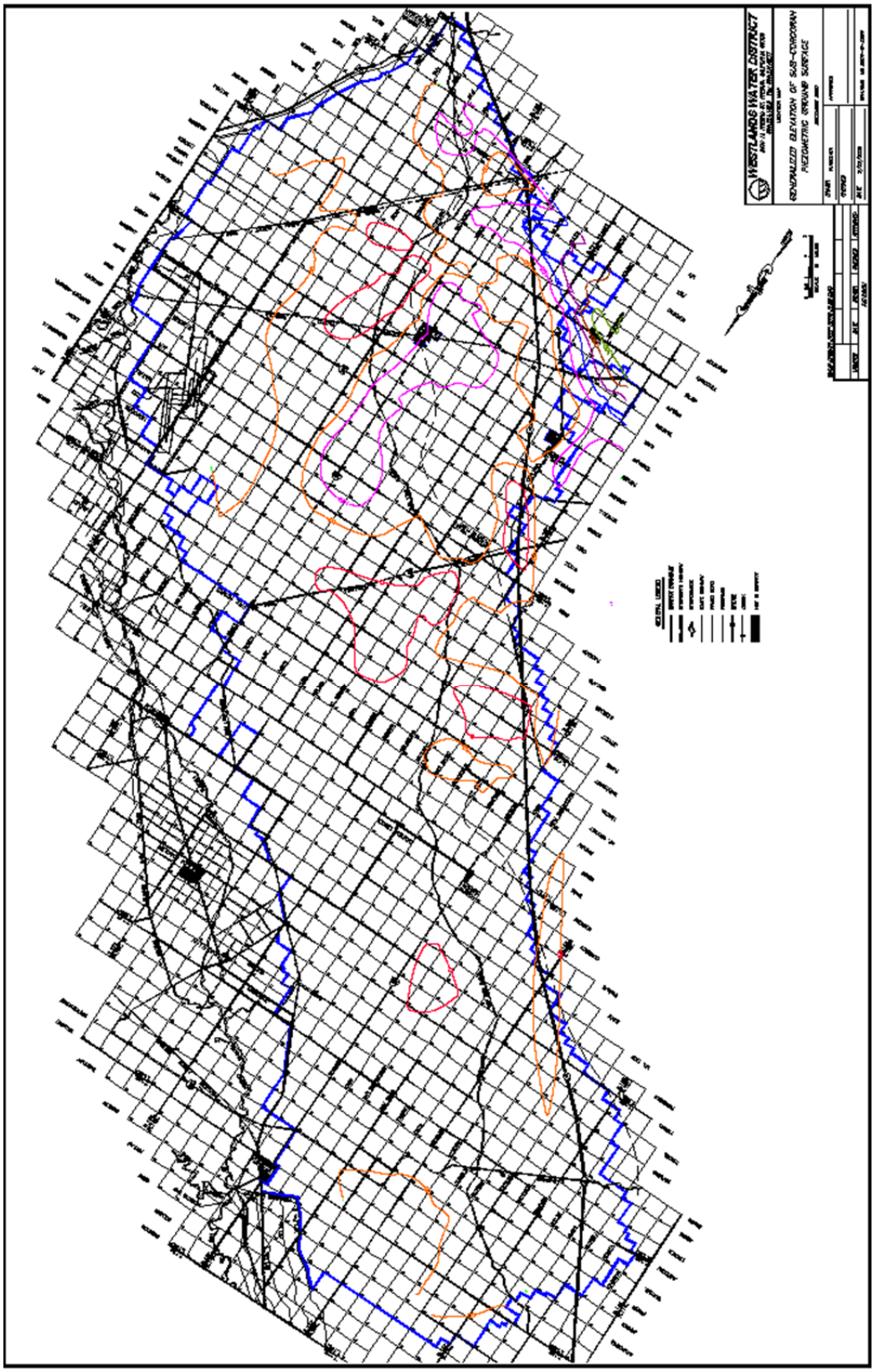

D 8 Confined aquifer groundwater contour map, December 2000.

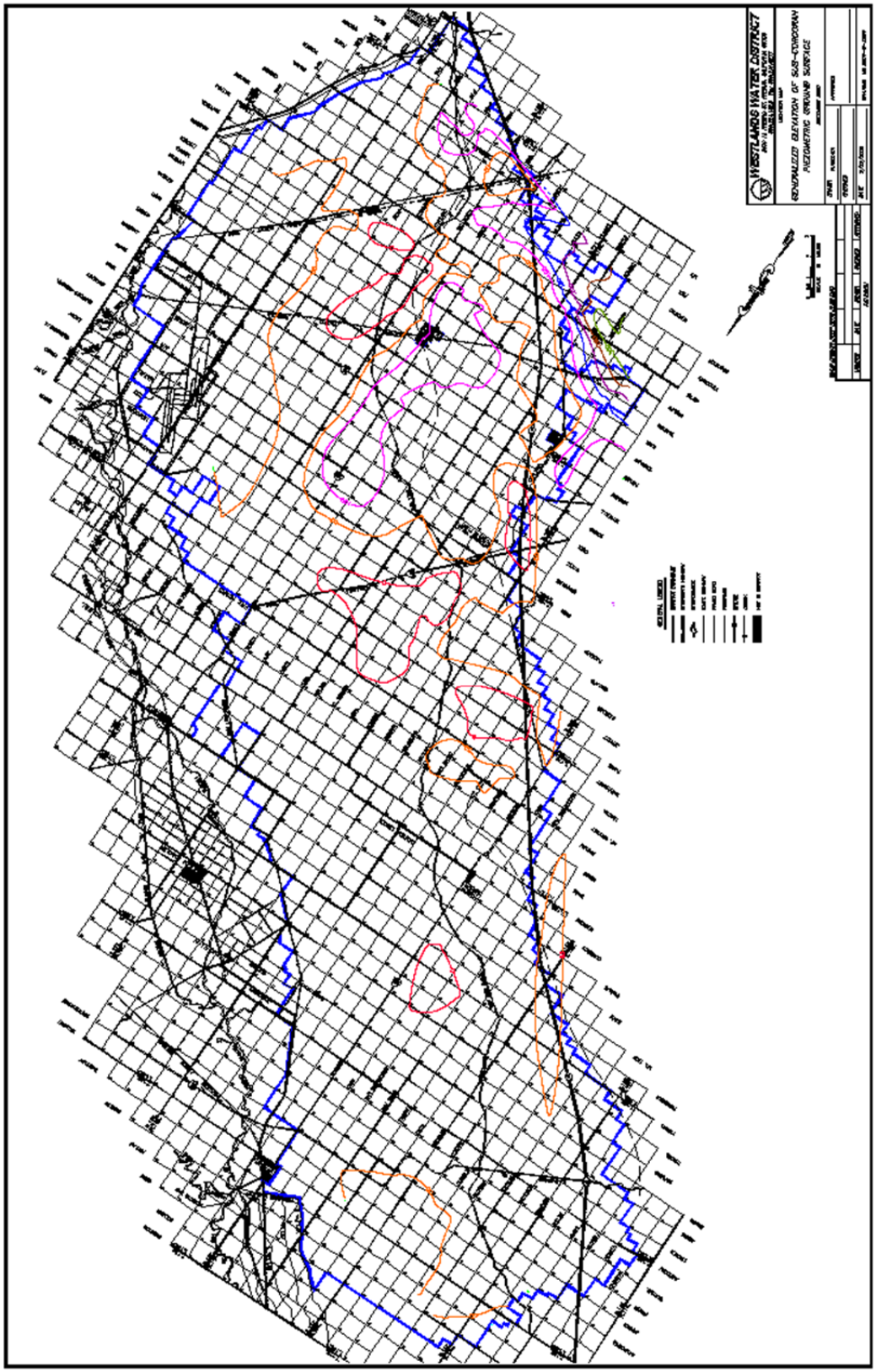

D 9 Confined aquifer groundwater contour map, December 2001.

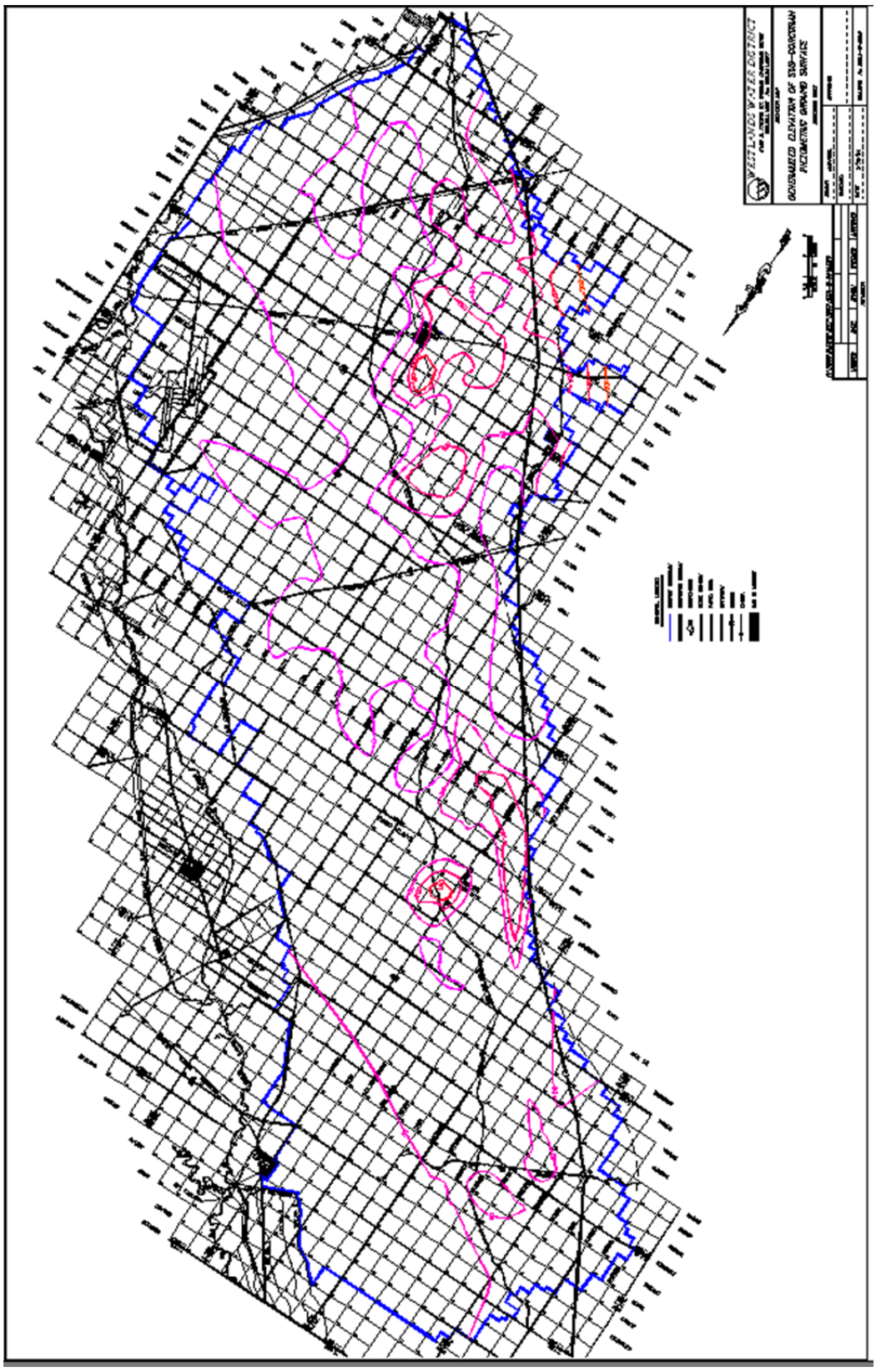

D 11 Confined aquifer groundwater contour map, December 2003.

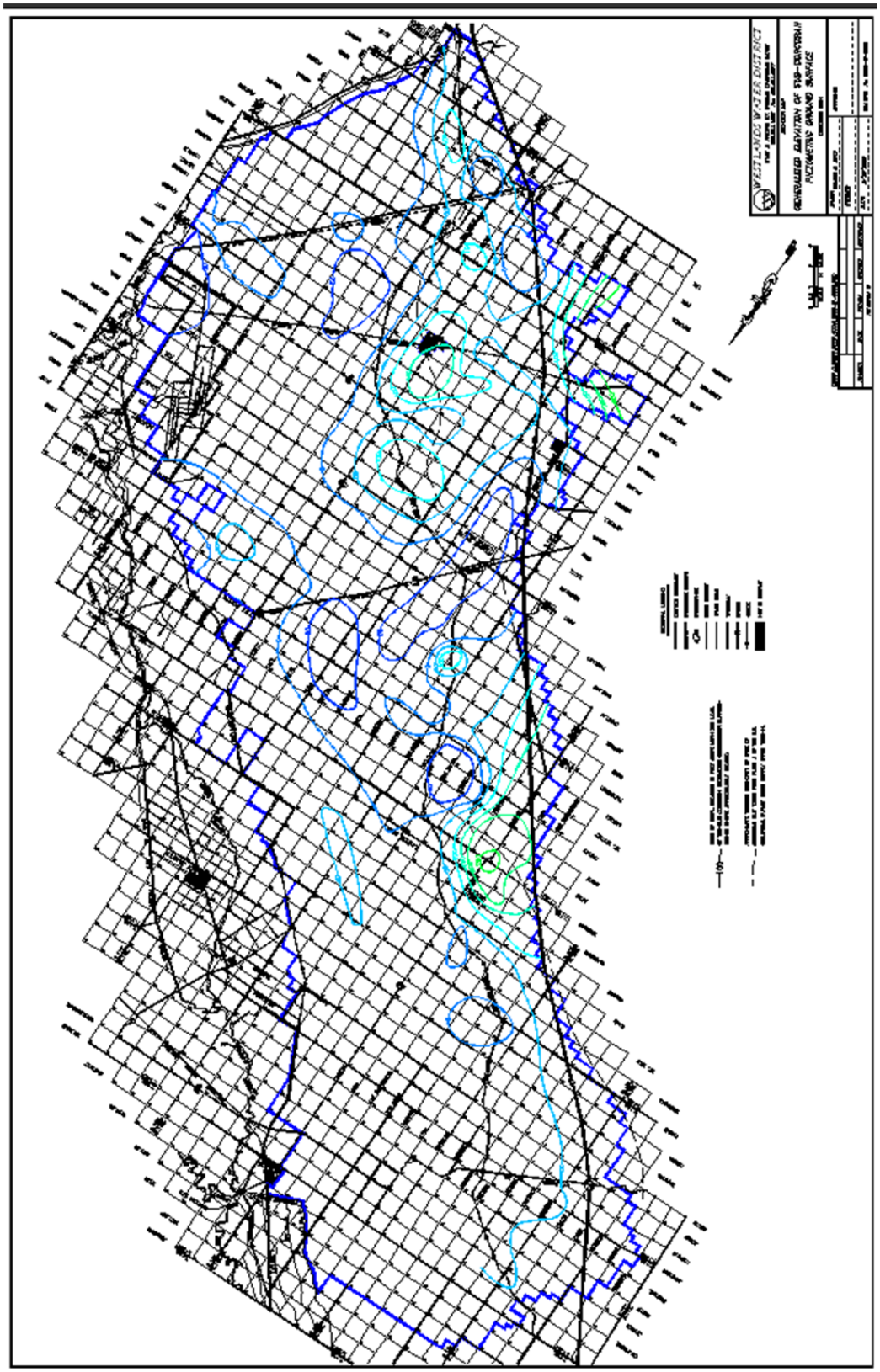

D 12 Confined aquifer groundwater contour map, December 2004.

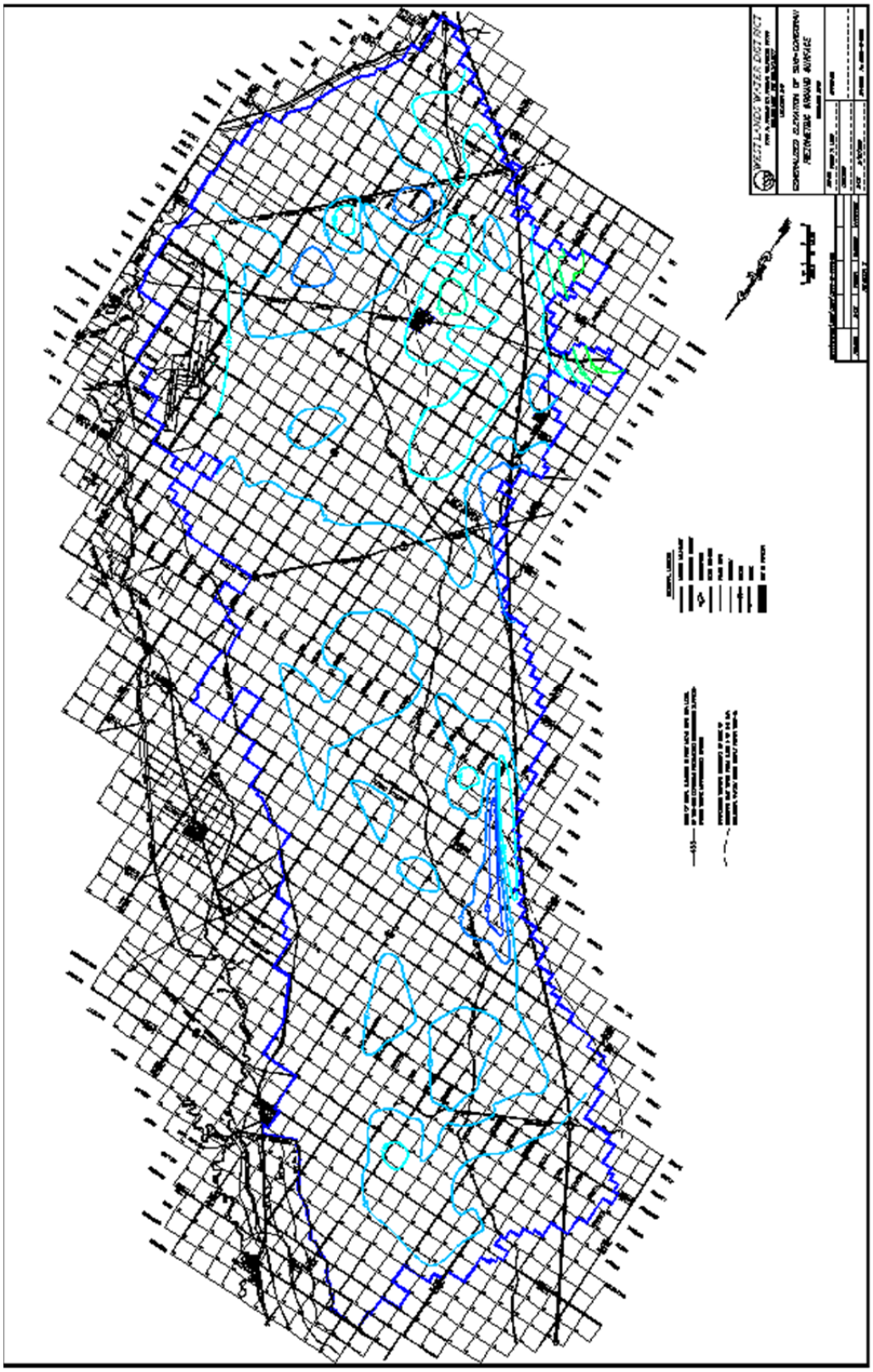

D 13 Confined aquifer groundwater contour map, December 2005.

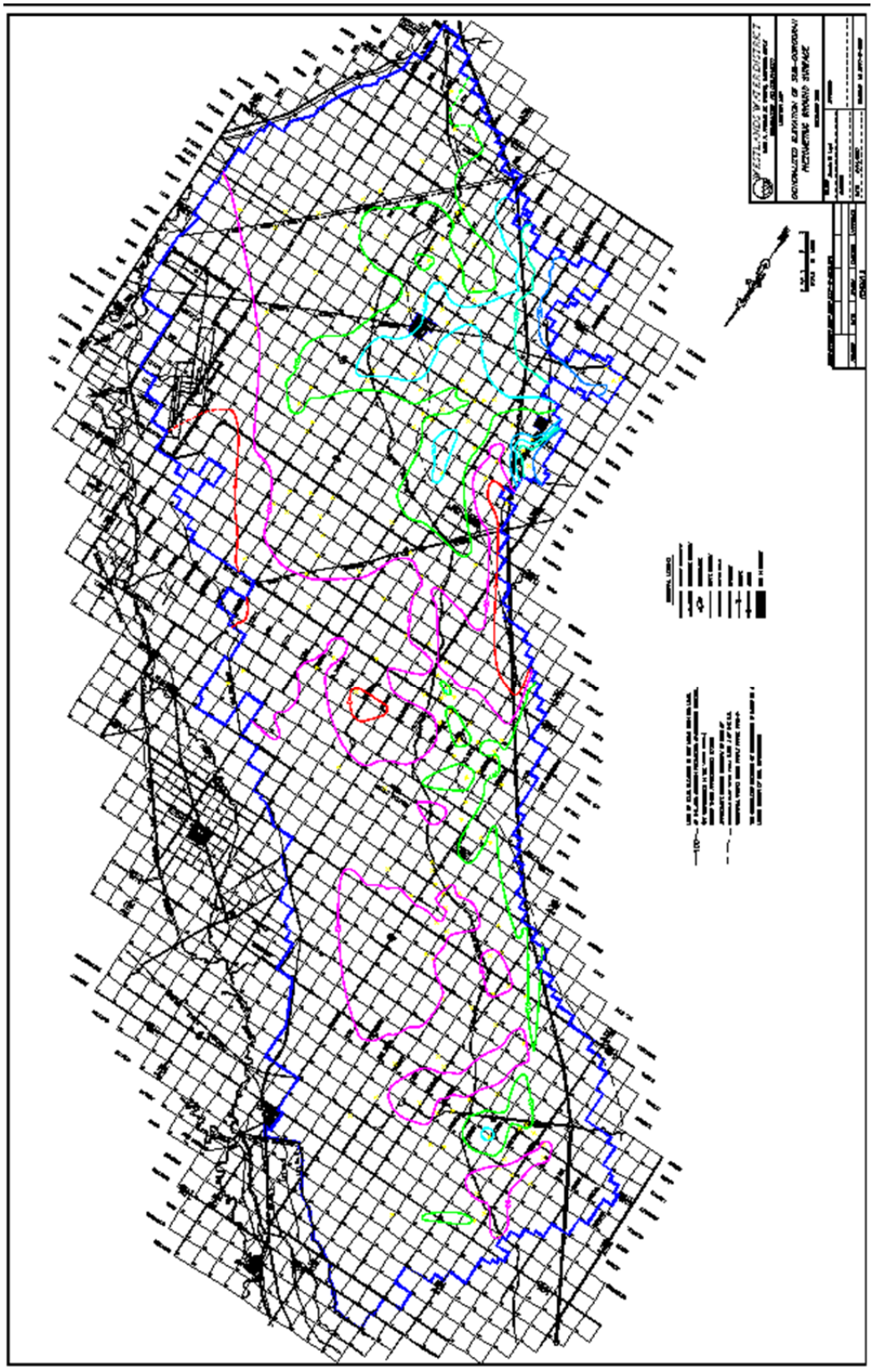

D 14 Confined aquifer groundwater contour map, December 2006.

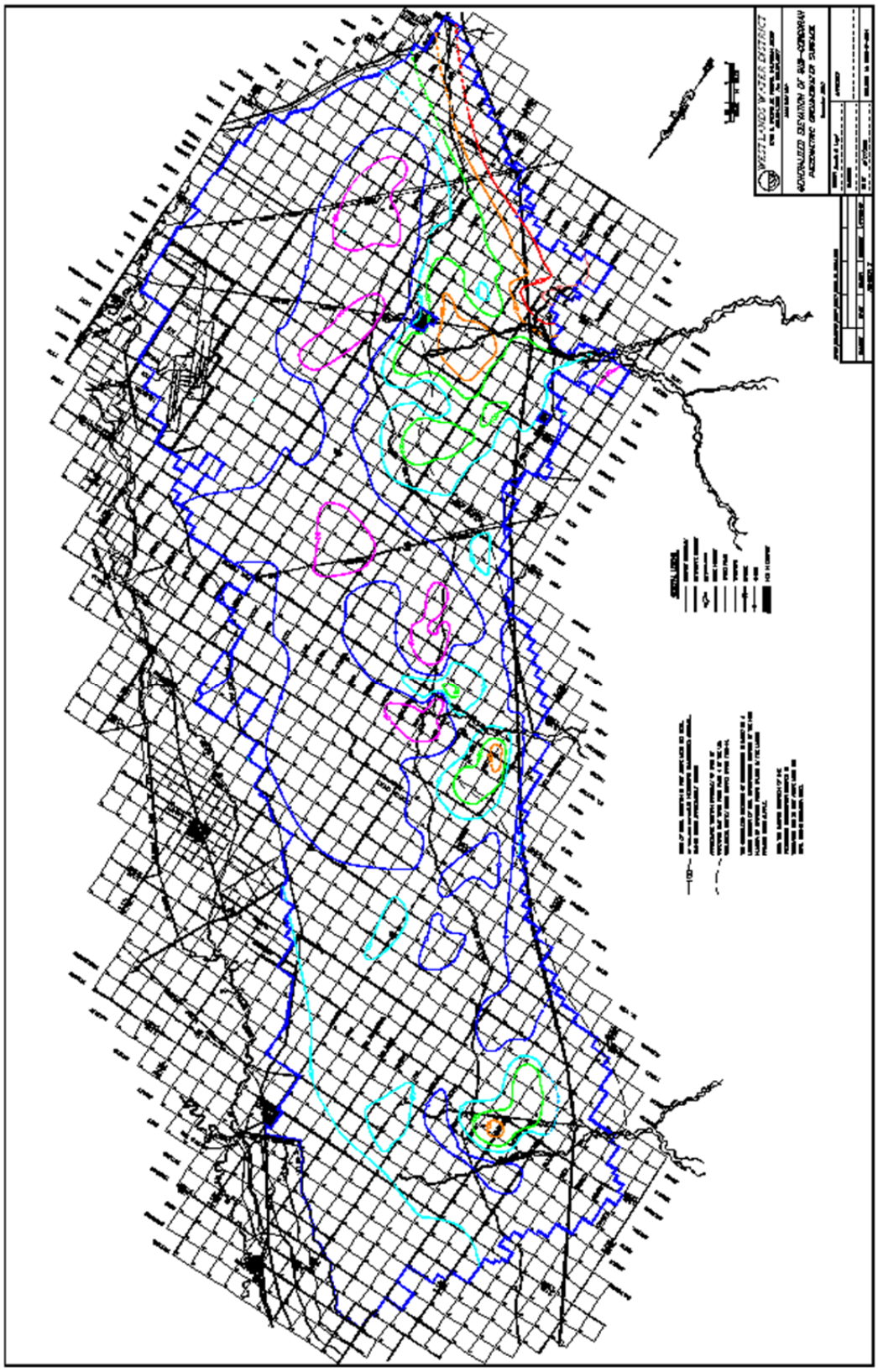

D 15 Confined aquifer groundwater contour map, December 2007.

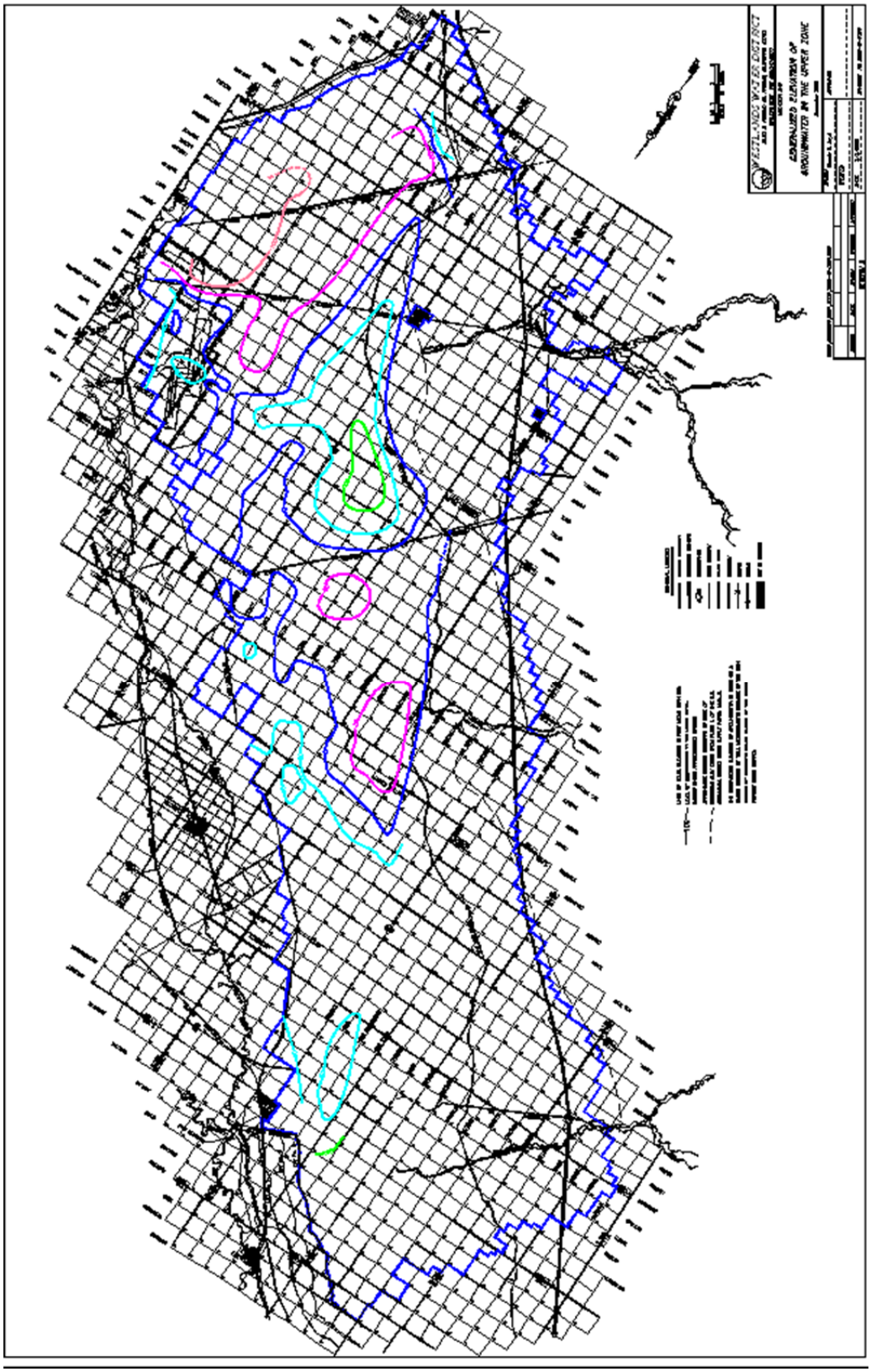

D 16 Confined aquifer groundwater contour map, December 2008.

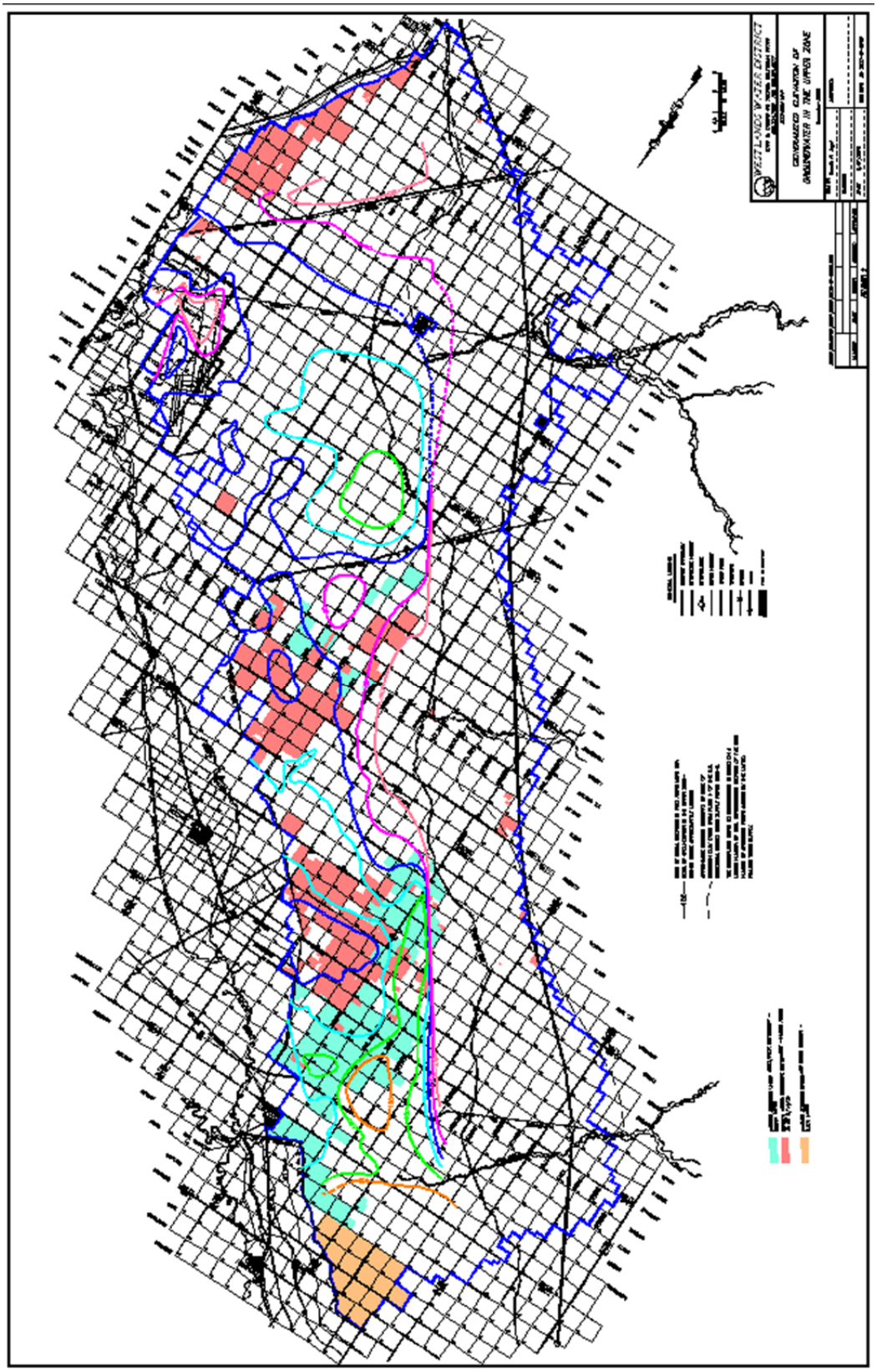

D 17 Confined aquifer groundwater contour map, December 2009.

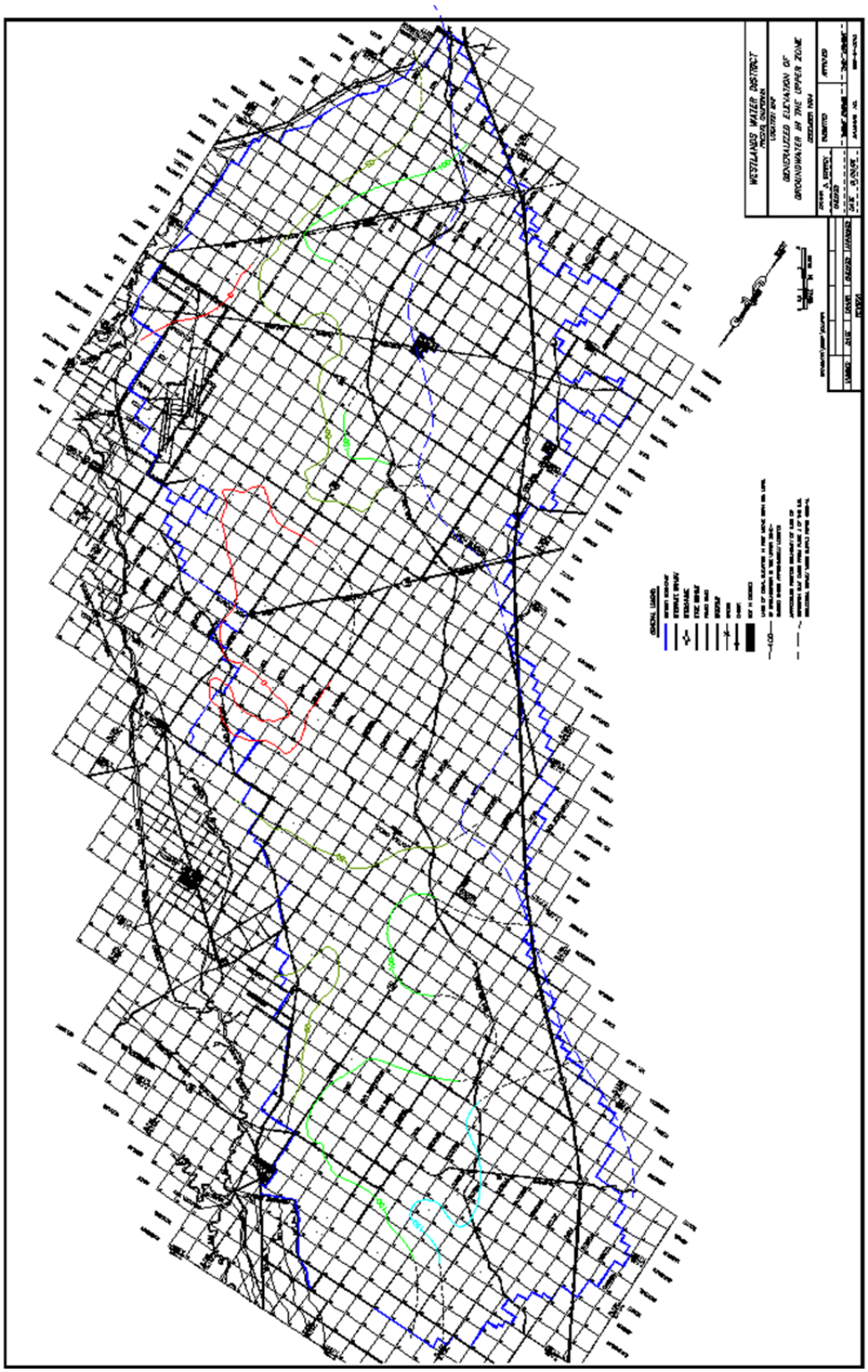

D 18 Unconfined aquifer groundwater contour map, December 1994.

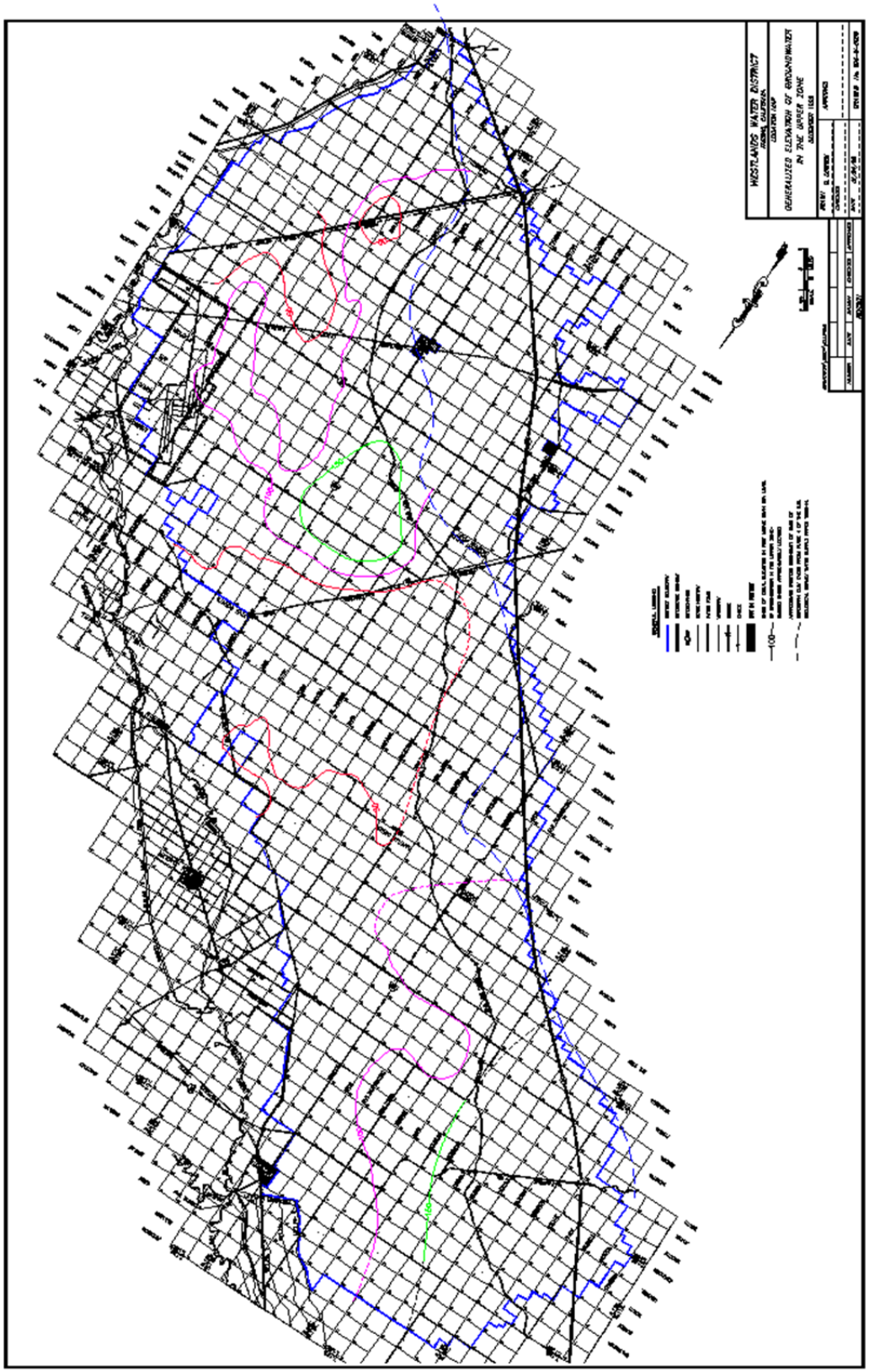

D 19 Unconfined aquifer groundwater contour map, December 1995.

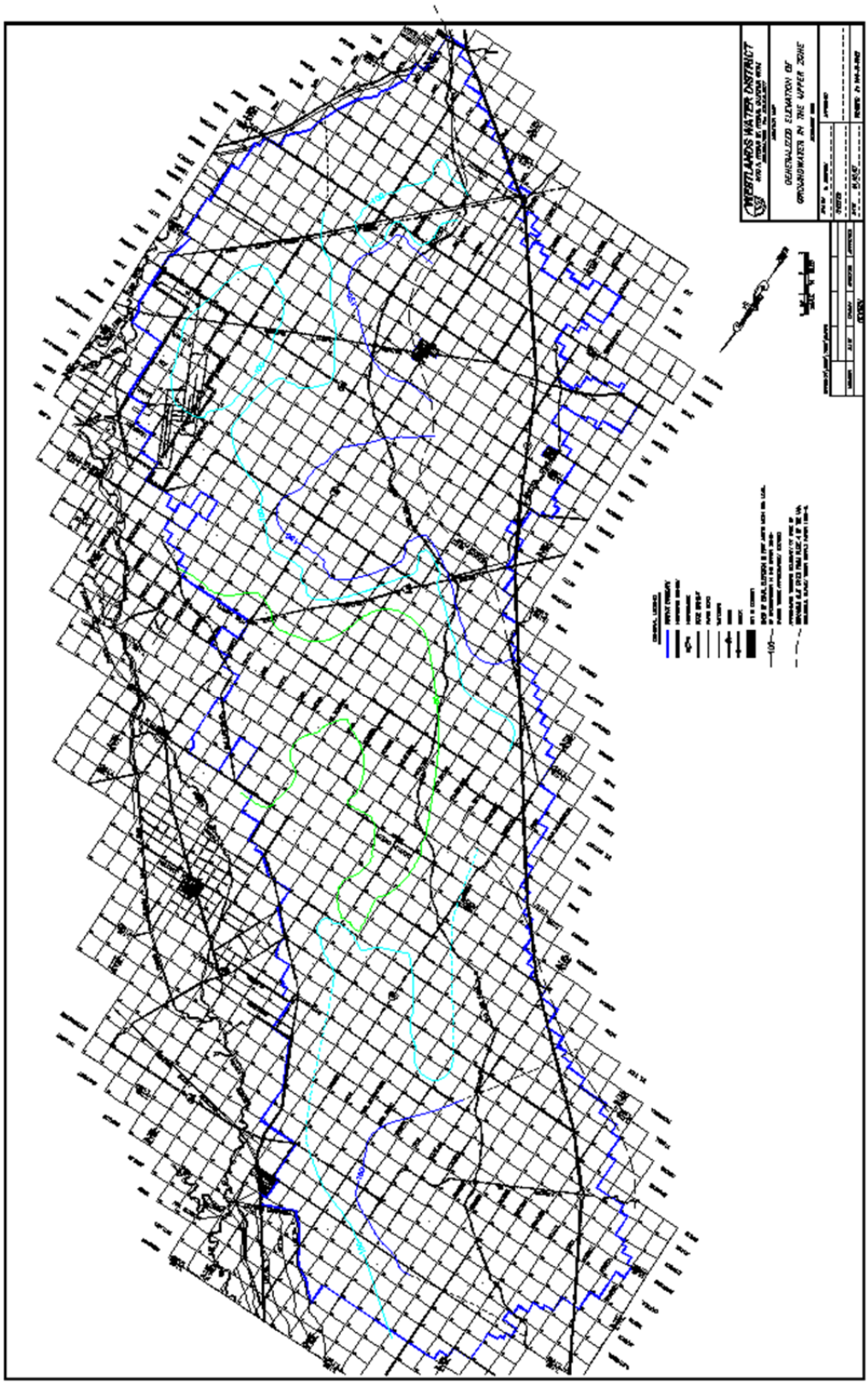

D 20 Unconfined aquifer groundwater contour map, December 1996.

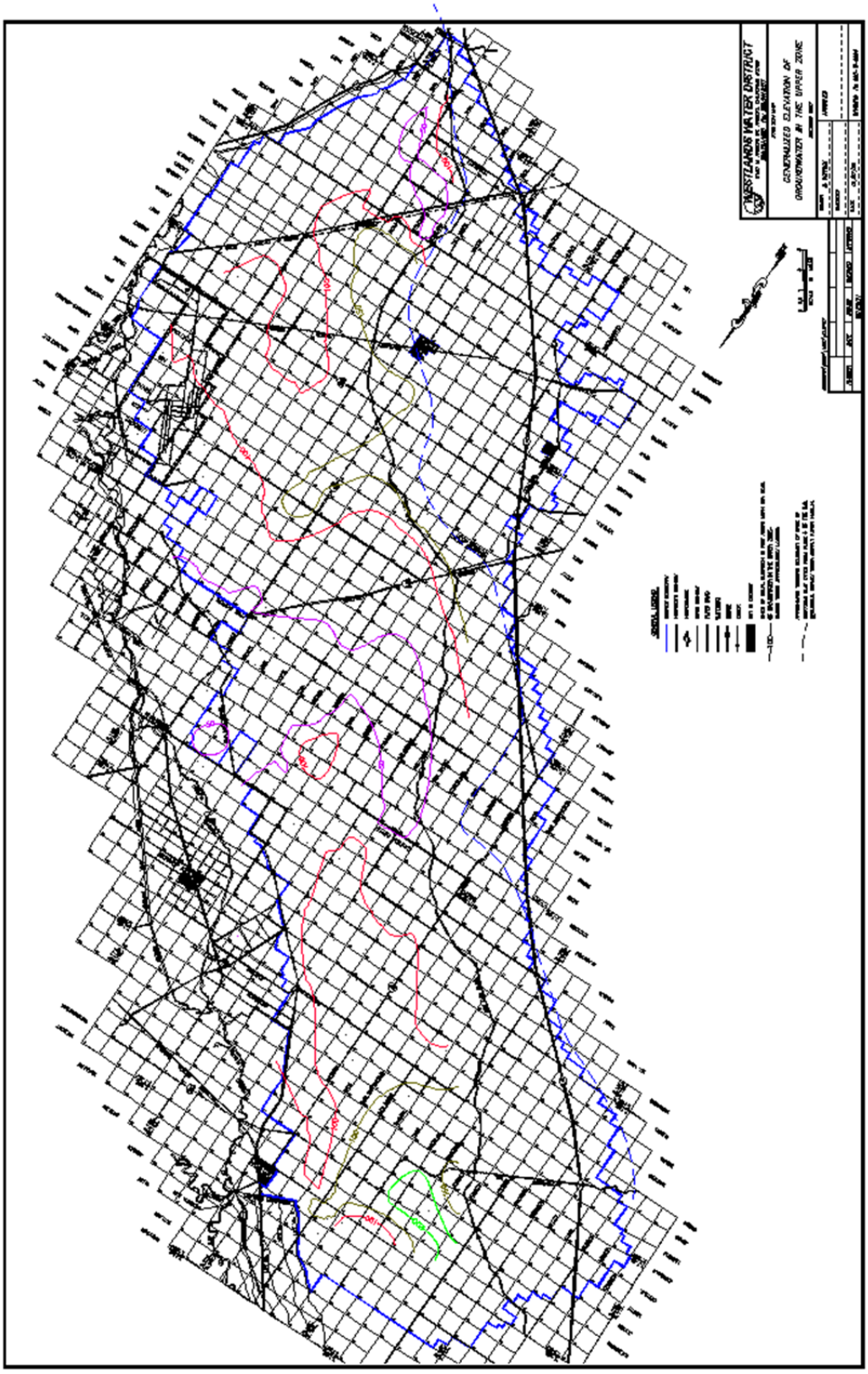

D 21 Unconfined aquifer groundwater contour map, December 1997.

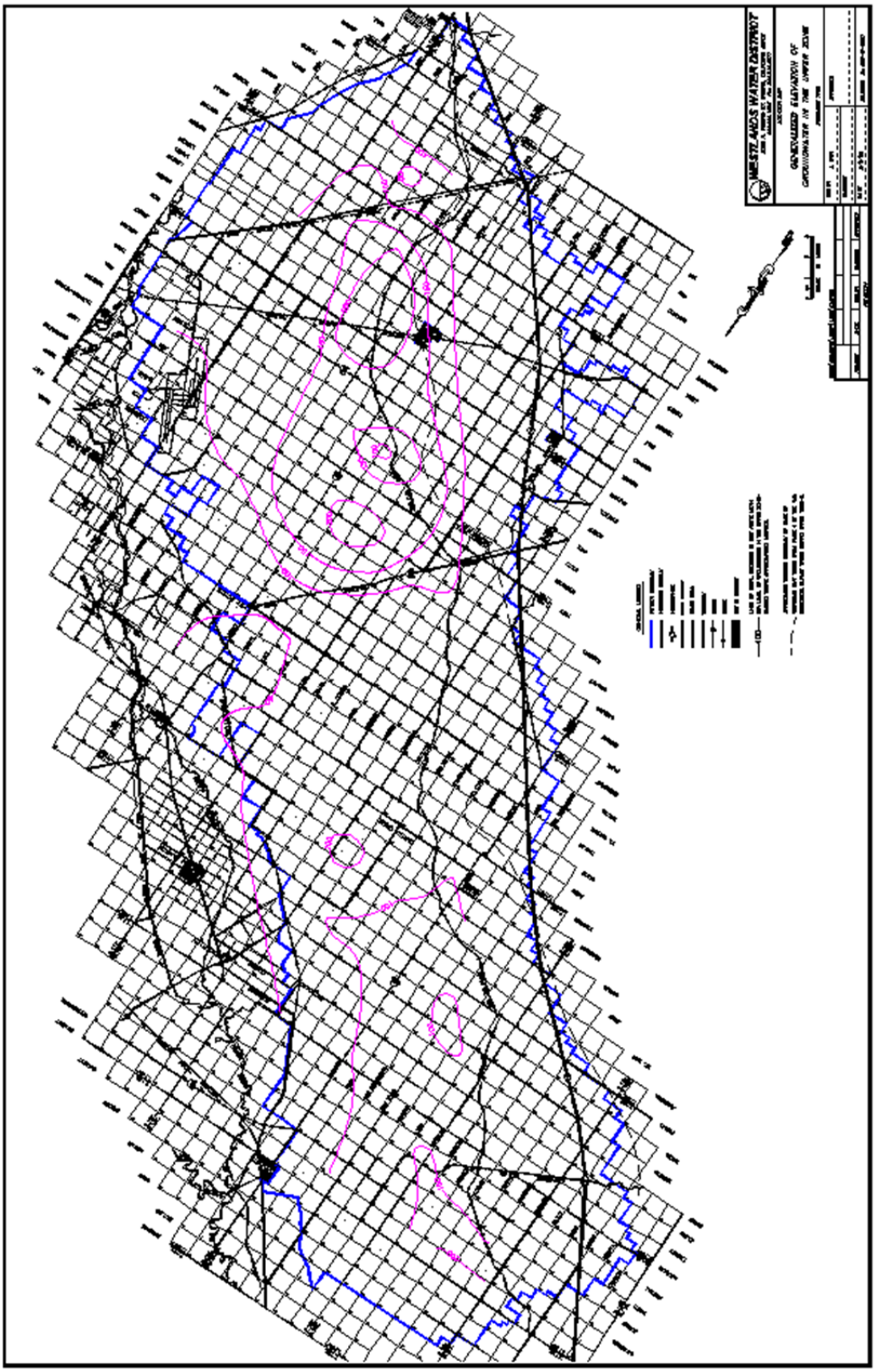

D 22 Unconfined aquifer groundwater contour map, December 1998.

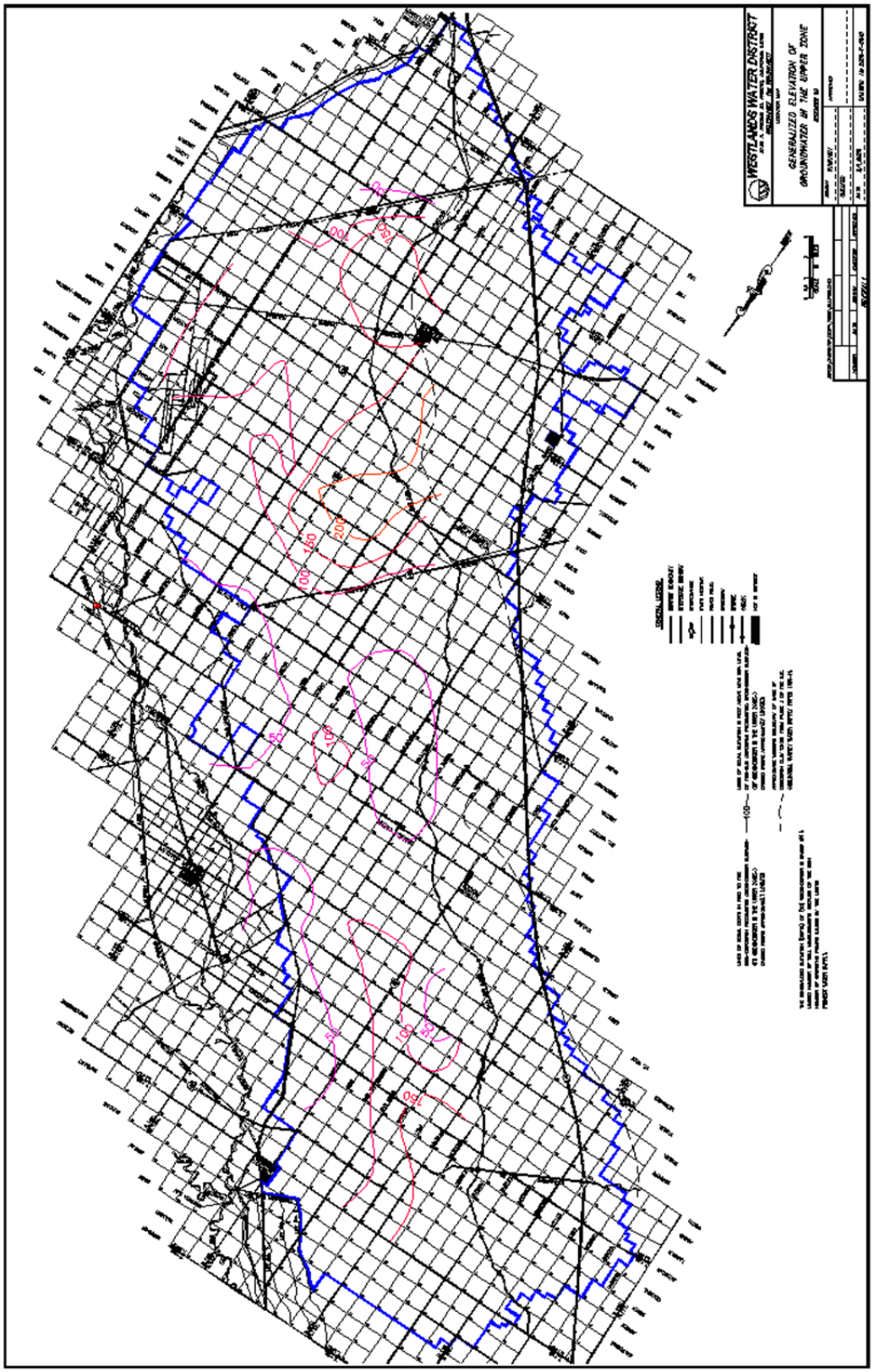

D 23 Unconfined aquifer groundwater contour map, December 1999.

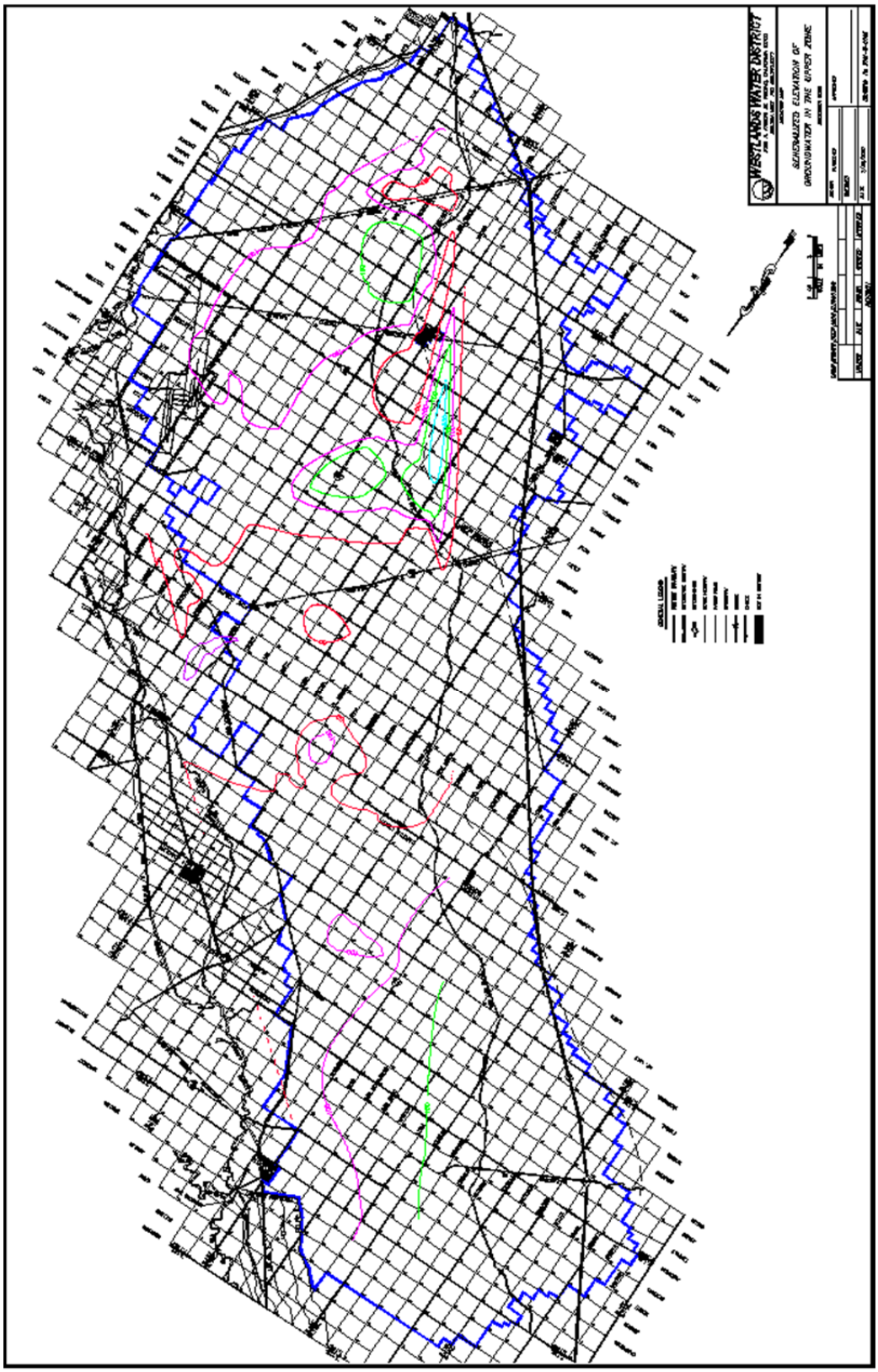

D 24 Unconfined aquifer groundwater contour map, December 2000.

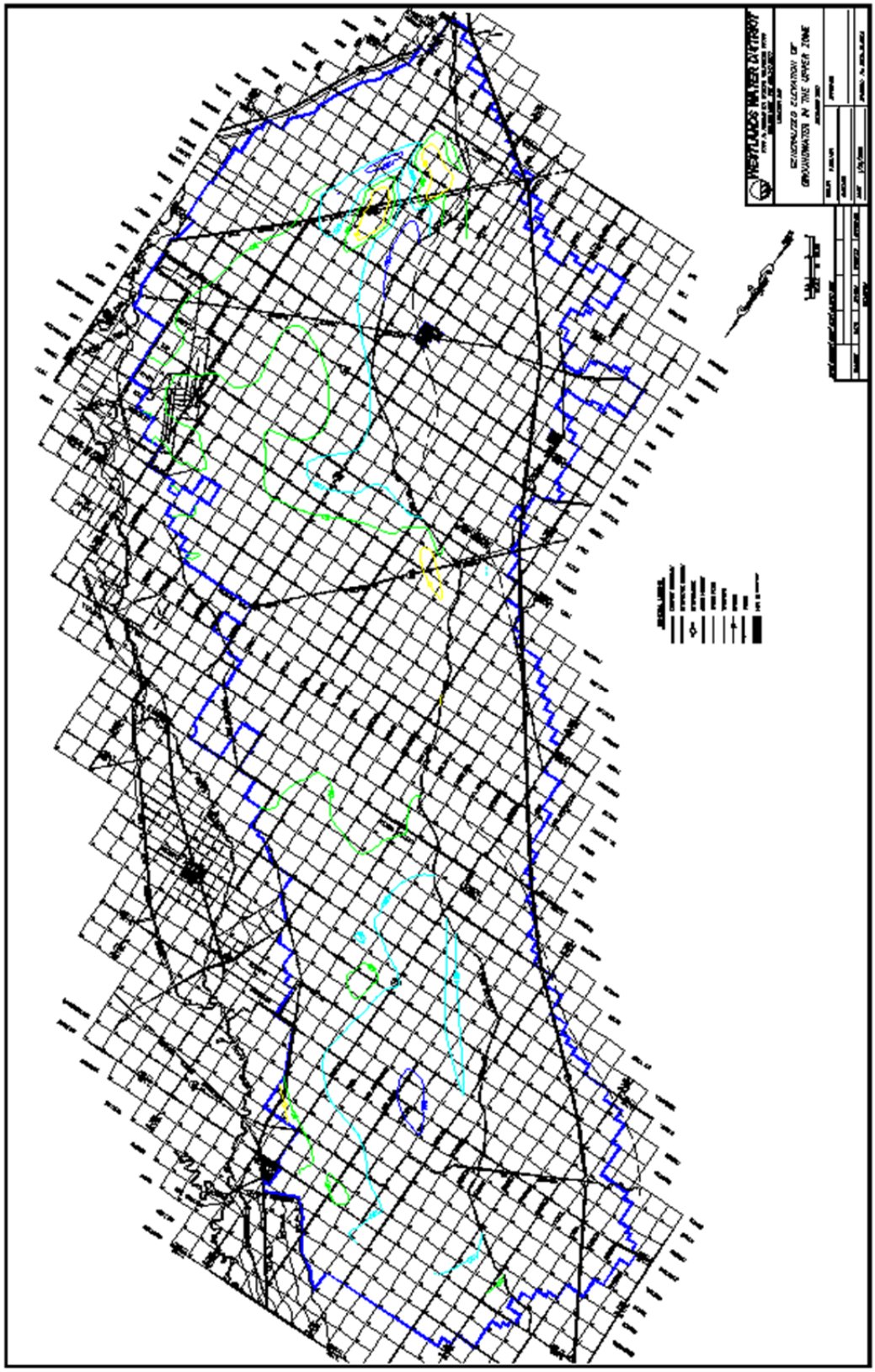

D 25 Unconfined aquifer groundwater contour map, December 2001.

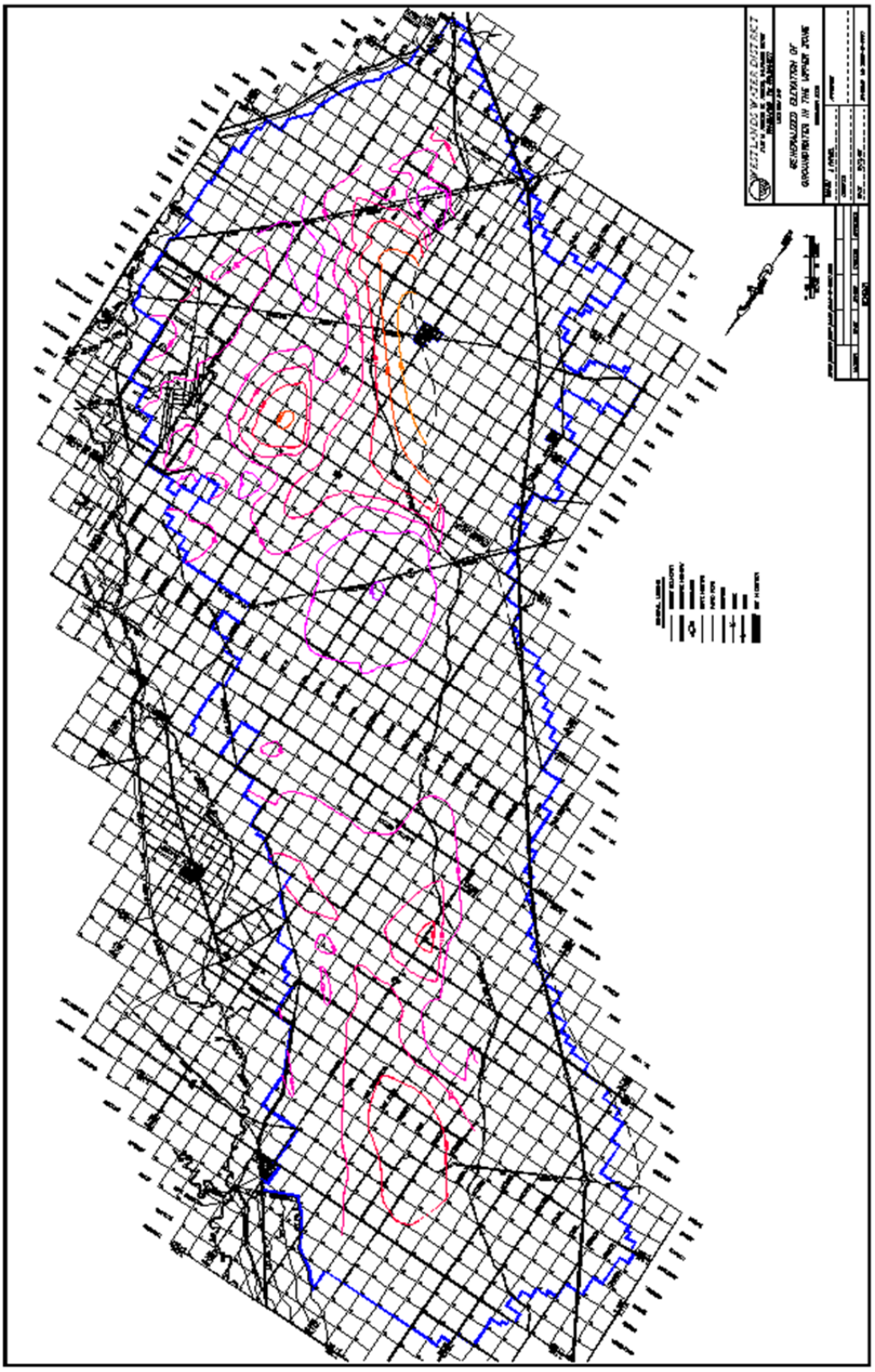

D 26 Unconfined aquifer groundwater contour map, December 2002.

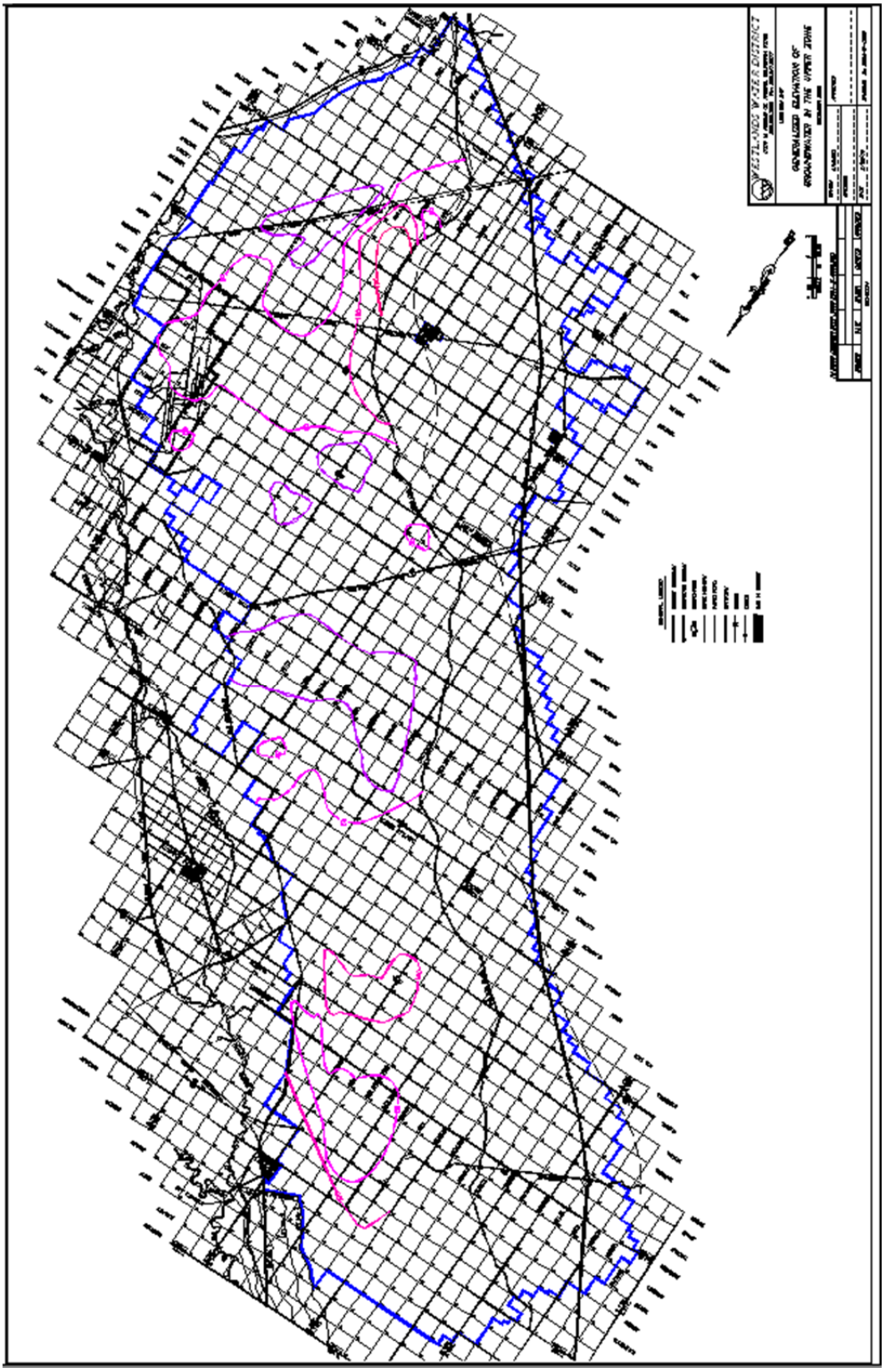

D 27 Unconfined aquifer groundwater contour map, December 2003.

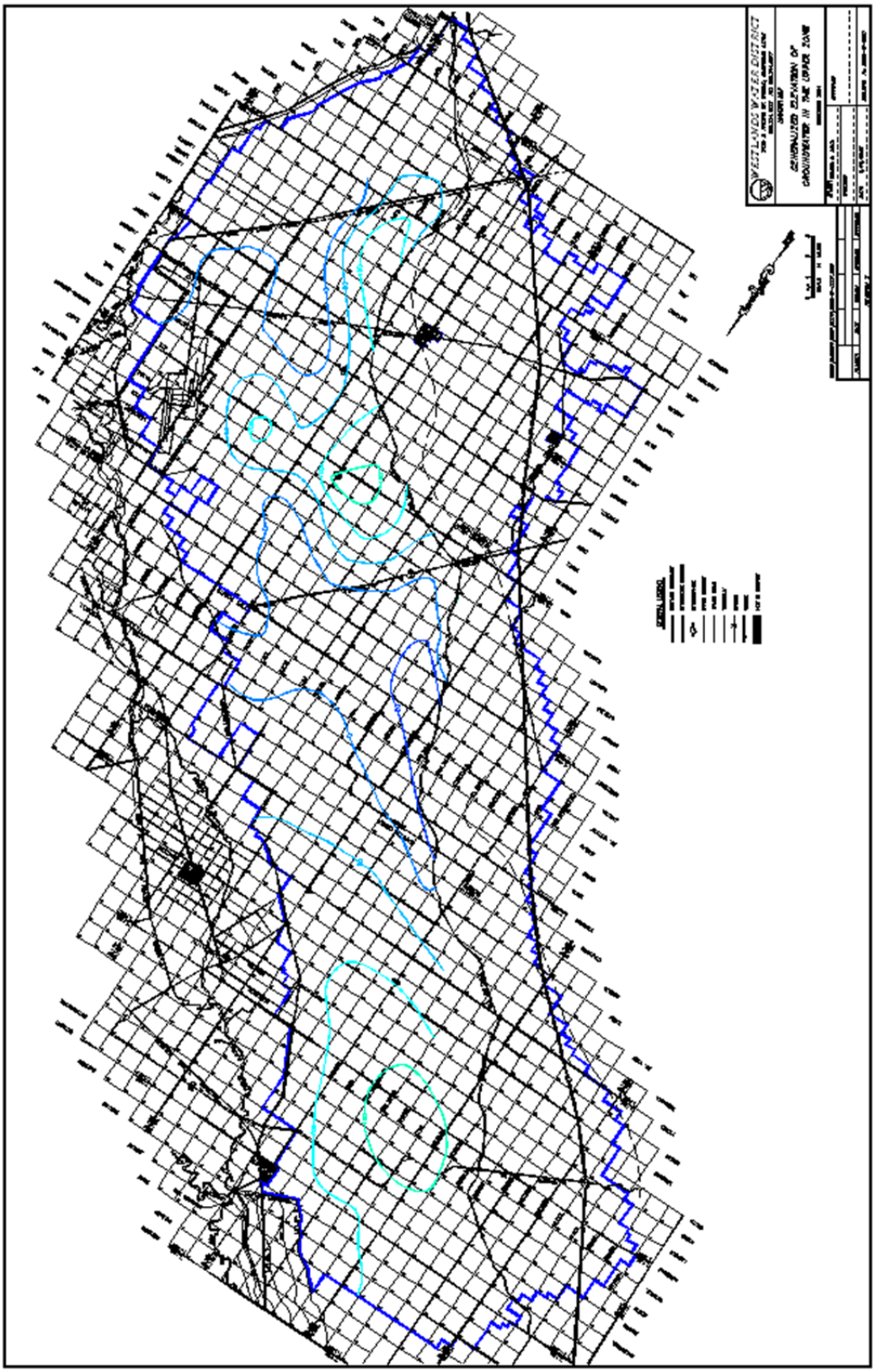

D 28 Unconfined aquifer groundwater contour map, December 2004.

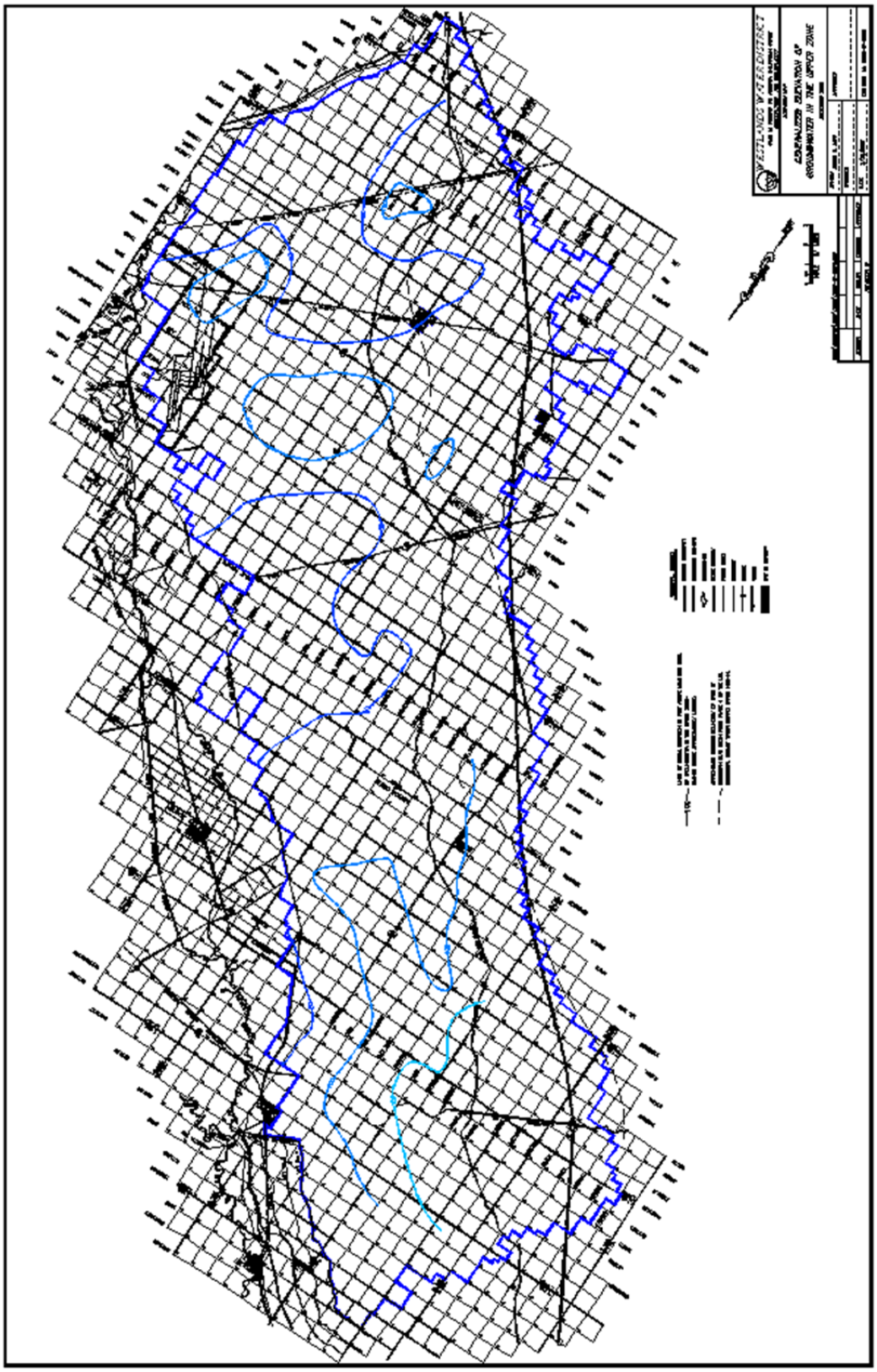

D 29 Unconfined aquifer groundwater contour map, December 2005.

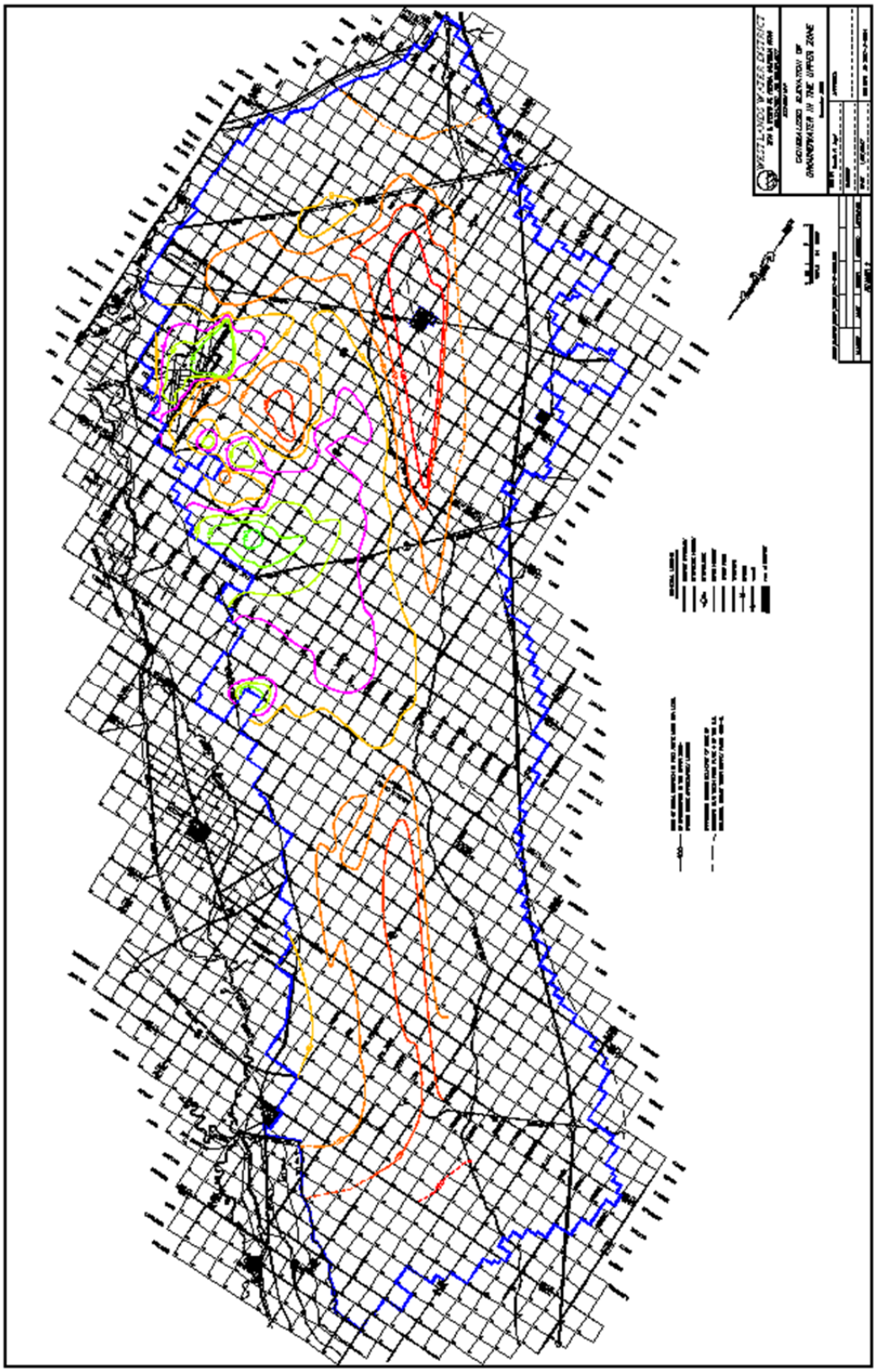

D 30 Unconfined aquifer groundwater contour map, December 2006.

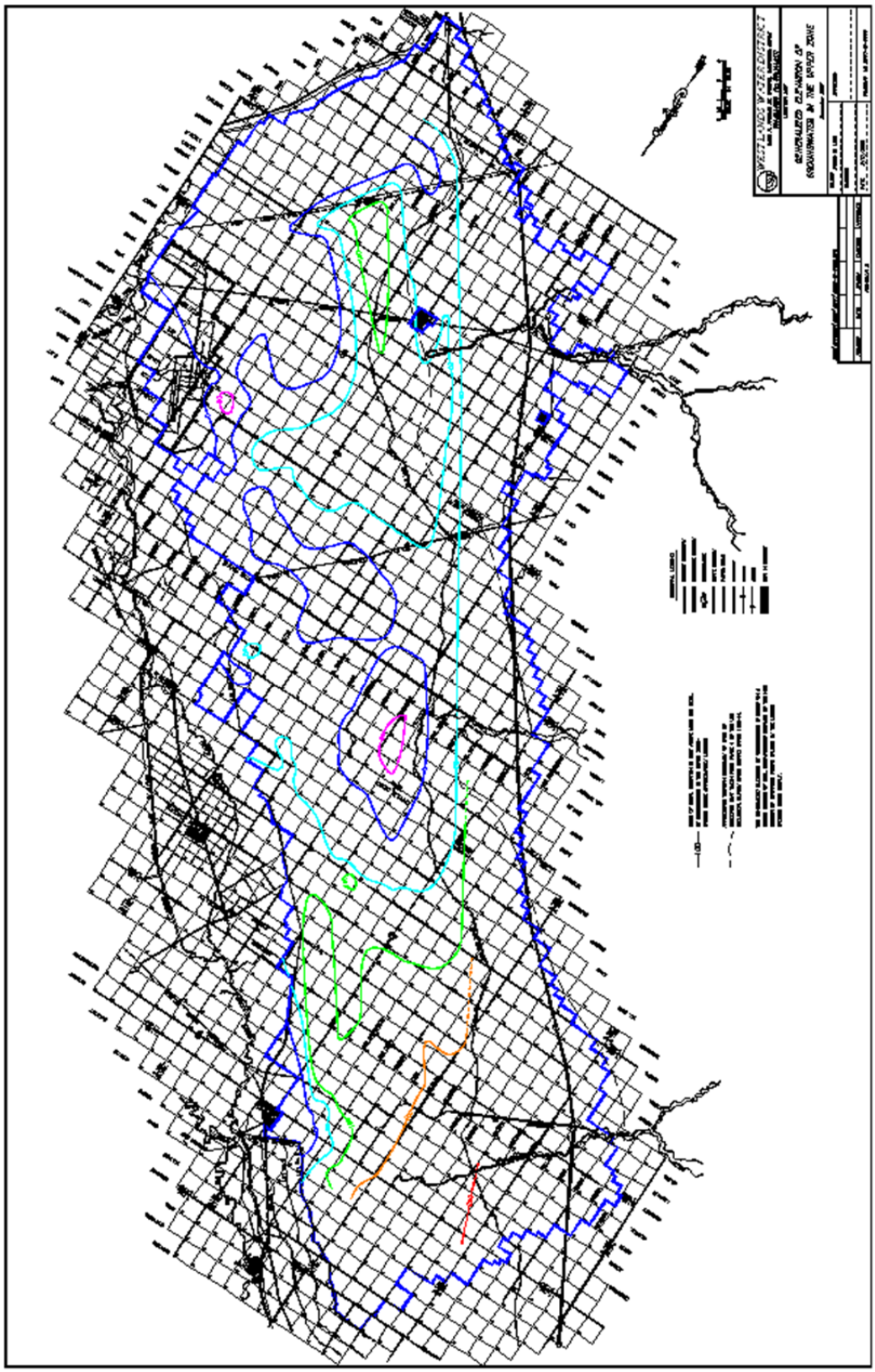

D 31 Unconfined aquifer groundwater contour map, December 2007.

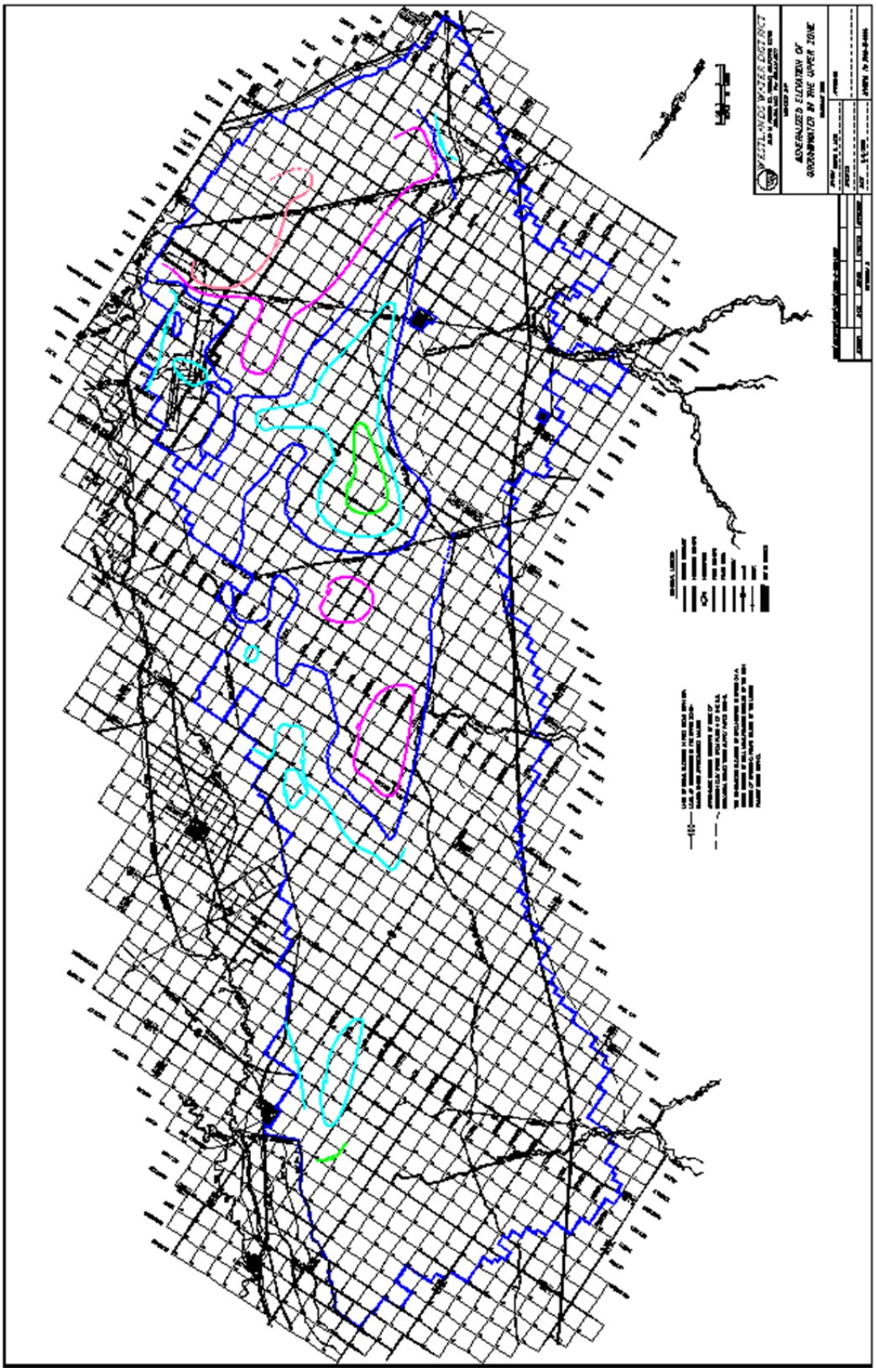

D 32 Unconfined aquifer groundwater contour map, December 2008.

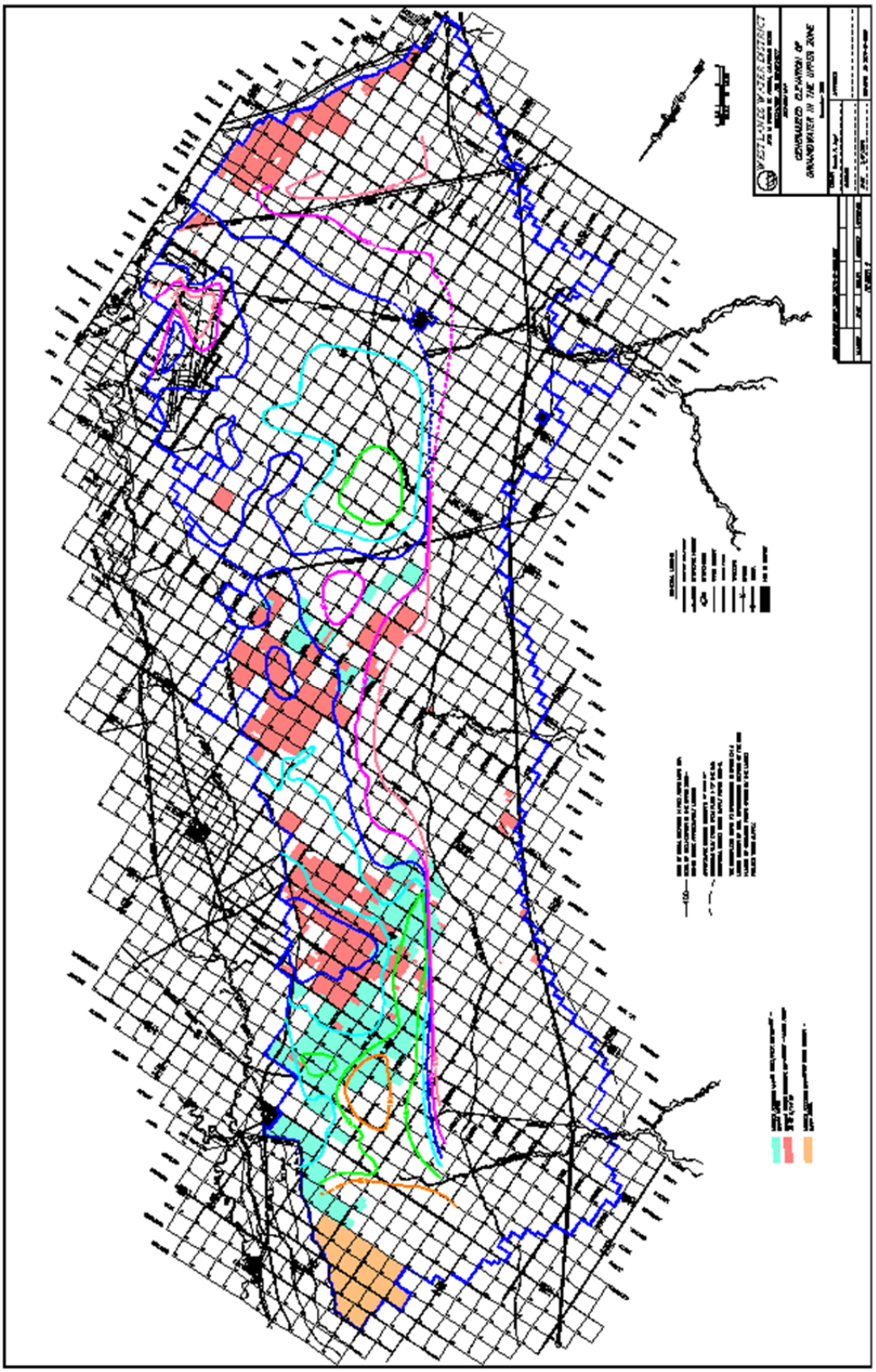

D 33 Unconfined aquifer groundwater contour map, December 2009.

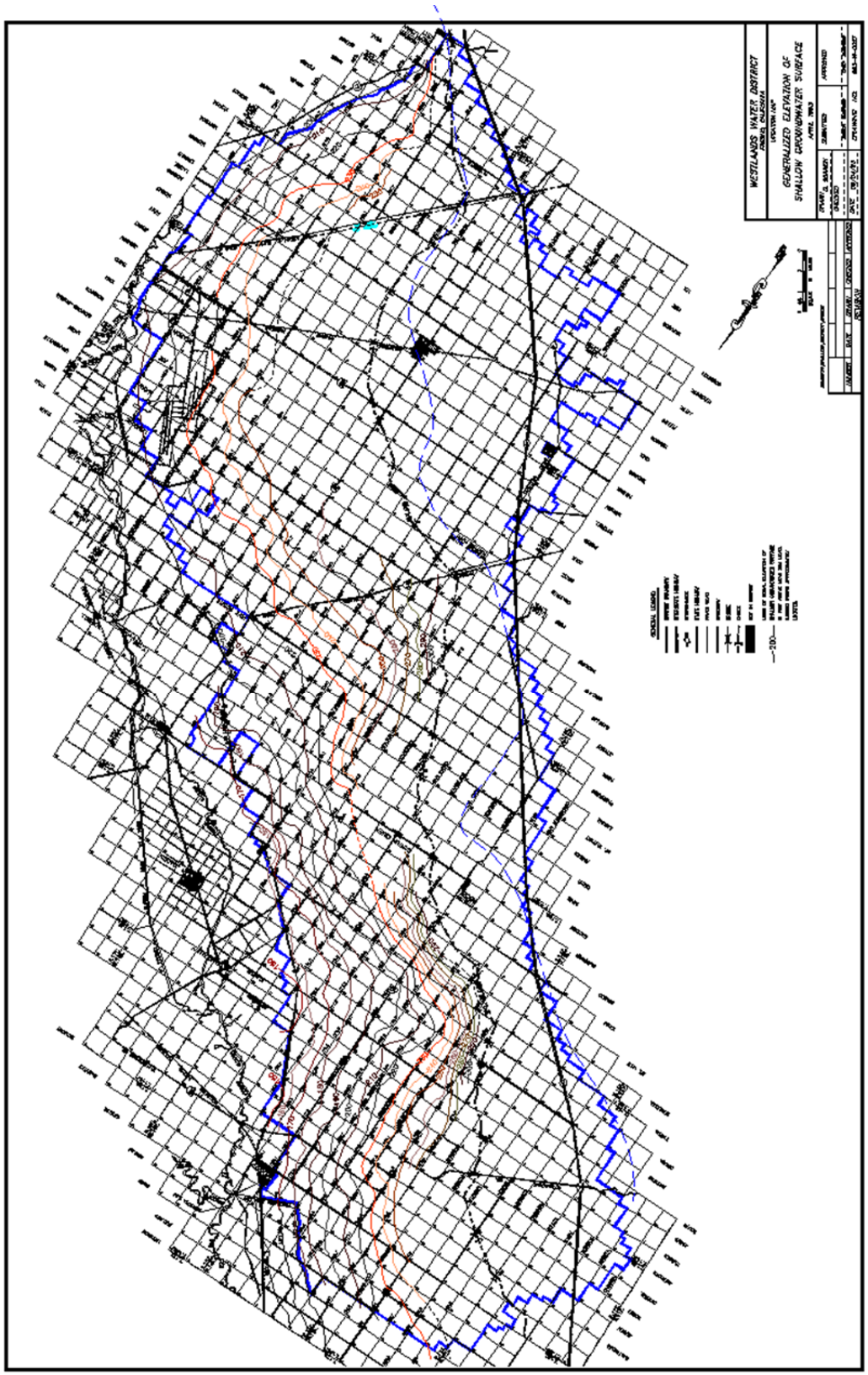

D 34 Shallow aquifer groundwater contour map, April 1993.

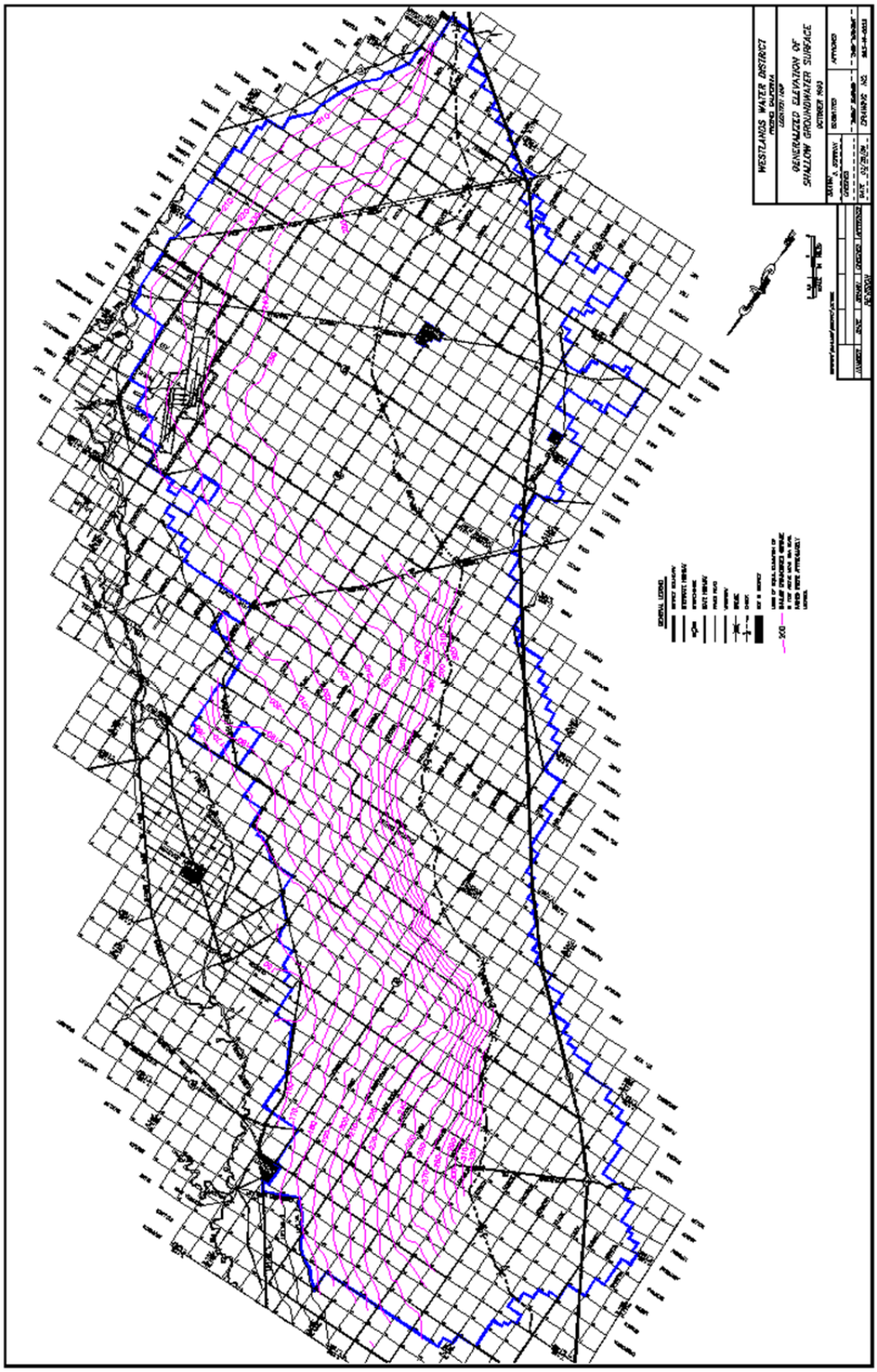

D 35 Shallow aquifer groundwater contour map, October 1993.

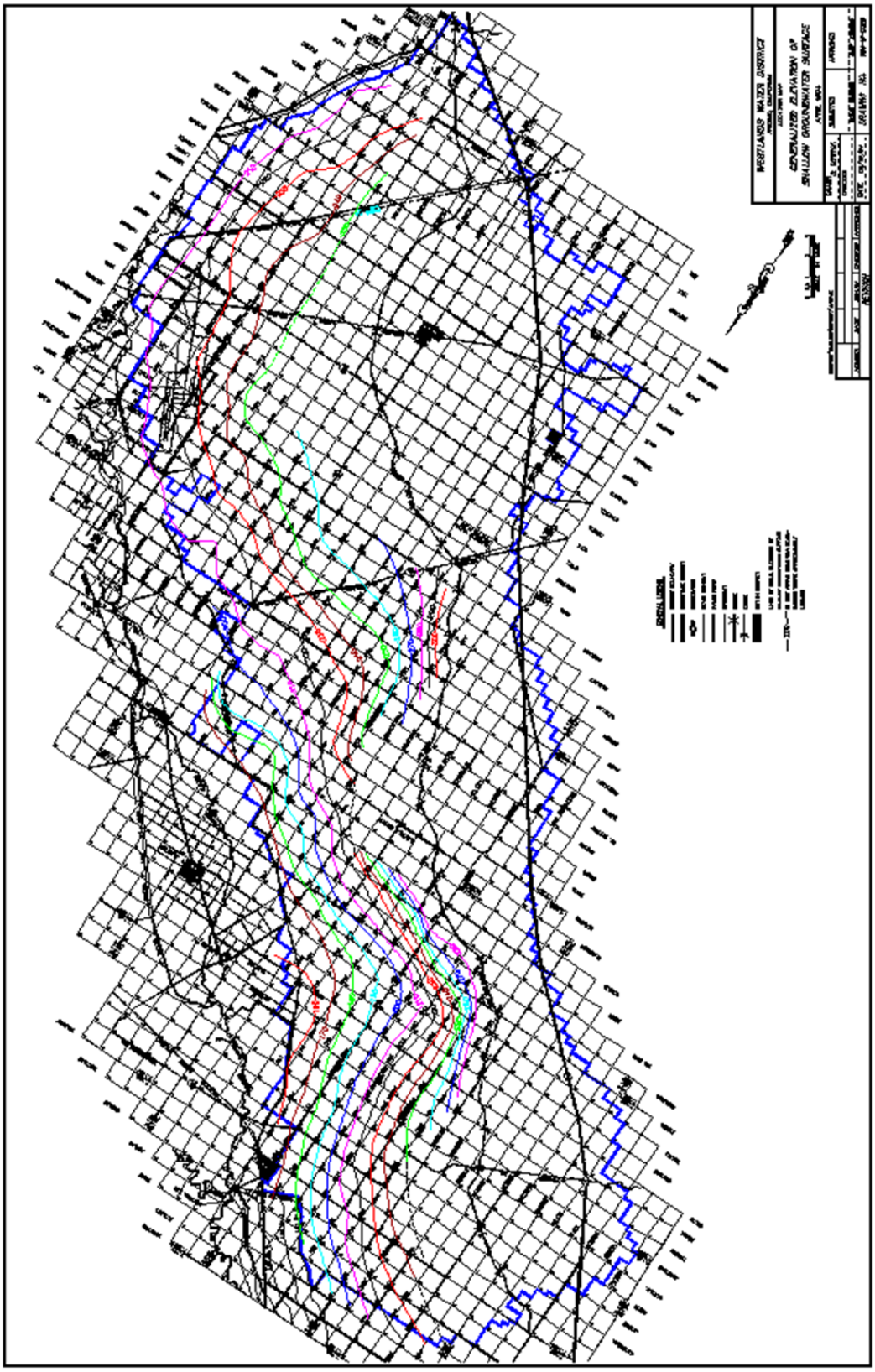

D 36 Shallow aquifer groundwater contour map, April 1994.

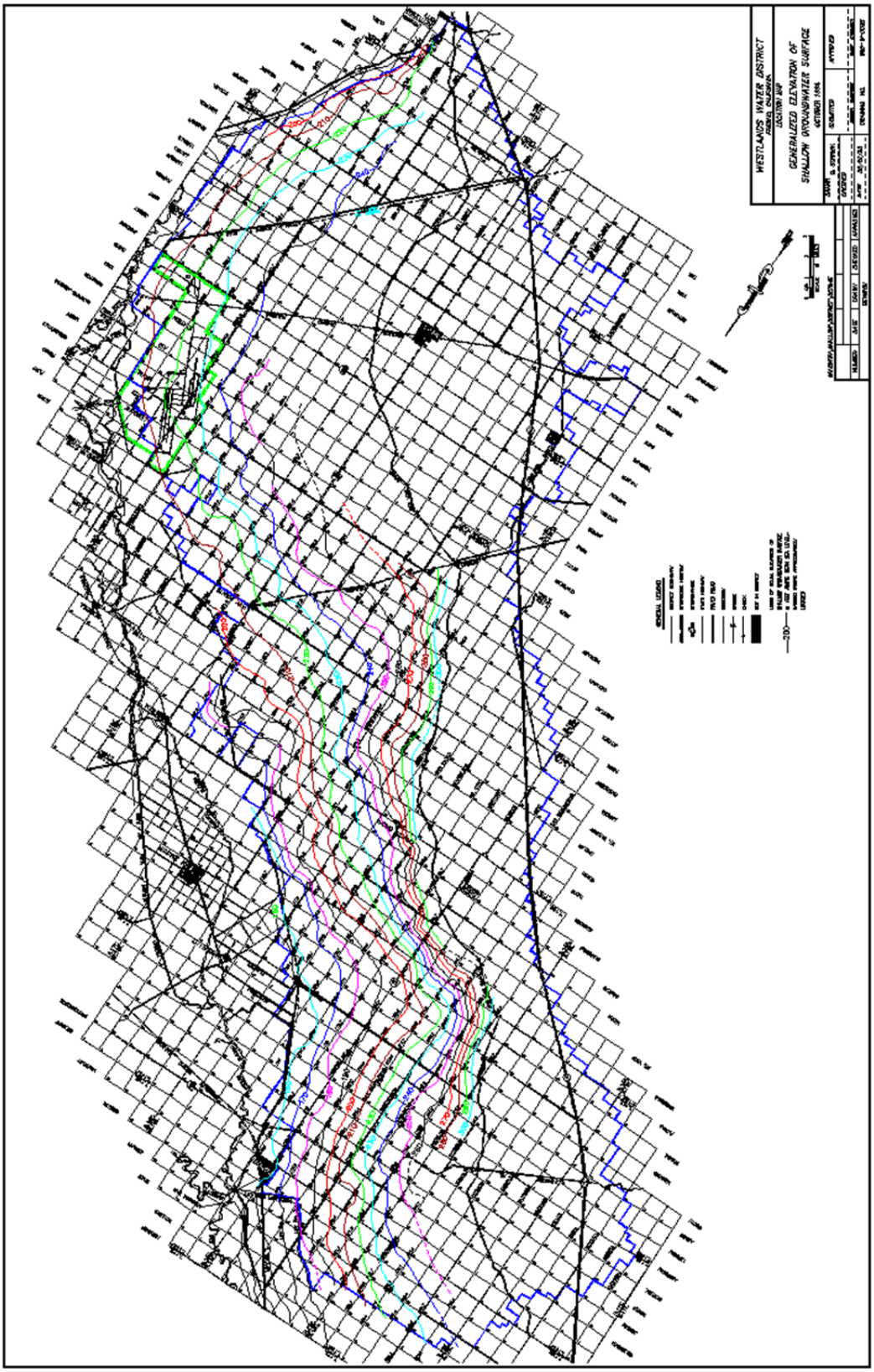

D 37 Shallow aquifer groundwater contour map, October 1994.

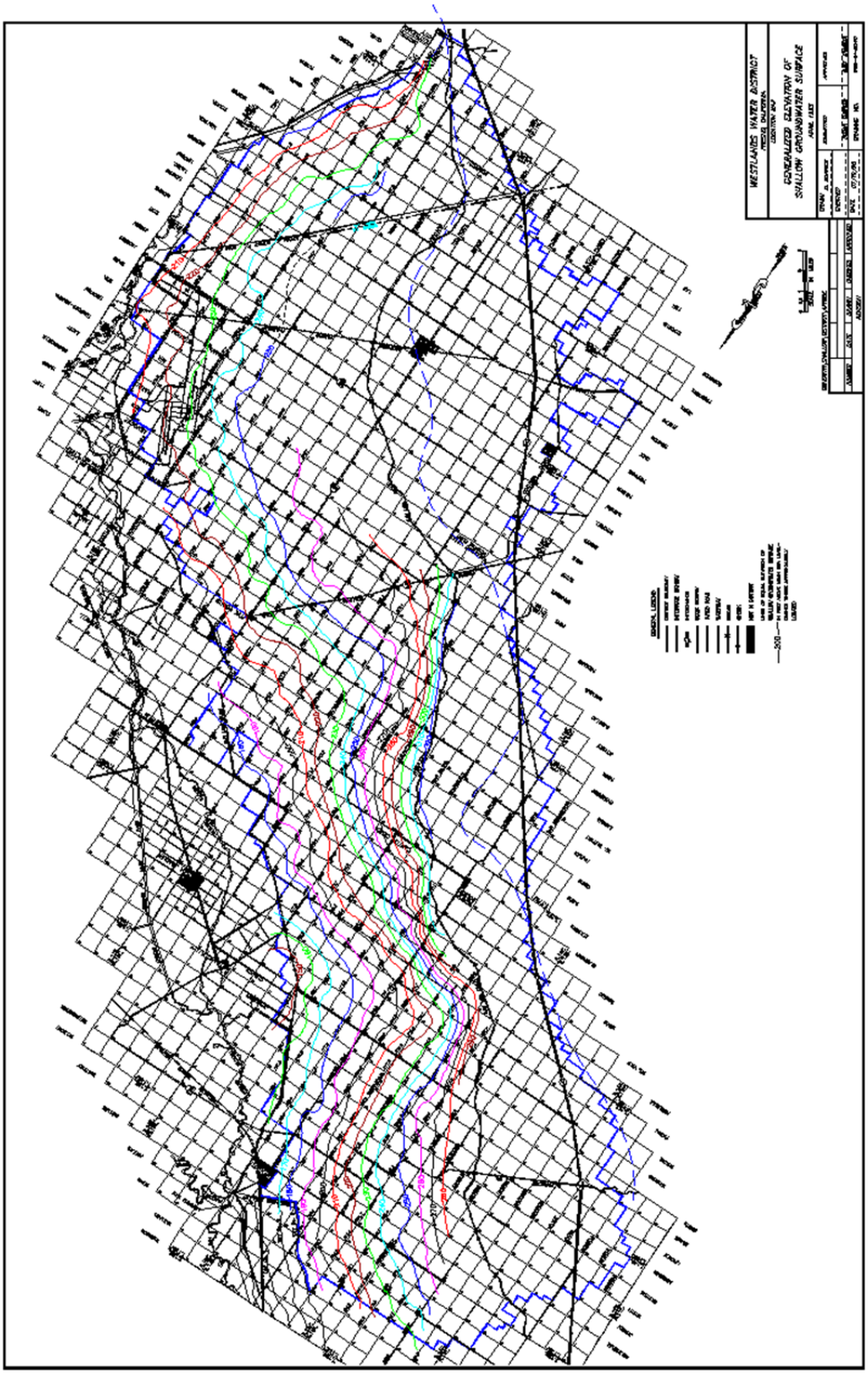

D 38 Shallow aquifer groundwater contour map, April 1995.

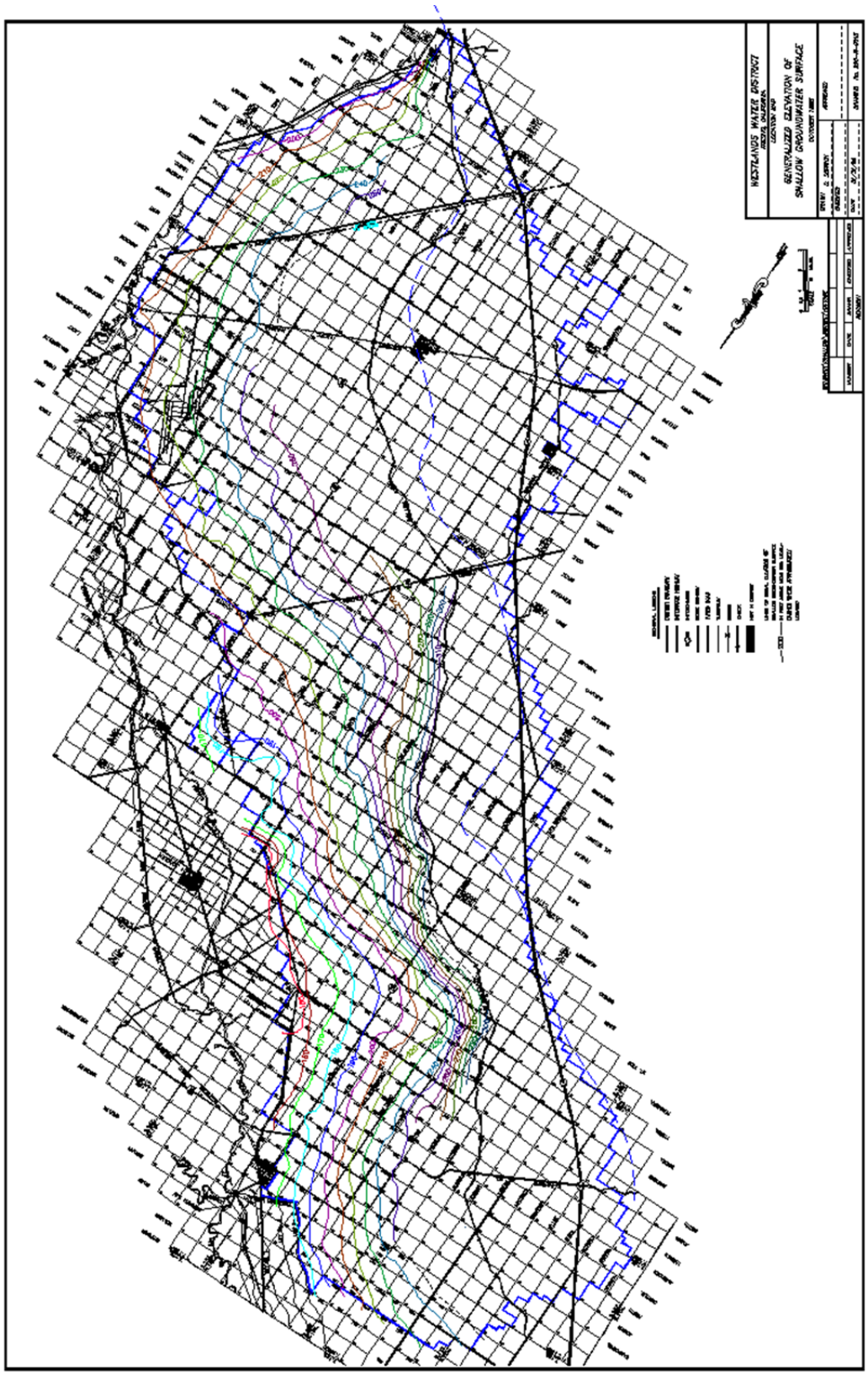

D 39 Shallow aquifer groundwater contour map, October 1995.

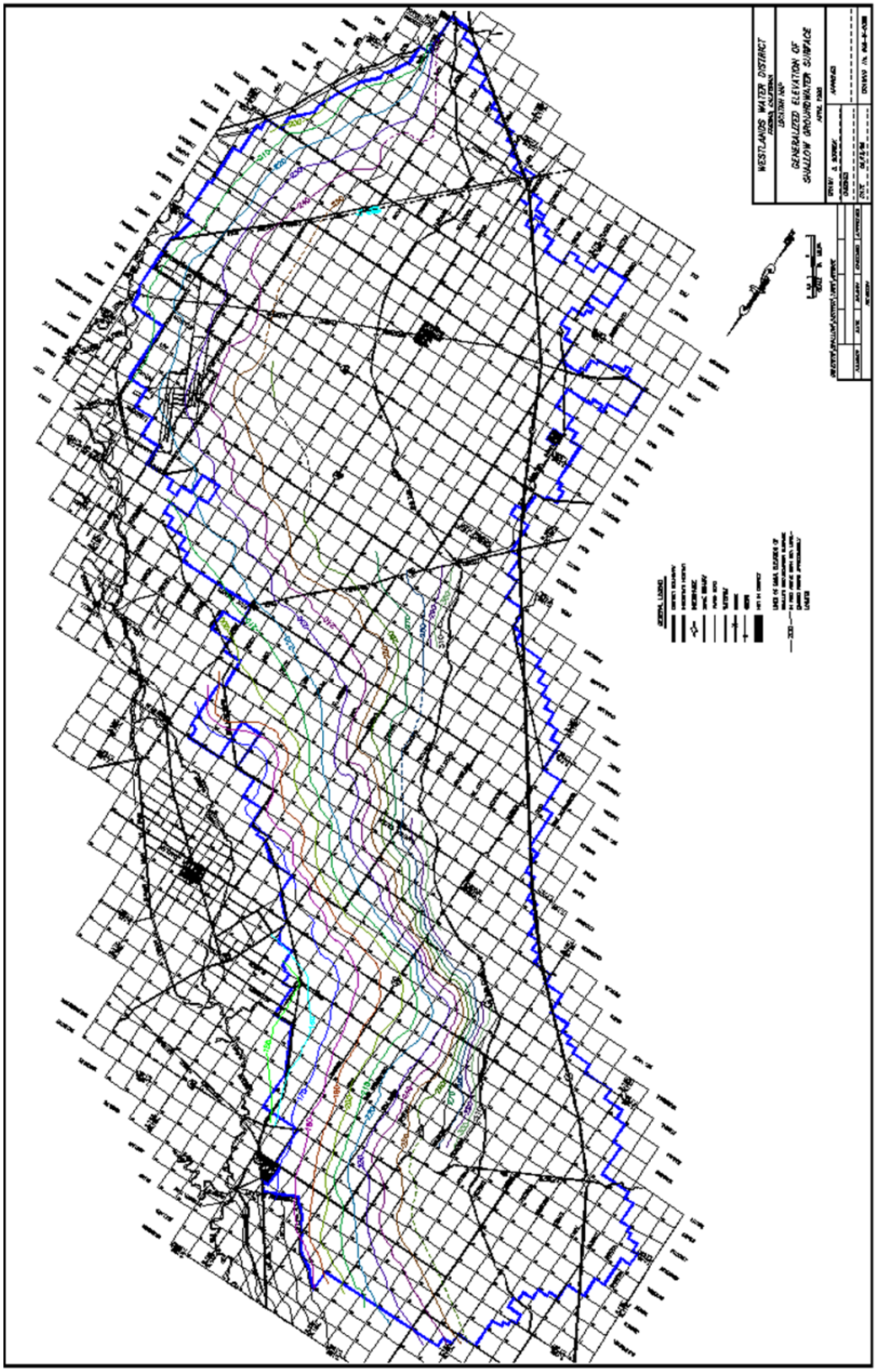

D 40 Shallow aquifer groundwater contour map, April 1996.

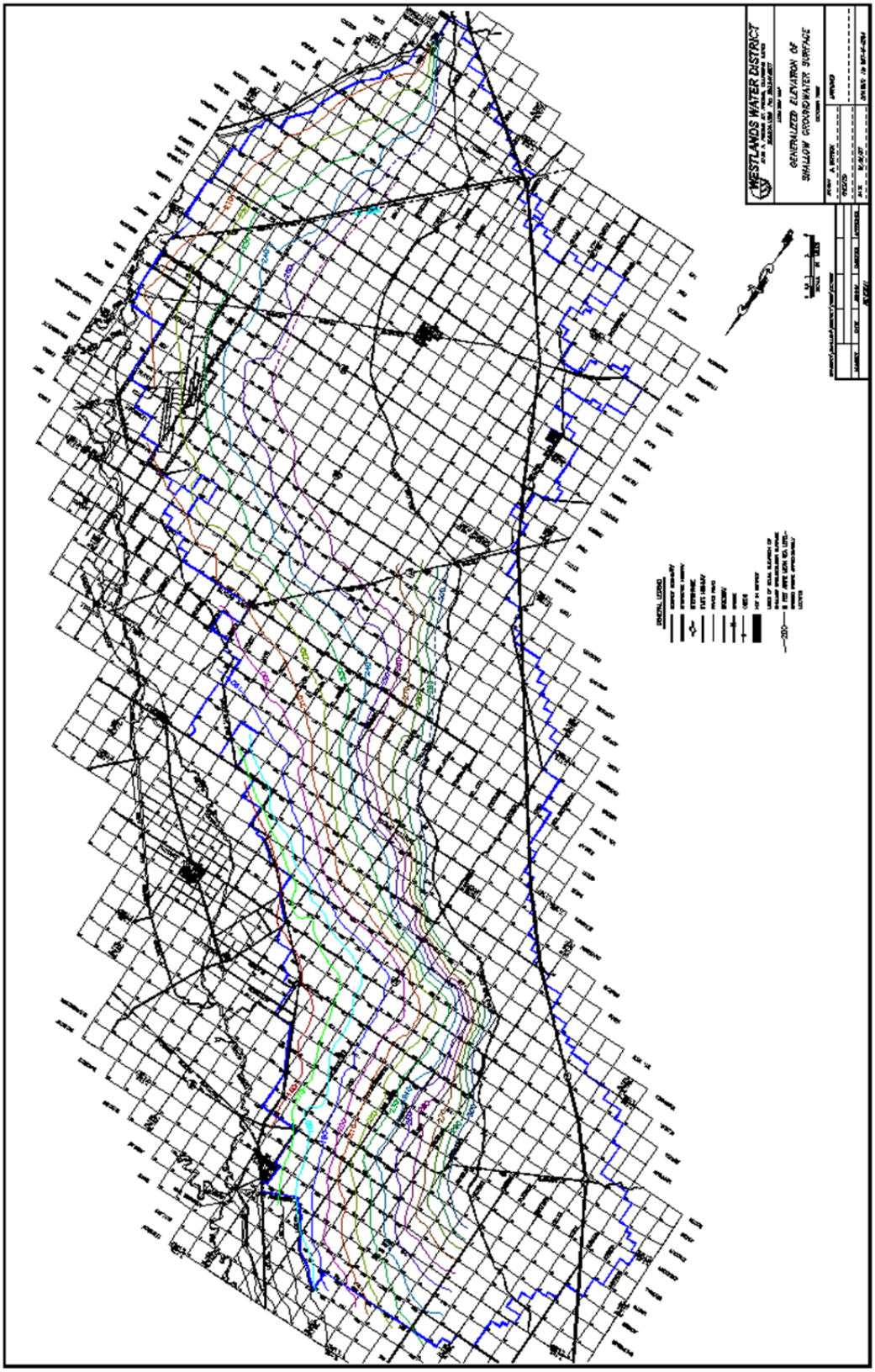

D 41 Shallow aquifer groundwater contour map, October 1996.

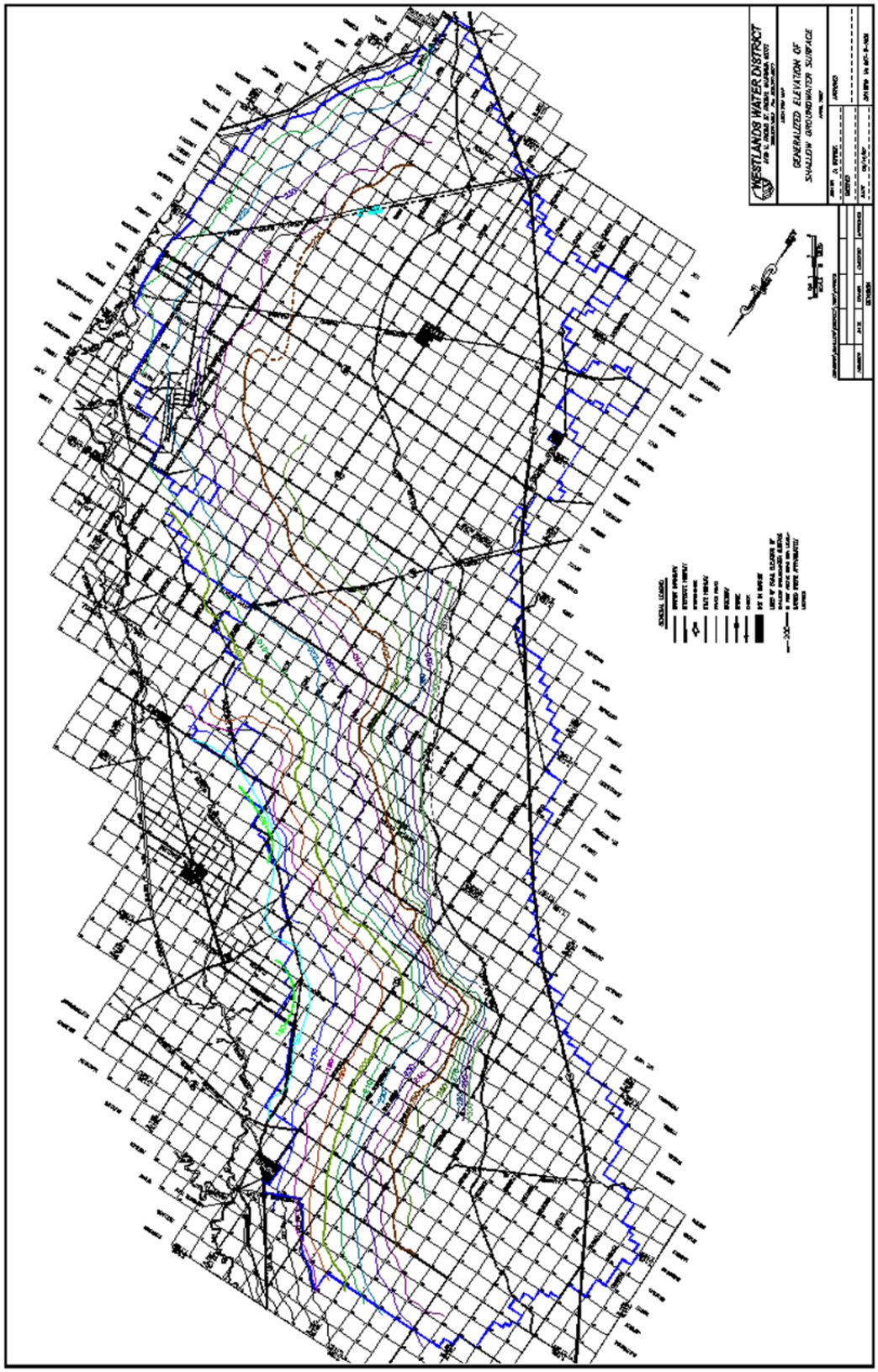

D 42 Shallow aquifer groundwater contour map, April 1997.

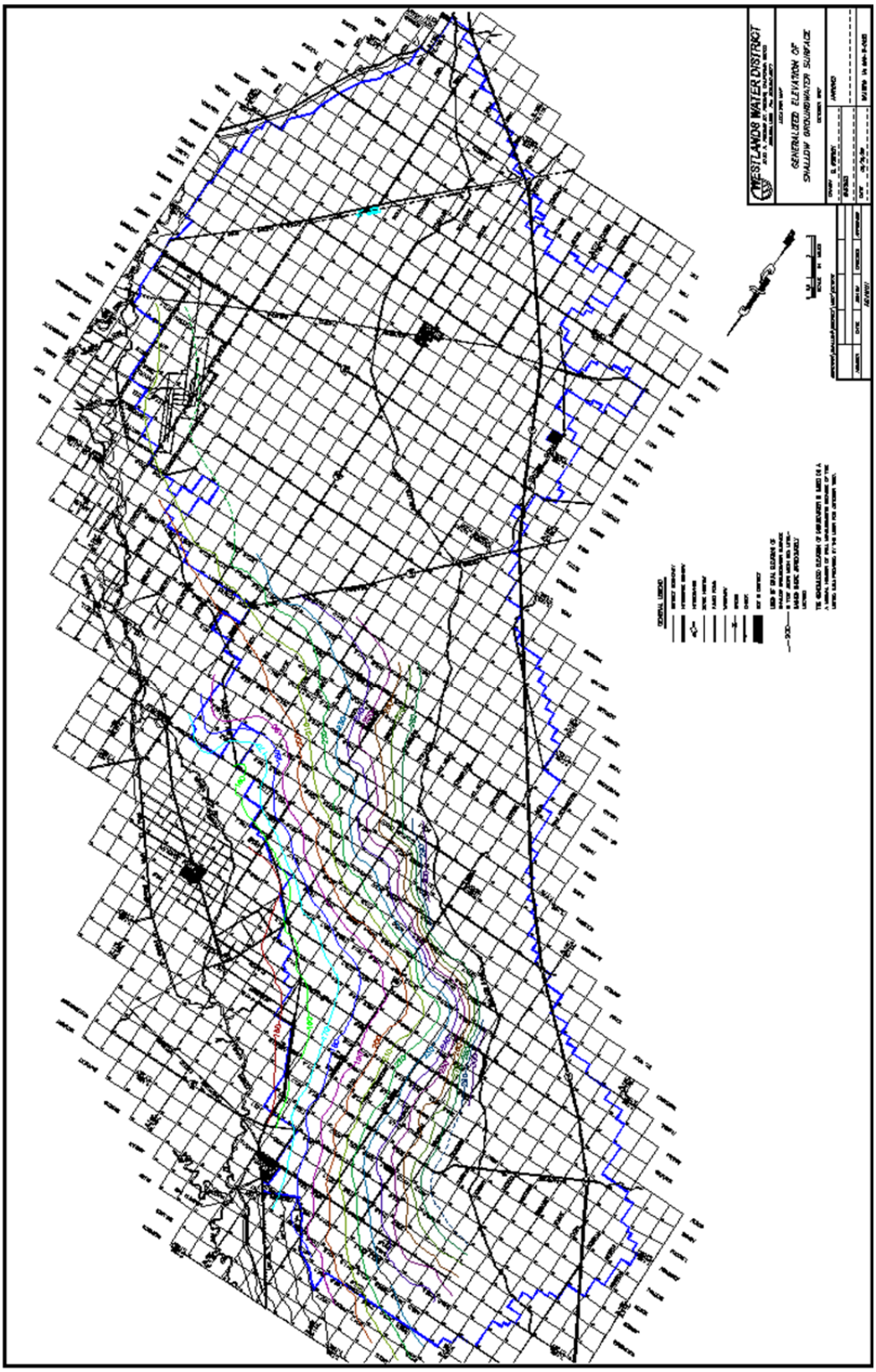

D 43 Shallow aquifer groundwater contour map, October 1997.

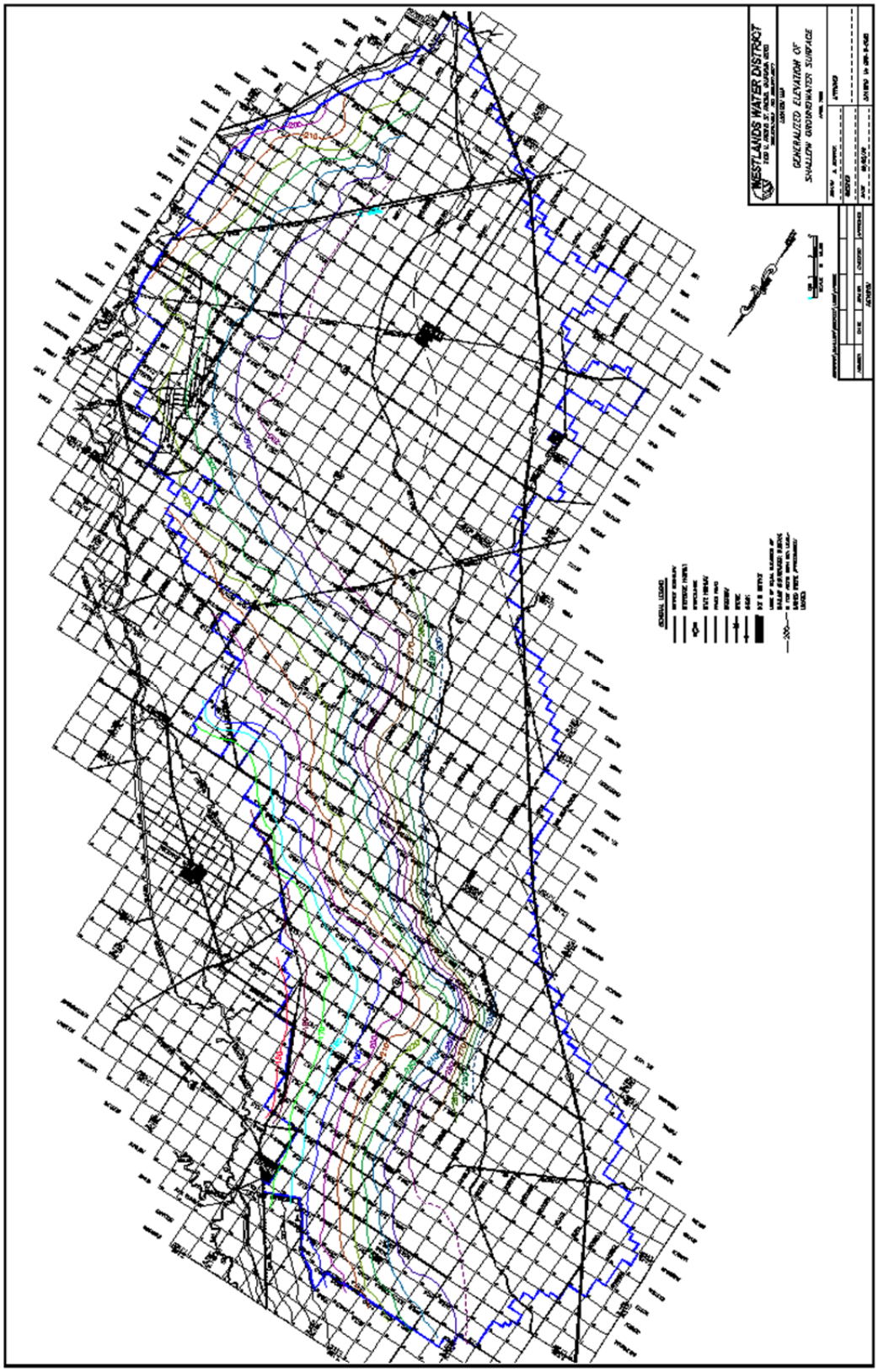

D 44 Shallow aquifer groundwater contour map, April 1998.

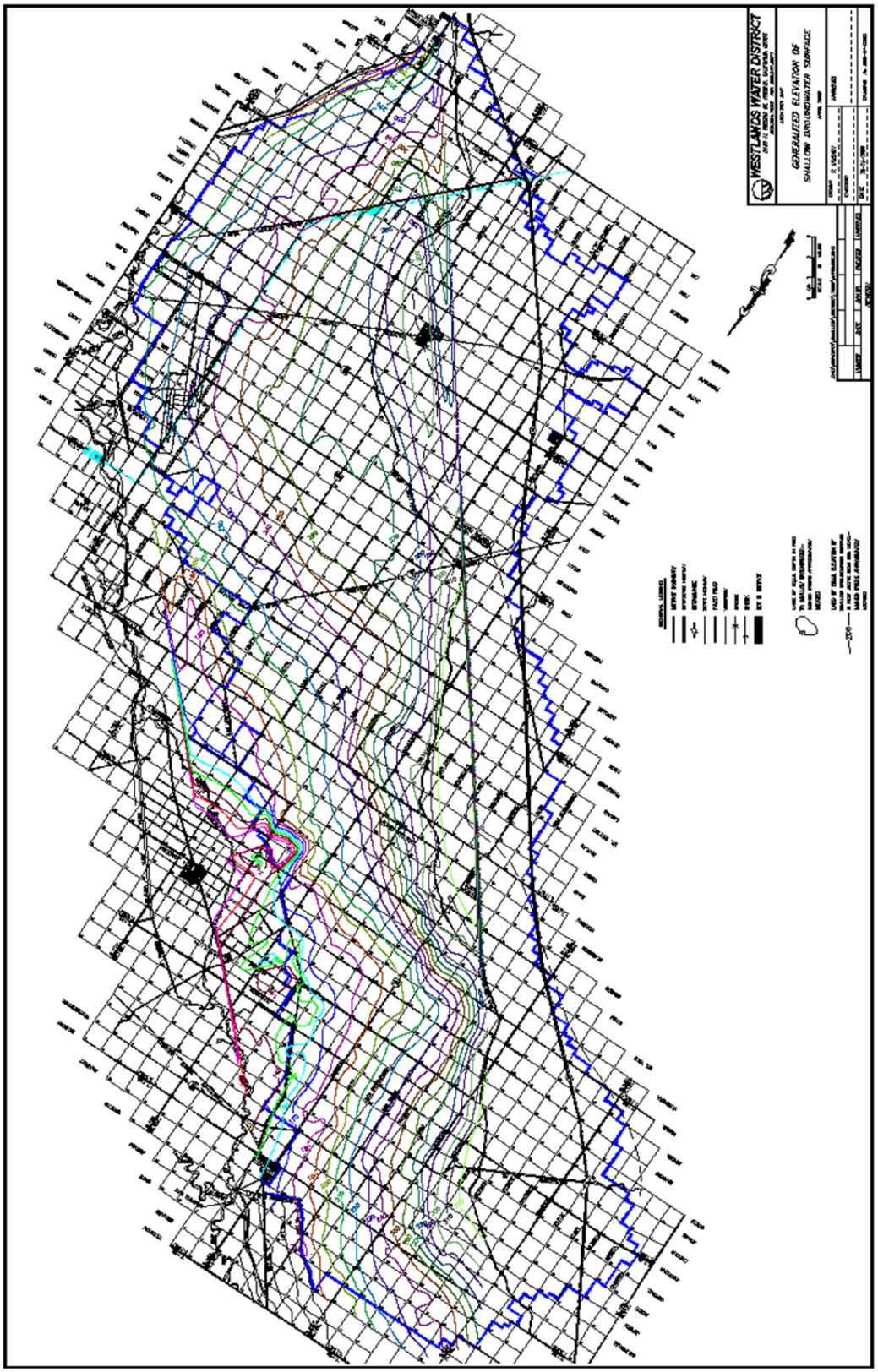

D 45 Shallow aquifer groundwater contour map, April 1999.

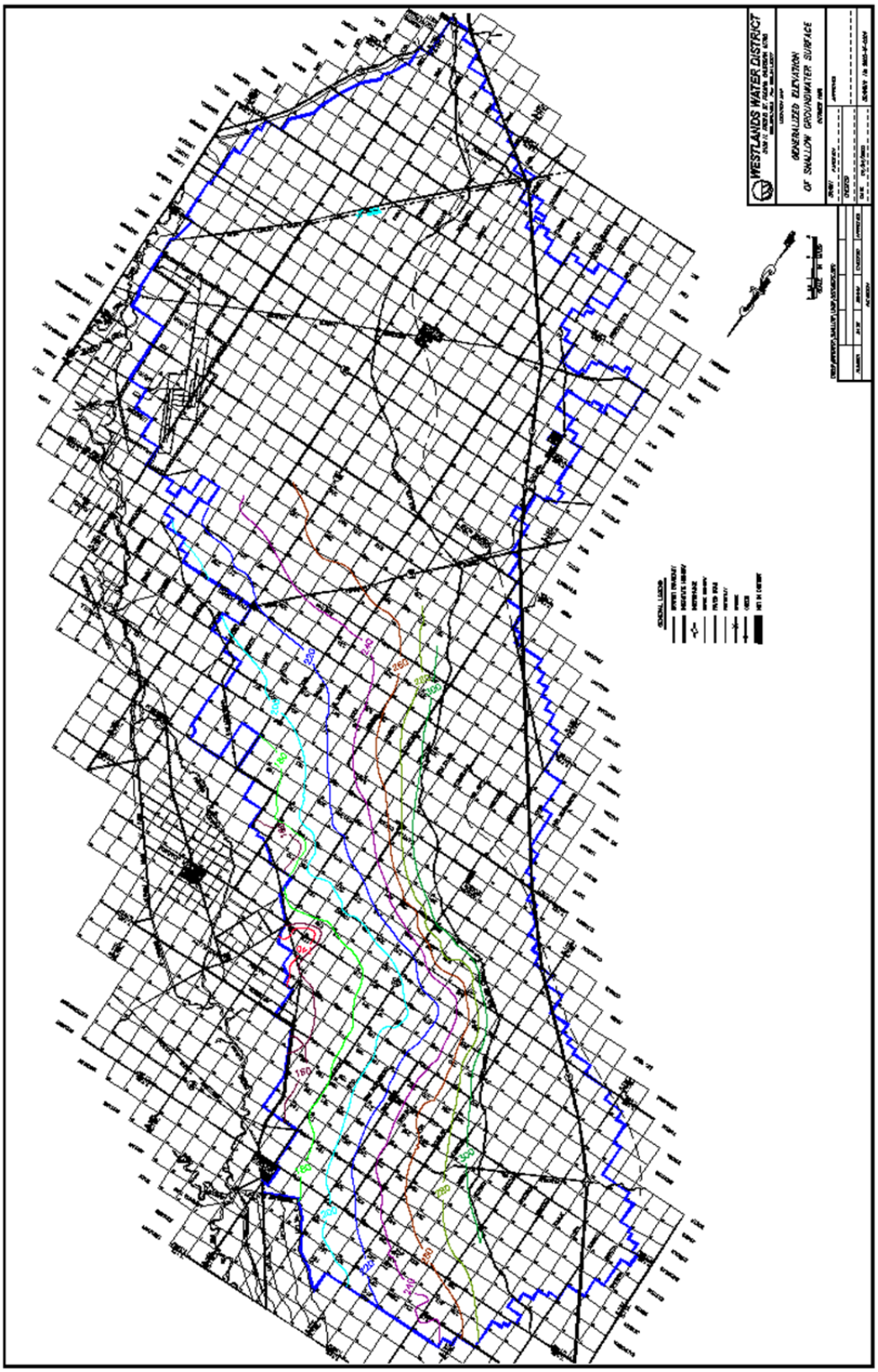

D 46 Shallow aquifer groundwater contour map, October 1999.

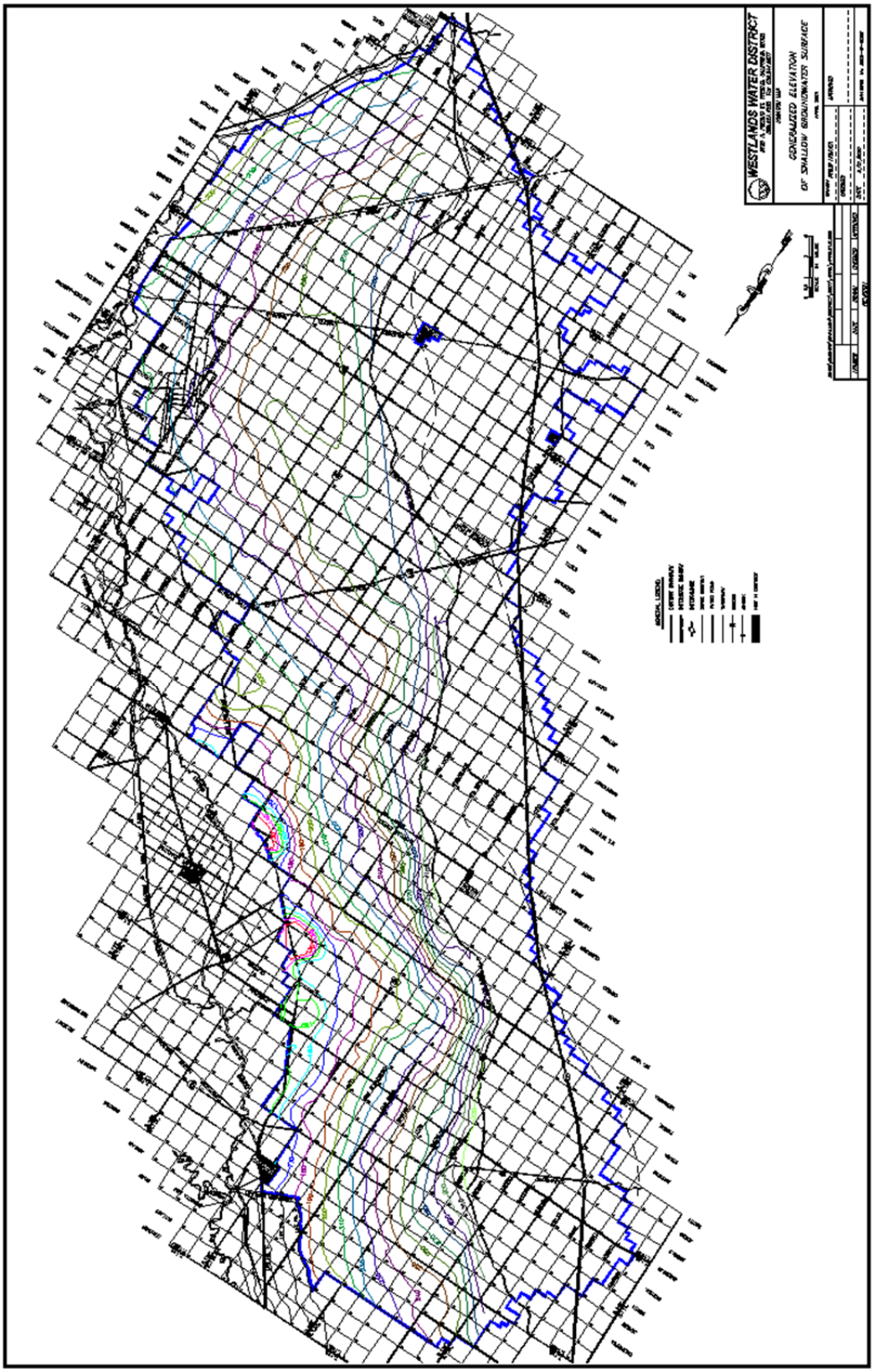

D 47 Shallow aquifer groundwater contour map, April 2001.

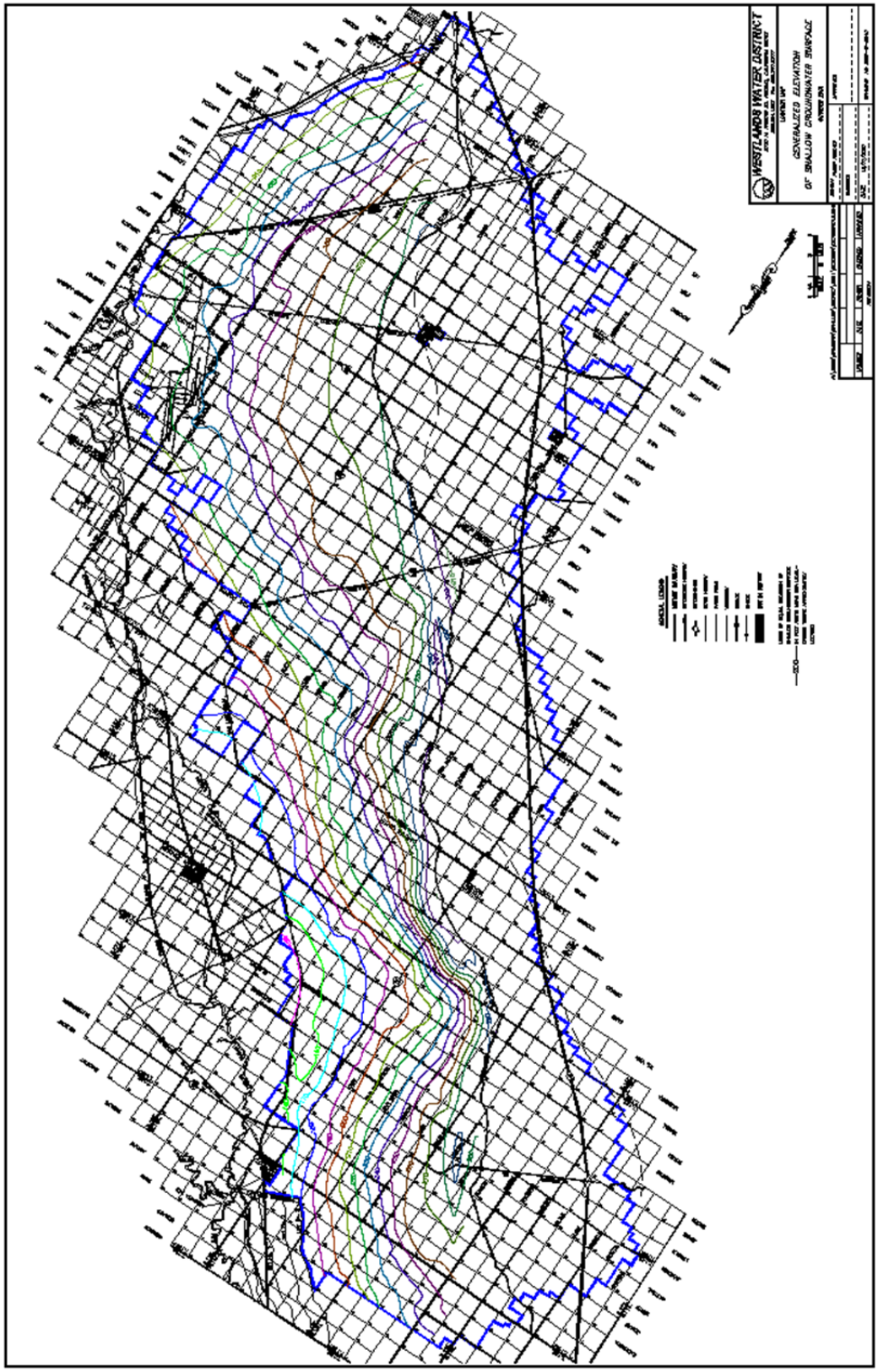

D 48 Shallow aquifer groundwater contour map, October 2001.

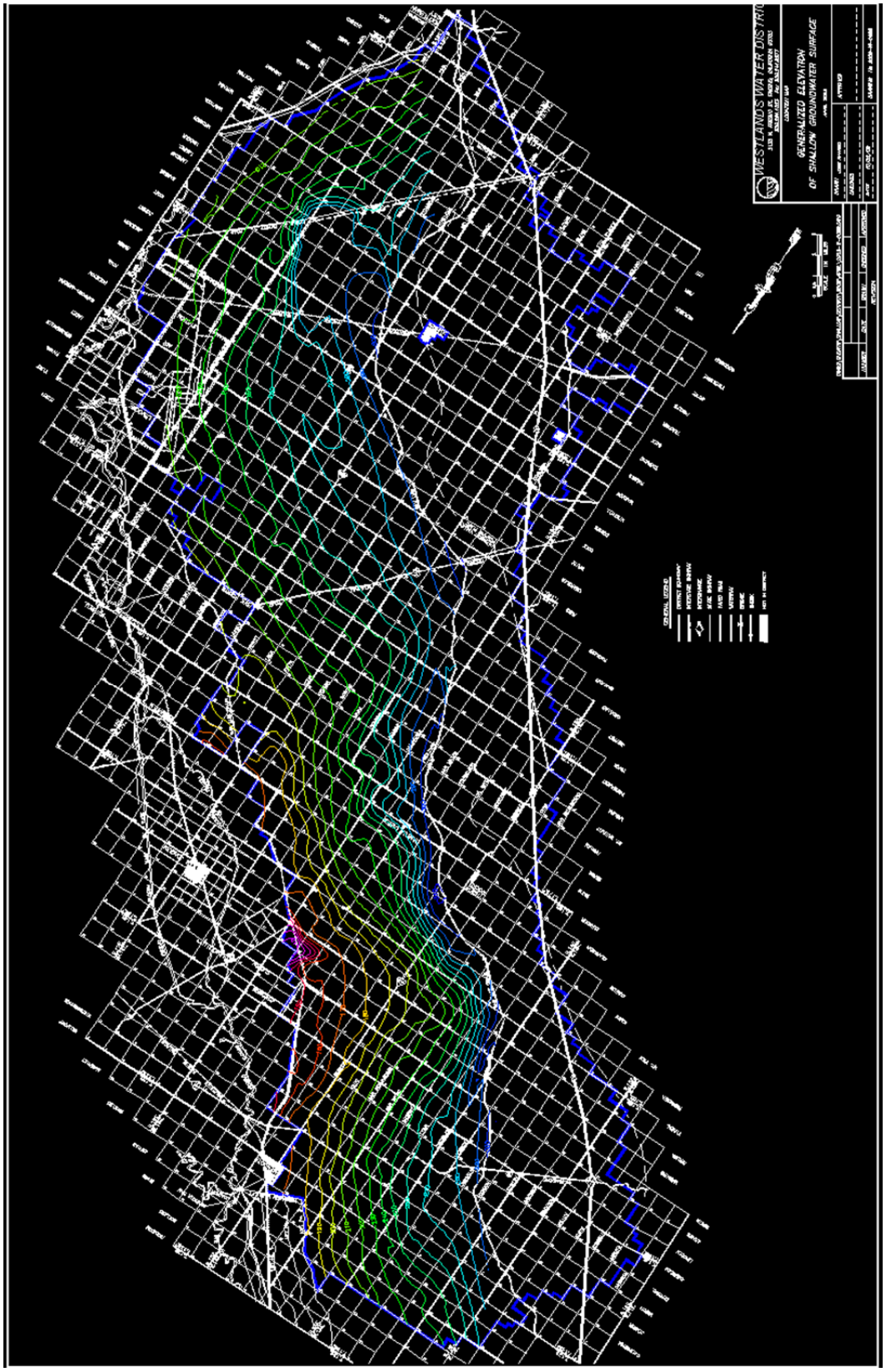

D 49 Shallow aquifer groundwater contour map, April 2002.

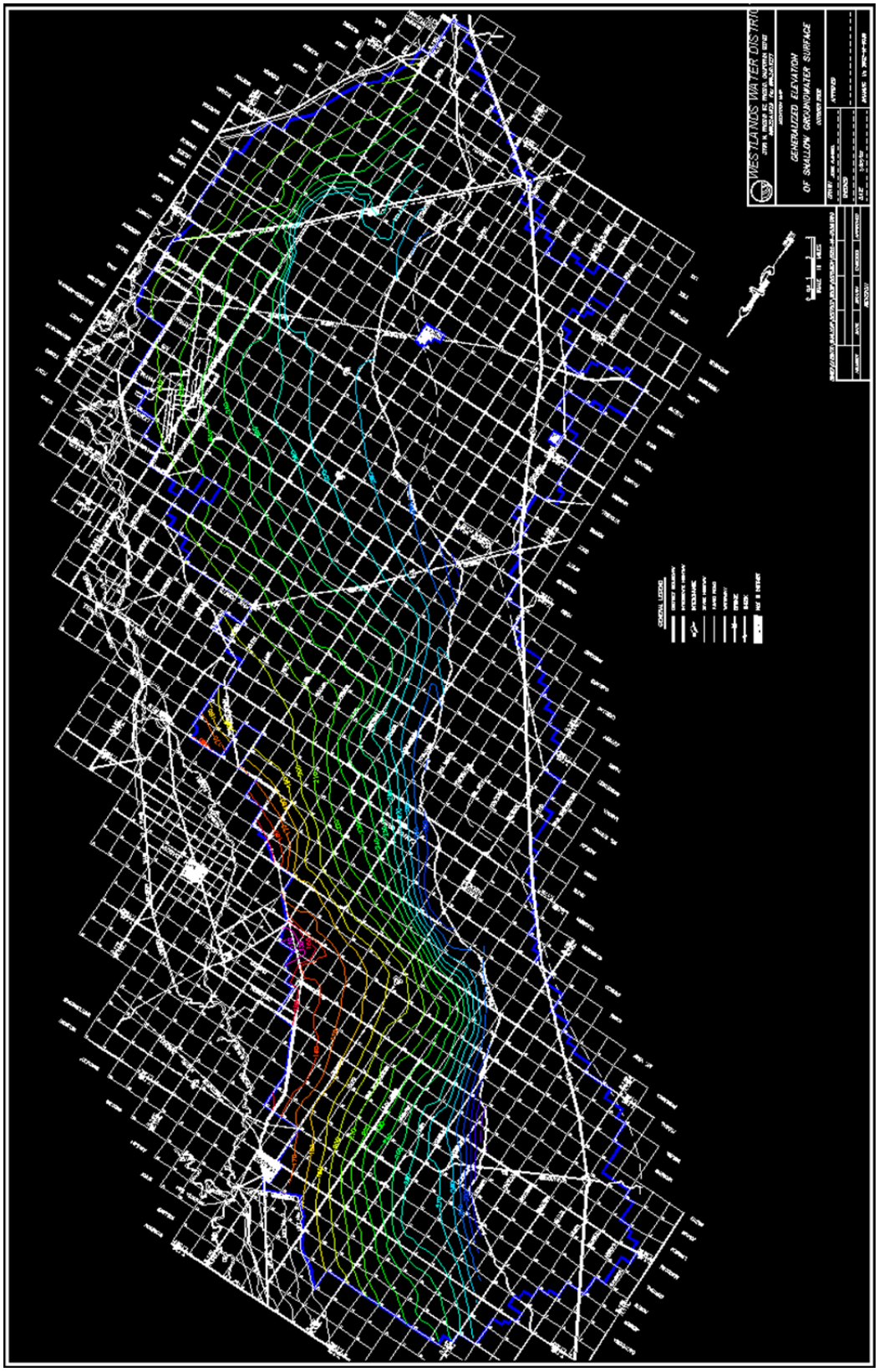

D 50 Shallow aquifer groundwater contour map, October 2002.

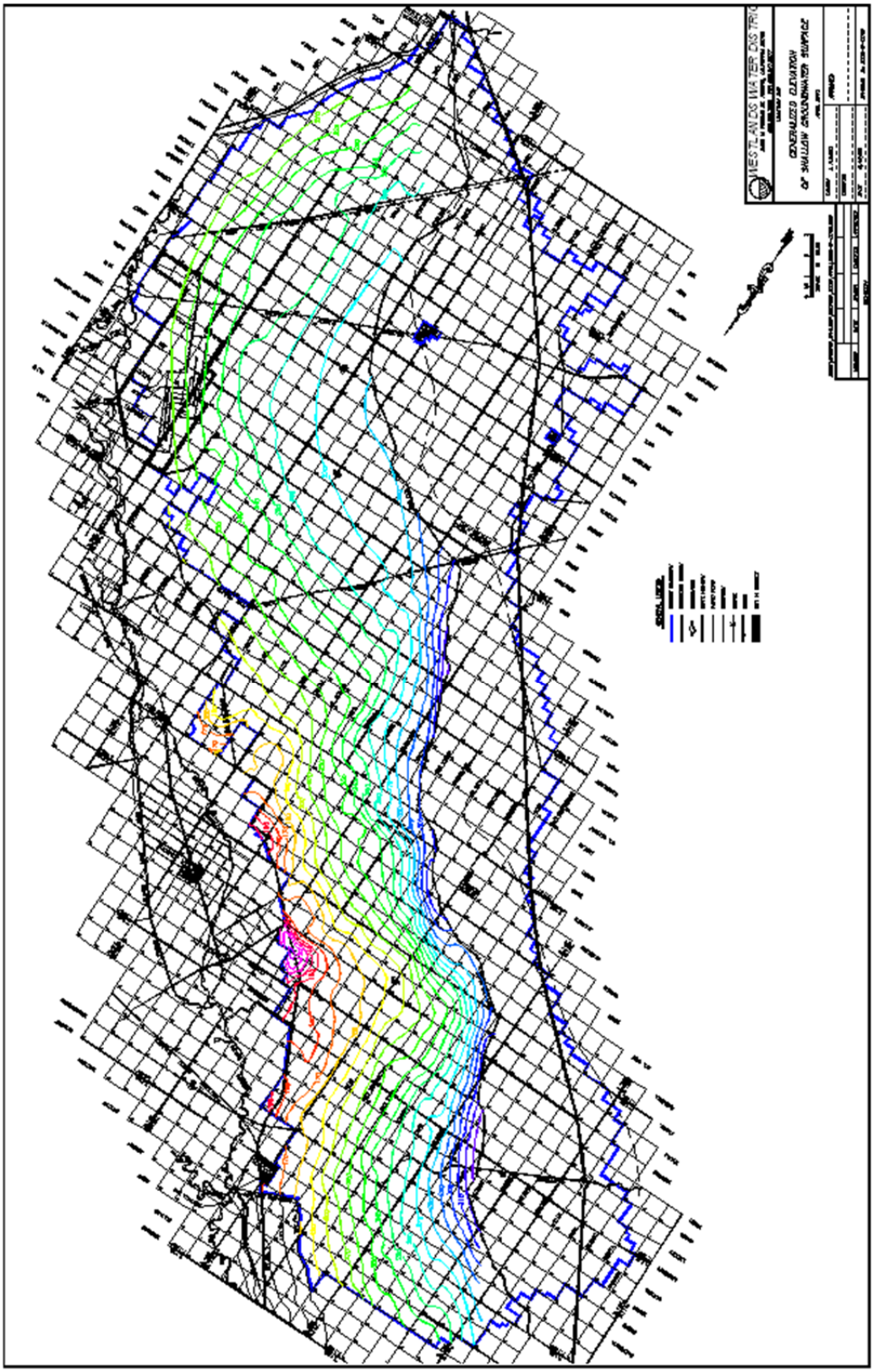

D 51 Shallow aquifer groundwater contour map, April 2003.

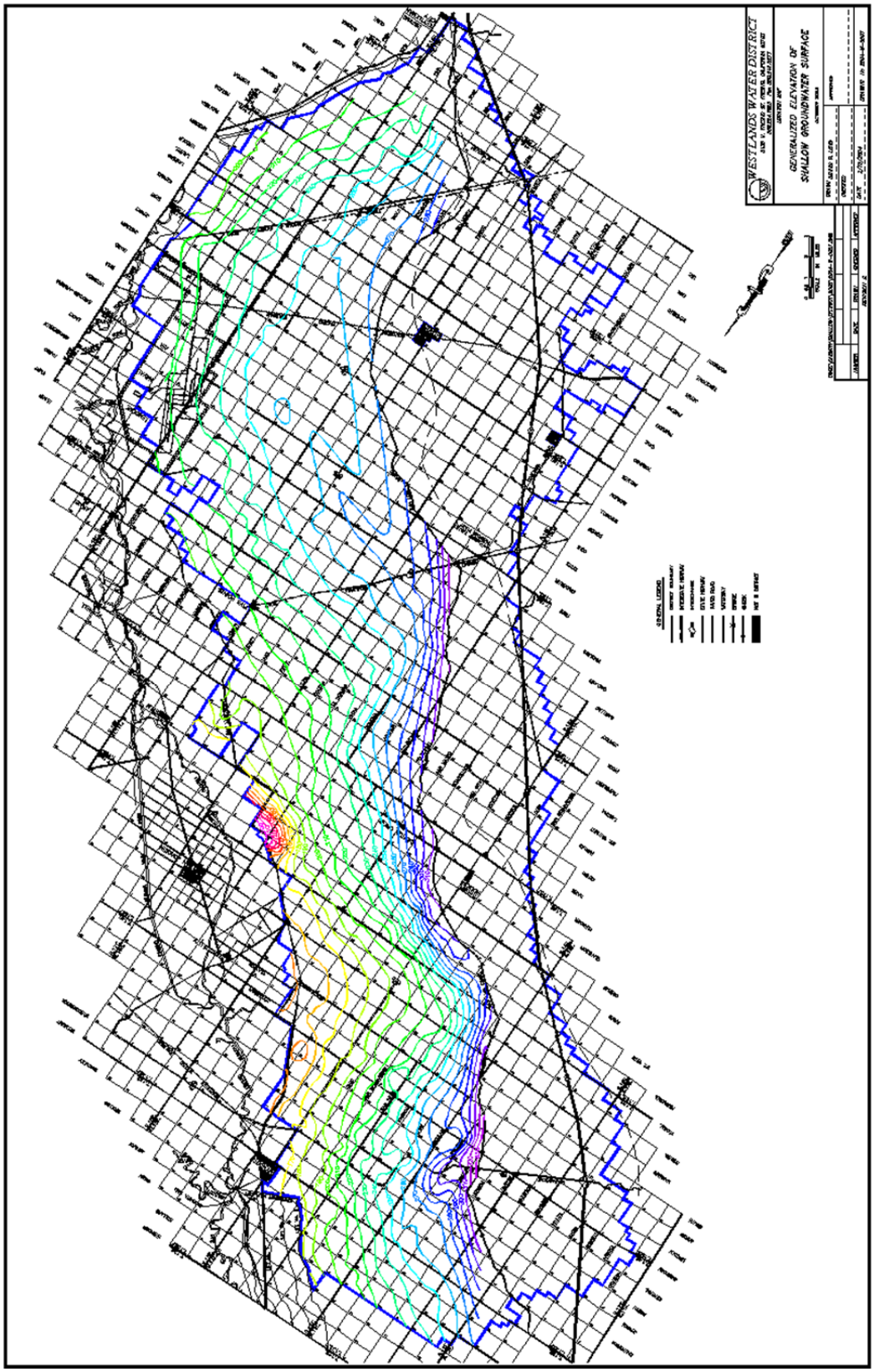

D 52 Shallow aquifer groundwater contour map, October 2003.

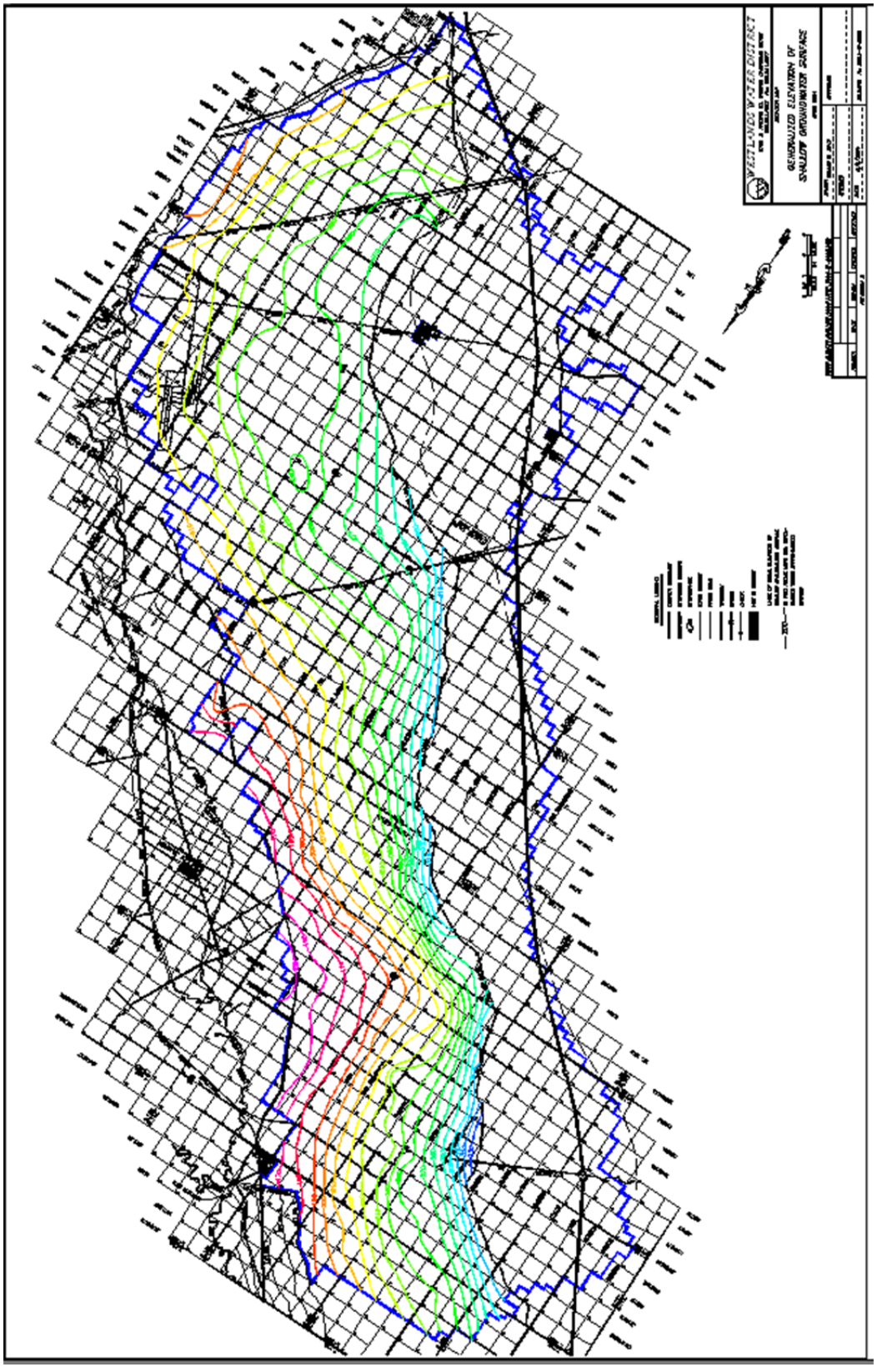

D 53 Shallow aquifer groundwater contour map, April 2004.

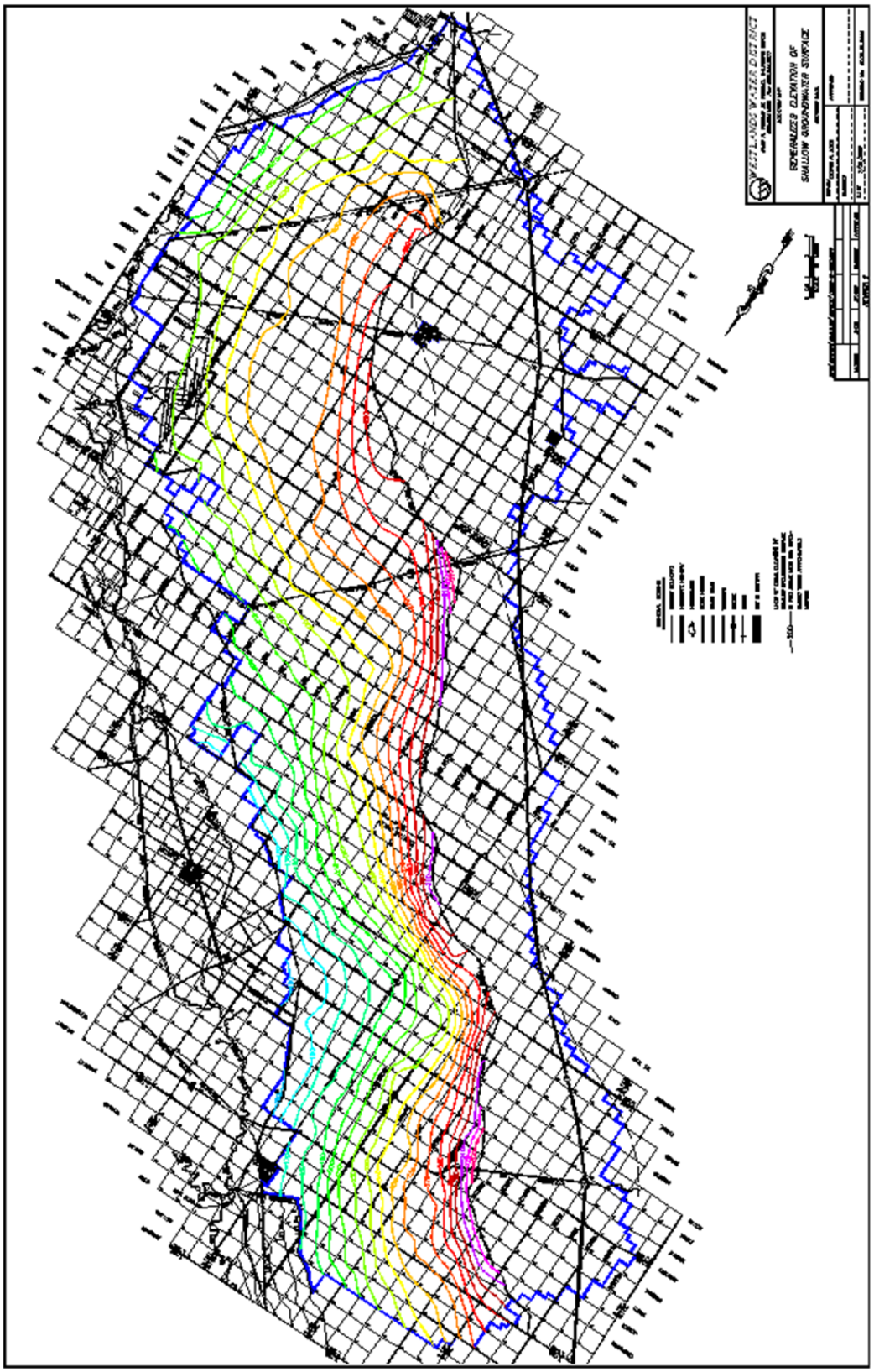

D 54 Shallow aquifer groundwater contour map, October 2004.

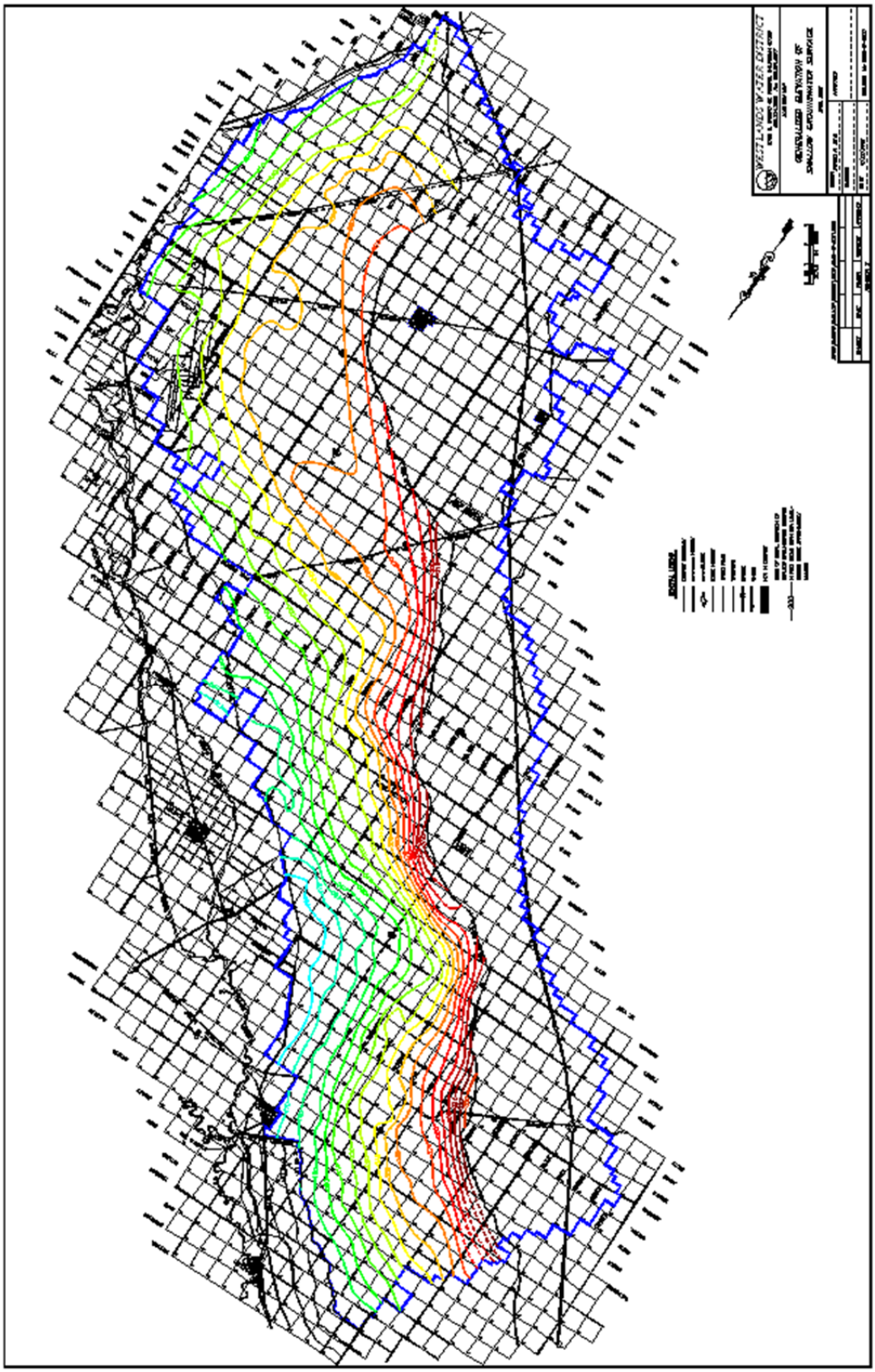

D 55 Shallow aquifer groundwater contour map, April 2005.

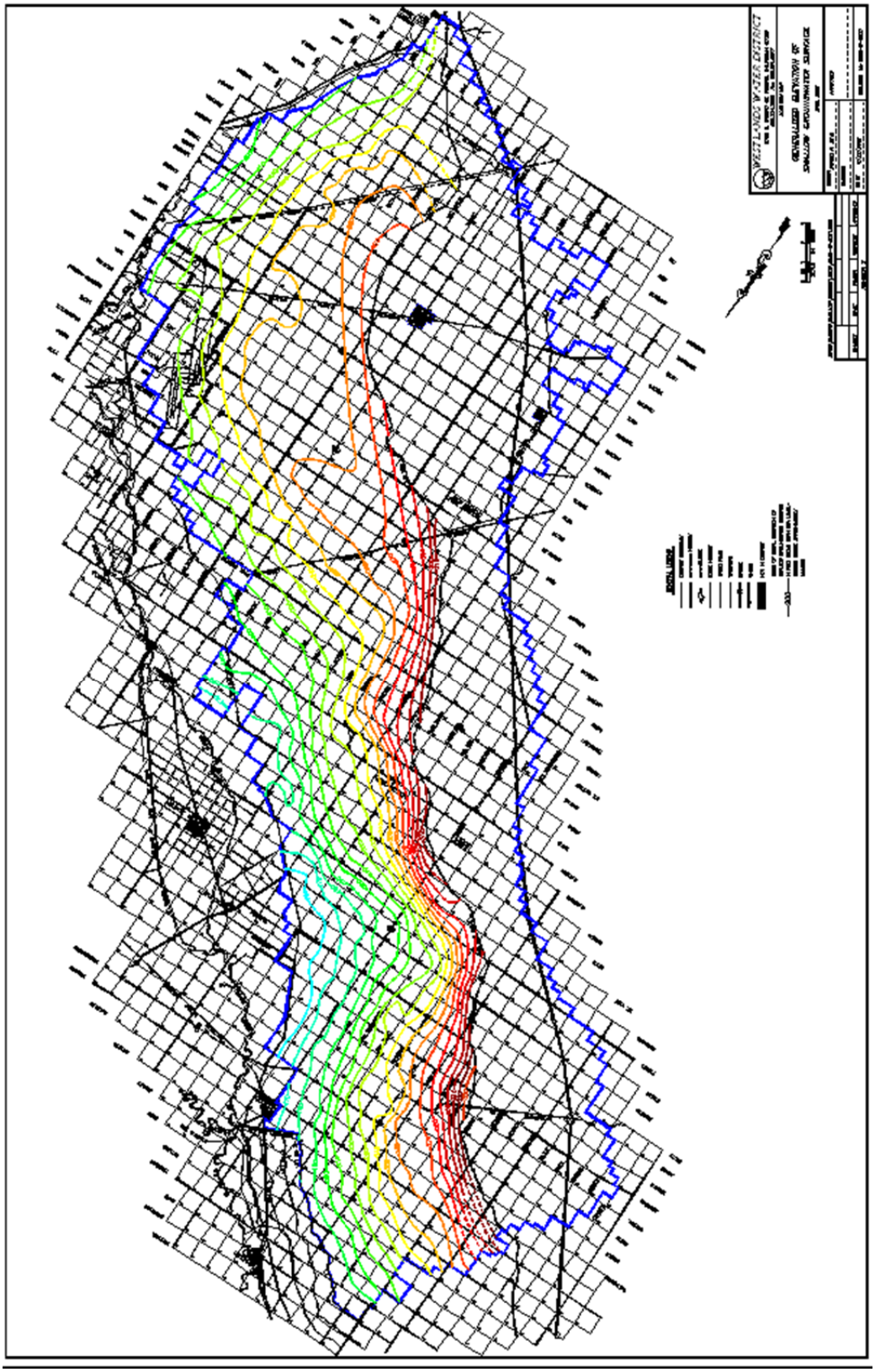

D 56 Shallow aquifer groundwater contour map, October2005.

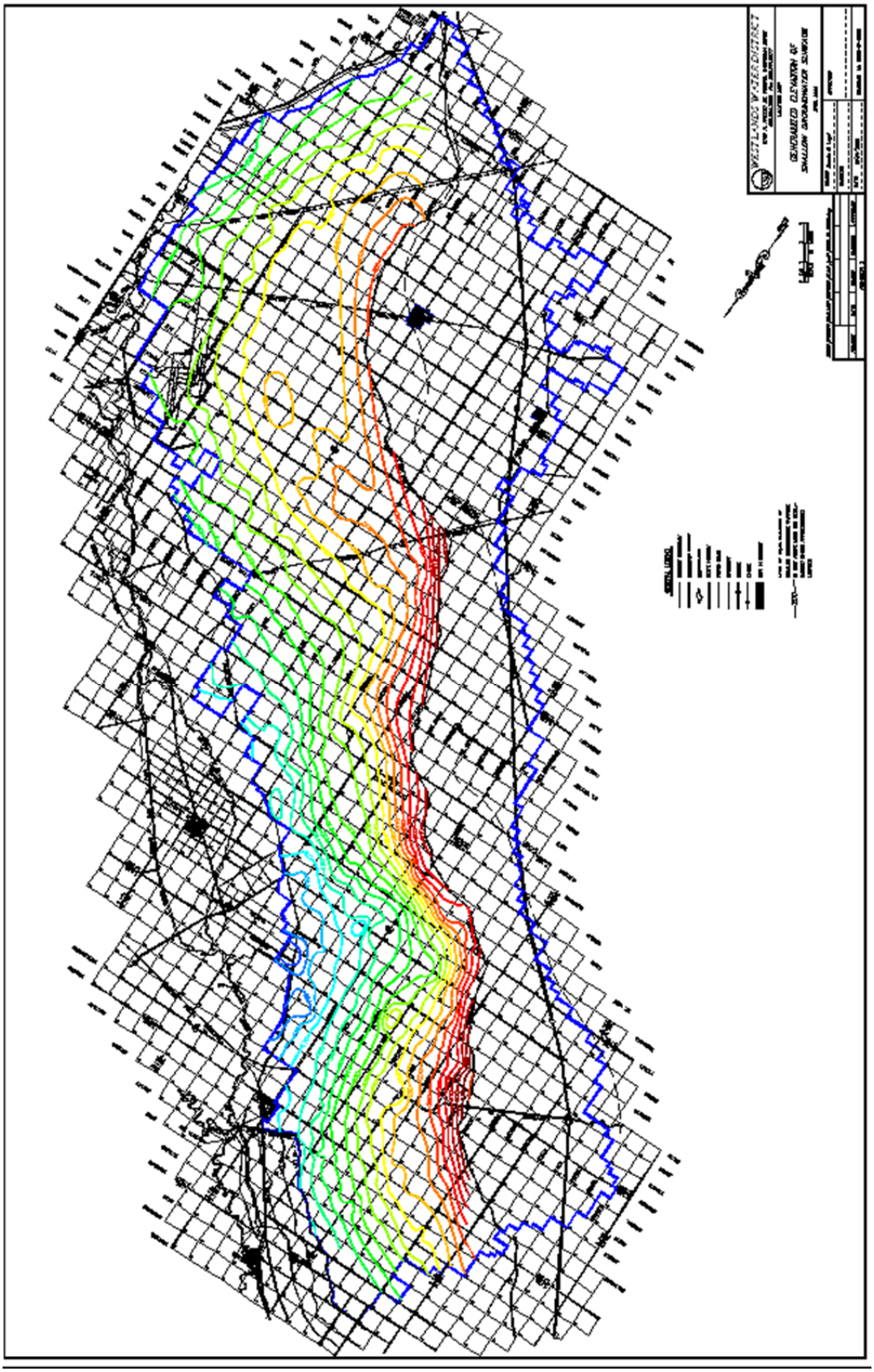

D 57 Shallow aquifer groundwater contour map, April 2006.

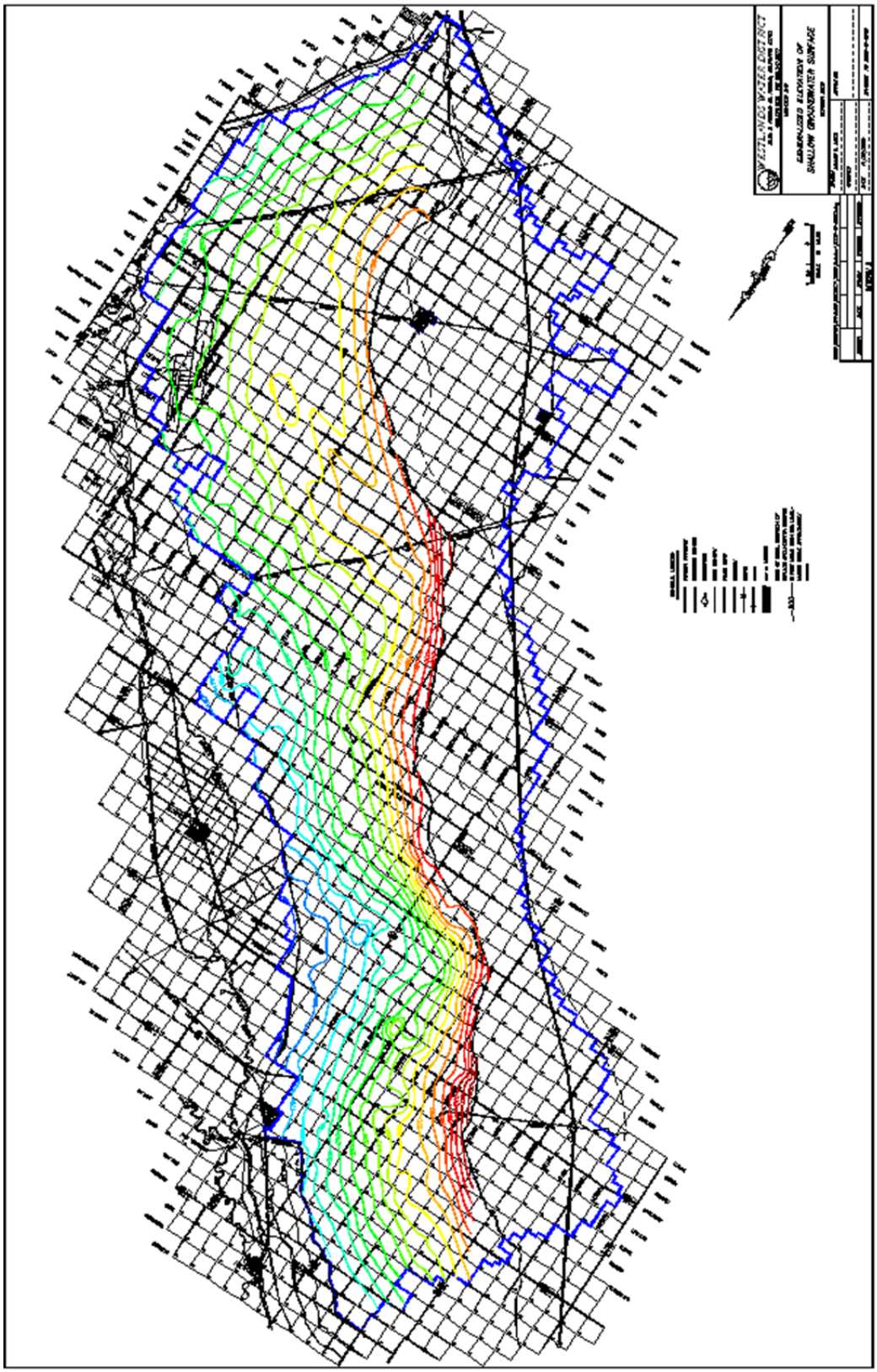

D 58 Shallow aquifer groundwater contour map, October 2006.

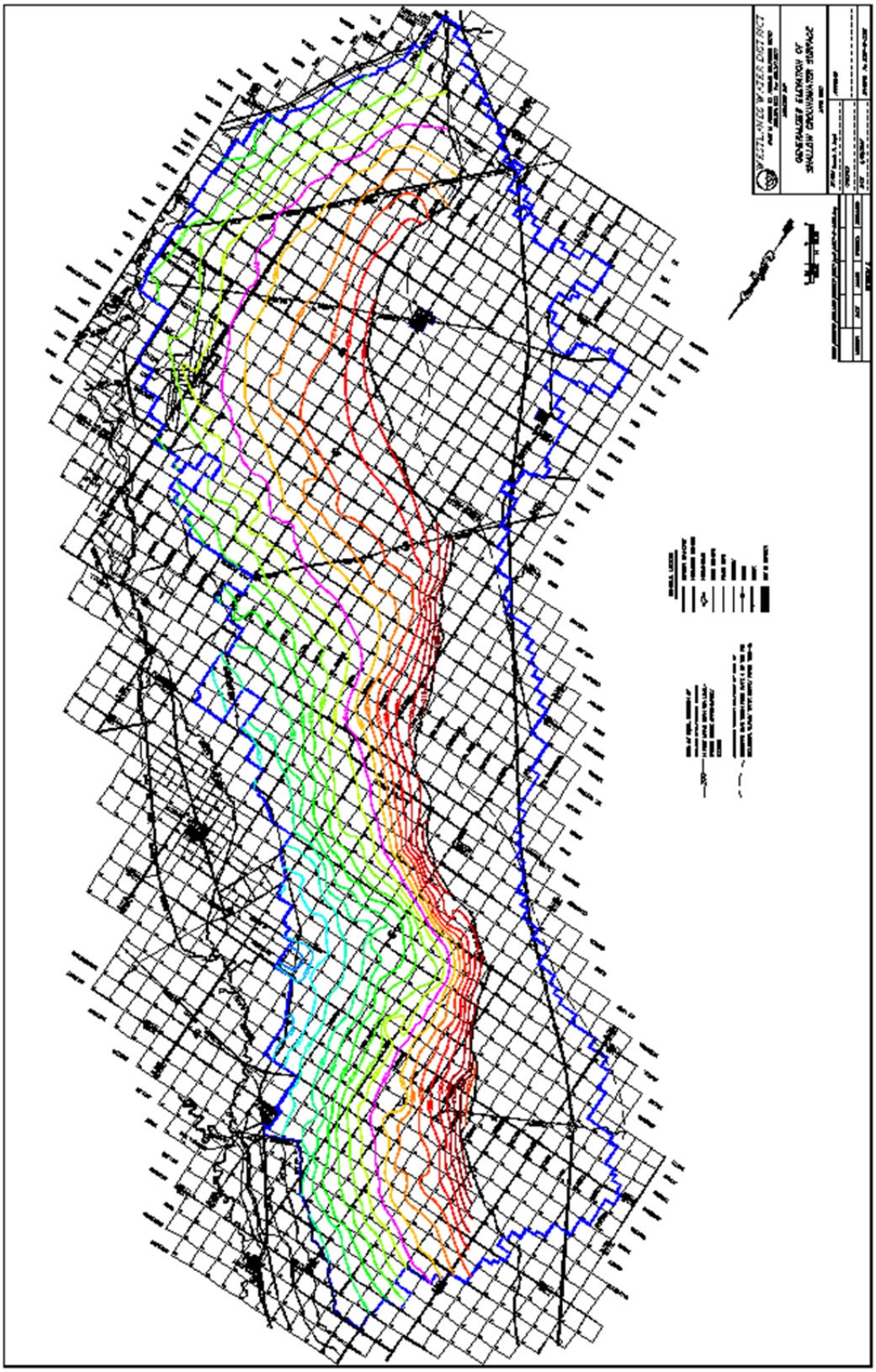

D 59 Shallow aquifer groundwater contour map, April 2007.

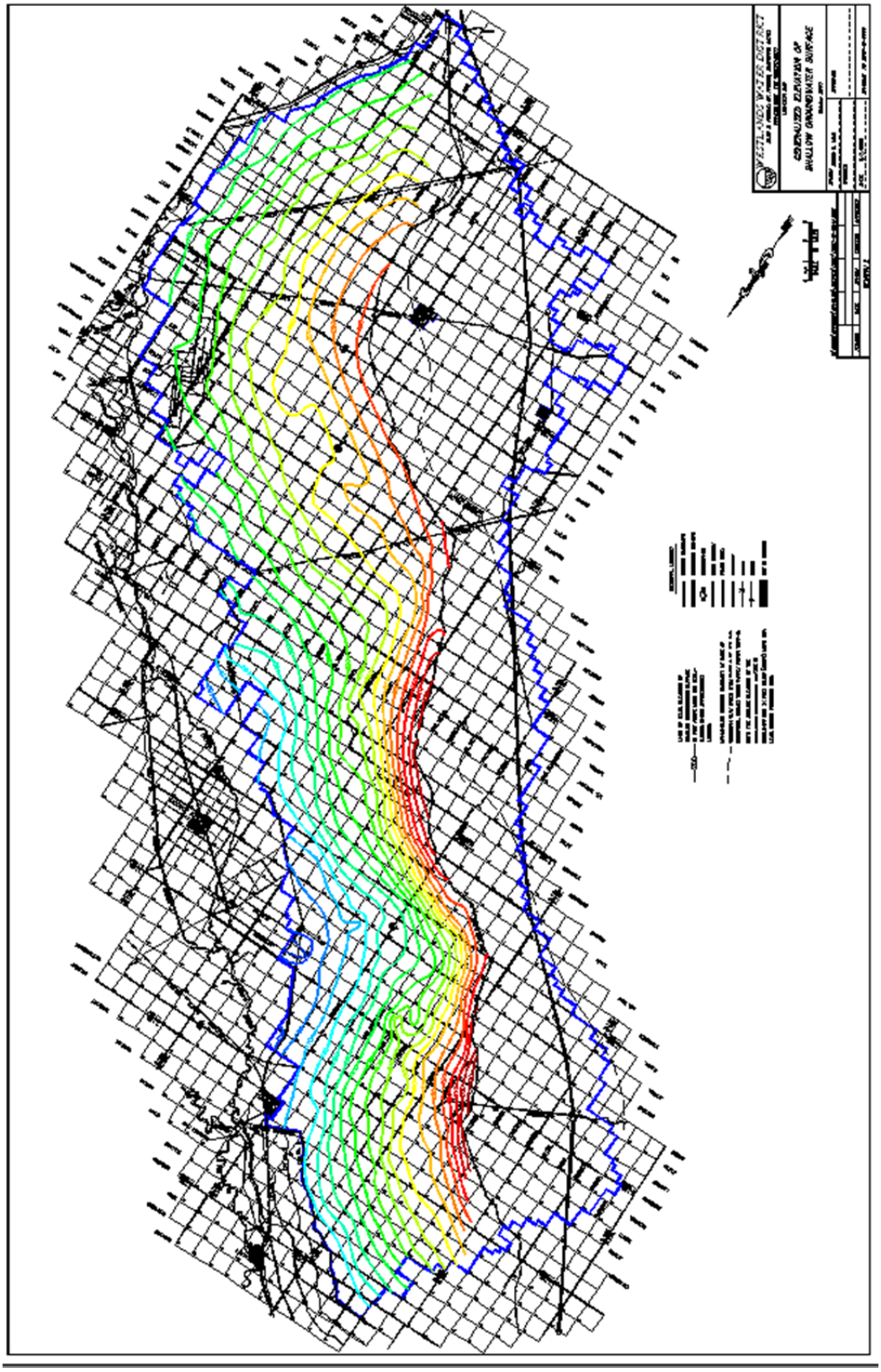

D 60 Shallow aquifer groundwater contour map, October 2007.

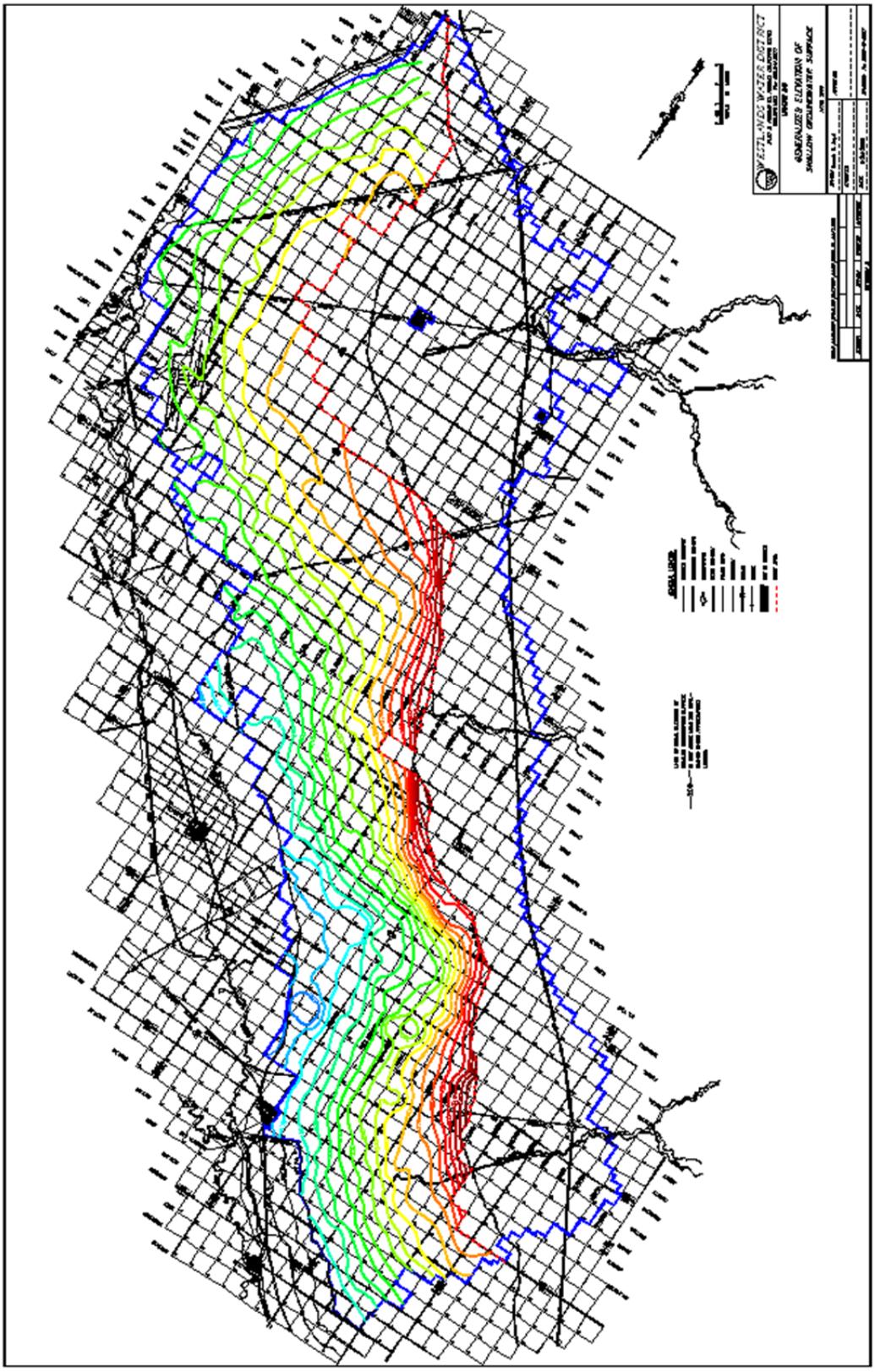

D 61 Shallow aquifer groundwater contour map, April 2008.

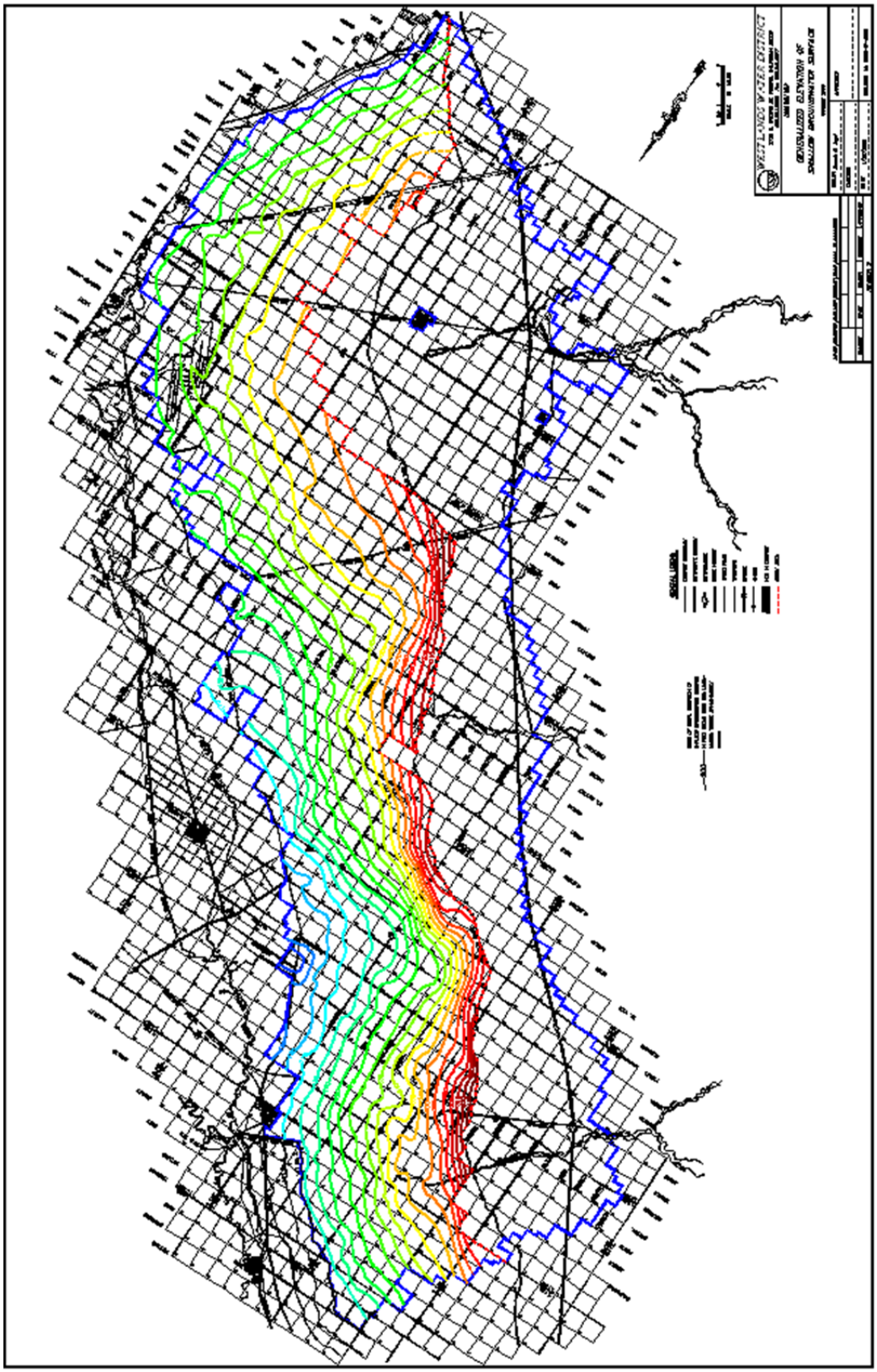

D 62 Shallow aquifer groundwater contour map, October 2008.

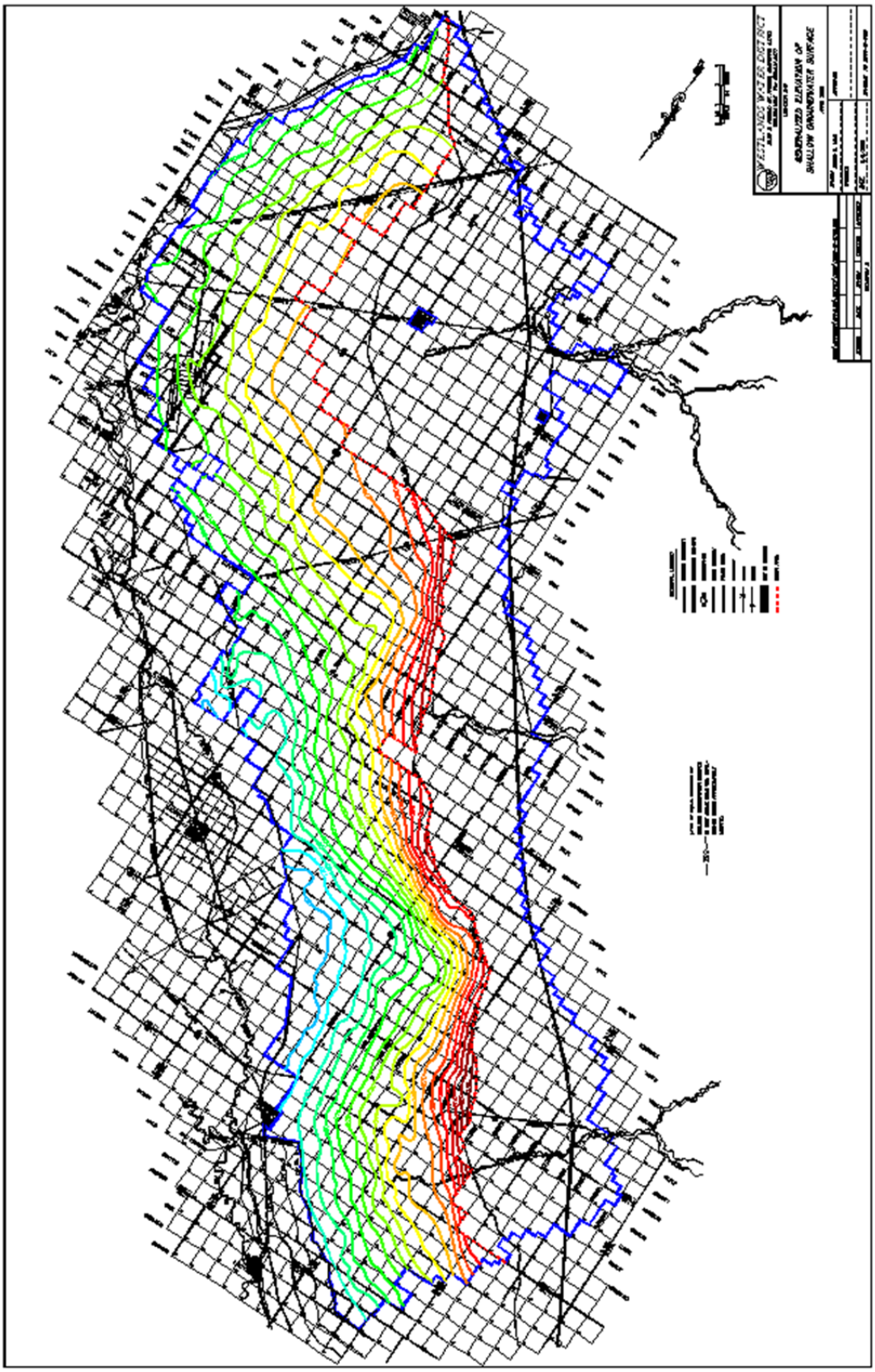

D 63 Shallow aquifer groundwater contour map, April 2009.

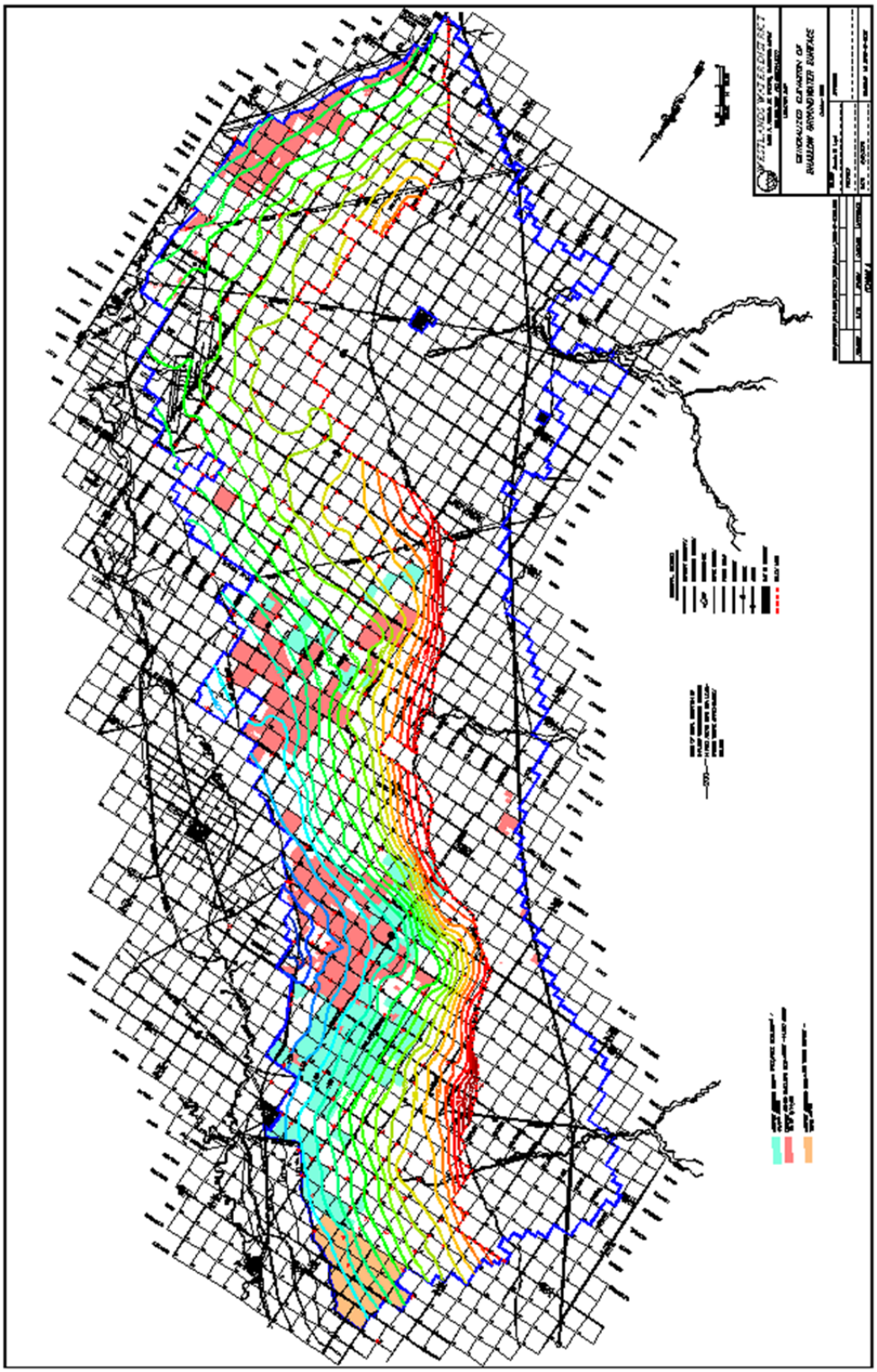

D 64 Shallow aquifer groundwater contour map, October 2009.

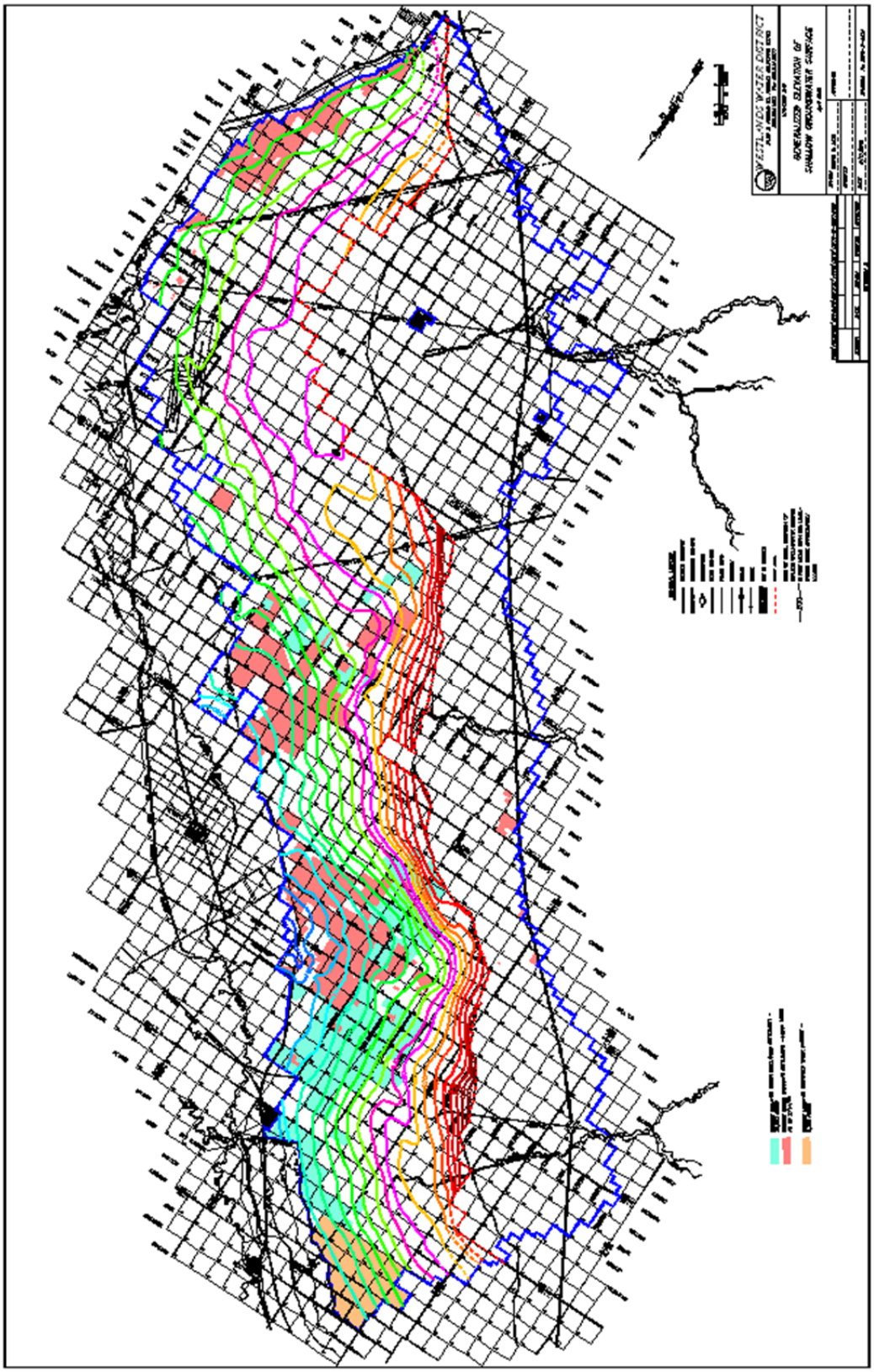

D 65 Shallow aquifer groundwater contour map, April 2010.

Appendix E CDWR groundwater elevation contour maps

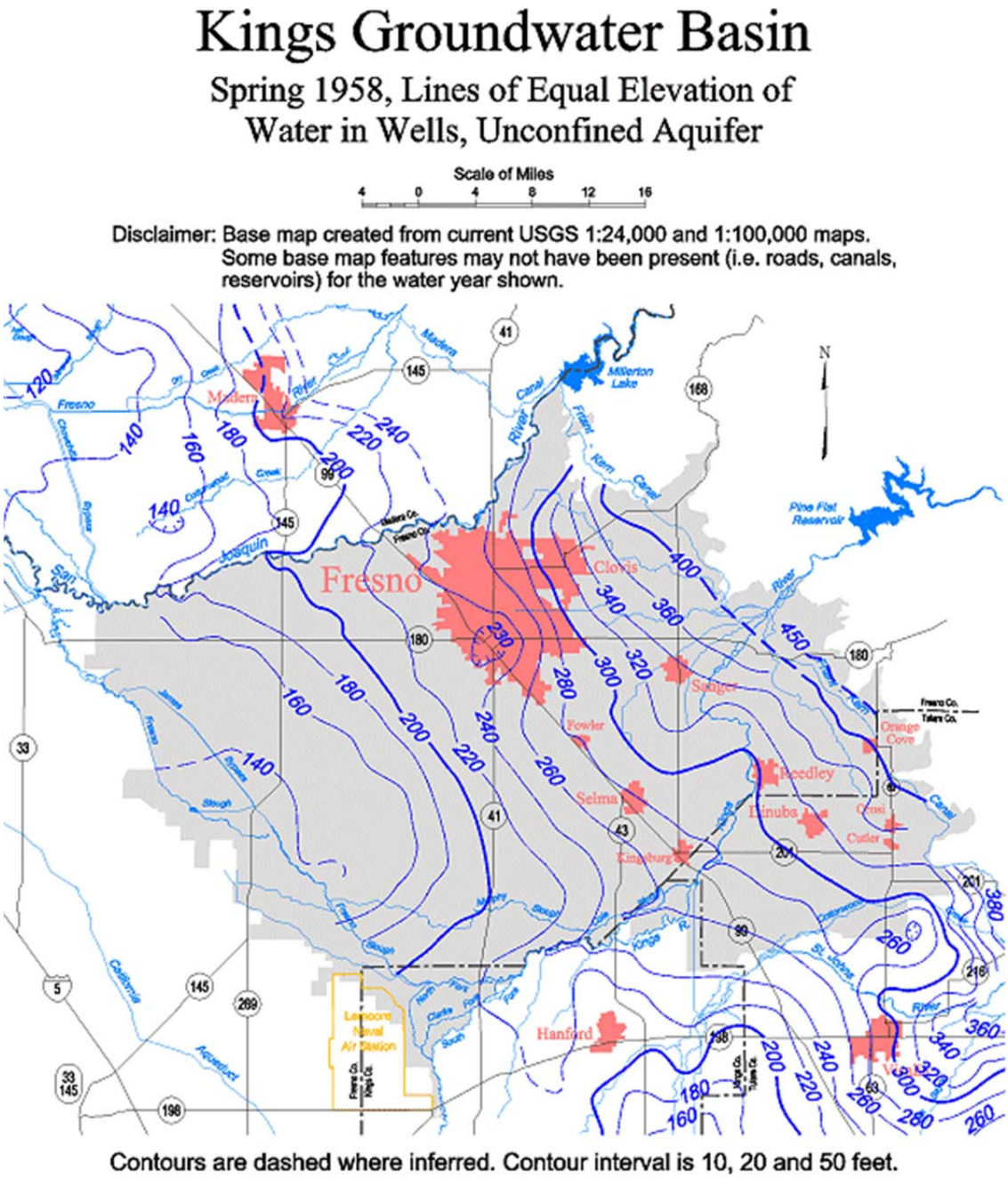

E 1 Unconfined aquifer groundwater contour map, Kings groundwater basin, Spring 1958.

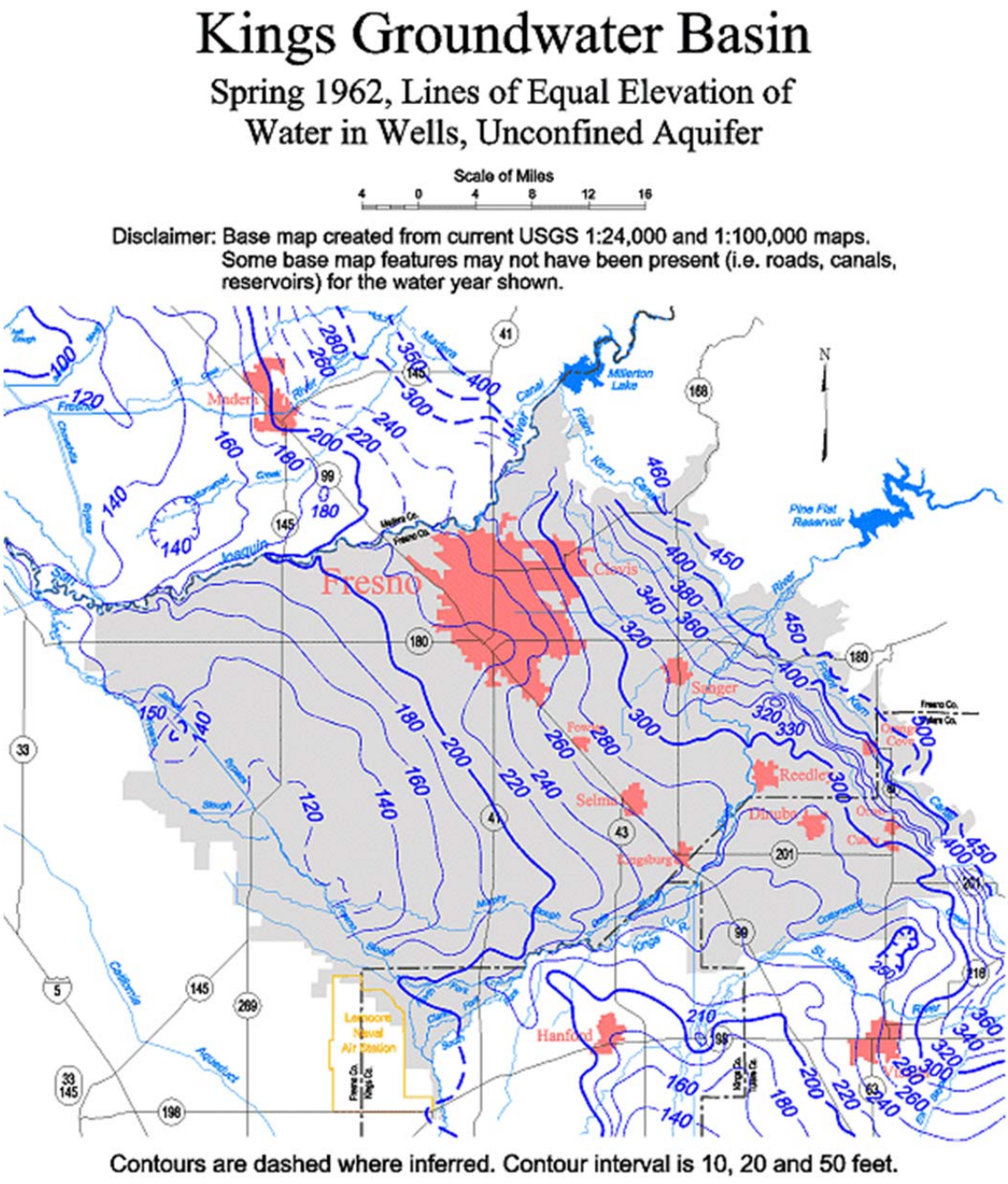

E 2 Unconfined aquifer groundwater contour map, Kings groundwater basin, Spring 1962.

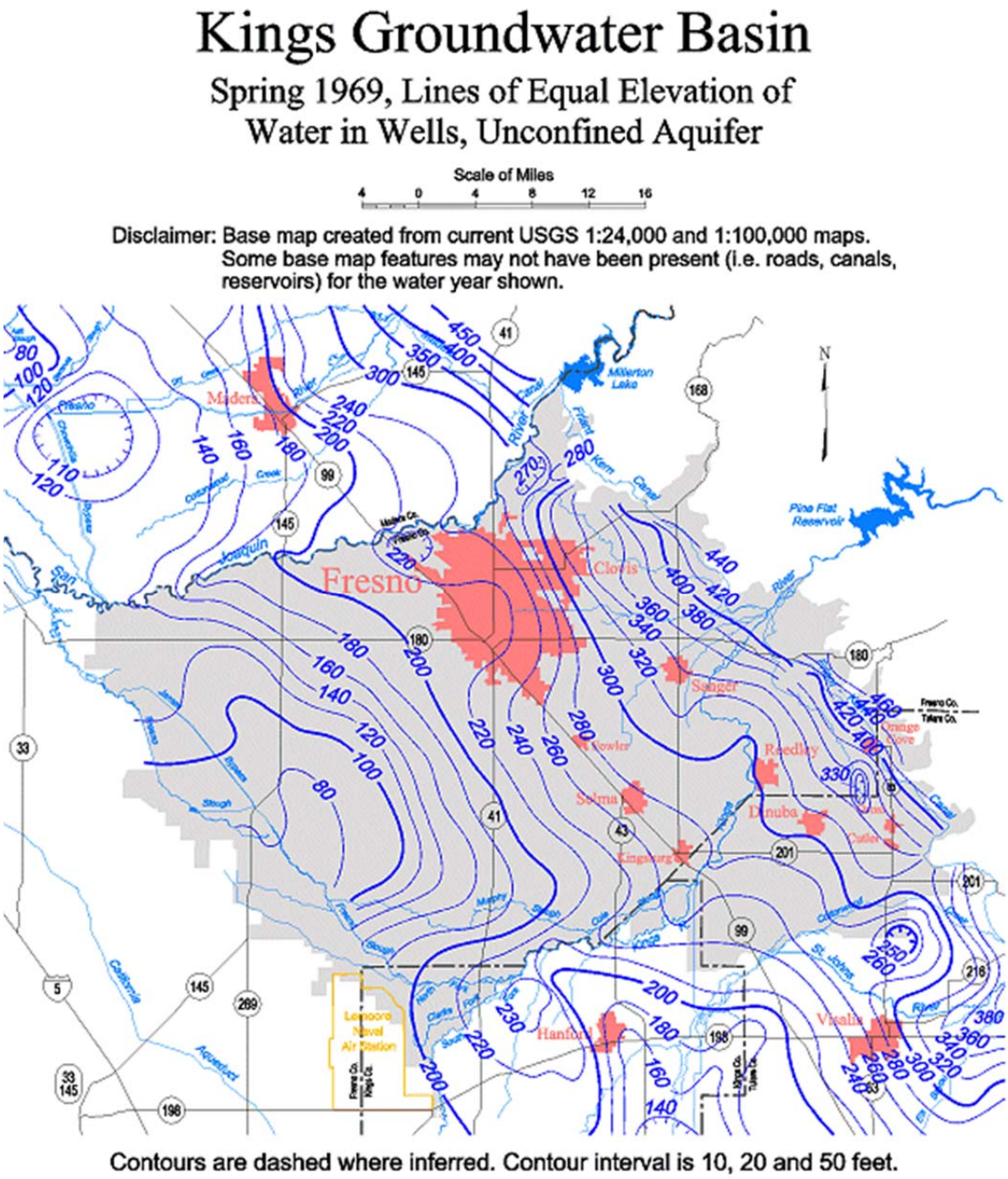

E 3 Unconfined aquifer groundwater contour map, Kings groundwater basin, Spring 1969.

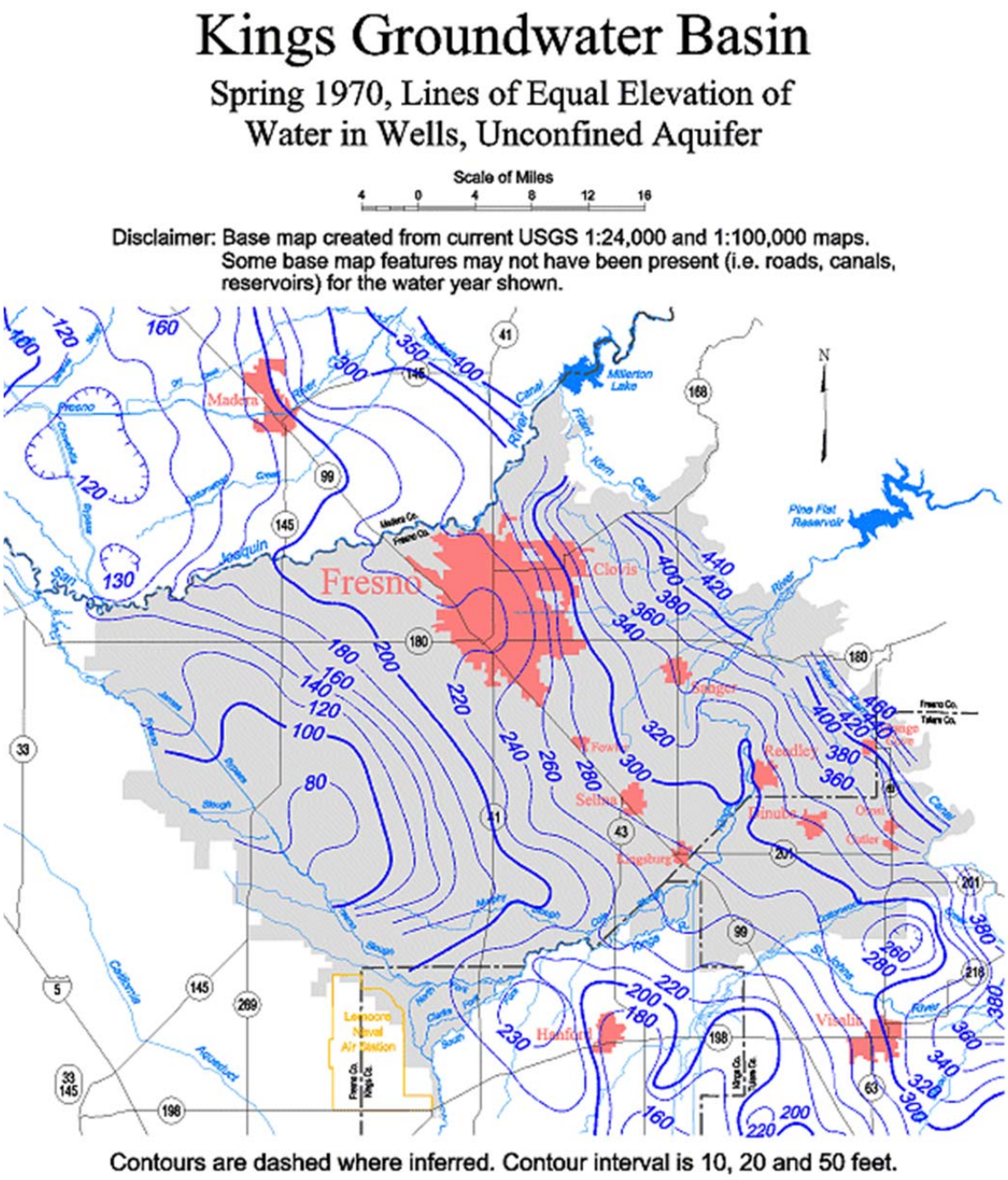

E 4 Unconfined aquifer groundwater contour map, Kings groundwater basin, Spring 1970.

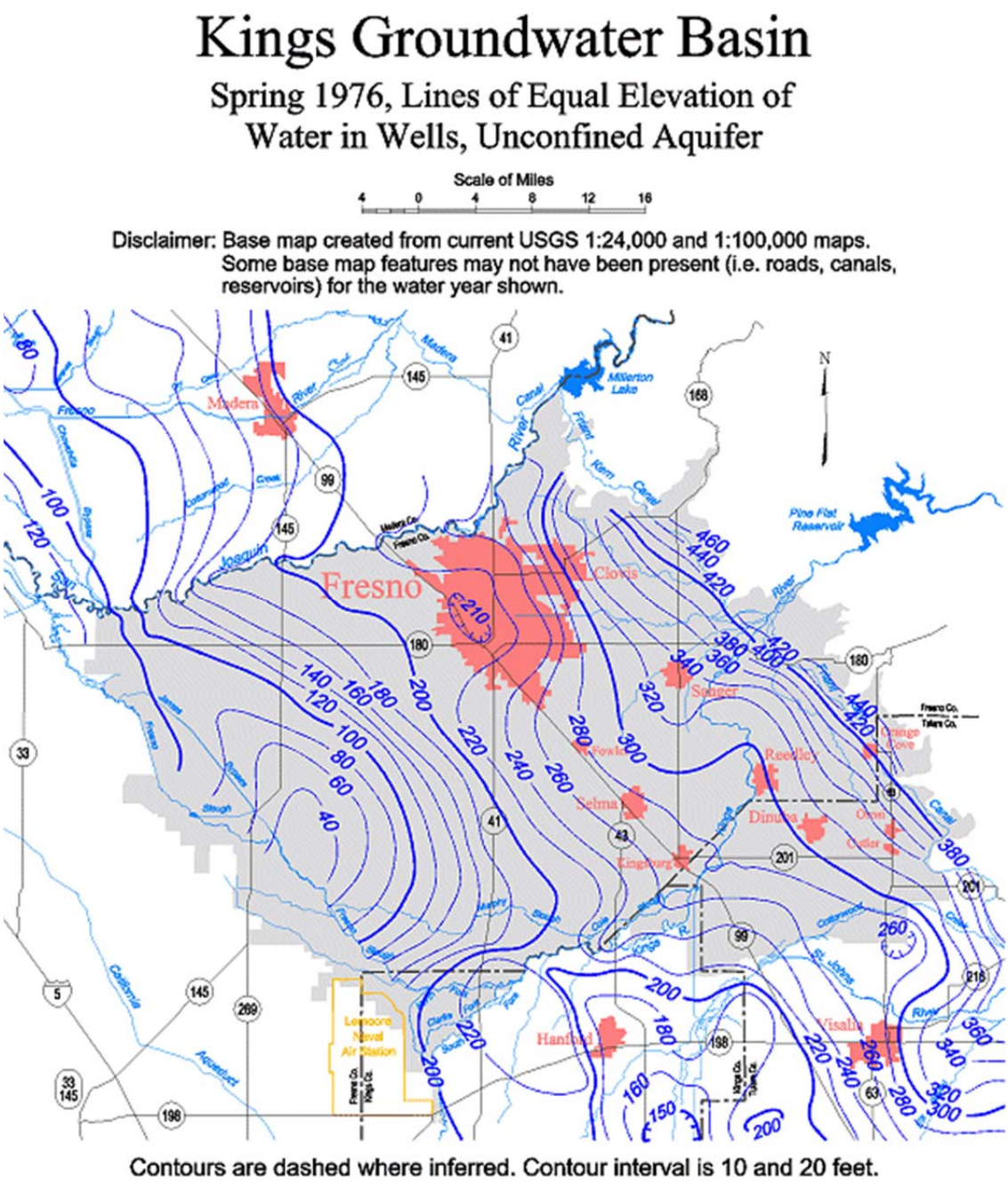

E 5 Unconfined aquifer groundwater contour map, Kings groundwater basin, Spring 1976.

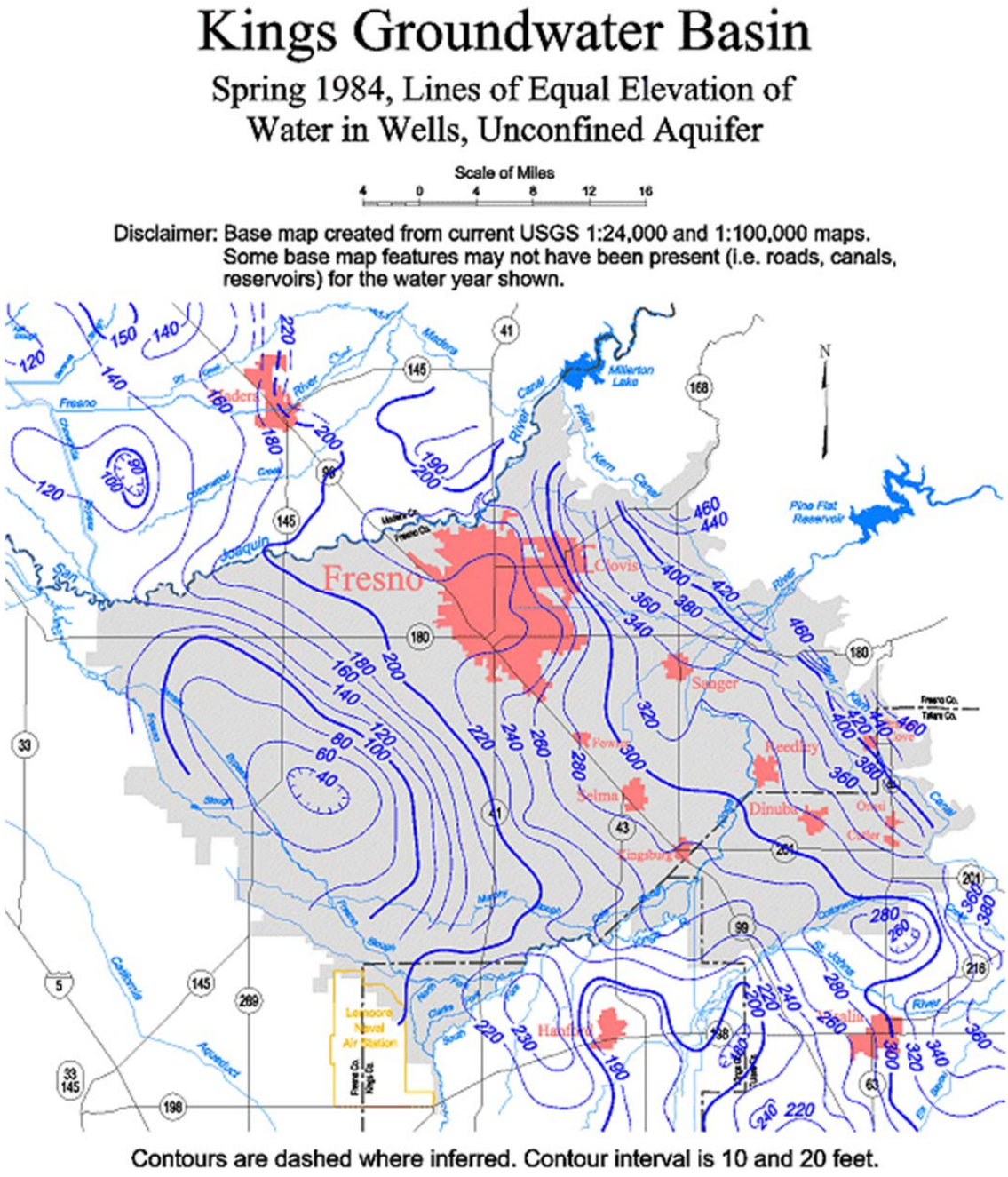

E 6 Unconfined aquifer groundwater contour map, Kings groundwater basin, Spring 1984.

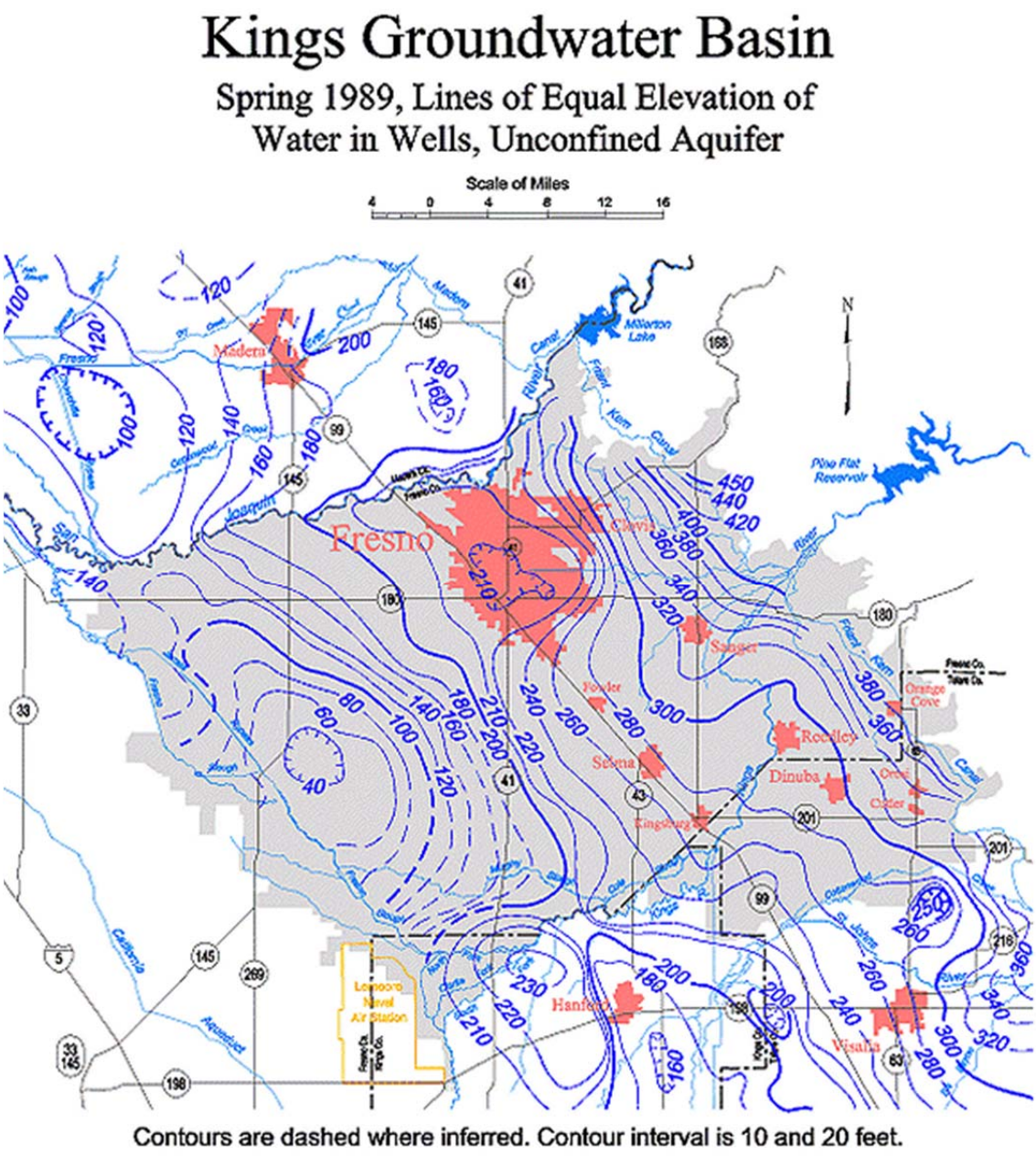

E 7 Unconfined aquifer groundwater contour map, Kings groundwater basin, Spring 1989.

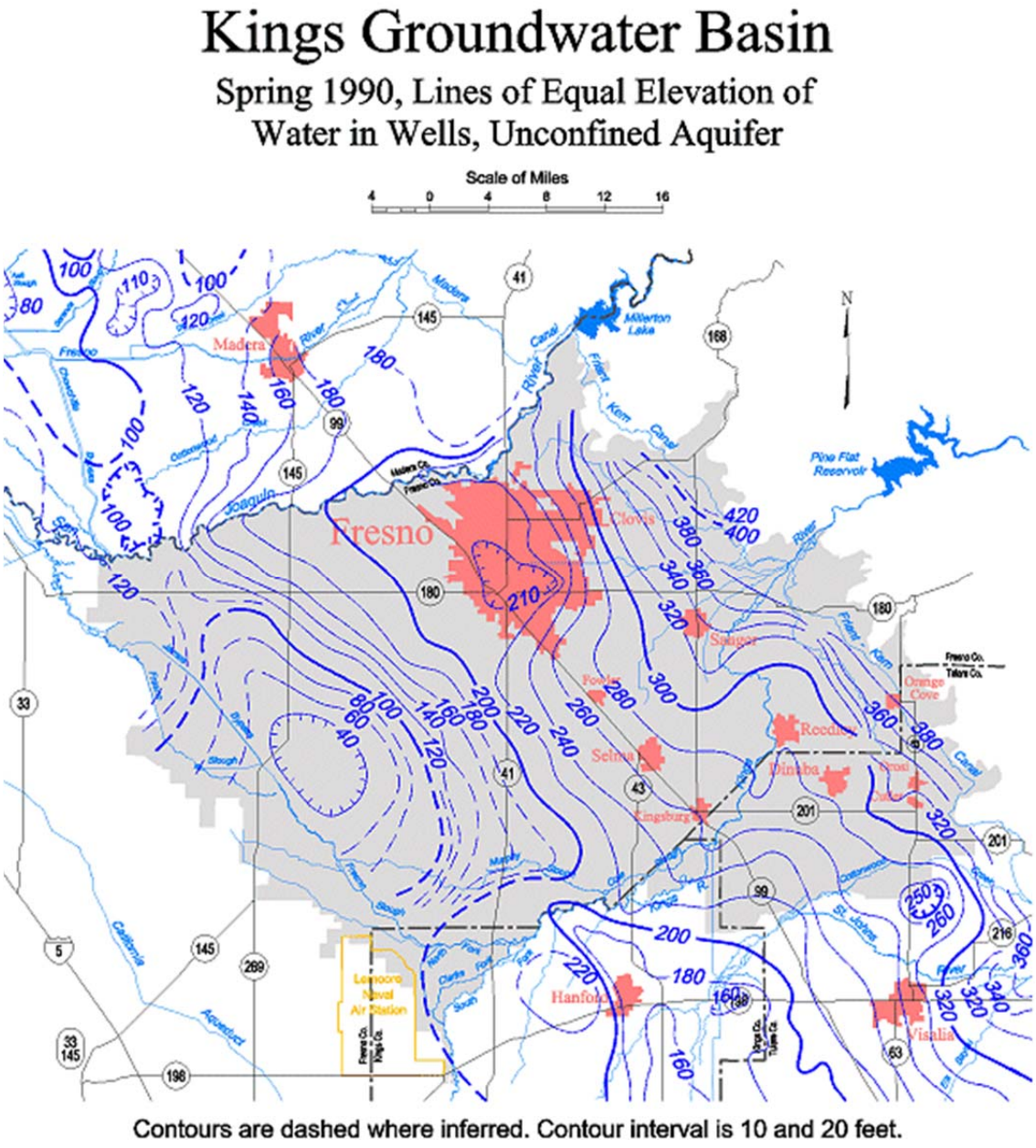

E 8 Unconfined aquifer groundwater contour map, Kings groundwater basin, Spring 1990.

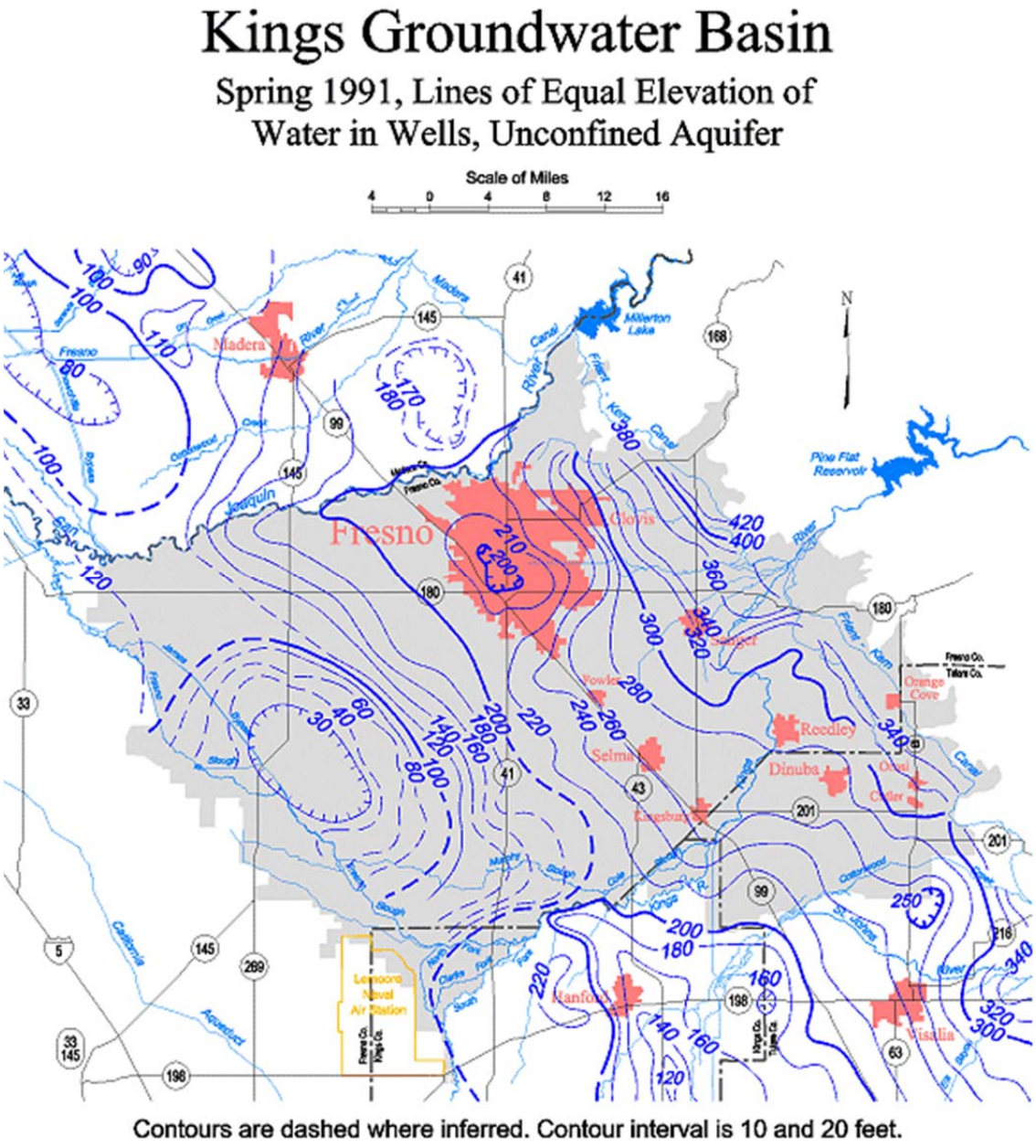

E 9 Unconfined aquifer groundwater contour map, Kings groundwater basin, Spring 1991.

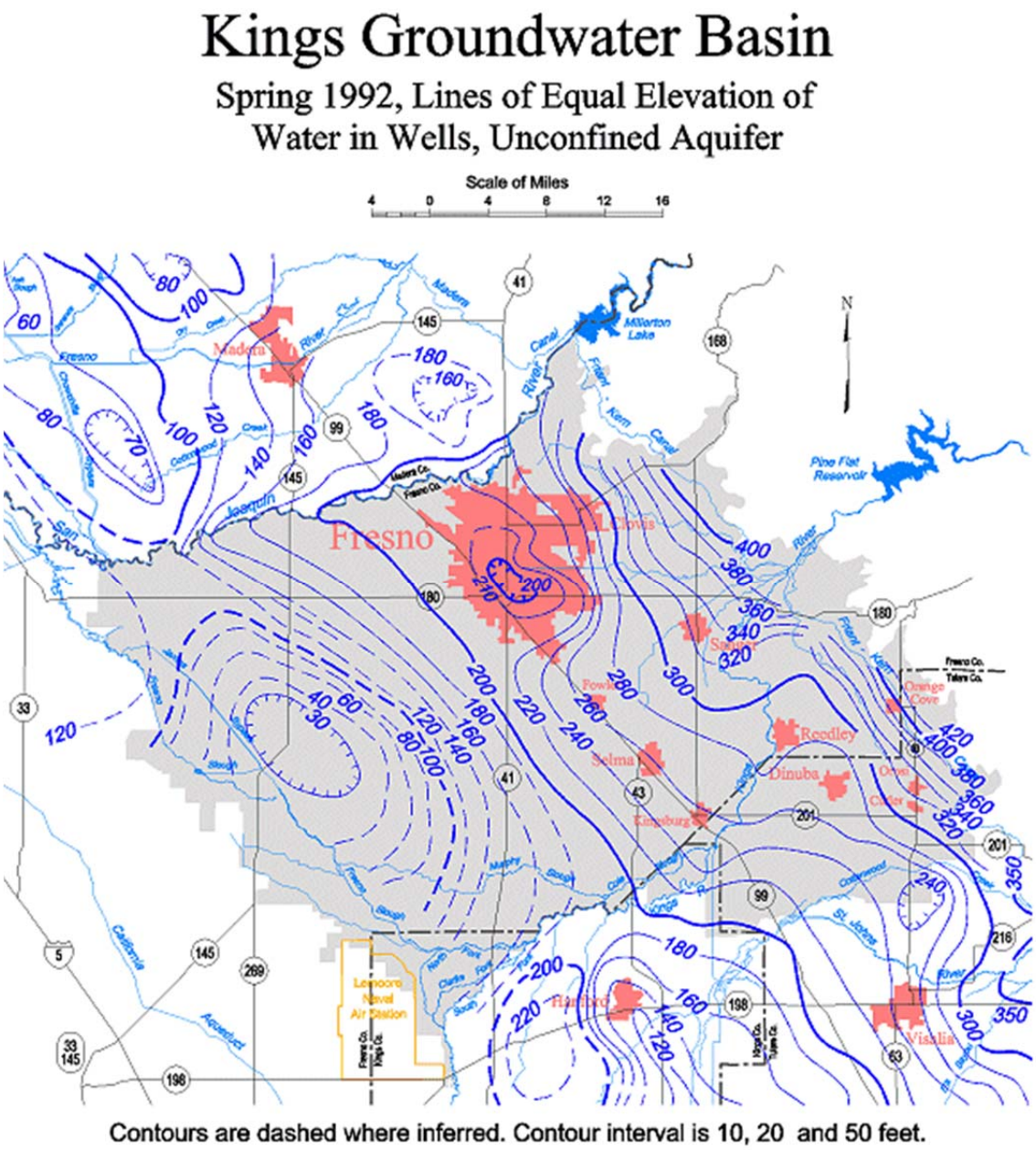

E 10 Unconfined aquifer groundwater contour map, Kings groundwater basin, Spring 1992.

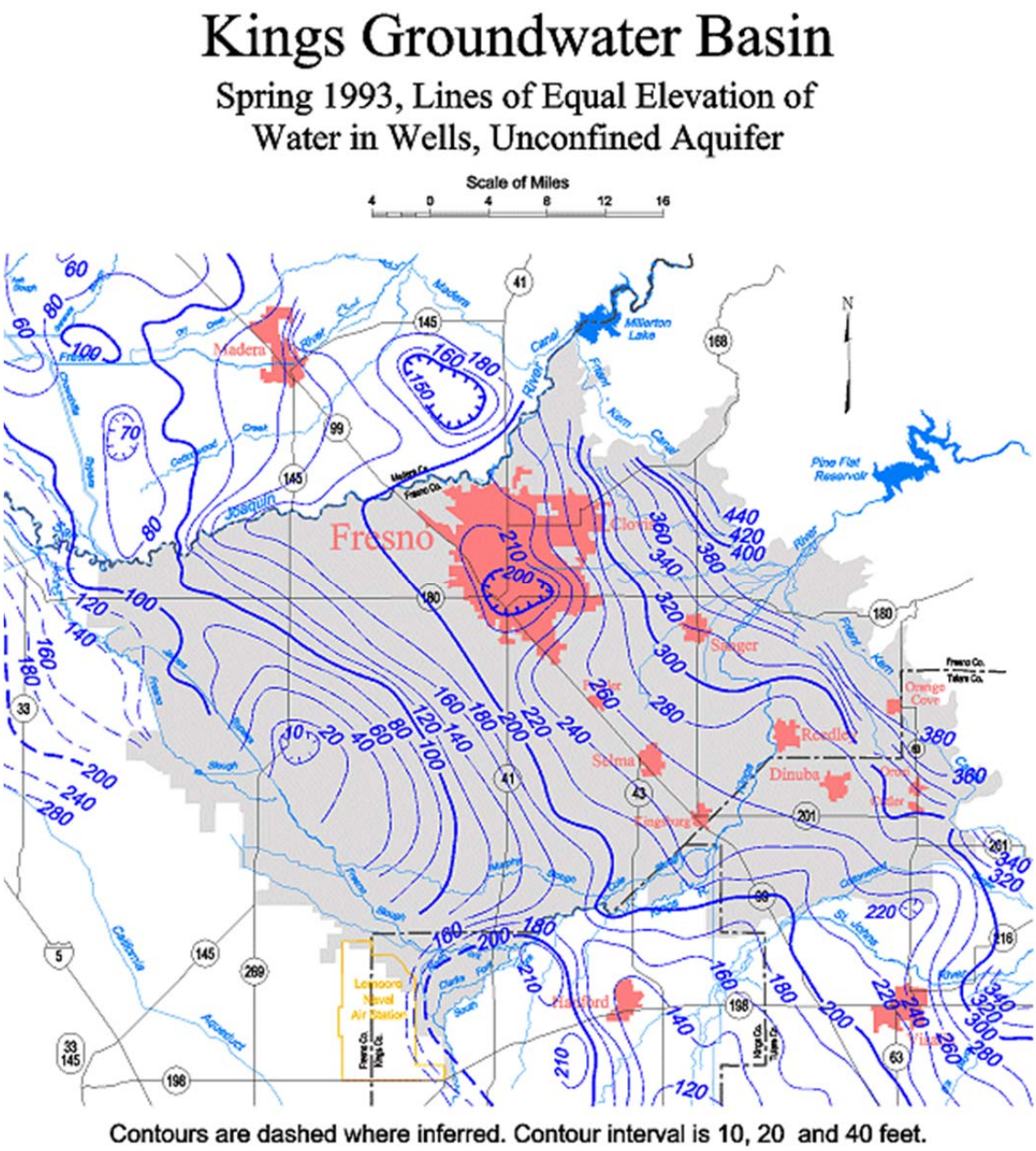

E 11 Unconfined aquifer groundwater contour map, Kings groundwater basin, Spring 1993.

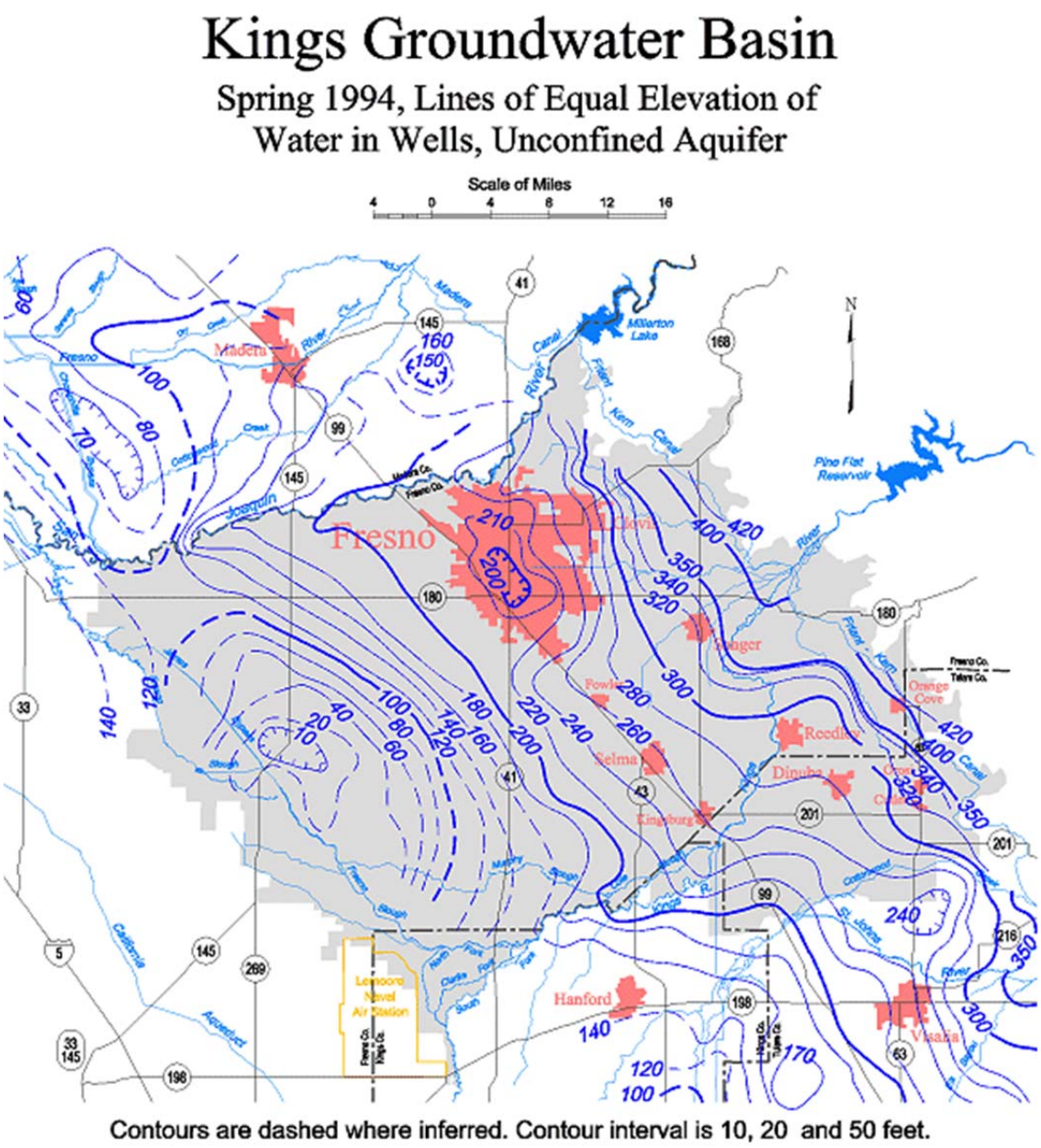

E 12 Unconfined aquifer groundwater contour map, Kings groundwater basin, Spring 1994.

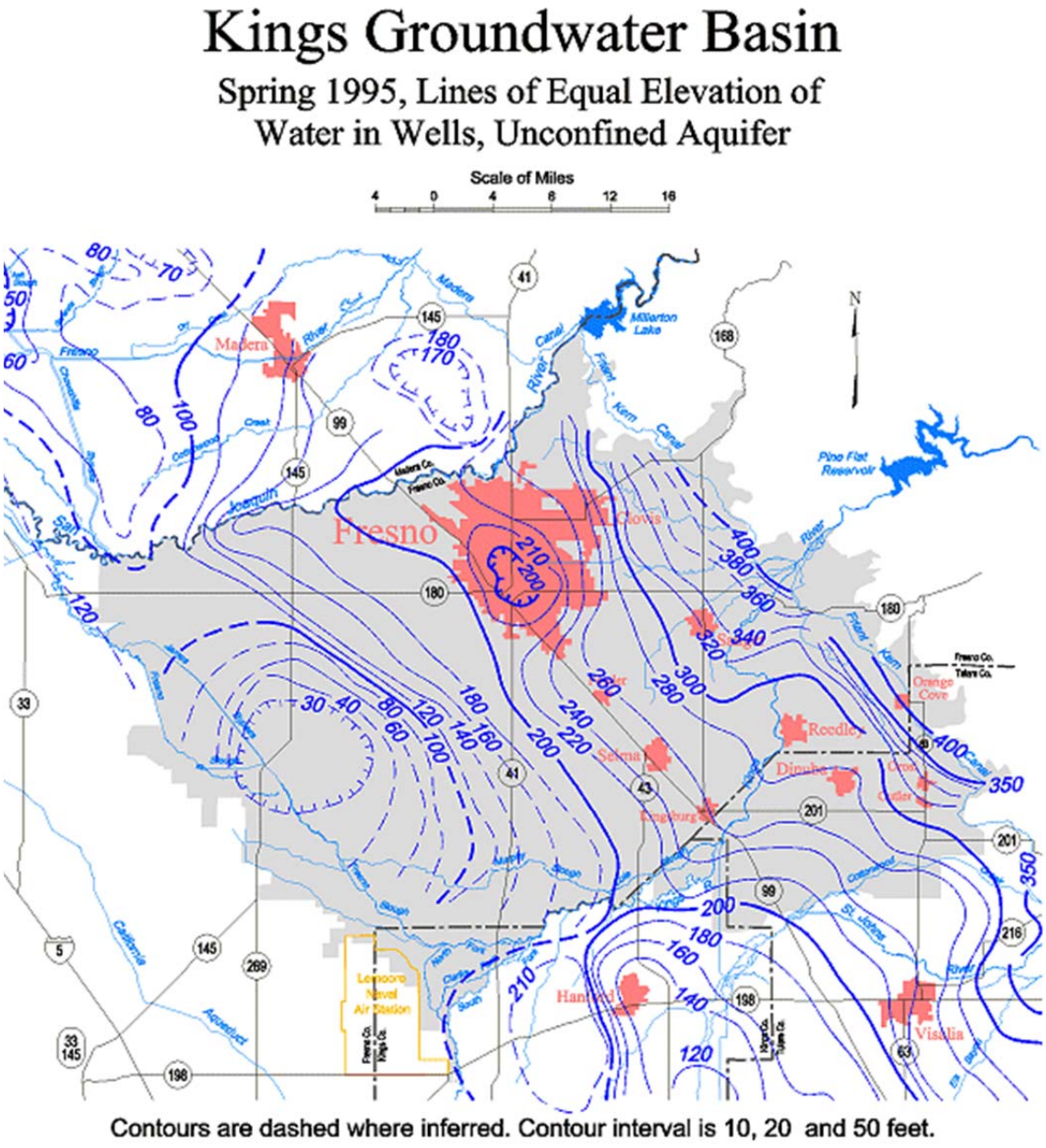

E 13 Unconfined aquifer groundwater contour map, Kings groundwater basin, Spring 1995.

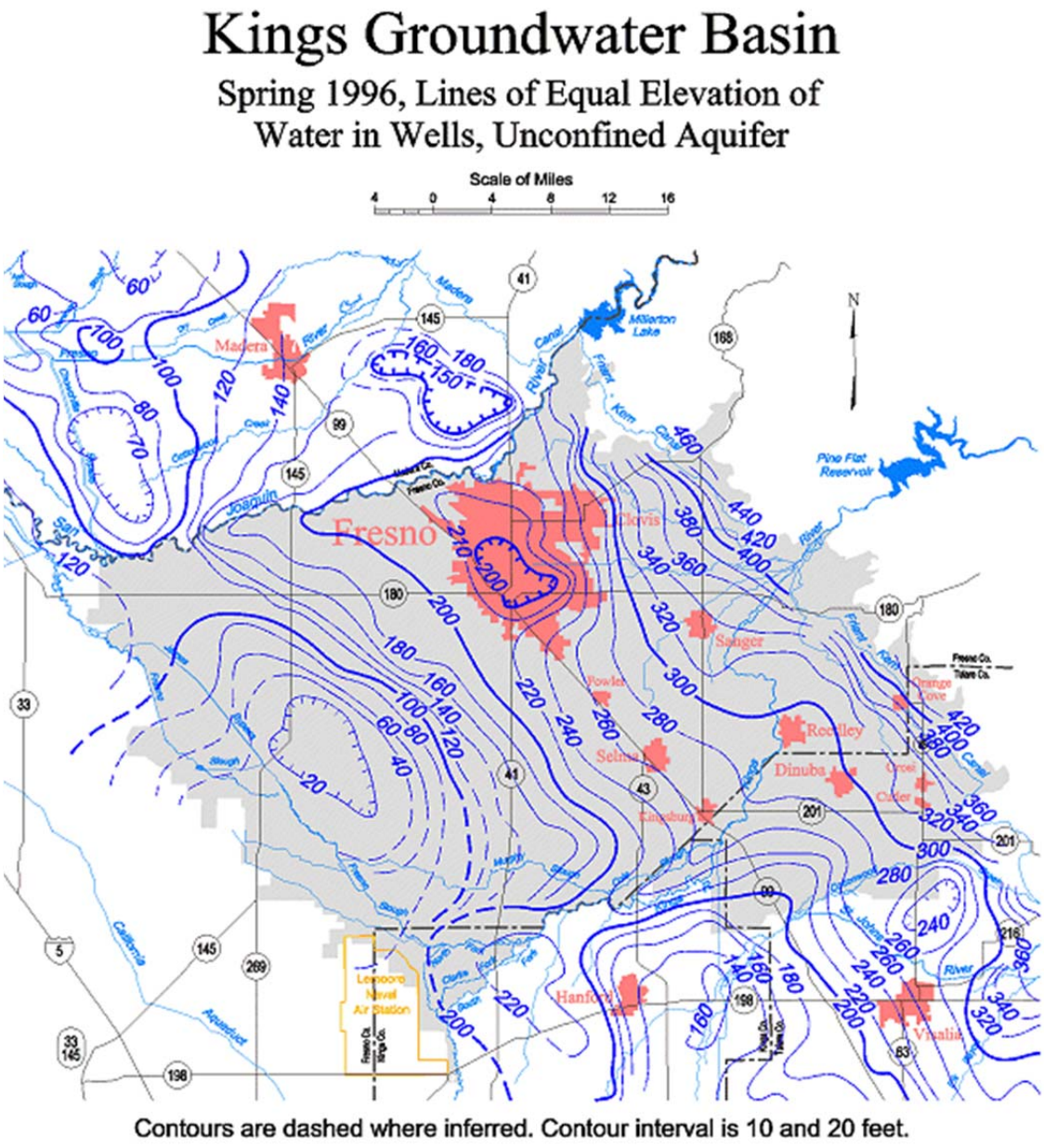

E 14 Unconfined aquifer groundwater contour map, Kings groundwater basin, Spring 1996.

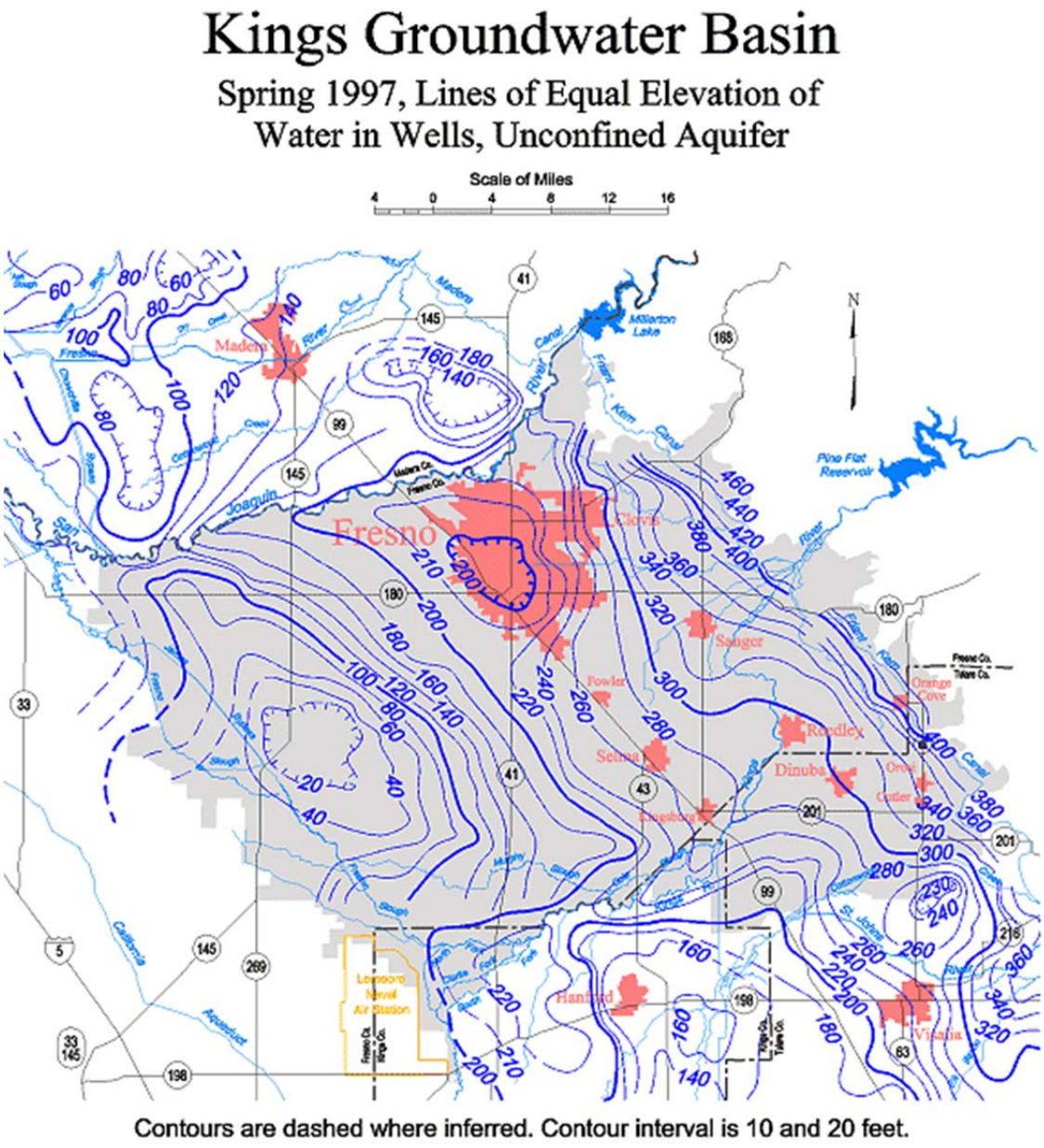

E 15 Unconfined aquifer groundwater contour map, Kings groundwater basin, Spring 1997.

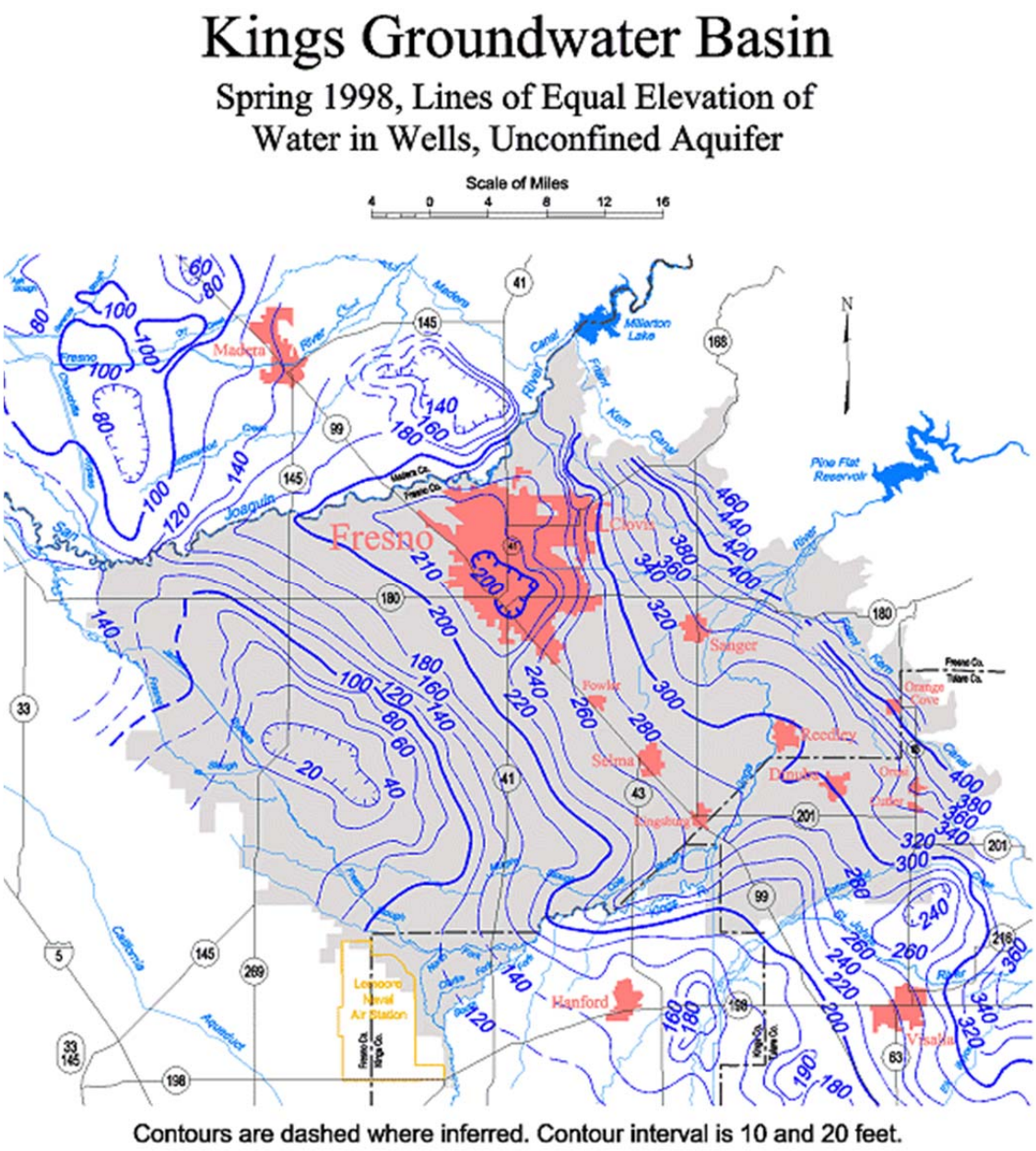

E 16 Unconfined aquifer groundwater contour map, Kings groundwater basin, Spring 1998.

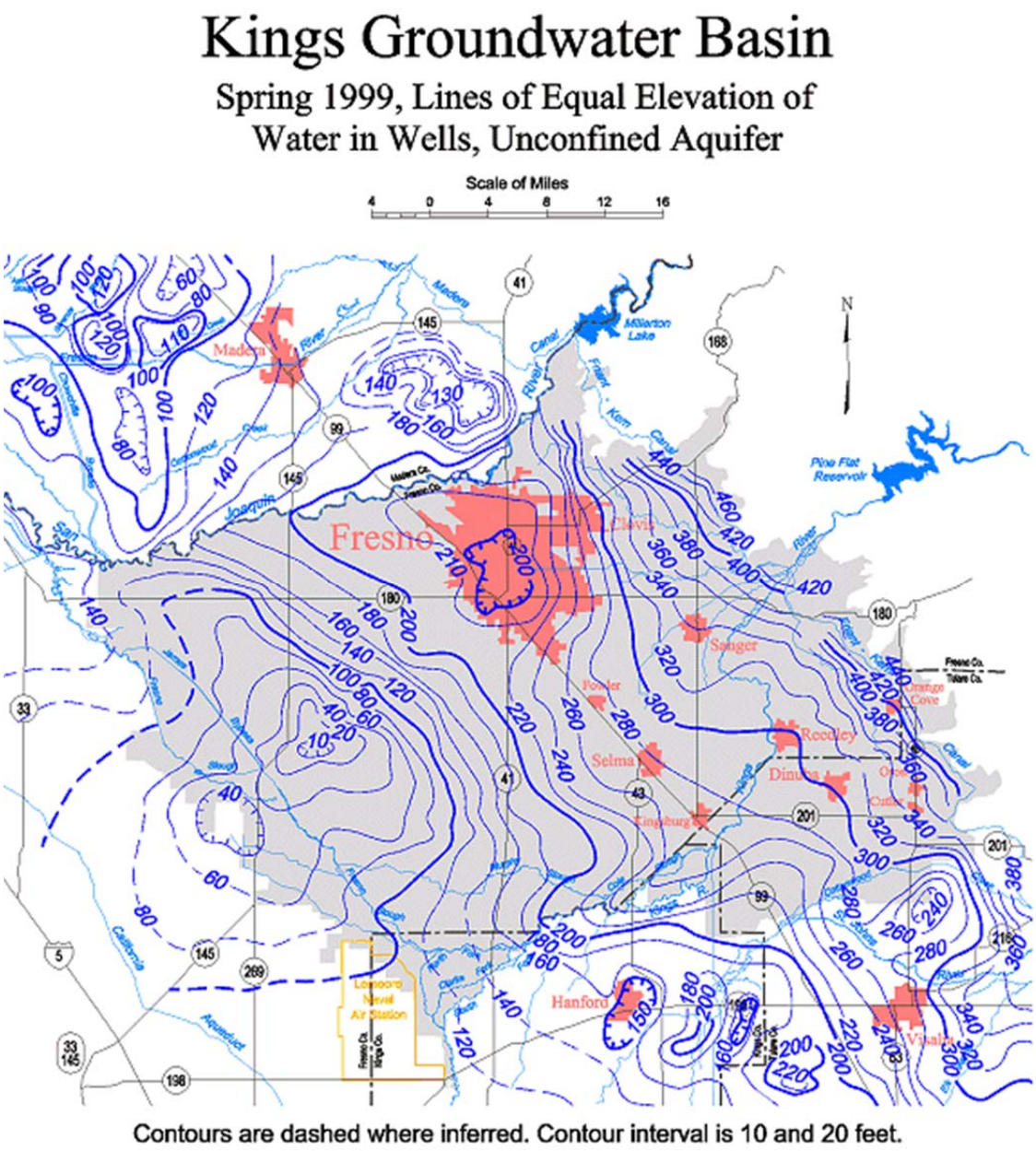

E 17 Unconfined aquifer groundwater contour map, Kings groundwater basin, Spring 1999.

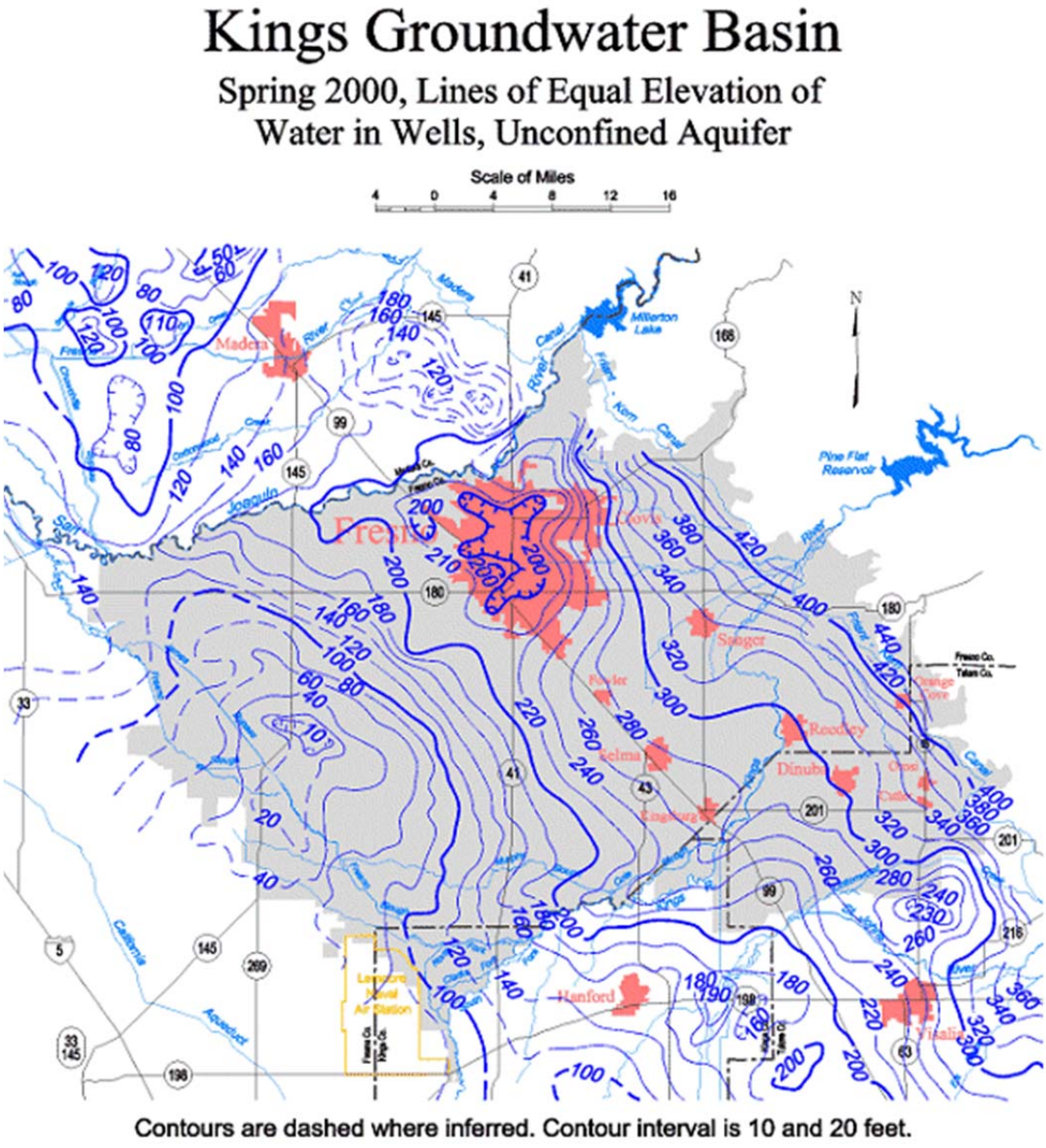

E 18 Unconfined aquifer groundwater contour map, Kings groundwater basin, Spring 2000.

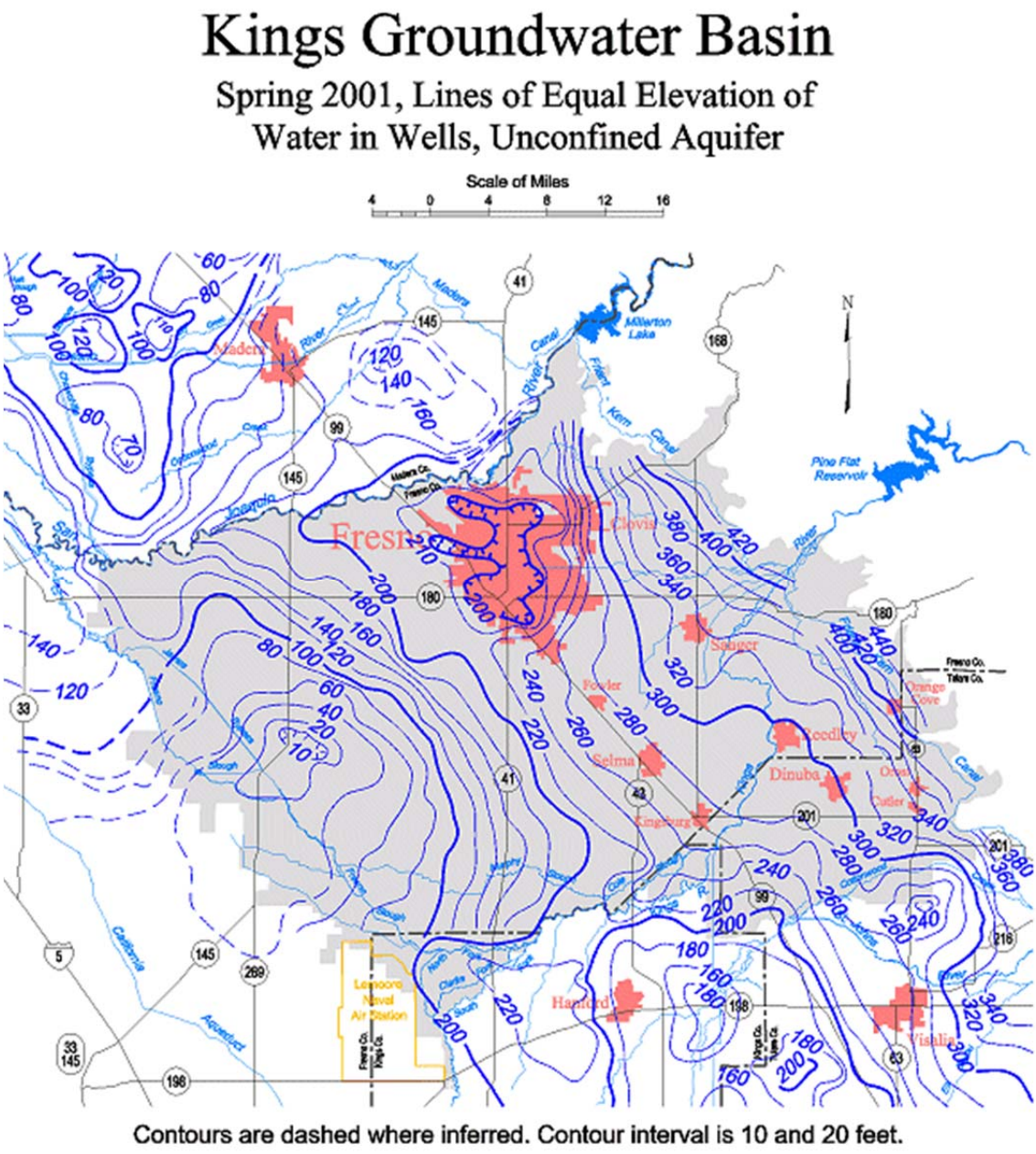

E 19 Unconfined aquifer groundwater contour map, Kings groundwater basin, Spring 2001.

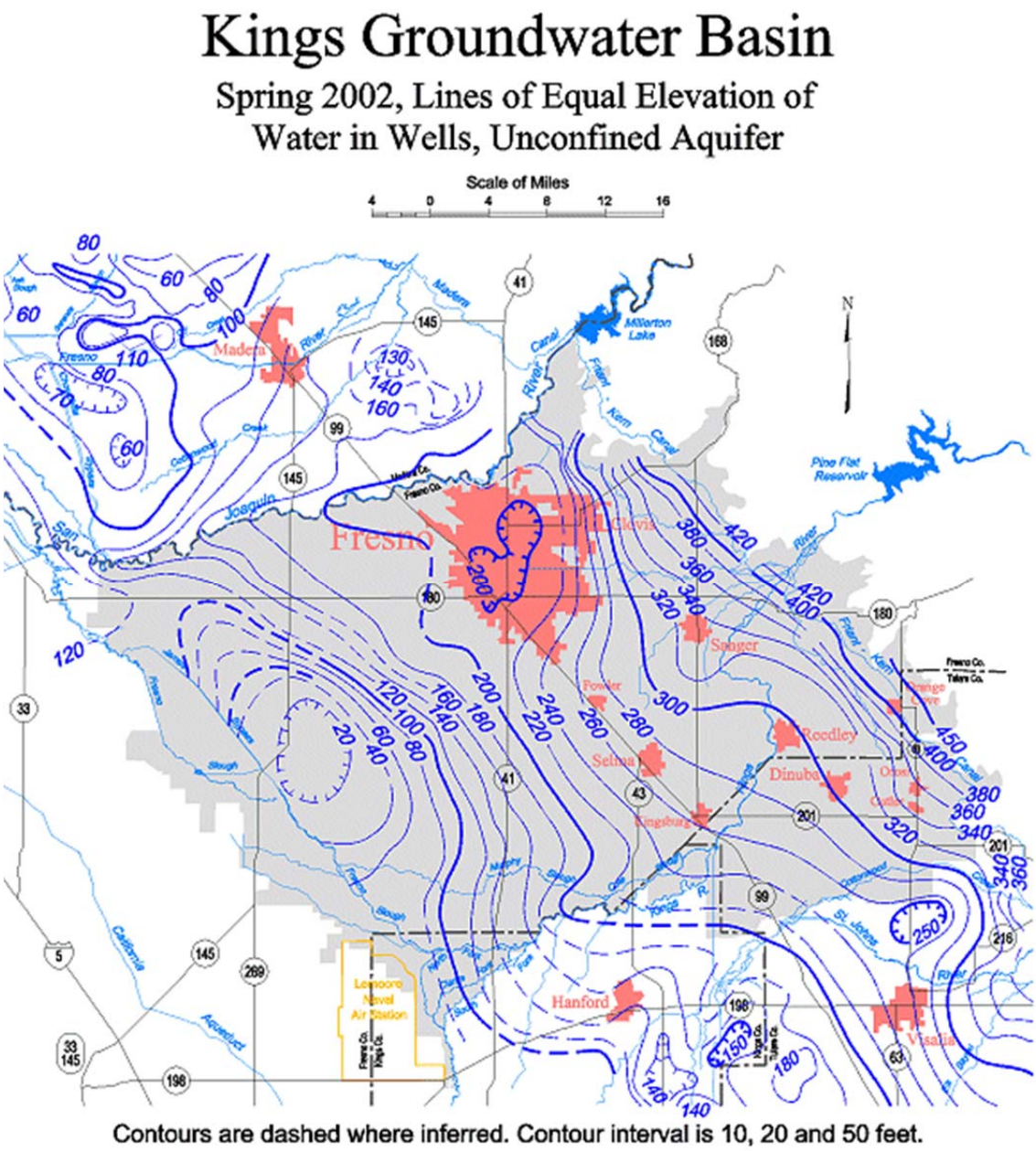

E 20 Unconfined aquifer groundwater contour map, Kings groundwater basin, Spring 2002.

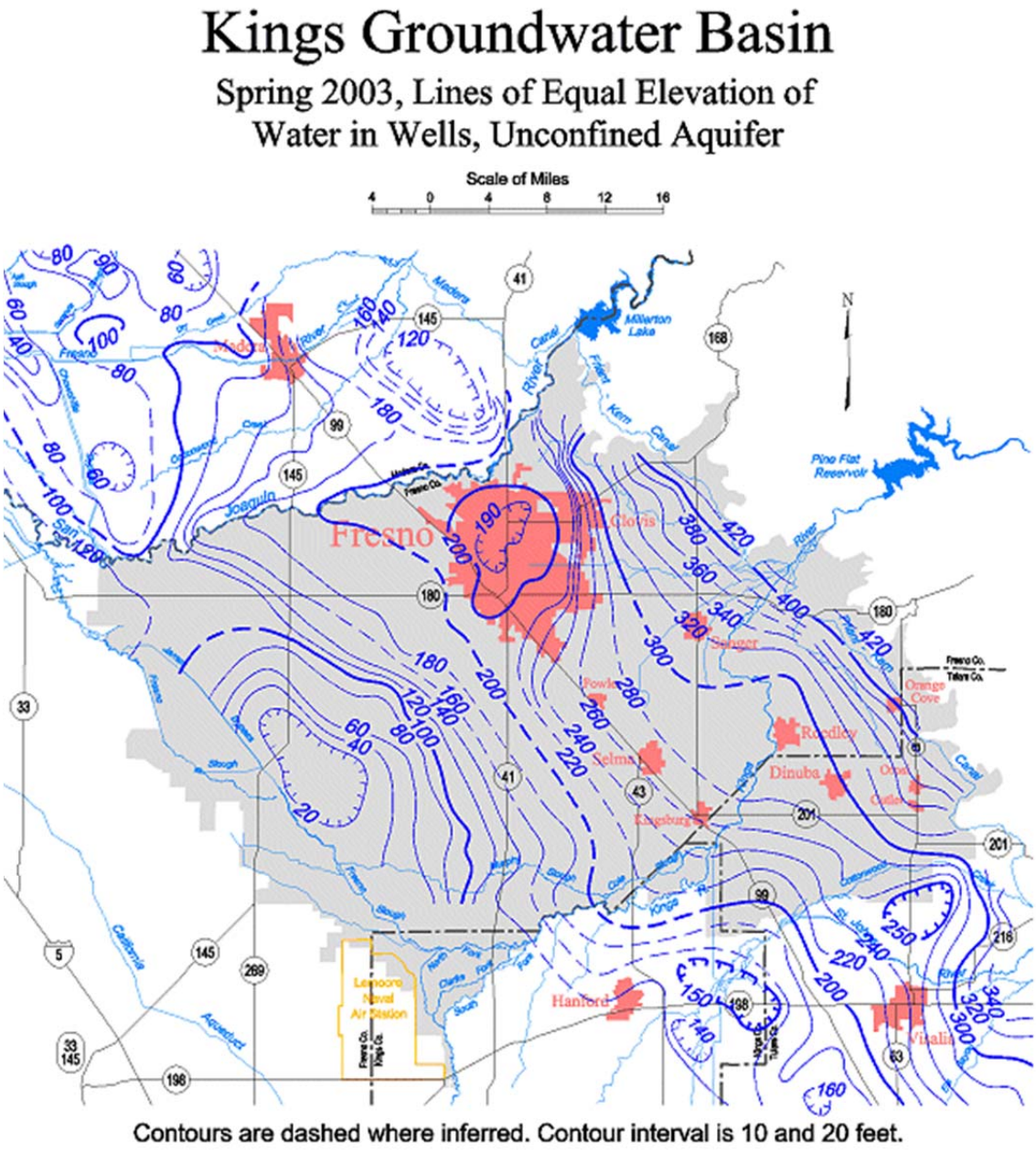

E 21 Unconfined aquifer groundwater contour map, Kings groundwater basin, Spring 2003.

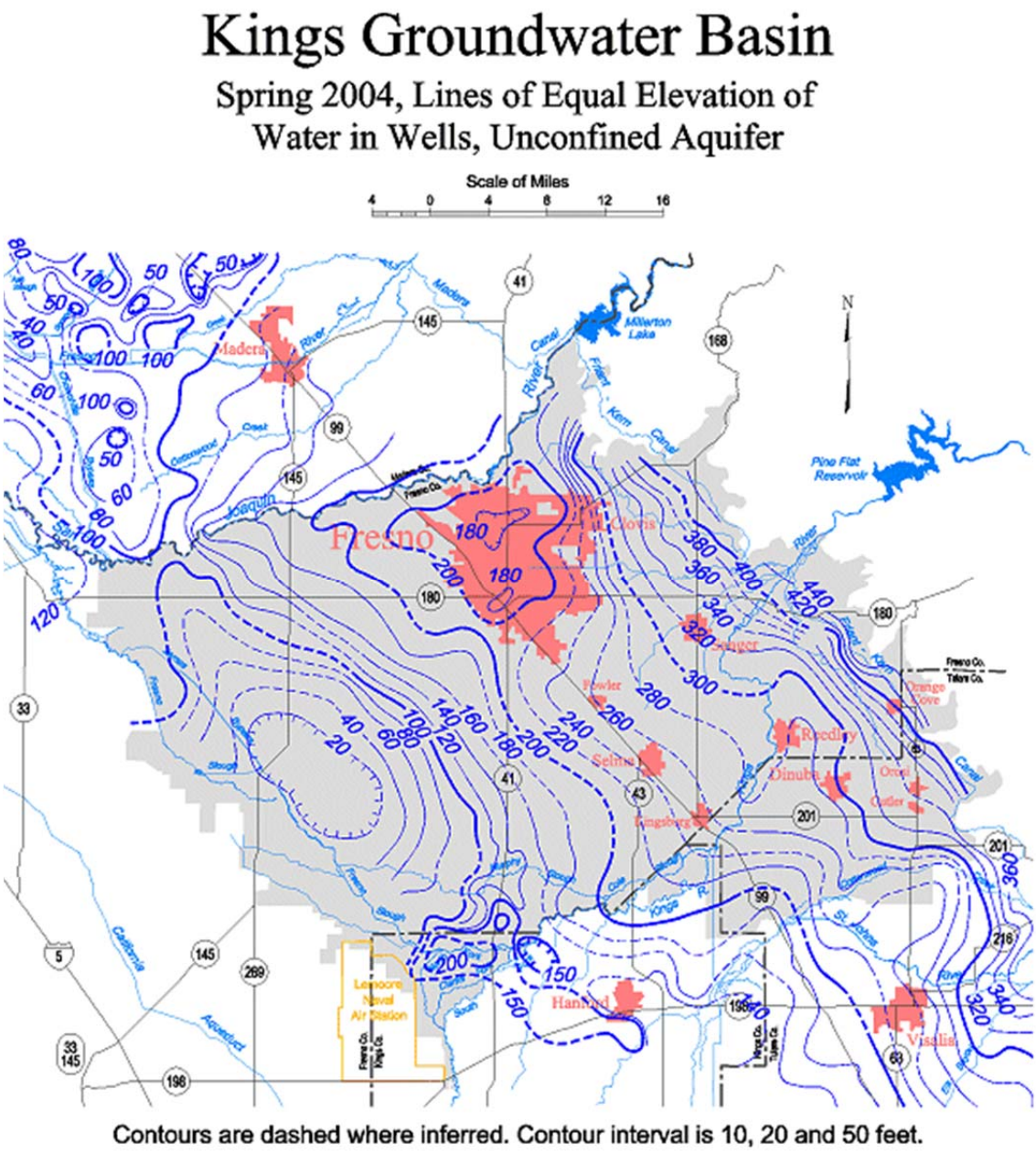

E 22 Unconfined aquifer groundwater contour map, Kings groundwater basin, Spring 2004.

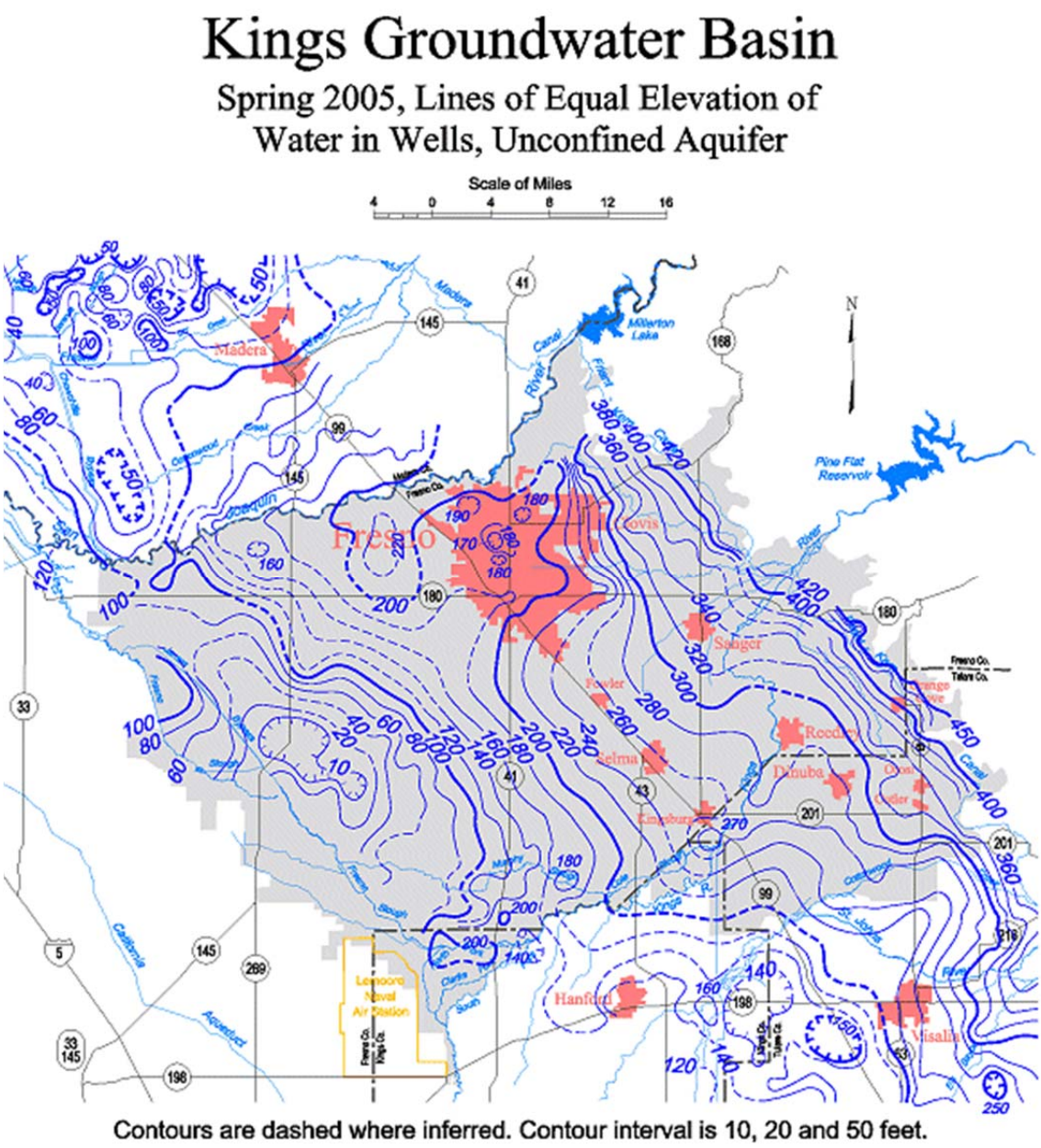

E 23 Unconfined aquifer groundwater contour map, Kings groundwater basin, Spring 2005.

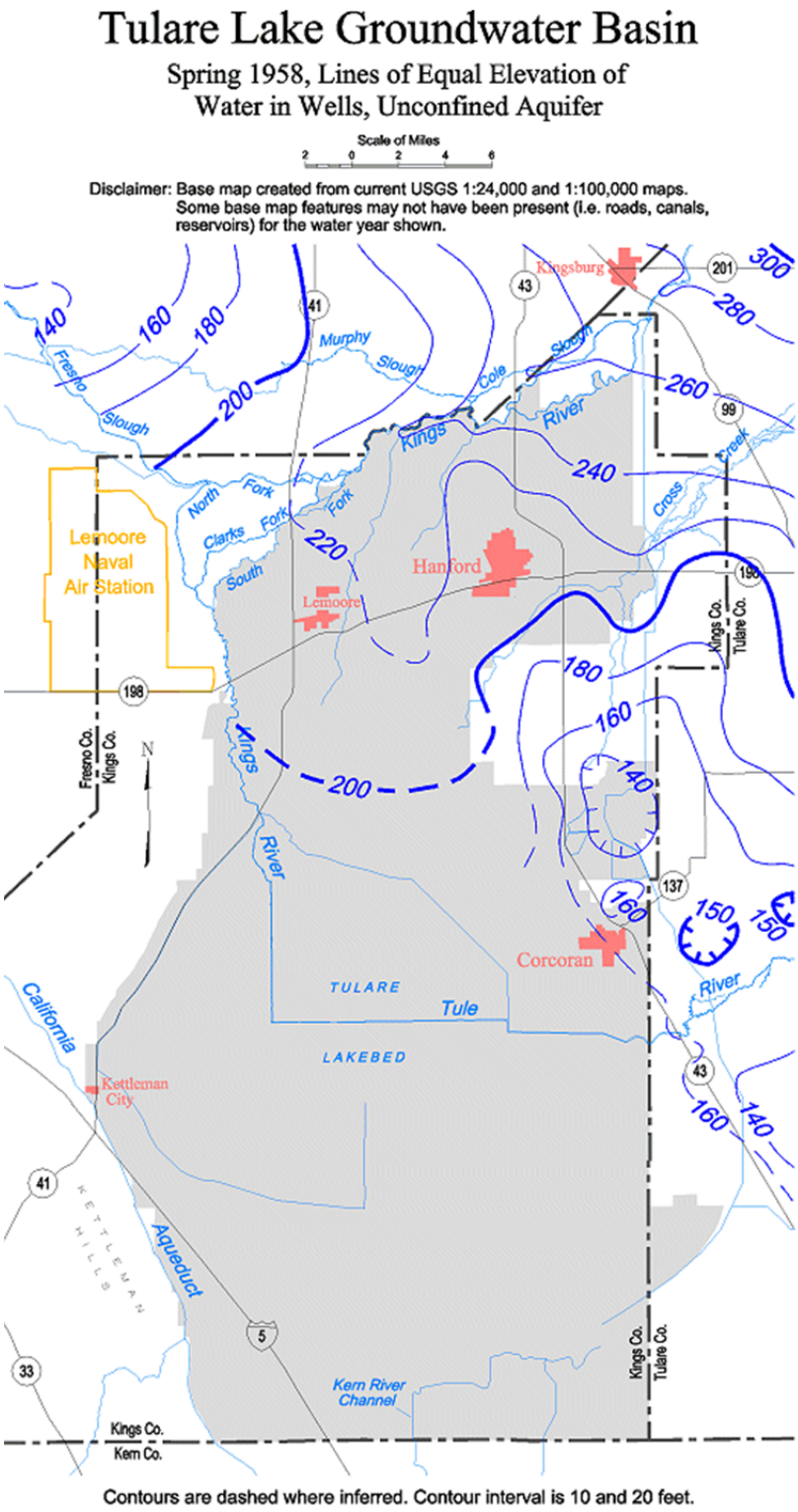

E 24 Unconfined aquifer groundwater contour map, Tulare Lake groundwater basin, Spring 1958.

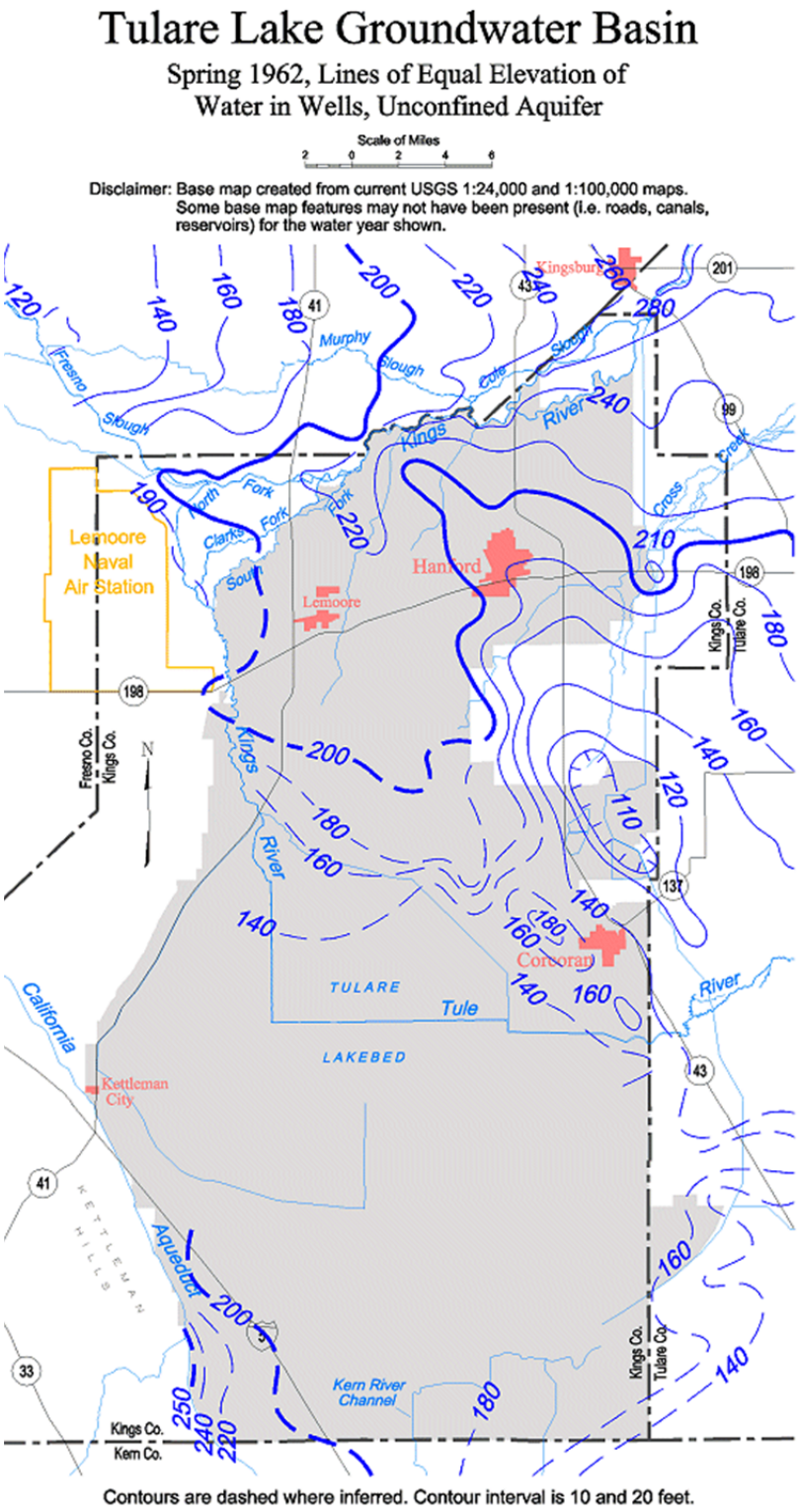

E 25 Unconfined aquifer groundwater contour map, Tulare Lake groundwater basin, Spring 1962.

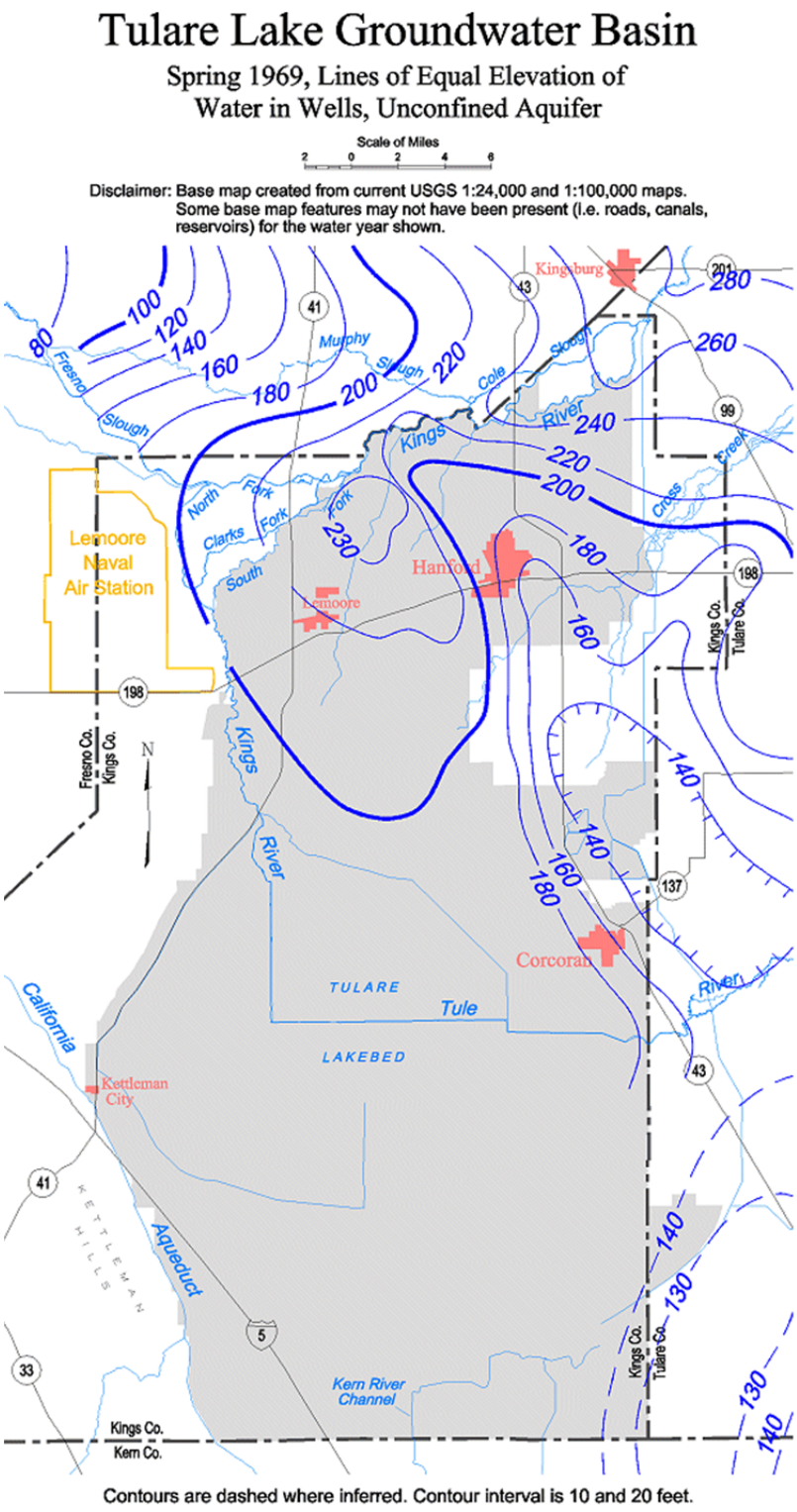

E 26 Unconfined aquifer groundwater contour map, Tulare Lake groundwater basin, Spring 1969.

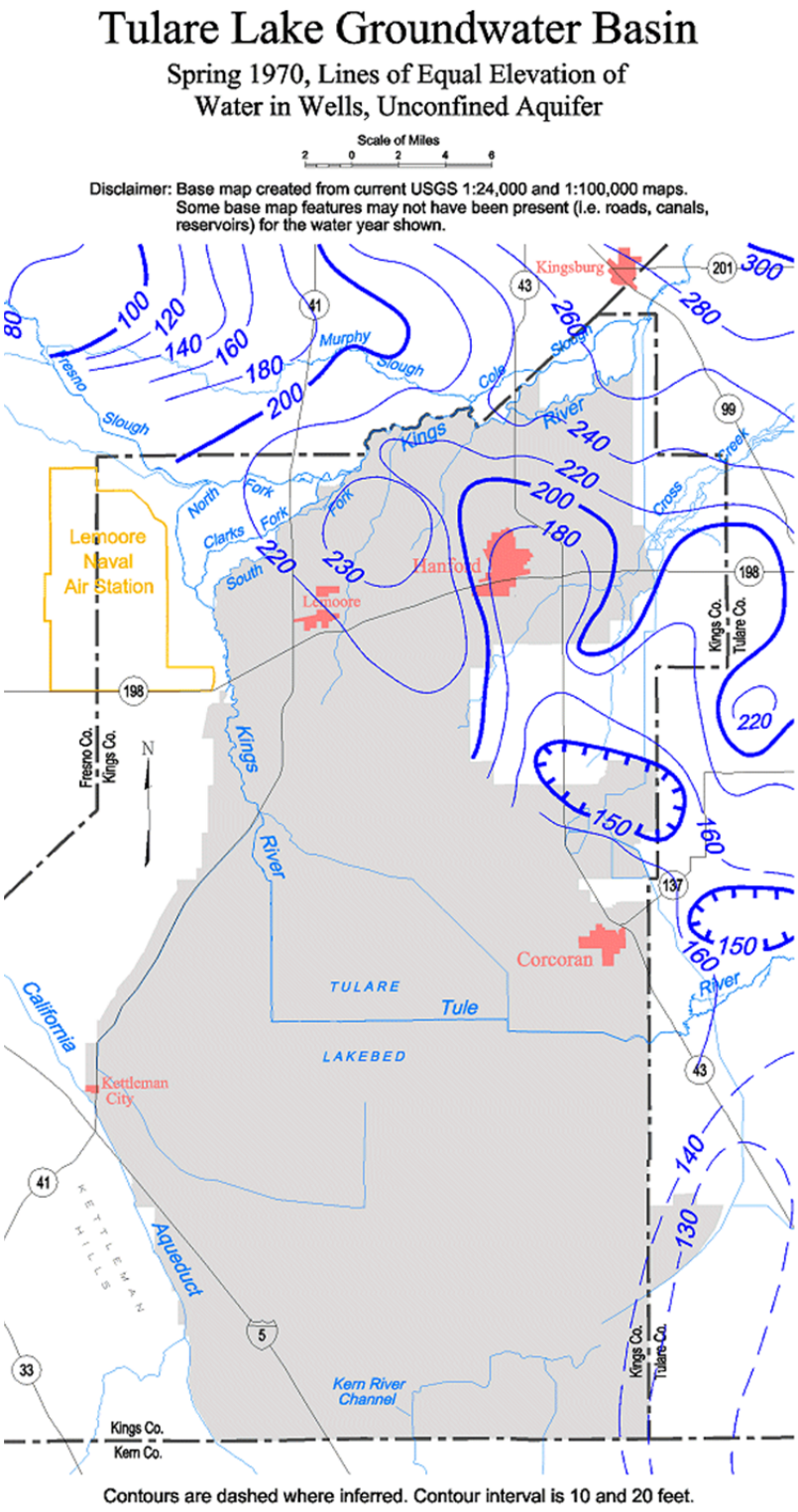

E 27 Unconfined aquifer groundwater contour map, Tulare Lake groundwater basin, Spring 1970.

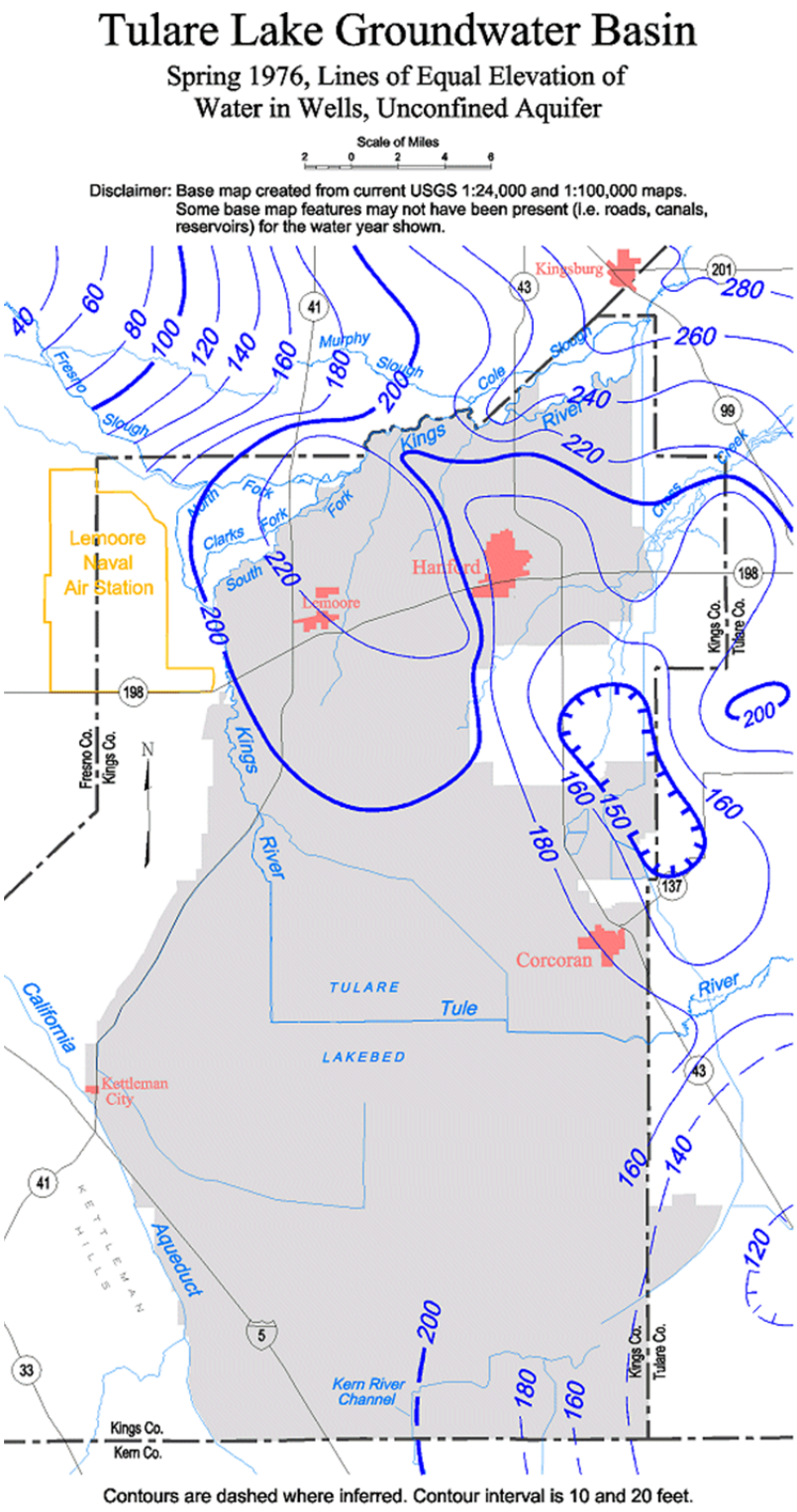

E 28 Unconfined aquifer groundwater contour map, Tulare Lake groundwater basin, Spring 1976.

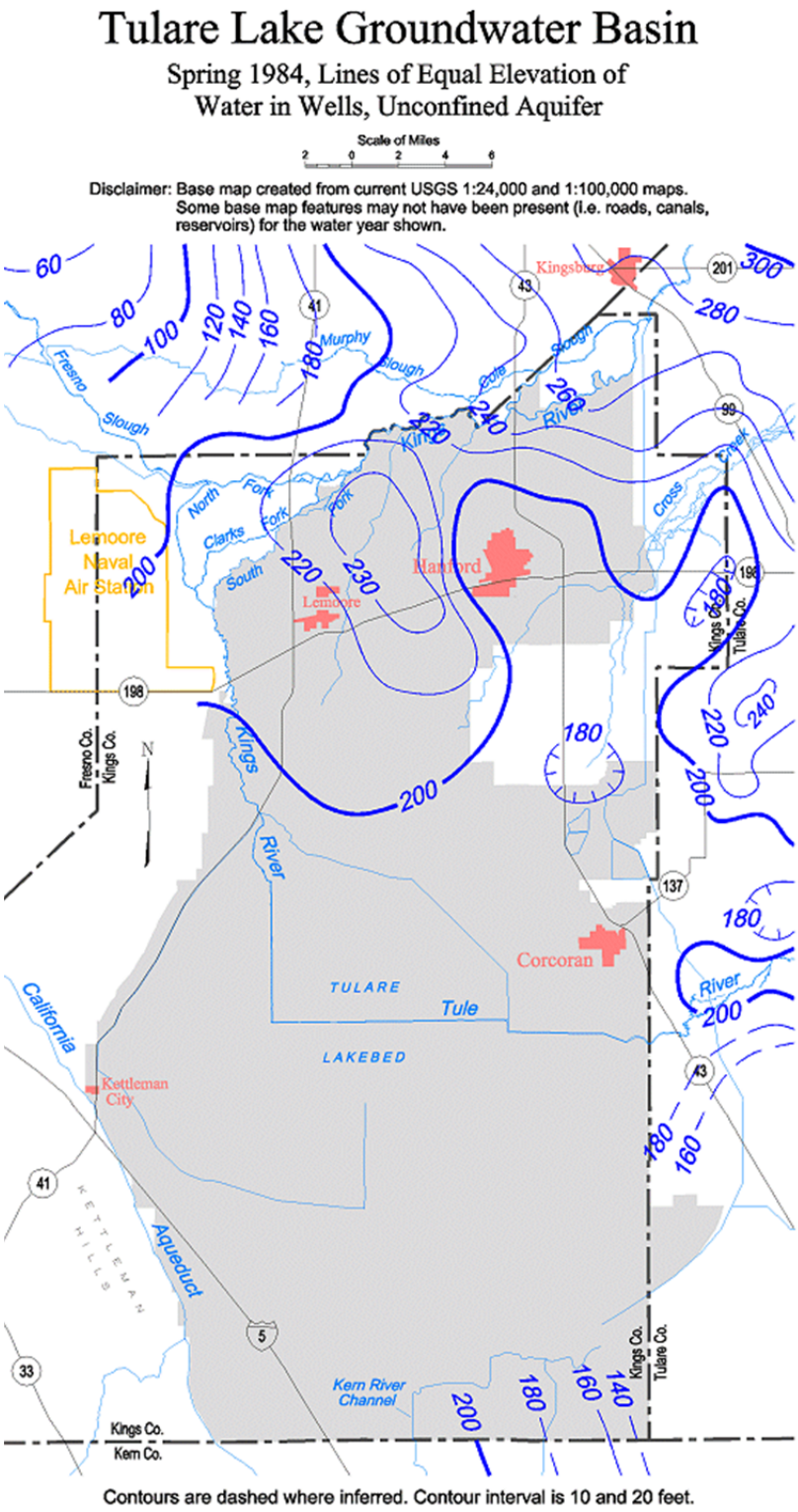

E 29 Unconfined aquifer groundwater contour map, Tulare Lake groundwater basin, Spring 1984.

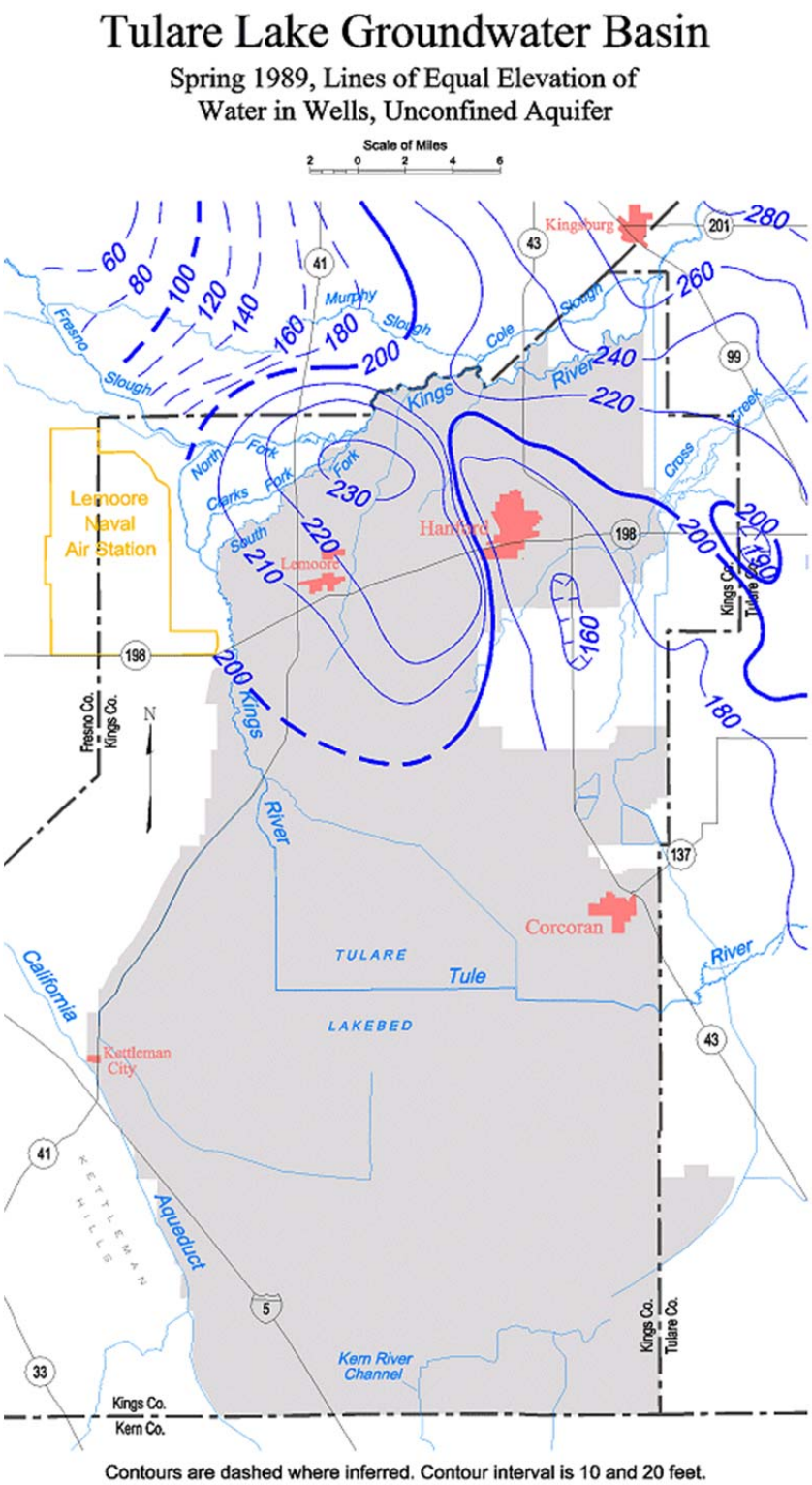

E 30 Unconfined aquifer groundwater contour map, Tulare Lake groundwater basin, Spring 1989.

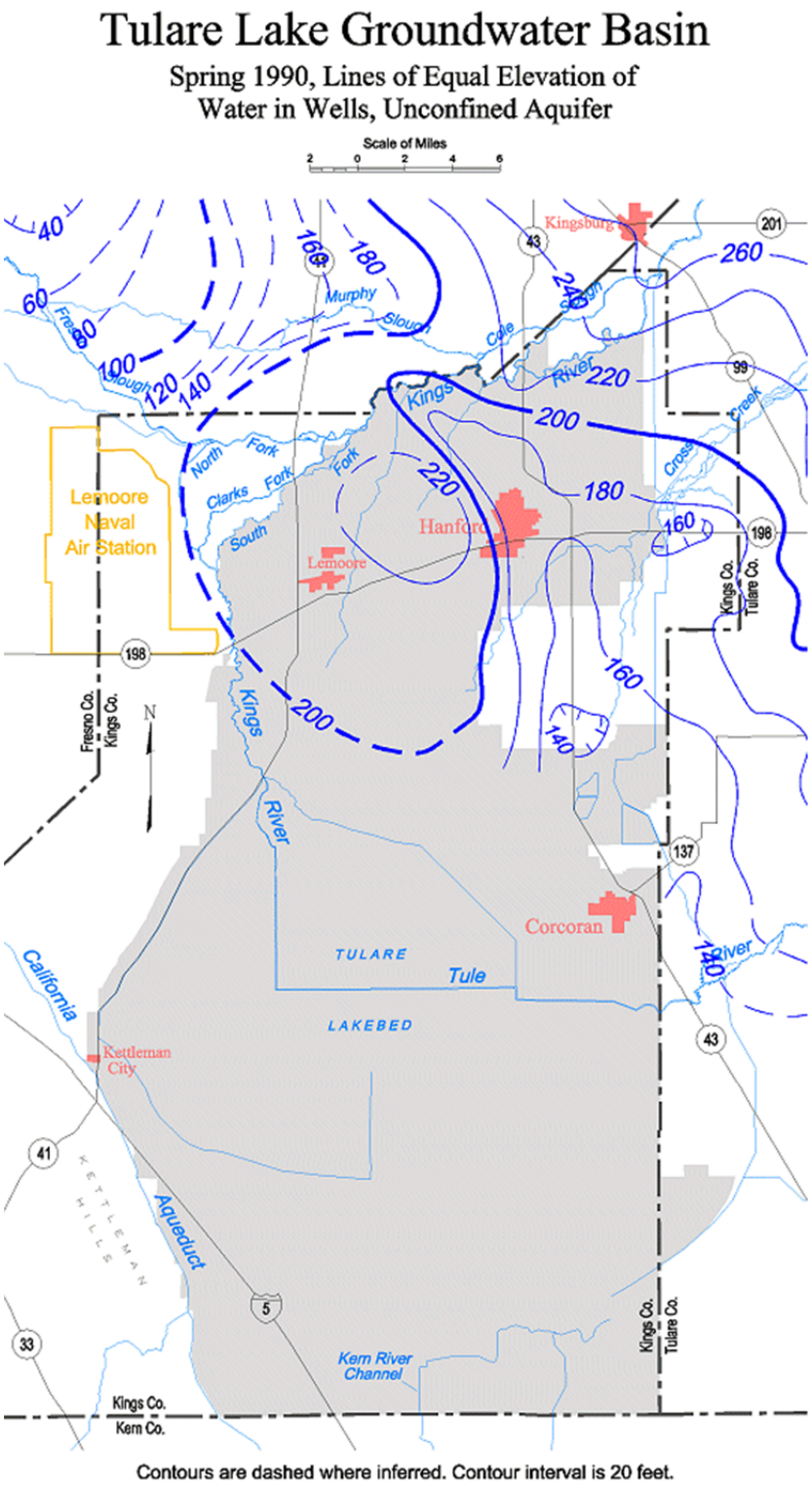

E 31 Unconfined aquifer groundwater contour map, Tulare Lake groundwater basin, Spring 1990.

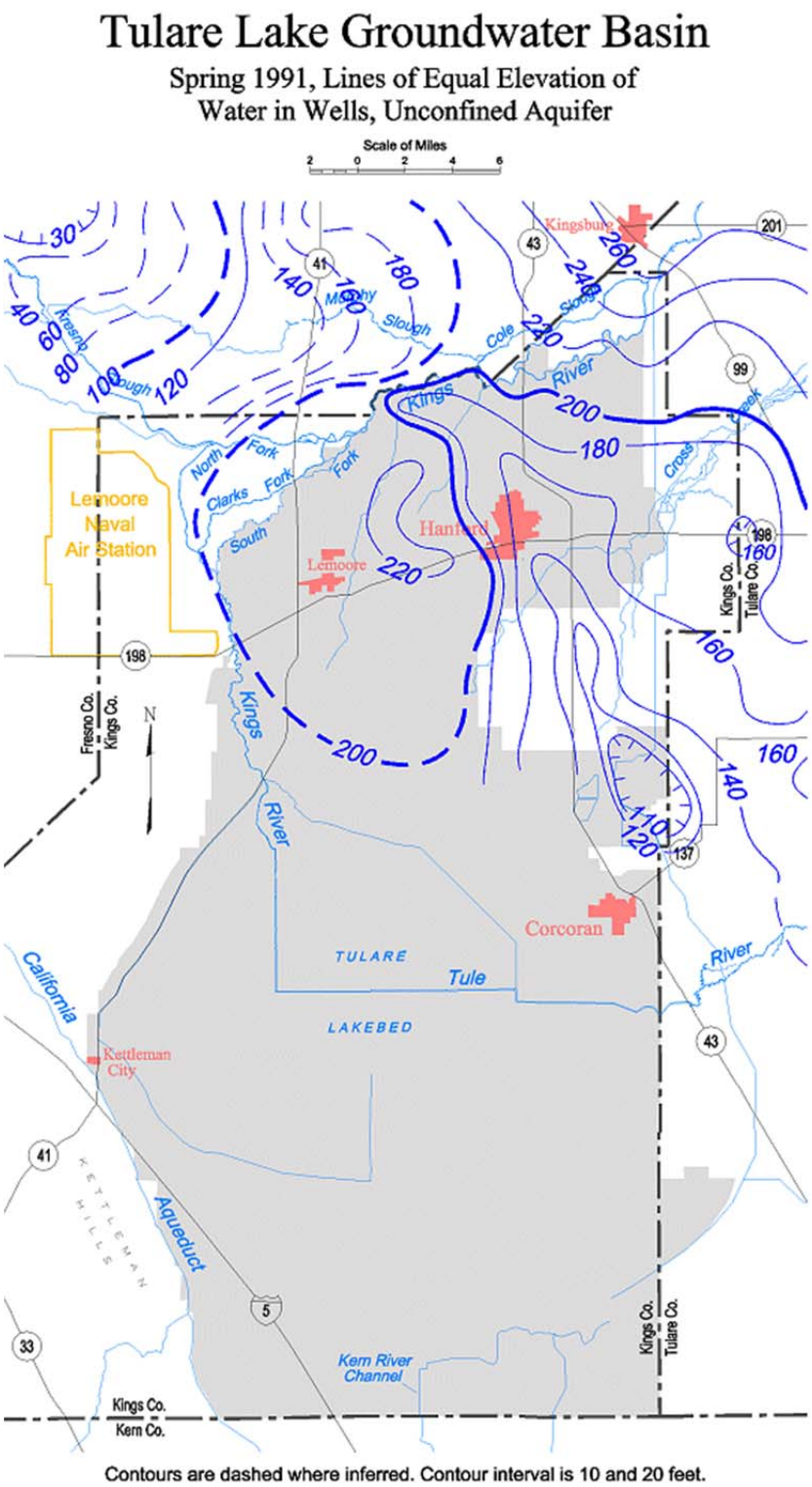

E 32 Unconfined aquifer groundwater contour map, Tulare Lake groundwater basin, Spring 1991.

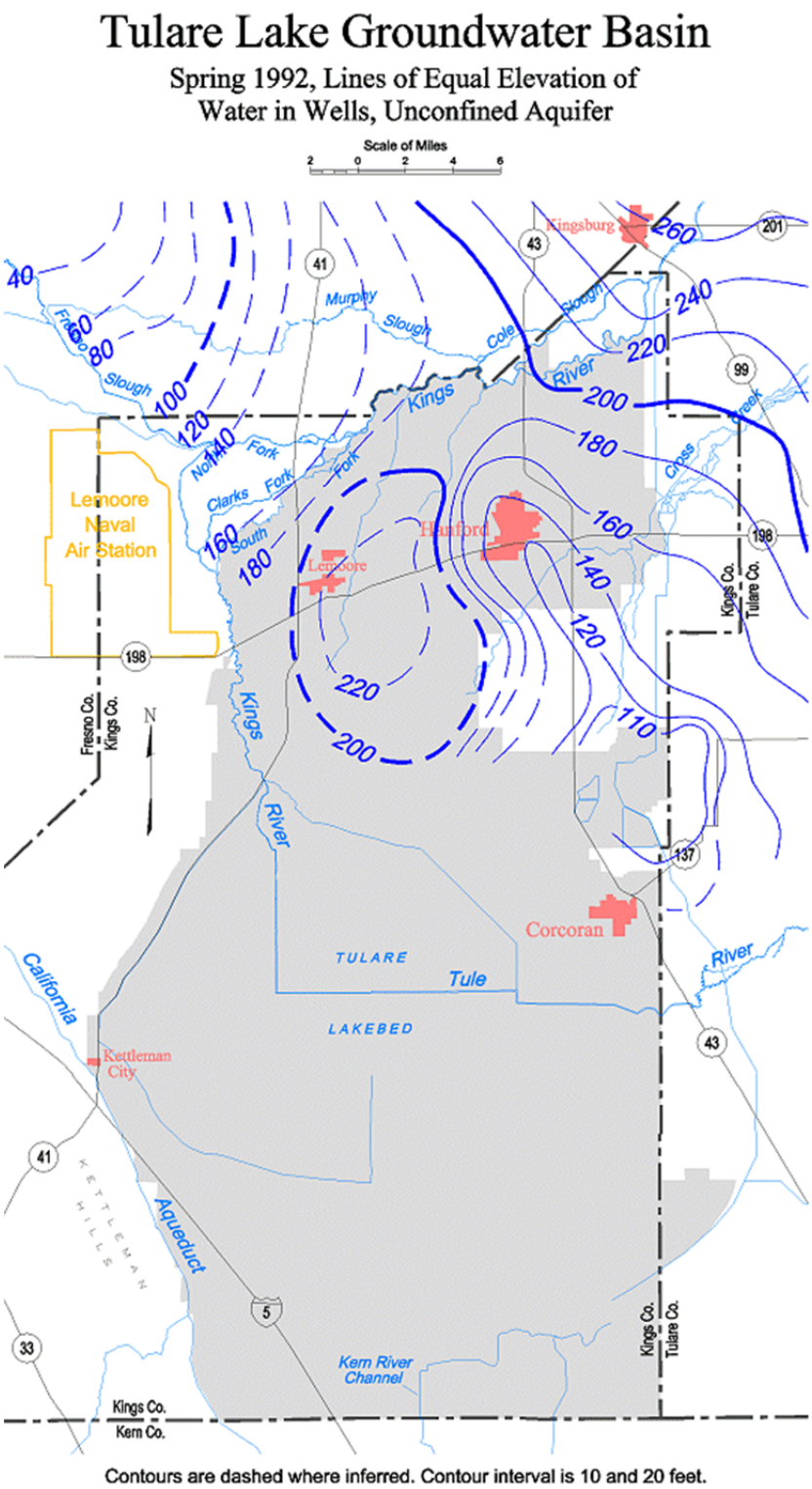

E 33 Unconfined aquifer groundwater contour map, Tulare Lake groundwater basin, Spring 1992.

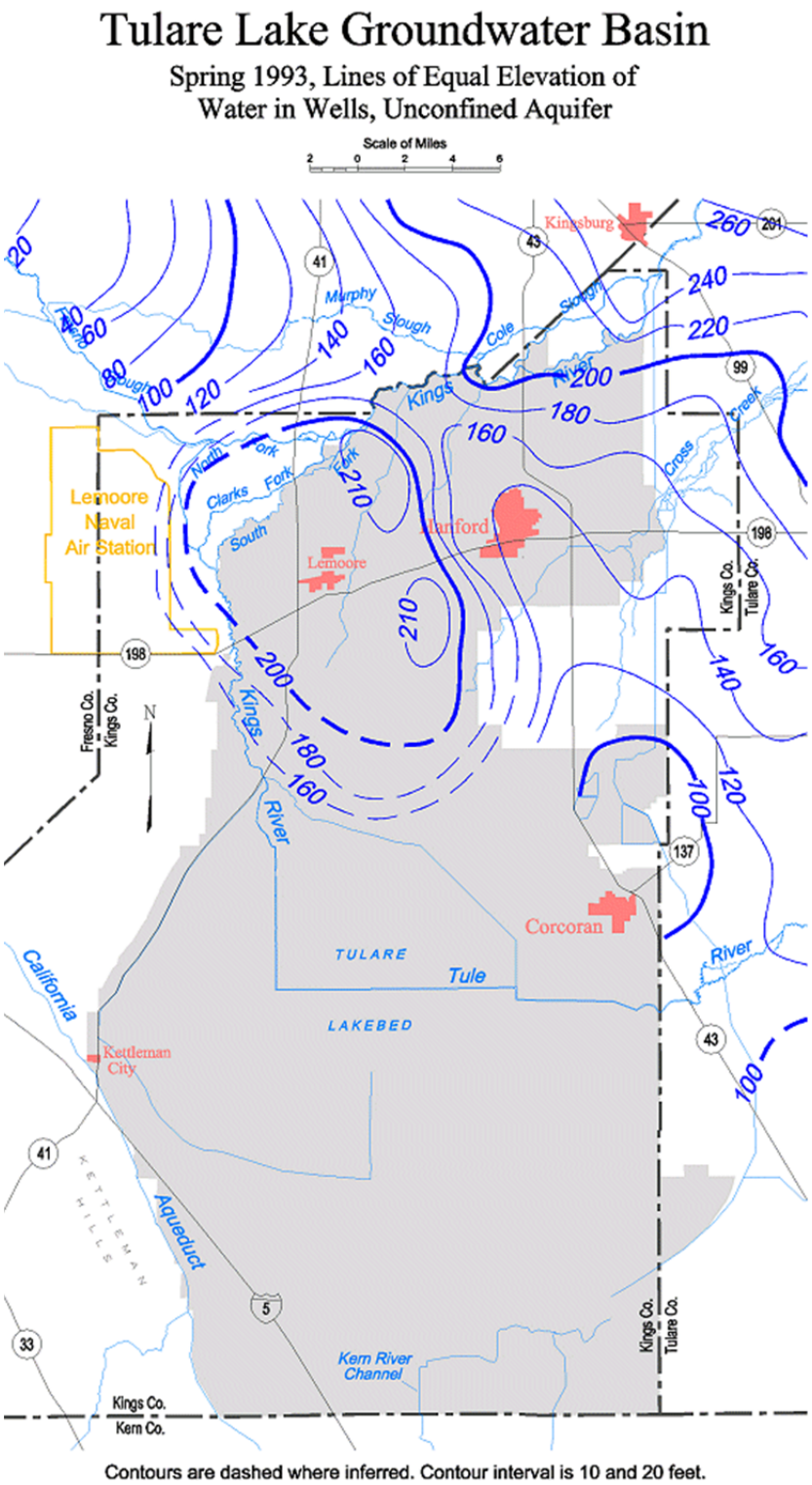

E 34 Unconfined aquifer groundwater contour map, Tulare Lake groundwater basin, Spring 1993.

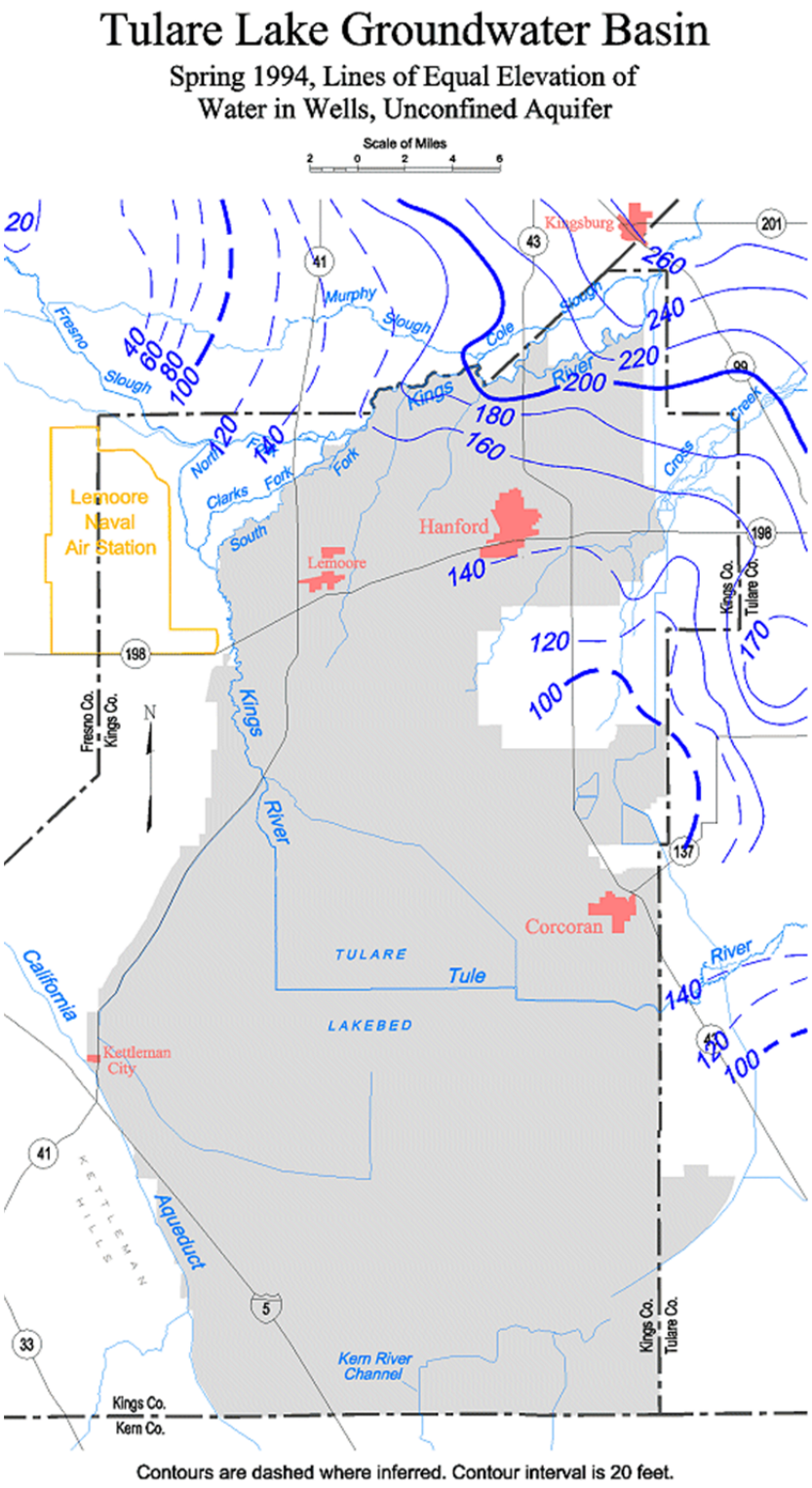

E 35 Unconfined aquifer groundwater contour map, Tulare Lake groundwater basin, Spring 1994.

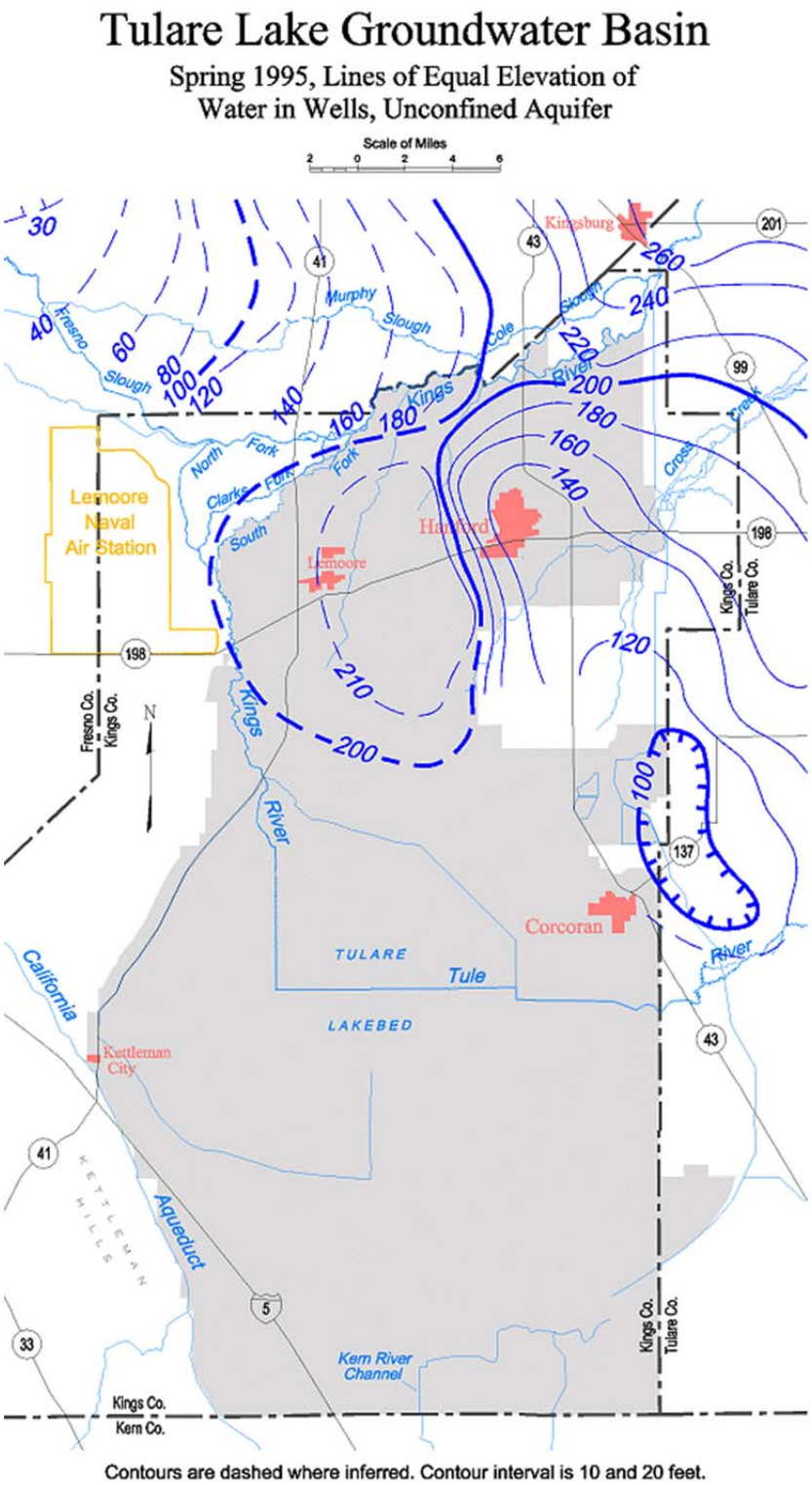

E 36 Unconfined aquifer groundwater contour map, Tulare Lake groundwater basin, Spring 1995.

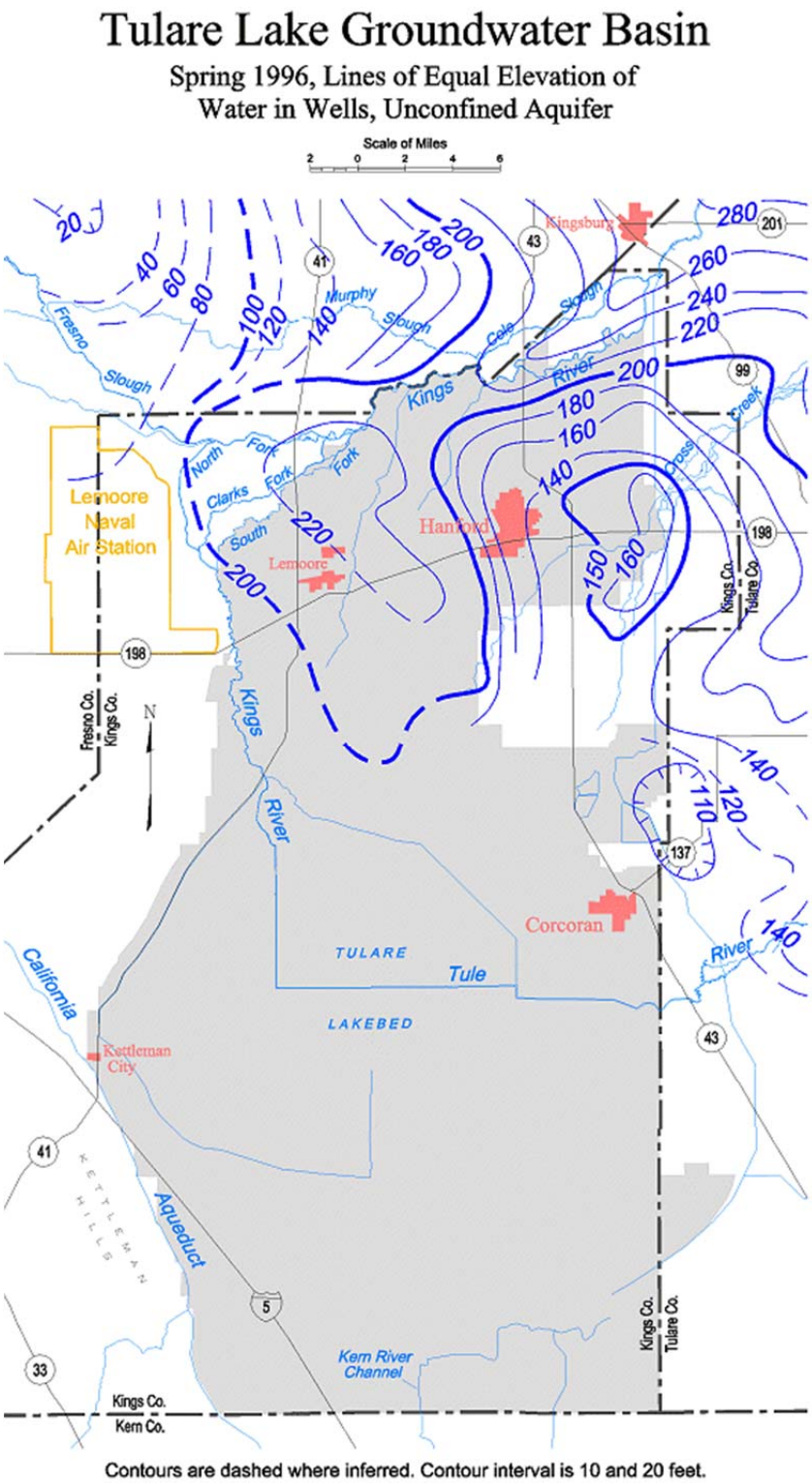

E 37 Unconfined aquifer groundwater contour map, Tulare Lake groundwater basin, Spring 1996.

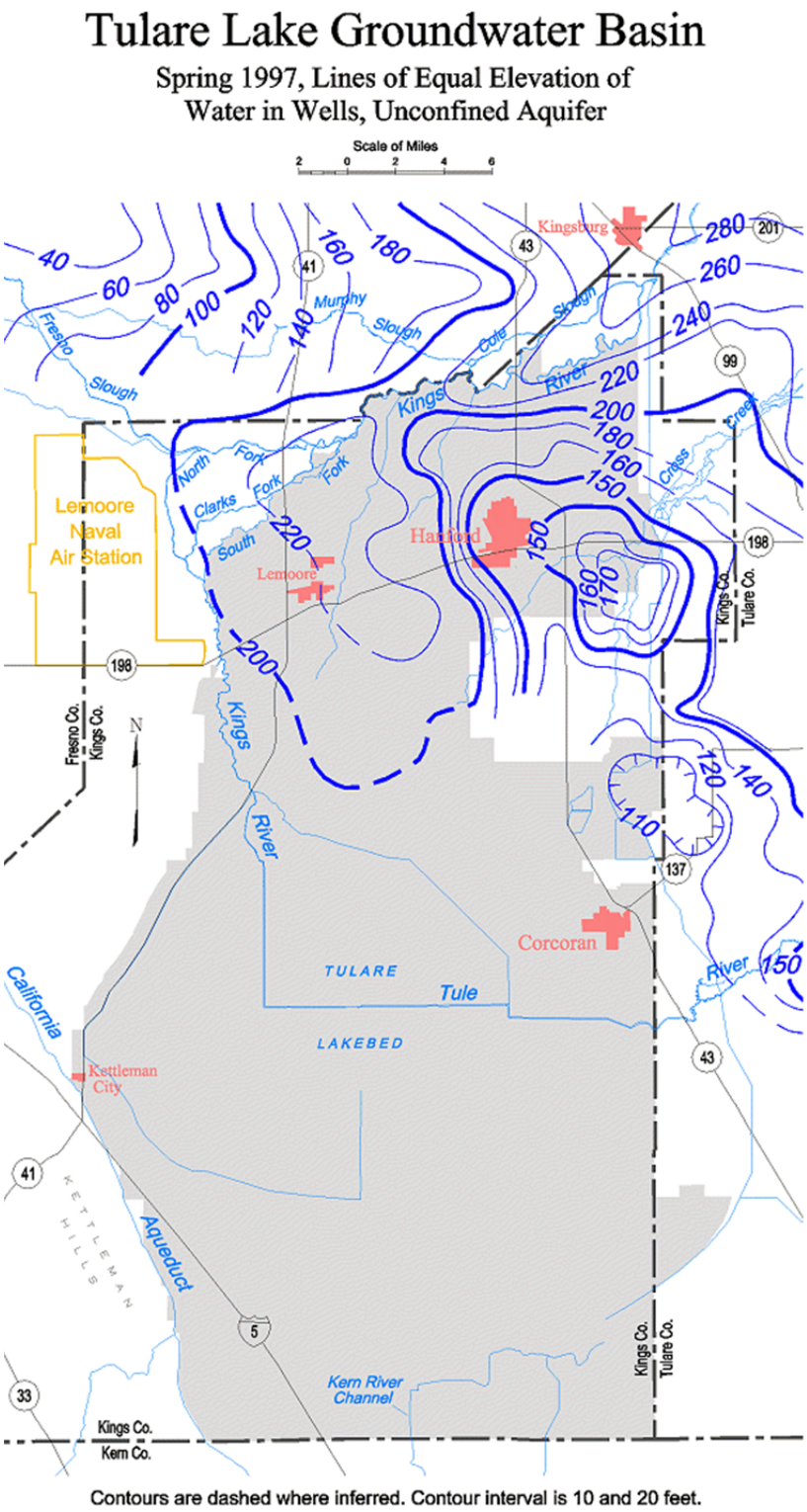

E 38 Unconfined aquifer groundwater contour map, Tulare Lake groundwater basin, Spring 1997.

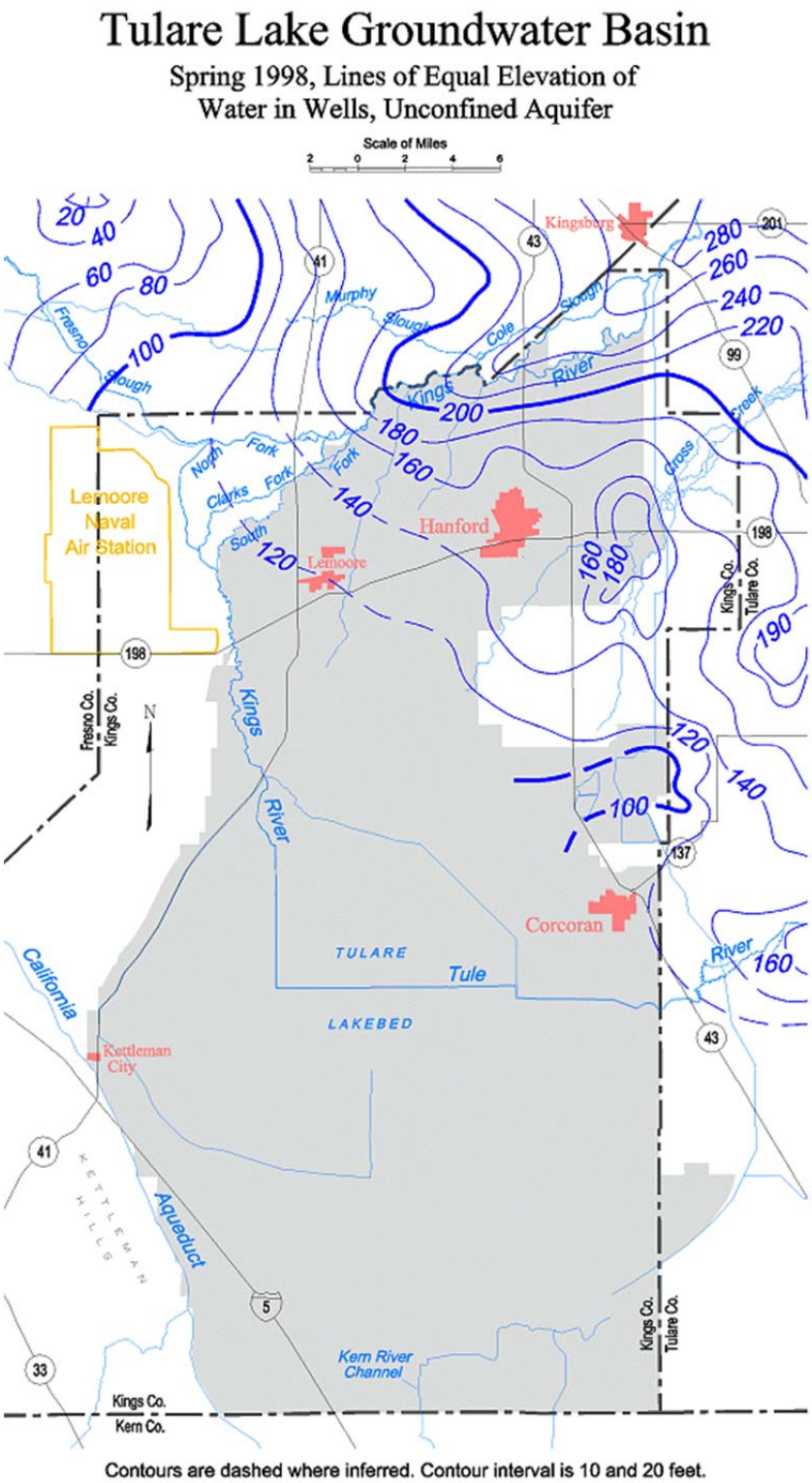

E 39 Unconfined aquifer groundwater contour map, Tulare Lake groundwater basin, Spring 1998.

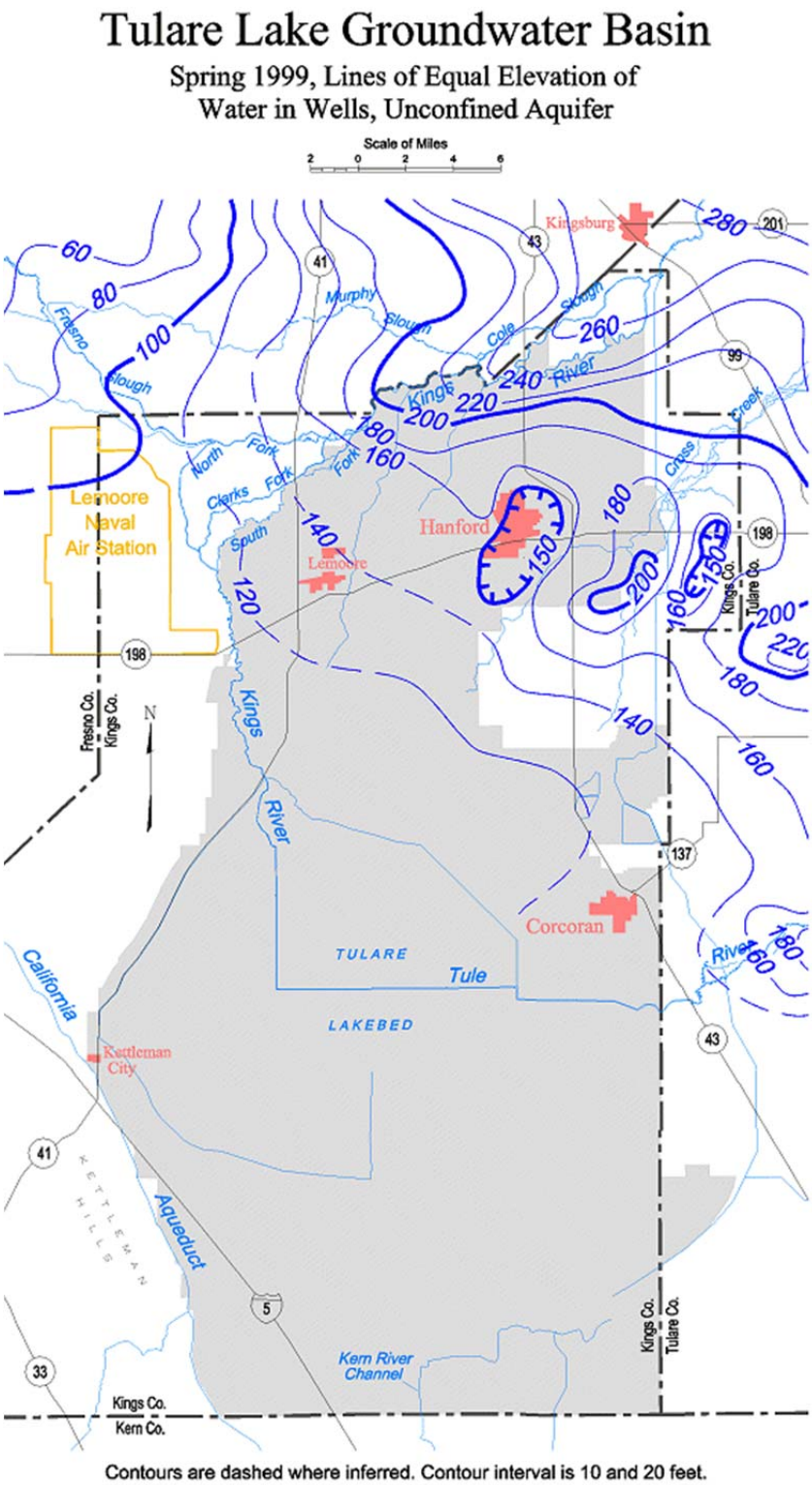

E 40 Unconfined aquifer groundwater contour map, Tulare Lake groundwater basin, Spring 1999.

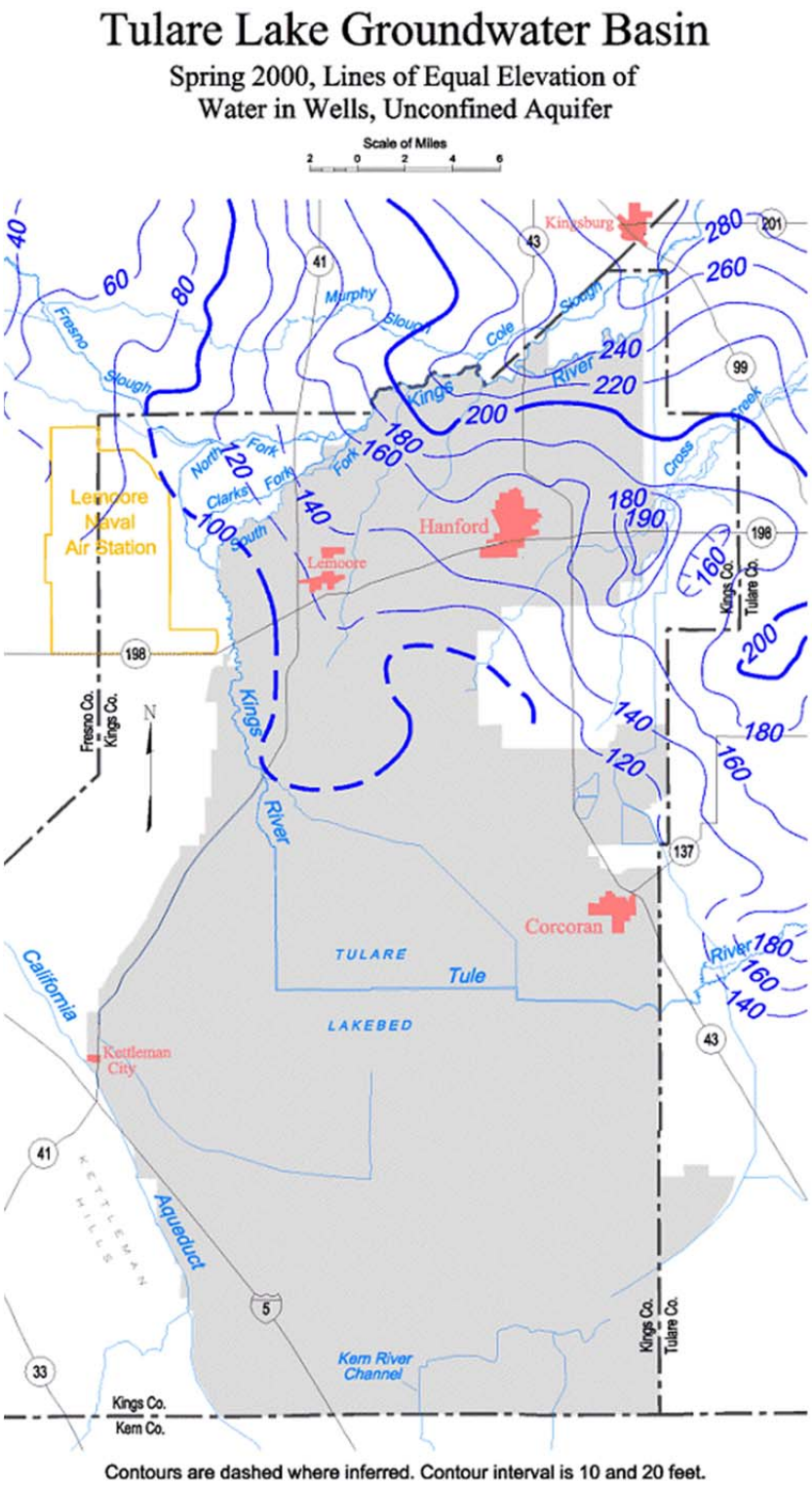

E 41 Unconfined aquifer groundwater contour map, Tulare Lake groundwater basin, Spring 2000.

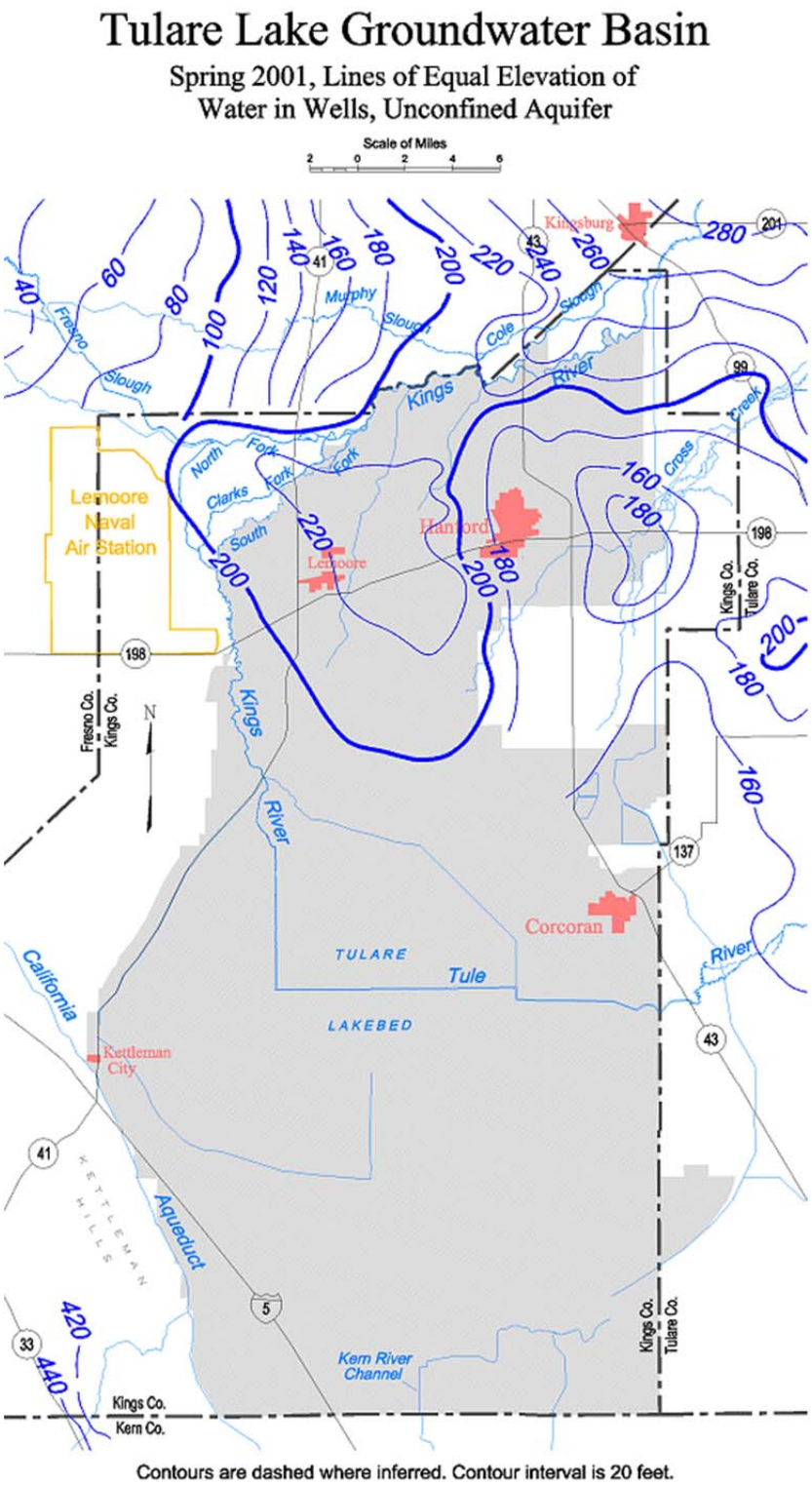

E 42 Unconfined aquifer groundwater contour map, Tulare Lake groundwater basin, Spring 2001.

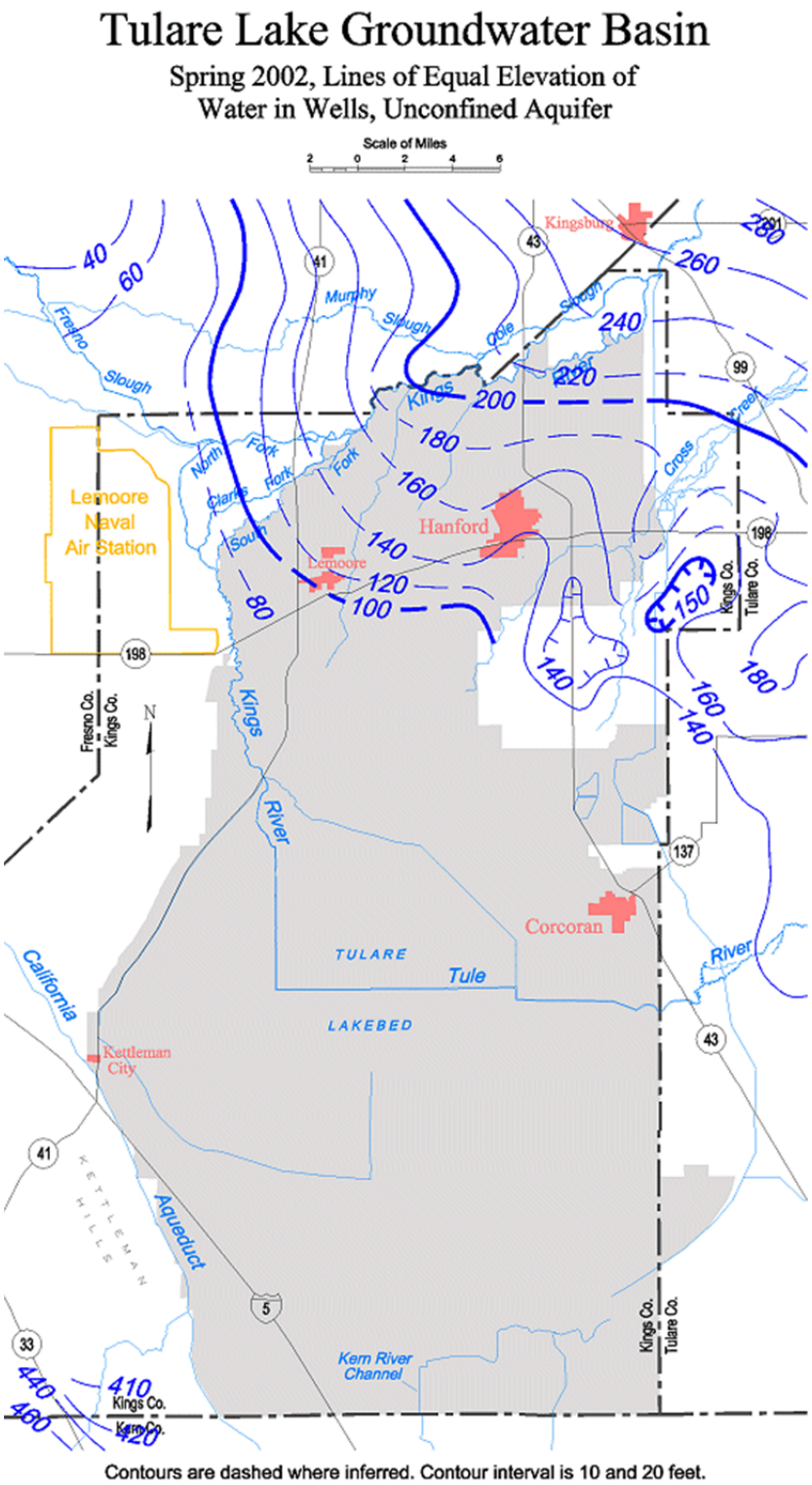

E 43 Unconfined aquifer groundwater contour map, Tulare Lake groundwater basin, Spring 2002.

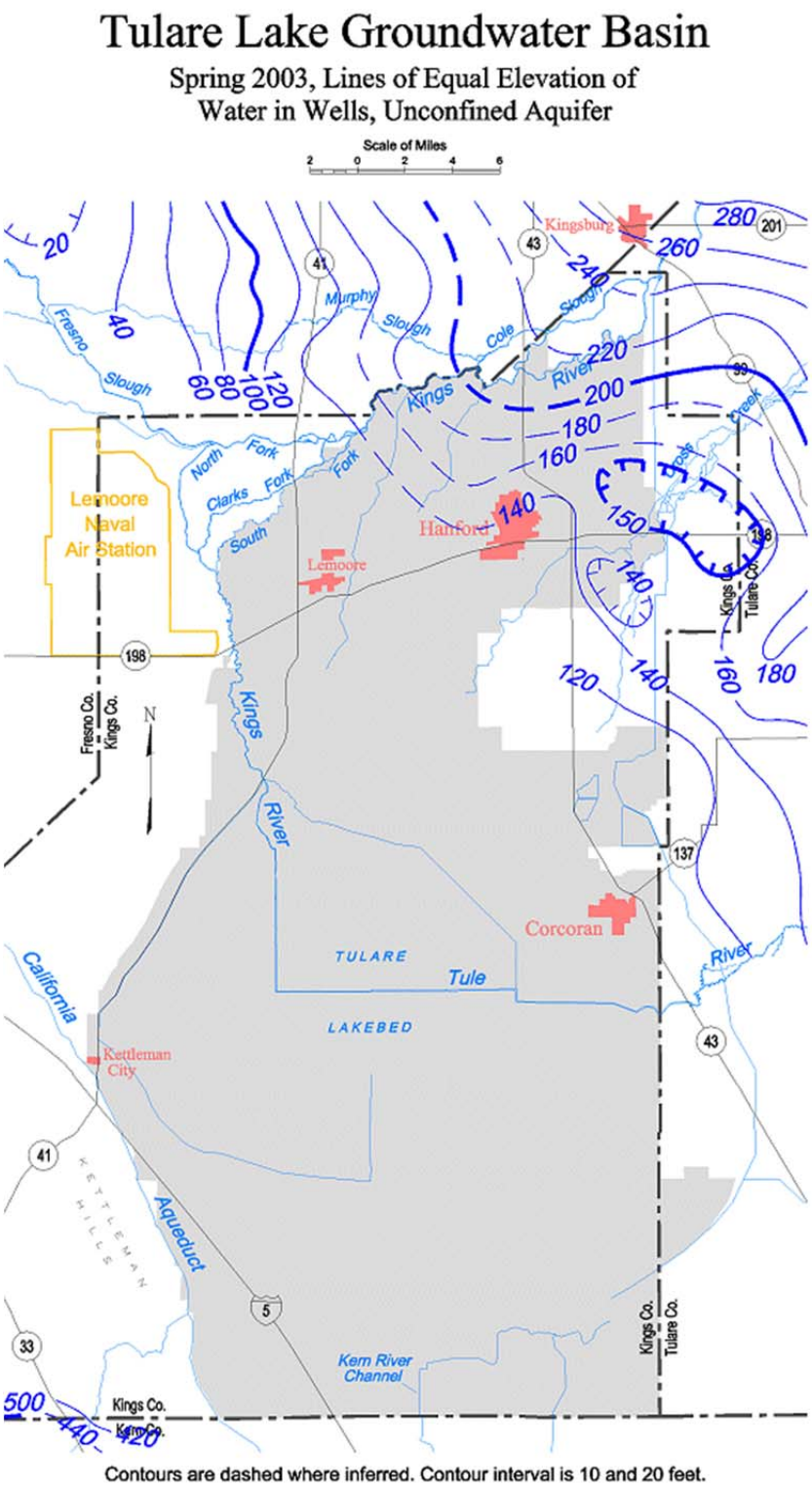

E 44 Unconfined aquifer groundwater contour map, Tulare Lake groundwater basin, Spring 2003.

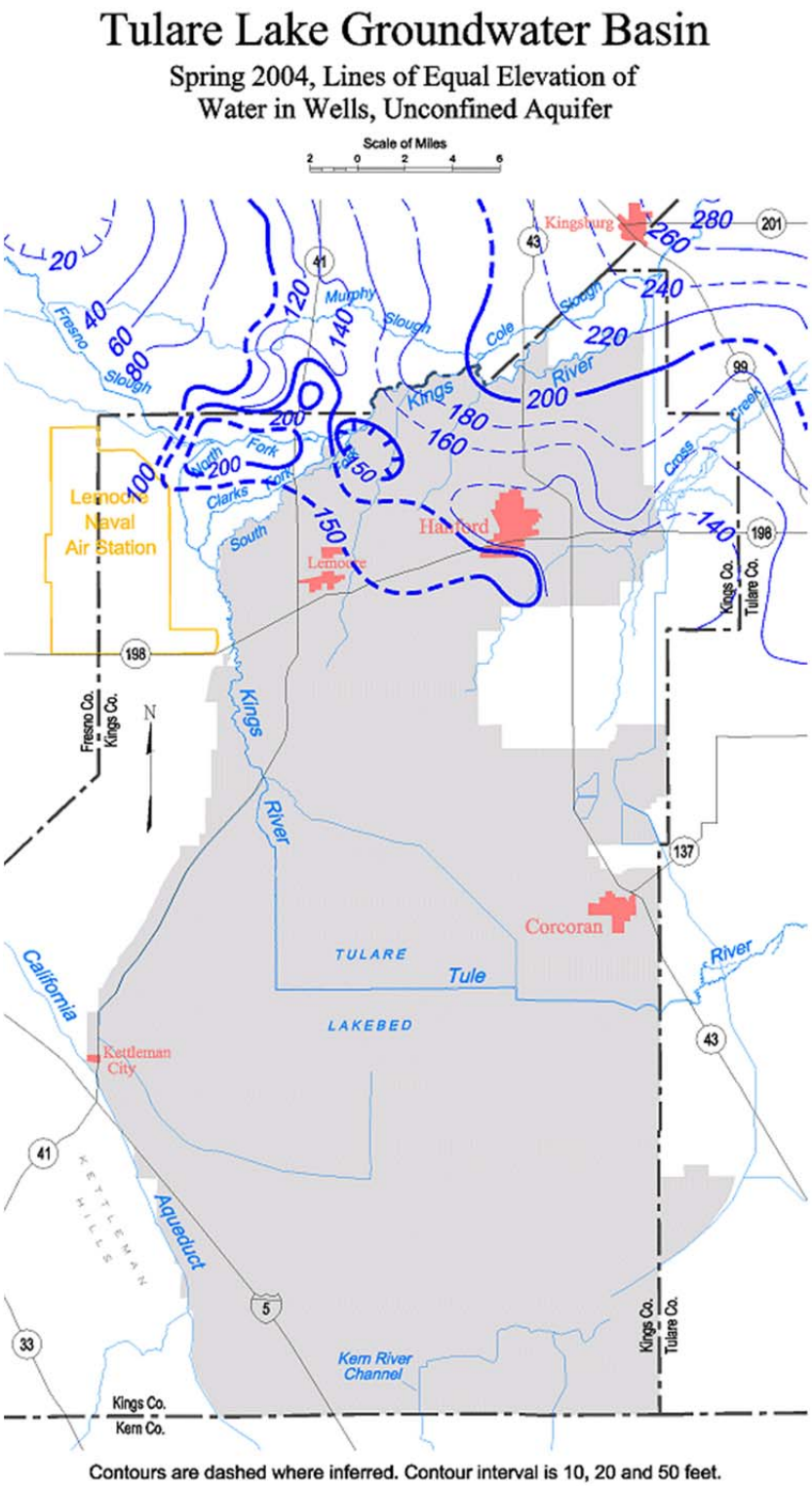

E 45 Unconfined aquifer groundwater contour map, Tulare Lake groundwater basin, Spring 2004.

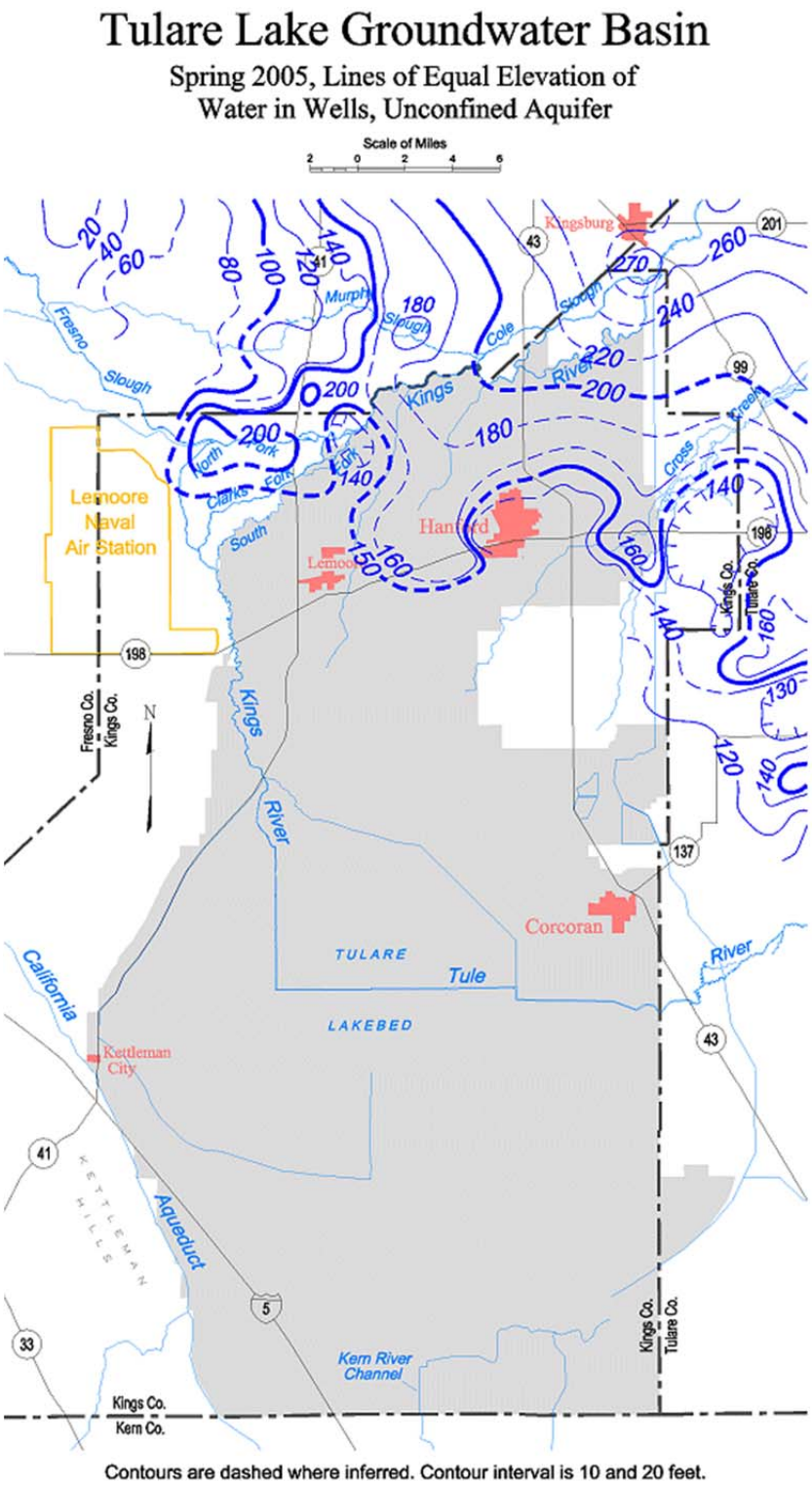

E 46 Unconfined aquifer groundwater contour map, Tulare Lake groundwater basin, Spring 2005.

Appendix F ArcGIS© databases

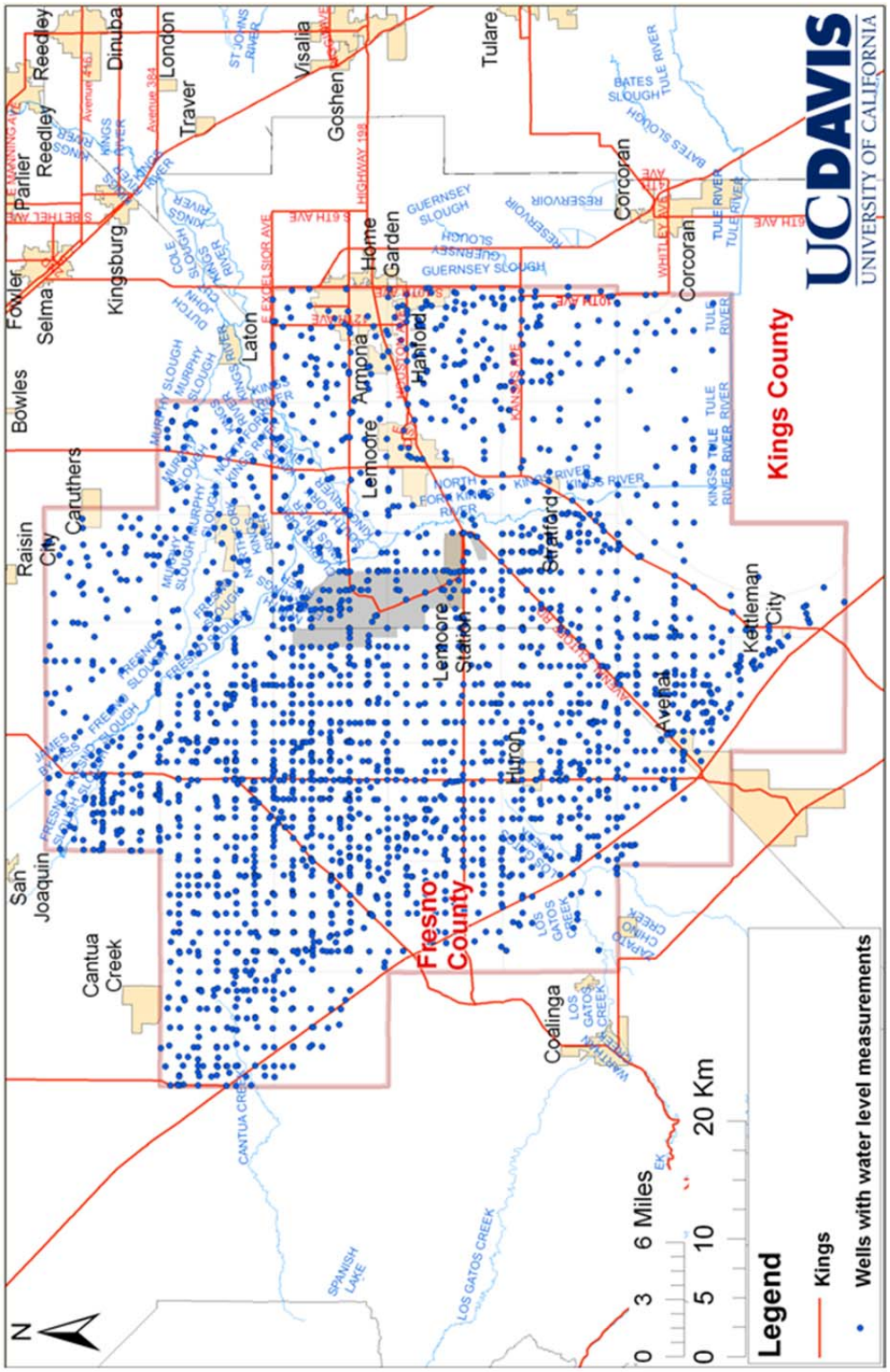

F 1 Wells with water level measurements available (CDWR WDL website, 2010).

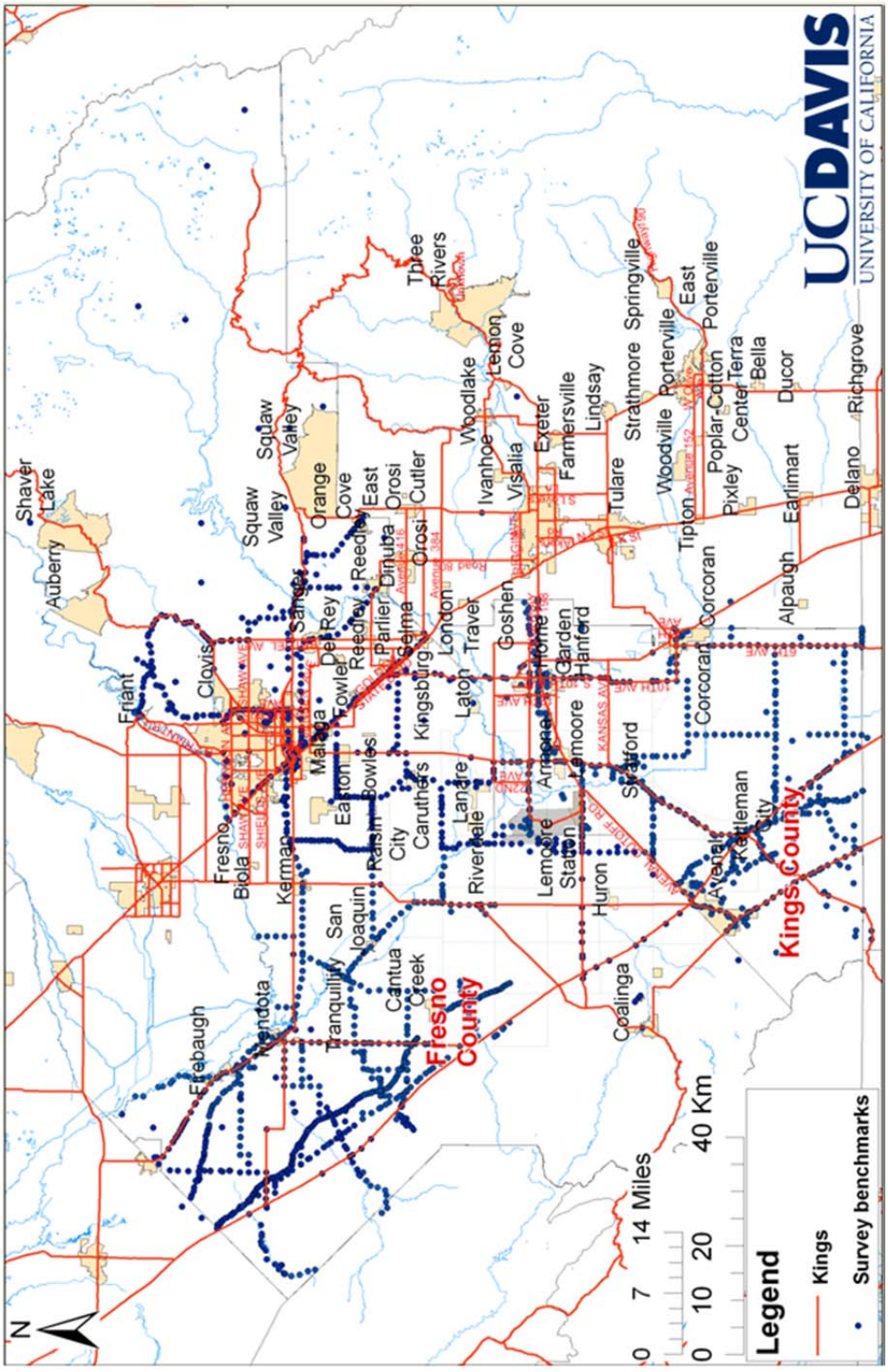

F 2 All survey benchmarks within Fresno and Kings Counties, California (obtained from NGS website, 2010).

Appendix G: Crop maps at Naval Air Station Lemoore, 1974 – 2010

[Shown on the following unnumbered pages]

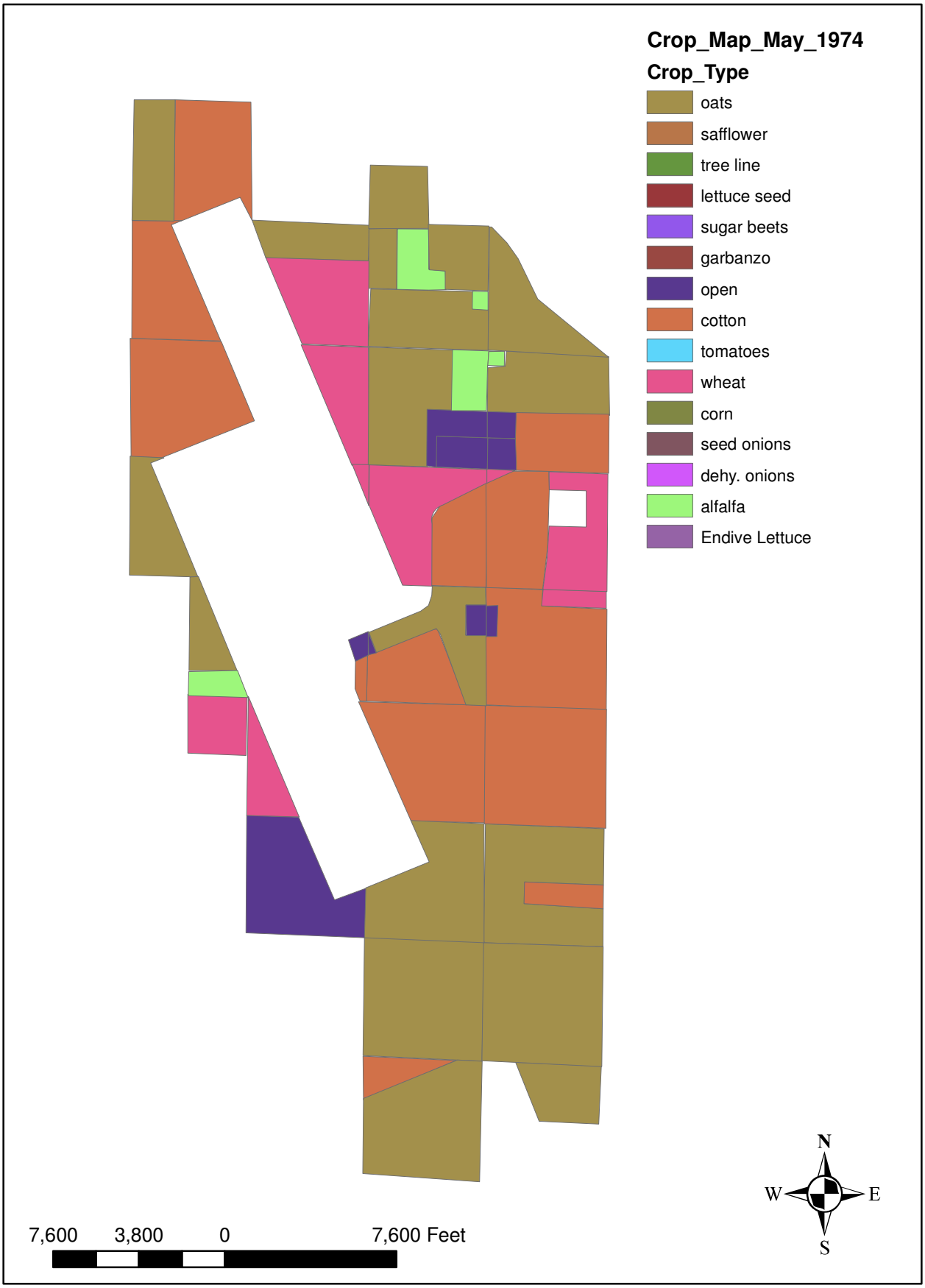
Crop_Map_May_1974
Crop_Type
oats
safflower
tree line
lettuce seed
sugar beets
garbanzo
open
cotton
tomatoes
wheat
corn
seed onions
dehy. onions
alfalfa
Endive Lettuce
N
W
E
S
7,600
3,800
0
7,600 Feet

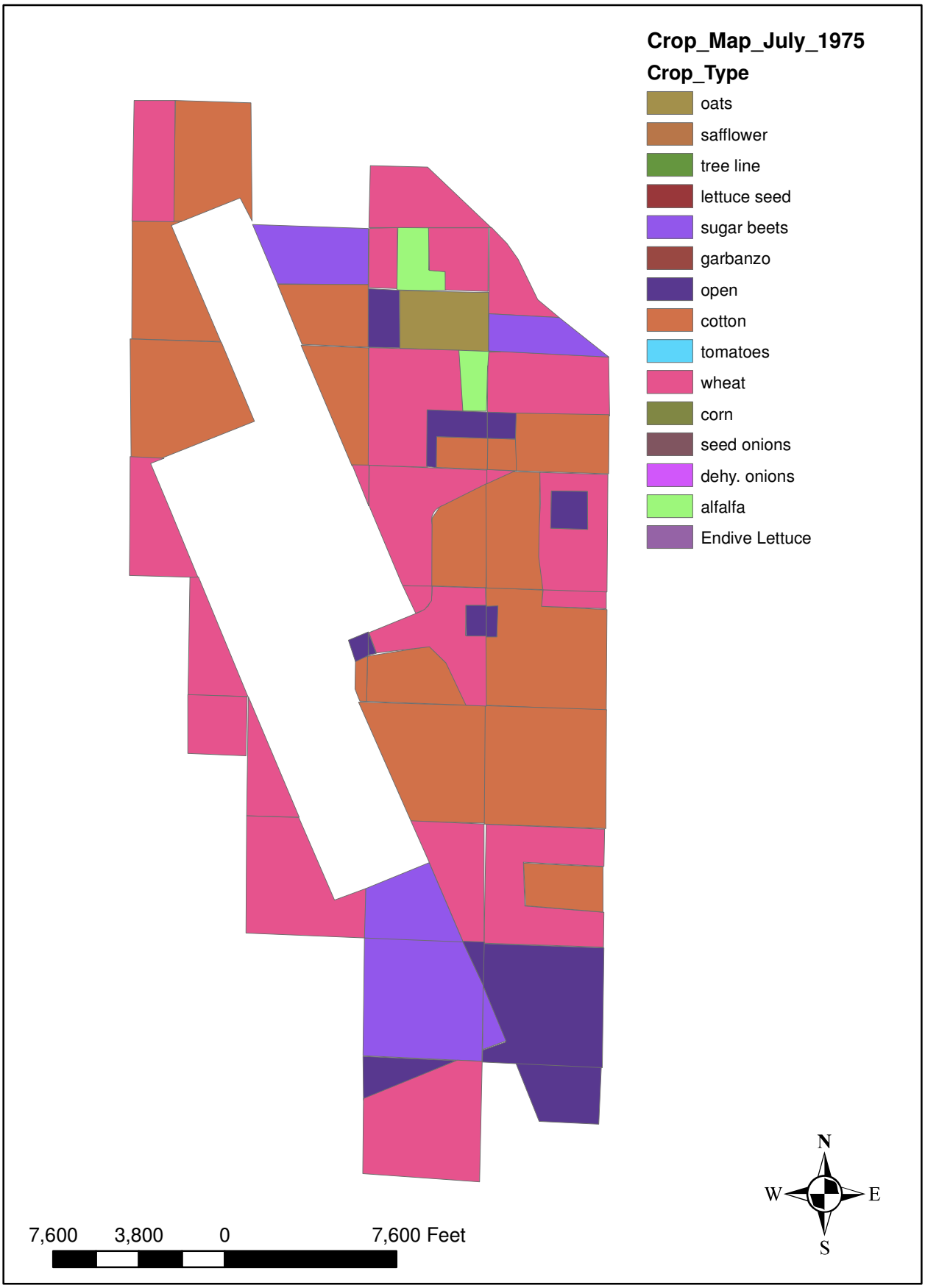
Crop_Map_July_1975
Crop_Type
oats
safflower
tree line
lettuce seed
sugar beets
garbanzo
open
cotton
tomatoes
wheat
corn
seed onions
dehy. onions
alfalfa
Endive Lettuce
N
W
E
S
7,600
3,800
0
7,600 Feet

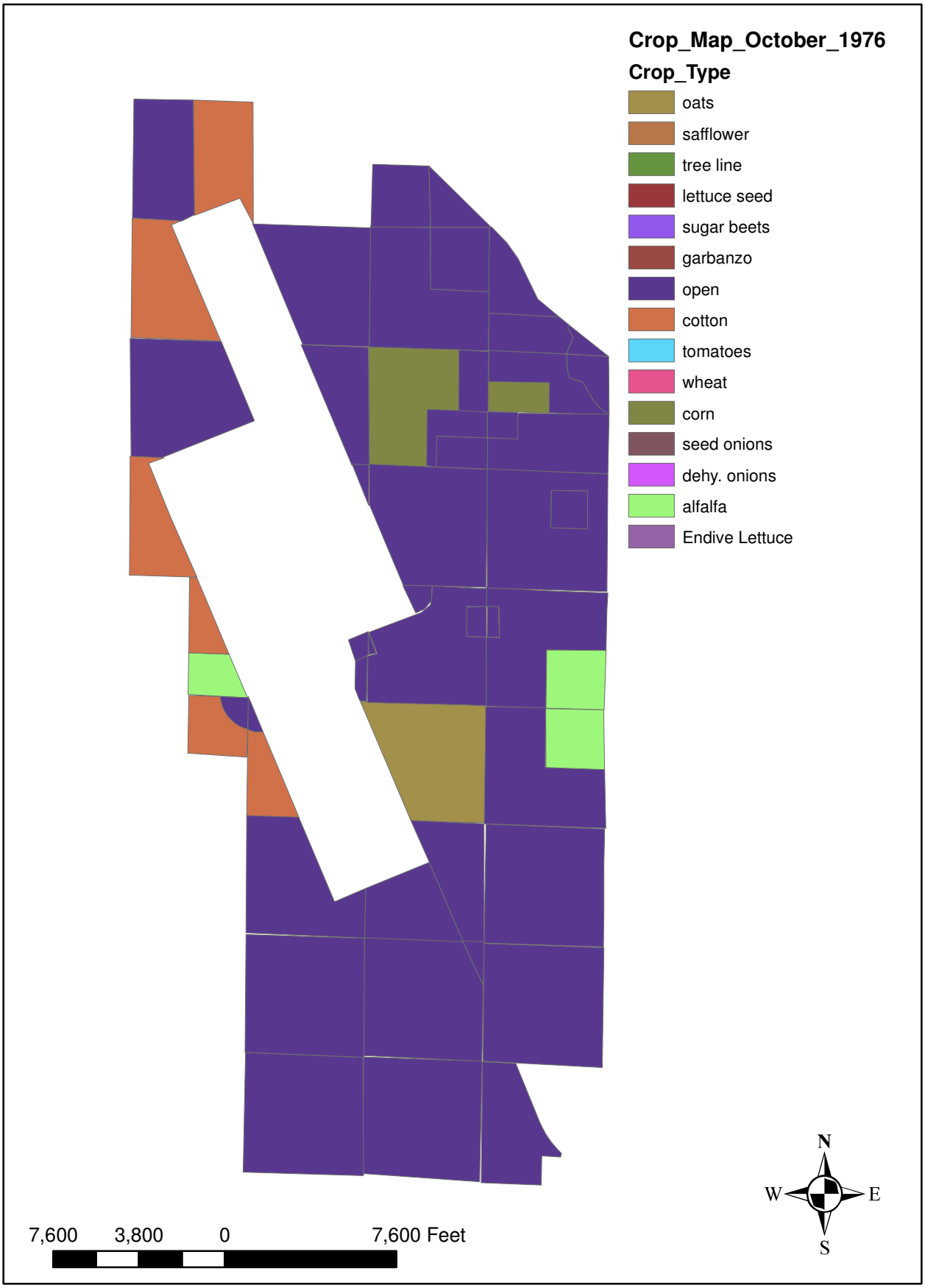
Crop_Map_October_1976
Crop_Type
oats
safflower
tree line
lettuce seed
sugar beets
garbanzo
open
cotton
tomatoes
wheat
corn
seed onions
dehy. onions
alfalfa
Endive Lettuce
7,600
3,800
0
7,600 Feet
N
W
E
S

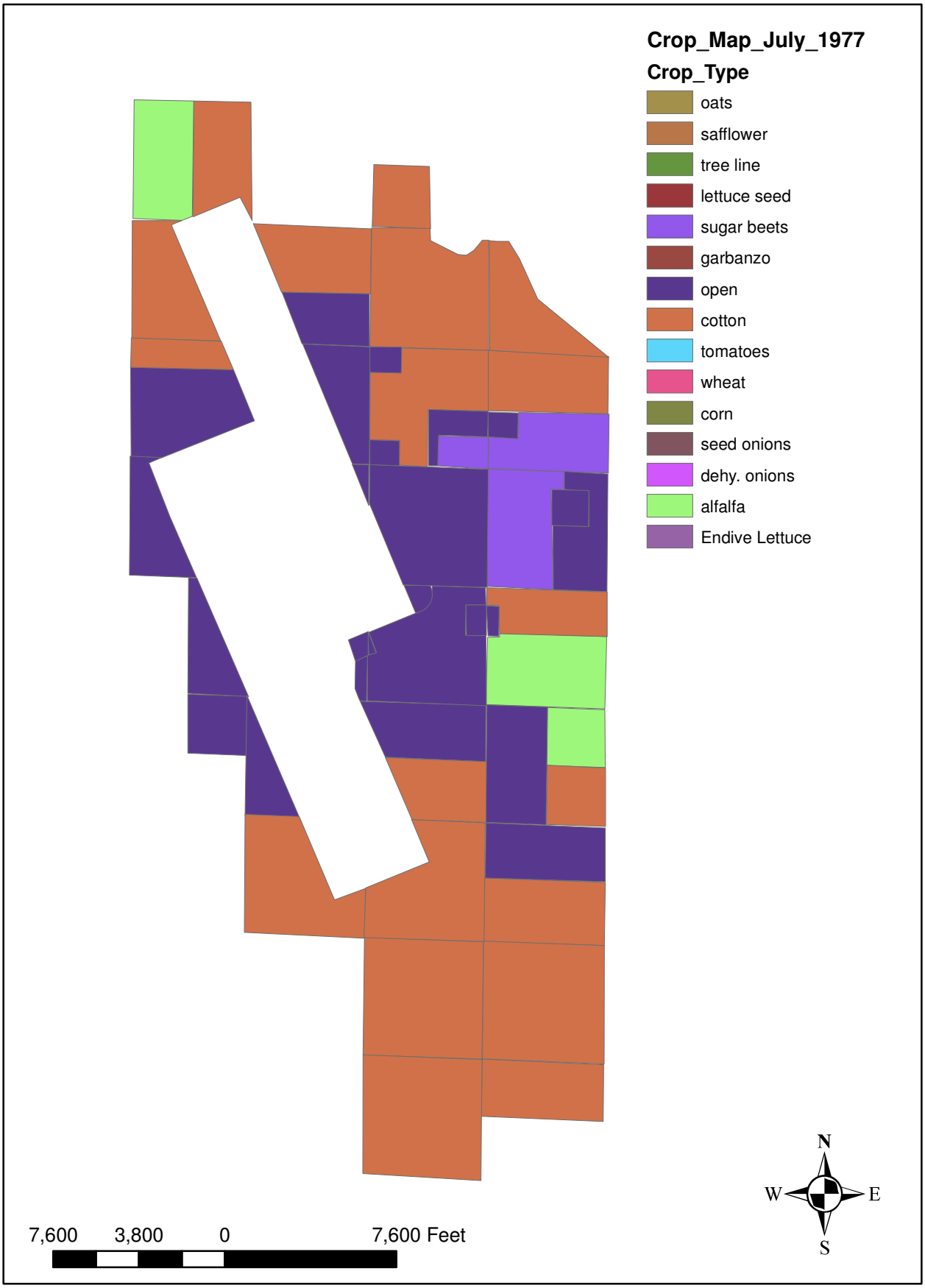
Crop_Map_July_1977
Crop_Type
oats
safflower
tree line
lettuce seed
sugar beets
garbanzo
open
cotton
tomatoes
wheat
corn
seed onions
dehy. onions
alfalfa
Endive Lettuce
7,600
3,800
0
7,600 Feet
N
W
E
S

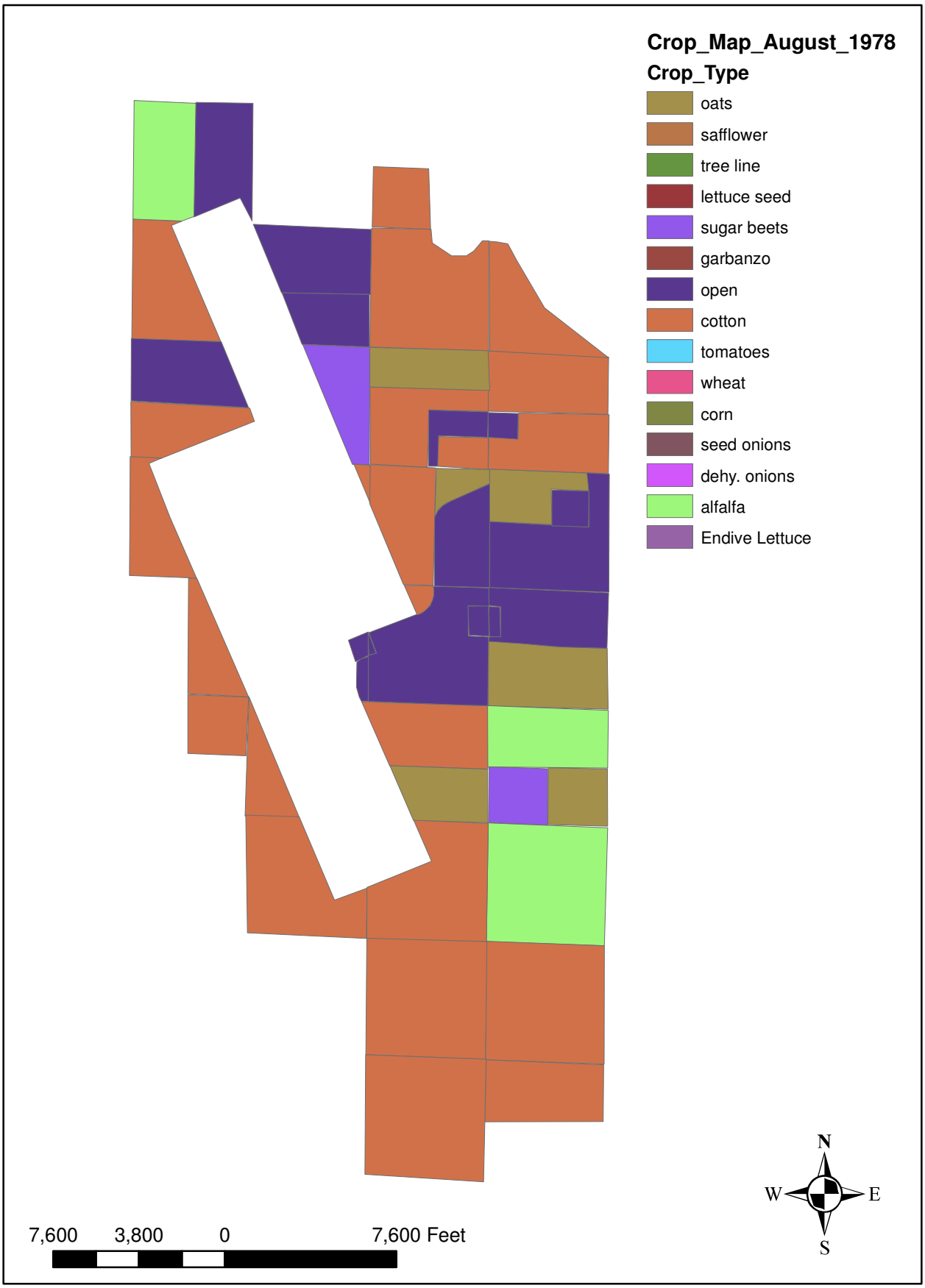
Crop_Map_August_1978
Crop_Type
oats
safflower
tree line
lettuce seed
sugar beets
garbanzo
open
cotton
tomatoes
wheat
corn
seed onions
dehy. onions
alfalfa
Endive Lettuce
7,600
3,800
0
7,600 Feet
N
W
E
S

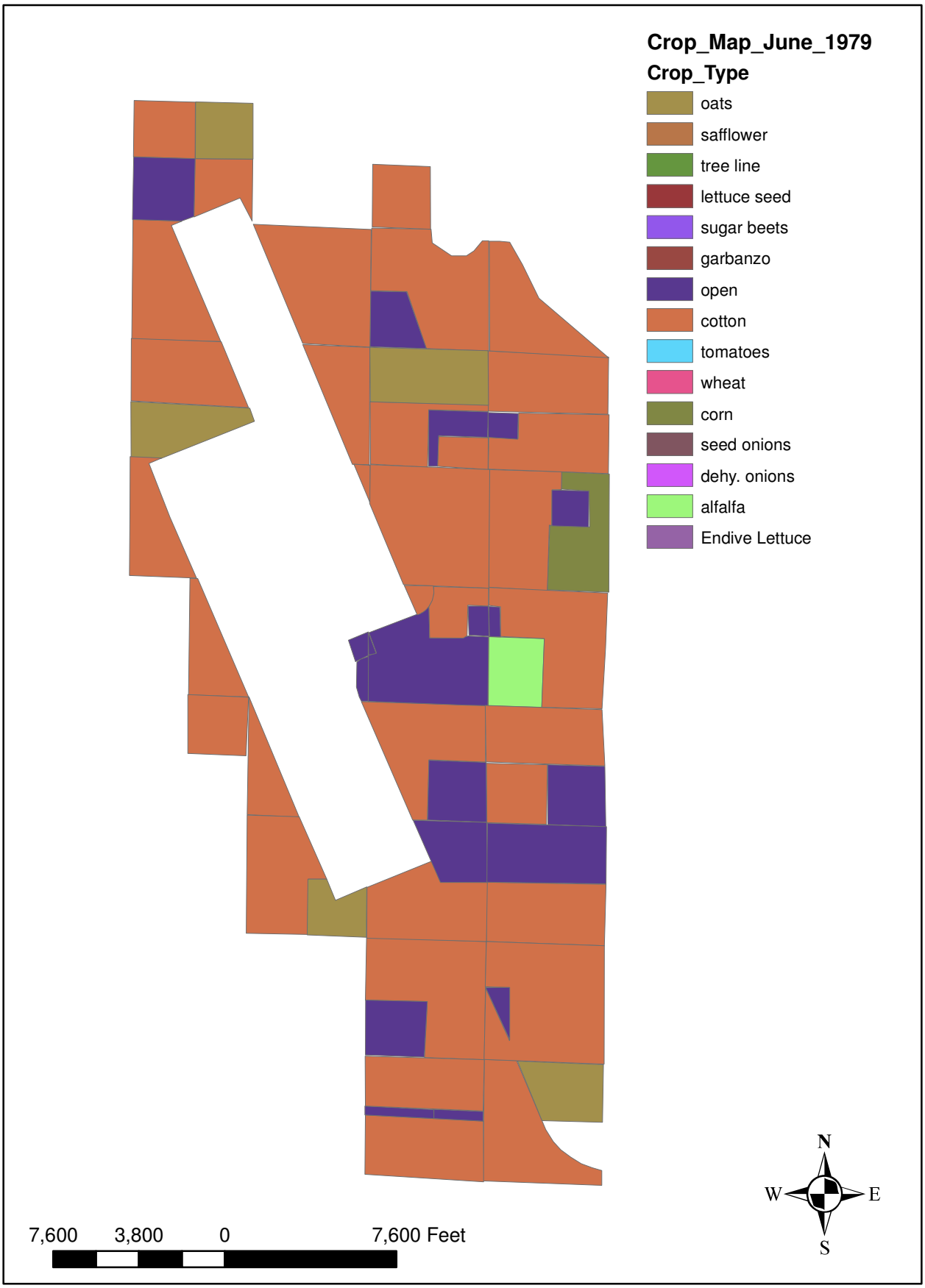
Crop_Map_June_1979
Crop_Type
oats
safflower
tree line
lettuce seed
sugar beets
garbanzo
open
cotton
tomatoes
wheat
corn
seed onions
dehy. onions
alfalfa
Endive Lettuce
7,600
3,800
0
7,600 Feet
N
W
E
S

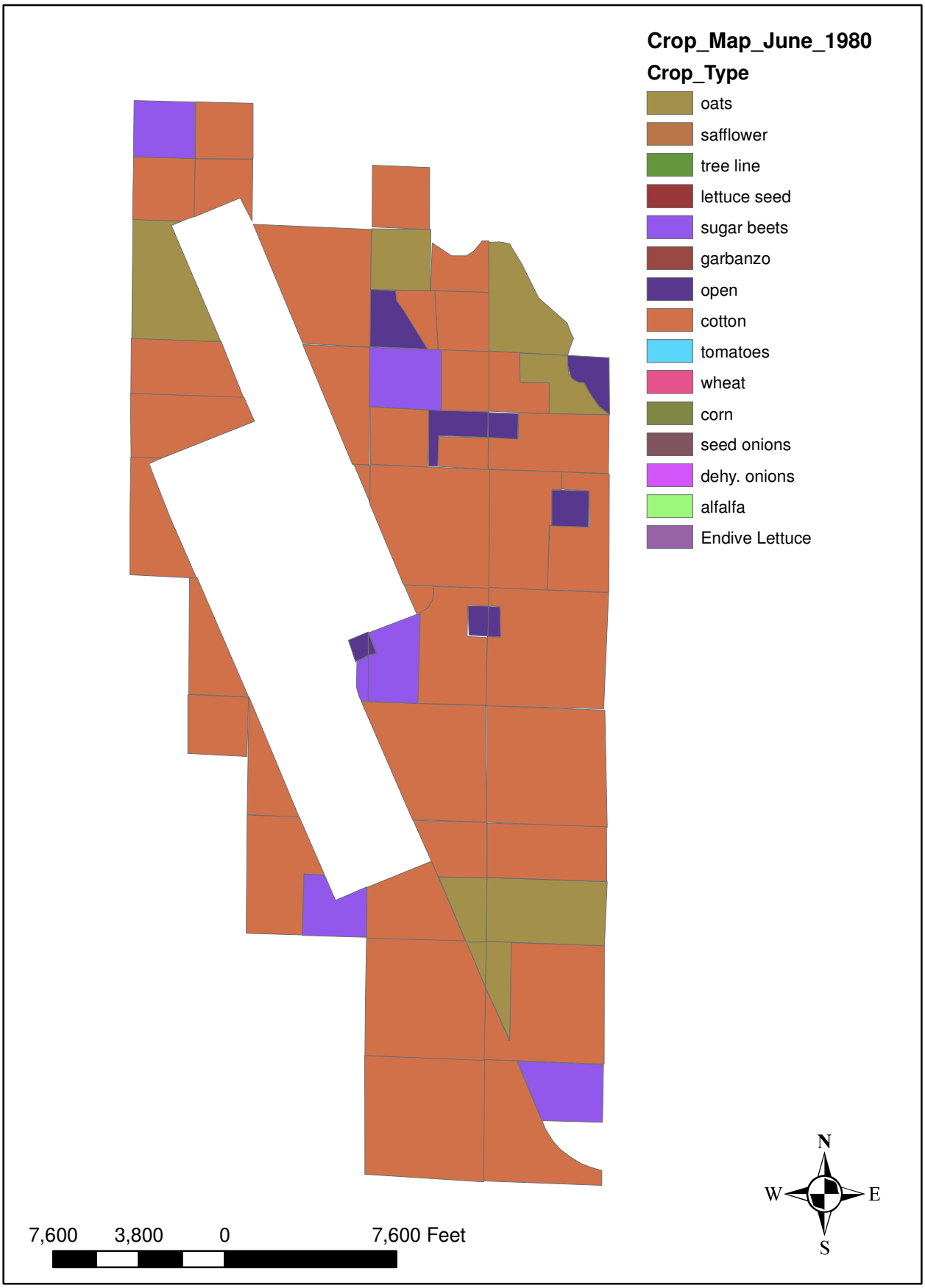
Crop_Map_June_1980
Crop_Type
oats
safflower
tree line
lettuce seed
sugar beets
garbanzo
open
cotton
tomatoes
wheat
corn
seed onions
dehy. onions
alfalfa
Endive Lettuce
7,600
3,800
0
7,600 Feet
N
W
E
S

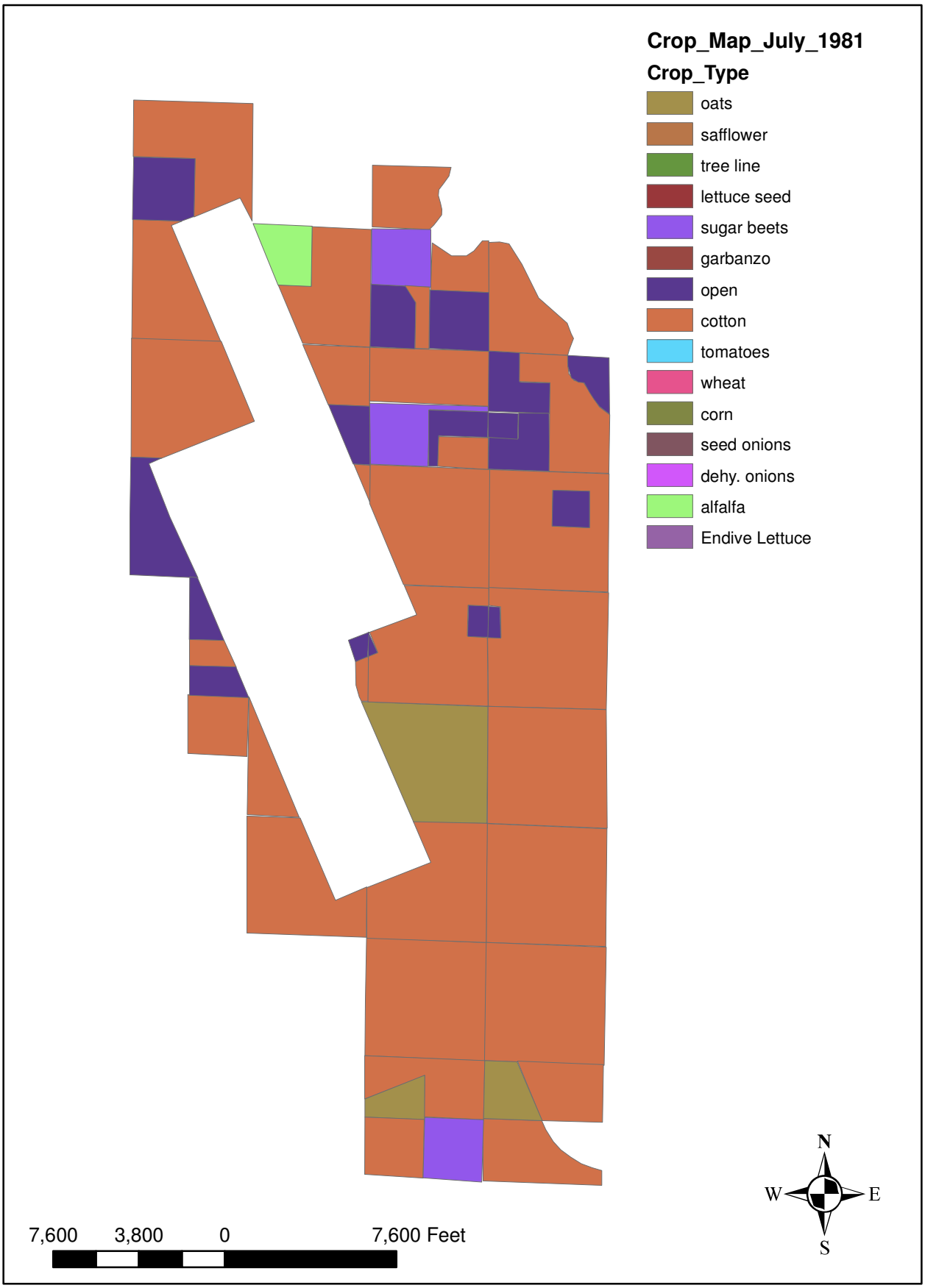
Crop_Map_July_1981
Crop_Type
oats
safflower
tree line
lettuce seed
sugar beets
garbanzo
open
cotton
tomatoes
wheat
corn
seed onions
dehy. onions
alfalfa
Endive Lettuce
N
W
E
S
7,600
3,800
0
7,600 Feet

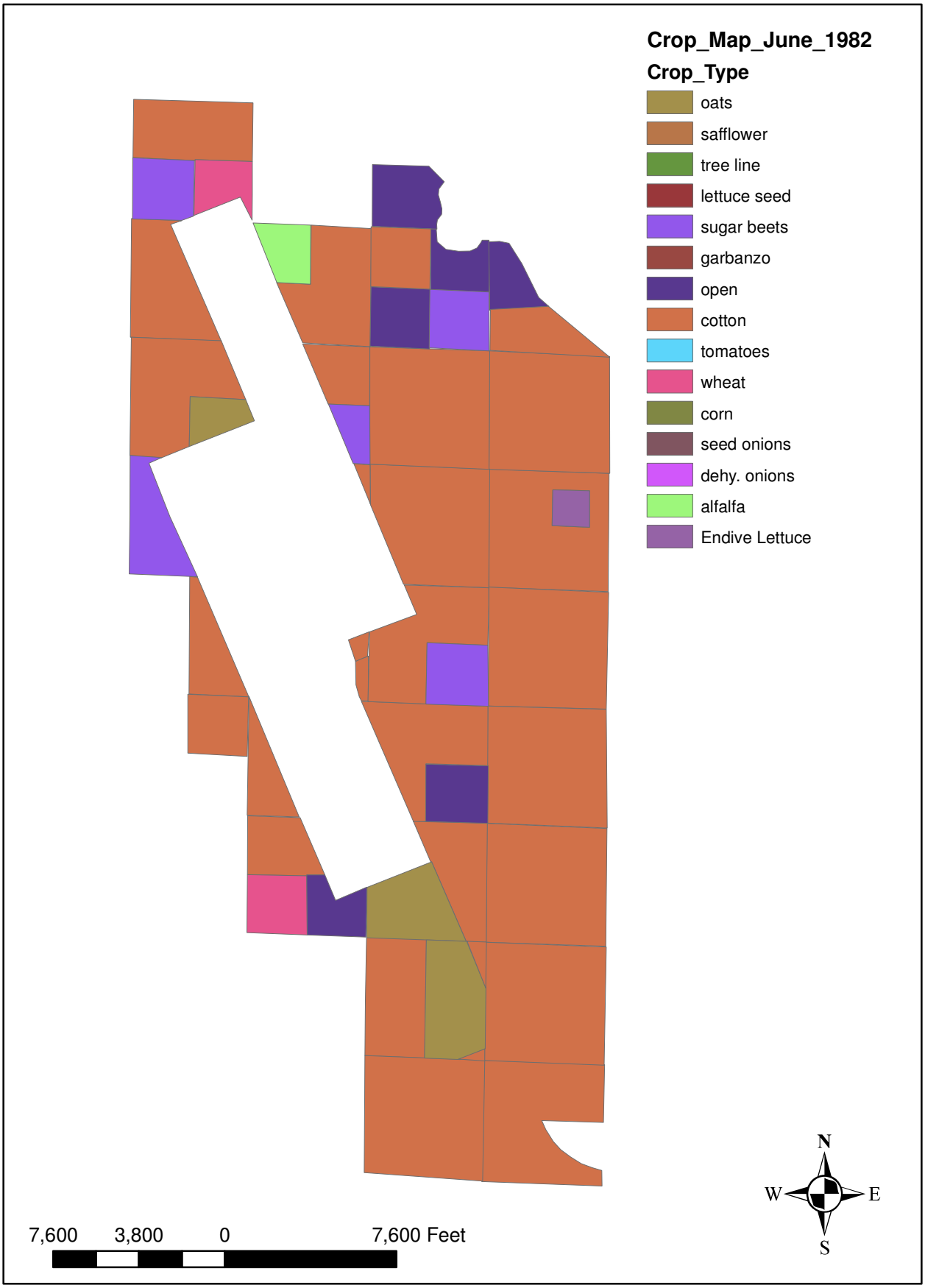
Crop_Map_June_1982
Crop_Type
oats
safflower
tree line
lettuce seed
sugar beets
garbanzo
open
cotton
tomatoes
wheat
corn
seed onions
dehy. onions
alfalfa
Endive Lettuce
7,600
3,800
0
7,600 Feet
N
W
E
S

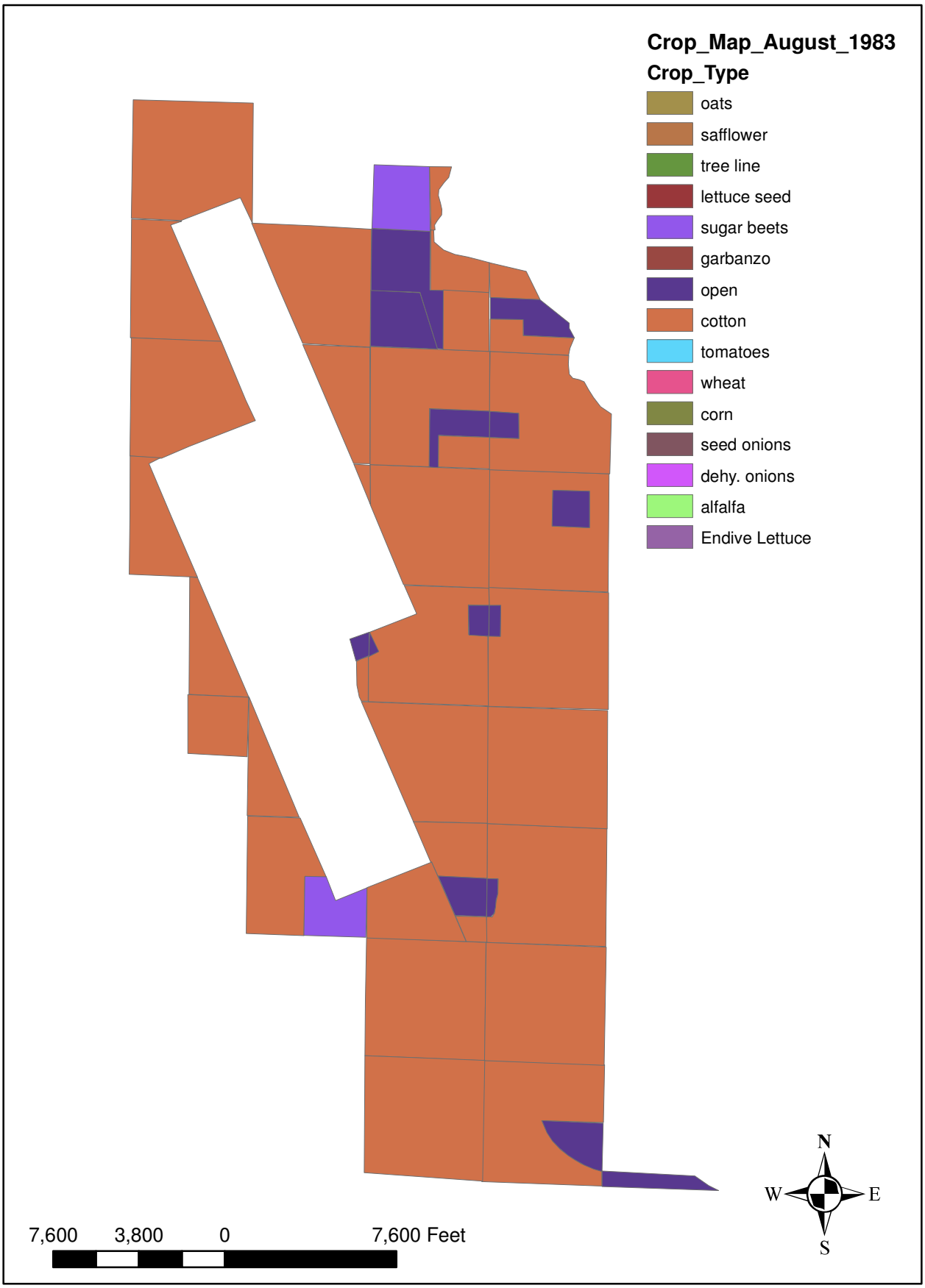
Crop_Map_August_1983
Crop_Type
oats
safflower
tree line
lettuce seed
sugar beets
garbanzo
open
cotton
tomatoes
wheat
corn
seed onions
dehy. onions
alfalfa
Endive Lettuce
N
W
E
S
7,600
3,800
0
7,600 Feet

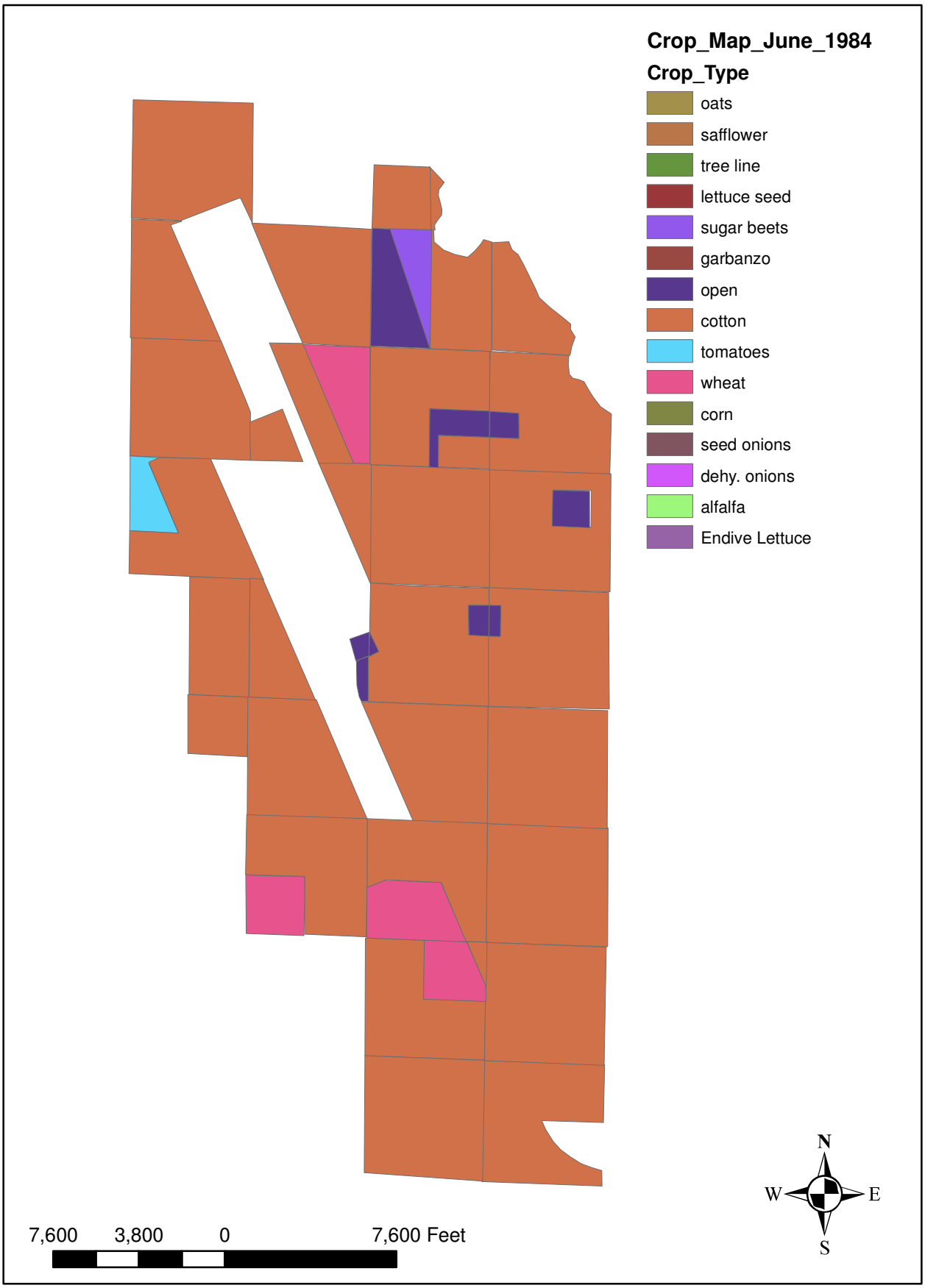
Crop_Map_June_1984
Crop_Type
oats
safflower
tree line
lettuce seed
sugar beets
garbanzo
open
cotton
tomatoes
wheat
corn
seed onions
dehy. onions
alfalfa
Endive Lettuce
7,600
3,800
0
7,600 Feet
N
W
E
S

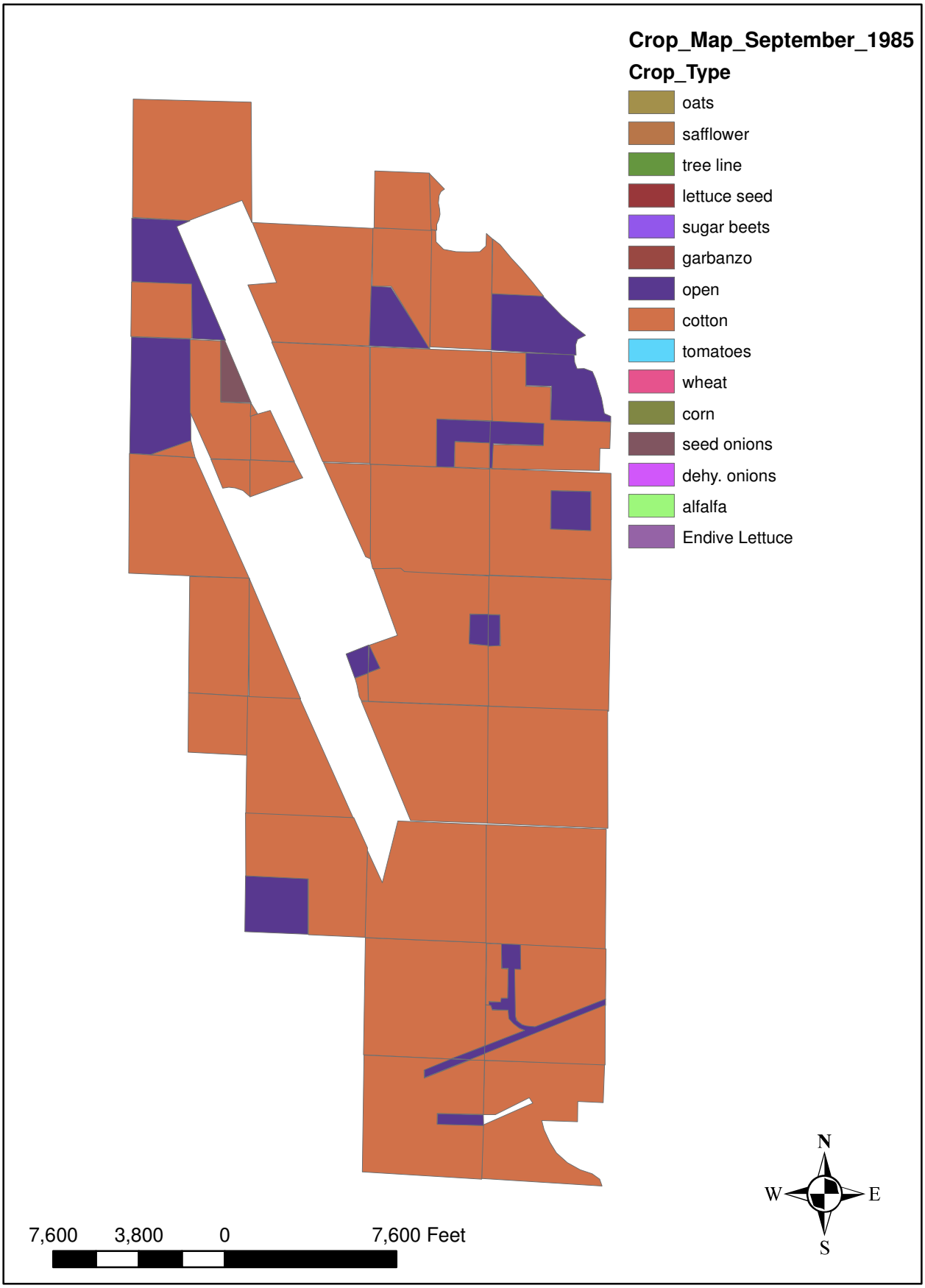
Crop_Map_September_1985
Crop_Type
oats
safflower
tree line
lettuce seed
sugar beets
garbanzo
open
cotton
tomatoes
wheat
corn
seed onions
dehy. onions
alfalfa
Endive Lettuce
N
W
E
S
7,600
3,800
0
7,600 Feet

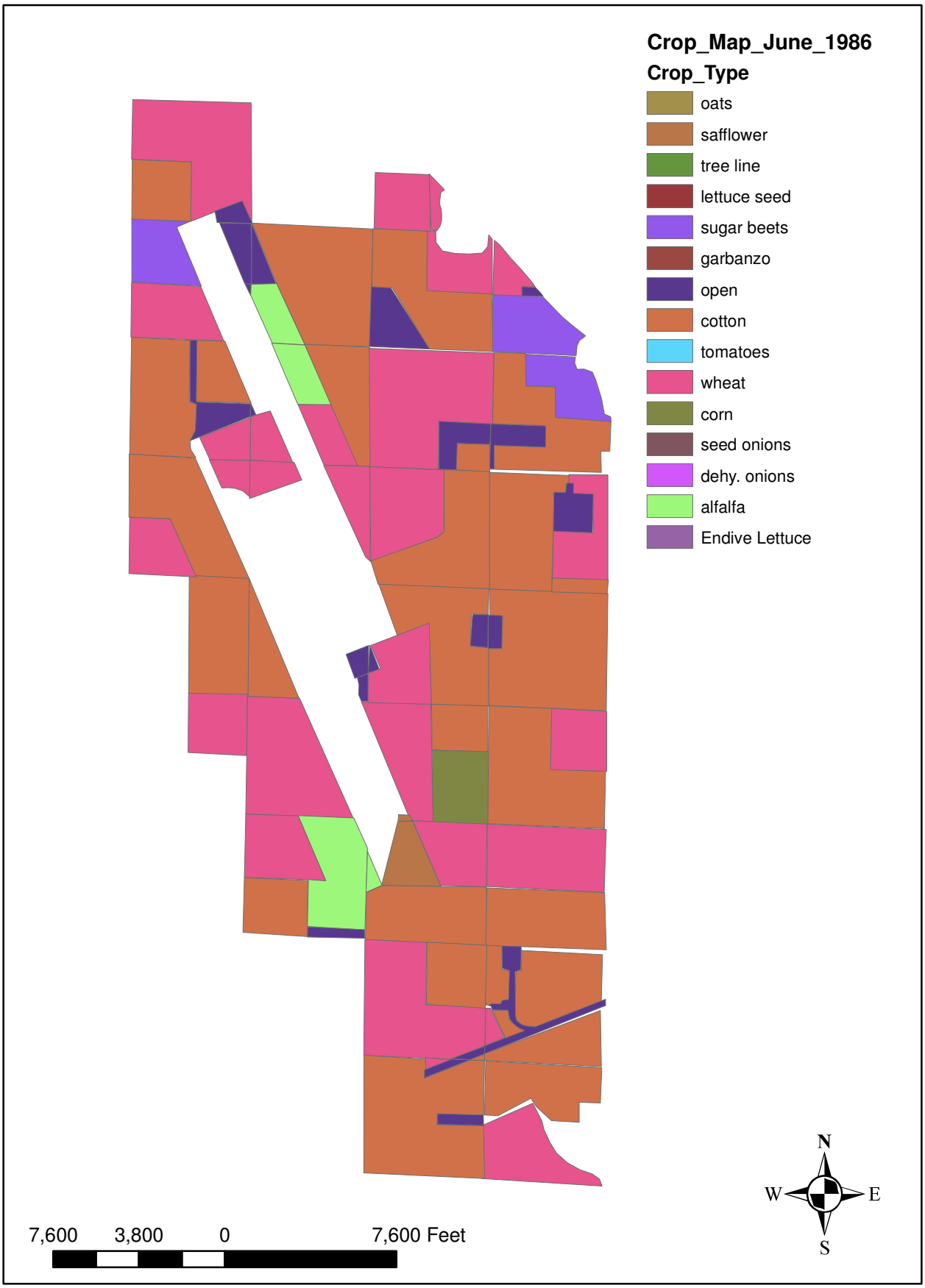
Crop_Map_June_1986
Crop_Type
oats
safflower
tree line
lettuce seed
sugar beets
garbanzo
open
cotton
tomatoes
wheat
corn
seed onions
dehy. onions
alfalfa
Endive Lettuce
7,600
3,800
0
7,600 Feet
N
W
E
S

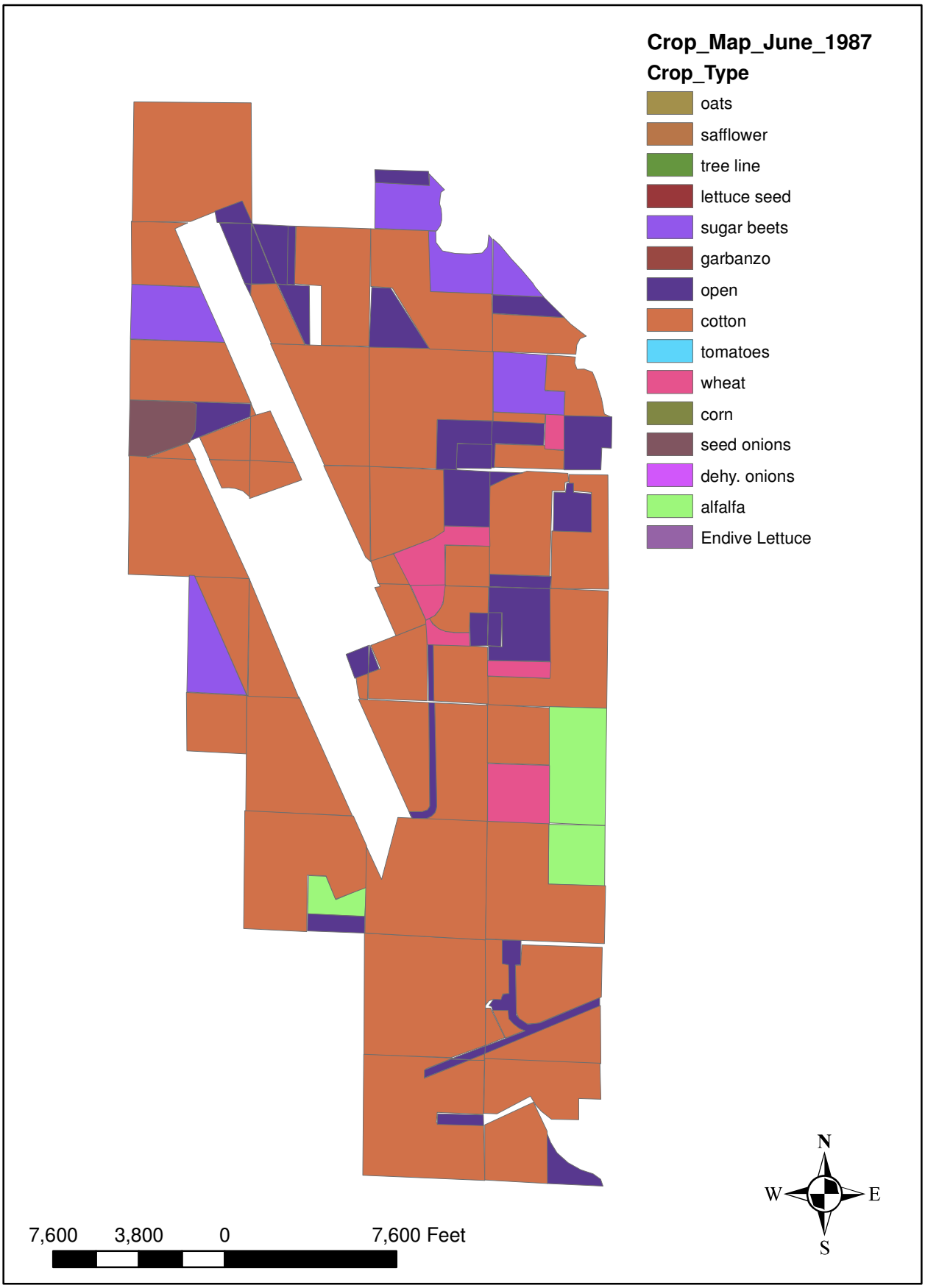
Crop_Map_June_1987
Crop_Type
oats
safflower
tree line
lettuce seed
sugar beets
garbanzo
open
cotton
tomatoes
wheat
corn
seed onions
dehy. onions
alfalfa
Endive Lettuce
7,600
3,800
0
7,600 Feet
N
W
E
S

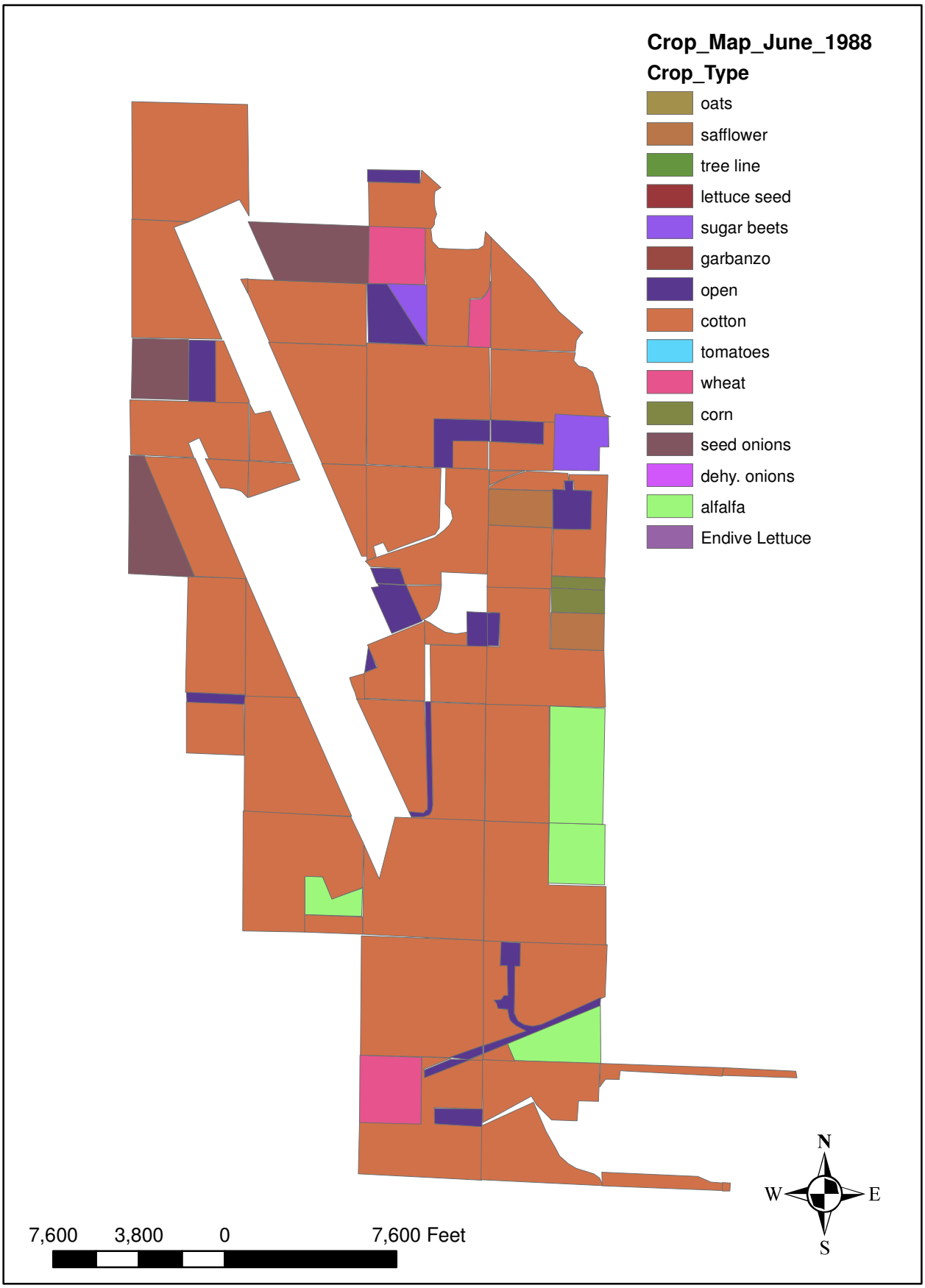
Crop_Map_June_1988
Crop_Type
oats
safflower
tree line
lettuce seed
sugar beets
garbanzo
open
cotton
tomatoes
wheat
corn
seed onions
dehy. onions
alfalfa
Endive Lettuce
N
W
E
S
7,600
3,800
0
7,600 Feet

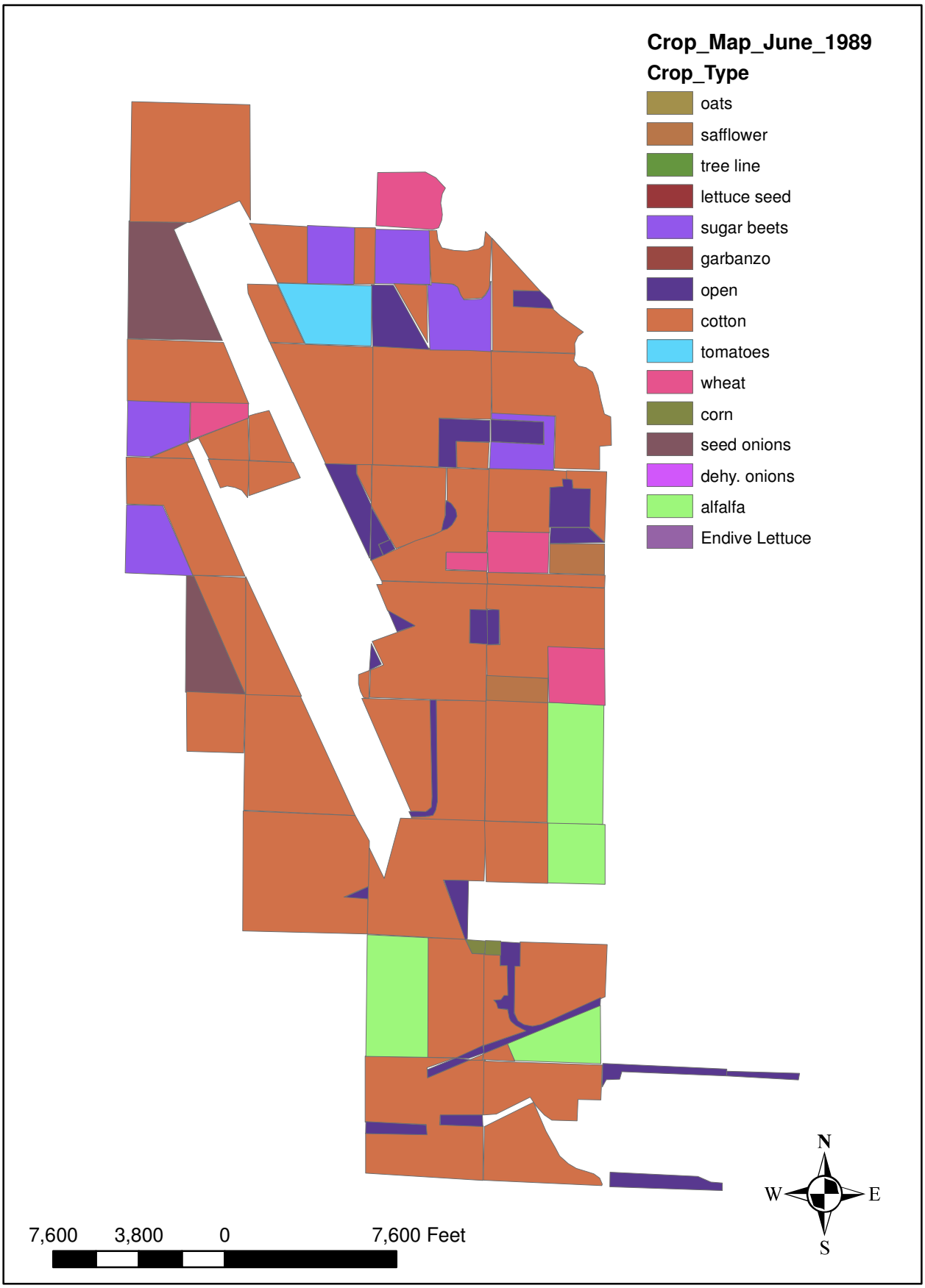
Crop_Map_June_1989
Crop_Type
oats
safflower
tree line
lettuce seed
sugar beets
garbanzo
open
cotton
tomatoes
wheat
corn
seed onions
dehy. onions
alfalfa
Endive Lettuce
N
W
E
S
7,600
3,800
0
7,600 Feet

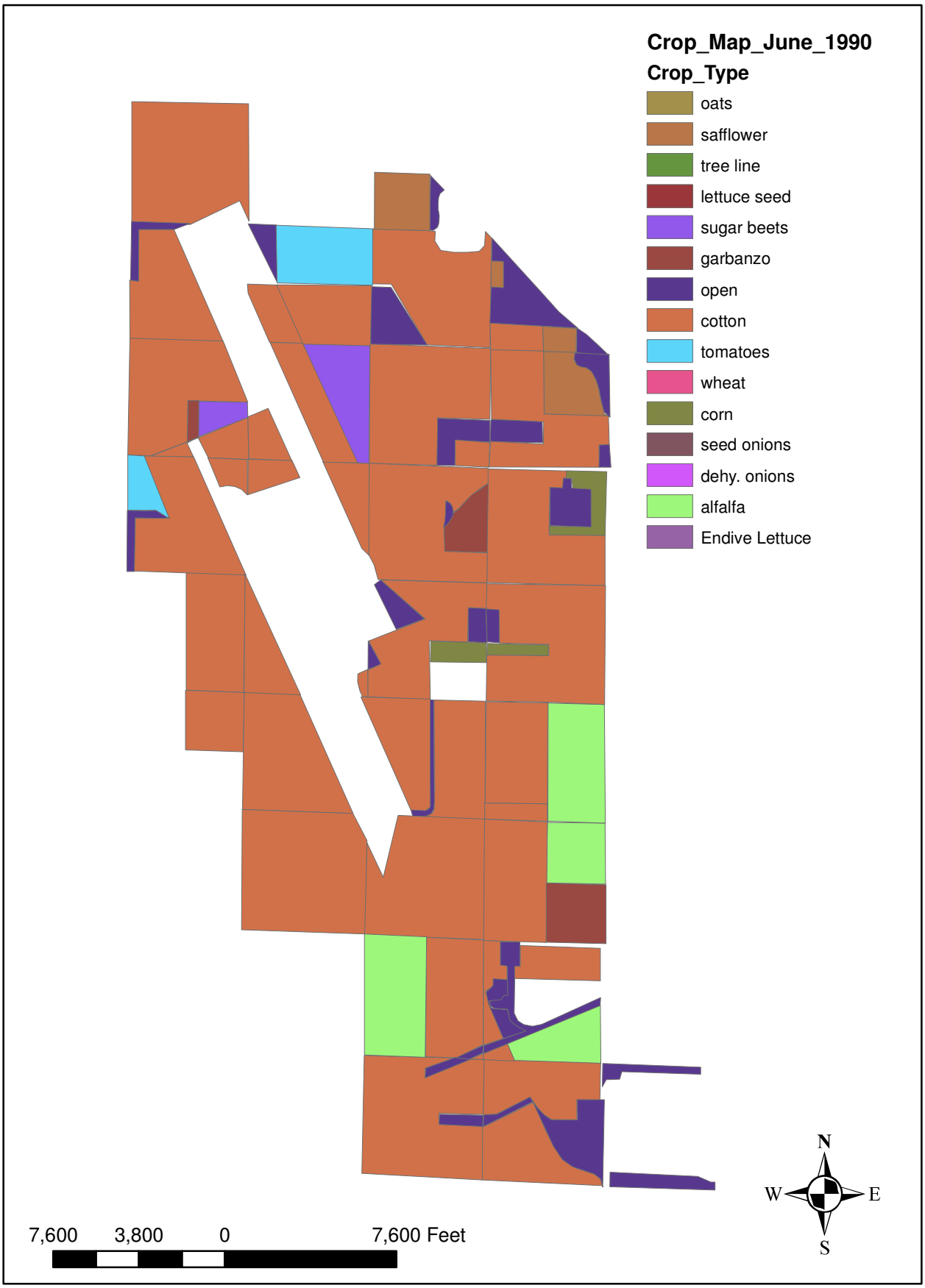
Crop_Map_June_1990
Crop_Type
oats
safflower
tree line
lettuce seed
sugar beets
garbanzo
open
cotton
tomatoes
wheat
corn
seed onions
dehy. onions
alfalfa
Endive Lettuce
N
W
E
S
7,600
3,800
0
7,600 Feet

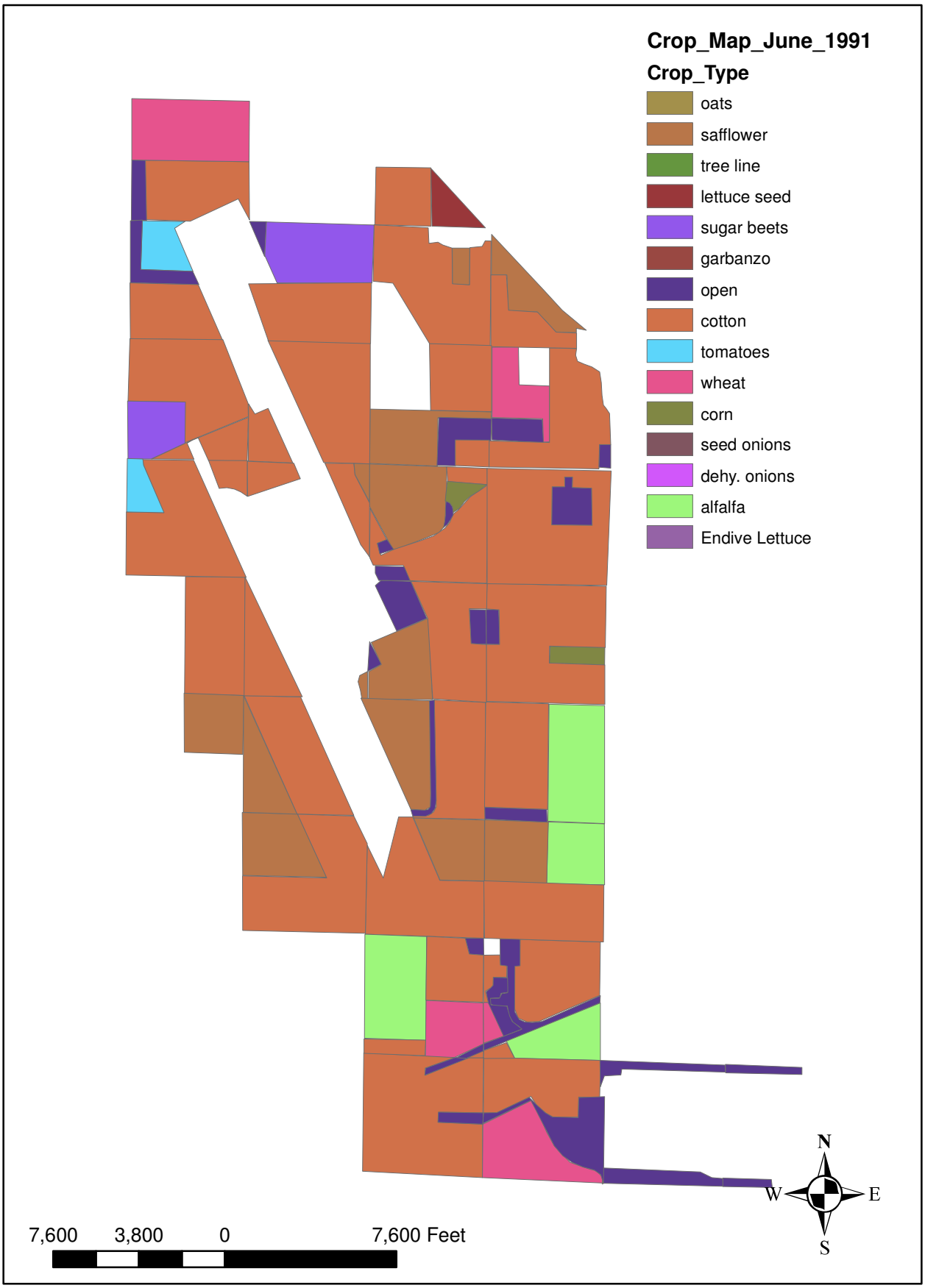
Crop_Map_June_1991
Crop_Type
oats
safflower
tree line
lettuce seed
sugar beets
garbanzo
open
cotton
tomatoes
wheat
corn
seed onions
dehy. onions
alfalfa
Endive Lettuce
N
W
E
S
7,600
3,800
0
7,600 Feet

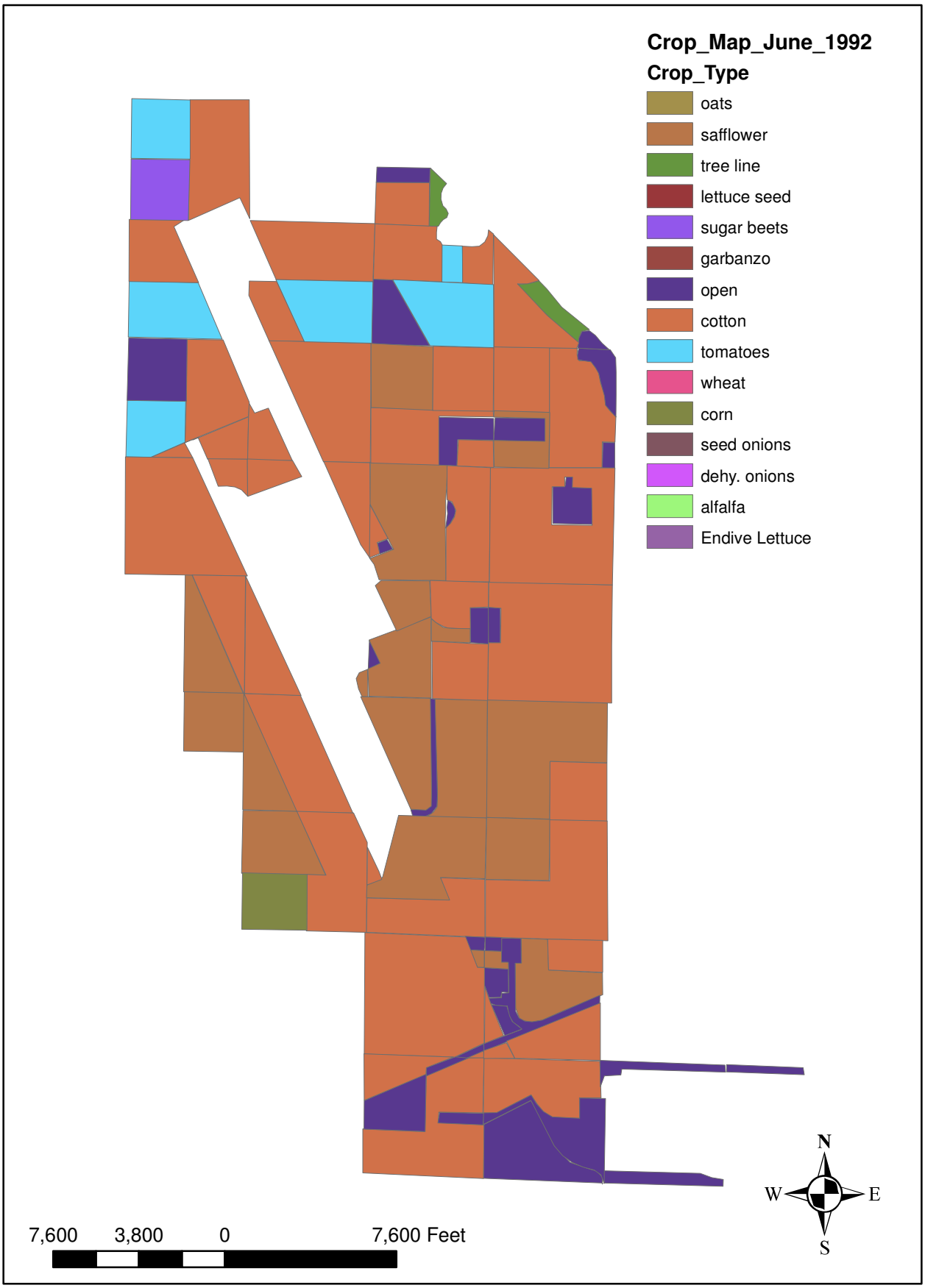
Crop_Map_June_1992
Crop_Type
oats
safflower
tree line
lettuce seed
sugar beets
garbanzo
open
cotton
tomatoes
wheat
corn
seed onions
dehy. onions
alfalfa
Endive Lettuce
N
W
E
S
7,600
3,800
0
7,600 Feet

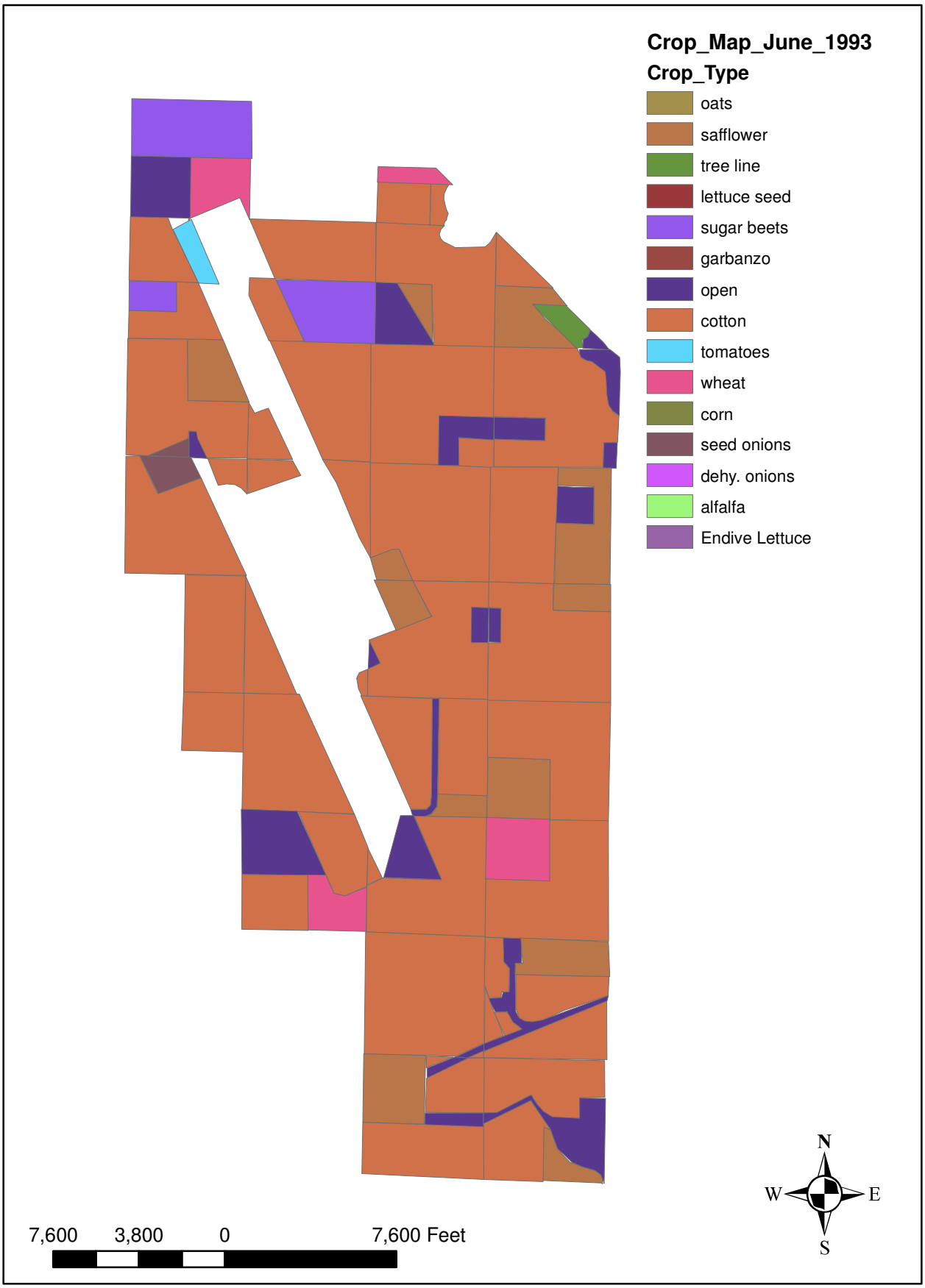
Crop_Map_June_1993
Crop_Type
oats
safflower
tree line
lettuce seed
sugar beets
garbanzo
open
cotton
tomatoes
wheat
corn
seed onions
dehy. onions
alfalfa
Endive Lettuce
7,600
3,800
0
7,600 Feet
N
W
E
S

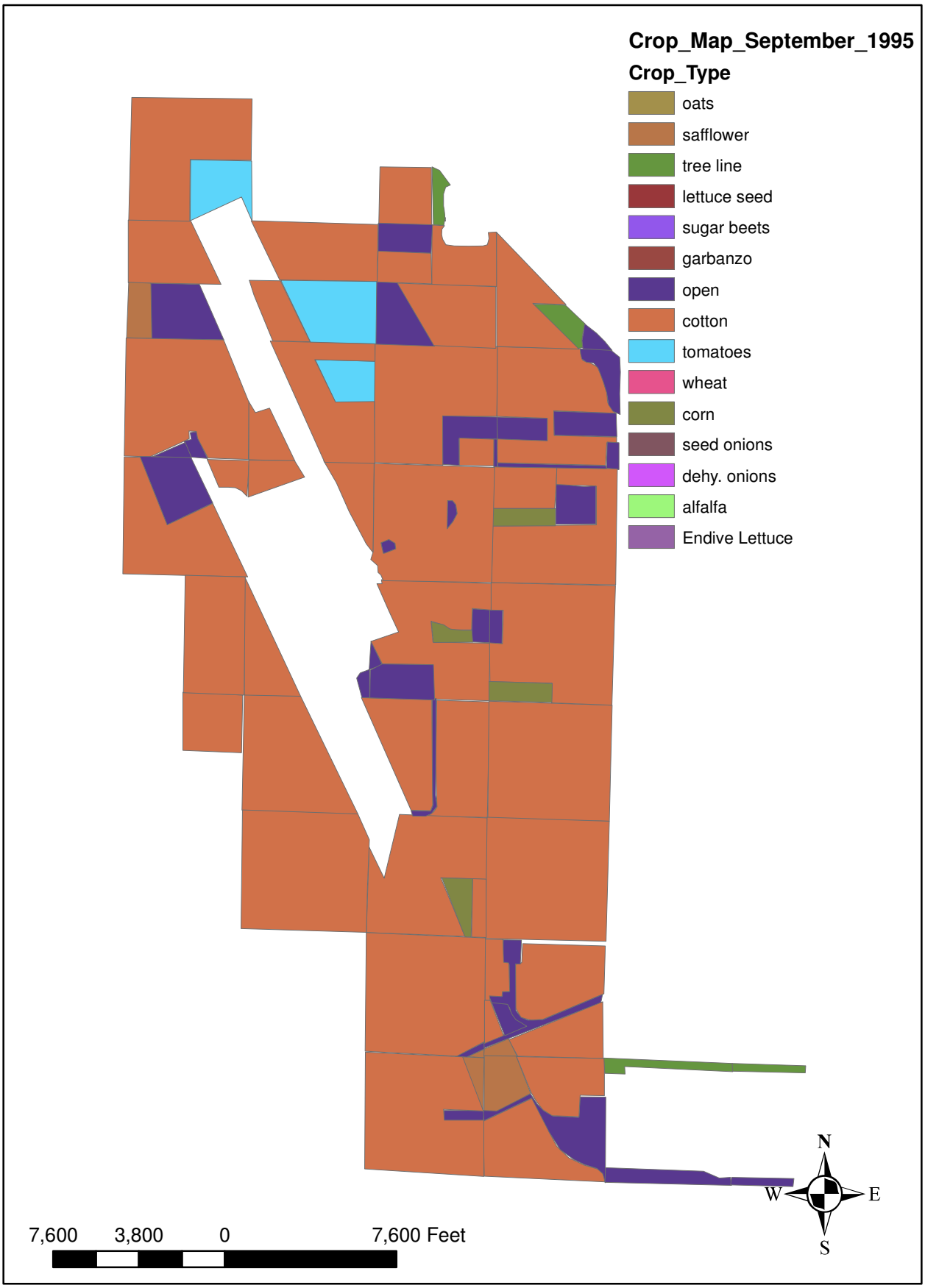
Crop_Map_September_1995
Crop_Type
oats
safflower
tree line
lettuce seed
sugar beets
garbanzo
open
cotton
tomatoes
wheat
corn
seed onions
dehy. onions
alfalfa
Endive Lettuce
N
W
E
S
7,600
3,800
0
7,600 Feet

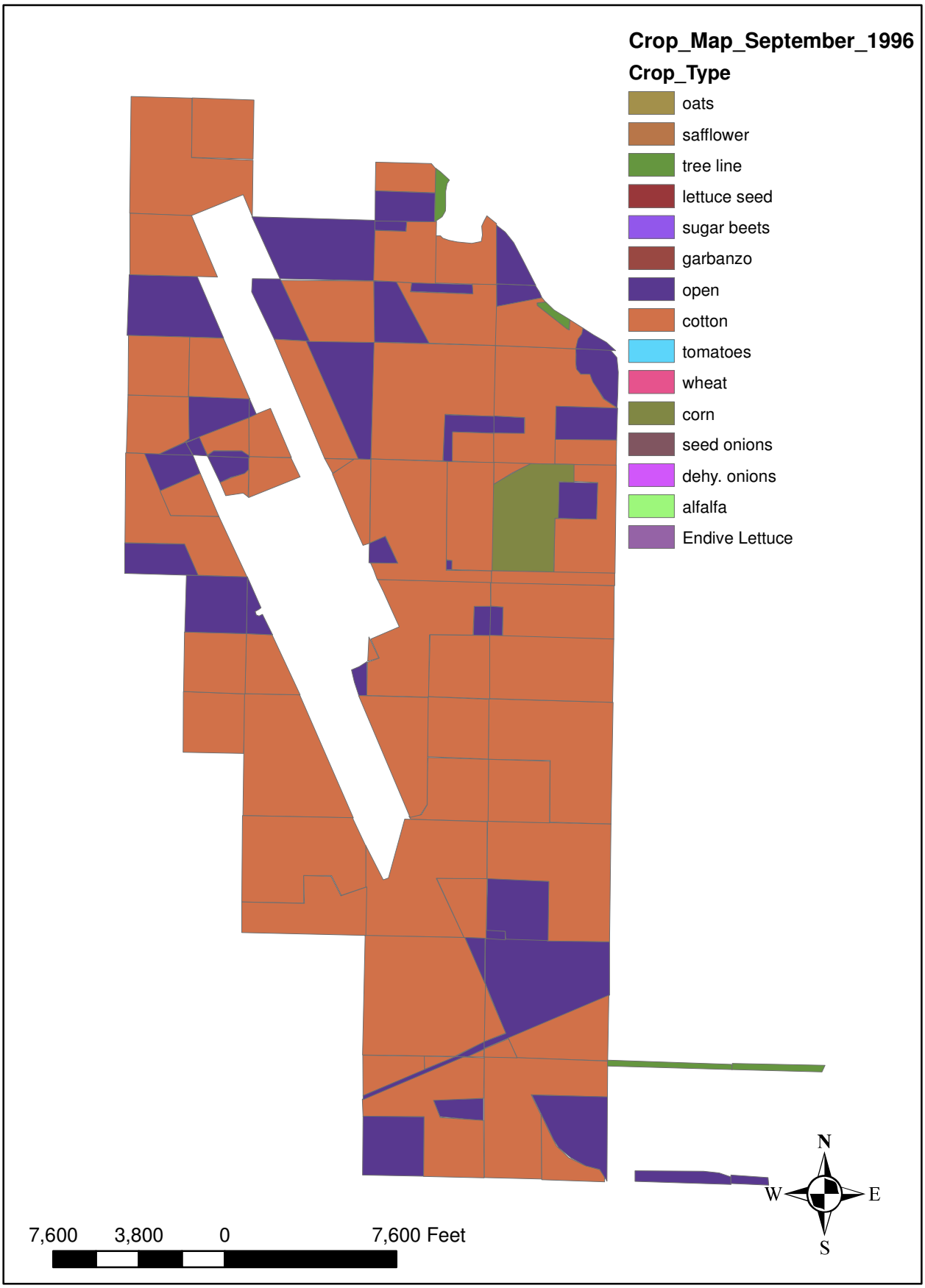
Crop_Map_September_1996
Crop_Type
oats
safflower
tree line
lettuce seed
sugar beets
garbanzo
open
cotton
tomatoes
wheat
corn
seed onions
dehy. onions
alfalfa
Endive Lettuce
N
W
E
S
7,600
3,800
0
7,600 Feet

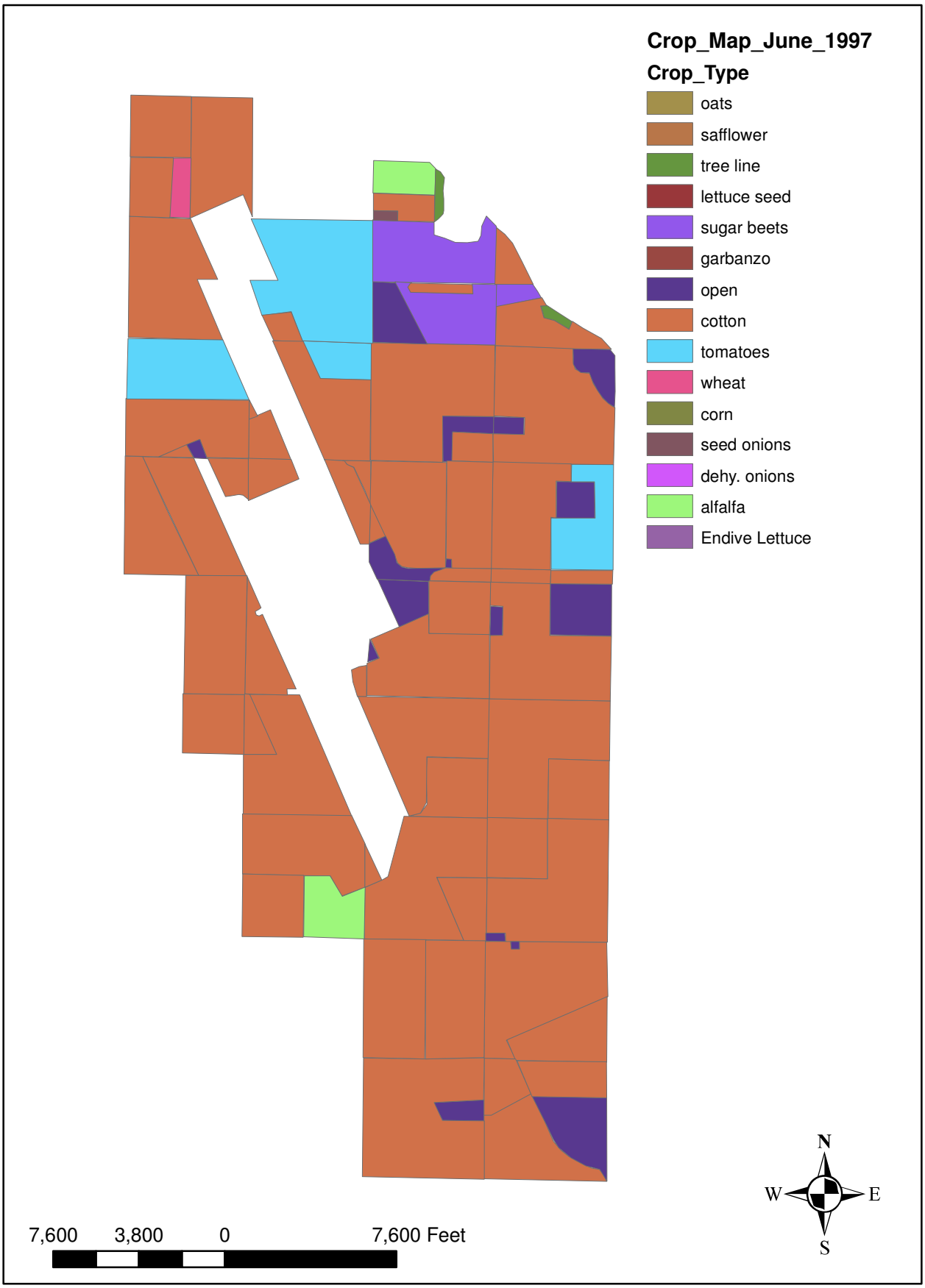
Crop_Map_June_1997
Crop_Type
oats
safflower
tree line
lettuce seed
sugar beets
garbanzo
open
cotton
tomatoes
wheat
corn
seed onions
dehy. onions
alfalfa
Endive Lettuce
7,600
3,800
0
7,600 Feet
N
W
E
S

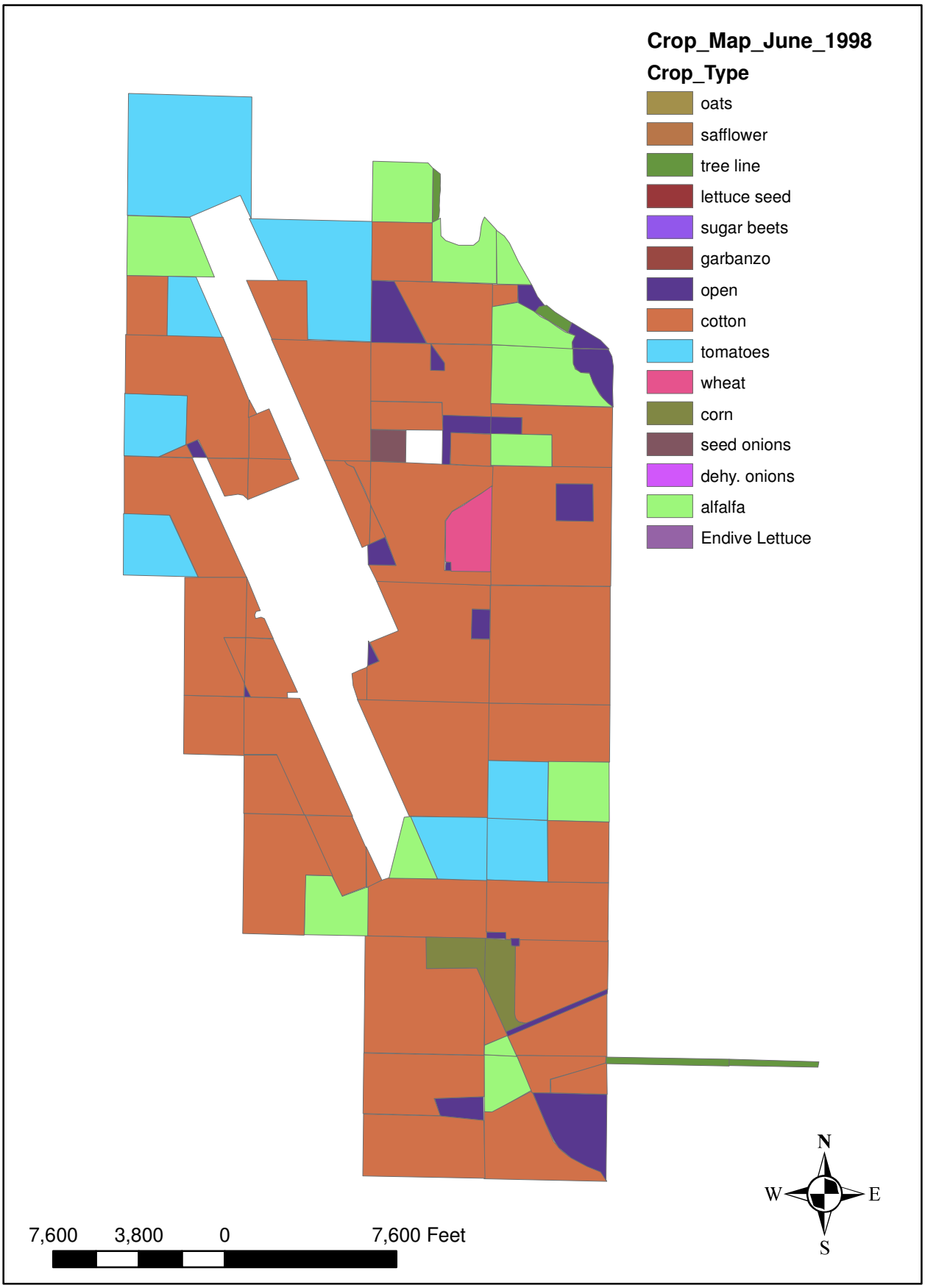
Crop_Map_June_1998
Crop_Type
oats
safflower
tree line
lettuce seed
sugar beets
garbanzo
open
cotton
tomatoes
wheat
corn
seed onions
dehy. onions
alfalfa
Endive Lettuce
N
W
E
S
7,600
3,800
0
7,600 Feet

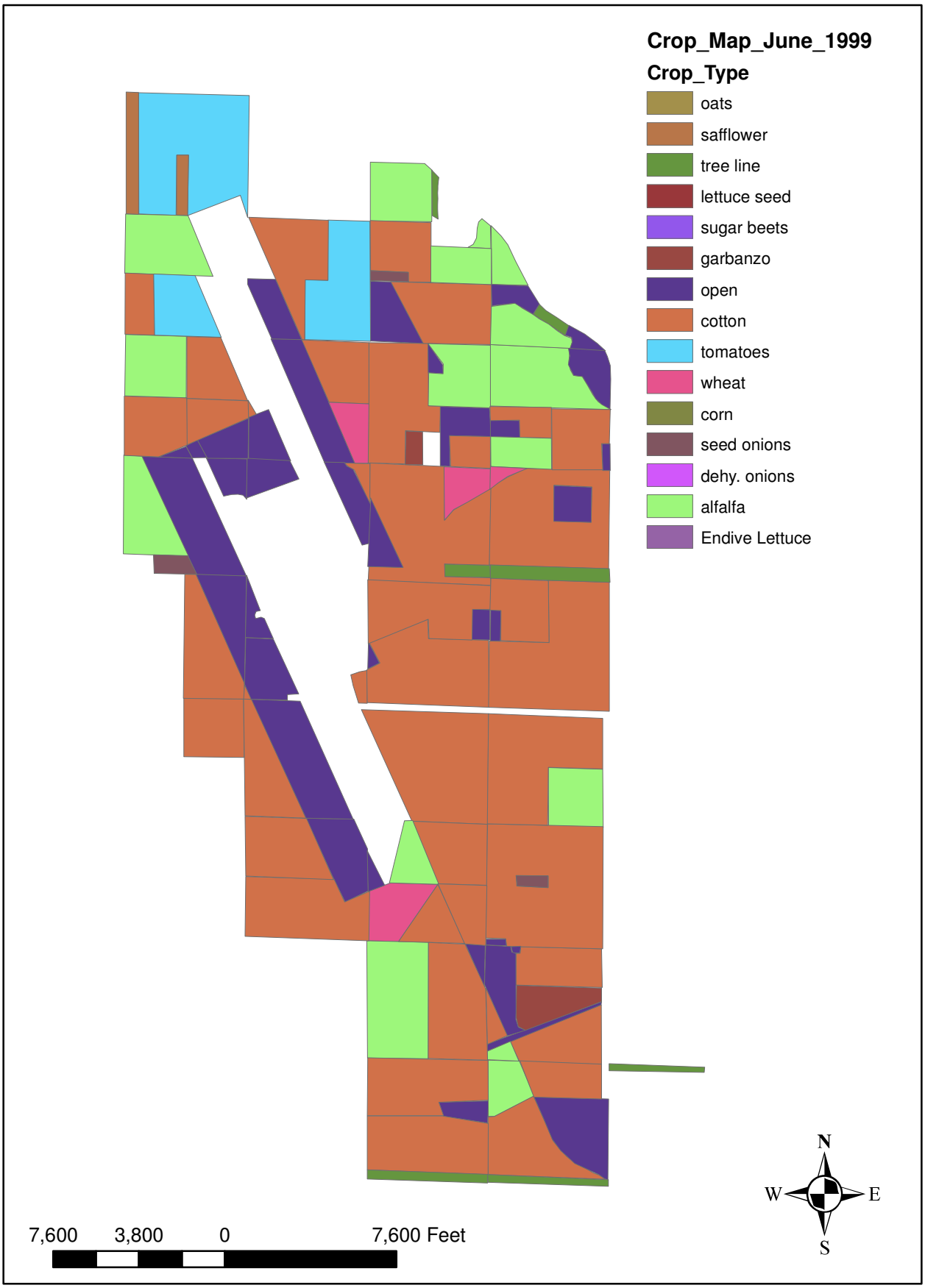
Crop_Map_June_1999
Crop_Type
oats
safflower
tree line
lettuce seed
sugar beets
garbanzo
open
cotton
tomatoes
wheat
corn
seed onions
dehy. onions
alfalfa
Endive Lettuce
N
W
E
S
7,600
3,800
0
7,600 Feet

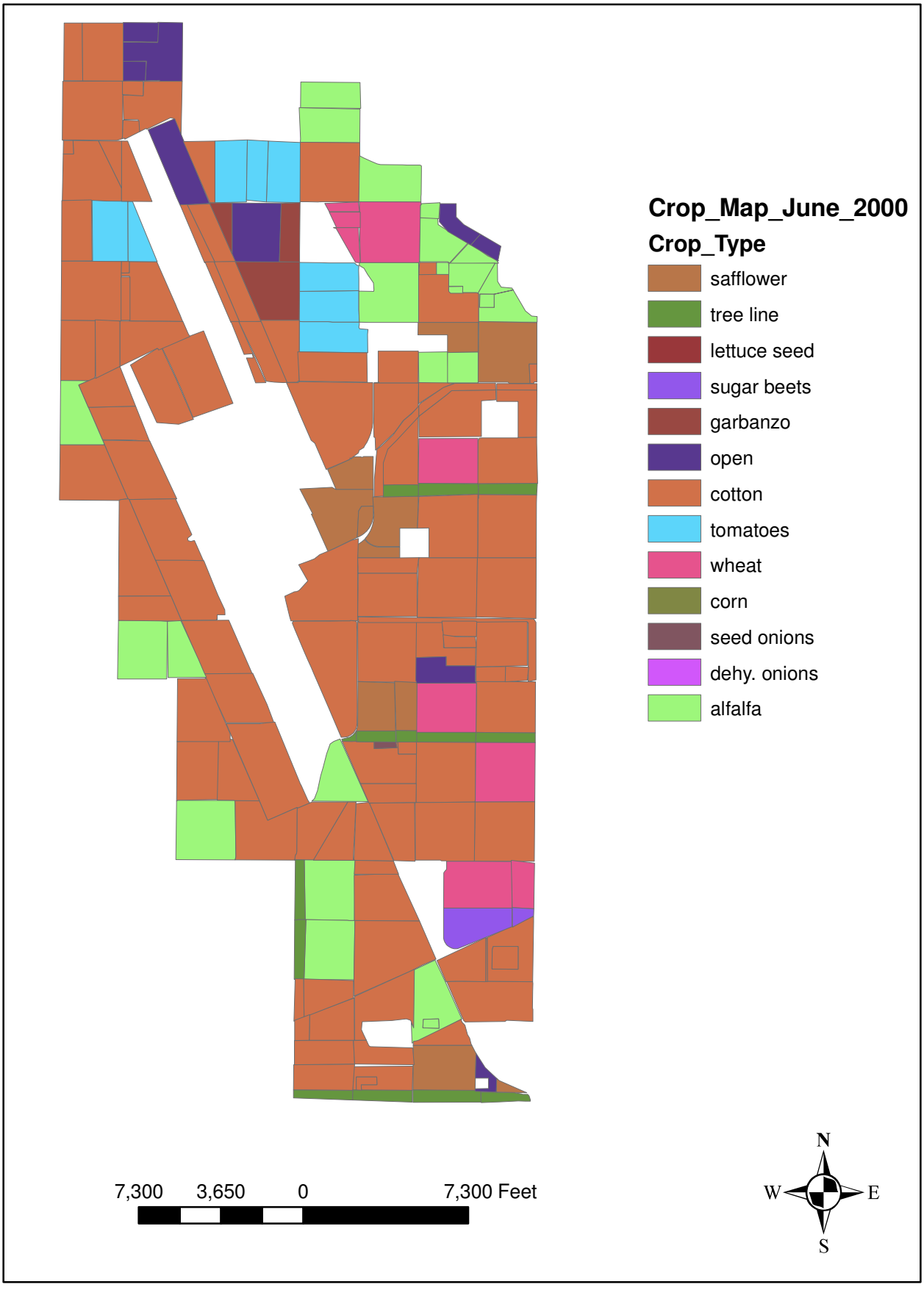
Crop_Map_June_2000
Crop_Type
safflower
tree line
lettuce seed
sugar beets
garbanzo
open
cotton
tomatoes
wheat
corn
seed onions
dehy. onions
alfalfa
7,300
3,650
0
7,300 Feet
N
W
E
S


Crop_Map_Sept_2001
Crop_Type
safflower
tree line
lettuce seed
sugar beets
garbanzo
open
cotton
tomatoes
wheat
corn
seed onions
dehy. onions
alfalfa
Endive Lettuce
7,500 3,750 0 7,500 Feet
N
W
E
S

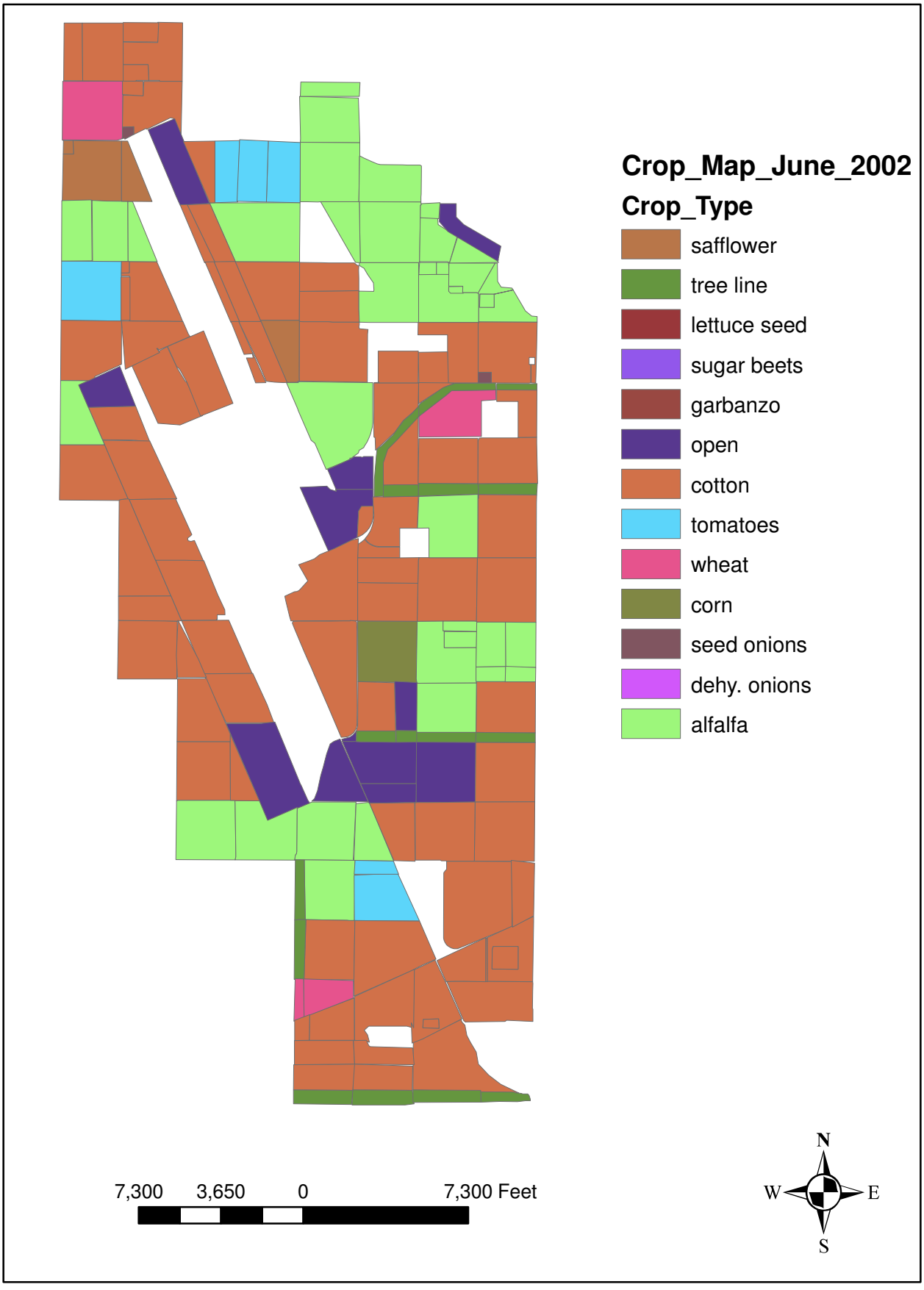
Crop_Map_June_2002
Crop_Type
safflower
tree line
lettuce seed
sugar beets
garbanzo
open
cotton
tomatoes
wheat
corn
seed onions
dehy. onions
alfalfa
7,300 3,650 0 7,300 Feet
N
W
E
S


Crop_Map_June_2003
Crop_Type
safflower
tree line
lettuce seed
sugar beets
garbanzo
open
cotton
tomatoes
wheat
corn
seed onions
dehy. onions
alfalfa
7,300 3,650 0 7,300 Feet
N
W
E
S


Crop_Map_June_2004
Crop_Type
safflower
tree line
lettuce seed
sugar beets
garbanzo
open
cotton
tomatoes
wheat
corn
seed onions
dehy. onions
alfalfa
7,300
3,650
0
7,300 Feet
N
W
E
S


Crop_Map_June_2005
Crop_Type
safflower
tree line
lettuce seed
sugar beets
garbanzo
open
cotton
tomatoes
wheat
corn
seed onions
dehy. onions
alfalfa
7,300 3,650 0 7,300 Feet
N
W
E
S

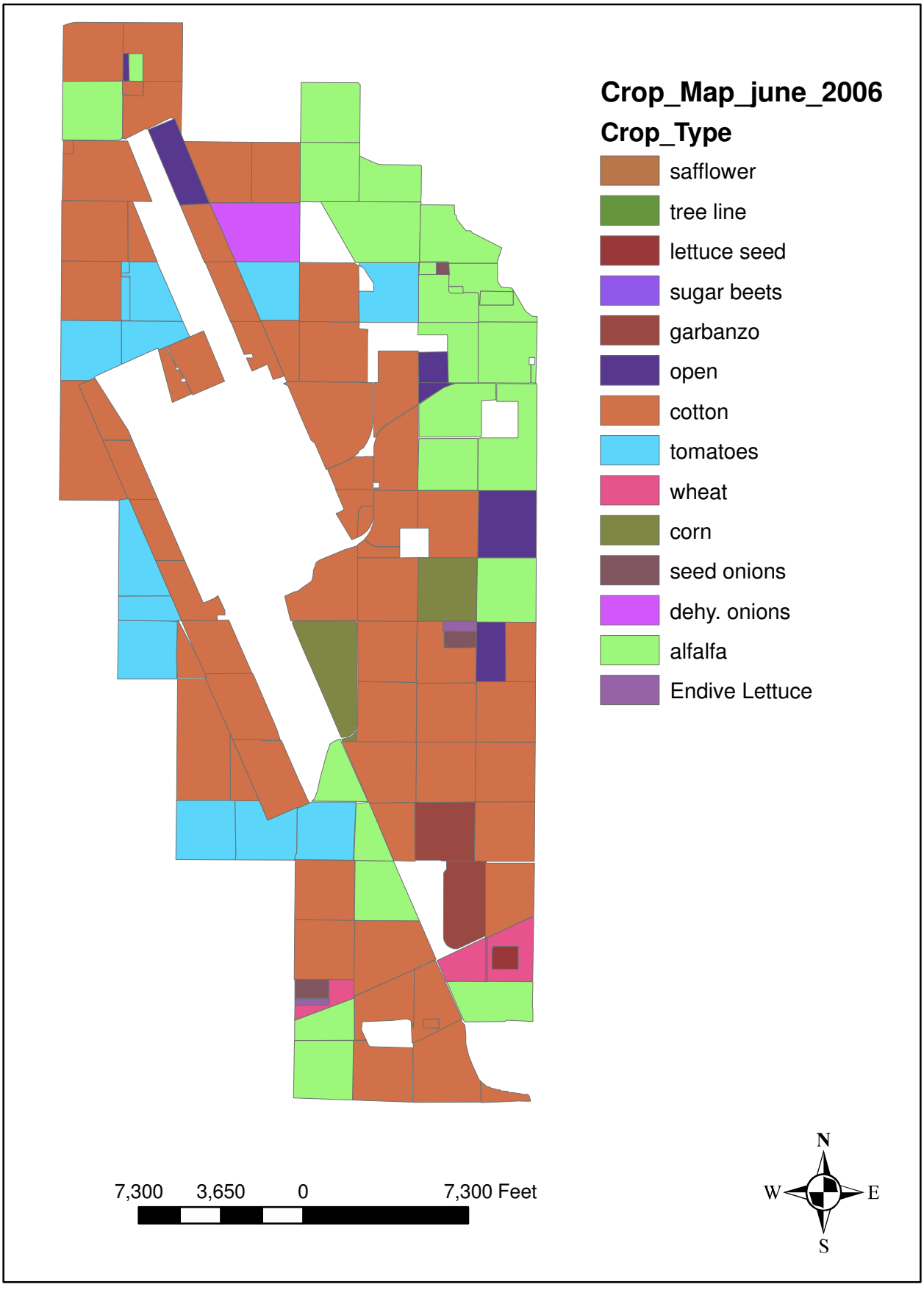
Crop_Map_june_2006
Crop_Type
safflower
tree line
lettuce seed
sugar beets
garbanzo
open
cotton
tomatoes
wheat
corn
seed onions
dehy. onions
alfalfa
Endive Lettuce
7,300 3,650 0 7,300 Feet
N
W
E
S


Crop_Map_Summer_2008
Crop_Type
safflower
tree line
lettuce seed
sugar beets
garbanzo
open
cotton
tomatoes
wheat
corn
seed onions
dehy. onions
alfalfa
7,300 3,650 0 7,300 Feet
N
W
E
S

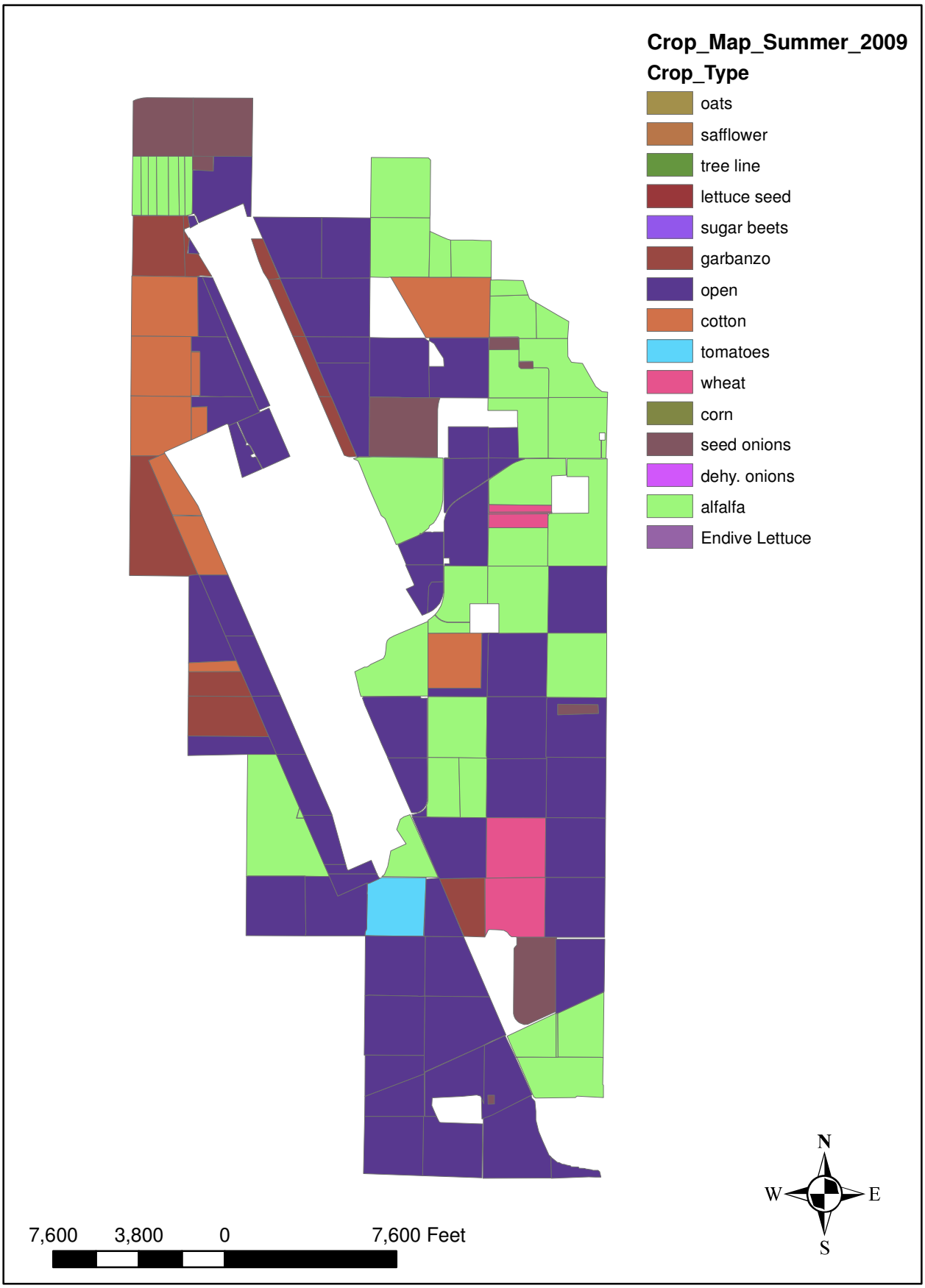
Crop_Map_Summer_2009
Crop_Type
oats
safflower
tree line
lettuce seed
sugar beets
garbanzo
open
cotton
tomatoes
wheat
corn
seed onions
dehy. onions
alfalfa
Endive Lettuce
N
W
E
S
7,600
3,800
0
7,600 Feet

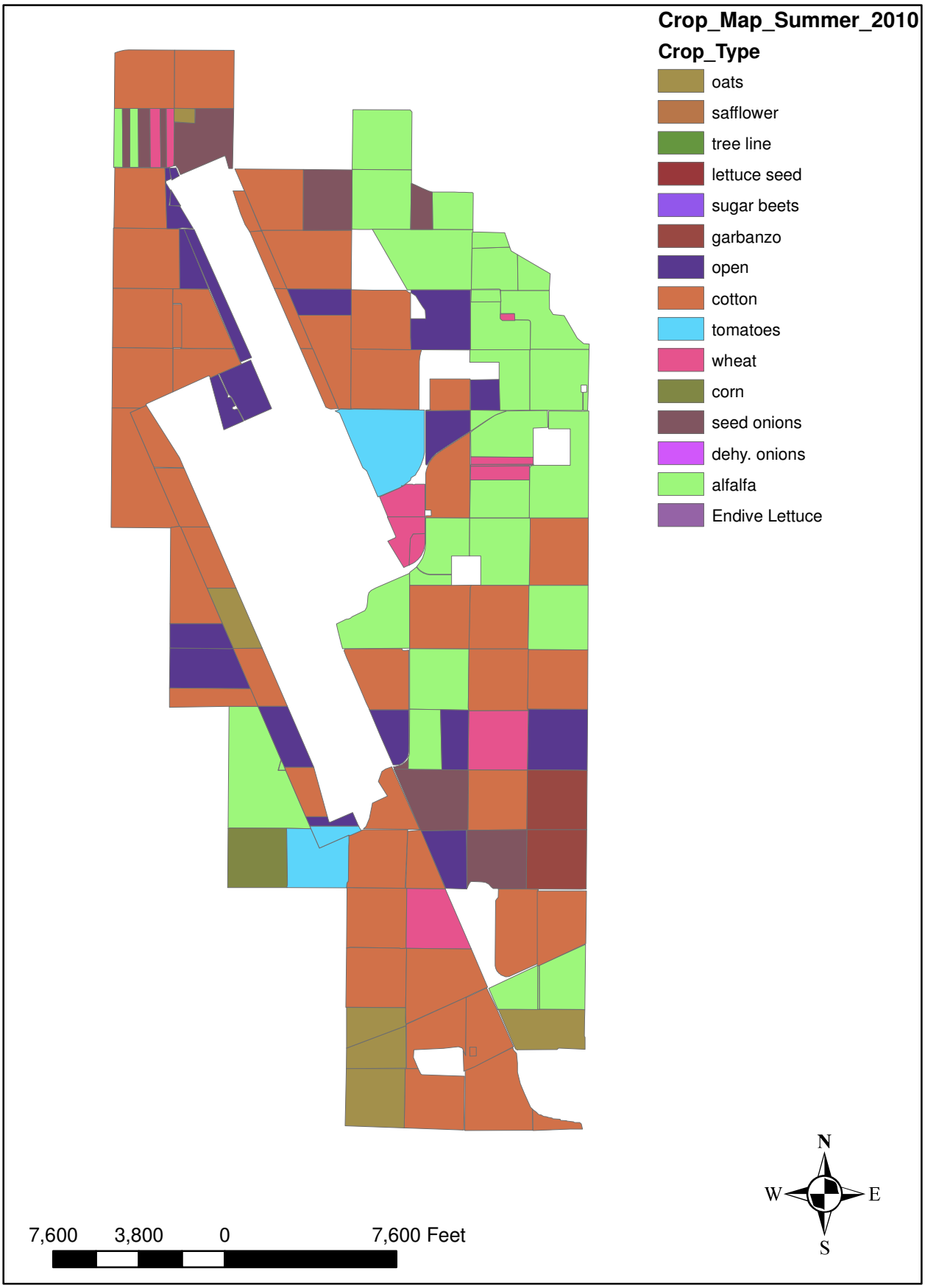
Crop_Map_Summer_2010
Crop_Type
oats
safflower
tree line
lettuce seed
sugar beets
garbanzo
open
cotton
tomatoes
wheat
corn
seed onions
dehy. onions
alfalfa
Endive Lettuce
N
W
E
S
7,600
3,800
0
7,600 Feet